Université de Montréal

Les azasulfurylpeptides :
Synthèse, analyse conformationnelle et applications biologiques

par
Stéphane Turcotte

Département de Chimie
Faculté des Arts et des Sciences

Thèse présentée à la Faculté des études supérieures et postdoctorales
en vue de l'obtention du grade de
Philosophiae Doctor (Ph. D.)
en Chimie

Avril, 2015

Résumé

Les azasulfurylpeptides sont des mimes peptidiques auxquels le carbone en position alpha et le carbonyle d'un acide aminé sont respectivement remplacés par un atome d'azote et un groupement sulfonyle (SO_2). Le but premier de ce projet a été de développer une nouvelle méthode de synthèse de ces motifs, également appelés *N*-aminosulfamides. À cette fin, l'utilisation de sulfamidates de 4-nitrophénol s'est avérée importante dans la synthèse des azasulfuryltripeptides, permettant le couplage d'hydrazides avec l'aide d'irradiation aux micro-ondes (Chapitre 2). Par la suite, en quantité stœchiométrique d'une base et d'un halogénure d'alkyle, les azasulfurylglycines (AsG) formés peuvent être chimiosélectivement alkylés afin d'y insérer diverses chaînes latérales. Les propriétés conformationnelles des *N*-aminosulfamides à l'état solide ont été élucidées grâce à des études cristallographiques par rayons X : elles possèdent une structure tétraédrique autour de l'atome de soufre, des traits caractéristiques des azapeptides et des sulfonamides, ainsi que du potentiel à favoriser la formation de tours γ (Chapitre 3).

Après le développement d'une méthode de synthèse des *N*-aminosulfamides en solution, une approche combinatoire sur support solide a également été élaborée sur la résine amide de Rink afin de faciliter la génération d'une librairie d'azasulfurylpeptides. Cette étude a été réalisée en employant le g*rowth hormone releasing peptide 6* (GHRP-6, His-D-Trp-Ala-Trp-D-Phe-Lys-NH_2). Ce dernier est un hexapeptide possédant une affinité pour deux récepteurs, le *growth hormone secretagogue receptor 1a* (GHS-R1a) et le récepteur *cluster of differenciation 36* (CD36). Une affinité sélective envers le récepteur CD36 confère des propriétés thérapeutiques dans le traitement de la dégénérescence maculaire liée à l'âge (DMLA). Six analogues d'azasulfurylpeptides de GHRP-6 utilisés comme ligands du CD36 ont été synthétisés sur support solide, mettant en évidence le remplacement du tryptophane à la position 4 de GHRP-6 (Chapitre 4).

Les analogues de GHRP-6 ont été ensuite analysés pour leur capacité à moduler les effets de la fonction et de la cascade de signalisation des ligands spécifiques au *Toll-like receptor 2* (TLR2), en collaboration avec le Professeur Huy Ong du département de Pharmacologie à la Faculté de Pharmacie de l'Université de Montréal. Le complexe TLR2-TLR6 est reconnu pour

être co-exprimé et modulé par CD36. En se liant au CD36, certains ligands de GHRP-6 ont eu un effet sur la signalisation du TLR2. Par exemple, les azasulfurylpeptides [AsF(4-F)^4]- et [AsF(4-MeO)^4]-GHRP-6 ont démontré une capacité à empêcher la surproduction du monoxyde d'azote (NO), un sous-produit réactif formé suite à l'induction d'un signal dans les macrophages par des ligands spécifiques liés au TLR2, tel le *fibroblast-stimulating lipopeptide 1* (R-FSL-1) et l'acide lipotéichoïque (LTA). En addition, la sécrétion du *tumor necrosis factor alpha* (TNFα) et du *monocyte chemoattractant protein 1* (MCP-1), ainsi que l'activation du *nuclear factor kappa-light-chain-enhancer of activated B cells* (NF-κB), ont été réduites. Ces résultats démontrent le potentiel de ces azasulfurylpeptides à pouvoir réguler le rôle du TLR2 qui déclenche des réponses inflammatoires et immunitaires innées (Perspectives).

Finalement, le potentiel des azasulfurylpeptides d'inhiber des métallo-β-lactamases, tels le *New-Delhi Metallo-β-lactamase 1* (NDM-1), IMP-1 et le *Verona Integron-encoded Metallo-β-lactamase* 2 (VIM-2), a été étudié en collaboration avec le Professeur James Spencer de l'Université de Bristol (Royaumes-Unis). Certains analogues ont été des inhibiteurs micromolaires du IMP-1 (Perspectives).

Ces nouvelles voies de synthèse des azasulfurylpeptides en solution et sur support solide devraient donc permettre leur utilisation dans des études de relations structure-activité avec différents peptides biologiquement actifs. En plus d'expandre l'application des azasulfurylpeptides comme inhibiteurs d'enzymes, cette thèse a révélé le potentiel de ces *N*-aminosulfamides à mimer les structures secondaires peptidiques, tels que les tours γ. À cet égard, l'application des azasulfurylpeptides a été démontrée par la synthèse de ligands du CD36 présentant des effets modulateurs sur le TLR2. Compte tenu de leur synthèse efficace et de leur potentiel en tant qu'inhibiteurs, les azasulfurylpeptides devraient trouver une large utilisation dans les sciences de peptides pour des applications dans la médecine et de la chimie biologique.

Mots-clés : Mimes peptidiques, Azasulfurylpeptides, *N*-Aminosulfamides, Alkylation chimio-sélective, GHRP-6, CD36, TLR2, Régulation des réponses inflammatoires et immunitaires innées, Inhibiteurs de métallo-β-lactamases.

Abstract

The azasulfurylpeptides are peptide mimics in which the alpha carbon and the carbonyl of an amino acid residue are respectively replaced by a nitrogen atom and a sulfonyl group (SO_2). The primary goal of this doctorate project was to develop a new effective method for the synthesis of these motifs, also called *N*-aminosulfamides. Towards this aim, the use of 4-nitrophenyl sulfamidates turned out to be important in the synthesis of azasulfuryltripeptides, allowing hydrazide couplings under micro-wave irradiation (Chapter 2). Side-chain diversity was then added using a stoichiometric amount of base and different alkyl halides to alkylate chemoselectively the azasulfurylglycine (AsG) residue. The conformational properties of the *N*-aminosulfamides in the solid state were studied using X-Ray crystallography, which showed a tetrahedral geometry about the sulfur atom, features of azapeptides and sulfonamides, as well as potential to favor the formation of γ turns (Chapter 3).

Following the development of the synthesis of these *N*-aminosulfamides in solution, a combinatorial approach on solid support was elaborated on Rink amide resin to generate a library of azasulfurylpeptides. The study was performed using the Growth Hormone Releasing Peptide 6 (GHRP-6, His-D-Trp-Ala-Trp-D-Phe-Lys-NH_2). The latter is a hexapeptide that has affinity for two receptors, the Growth Hormone Secretagogue Receptor 1a (GHS-R1a) and the Cluster of Differenciation 36 (CD36) receptor. Selective binding to the CD36 receptor has therapeutic potential in the treatment of age-related macular degeneration (AMD). Six azasulfurylpeptide analogs were synthesized on solid support by replacing tryptophan at the 4^{th} position of GHRP-6 with different *N*-aminosulfamide residues (Chapter 4).

The GHRP-6 analogs were tested for their ability to mediate the effects of receptor-specific ligands on the function and downstream signaling of the Toll-Like Receptor 2 (TLR2), in collaboration with Professor Huy Ong at the department of Pharmacology in the Faculty of Pharmacy at the Université de Montréal. The TLR2-TLR6 complex is known to be co-expressed and modulated by CD36. On binding to CD36, certain GHRP-6 ligands exhibited effects on the signaling of TLR2. For example, the azasulfurylpeptides [4-F-AsF^4]- and [4-MeO-AsF^4]-GHRP-6 prevented the overproduction of nitric oxide (NO), a reactive oxygen species formed following the induction of signal in macrophages on binding of TLR2-specific ligands, such as

the Fibroblast-Stimulating Lipopeptide 1 (R-FSL-1) and lipoteichoic acid (LTA). Furthermore, the secretion of the Tumor Necrosis Factor Alpha (TNFα) and Monocyte Chemoattractant Protein 1 (MCP-1), as well as the activation of the Nuclear Factor Kappa-light-chain-enhancer of activated B cells (NF-κB), all were reduced. These results offer promise for regulating Toll-like receptor roles in triggering innate immunity and inflammatory responses (Perspectives).

Finally, the potential of the azasulfurylpeptides to inhibit metallo-β-lactamases, such as the New-Delhi Metallo-β-lactamase 1 (NDM-1), IMP-1 and the Verona Integron-encoded Metallo-β-lactamase 2 (VIM-2), has been studied in collaboration with Professor James Spencer at the University of Bristol (United-Kingdom). Some analogs were micromolar inhibitors of IMP-1 (Perspectives).

These new approaches for the synthesis of azasulfurylpeptides in solution and on solid support should enable their use in studies of structure-activity relationships with different biologically active peptides. In addition to expanding the application of azasulfurylpeptides as enzyme inhibitors, this thesis has revealed the potential of these *N*-aminosulfamides to mimic the peptide secondary structures, such as γ turns. Application of azasulfurylpeptides in this respect has been demonstrated by the synthesis of CD36 ligands exhibiting modulatory effects on the TLR2. Considering their effective synthesis and potential as inhibitors, azasulfurylpeptides should find broad use in peptide science for applications in medicine and chemical biology.

Keywords: Peptide mimicry, Azasulfurylpeptides, *N*-Aminosulfamides, Chemoselective alkylation, GHRP-6, CD36, TLR2, Regulation of innate immunity and inflammatory responses, Metallo-β-lactamases inhibitors.

Notes

Je tiens à préciser ma contribution pour chacun des chapitres qui composent cette thèse par articles :

- Chapitre 1 : J'ai entièrement rédigé l'introduction de ma thèse.
- Chapitre 2 : Les sulfamidates présentés dans l'article 1 (Org. Lett. **2012**) ont été synthétisés avec l'aide de Samir Bouayad-Gervais. Par la suite, les couplages des hydrazides aux sulfamidates, ainsi que les alkylations chimiosélectives sur les azasulfurylglycines, ont entièrement été réalisés par moi. J'ai finalement écrit la première version de l'article, auquel le Professeur William D. Lubell a commenté et corrigé avant soumission. Dans l'article 2 (Proceedings **2012**), la comparaison entre le BTPP et l'hydroxyde de tétraéthylammonium (Et_4NOH) a été réalisé avec l'aide de Thierry Havard. J'ai par la suite participé au *32nd European Peptide Symposium* en Grèce où cet abrégé de conférence a été rédigé par moi, sous la supervision du Pr. Lubell.
- Chapitre 3 : La rédaction de l'article 3 [Biopolymers (Pept. Sci.) **2015**] a également été rédigée par moi, sous la supervision du Pr. Lubell. L'utilisation de l'appareil à rayons X pour la résolution des structures des deux cristaux présentés dans cet article a été réalisée par Francine Bélanger à l'Université de Montréal.
- Chapitre 4 : L'article 4 (en préparation pour Org. Lett.) présente la synthèse sur support solide de six analogues [azasulfuryl^4]-GHRP-6. Bien que la méthodologie ait été développée par moi, Lylia Dif-Yaiche a synthétisé entièrement l'analogue [Ala^1, AsF(4-F)^4]-GHRP-6] (**134**). Les 5 autres ont été accomplis par moi. La préparation de cet article a été rédigée par moi, sous la supervision du Pr. Lubell.
- Chapitre 5 : La rédaction de ce chapitre présentant les analyses biologiques réalisées à ce jour sur les azasulfurylpeptides a entièrement été effectuée par moi. Toutefois, les résultats présentés dans ce chapitre n'ont pas été réalisés par moi. Les tests biologiques sur la modulation du *Toll-like receptor 2* (TLR2) ont été accomplis par Katia Mellal et Mukandila Mulumba, sous la supervision du Professeur Huy Ong à l'Université de Montréal. Les tests d'affinité envers CD36 par résonance des plasmons de surface ont été accomplis par Jérémie

Labrecque-Carbonneau, sous la supervision du Professeur Jean-François Masson à l'Université de Montréal. Finalement, l'analyse computationnelle d'une série d'inhibiteurs potentiels de métallo-β-lactamases a été effectuée par Ricky Cain dans le groupe du Pr. Colin Fishwick à l'Université de Leeds, tandis que les tests biologiques ont été réalisés par Ramya Salimraj, sous la supervision du Professeur James Spencer à l'Université de Bristol.

- Chapitre 6 : J'ai entièrement rédigé la conclusion de cette thèse.

Table des matières

Liste des schémas

Liste des figures

Liste des tableaux

Liste des abréviations

[α]	Rotation spécifique [en (deg * mL / g * dm)
Ac	Acétyle
AcOH	Acide acétique
ADN	Acide désoxyribonucléique
Ala	Alanine
Alloc	Allyloxycarbonyle
AMD	*Age-related macular degeneration*
Ar	Aryle
AsF	Azasulfurylphénylalanine
AsG	Azasulfurylglycine
AsY	Azasulfuryltyrosine
Bn	Benzyle
Boc	*tert*-Butyloxycarbonyle
br	*Broad* (en RMN)
BTPP	*tert*-Butylimino-tri(pyrrolidino)phosphorane
°C	Degré Celsius
Cbz	Benzyloxycarbonyle
CD36	*Cluster of differenciation 36*
COSY	*Correlated spectroscopy*
CPA	Carboxypeptidase A
δ	Déplacement chimique en ppm (en RMN)
d	Doublet (en RMN)
DCE	1,2-Dichloroéthane
DCM	Dichlorométhane
dd	Doublet de doublet (en RMN)
deg	Degré
DIC	*N*,*N*-Diisopropylcarbodiimide
DIEA	*N*,*N*-Diisopropyléthylamine
DMF	N,N-Diméthylformamide

DMLA	Dégénérescence maculaire liée à l'âge
DMSO	Diméthylsulfoxyde
DMTr	4,4'-Diméthoxytrityle
ESI	*Electrospray ionization*
Et	Éthyle
Et_2O	Éther diéthylique
EtOAc	Acétate d'éthyle
EtOH	Éthanol
éq	Équivalent
FA	Acide formique
Fmoc	Fluorénylméthyloxycarbonyle
Fmoc-OSu	Hydroxysuccinimide de fluorénylméthyloxycarbonyle
g	Gramme(s)
GHRP-6	*Growth hormone releasing peptide 6*
GHS-R1a	*Growth hormone secretagogue receptor 1a*
h	Heure(s)
H_2SO_4	Acide sulfurique
HBTU	*O*-Benzotriazol-1-yl-*N*,*N*,*N'*,*N'*-tétraméthyluronium hexafluorophosphate
His	Histidine
HIV-1	*Human immunodeficiency virus 1*
HMBC	*Heteronuclear Multiple Bond Correlation*
HOBt	Hydroxybenzotriazole
HPLC	*High performance liquid chromatography*
HPV	*Human Papillomavirus*
HRMS	*High resolution mass spectrometry*
IBC	Chloroformate d'isobutyle
IBX	Acide *o*-iodobenzoïque
IFNγ	Interferon γ
IPNBSH	Hydrazide du *N*-isopropylidène-*N'*-2-nitrobenzènesulfonyle
*i*Pr	*iso*-Propyle

IR	Infrarouge
J	Constante de couplage (en RMN)
KO*t*Bu	*tert*-butoxyde de potassium
L	Litre
LCMS	*Liquid chromatography mass spectrometry*
Leu	Leucine
LTA	Acide lipotéichoïque
Lys	Lysine
M	Mole(s) par litre
m	Multiplet (en RMN)
MCP-1	*Monocyte chemoattractant protein 1*
Me	Méthyle
MeOH	Méthanol
MHz	Mégahertz (en RMN)
mp	*Melting point*
NaOMe	Méthoxyde de sodium
NDM-1	*New-Delhi Metallo-β-lactamase 1*
NEt_3	Triéthylamine
NEt_4OH	Hydroxyde de tétraéthylammonium
NF-κB	*Nuclear factor kappa-light-chain-enhancer of activated B cells*
NMM	*N*-méthylmorpholine
NMR	*Nuclear magnetic resonance*
NO	Monoxyde d'azote
Ph	Phényle
Phe	Phénylalanine
ppm	Partie par million (en RMN)
Pro	Proline
Pyr	Pyridine
q	Quadruplet (en RMN)
R5L	Règles de cinq de Lipinski
R-FSL-1	*Fibroblast-Stimulating Lipopeptide 1*

R*f*	Facteur de rétention (en chromatographie)
RMN	Résonance magnétique nucléaire
RP	*Reverse phase*
RT	*Retention time*
rt	*Room temperature*
s	Singulet (en RMN)
$SbCl_5$	Chlorure d'antimoine (V)
SO_2	Dioxyde de soufre
SO_2Cl_2	Chlorure de sulfuryle
SPSS	Synthèse peptidique sur support solide
T	Thymine (ADN)
t	Triplet (en RMN)
TBDMS	*tert*-Butyldiméthylsilyle
TBTU	*O*-Benzotriazol-1-yl-*N*,*N*,*N'*,*N'*-tétraméthyluronium tetrafluoroborate
*t*Bu	*tert*-Butyle
*t*BuOAc	Acétate de *tert*-butyle
TEA	Triéthylamine
TES	Triéthylsilane
TFA	Acide trifluoroacétique
THF	Tétrahydrofurane
TLC	*Thin layer chromatography*
TLR2	*Toll-Like Receptor 2*
TM	Tamis moléculaire
TNF(α)	*Tumor necrosis factor (alpha)*
Tr	Trityle
Val	Valine
VIM-2	*Verona Integron-encoded Metallo-β-lactamase 2*

À ma grand-mère, atteinte de la dégénérescence maculaire liée à l'âge.

Remerciements

Je tiens tout d'abord à remercier mon directeur de recherche, le Professeur William D. Lubell de m'avoir accepté dans son groupe dans le but d'obtenir mon doctorat. Le début de ce projet a été particulièrement difficile dans le développement de la méthodologie et pour mon moral… Sans son soutien continuel, je n'aurai probablement pas pu compléter ce projet.

Je remercie mes deux étudiants d'été, Samir Bouayad-Gervais et Thierry Havard, avec lesquels j'ai eu la chance de travailler ensemble et d'inclure comme co-auteurs dans mes publications. Merci également au Professeur Shawn Collins de m'avoir proposé l'étape d'alkylation durant mon séminaire étudiant. Cette étape a été un point tournant dans ce projet.

Merci à Julien Poupart, Antoine Douchez et Mohamed Atfani pour avoir révisé et apporté leurs corrections lors de la rédaction de cette thèse. J'apprécie également l'ambiance dynamique que ma collègue de laboratoire, Yésica Garcia-Ramos, a apportée, ainsi que les autres membres du groupe que j'ai eu le plaisir de côtoyer.

Je remercie le personnel du centre régional de spectrométrie de masse (Dr. Alexandra Fürtos, Karine Venne et Marie-Christine Tang) pour les analyses HRMS, du centre régional de RMN (Dr. Minh Tan Phan Viet, Sylvie Bilodeau, Antoine Hamel et Cédric Malveau) pour leur aides dans l'analyse de certains composés, et du laboratoire de diffraction des rayons X (Françine Bélanger) pour la résolution des structures des cristaux.

J'éprouve une grande reconnaissance envers la Faculté des études supérieures et postdoctorales (FESP) et les Fonds Québécoises en Recherche Nature et Technologies (FQRNT) pour le support financier durant mes études graduées.

Un grand merci également à mes parents qui m'ont supporté tout au long de mes études, et qui m'ont écouté lorsque je traversais des périodes difficiles au laboratoire.

Chapitre 1 : Introduction

1.1. Les peptides en tant que médicaments

1.1.1. Début du 20e siècle

En comparaison avec les protéines, un peptide est arbitrairement défini comme une molécule contenant moins de 50 acides aminés. Au début du 20e siècle, les peptides n'étaient pas considérés comme de bons candidats dans le développement de médicaments. En effet, les petits peptides ayant une faible masse moléculaire (< 500 Da) souffrent souvent de faibles sélectivités envers les récepteurs, ce qui se manifeste généralement par la présence d'effets secondaires.[1] De plus, les peptides sont généralement connus pour être instables métaboliquement, être éliminés rapidement, avoir une faible perméabilité avec les membranes et ne pouvant pas être administrés oralement. Quant aux protéines (> 5000 Da), malgré leur spécificité envers leurs récepteurs, elles sont généralement peu biodisponibles.[1] Également, d'après les « règles de cinq de Lipinski » (R5L), une substance aura une forte probabilité d'être peu absorbée ou de difficilement pénétrer la membrane si :[2, 3]

1. Sa masse moléculaire est supérieure à 500 Da;
2. Elle possède plus de 5 donneurs de liaisons hydrogène (somme des groupements OH et NH);
3. Elle possède plus de 10 accepteurs de liaisons hydrogène (somme des atomes N et O);
4. Sa valeur de log *P* est supérieure à 5.

Considérant qu'un peptide dépasse rapidement les 500 Da après seulement cinq acides aminés, il n'est pas surprenant que les peptides n'étaient pas considérés par les compagnies pharmaceutiques au début du 20e siècle dans le développement de médicaments.

1.1.2. Fin du 20e siècle

Toutefois, avec les nouvelles techniques d'expressions, de purification et d'analyse de protéines de plus en plus efficaces, de nouvelles classes de molécules thérapeutiques ont commencé à émerger vers la fin du 20e siècle.[1] Dans la classe des anticorps et protéines, on retrouve comme exemples : Adalimumab / Humira Pen,[4] Etanercept ⁄ Enbrel[5] et Infliximab ⁄ Remicade[6] (arthrite rhumatoïde), Rituximab ⁄ Rituxan[7] (lymphomes non-Hodgkinien), Bevacizumab⁄Avastin[8] (cancer colorectal), ainsi que Trastuzumab⁄Herceptin[9] (cancer du sein).

Dans la classe des protéines injectables, on retrouve entre autres : l'insuline Glargine / Lantus[10] (diabètes de type I et II), Neulasta / Pegfilgrastim[11] (neutropénie, c'est-à-dire un déficit dans la quantité de neutrophiles causé par la chimiothérapie), Epogen[12] (anémie rénale) et Avonex[13] (sclérose en plaques). Finalement, dans la classe des peptides injectables, des exemples comprennent : Copaxone / Glatiramer acetate[14] (sclérose en plaques), Lupron / Leuprorelin[15] et Zoladex / Goserelin[16] (cancers du sein et de la prostate), ainsi que Sandostatin / Octreotide[17] (inhibiteur de la sécrétion de l'hormone de croissance) et Velcade / Bortezomib[18] (myélome multiple et leucémie).

Ces molécules, correspondant à la classe des « biologiques », ne respectent pas les R5L et doivent par conséquent être administrées par des injections intraveineuses. Ces biologiques font désormais parti des différentes catégories de molécules ayant connu et connaissant du succès en tant que médicaments. Dans la classe des peptides, suite au développement de la synthèse peptidique sur support solide (SPSS) par Merrifield en 1963,[19] l'exploration des peptides en tant que médicaments a connu un essor remarquable étant donné leur plus grande facilité de synthèse. Bons nombres d'efforts se tournent vers la recherche de nouveaux médicaments auxquels les masses moléculaires des peptides synthétisés se situeraient entre les petites molécules (< 500 Da) et les biologiques (> 5000 Da). Ceci serait dans le but d'éviter les problèmes de sélectivité et de biodisponibilité qui sont respectivement associés aux petites et grosses molécules.

Afin de surmonter les problèmes liés à l'utilisation des peptides comme médicaments, une chimie visant à modifier certaines propriétés des peptides, comme par exemples leur profil pharmacocinétique (absorption, biodisponibilité, temps de demi-vie), leur structure secondaire (ou tridimensionnelle) et leur activité biologique, à rapidement connu un essor, soit la chimie peptidomimétique.

1.2. Inhibiteurs d'enzymes

Dans la recherche d'inhibiteurs d'enzymes, le concept de mimer l'état de transition dans l'hydrolyse des amides a grandement été étudié. Par exemple, la modification du lien amide des peptides a pour but de créer des inhibiteurs compétitifs dont la géométrie structurelle

tétraédrique ressemble à l'intermédiaire *gem*-diolate formé dans le mécanisme de l'hydrolyse des amides catalysés par les enzymes.

1.2.1. Les phosphonamidates, phosphinates et phosphonates

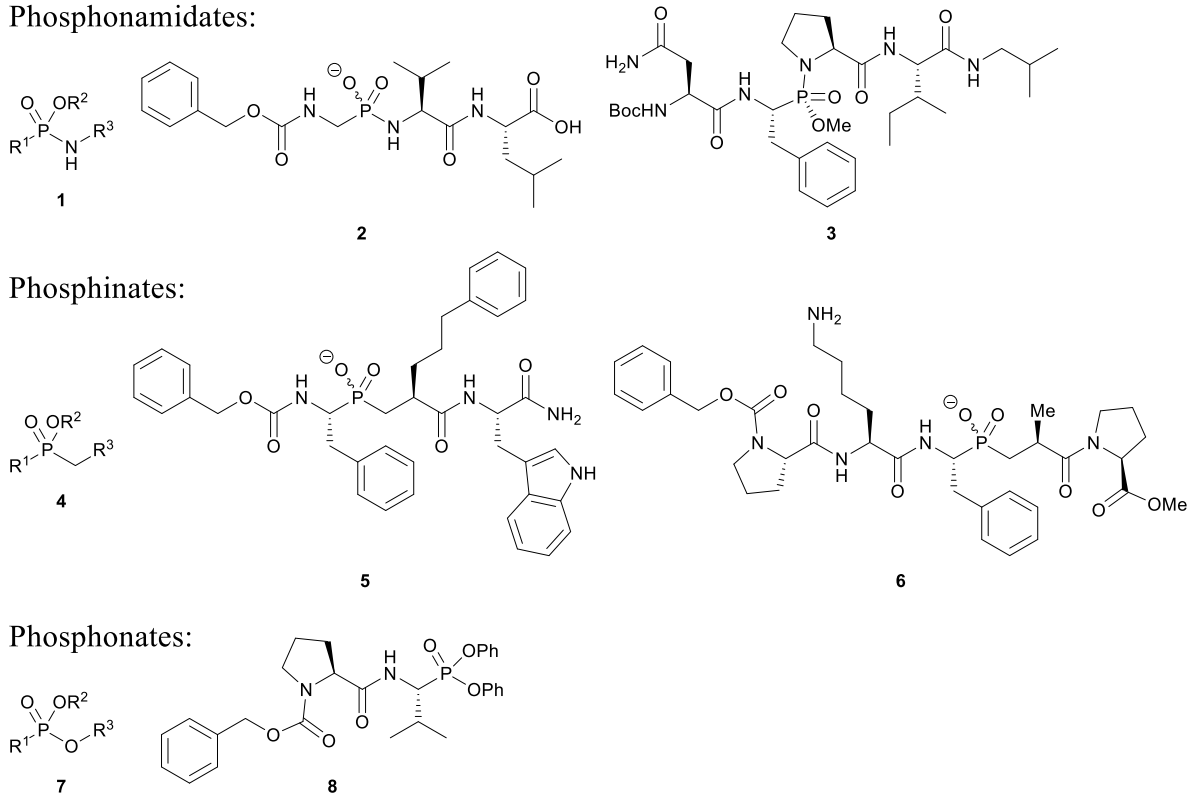

Figure 1.1. Exemples d'inhibiteurs phosphorés : les phosphonamidates, phosphinates et phosphonates.

À titre d'exemples, les phosphonamidates (**1**), les phosphinates (**4**) et les phosphonates (**7**) font parties des classes importantes de mimes peptidiques contenant un atome de phosphore pouvant mimer les états de transition dans l'hydrolyse des amides (Figure 1.1). Les phosphonamidates ont servi d'inhibiteurs de protéases de zinc, telle la carboxypeptidase A (CPA),[20, 21] la collagénase neutrophile humaine[22] et la thermolysine (**2**),[23, 24] car ils peuvent coordonner avec le zinc afin d'inhiber leur fonction dans la processus d'hydrolyse. Ils ont également permis de développer des inhibiteurs de la protéinase de l'immunodéficience humaine-1 (HIV-1, **3**)[25, 26] et du peptidyl-prolyl *cis-trans* isomérase.[27] Les phosphinates ont été illustrés dans des exemples d'inhibition de la famille des matrixines (**5**)[28] et de l'astacine (**6**),[29]

d'autres classes de métallopeptidases. Quant aux phosphonates, ils ont été utilisés dans des inhibiteurs irréversibles de protéases à sérines, comme la chymotrypsine (**8**).[30]

1.2.2. Les sulfonamides et sulfinamides

Sulfonamides:

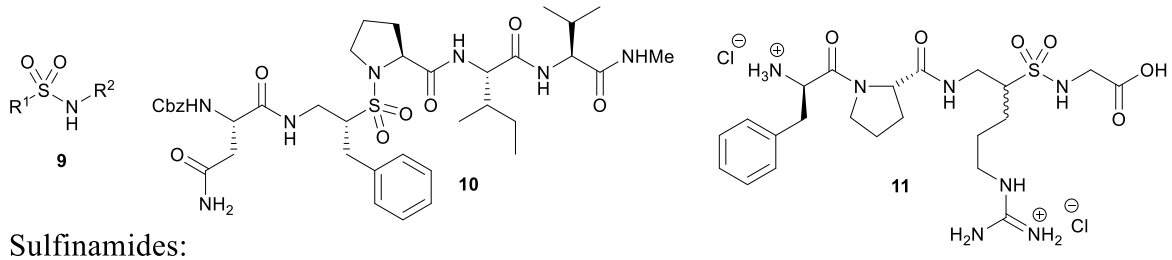

Sulfinamides:

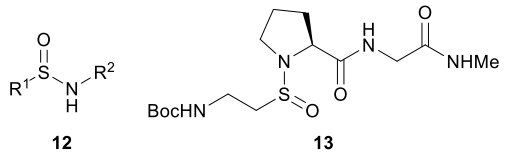

Figure 1.2. Exemples d'inhibiteurs soufrés : les sulfonamides et sulfinamides.

En revanche, les sulfonamides (**9**) et les sulfinamides (**12**) contiennent un atome de soufre pouvant avoir la géométrie tétraédrique désirée (Figure 1.2). Tout comme les dérivés phosphorylés, des recherches ont été effectuées dans la synthèse d'inhibiteurs de la protéinase de HIV-1 (**10**)[31, 32] et de la thermolysine.[33] D'autres exemples de sulfonamides impliquent des inhibiteurs de la thrombine (**11**),[34] une protéase à sérine, et de ligases de muramyle,[35] responsables dans la biosynthèse de peptidoglycanes. La synthèse des sulfonamides dérive des sulfinamides auxquels une étape d'oxydation est nécessaire.[31-36] Les sulfinamides peuvent également être utilisés dans la synthèse potentielle d'inhibiteurs de HIV-1 (**13**).[32] Il est important de mentionner que la synthèse des α-aminosulfonamides (**14**) est impossible, car une β-élimination survient, menant à la formation d'imines *N*-acylés (**15**, Schéma 1.1).[37]

Schéma 1.1. Décomposition des α-aminosulfonamides.

α-Aminosulfonamides

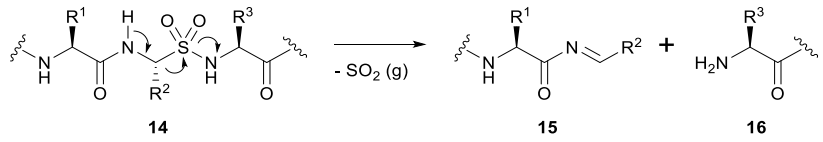

1.3. Contraintes covalentes pour favoriser des tours

Dans le but de synthétiser des inhibiteurs ayant une conformation précise, plusieurs contraintes covalentes insérées dans les peptides ont été développées afin de favoriser la formation de tours β et γ. La présence de tels tours peut influencer l'activité biologique des peptides. Un tour est une structure secondaire d'un peptide ou d'une protéine et correspond à une inversion de la direction de la chaîne peptidique. Il implique 4 acides aminés pour un tour β (*i* à *i*+3) et 3 acides aminés pour un tour γ (*i* à *i* + 2), auquel la distance entre le premier et le dernier acide aminé du tour est inférieur à 7Å. De plus, les tours possèdent généralement une liaison hydrogène entre le carbonyle du premier résidu et l'amide du dernier acide aminé.

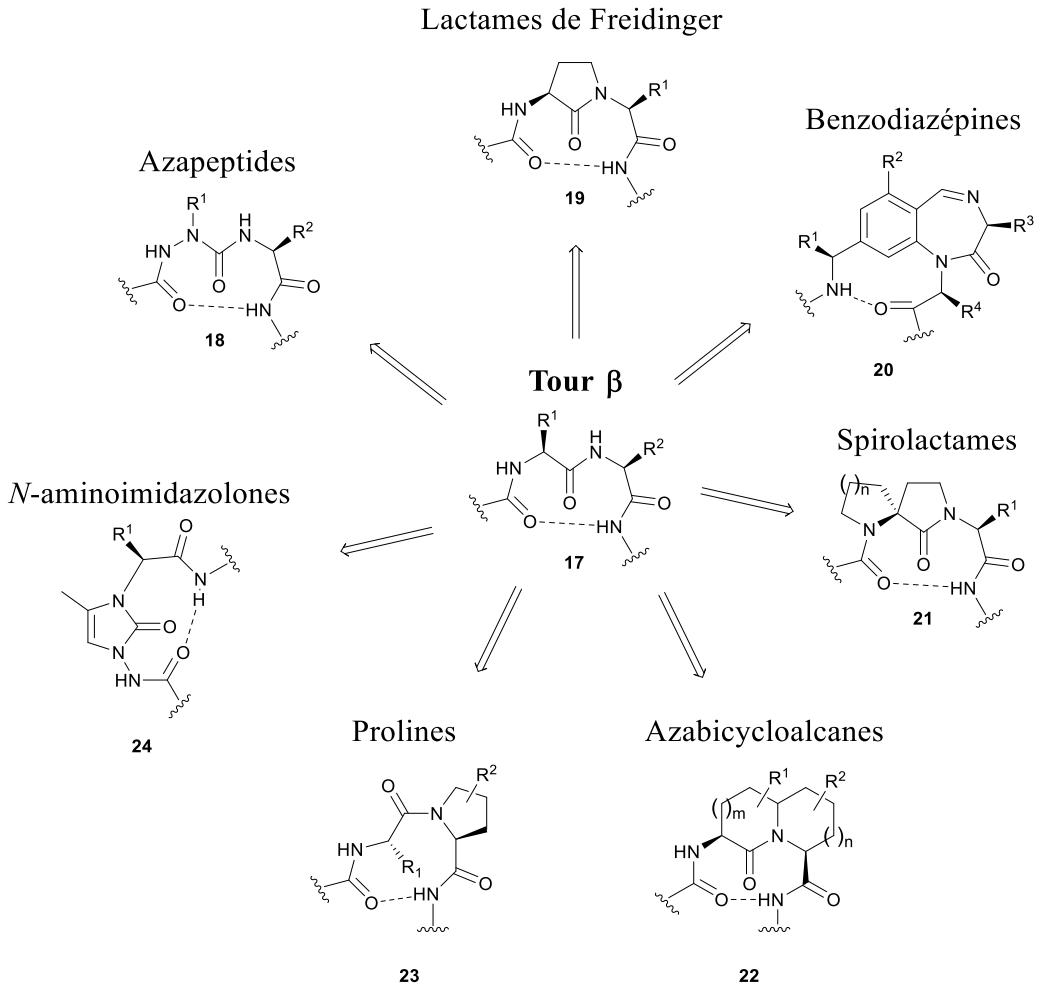

Figure 1.3. Exemples de contraintes covalentes utilisées dans la formation de tours β.

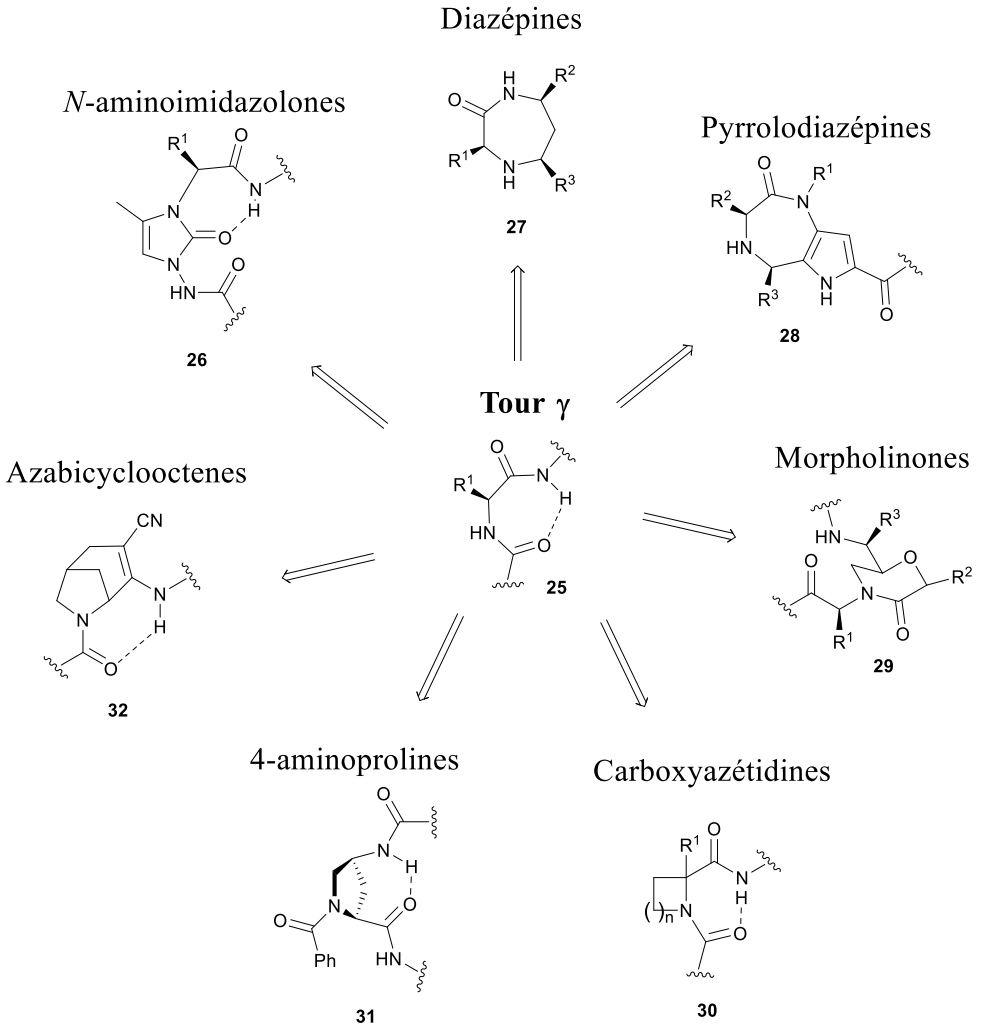

Figure 1.4. Exemples de contraintes covalentes utilisées dans la formation de tours γ.

Les azapeptides (**18**),[38-40] les lactames de Freidinger (**19**),[41-45] les benzodiapépines (**20**),[46] les spirolactames (**21**),[47-49] les azabicycloalcanes (**22**),[50-54] les dérivés de prolines (**23**)[55-57] et les *N*-aminoimidazolones (**25**)[58-60] sont tous des exemples impliqués dans la formation de tours β (Figure 1.3). Les tours β sont essentiels à la reconnaissance lors de la liaison d'un ligand à son récepteur.[61] Quant aux mimes de tours γ, on retrouve les *N*-aminoimidazolones (**26**)[58, 59], les diazépines (**27**),[62-64] les pyrrolodiazépines (**28**),[65] les morpholinones (**29**),[66] les carboxy-azétidines (**30**),[67] les 4-aminoprolines (**31**)[68] et les azabicyclooctène (**32**)[69] (Figure 1.4). Les tours γ sont particulièrement importants dans l'activité biologique de récepteurs couplés à la protéine G.[1] Tous ces exemples illustrent bien l'intérêt porté au développement de nouvelles conformations qui seront utilisées dans des peptides biologiquement actifs.

1.4. Les azasulfurylpeptides

Les azasulfurylpeptides (**33**), ou *N*-aminosulfamides, ont été introduits par le professeur John Jones à l'université de Oxford en 1994 et constituent une nouvelle classe de mimes peptidiques auxquels le carbone en position alpha et le carbonyle d'un acide aminé sont respectivement remplacés par un atome d'azote et un groupement sulfonyle (Figure 1.5).[70] La capacité des azasulfurylpeptides de pouvoir mimer l'intermédiaire tétraédrique dans l'hydrolyse des liens amides a été exploitée par l'insertion d'un azasulfurylphénylalanine (AsF) dans une séquence d'un substrat de HIV-1. Cette modification a eu comme effet d'engendrer un inhibiteur de HIV-1 possédant une constante d'inhibition de 27 μM (**34**, Figure 1.5).[71] Ces motifs constituent donc une alternative intéressante aux α-aminosulfonamides qui se dégradent spontanément.

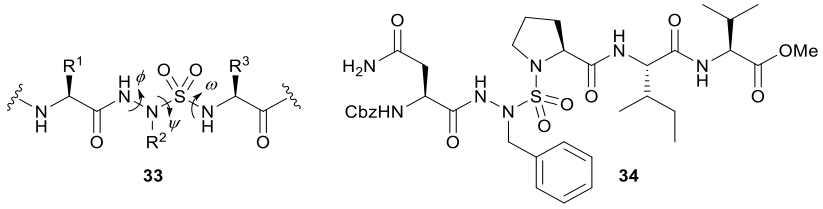

Figure 1.5. Structure générale des azasulfurylpeptides (**33**) et d'un inhibiteur de HIV-1 (**34**).

1.4.1. Méthode initiale de synthèse des azasulfurylpeptides

La méthode initiale de synthèse des azasulfurylpeptides utilise du chlorure du sulfuryle (SO_2Cl_2) avec une quantité catalytique de chlorure d'antimoine (V) ($SbCl_5$) pour combiner une amine (**35**) avec un dérivé d'hydrazide (**38** ou **39**). Toutefois, cette approche peut mener à la formation d'un sulfamide symétrique (**37d**). De plus, afin d'insérer des chaînes latérales sur les azasulfurylpeptides, des dérivés d'hydrazides *N*-benzylés (**39**) ont été utilisés comme exemple, requérant la synthèse préalable de ces précurseurs.[70] Depuis, aucune autre approche n'a été développée démontrant une possible difficulté dans la synthèse de ces composés.

Schéma 1.2. Méthode initiale de synthèse des azasulfurylpeptides.

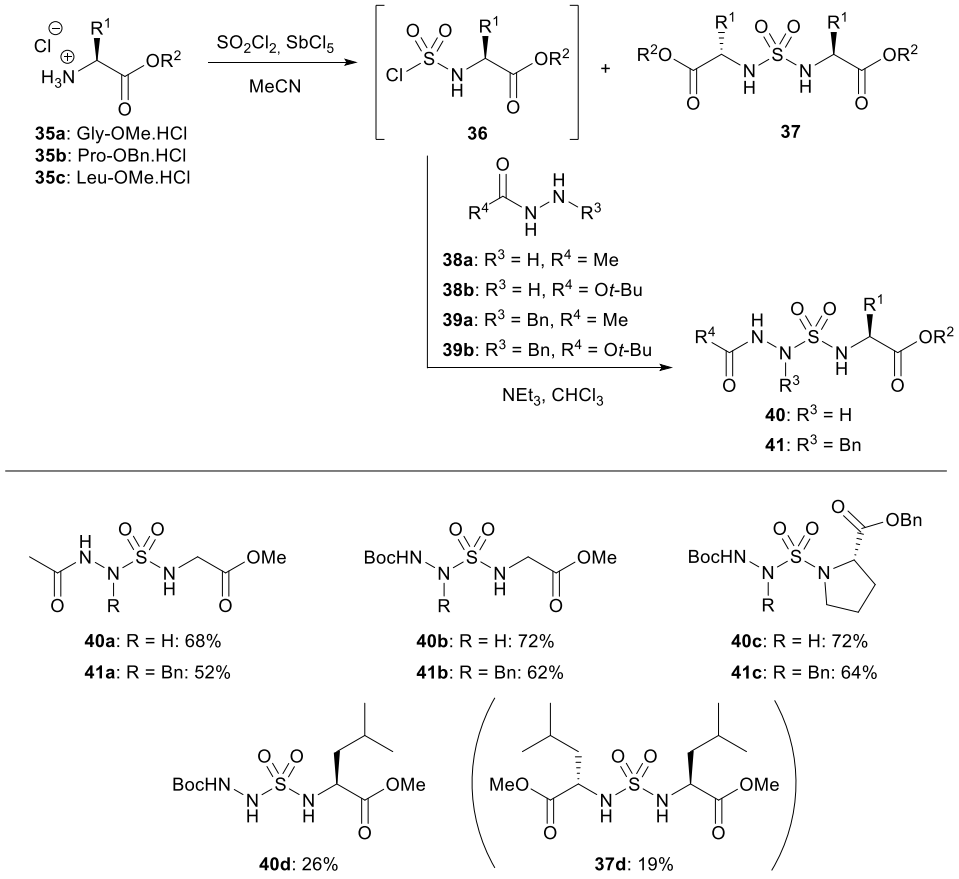

1.4.2. Propriétés conformationnelles attendues

En théorie, les azasulfurylpeptides combinent les propriétés relatives aux azapeptides[38] et aux sulfonamides.[72] Ceci inclus :

1. Une répulsion électronique entre les paires d'électrons des deux atomes d'azotes adjacents, favorisant des angles de torsion ϕ de ± 90°;[38]
2. Des angles de torsion ψ et ω de ± 60° ou ± 100° correspondant respectivement aux conformations décalées et éclipsées des sulfonamides (Figure 1.6). Le conformère éclipsé est plus stable d'environ 5 à 10 kJ/mol, attribuable à la minimisation de la répulsion électronique entre les doublets électroniques des oxygènes et de l'azote qui sont dans le même plan pour le conformère décalé;[72]

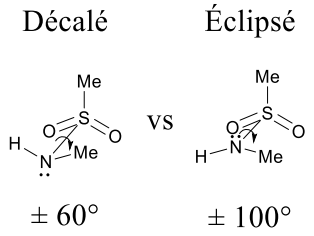

Figure 1.6. Représentation du conformère décalé et éclipsé des sulfonamides.

3. Une meilleure flexibilité en raison de la barrière de rotation plus faible autour du lien S−N ($\Delta G^{\ddagger} \approx$ 30 kJ/mol pour le conformère décalé et 40 kJ/mol pour le conformère éclipsé), relativement au lien C−N des amides ($\Delta G^{\ddagger} \approx$ entre 65 et 90 kJ/mol);[72]

4. Une hyperconjugaison, appelée interaction anomérique π, entre l'orbitale non-liante de l'azote et l'orbitale σ* de la liaison S-C du sulfonamide ($n_N \rightarrow \sigma^*_{S\text{-}C}$). Ceci se caractérise par des longueurs de liaisons S-N dans les sulfonamides plus courtes (autour de 1.65 Å) que les longueurs de liaisons S-N simples (autour de 1.75 Å);[73]

5. Une géométrie tétraédrique du sulfamide caractérisée par des longueurs de liaison S−N et S=O plus longues qu'un lien amide;[72]

6. Une plus grande acidité de Brønsted du proton du sulfamide et une meilleure basicité de Lewis des oxygènes du groupement sulfonyle, en raison de l'effet inductif du lien sulfonyle,[74] favorisant la formation de liaisons hydrogène.[75-77] En effet, la double liaison S=O implique une liaison σ et une délocalisation π (ou rétrodonation $p\pi$-$d\pi$) entre une paire d'électrons de l'oxygène et l'orbitale *d* du soufre (Figure 1.7). Cette rétrodonation est cependant faible dans le cas du lien S−N.[74]

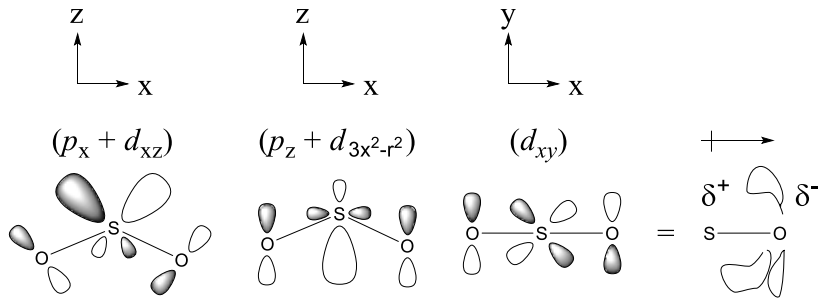

Figure 1.7. Représentation de la délocalisation π de la liaison S=O.

Si les azasulfurylpeptides respectent les contraintes conformationnelles énumérés ci-dessus, la combinaison des angles ϕ et ψ seront relativement proches des angles de torsion idéales de tours γ classiques ($\phi^{i+1} = 75°$, $\psi^{i+1} = -65°$) ou inversés ($\phi^{i+1} = -75°$, $\psi^{i+1} = 65°$), ou de tours β de type II ($\phi^{i+1} = -60°$, $\psi^{i+1} = 120°$) ou II' ($\phi^{i+1} = 60°$, $\psi^{i+1} = -120°$), et ces mimes peptidiques pourraient être un atout important dans la formation de ces tours.

1.4.3. Analyses cristallographiques de deux azasulfuryldipeptides

Tableau 1.1. Longueurs de liaison et angles de torsion sélectionnés pour *N*-(Ac)-AsF-Gly-OMe (**42**) et *N*-(Boc)-AsF-Pro-OMe (**43**).[70]

N-(Ac)-AsF-Gly-OMe (**42**)		*N*-(Boc)-AsF-Pro-OMe (**43**)	
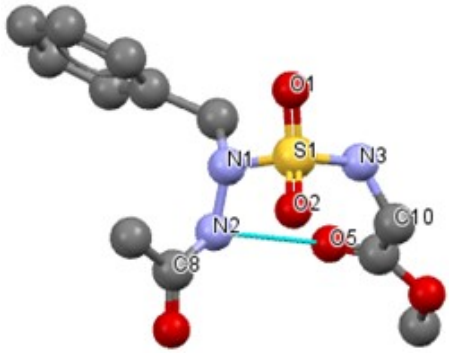		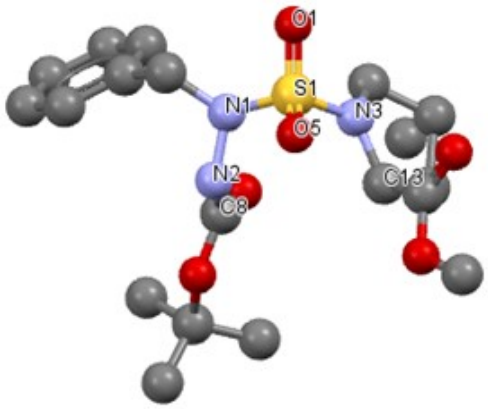	
Atomes	**Longueur (Å)**	**Atomes**	**Longueur (Å)**
N(2)−N(1)	1.396	N(2)−N(1)	1.396
N(1)−S(1)	1.677	N(1)−S(1)	1.664
S(1)−N(3)	1.599	S(1)−N(3)	1.600
S(1)=O(1)/S(1)=O(2)	1.421/1.420	S(1)=O(1) / S(1)=O(5)	1.422/1.419
Angles de torsion	**Angle (°)**	**Angle de torsion**	**Angle (°)**
ϕ [C(8)−N(2)−N(1)−S(1)]	94.3	ϕ [C(8)−N(2)−N(1)−S(1)]	−112.7
ψ [N(2)−N(1)−S(1)−N(3)]	76.1	ψ [N(2)−N(1)−S(1)−N(3)]	73.5
ω [N(1)−S(1)−N(3)−C(10)]	−89.2	ω [N(1)−S(1)−N(3)−C(13)]	−90.7

Des études cristallographiques ont été réalisées sur deux azasulfuryldipeptides contenant chacun un AsF, l'analogue de la phénylalanine.[70] En examinant le tableau 1.1 ci-dessus, on remarque que les restrictions conformationnelles des azapeptides de l'angle ϕ (i.e. de ± 90°) et des sulfonamides de l'angle ψ et ω (i.e. de ± 60° ou ± 100°) ont été conservées. Les angles de torsion ψ et ω dans ces exemples correspondent donc respectivement aux conformères décalés et éclipsés des sulfonamides. La structure géométrique autour de l'atome du soufre a confirmé l'hypothèse que ces types de structures peuvent être des mimes des états de transition dans l'hydrolyse des amides. Toutefois, cette structure est légèrement asymétrique car les longueurs de liaison S−N ne sont pas égales (ie. 1.60 Å et 1.67 Å). De plus, une liaison hydrogène intramoléculaire à huit membres a été observée pour **42** entre le proton du lien amide et le carbonyle de l'ester méthylique, démontrant la capacité des azasulfurylpeptides à s'engager dans de telles liaisons. Ces résultats suscitent donc un grand intérêt à poursuivre la recherche sur les effets des azasulfurylpeptides comparativement à leur peptide parent.

1.5. Description de la thèse

Le but premier de cette thèse a été de développer une nouvelle voie de synthèse en solution des azasulfurylpeptides (Chapitre 2). Cette méthode met en évidence l'utilisation de radiations aux micro-ondes dans le couplage de différents hydrazides avec des sulfamidates de 4-nitrophénol dérivés d'acides aminés. De plus, des alkylations chimiosélectives ont été réalisées sur les azasulfurylglycines (AsG), afin d'y insérer diverses chaînes latérales.

Désirant en apprendre d'avantage sur les préférences conformationnelles des azasulfurylpeptides, deux modèles de tripeptides contenant un AsG ont été analysés par des études cristallographiques (Chapitre 3). Les résultats ont démontré un grand potentiel dans la stabilisation de tours γ par contraintes électroniques, c'est-à-dire grâce aux restrictions conformationnelles respectives des angles de torsion.

Par la suite, une approche combinatoire sur support solide a été effectuée sur la résine de Rink, mettant en évidence l'utilisation d'azasulfurylglycines protégés par un groupement Fmoc, suivi d'alkylations chimiosélectives sur la résine (Chapitre 4). Le peptide étudié est le *growth hormone releasing peptide 6* (GHRP-6, His-D-Trp-Ala-Trp-D-Phe-Lys-NH_2). Ce peptide synthétique est un hexapeptide possédant une affinité pour deux récepteurs, soit le

growth hormone secretagogue receptor 1a (GHS-R1a) et le récepteur *cluster of differenciation 36* (CD36). Un composé présentant une affinité sélective pour le récepteur CD36 pourrait s'avérer efficace pour le développement d'un traitement contre la dégénérescence maculaire liée à l'âge (DMLA).

Suite à la synthèse de six analogues contenant un *N*-aminosulfamide dérivé de l'AsF à la position 4 de GHRP-6, en perspectives à ce projet de doctorat, des études biologiques sur le *Toll-like receptor 2* (TLR2) ont été effectués en collaboration avec le professeur Huy Ong au département de Pharmacologie à la Faculté de Pharmacie de l'Université de Montréal. Le complexe TLR2-TLR6 est reconnu pour être co-exprimé et modulé par CD36. En se liant au CD36, ces études ont démontrées le potentiel des azasulfurylpeptides à pouvoir réguler le rôle du TLR2 qui déclenche des réponses inflammatoires et immunitaires innées (Perspectives).

Finalement, en collaboration avec le Professeur James Spencer, différents azasulfurylpeptides ont été évalués pour leur capaciter à inhibiter des métallo-β-lactamases. Certains analogues ont été des inhibiteurs micromolaires du IMP-1.

Ces nouvelles méthodologies de synthèse des azasulfurylpeptides en solution et sur support solide devraient donc permettre des études de relations structure-activité avec différents peptides biologiquement actifs. En tant que mimes structurelles, les *N*-aminosulfamides ont démontré un potentiel à mimer les structures secondaires peptidiques, tels que les tours γ. De plus, l'application des azasulfurylpeptides a été démontrée par la synthèse de ligands du CD36 présentant des effets modulateurs sur le TLR2. En tant que mimes des états de transition dans l'hydrolyse des liens amides, les azasulfurylpeptides ont servi d'inhibiteurs de métallo-β-lactamases.

Chapitre 2 : Synthèse en solution des azasulfurylpeptides

2.1. Mise en contexte de l'article 1

Bien que la seule méthode existante pour la synthèse des *N*-aminosulfamides au début de ce projet implique l'utilisation de SO_2Cl_2 et d'une quantité catalytique de $SbCl_5$, certains couplages entre les carbazates et les amines demeurent problématiques (Introduction). Les premières investigations de recherches effectuées ont eu pour but de développer une nouvelle méthodologie de synthèse des azasulfurylpeptides, sans catalyseur potentiellement nocif.

2.2. Hypothèse de base : activation des hydrazones

L'activation des carbazates (**44**) avec le SO_2Cl_2 a été publiée comme infaisable, en raison de la formation des hydrazones (**46**) par élimination β, suivi d'une tautomérisation (Schéma 2.1).[70]

Schéma 2.1. Formation des hydrazones par élimination β et tautomérisation, suite à l'activation des carbazates avec le chlorure de sulfuryle.

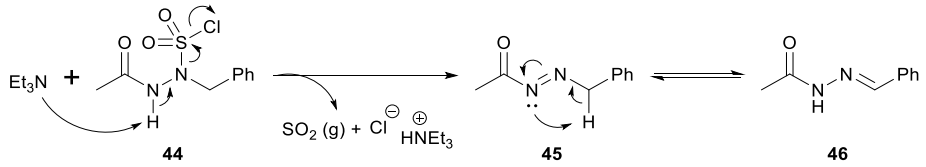

Par conséquent, l'activation des hydrazones a tout d'abord été proposée, en raison de l'absence du proton responsable de l'élimination β observée avec les carbazates (Schéma 2.2). L'activation des hydrazones a grandement été développée dans le groupe de recherche du professeur Lubell pour la synthèse combinatoire des azapeptides,[78-83] et a fait sujet d'un article de révision présentant les synthèses et les potentiels thérapeutiques des azapeptides.[38] Par exemple, suite à l'activation du benzophénone hydrazone (**47**) avec le chloroformate de 4-nitrophénol (**48**), le carbazate **49** obtenu peut être couplé avec un acide aminé afin d'obtenir le benzophénone semicarbazone **50** (Schéma 2.2).[78] Par analogie à cette voie de synthèse, l'utilisation du chlorosulfate de 4-nitrophénol (**51**) ou du SO_2Cl_2 pour activer l'hydrazone **47** a tout d'abord été envisagée pour la synthèse des azasulfurylpeptides.

Schéma 2.2. L'activation des hydrazones comme hypothèse de base, par analogie à la synthèse des azapeptides en solution.

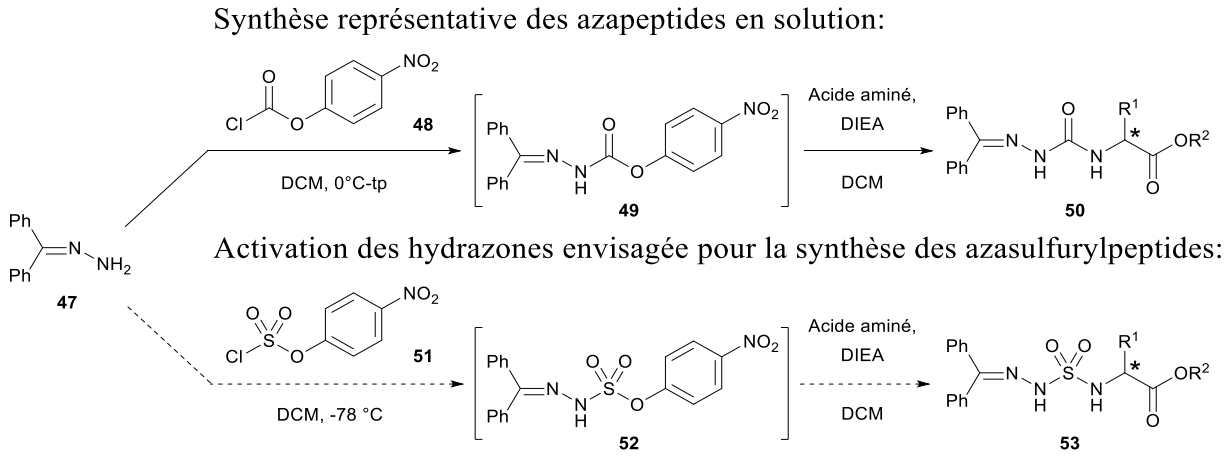

Cependant, les expériences effectuées pour activer l'hydrazone **47** avec le SO_2Cl_2 ou le chlorosulfate **51** ont conduit à la formation de l'azine **54** (Schéma 2.3). Le mécanisme proposé pour la formation de ce dernier est similaire à une oxydation des hydrazones avec l'acide *o*-iodobenzoïque (IBX).[84] De plus, la décomposition des sels d'hydrazones sulfonylés a déjà été observée auparavant.[85, 86] Ainsi, suite à l'activation de l'hydrazone **47** avec le chlorosulfate **51**, le 4-nitrophénolate est libéré pour obtenir le chlorure de sulfonyle **55**. Cet intermédiaire instable se décompose rapidement pour former le composé diazo **57** en présence d'une base. Ce dernier dimérise et suite à la libération d'azote gazeux (N_2), l'azine **54** est obtenu.

La libération du phénolate au lieu de l'anion chlorure est expliquée par une étude cinétique sur le chlorosulfate **51**. En effet, il a été démontré que la scission du lien S−OAr est plus rapide que celle du lien S−Cl, par réaction avec le méthoxyde de sodium (NaOMe) en milieu méthanolique.[87] Ceci illustre bien que le phénolate est un meilleur groupe partant que le chlorure, en raison de la stabilisation par résonance du phénolate.

Schéma 2.3. Mécanisme proposé pour la formation de l'azine **54**, suite à l'activation de l'hydrazone **47** avec le chlorosulfate **51**.

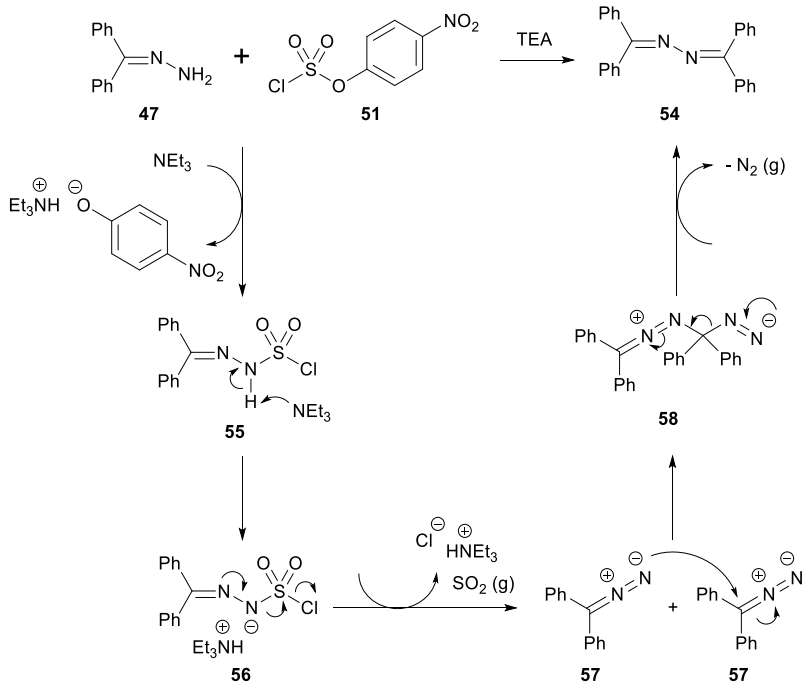

2.3. Activation des acides aminés

L'obtention des azines par activation des hydrazones permet d'écarter l'hypothèse de base et l'approche envisagée par analogie avec les azapeptides. Ainsi, la deuxième approche suggérée a été l'activation des acides aminés, en utilisant également le chlorosulfate de 4-nitrophénol.

Le chlorosulfate **51** a été choisi car il est un solide cristallin stable qui peut être conservé pour une longue période de temps. Comparativement au SO_2Cl_2, qui est un liquide incolore après distillation fractionnée, ce dernier jaunit rapidement par décomposition en SO_2 et HCl, qui graduellement forme de l'acide sulfurique (H_2SO_4) avec l'humidité de l'air.[88] De plus, considérant la ressemblance des *N*-aminosulfamides avec les sulfamides, le chlorosulfate **51** a permis la synthèse de mimes d'ADN contenant un groupement sulfamide, en remplacement au groupement phosphate.[89, 90]

Dans cette approche, l'amine **59** de départ est convertie en sulfamidate **61** correspondant par traitement avec le chlorosulfate **51** (2 éq.). Il est important de mentionner que l'ajout en

large excès, de 4-nitrophénol (**60**, 10 éq.) et de triéthylamine (12 éq.), a permis d'empêcher la formation du sulfamide symétrique **62**, en interceptant le chlorure de sulfonyle préalablement formé. Finalement, le sulfamidate **61** est couplé avec une deuxième amine (**63**) pour former le sulfamide **64**, en présence de tamis moléculaire.[90]

Schéma 2.4. Utilisation du chlorosulfate de 4-nitrophénol dans la synthèse de mimes d'ADN contenant un groupement sulfamide en remplacement au groupement phosphate.

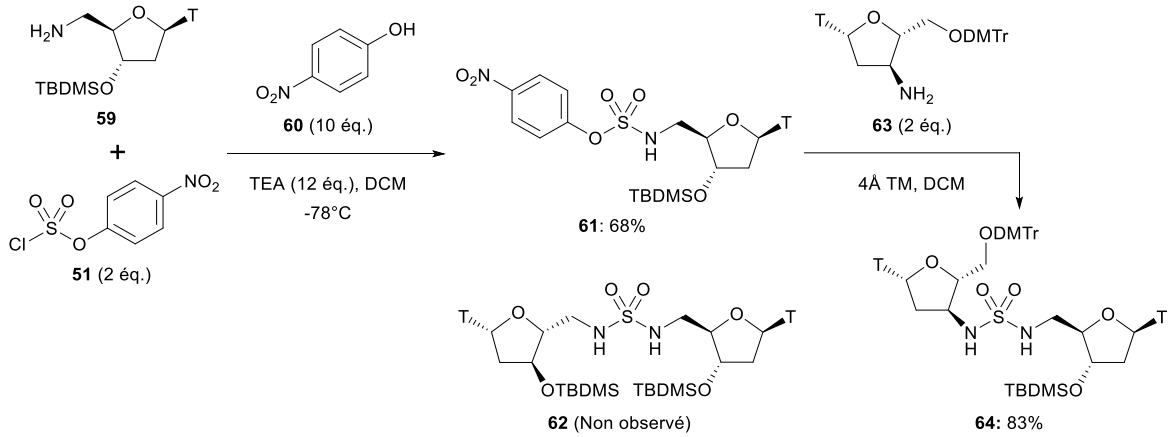

Les sulfamidates de 4-nitrophénol présentés dans l'article 1 ont été synthétisés par une approche similaire, en activant cette fois-ci un acide aminé.[91] Afin de faciliter la purification de ces sulfamidates, les quantités de 4-nitrophénol (2 éq.) et de triéthylamine (6 éq.) ont été drastiquement réduites. Aucune formation de sulfamide symétrique n'a également été détectée dans ces conditions expérimentales. Ceci constitue donc une avancé extrêmement intéressante en comparaison à l'utilisation du SO_2Cl_2.

2.4. Utilisation des sulfamidates

Suite à la formation des sulfamidates, les premiers essais de couplage ont été réalisés avec l'hydrazone **47**. Celle-ci possédant un proton plus acide en raison de la stabilisation par résonance de l'anion, les hydrazones sont reconnus pour favoriser les alkylations régiosélectives sur la fonction urée, présente dans les azapeptides.[38]

L'utilisation d'irradiation aux micro-ondes a été utilisée dès les premières tentatives de synthèse, pour le développement des conditions expérimentales de couplage avec l'hydrazone **47**. En effet, de telles conditions expérimentales ont été utilisées sur support solide, dans la

synthèse des β-amino γ-lactames, auquel un peptide est couplé au sulfamidate cyclique **46**, dérivé de l'acide aspartique (Schéma 2.5).[92]

Schéma 2.5. Utilisation d'irradiation aux micro-ondes dans la synthèse des β-amino γ-lactames.

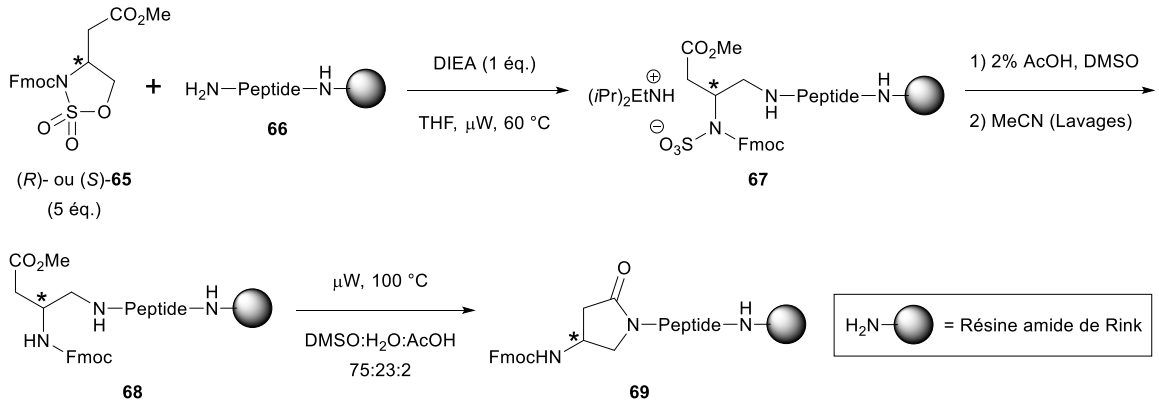

Ainsi, l'utilisation d'irradiation aux micro-ondes, à 60 °C pour 2.5 h, a grandement favorisé le couplage de l'hydrazone **47** avec l'ester *tert*-butylique de la L-phénylalanine avec l'obtention d'un rendement de 80% (Article 1).[91] Comme réaction de contrôle, ce même couplage a été réalisé en chauffant à 60 °C par chauffage conventionnel (bain d'huile) et est demeuré incomplet après 24 h de réaction.

Toutefois, les tentatives effectuées pour cliver l'hydrazone, c'est-à-dire par hydrolyse acide (1N HCl) ou par l'emploi de l'hydrochlorure d'hydroxylamine dans la pyridine,[38] ont rapidement mené à la décomposition des dipeptides. Cette forme de décomposition a également été observée dans l'emploi de l'hydrazide du *N*-isopropylidène-*N'*-2-nitrobenzènesulfonyle (**71**, IPNBSH), servant à réduire des alcools allyliques, suite à un réarrangement sigmatropique du diazène **75**, libérant de l'azote gazeux et l'alcène **76** (Schéma 2.6).[93]

En raison de cette décomposition, des hydrazides dérivés d'acides aminés ont été utilisés afin d'éviter l'étape de clivage problématique (Article 1). Par cette méthode, il est donc possible de synthétiser des tripeptides dont un azasulfurylglycine (AsG) est présent à la position 2.

Schéma 2.6. Exemple de la réduction des alcools en employant l'hydrazide **71**.

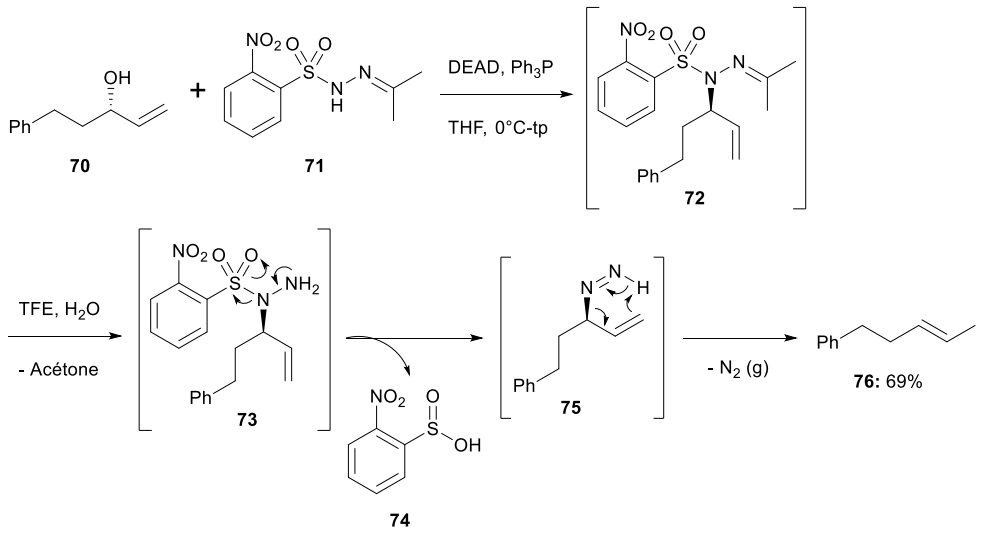

2.5. Mise en contexte de l'article 2

Dans le but de diversifier les tripeptides formés, de manière combinatoire, des alkylations chimiosélectives sur les tripeptides contenant l'AsG ont tout d'abord été réalisées. Pour ce faire le *tert*-butylimino-tri(pyrrolidino)phosphorane (BTPP), une base forte non nucléophile de type phosphazène (pKa de l'acide conjugué = 28.35 dans l'acétonitrile), a été utilisé (Article 1).[91] Le BTPP a déjà été utilisé dans le passé pour des alkylations sur support solide des azapeptides.[81, 94] Cependant, cette base provenant de Sigma-Aldrich est relativement dispendieuse (548,00 $ pour 25 mL). D'autres essais ont été réalisés menant à de faibles rendements (aux alentours de 30%) avec des réactions de type Mitsunobu ou par l'emploi du *tert*-butoxyde de potassium (KO*t*Bu), également employé dans les alkylations régiosélectives des azapeptides.[38]

Dans des travaux réalisés sur différents hydrazones, l'emploi de l'hydroxyde de tetraéthylammonium (NEt_4OH, Sigma-Aldrich, solution de 40% dans l'eau, 73,00$ pour 100 mL), une base plus douce (pKa de l'acide conjugué = 15.75 dans l'eau), a été utilisée avec succès pour des alkylations sur des fluorénylidènes[82] et dipeptides.[95] De plus, dans une analyse de prédiction des pKa des dérivés d'hydrazines (Figure 2.1), le pKa prédit pour le sulfonamide **77** est de 7.93.[96] Similairement, les *N*-aminosulfamides devraient posséder un pKa semblable. Par conséquent, l'emploi du NEt_4OH devrait s'avérer suffisamment basique pour pouvoir

déprotonner l'AsG et a donc été validé dans une petite analyse complémentaire présentée dans l'article 2.[97] Une limitation de cette base est la nécessité d'utiliser des esters non hydrolysables par l'anion hydroxyde.

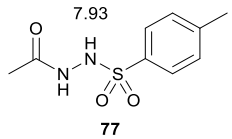

77

Figure 2.1. Prédiction des pKa du dérivé sulfonamide de l'hydrazine acylé **77**.

2.6. Conclusion

Le développement d'une nouvelle voie de synthèse des azasulfurylpeptides en solution, a été étudié, développé et décrit avec succès. L'utilisation des sulfamidates de 4-nitrophénol, le couplage des hydrazides avec l'aide d'irradiation aux micro-ondes, et les alkylations chimiosélectives effectués sur les tripeptides contenant un AsG sont les trois étapes clés qui se démarquent de la première voie de synthèse des *N*-aminosulfamides. De plus, aucune formation de sulfamides symétriques n'a été détectée lors de l'activation des acides aminés aux sulfamidates de 4-nitrophénol et aucun catalyseur n'a été employé dans cette approche. En utilisant cette nouvelle voie de synthèse, des modèles de tripeptides pourront être synthétisés, afin d'en étudier leurs propriétés conformationnelles (Chapitre 3). Enfin, cette approche a servi d'introduction dans le développement d'une synthèse sur support solide d'analogues de GHRP-6 (Chapitre 4).

La grande difficulté de purification des sulfamidates en raison de l'excès de 4-nitrophénol est une limitation à cette méthodologie. En effet, dans le cas du sulfamidate de 4-nitrophénol de l'alanine, ce composé se décompose légèrement en effectuant les extractions basiques avec le bicarbonate de sodium pour retirer le 4-nitrophénol (Article 1, Partie expérimentale). Dans les cas où les sulfamidates seraient instables, il est préférable de ne pas effectuer ces extractions et de poursuivre la prochaine réaction désirée en présence de cet excès de 4-nitrophénol dans le milieu réactionnel.

Article 1

Turcotte, S.; Bouayad-Gervais, S. H.; Lubell, W. D. *N*-Aminosulfamide Peptide Mimic Synthesis by Alkylation of Azasulfurylglycinyl Peptides. *Org. Lett.* **2012**, *14*, 1318-1321.

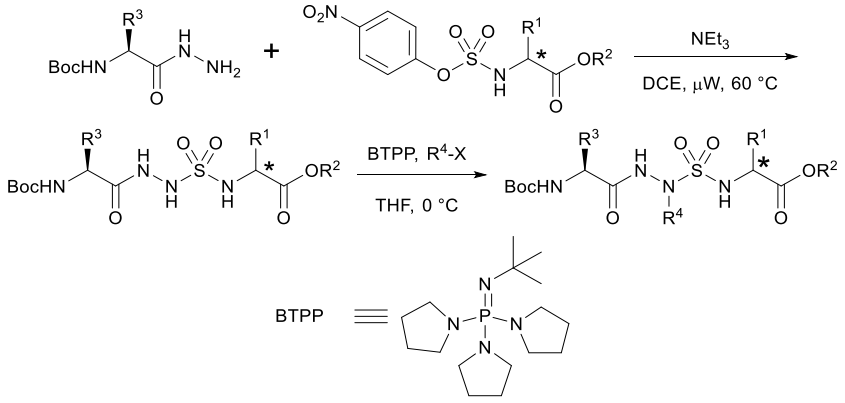

N-Aminosulfamide Peptide Mimic Synthesis by Alkylation of Azasulfurylglycinyl Peptides

Stéphane Turcotte, Samir H. Bouayad-Gervais, William D. Lubell*

Department of Chemistry, University of Montreal, C.P. 6128,

Succursale Centre-Ville, Montréal, Québec, H3C 3J7

Abstract

N-Aminosulfamides are peptidomimetics in which the $C_\alpha H$ and the carbonyl of an amino acid residue are both respectively replaced by a nitrogen atom and a sulfonyl group. Azasulfurylglycinyl tripeptide analogs were effectively synthesized from amino acid building blocks by condensations of *N*-protected amino hydrazides and *p*-nitrophenylsulfamidate esters. The installation of *N*-alkyl chains and access to other azasulfuryl amino acid residues were effectively achieved by chemoselective alkylation.

Introduction

The biological activity and physical properties of peptide structures are inherently contingent on backbone geometry and side chain functionality, such that attempts to modulate natural function are challenged to consider innate form. For example, replacement of a peptide amide by a phosphonamide[98] or a silanediol[99] may effectively mimic the tetrahedral transition states common in enzyme-catalyzed reactions and produce enzyme inhibitors. Although the respective amide to sulfonamide exchange may appear promising, the resulting α-sulfonamido peptides have been reported to be unstable.[37]

N-Aminosulfamido peptides **33** in which both the $C_\alpha H$ and the carbonyl of an amino acid residue are respectively replaced by a nitrogen atom and a sulfonyl group have proven to be more stable (Figure 2.2). Moreover, azasulfurylphenylalaninyl (Asf) peptide **34** was reported to

inhibit the human immunodeficiency virus-1 (HIV-1) proteinase, presumably by imitating the transition-state for amide bond hydrolysis.[71]

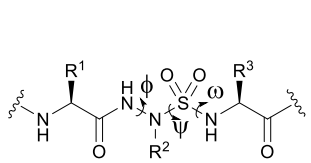

N-aminosulfamido peptide **33**

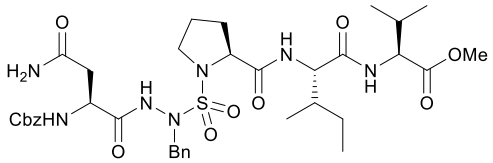

Cbz-L-Asn-Asf-L-Pro-L-Ile-L-Val-OMe **34**

Figure 2.2. *N*-Aminosulfamido peptide **33** and proteinase inhibitor **34**.

Azasulfuryl peptide analogs combine the characteristics of aza- and α-sulfonamido peptides, thus offering interesting potential for modifying backbone geometry. The sulfonyl group possesses a tetrahedral sulfur,which adopts ω torsion angle values around ± 60° and ± 100° (instead of amide cis-(*E*) and trans-(*Z*) conformations at respectively 0° and ± 180°) separated by a lower S−N rotational barrier ($\Delta G^{\ddagger} \approx 35$ kJ/mol), relative to the amide C−N ($\Delta G^{\ddagger} \approx 75$ kJ/mol).[72] Furthermore, the S−N bond length is longer than the C−N, due to lack of an amide bond resonance and greater sp^3 versus sp^2 character of the sulfonamide nitrogen (Figure 2.3).

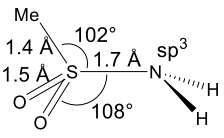

Methanesulfonamide **78**

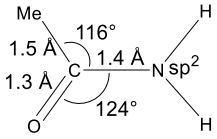

Acetamide **79**

Figure 2.3. Sulfonamide[73] and amide[100] bond lengths and angles.

In light of their interesting conformational and biological properties, the synthesis of *N*-aminosulfamides has apparently restricted their application in peptidemimicry.[71] To the best of our knowledge, only one method has been reported for constructing acyclic *N*-aminosulfamides and employs sulfuryl chloride (SO_2Cl_2) to combine hydrazide and amine components (Scheme 2.7).[70] Coupling was relatively sluggish, in spite of the addition of catalytic amounts of toxic antimony pentachloride ($SbCl_5$), such that, in the synthesis of *N*-aminosulfamide **40d**, reaction of 2 equiv of the amine component with sulfuryl chloride competed to produce symmetric sulfamide **37d** as a major side product. In addition, introduction

of side chains onto the *N*-aminosulfamide residue required synthesis of *N*-alkyl protected hydrazide precursors.[70]

Scheme 2.7. Reported synthesis of *N*-aminosulfamides.

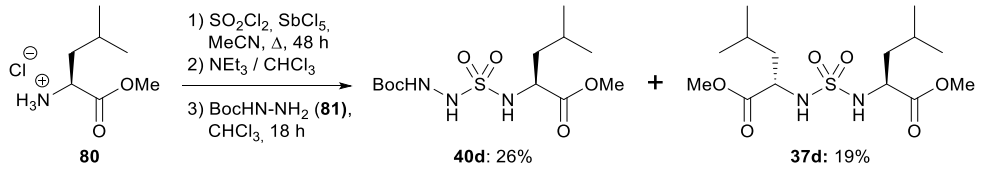

Results and Discussion

Inspired by our past applications of sulfamidates as synthetic intermediates,[42, 92, 101, 102] as well as the application of azaglycine alkylation in the submonomer synthesis of azapeptides,[79-81] we have pursued an approach to *N*-aminosulfamide peptides featuring convergent synthesis of an azasulfurylglycine intermediate and subsequent chemoselective alkylation. 4-Nitrophenyl chlorosulfate **51** has been used effectively in the synthesis of sulfamides[90] and was thus studied for the selective synthesis of *N*-aminosulfamides.

Scheme 2.8 Synthesis of the *p*-nitrophenylsulfamidate esters **87-91**.

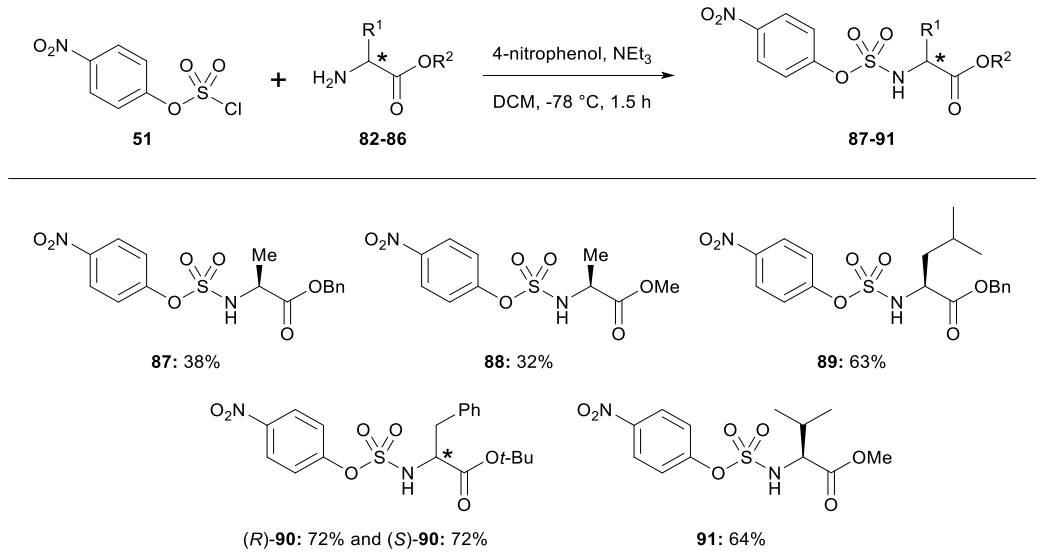

Initial attempts to prepare sulfamidates from hydrazones and chlorosulfate **51** gave however azines. On the contrary, the corresponding sulfamidates were prepared successfully from various amino esters; i.e., L-Ala-OBn (**82**), L-Ala-OMe **(83)**, L-Leu-OBn (**84**), D- and

L-Phe-O*t*-Bu [(*R*)- and (*S*)-**85**], and L-Val-OMe (**86**) (Scheme 2.8). Two equivalents of 4-nitrophenol were necessary as additive to avoid formation of symmetric sulfamide. Additionally, two equivalents of chlorosulfate **51** were also crucial for sulfamidate formation. Lower yields of **87** and **88** were incurred during purification on silica gel and using aq. $NaHCO_3$ washings to remove nitrophenol (Experimental Section). Relative to sulfuryl chloride, which needs to be distilled prior to use, chlorosulfate **51** was a convenient solid. Similarly, except for sulfamidate **90**, the *p*-nitrophenylsulfamidates were solids, which could be stored for several months without decomposition.

To further examine conformational properties, sulfamidate **91** was crystallized from EtOAc on diffusion of hexane vapors (Figure 2.4 and Experimental Section). The crystal structure shows that the sulfamidate (−N−S(O_2)−O−) adopts a distorted tetrahedral structure and that the N−S bond length (1.593 Å) is longer than an amide bond (Figure 2.3). Furthermore, the ω torsion angle (62.2°) was close to the ideal theoretical value (60°) for sulfonamides.[72]

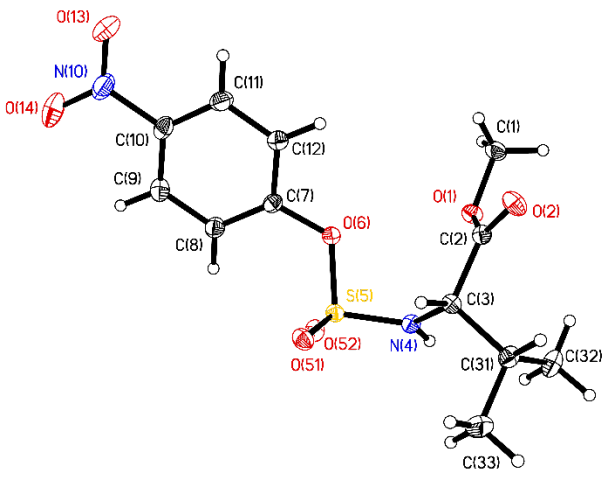

Figure 2.4. Crystal structure of sulfamidate **91**, showing the atomic numbering system employed.

N-Aminosulfamides **96-105** were synthesized by reaction of sulfamidates **88-91** respectively with benzophenone hydrazone (**47**), *tert*-butyl and benzyl carbazates (**81** and **92**), as well as *N*-(Boc)-L-Ala, L-Phe and L-Pro hydrazides (**93-95**) (Scheme 2.9). Microwave irradiation proved important in the formation of the *N*-aminosulfamides and favoured coupling between the two precursors. In contrast to the 80% yield using microwave heating, synthesis of

N-aminosulfamide **96** in DCM using conventional heating at reflux for 24 h gave only 36% yield and recovered starting material.

Scheme 2.9. Synthesis of the *N*-aminosulfamides **96-105**.

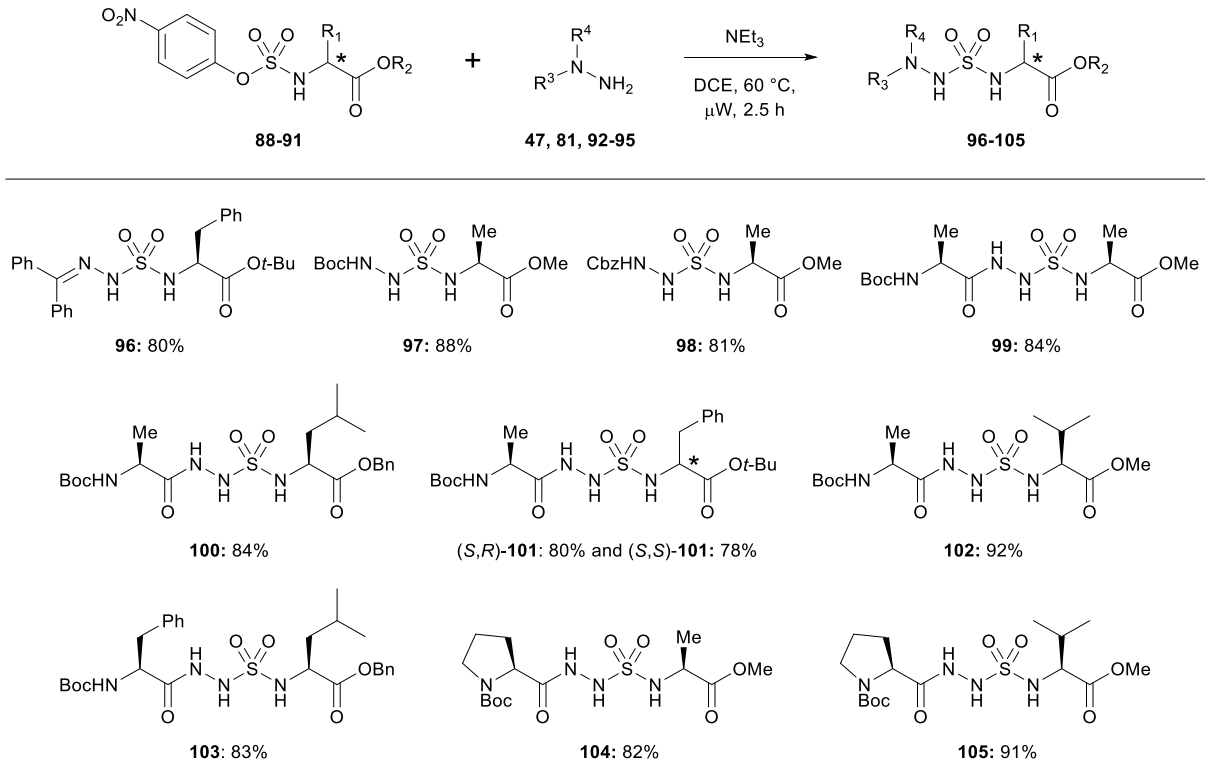

Although side chains may in principle be introduced onto the *N*-aminosulfamide moiety by employing *N'*-alkylhydrazides, inspired by our submonomer approach to azapeptides,[79-81] chemoselective alkylation was pursued to provide a combinatorial approach to azasulfuryl amino acid residues. Initially, attempts to employ hydrazone and carbazate derivatives **96-98** in chemoselective alkylation/deprotection sequences failed, likely due to sulfonyl hydrazide decomposition.[93]

Chemoselective alkylation of azasulfurylglycinyl (Asg) peptides **99-101** and **103** proved effective for preparing orthogonally protected building blocks **106-112** for incorporation into longer peptides (Scheme 2.10). Initially, *N*-Boc-Ala-Asg-Ala-OMe (**99**) was treated with potassium *tert*-butoxide and propargylbromide to provide azasulfuryl tripeptide **106**, albeit in 20% yield with recovered starting material. By switching to the phosphazene base, *tert*-butylimino-tri(pyrrolidino)-phosphorane (BTPP), alkylation yield was improved to 73%.

Subsequent reactions were performed with BTPP. *Bis*-alkylation was minimized by employing stoichiometric amounts of base and alkylating reagent.

Scheme 2.10. Chemoselective alkylation of azasulfurylglycinyl peptides.

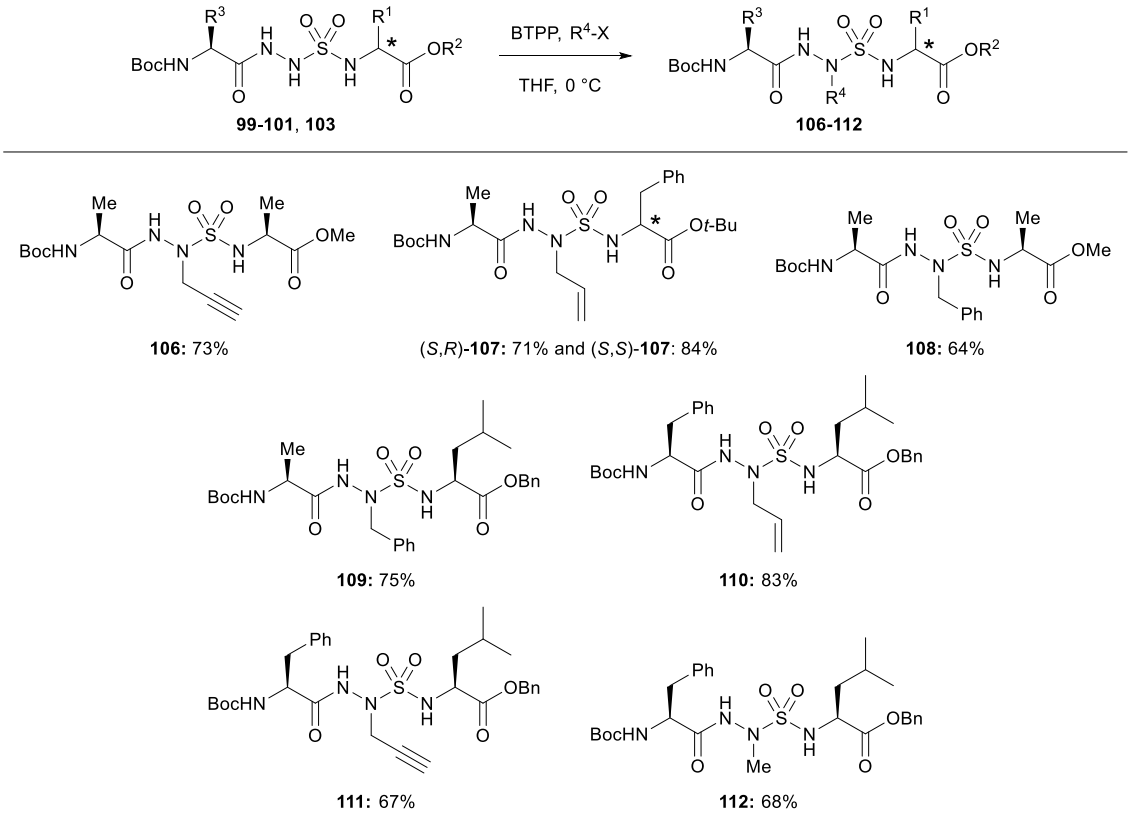

The position of alkylation was ascertained by NMR experiments on tripeptide **106** (Experimental Section). In the 2D COSY spectrum, through-bond correlations were observed between the alanine N-H and C_α-H protons. In the 2D HMBC spectrum, through-bond correlation was observed between the hydrazide NH and carbonyl carbon. The position of alkylation was assigned for analogs **107-112** based on analogy to **106**, because of the relatively similar chemical shifts for the N-H signals in the ^{1}H NMR spectra.

In order to ascertain if epimerization had occured during the alkylation of azasulfurylallylglycine, (S,R)- and (S,S) diastereoisomers of azasulfurylallylglycinyl tripeptide **107** were synthesized and analyzed by 1H NMR spectroscopy. The diastereoisomeric ratio observed for the alkylated product **107** was consistent with the starting azasulfurylglycinyl tripeptide diastereomers **101**, indicating no epimerization.[103] Furthermore, treatment of

azasulfurylallylglycinyl tripeptide (S,R)-**107** with one equivalent of BTPP at room temperature for 3h failed to cause epimerization.

Conclusion

In conclusion, a new method for the synthesis of *N*-aminosulfamides has been developed featuring the coupling of *p*-nitrophenylsulfamidates and *N*-(Boc)-amino acid hydrazides under microwave irradiation. Chemoselective alkylation of the azasulfurylglycinyl peptides was used to add side-chain diversity and prepare other azasulfuryl amino acid residues. This method avoids symmetric sulfamide formation as well as the use of *N*'-alkyl hydrazides in the synthesis of the *N*-aminosulfamide peptides. The crystallization of sulfamidate **91** confirmed the tetrahedral nature of the sulfur and the 60° ω-torsion angle. We are currently working on crystallizing the *N*-aminosulfamides, in order to validate potential for mimicry of the transition state of amide bond hydrolysis. In addition, insertion of the *N*-aminosulfamide tripeptide building blocks into biologically active peptides is being pursued to study structure-activity relationships.

Acknowledgment

This research was supported by the Natural Sciences and Engineering Research Council of Canada (NSERC) and the Fonds Québecois de la Recherche sur la Nature et les Technologies (FQRNT). ST would like to thank the FQRNT for graduate student fellowships. The authors also thank Dr. A. Furtos, K. Venne, and M-C. Tang (University of Montreal) for the HR-MS analysis and to Francine Bélanger (University of Montreal) for the crystallographic data.

Article 2

Turcotte, S.; Havard, T.; Lubell, W. D. Mild chemoslective alkylation of azasulfurylglycinyl peptides. In *Proceedings to the 32nd European Peptide Symposium*; Kokotos, G., Constantinou-Kokotou, V., Matsoukas, J., Eds. Athens, Grece, **2012**, 140-141.

Mild chemoselective alkylation of azasulfurylglycinyl peptides.

Stéphane Turcotte, Thierry Havard, William D. Lubell*

Département de chimie, Université de Montréal, C.P. 6128,

Succursale Centre-Ville, Montréal, Québec, H3C 3J7, Canada

Introduction

Mimics of the tetrahedral transition states common in enzyme-catalyzed reactions, such as phosphonamides[98] and silanediols,[99] have served as enzyme inhibitors. In this vein, the analogous α-aminosulfonamido peptide would offer potential; however, such α-amino-sulfonamides were found to rapidly decompose.[37] On the contrary, reasonable stability has been exhibited by *N*-aminosulfamido peptides, in which a nitrogen and a sulfonyl group replace respectfully both the CH_α and the carbonyl of an amino acid residue. To the best of our knowledge, prior to our research, only one method had been reported for constructing acyclic *N*-aminosulfamides.[70] This method suffered, however, from sluggish couplings leading to formation of symmetric sulfamides, due to the use of sulfuryl chloride and catalytic amounts of antimony pentachloride to combine the hydrazide and amine components (Scheme 2.11).[70] Moreover, *N*-alkyl hydrazide synthesis was required for the introduction of side chains onto the *N*-aminosulfamide residue.

Scheme 2.11. Symmetric sulfamide formation competes with *N*-aminosulfamide synthesis.

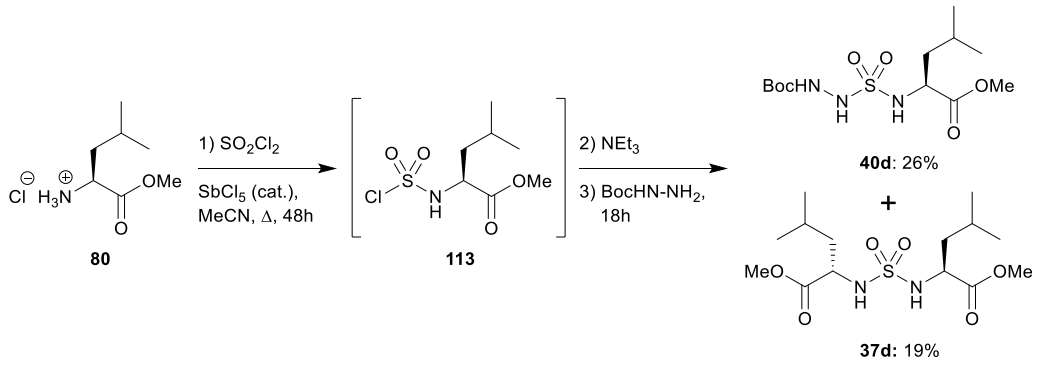

We reported recently a three-step method for the synthesis of *N*-aminosulfamides.[91] In the first step, crystalline 4-nitrophenyl sulfamidates are produced by acylation of the amino acid component with 4-nitrophenyl chlorosulfate. Sulfamidates (*R*)-**90** and **88** provide an effective means for preventing formation of symmetric sulfamide during *N*-aminosulfamide synthesis, such that in the second step, reaction with hydrazide **93** under microwave irradiation at 60°C gives selectively azasulfamido tripeptides (*S*,*R*)-**101** and **99**. Although side chains may be introduced by employment of *N*-alkyl hydrazides, we have also shown that chemoselective alkylation of the azasulfurylglycinamides can be accomplished to install effectively *N*-alkyl side-chains, using the phosphazene base BTPP (Scheme 2.12).

Scheme 2.12. Azasulfamido peptide synthesis.

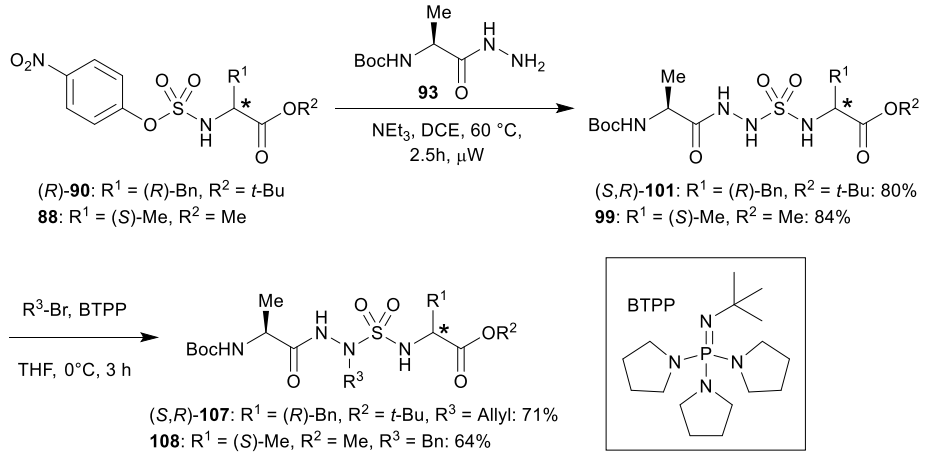

Results and Discussion

Alkylation of azasulfurylglycinamides (*S*,*R*)-**101** and **99** provides an effective method for adding diverse side chains to expand the scope of azasulfamido peptide diversity; however, the expense of BTPP as base may be prohibitive. Exploring alternative bases, we have found that the inexpensive and milder base, NEt_4OH can be effectively used to achieve the desired chemoselective alkylation (Table 2.1). In the alkylation of *N*-(Boc)alaninyl-azasulfurylglycinyl-D-phenylalanine *tert*-butyl ester [(*S*,*R*)-**101**] with allyl bromide, NEt_4OH at 40°C gave superior yield of (*S*,*R*)-**107** over BTPP at 0°C after 3h in THF. On the other hand, the alkylation of azasulfurylglycinamide **99** with benzyl bromide was less successful using the NEt_4OH conditions, likely due to competing methyl ester hydrolysis. To ascertain if epimerization

occurred during the alkylation of (*S*,*R*)-**101** using Et_4NOH, the diastereoisomeric ratio of (*S*,*R*)- and (*S*,*S*)-**107** were compared in MeOD. Observation of the respective *tert*-butyl ester signals at 1.41 ppm and 1.47 ppm in the ^1H NMR spectra revealed that no epimerization occurred.

Table 2.1. Head-to-head comparison of BTPP with Et_4NOH.

Product	Yield (BTPP, 0 °C, 3h)	Yield (Et_4NOH, 40 °C, 3h)
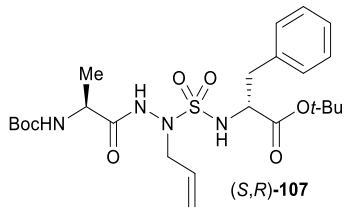 (*S*,*R*)-**107**	71%	81%
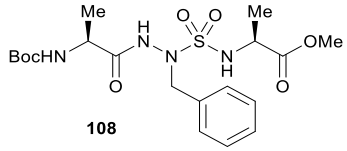 **108**	64%	40%

Conclusion

In conclusion, NEt_4OH has been used as an inexpensive milder replacement for the costly base BTPP in the chemoselective alkylation of azasulfurylglycinyl peptides.

Acknowledgments

This research was supported by the Natural Sciences and Engineering Research Council of Canada (NSERC) and the Canadian Institutes of Health Research (CIHR) grant No. TGC-114046. S.T. thanks the FQRNT for a graduate student fellowship.

Chapitre 3 : Analyse conformationnelle des azasulfurylpeptides

3.1. Mise en contexte de l'article 3

Avec la nouvelle méthode de synthèse en solution développée, une étude plus approfondie sur les préférences conformationnelles des azasulfurylpeptides a été élaborée. Deux modèles de tripeptides contenant un AsG ont donc été cristallisés et examinés pour leur capacité à induire des tours γ.

Article 3

Turcotte, S.; Lubell, W. D. Crystal Structure Analyses of Azasulfuryltripeptides Reveal Potential for γ-Turn Mimicry. Biopolymers (Pept. Sci.), **2015**, Accepté,

DOI: 10.1002/bip.22632.

Crystal Structure Analyses of Azasulfuryltripeptides Reveal Potential for γ-Turn Mimicry†

Stéphane Turcotte, William D. Lubell*

Department of Chemistry, Université de Montréal, P.O. Box 6128,

Downtown Station, Montréal, QC, H3C 3J7, Canada

† Dedicated to two giant pioneers in the study of peptide conformation and dynamics, Professors Claudio Toniolo and Luis Moroder.

Abstract

Azasulfurylpeptides feature an amino acid residue in which the CαH and the carbonyl are replaced respectively by a nitrogen atom and a sulfonyl group. Insight into the conformational preferences of azasulfurylpeptides containing an azasulfurylglycine (AsG) residue has been pursued using X-ray analysis in the solid state. Crystals of *N*-(Boc)-Pro-AsG-Val-OMe (**105**) and *N*-(Cbz)-Ala-AsG-D-Phe-O*t*-Bu (**119**) showed tetrahedral geometries about the sulfur atom with the ω torsion angle preferring a staggered conformation. Furthermore, the ϕ and ψ torsion angles of the central azasulfuryl residue were respectively within close proximity to those of ideal inverse and classical γ-turns. In the crystal lattice, azasulfurylpeptide **119** engaged in intermolecular hydrogen bonds between the sulfonyl oxygen and hydrazide hydrogen in an antiparallel orientation.

Introduction

Peptide analogs that can effectively mimic the tetrahedral transition states found in enzyme-catalyzed amide bond hydrolysis have been pursued for use as enzyme inhibitors. For example, replacement of the amide carbonyl by a tetrahedral phosphorus atom using α-amino-phosphonamides and α-aminophosphonamidates has provided inhibitors of human cyclophilin,[27] HIV-1 proteinase,[26, 104] human neutrophil collagenase,[22] enkephalinase and angiotensin-converting enzyme.[105] On the other hand, attempts have been less successful at employing β-aminosulfonamides as tetrahedral mimics in enzyme inhibitors of HIV protease,

thermolysin, and thrombin, as well as antigens for raising catalytic antibodies.[33] Notably, the application of α-aminosulfonamides as tetrahedral mimics in enzyme inhibitors has failed due to their rapid decomposition.[37]

Azasulfurylpeptides **33** possess an amino acid residue from which the $C_\alpha H$ and carbonyl have been respectively replaced by nitrogen and a sulfonyl group (Figure 3.1).[70] Although few examples of these peptidomimetics have been reported, their potential to mimic the tetrahedral geometry during amide bond hydrolysis was exploited by the insertion of azasulfurylphenylalanine (AsF) into a transition-state mimic, micromolar inhibitor of the human immunodeficiency virus-1 (HIV-1) proteinase, azasulfurylpeptide **34** (Figure 3.1).[71] Although their physical characterization has been limited, azasulfurylpeptides may likely combine properties of azapeptides[38] and sulfonamides,[72, 73] including (1) lone pair-lone pair repulsion between adjacent nitrogen favoring a ϕ-torsion angle of ±90°,[38] (2) ω-torsion angle geometry favored at ±60° and ±100° respectively for the staggered and eclipsed conformations,[72] (3) enhanced flexibility due to a lower S−N rotational barrier,[72] and (4) a tetrahedral geometry about the sulfonyl group with S−N and S=O bond lengths that are relatively longer than amide bond lengths.[72] Furthermore, the greater Brønsted acidity of the sulfamide proton and greater Lewis basicity of sulfuryl oxygens may offer interesting potential for favoring hydrogen bonding, similar to the related sulfonamides as demonstrated in their crystal structures.[75-77]

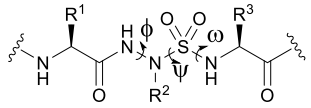

N-aminosulfamido peptide **33**

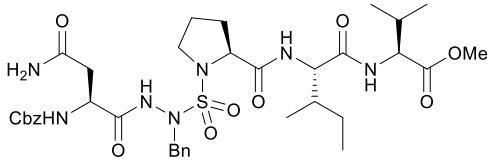

Cbz-L-Asn-Asf-L-Pro-L-Ile-L-Val-OMe **34**

Figure 3.1. General structure of an azasulfurylpeptide (**33**) and HIV-1 proteinase inhibitor **34**.

In the first reported syntheses of azasulfurylpeptides, amine and hydrazide building blocks **114** and **115** were combined with sulfuryl chloride using a catalytic amount of antimony pentachloride ($SbCl_5$); however, symmetric sulfamide **117** was often formed as side product.[70] *N*-Benzyl protected hydrazide precursors **115b** could be employed to introduce a side-chain onto the *N*-aminosulfamide residue (Scheme 3.1).[70]

Hydrazide acylation with amino acid-derived 4-nitrophenyl sulfamidates **118** has provided azasulfuryltripeptides without formation of symmetric sulfamide side product.[91] Furthermore, chemoselective alkylations of azasulfurylglycine (AsG) tripeptides **116a** have facilitated the insertion of various side-chains onto the *N*-aminosulfamide residue (Scheme 3.1).[91, 97]

Scheme 3.1. Solution-phase synthesis of *N*-aminosulfamides.

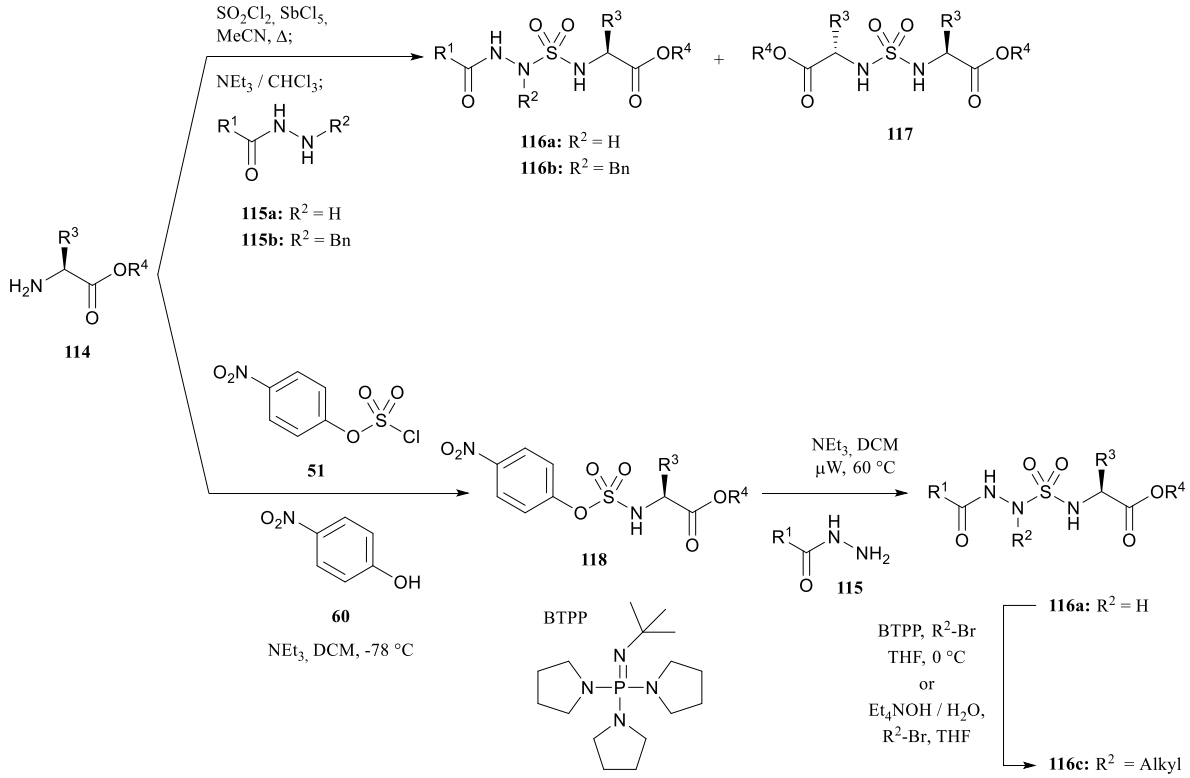

With effective means for making azasulfuryltripeptides in hand, attention has turned to study their conformational preferences. Herein, the crystal structures are now reported for two azasulfurylglycinyl tripeptides: *N*-(Boc)-Pro-AsG-Val-OMe (**105**) and *N*-(Cbz)-Ala-AsG-D-Phe-O*t*Bu (**119**). The crystal structures for both azasulfuryltripeptides exhibited properties characteristic of sulfonamides and azapeptides. Furthermore, they were found to adopt dihedral angles about the aminosulfamide residue that were similar to the central amino acid in a γ-turn secondary structure. γ-Turn conformations have been recognized to be important for the biological activity of various peptides,[63, 66, 72, 106-114] particularly ligands of G-protein-coupled receptors.[1] In spite of their importance in various recognition events,[111, 115-119] relatively few

examples of γ-turn mimics have been reported; most involving conformational constraint by structural linkages such as benzodiazepine,[63] pyrrolodiazepine,[65] diazepine,[62-64] morpholin-3-one,[66] 4-aminoproline,[68] 2-alkyl-2-carboxyazetidine,[67] 4-alkyamino-3-cyano-azabicyclo[3.2.1.] oct-3-ene,[69] as well as *N*-aminoimidazol-2-one heterocycles.[58, 59] Considering the relevance of γ-turns in biologically active peptides, mimics derived from azasulfurylpeptides may find interesting utility.

Results and Discussion

Insight into the conformational preferences of azasulfurylpeptides has been obtained by using X-ray analysis in the solid state of two azasulfuryltripeptide models. The Pro-AsG-Val (AsG = azasulfurylglycine) sequence was examined, because of the importance of the Pro-Gly dipeptide as the central residue of type II β-turn conformations.[120] The Pro-Gly-Val tripeptide is part of the repeating peptide sequence in elastin that has been shown to be a chemotactic factor for fibroblasts and monocytes.[121] In addition, Boc-Pro-Gly-Val-OH has been shown to adopt a preferred β-turn conformation in solution and to act as an inhibitor of the prolyl hydroxylase.[122] The Ala-AsG-D-Phe sequence was examined, because of its relationship to a key portion of azapeptide analogs of growth hormone releasing peptide-6 that we have previously shown to exhibit affinity and capacity to modulate the cluster of differentiation-36 receptor.[81, 123]

Crystals of *N*-(Boc)-Pro-AsG-Val-OMe (**105**)[91] and *N*-(Cbz)-Ala-AsG-D-Phe-O*t*-Bu (**119**) (Table 3.1) were both respectively grown from hexanes in ethyl acetate. The synthesis of azasulfuryltripeptide **105** was previously reported by coupling of hydrazide **95** and sulfamidate **91** in 1,2-dichloroethane (DCE) using microwave irradiation.[91] On the other hand, the synthesis of azasulfuryltripeptide **119** was achieved using an analogous microwave method as that described for **105** with the exception that hydrazide **122** and sulfamidate (*R*)-**90** were reacted in chloroform ($CHCl_3$) instead of DCE (Scheme 3.2).

Scheme 3.2. Synthesis of azasulfuryltripeptides **118** and **119**.

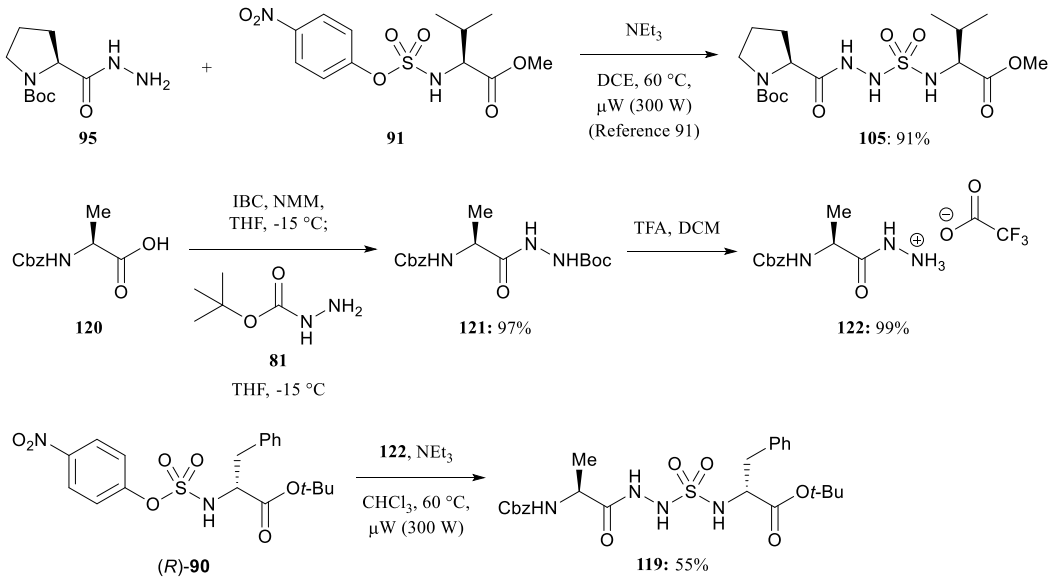

X-ray crystallographic analyses have been previously reported only for azasulfuryldipeptides: *N*-(Ac)-AsF-Gly-OMe (**42**) and *N*-(Boc)-AsF-Pro-OMe (**43**).[70] In comparing the X-ray structures of the azasulfuryltripeptides **105** and **119** with dipeptides **42** and **43**, the ω dihedral angles for the former were respectively 72.5° and −55.5°, consistent with the preferred staggered conformation (±60°) found in X-ray analyses of sulfonamides; however, those of the latter were −90°,[70] and closer to the eclipsed conformation (±100°) of sulfonamides. The ϕ dihedral angle of the azasulfuryltripeptides **105** and **119** were respectively –107.8° and 105.1°, consistent with the theoretical value of ±90° predicted for diacylhydrazines and found in X-ray structures of azapeptides.[124-129] The ψ torsion angle values of the azasulfuryltripeptides **105** and **119** were also similar (respectively 51.1° and −61.4°). The ϕ and ψ dihedral angle combination of the azasulfuryltripeptides **105** (–107.8°, 51.1°) and **119** (105.1°, −61.4°) were respectively within close proximity to the ideal torsion angle values of the central residues found in inverse (–75°, 65°) and classical (75°, –65°) γ-turns.

Table 3.1. Selected Bonds Length and Torsion Angles for *N*-(Boc)-Pro-AsG-Val-OMe (**105**) and *N*-(Cbz)-Ala-AsG-D-Phe-O*t*–Bu (**119**)

N-(Boc)-Pro-AsG-Val-OMe (**105**)		*N*-(Cbz)-Ala-AsG-D-Phe-O*t*-Bu (**119**)	
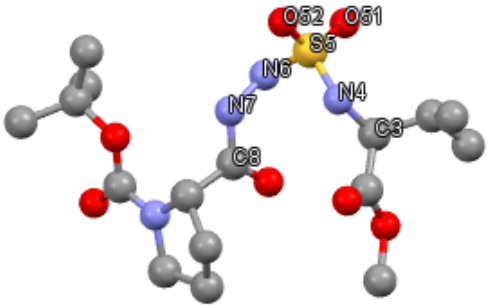		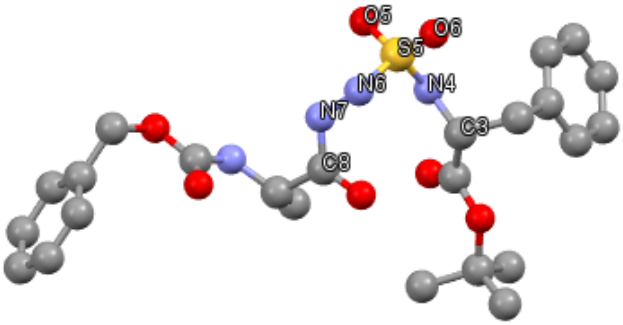	
Atoms	**Length (Å)**	**Atoms**	**Length (Å)**
N(7)−N(6)	1.387	N(7)−N(6)	1.393
N(6)−S(5)	1.678	N(6)−S(5)	1.662
S(5)−N(4)	1.603	S(5)−N(4)	1.618
S(5)=O(51)/S(5)=O(52)	1.428/1.421	S(5)=O(5) / S(5)=O(6)	1.433/1.421
Torsion angles	**Angle (°)**	**Torsion angles**	**Angle (°)**
ϕ [C(8)−N(7)−N(6)−S(5)]	−107.8	ϕ [C(8)−N(7)−N(6)−S(5)]	105.1
ψ [N(7)−N(6)−S(5)−N(4)]	51.1	ψ [N(7)−N(6)−S(5)−N(4)]	−61.4
ω [N(6)−S(5)−N(4)−C(3)]	72.5	ω [N(6)−S(5)−N(4)−C(3)]	−55.5

Stabilization of the γ-turn geometry appears to arise from the combination of lone pair-lone pair repulsion between the adjacent nitrogen of the hydrazine,[129] and the conformational preferences of the sulfamide.[74] In contrast to γ-mimics based on covalent constraint,[58, 59, 62-69] to the best of our knowledge, the azasulfuryltripeptides presented herein represent the first examples of stabilization of a γ-turn conformation by electronic interactions of neighboring heteroatoms. Of particular note, introduction of azasulfurylglycine for glycine in the Pro-Gly motif altered the commonly preferred type II β-turn geometry in favor of a γ-turn conformation. Azasulfuryltripeptides may thus have potential to exhibit biological activity by mimicking such natural turn geometry. Although the solid state conformations may not necessarily represent the

population of conformers in solution or when bound to a receptor, the application of azasulfurylpeptide in γ-turn mimicry merits further consideration.

The sulfur to oxygen and sulfur to nitrogen bond lengths in the azasulfurylpeptides **42**, **43**, **105** and **119** were similar (Table 3.1). Furthermore, the S=O bond length (1.42 Å) was similar to the C-O bond lengths calculated in the tetrahedral intermediate of amide bond hydrolysis (Figure 3.2, **123**).[130] The two S−N bond lengths (1.61 Å and 1.68 Å) observed in the crystal structures were however longer than the respective C−C and C−N bond lengths predicted for the transition state of amide bond hydrolysis (Figure 3.2). The sulfur adopts a tetrahedral geometry, supporting the hypothesis that the azasulfurylpeptides may mimic the tetrahedral transition state found in amide bond hydrolysis, and the rationale behind the activity of HIV-1 proteinase inhibitor **34**.[71]

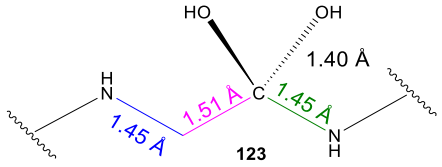

Figure 3.2. Calculated bond lengths of the tetrahedral intermediate in amide bond hydrolysis.

In addition, the crystal lattice of azasulfuryltripeptide **119** exhibited intermolecular hydrogen bonds between the sulfonyl oxygen and the hydrazide amide hydrogen [i.e. N(37)−H(37)...O(5) and N(7)−H(7)...O(35)] in an antiparallel orientation (Figure 3.3).

Conclusion

X-Ray crystallography has been used to characterize *N*-(Boc)-Pro-AsG-Val-OMe (**105**) and *N*-(Cbz)-Ala-AsG-D-Phe-O*t*-Bu (**119**) in order to better understand the conformational properties of azasulfurylpeptides. The dihedral angles, bond lengths and bond angles of **105** and **119** illustrated that features of azapeptides and sulfonamides are found in their *N*-aminosulfamide structures. For example, the tetrahedral geometry about the sulfur of the azasulfurylpeptides resembled the transition state found in amide bond hydrolysis. Moreover, the *N*-aminosulfamide residue in azasulfurylpeptides **105** and **119** adopted backbone dihedral angles that respectively mimicked the central residue of inverse and classical γ-turns, suggesting their potential to serve as surrogates of this important biological active turn geometry. In

addition, crystal packing of tripeptide **119** indicated significant intermolecular hydrogen bonding between sulfonyl oxygen and hydrazide hydrogen. Considering these features, structure-activity relationships of azasulfurylpeptides are now being studied in larger biologically active peptides.

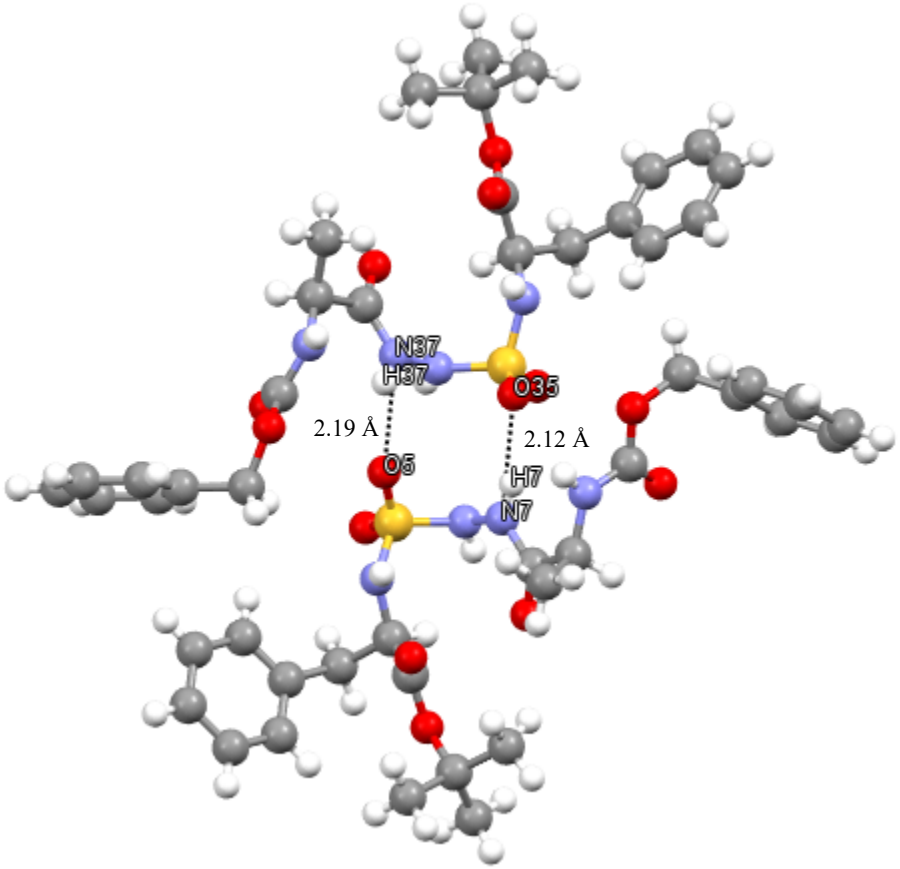

Figure 3.3. Packing structure of *N*-(Cbz)-Ala-AsG-D-Phe-O*t*-Bu (**119**).

Acknowledgment

S.T. would like to thank the FQRNT for a graduate student fellowship. The authors also thank Dr. Alexandra Furtos, Karine Venne and Marie-Christine Tang (Université de Montréal) for HR-MS analyses, and Francine Bélanger (Université de Montréal) for crystallographic analyses of azasulfurylpeptides **105** and **119**. This research was supported by the Natural Sciences and Engineering Research Council of Canada (NSERC), the Ministère du développement économique de l'innovation et de l'exportation du Québec (#878-2012, Traitement de la dégénerescence maculaire) and Amorchem.

Chapitre 4 : Synthèse sur support solide des azasulfurylpeptides

4.1. Mise en contexte de l'article 4

Dans le but de développer une synthèse combinatoire sur support solide des azasulfurylpeptides, deux voies de synthèse sont proposées. La première approche utilise des azasulfuryltripeptides alkylés avant leur insertion sur support solide pour pouvoir compléter des analogues de GHRP-6. Dans la deuxième approche, suite à une protection préalable des AsG par un groupement Fmoc, les alkylations chimiosélectives sont réalisées sur résine. Six analogues [azasulfuryl^{4}]-GHRP-6 ont ainsi été synthétisés, tandis que la synthèse des analogues [azasulfuryl^{3}]-GHRP-6 demeure toujours en investigation.

Article 4

Turcotte, S.; Dif-Yaiche, L.; Lubell, W. D. Solid-Phase Azasulfurylpeptide Synthesis.

En préparation pour Org. Lett.

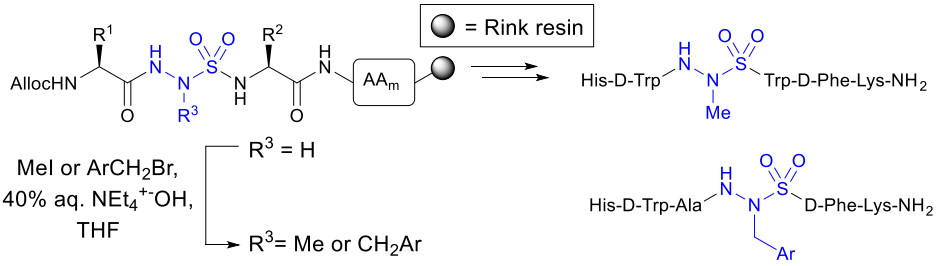

Solid-Phase Azasulfurylpeptide Synthesis

Stéphane Turcotte, Lylia Dif-Yaiche, William D. Lubell*

Département de Chimie, Université de Montréal, C.P. 6128,

Succursale Centre-Ville, Montréal, QC, H3C 3J7, Canada

Abstract

Featuring an amino acid surrogate in which the CαH and carbonyl are replaced respectively by nitrogen and a sulfonyl group, azasulfurylpeptides offer interesting potential for transition and ground state peptide mimicry. Employing azasulfuryltripeptide building blocks and the alkylation of the azasulfurylglycine (AsG) residue on Rink resin, a diversity-oriented approach for azasulfurylpeptide synthesis has been conceived and used to prepare six analogs of growth hormone releasing peptide-6 (GHRP-6).

Introduction

Combining the properties of azapeptides[38] and sulfonamides,[72, 73] azasulfurylpeptides possess an amino acid surrogate in which the $C_\alpha H$ and carbonyl components are respectively replaced by nitrogen and a sulfonyl group.[70, 71, 91, 97] Conformational analysis of azasulfuryltripeptide analogs have recently demonstrated their potential to mimic both the tetrahedral transition state of amide bond hydrolysis, as well as the backbone geometry of peptide turns.[131] In particular, the combination of lone pair-lone pair repulsion between their adjacent nitrogen,[38] and the potential for staggered (±60°) and eclipsed (±100°) sulfonamide conformers[72] favors the aminosulfamide residue to adopt backbone geometry characteristic of the ϕ^{i+1} and ψ^{i+1} dihedral angles of ideal γ- and type II β-turns. The *N*-aminosulfamide residue has served as a transition state mimic of amide hydrolysis in a micromolar human immunodeficiency virus-1 (HIV-1) proteinase inhibitor;[71] however, azasulfurylpeptide utility in turn mimicry of biological active peptides has yet to be explored. The latter concept is intriguing because of the expected greater Brønsted acidity of the sulfamide protons and greater Lewis basicity of the sulfuryl oxygens.[75-77]

The absence of a solid-phase approach for the synthesis of azasulfurylpeptides has limited such studies. The synthesis of azasulfuryltripeptides in solution was enhanced by employment of amino acid-derived *p*-nitrophenyl-sulfamidates (e.g., (*R*)-**90**) for hydrazide (e.g., **124** and **93**) acylation (Scheme 4.1),[91] because symmetric sulfamide side-product was avoided.[70] Furthermore, chemoselective alkylation of azasulfurylglycine (AsG) in tripeptide analogs (e.g., (*S*,*R*)-**101**) empowered installment of side-chains onto the *N*-aminosulfamide residue.[91]

In the context of our program to develop cluster of differentiation-36 modulators, we have studied analogs of growth hormone releasing peptide-6 (GHRP-6, His-D-Trp-Ala-Trp-D-Phe-Lys-NH_2).[81, 123, 132] For example, the azapeptides [azaTyr^4]-GHRP-6 and [Ala^1, azaPhe^4]-GHRP-6 exhibited respectively pro- and anti-angiogenic activity.[123] Targeting to improve receptor interactions, azasulfurylpeptide analogs of GHRP-6 have now been pursued.

Building on the methods for solution-phase synthesis, solid-phase azasulfurylpeptide synthesis has been elaborated with the goal of developing a diversity-oriented approach for making libraries to study structure-activity relationships. Employing Rink resin and an Fmoc-protection strategy, GHRP-6 analogs were prepared with *N*-aminosulfamide residues respectively at the 3- and 4-positions.

Scheme 4.1. Solution-phase syntheses of azasulfuryltripeptides *N*-(Alloc)-Ala-AsF(4-F)-D-Phe (**127**) and *N*-(Fmoc)-Ala-AsF-D-Phe (**128**).

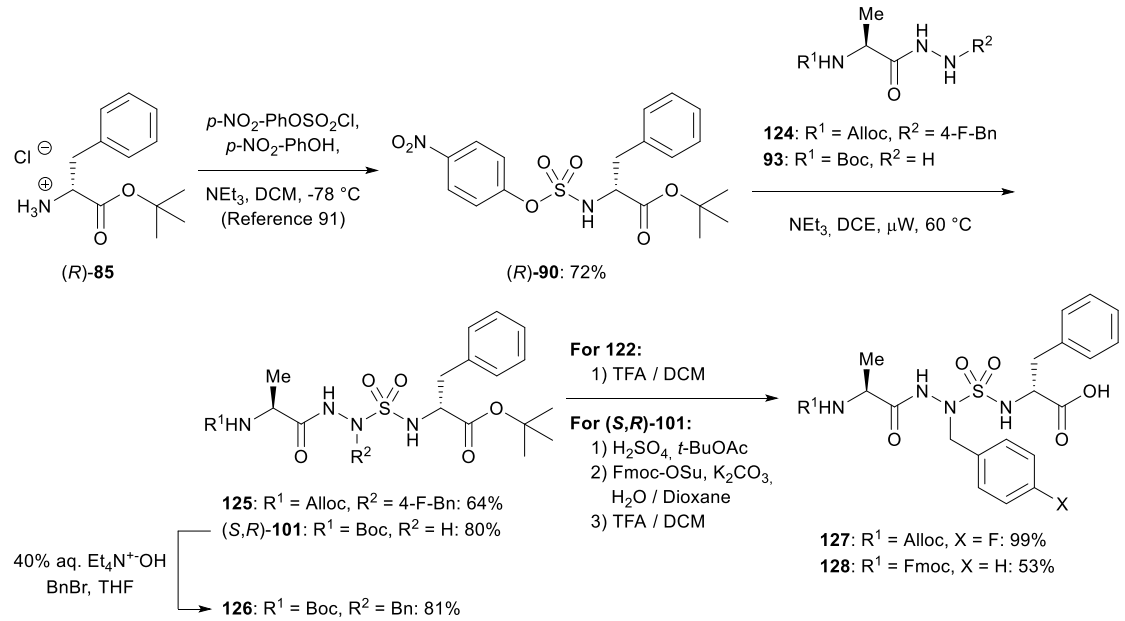

Results and Discussion

Attempts to prepare *N*-aminosulfamide from a supported peptide by the synthesis of the corresponding resin-bound sulfamidate using *p*-nitrophenyl chlorosulfate followed by coupling to a hydrazide failed. In solution, activation of valine *iso*-propylamide with *p*-nitrophenyl chlorosulfate gave the desired sulfamidate in only 15% yield, presumably, because intramolecular cyclization occurred on the *C*-terminal amide nitrogen to form a sulfahydantoin analog (not isolated).[133]

Subsequently, azasulfuryltripeptides were used as building blocks to install amino-sulfamide residues into longer peptides. Initially, *N*-(Alloc)-alaninyl-azasulfuryl-4-fluorophenylalaninyl- and *N*-(Fmoc)-alaninyl-azasulfurylphenylalaninyl-D-phenylalanines (**127** and **128**) were respectively synthesized in solution by approaches featuring the introduction of the arylmethyl moiety by coupling of 4-fluorobenzyl hydrazide **124** to sulfamidate (*R*)-**90**, as well as alkylation of azasulfurylglycinyl tripeptide (*S*,*R*)-**101** (Scheme 4.1, Experimental Section).[91, 97]

The AsF-tripeptide building blocks **127** and **128** were respectively coupled onto Lys(Boc) Rink resin **129** (Scheme 4.2). After respective removal of the Fmoc and Alloc groups using piperidine in DMF, and $Pd(PPh_3)_4$ with 1,3-dimethylbarbituric acid (DMBA), conventional Fmoc-based solid-phase synthesis was used to elongate the peptides. Couplings were performed with HBTU and DIEA in DMF employing Fmoc-D-Trp(Boc), followed by Fmoc-Ala or Fmoc-His(Trt). Cleavage of the peptides from the resin using a solution of TFA:H_2O:TES (95:2.5:2.5) in a cold room (4 °C), and purification by HPLC afforded respectively [Ala^1, $AsF(4\text{-}F)^4$]-GHRP-6 (**134**) and [AsF^4]-GHRP-6 (**135**) in 23% and 12% overall yields from tripeptides **127** and **128** (Table 4.1).

Scheme 4.2. Solid-phase peptide synthesis of [Ala[1], AsF(4-F)[4]]-GHRP-6 (**134**) and [AsF[4]]-GHRP-6 (**135**).

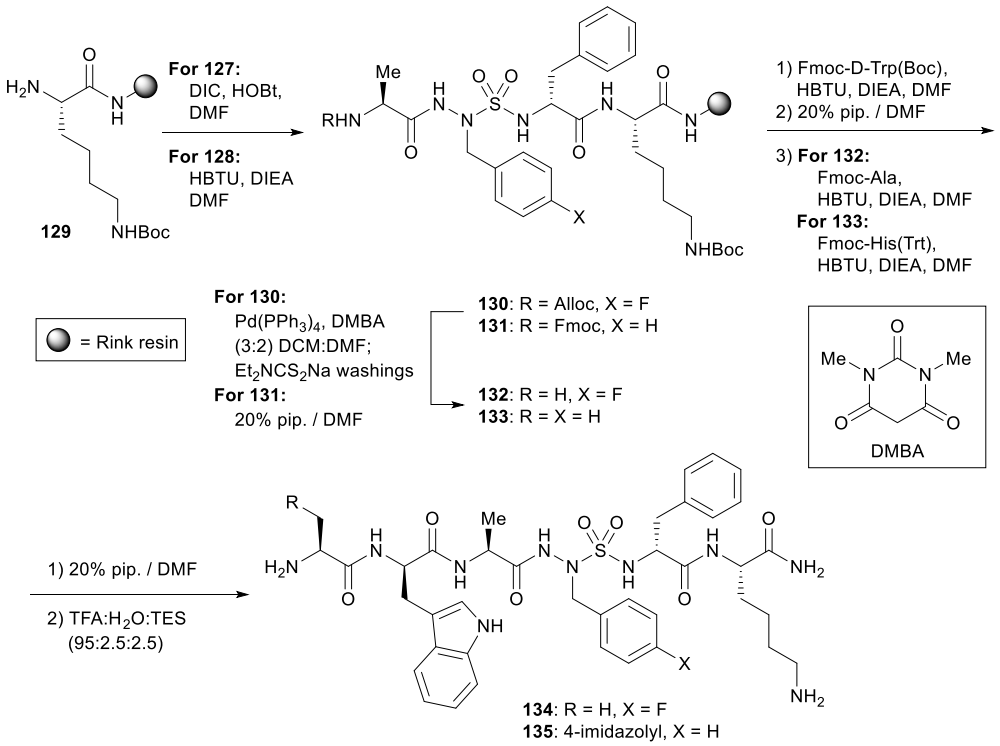

Although the fragment approach for solid-phase synthesis provided access to AsF[4]-GHRP-6 analogs **134** and **135**, alkylation of a resin-bound AsG peptide was pursued to facilitate introduction of side-chain diversity for structure-activity relationship studies. Attempts to couple *N*-(Fmoc)-Ala-AsG-D-Phe (**136**) to Lys(Boc) amide resin **129** met however with failure. Instead of the formation of AsG peptide **137**, analysis of an aliquot of resin by LC-MS after cleavage with TFA:H_2O:TES (95:2.5:2.5) indicated that the major product was the deletion sequence Fmoc-Ala-Lys-NH_2 from formation and cleavage of peptide **138** (Scheme 4.3). Considering AsF- and AsG-tripeptides **128** and **136** were respectively coupled effectively and unsuccessfully, the presence of the sulfamide proton was hypothesized to account for the degradation of the building block leading to the deletion product **138**.[134] Strategies were thus pursued to protect the AsG residue prior to coupling. Although allyl and phenylsulfonylethyl protection of the *N*-aminosulfamide residue could be introduced on the AsG residue to give azasulfuryltripeptide building blocks that were coupled successfully onto resin **129**, attempts to

remove these alkyl groups were unsuccessful, using $Pd(PPh_3)_4$ and DMBA, and piperidine in DMF, to effect respectively allyl transfer and β-elimination.

Scheme 4.3. Attempted coupling of azasulfurylglycinyl tripeptide **136** to resin **129**.

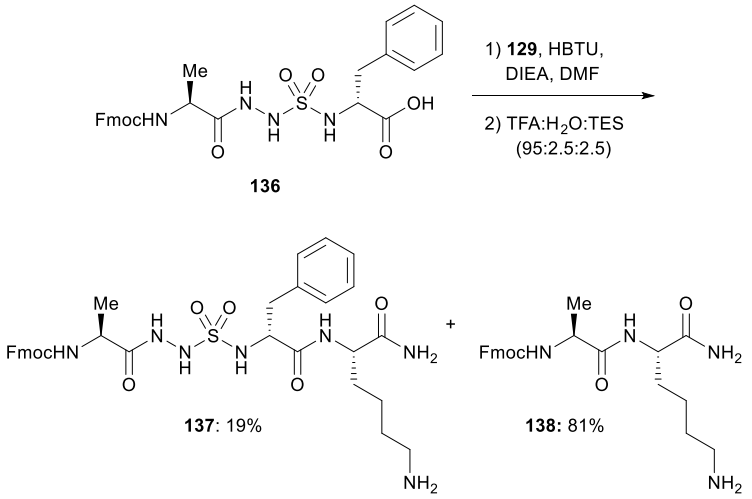

On the other hand, Fmoc protection of the *N*-aminosulfamide residue provided a successful means for introducing AsG residues into peptides. Acylation of azasulfurylglycine peptide **139** with Fmoc-OSu and sodium carbonate gave *N*-(Alloc)-Ala-AsG(Fmoc)-D-Phe-O*t*Bu (**140)** in 86% yield (Scheme 4.4). Removal of the *tert*-butyl ester provided acid **141**, which was coupled to Lys(Boc) resin **129** employing DIC and HOBt in DMF. Liberation of the *N*-aminosulfamide by removal of the Fmoc protection was achieved using piperidine in DMF to give AsG peptide resin **143**.

With AsG peptide **143** in hand, a proof-of-concept synthesis was performed by alkylation with benzyl bromide using tetraethylammonium hydroxide in THF to afford cleanly AsF peptide **144a** (Scheme 4.4). After alloc group removal, sequence elongation, and cleavage, peptide **134** was obtained in 78% crude purity, as assessed by LC-MS analysis and demonstrated to have identical retention time as material made by the building block approach described above.

Having validated the alkylation method by making [AsF^4]-GHRP-6 (**134**), diverse [azasulfuryl^4]-GHRP-6 analogs were pursued using similar conditions with a series of arylmethyl halides (Scheme 4.4): 4-fluoro-, 4-methoxy- and 4-dimethyl-*tert*-butylsilyloxybenzyl bromides, as well as 2-naphthylmethyl bromide. Conversion after

alkylation was assessed by cleavage of an aliquot of resin and LC-MS analysis, which detected 53-81% of **144a-e** contaminated with 5-11% of *bis*-alkylated product **145b-e**. After removal of the alloc protection, washing with sodium diethyldithiocarbamate, elongation of the peptide sequence, and cleavage as described above for **134**, azasulfurylpeptides **146b-e** were obtained in 52-70% crude purities and isolated by HPLC in 3-10% overall yields (Table 4.1).

Scheme 4.4. Diversity-oriented azasulfurylpeptide synthesis.

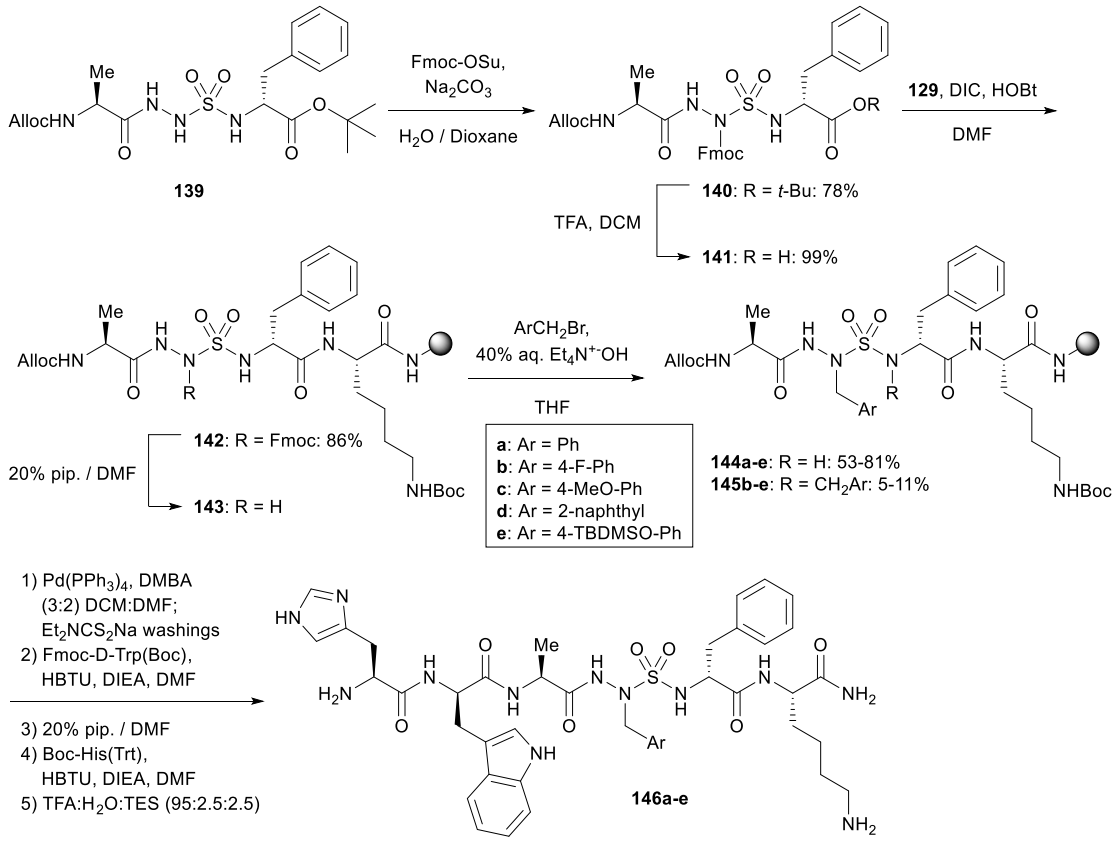

Table 4.1. Yields and purities of [azasulfuryl[4]]-GHRP 6 analogs.

Peptides	Crude purity[a]	Isolated Purity[b]	Isolated yields[c]	HRMS	
				m / z (cal)	m / z (obs)
Ala-D-Trp-Ala-AsF(4-F)-D-Phe-Lys-NH_2 (**134**)	59%	>99%	23%	845.3647	845.3539
His-D-Trp-Ala-AsF-D-Phe-Lys-NH_2 (**135**)	73%	99%	12%	893.3851	893.3832
His-D-Trp-Ala-AsF(4-F)-D-Phe-Lys-NH_2 (**146b**)	63%	>99%	3%	911.3757	911.3769
His-D-Trp-Ala-AsF(4-MeO)-D-Phe-Lys-NH_2 (**146c**)	70%	>99%	10%	923.3957	923.3936
His-D-Trp-Ala-AsA(2-naphthyl)-D-Phe-Lys-NH_2 (**146d**)	52%	98%	10%	943.4008	943.4007
His-D-Trp-Ala-AsY-D-Phe-Lys-NH2 (**146e**)	63%	>99%	9%	909.3801	909.3805

[a] Crude peptide purity ascertained by LC-MS analysis using 5-80% MeOH (0.1% FA) in H_2O (0.1% FA) as eluent. [b] Isolated peptide purity ascertained by LC-MS analysis in two systems: MeOH (0.1% FA) in H_2O (0.1% FA), and MeCN (0.1% FA) in H_2O (0.1% FA). [c] Isolated yields calculated based on resin loading.

To validate solid-phase synthesis of azasulfuryl residues without substituent and with simple alkyl substituents, the Ala^3 position of GHRP-6 was modified. The synthesis of the requisite building block, *N*-(Alloc)-D-Trp(Boc)-AsG(Fmoc)-Trp(Boc) (**154**) was accomplished by employing cumyl carbazate (**148**) to make hydrazide **150** and 2,4-dimethoxybenzyl (Dmb) ester protection of sulfamidate **151**, because of their removal with mild acid conditions that preserved the Boc side chain protection (Scheme 4.5). Employing D-Phe-Lys(Boc) resin **155**, AsG tripeptide **154** was coupled using DIC and HOBt in DMF to provide pentapeptide **156** in 40% crude purity. Alkylation of AsG **157** with iodomethane and tetraethylammonium hydroxide in THF for 5 h gave azasulfurylalanine (AsA) in 60% conversion. After the removal of the Alloc protecting group, analysis of an aliquot of resin by LC-MS after cleavage gave a mass indicative that the Alloc was cleaved, albeit in 17% crude purity. However, in the hopes of completing [AsA^3]- (**159**) and [AsG^3]-GHRP-6 (**160**) from unalkylated AsG **157**, no reaction occurred when the coupling of Fmoc- or Boc-His(Trt) with HBTU and DIEA was attempted. Other experiments are currently under investigation in order to understand why these couplings failed.

Scheme 4.5. Synthesis of [AsA^3]-GHRP-6 (**159**) and [AsG^3]-GHRP-6 (**160**).

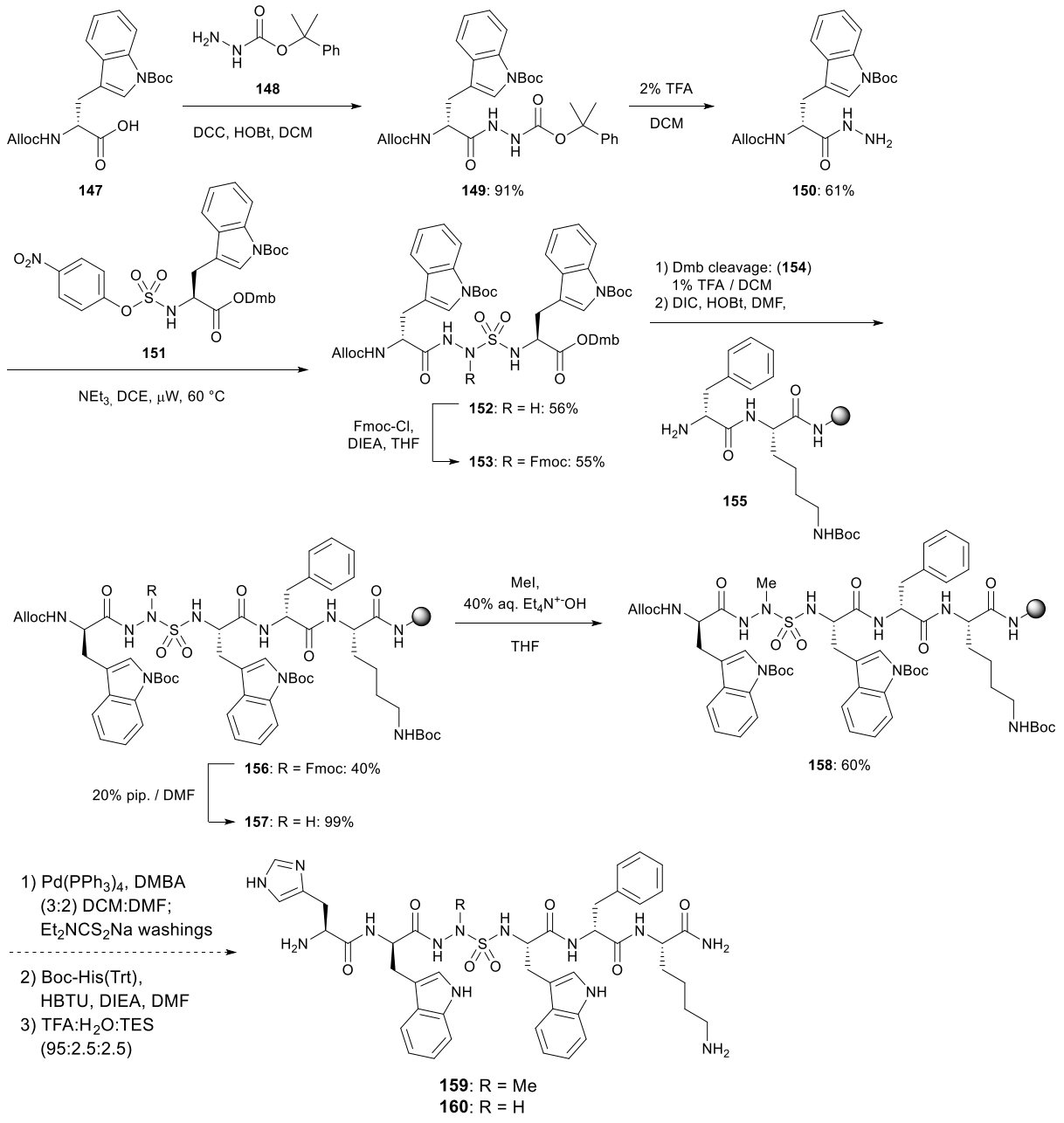

Conclusion

In conclusion, solid-phase methods were developed for the synthesis of azasulfurylpeptides. Six [azasulfuryl^4]-GHRP-6 analogs were prepared using azasulfuryltripeptide building blocks. Employing *N*-alkylsulfamides **127** and **128**, [Ala^1, AsF(4-F)^4]- and [AsF^4]-GHRP-6 (**134** and **135**) were synthesized using a modified Fmoc

strategy for solid-phase peptide synthesis. Although coupling of azasulfurylglycine tripeptide **136** gave mostly deletion sequence **138**, Fmoc protection of the *N*-aminosulfamide residue in peptides **141** and **154** empowered introduction of AsG residues. Alkylation of the AsG residue with different arylhalides provided a set of [azasulfuryl^4]-GHRP-6 analogs, which are currently being investigated for biological activity.

Chapitre 5 : Perspectives

6.1. Modulateurs du Toll-like receptor 2 (TLR2)

Les *Toll-like receptors* (TLRs) jouent un rôle important dans les réponses inflammatoires et immunitaires.[135, 136] Ces récepteurs sont impliqués dans un processus de signalisation dans lequel la biosynthèse des cytokines proinflammatoires est promue suite à l'activation du *Nuclear Factor Kappa-light-chain-enhancer of activated B cells* (NF-κB).[137] La modulation des TLRs a donc du potentiel dans le traitement de maladies immunitaires, en modulant la réponse inflammatoire.[138, 139]

Par exemple, des agonistes immunostimulants des TLRs sont présentement sur le marché, comme l'Imiquimod (**187**), un dérivé d'imidazoquinoline (Figure 5.1), impliqué dans le combat contre le *human papillomavirus* (HPV), une maladie transmissible sexuellement, et comme agoniste du TLR7.[138] L'agoniste du TLR4, le monophosphoryl lipid A, a été approuvé comme additif dans plusieurs vaccins.[138] En addition, plusieurs composés dérivés d'acides nucléiques sont recherchés pour moduler les TLRs.[138]

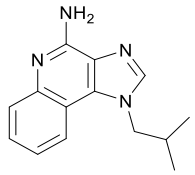

Figure 5.1. Agoniste des TLRs, l'Imiquimod (**187**).

L'inhibition du processus de signalisation des TLRs est impliquée dans le traitement de lésions ischémiques, suite à des crises cardiaques,[140] ainsi que dans la maladie neuro-dégénérative de l'Alzheimer.[141] D'une importance particulière, un anticorps antagoniste du TLR2 a été impliqué dans la réduction des risques des lésions ischémiques[142] et de l'inflammation rencontrée suite à une transplantation rénale.[143] La recherche de composés capables de moduler les fonctions du TLR2 est donc d'un grand intérêt.

Le complexe hétérodimère TLR2-TLR6 est présent avec le CD36 dans des cellules microvasculaires endothéliales et les macrophages qui agit comme co-récepteur.[144] Le processus de signalisation est donc dépendant du CD36 (Figure 5.2).[145] Des ligands pouvant interagir avec le récepteur CD36 auraient donc un potentiel à réguler les fonctions de ce complexe des TLRs par un mécanisme allostérique.

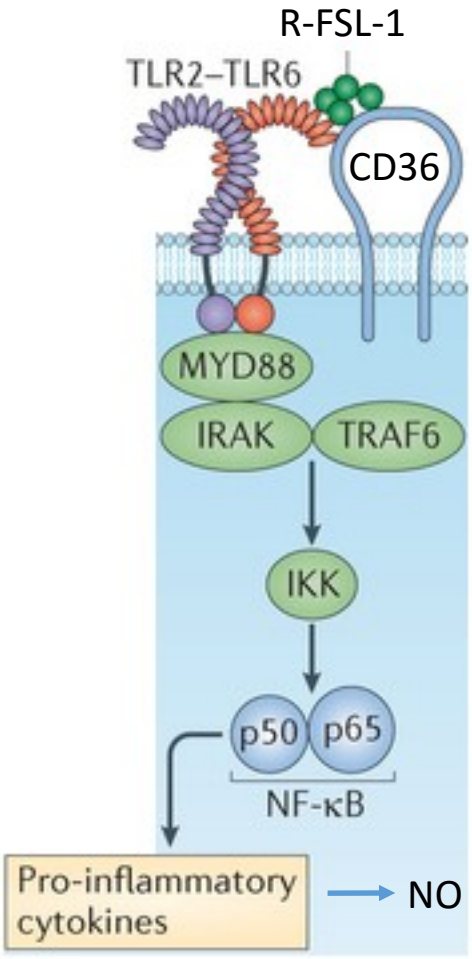

Figure 5.2. Processus de signalement du complexe TLR2-TLR6.[145]

Suite à la synthèse des [azasulfuryl[4]]-GHRP-6, l'affinité de liaison des azasulfurylpeptides au CD36 a tout d'abord été déterminée par résonance des plasmons de surface[146] (par Jérémie Labrecque-Carbonneau) en collaboration avec le Professeur Jean-François Masson à l'Université de Montréal, pour leur affinité envers CD36 (Tableau 5.1). Tous les analogues synthétisés ont démontré une affinité légèrement supérieure au GHRP-6.

Tableau 5.1. Constantes d'affinité envers CD36 des [azasulfuryl^4]-GHRP-6.

Peptides	k_D (μM)
His-D-Trp-Ala-Trp-Phe-Lys-NH_2 (**GHRP-6**)	25.6
His-D-Trp-Ala-AsF-D-Phe-Lys-NH_2 (**135**)	4.5
His-D-Trp-Ala-AsF(4-F)-D-Phe-Lys-NH_2 (**146b**)	20.0
His-D-Trp-Ala-AsF(4-MeO)-D-Phe-Lys-NH_2 (**146c**)	9.8
His-D-Trp-Ala-AsA(2-naphthyl)-D-Phe-Lys-NH_2 (**146d**)	13.9
His-D-Trp-Ala-AsY-D-Phe-Lys-NH2 (**146e**)	12.0

Étant donné leur bonne affinité pour CD36 *in vitro*, les azasulfurylpeptides ont ensuite été analysés par essais cellulaires pour leur capacité à moduler l'activité des TLR2 stimulés par des ligands spécifiques comme le *fibroblast-stimulating lipopeptide 1* (R-FSL-1) ou l'acide lipotéichoïque (LTA) (par Katia Mellal et Mukandila Mulumba) en collaboration avec le Professeur Huy Ong du département de Pharmacologie à la Faculté de Pharmacie de l'Université de Montréal.

Dans une première analyse visant à mesurer la modulation de la production de monoxyde d'azote (NO), un sous-produit réactif formé suite à l'induction dans les macrophages de ligands du TLR2, stimulé par le R-FSL-1 ou LTA, les azasulfurylpeptides [AsF(4-F)^4]- (**146b**) et [AsF(4-MeO)^4]-GHRP-6 (**146c**) ont démontré une capacité d'atténuer cette production de NO (Figure 5.3) dans les macrophages, lorsque stimulés avec le R-FSL-1; [AzaLys^6]-GHRP-6 (**188**) a servi de contrôle négatif. Le terme « vehicle » est attribué à des macrophages de contrôle auquel le TLR2 n'a pas été stimulé par le R-FSL-1. L'analyse a été poursuivie pour la sécrétion du *tumor necrosis factor alpha* (TNFα) et du *monocyte chemoattractant protein 1* (MCP-1) par les cytokines proinflammatoires. Les azasulfurylpeptides **146b** et **146c** ont également réduit la sécrétion de ces derniers par 23% (Figure 5.4). Il est important de mentionner que l'atténuation de la réponse inflammatoire induite par l'activation des TLR2 est recherchée sans toutefois inhiber complètement leur activation, causant un problème d'immunodéficience.

Par la suite, le profil cinétique de la modulation du TLR2 sur NF-κB, suite à son induction avec l'*Interferon γ* (IFN g) a été mesuré pour **146b**. Cet azasulfurylpeptide a donc

diminué l'activation de NF-κB par 11% à 5 min, par 29% à 10 min et par 25% à 15 min, après leur exposition au R-FSL-1 (Figure 5.5).

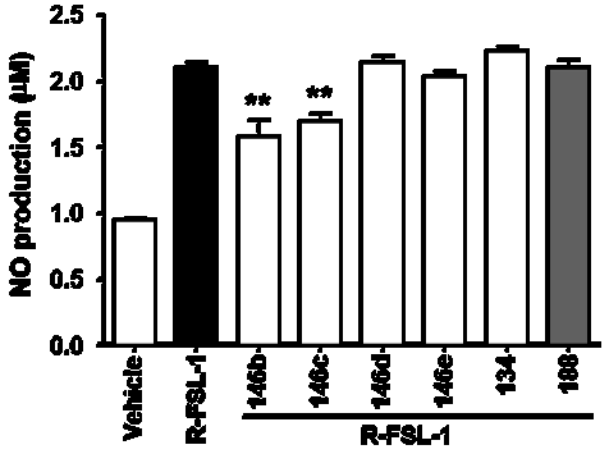

Figure 5.3. Modulation de la surproduction de NO induite par l'activation du TLR2 avec R-FSL-1 par les azasulfurylpeptides après 24 h.

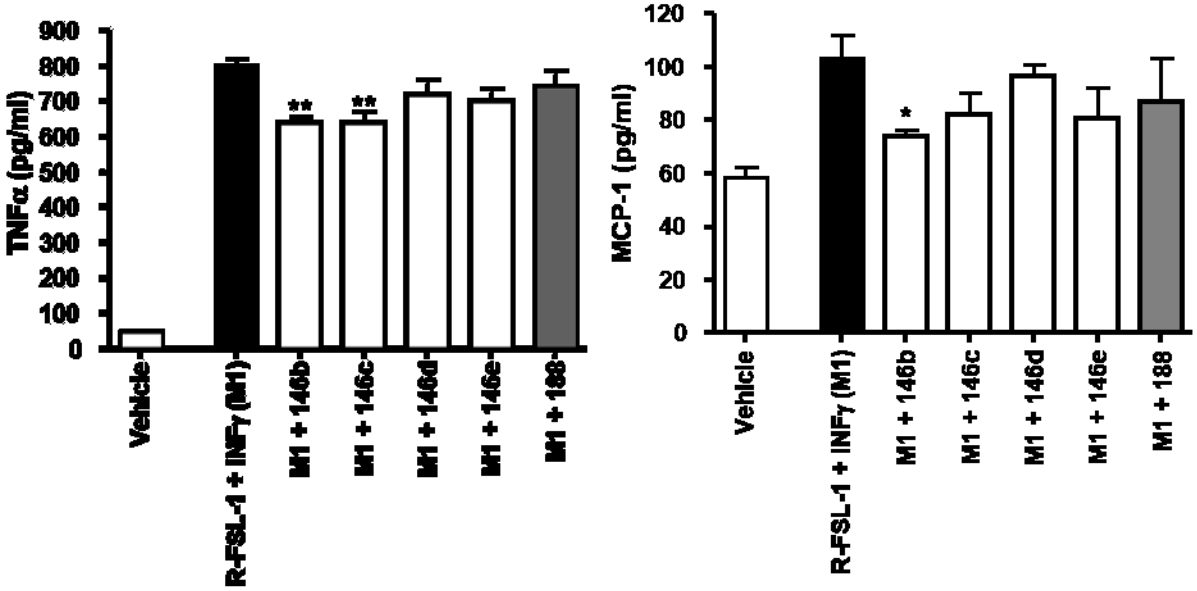

Figure 5.4. Modulation de la sécrétion de TNFα et MCP-1 induite par l'activation du TLR2 avec R-FSL-1 par les azasulfurylpeptides.

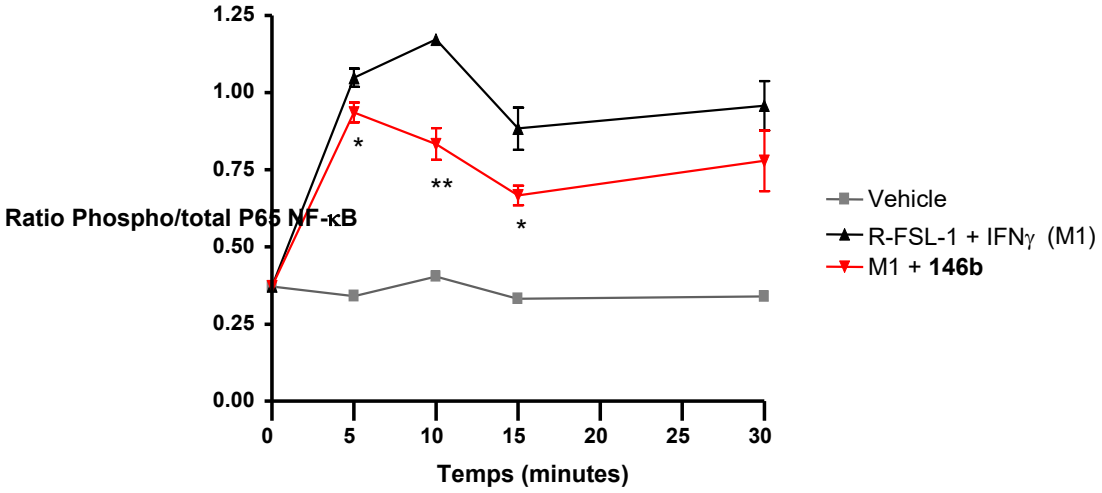

Figure 5.5. Profil cinétique de l'activation de NF-κB induite par l'activation du TLR2 avec R-FSL-1 par l'azasulfurylpeptide **146b**.

Afin de démontrer la dépendance du CD36 dans la modulation de la fonction du TLR2, des tests ont été réalisés sur des souris knockout (déficientes) du gène CD36. Les résultats n'ont démontré aucune influence des azasulfurylpeptides sur la modulation de la sécrétion de TNFα et MCP-1 induit par l'activation du TLR2 (Figure 5.6). De plus, dans une dernière étude sur l'activation du TLR2 avec le LTA (dépendante du CD36; agoniste du complexe TLR2/TLR6) et avec le PAM_3CSK_4 (indépendante du CD36; agoniste du complexe TLR1/TLR2), les azasulfurylpeptides **146b** et **146c** ont modulé la sécrétion du TNFα seulement pour l'activation avec le LTA (Figure 5.7).

Ces résultats démontrent le potentiel des azasulfurylpeptides **146b** et **146c** à pouvoir réguler le rôle du TLR2 qui induit les réponses inflammatoires et immunitaires innées.[147] D'autres tests sont présentement en cours quant à leur capacité à diminuer l'inflammation résultant de la formation de drusen (dépôt de lipoprotéines) dans l'espace sous rétinien; un des caractéristiques observé dans la dégénérescence maculaire liée à l'âge de type sec.[148] Cette réduction de l'inflammation permettrait de réduire le développement de la pathologie dont la phase avancée est caractérisée par une néovascularisation choroïdienne,[148] causant graduellement la cécité. Des tests sur la régulation de l'angiogenèse avec les azasulfurylpeptides seront également envisagés.

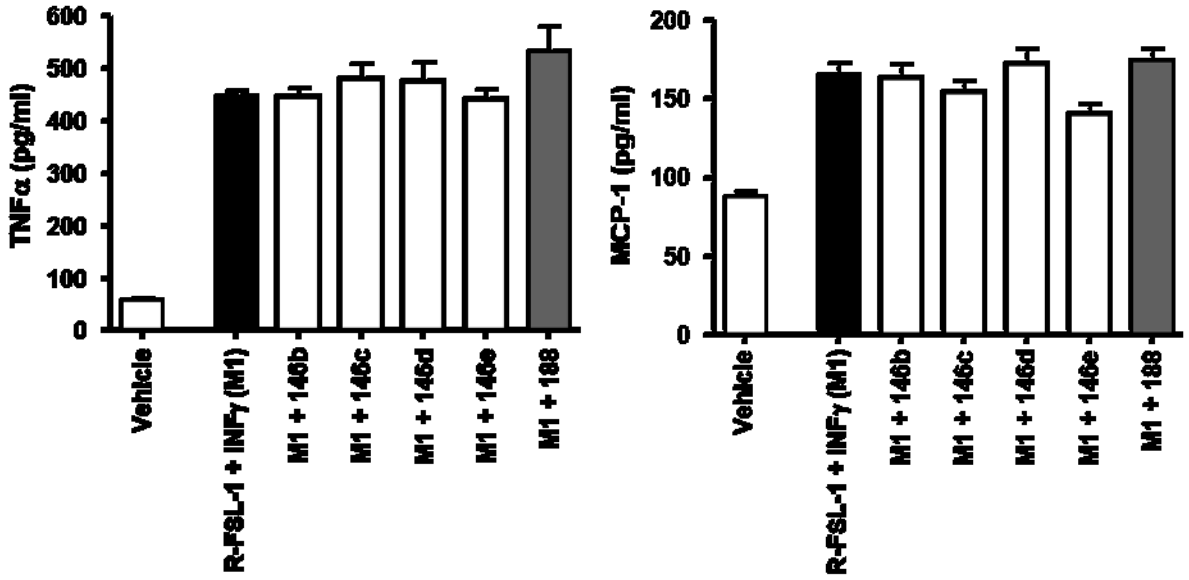

Figure 5.6. Modulation de la sécrétion de TNFα et MCP-1 induite par l'activation du TLR2 avec R-FSL-1 par les azasulfurylpeptides dans des souris déficientes du CD36.

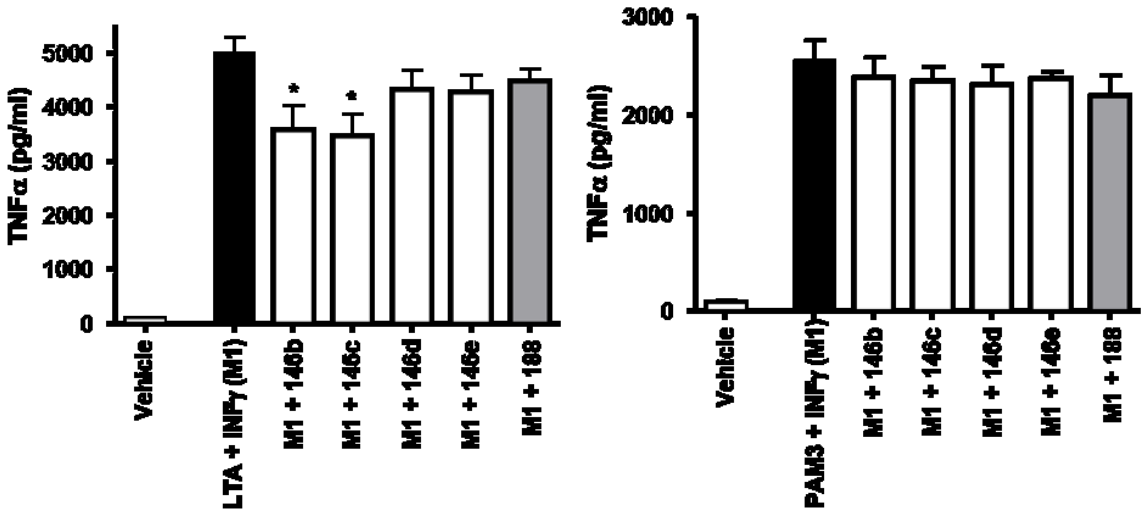

Figure 5.7. Modulation de la sécrétion de TNFα induite par l'activation du TLR2 avec LTA (Dépendant du CD36) ou PAM_3 (Indépendant du CD36) par les azasulfurylpeptides.

Finalement, dans le but d'explorer le mécanisme d'action des azasulfurylpeptides, la synthèse de [Tyr, Ala^0]-**146b** (**189**, figure 5.8) a été réalisée afin de développer un traceur radioactif avec I^{125}, sur la tyrosine du peptide.[149] Ce traceur radioactif permettra de monitorer la disposition intracellulaire de l'azasulfurylpeptide, suite à sa liaison au CD36 et de son internalisation dans les macrophages.

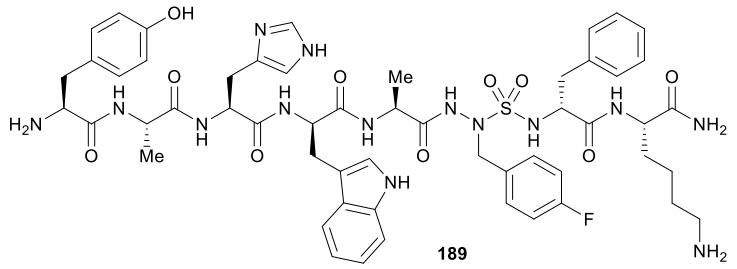

Figure 5.8. Représentation de [Tyr, Ala^0]-**146b** (**189**), servant à explorer l'affinité de **146b** envers le CD36.

6.2. Inhibiteurs de métallo-β-lactamases

Les β-lactames [tels les carbapénèmes (**190**), céphalosporines (**191**) et pénicillines (**192**), Figure 5.9] sont grandement utilisés de nos jours dans les antibiotiques contre les infections bactériennes. La fonction principale des β-lactames est d'empêcher la biosynthèse de la paroi bactérienne, appelé peptidoglycane. En effet, les antibiotiques β-lactames inhibent les enzymes transpeptidases responsables de l'insertion de la séquence terminale D-Ala-D-Ala dans le peptidoglycane, causant la mort des bactéries. Cette activité est attribuable au fait que la structure des β-lactames s'apparente à la portion terminale D-alaninyl-D-alanine du peptidoglycane.[150]

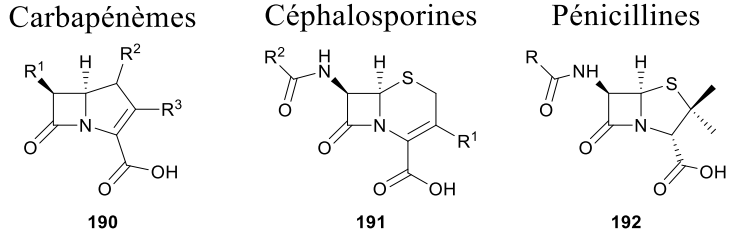

Figure 5.9. Représentation des carbapénèmes (**190**), des céphalosporines (**191**) et des pénicillines (**192**) dans les antibiotiques de types β-lactames.

Toutefois, plusieurs bactéries deviennent de plus en plus résistantes en développant des β-lactamases qui hydrolysent le lien amide des β-lactames. Il existe à ce jour quatre classes de β-lactamases.[151] Les classes A, C et D possèdent une sérine nucléophile dans leur site actif pour hydrolyser les β-lactames. La classe B correspond aux métallo-β-lactamases, possédant un atome de zinc dans leur site actif pour hydrolyser les β-lactames. Le *New Delhi Metallo-β-*

lactamase 1 (NDM-1) est un exemple de métallo-β-lactamases de la classe B,[151, 152] découvert chez un patient suédois d'origine indienne voyageant au New Delhi en 2009 et provenant de la bactérie *Klebsiella pneumoniae*.[153]

Il y a donc un grand intérêt à développer des inhibiteurs de β-lactamases pour contrer la résistance bactérienne. Ainsi, la capacité des azasulfurylpeptides de pouvoir inhiber différents métallo-β-lactamases, soit le NDM-1, ainsi que IMP-1 et le *Verona Integron-encoded Metallo-β-lactamase 2* (VIM-2) a été évaluée en collaboration avec le Professeur James Spencer à l'Université de Bristol.

Tout d'abord, une série de plusieurs azasulfuryltripeptides qui ont été synthétisés au courant de ce projet de doctorat a été soumise pour une analyse computationnelle effectuée par Ricky Cain dans le groupe du Pr. Colin Fishwick à l'Université de Leeds en utilisant le logiciel Sprout. Ce logiciel comporte 5 modules, soit : Cangaroo, Hippo, Elefant, Spider et Alligator. Cangaroo identifie un site de liaison potentiel dans le crystal de l'enzyme fournise. Hippo identifie les donneurs et accepteurs de ponts hydrogène, ainsi que les régions hydrophobiques dans le site de liaison trouvé. Elefant permet la sélection de fragments qui pourra s'insérer dans les sites de liaisons. Ces fragments sont ensuite connectés entre eux par des espaceurs déterminés par le module Spider. Finalement, les structures générées subissent des substitutions hétéroatomiques et un pointage arbitraire est généré par le module Alligator pour fournir les meilleurs candidats.[154]

Ayant fournis des structures précises pour un site de liaison connu dans le NDM-1, les dix meilleurs composés du résultat de cette analyse par le module Alligator ont donc été synthétisés et testés contre le NDM-1 (Figure 5.10). Malheureusement, aucun de ces composés n'agit comme inhibiteurs du NDM-1.

Par la suite, des analyses préliminaires ont été effectuées par Ramya Salimraj sous la supervision du Pr. James Spencer à l'Université de Bristol sur l'inhibition des azasulfurylpeptides envers IMP-1 et VIM-2. Les azasulfurylpeptides **136** (K_i = 110 μM), **112** (K_i = 300 μM) et **128** (K_i = 134 μM) ont démontré une activité inhibitrice micromolaire envers IMP-1. Ces résultats sont encourageants considérant qu'aucune analyse structure-activité n'a été établie préalablement avec les azasulfurylpeptides. Les azasulfurylpeptides ne sont toutefois

pas actifs envers VIM-2. La reproductibilité de ces résultats et les procédures expérimentales restent cependant à confirmer.

Un problème rencontré dans cette première série est que les azasulfurylpeptides synthétisés ne sont pas solubles dans l'eau. Ainsi, une deuxième série d'azasulfurylpeptides pourrait être présentée en retirant les protections *N*-terminales et *C*-terminales, afin de les rendre plus solubles dans l'eau.

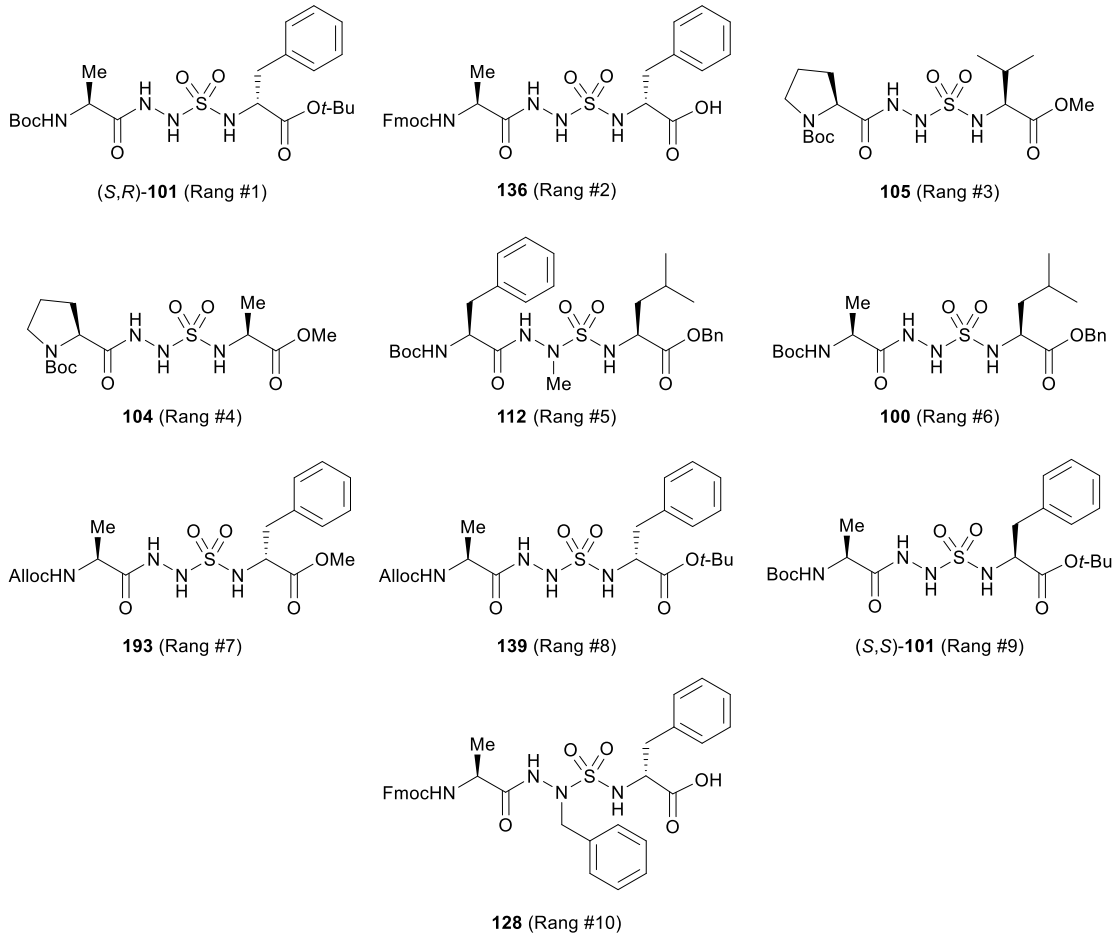

Figure 5.10. Représentation des dix meilleurs azasulfurylpeptides étudiés par analyse computationnelle pouvant se lier au site actif du NDM-1.

6.3. Conclusion

La synthèse des analogues d'azasulfurylpeptides de GHRP-6 utilisés comme ligands du CD36 ont permis d'établir une première relation structure-activité avec CD36 et le TLR2. Deux exemples, soit les azasulfurylpeptides [AsF(4-F)^4]- (**146b**) et [AsF(4-MeO)^4]-GHRP-6 (**146c**), ont démontré un potentiel à pouvoir réguler le rôle du TLR2 qui déclenche des réponses inflammatoires et immunitaires innées. De plus, la capacité des *N*-aminosulfamides à agir comme inhibiteurs d'enzymes a été validée par la synthèse d'inhibiteurs micromolaires du métallo-β-lactamase IMP-1. Ces résultats illustrent bien l'intérêt de poursuivre ces études sur les effets de l'utilisation des azasulfurylpeptides sur l'activité biologique de différents ligands et enzymes.

Chapitre 6 : Conclusion

En conclusion, une nouvelle méthodologie pour la synthèse des azasulfurylpeptides en solution a tout d'abord été développée. L'activation de dérivés d'acides aminés avec le chlorosulfate de 4-nitrophénol (**51**) a permis l'obtention de plusieurs sulfamidates de 4-nitrophénol. Ces sulfamidates ont par la suite été couplé à des hydrazides avec l'aide d'irradiation aux micro-ondes afin d'obtenir des azasulfuryltripeptides contenant l'analogue de la glycine, l'azasulfurylglycine. Puis, des alkylations chimiosélectives ont été effectuées sur les AsG pour y insérer diverses chaînes latérales.

Grâce à cette nouvelle approche, deux modèles d'azasulfuryltripeptides, soit le *N*-(Boc)-Pro-AsG-Val-OMe (**105**) et le *N*-(Cbz)-Ala-AsG-D-Phe-O*t*-Bu (**119**) ont été cristallisés et analysés. Ces modèles ont démontré des angles de torsion similaires à ceux observés pour les azapeptides et les sulfonamides. Également, ces azasulfurylpeptides ont démontré une capacité à induire des tours γ par contrainte électronique. La géométrie tétraédrique de l'atome de soufre valide l'hypothèse que ces composés peuvent mimer les états de transition dans l'hydrolyse des liens amides. Finalement, des liaisons hydrogènes intermoléculaires dans la matrice cristalline de **119** illustrent bien la capacité des azasulfurylpeptides à s'engager dans de telles liaisons.

Afin de promouvoir la synthèse des azasulfurylpeptides de façon combinatoire, une approche sur support solide a également été conçue. Six analogues [azasulfuryl^4]-GHRP-6 ont été synthétisés par deux approches différentes. En employant des azasulfuryltripeptides alkylés avant leur insertion sur support solide, [Ala^1, AsF(4-F)^4]- et [AsF^4]-GHRP-6 (**134** et **135**) ont été synthétisés. Puis, par l'emploi des AsG protégés par un groupement Fmoc, des alkylations chimiosélectives ont été réalisés sur résine pour compléter la synthèse des analogues [azasulfuryl^4]-GHRP-6.

Les analogues de GHRP-6 ont été ensuite analysés pour leur capacité à moduler les effets de la fonction du TLR2 dans le processus de signalisation des réponses inflammatoires. Les azasulfurylpeptides [AsF(4-F)^4]- et [AsF(4-MeO)^4]-GHRP-6 ont démontré une capacité à diminuer l'activation de NF-κB et la sécrétion de TNFα et de MCP-1 par les cytokines proinflammatoires. Ces résultats démontrent donc le potentiel de ces azasulfurylpeptides à pouvoir réguler le rôle du TLR2. Finalement, certains azasulfuryltripeptides ont démontré une activité inhibitrice envers IMP-1, un métallo-β-lactamase.

Depuis la méthode initiale de synthèse des azasulfurylpeptides, aucune étude n'avait été initiée pour l'utilisation des azasulfurylpeptides. Le développement des voies de synthèse en solution et sur support solide, présenté dans ce document de thèse, ainsi que leurs utilisations pour l'obtention de nouvelles familles de mimes peptidiques devraient permettre un nouvel essor de la recherche en chimie médicinale.

Bibliographie

(1) Craik, D. J.; Fairlie, D. P.; Liras, S.; Price, D., The future of peptide-based drugs. *Chem. Biol. Drug Des.* **2013,** *81*, 136-147.
(2) Voet, D.; Voet, J. G., *Biochimie*. 2e édition ed.; John Wiley & Sons, Inc. **2005**; p 1585.
(3) Lipinski, C. A.; Lombardo, F.; Dominy, B. W.; Feeney, P. J., Experimental and computational approaches to estimate solubility and permeability in drug discovery and development settings. *Adv. Drug Del. Rev.* **2012,** *64*, 4-17.
(4) Schiff, M. H.; Burmester, G. R.; Kent, J.; Pangan, A. L.; Kupper, H.; Fitzpatrick, S. B.; Donovan, C., Safety analyses of adalimumab (Humira) in global clinical trials and US postmarketing surveillance of patients with rheumatoid arthritis. *Ann. Rheum. Dis.* **2006,** *65*, 889-894.
(5) Fleischmann, R. M.; Baumgartner, S. W.; Tindall, E. A.; Weaver, A. L.; Moreland, L. W.; Schiff, M. H.; Martin, R. W.; Spencer-Green, G. T., Response to etanercept (Enbrel) in elderly patients with rheumatoid arthritis: a retrospective analysis of clinical trial results. *The Journal of rheumatology* **2003,** *30*, 691-696.
(6) Bondeson, J.; Maini, R., Tumour necrosis factor as a therapeutic target in rheumatoid arthritis and other chronic inflammatory diseases: the clinical experience with infliximab (Remicade). *Int. J. Clin. Pract.* **2001,** *55*, 211-216.
(7) Jazirehi, A. R.; Bonavida, B., Cellular and molecular signal transduction pathways modulated by rituximab (rituxan, anti-CD20 mAb) in non-Hodgkin's lymphoma: implications in chemosensitization and therapeutic intervention. *Oncogene* **2005,** *24*, 2121-2143.
(8) Ferrara, N.; Hillan, K. J.; Novotny, W., Bevacizumab (Avastin), a humanized anti-VEGF monoclonal antibody for cancer therapy. *Biochem. Biophys. Res. Commun.* **2005,** *333*, 328-335.
(9) Molina, M. A.; Codony-Servat, J.; Albanell, J.; Rojo, F.; Arribas, J.; Baselga, J., Trastuzumab (herceptin), a humanized anti-Her2 receptor monoclonal antibody, inhibits basal and activated Her2 ectodomain cleavage in breast cancer cells. *Cancer Res.* **2001,** *61*, 4744-4749.
(10) Wang, F.; Carabino, J. M.; Vergara, C. M., Insulin glargine: a systematic review of a long-acting insulin analogue. *Clin. Ther.* **2003,** *25*, 1541-1577.
(11) Biganzoli, L.; Untch, M.; Skacel, T.; Pico, J.-L. In *Neulasta (pegfilgrastim): a once-per-cycle option for the management of chemotherapy-induced neutropenia*, Semin. Oncol.2004 Elsevier; pp 27-34.
(12) Martin, G. R.; Ongkingo, J. R.; Turner, M. E.; Skurow, E. S.; Ruley, E. J., Recombinant erythropoietin (Epogen) improves cardiac exercise performance in children with end-stage renal disease. *Pediatr. Nephrol.* **1993,** *7*, 276-280.
(13) Galetta, S. L., The controlled high risk Avonex® multiple sclerosis trial (Champs study). *J. Neuroophthalmol.* **2001,** *21*, 292-295.
(14) Johnson, K.; Brooks, B.; Cohen, J.; Ford, C.; Goldstein, J.; Lisak, R.; Myers, L. W.; Panitch, H.; Rose, J.; Schiffer, R., Extended use of glatiramer acetate (Copaxone) is well tolerated and maintains its clinical effect on multiple sclerosis relapse rate and degree of disability. *Neurology* **1998,** *50*, 701-708.
(15) Okada, H., One- and three-month release injectable microspheres of the LH-RH superagonist leuprorelin acetate. *Adv. Drug Del. Rev.* **1997,** *28*, 43-70.

(16) Miller, R.; Frank, R., Zoladex® (goserelin) in the treatment of benign gynaecological disorders: an overview of safety and efficacy. *BJOG: Int. J. Obstet. Gy.* **1992,** *99*, 37-41.
(17) Arnold, R.; Neuhaus, C.; Benning, R.; Schwerk, W. B.; Trautmann, M. E.; Joseph, K.; Bruns, C., Somatostatin analog sandostatin and inhibition of tumor growth in patients with metastatic endocrine gastroenteropancreatic tumors. *World J. Surg.* **1993,** *17*, 511-519.
(18) Adams, J.; Kauffman, M., Development of the proteasome inhibitor Velcade™ (Bortezomib). *Cancer Invest.* **2004,** *22*, 304-311.
(19) Merrifield, R. B., Solid phase peptide synthesis. I. The synthesis of a tetrapeptide. *J. Am. Chem. Soc.* **1963,** *85*, 2149-2154.
(20) Christianson, D. W.; Lipscomb, W. N., Comparison of carboxypeptidase A and thermolysin: inhibition by phosphonamidates. *J. Am. Chem. Soc.* **1988,** *110*, 5560-5565.
(21) Jacobsen, N. E.; Bartlett, P. A., A phosphonamidate dipeptide analog as an inhibitor of carboxypeptidase A. *J. Am. Chem. Soc.* **1981,** *103*, 654-657.
(22) Mookhtiar, K. A.; Marlowe, C. K.; Bartlett, P. A.; Van Wart, H. E., Phosphonamidate inhibitors of human neutrophil collagenase. *Biochemistry* **1987,** *26*, 1962-1965.
(23) Bartlett, P. A.; Marlowe, C. K., Phosphonamidates as transition-state analog inhibitors of thermolysin. *Biochemistry* **1983,** *22*, 4618-4624.
(24) Holden, H. M.; Tronrud, D. E.; Monzingo, A. F.; Weaver, L. H.; Matthews, B. W., Slow- and fast-binding inhibitors of thermolysin display different modes of binding: crystallographic analysis of extended phosphonamidate transition-state analogs. *Biochemistry* **1987,** *26*, 8542-8553.
(25) McLeod, D. A.; Brinkworth, R. I.; Ashley, J. A.; Janda, K. D.; Wirsching, P., Phosphonamidates and phosphonamidate esters as HIV-1 protease inhibitors. *Bioorg. Med. Chem. Lett.* **1991,** *1*, 653-658.
(26) Camp, N. P.; Hawkins, P. C.; Hitchcock, P. B.; Gani, D., Synthesis of stereochemically defined phosphonamidate-containing peptides: inhibitors for the HIV-1 proteinase. *Bioorg. Med. Chem. Lett.* **1992,** *2*, 1047-1052.
(27) Demange, L.; Moutiez, M.; Dugave, C., Synthesis and evaluation of Glyψ (PO_2R-N) Pro-containing pseudopeptides as novel inhibitors of the human cyclophilin hCyp-18. *J. Med. Chem.* **2002,** *45*, 3928-3933.
(28) Gall, A.-L.; Ruff, M.; Kannan, R.; Cuniasse, P.; Yiotakis, A.; Dive, V.; Rio, M.-C.; Basset, P.; Moras, D., Crystal structure of the stromelysin-3 (MMP-11) catalytic domain complexed with a phosphinic inhibitor mimicking the transition-state. *J. Mol. Biol.* **2001,** *307*, 577-586.
(29) Grams, F.; Dive, V.; Yiotakis, A.; Yiallouros, I.; Vassiliou, S.; Zwilling, R.; Bode, W.; Stöcker, W., Structure of astacin with a transition-state analogue inhibitor. *Nat. Struct. Mol. Biol.* **1996,** *3*, 671-675.
(30) Oleksyszyn, J.; Powers, J. C., Irreversible inhibition of serine proteases by peptide derivatives of (α-aminoalkyl) phosphonate diphenyl esters. *Biochemistry* **1991,** *30*, 485-493.
(31) Moree, W. J.; van Gent, L. C.; van der Marel, G. A.; Liskamp, R. M., Synthesis of peptides containing a sulfinamide or a sulfonamide transition-state isostere. *Tetrahedron* **1993,** *49*, 1133-1150.
(32) Moree, W. J.; van der Marel, G. A.; Liskamp, R. J., Synthesis of peptidosulfinamides and peptidosulfonamides: peptidomimetics containing the sulfinamide or sulfonamide transition-state isostere. *J. Org. Chem.* **1995,** *60*, 5157-5169.

(33) Liskamp, R. M.; Kruijtzer, J. A., Peptide transformation leading to peptide-peptidosulfonamide hybrids and oligo peptidosulfonamides. *Mol. Divers.* **2004,** *8*, 79-87.
(34) Lowik, D. W.; Liskamp, R. M., Synthesis of α-and β-substituted aminoethane sulfonamide arginine-glycine mimics. *Eur. J. Org. Chem.* **2000,** *2000*, 1219-1228.
(35) Humljan, J.; Kotnik, M.; Boniface, A.; Šolmajer, T.; Urleb, U.; Blanot, D.; Gobec, S., A new approach towards peptidosulfonamides: synthesis of potential inhibitors of bacterial peptidoglycan biosynthesis enzymes MurD and MurE. *Tetrahedron* **2006,** *62*, 10980-10988.
(36) Moree, W.; Van der Marel, G.; Liskamp, R., Peptides containing a sulfinamide or a sulfonamide moiety: New transition-state analogues. *Tetrahedron Lett.* **1991,** *32*, 409-412.
(37) Gilmore, W. F.; Lin, H.-J., Synthesis of carbamates of α-amino sulfonamides. *J. Org. Chem.* **1978,** *43*, 4535-4537.
(38) Proulx, C.; Sabatino, D.; Hopewell, R.; Spiegel, J.; García Ramos, Y.; Lubell, W. D., Azapeptides and their therapeutic potential. *Future Med. Chem.* **2011,** *3*, 1139-1164.
(39) Zega, A., Azapeptides as pharmacological agents. *Curr. Med. Chem.* **2005,** *12*, 589-597.
(40) Gante, J., Azapeptides. *Synthesis* **1989**, 405-413.
(41) Boutard, N.; Jamieson, A. G.; Ong, H.; Lubell, W. D., Structure-activity analysis of the growth hormone secretagogue GHRP-6 by α-and β-amino γ-lactam positional scanning. *Chem. Biol. Drug Des.* **2010,** *75*, 40-50.
(42) Jamieson, A. G.; Boutard, N.; Beauregard, K.; Bodas, M. S.; Ong, H.; Quiniou, C.; Chemtob, S.; Lubell, W. D., Positional scanning for peptide secondary structure by systematic solid-phase synthesis of amino lactam peptides. *J. Am. Chem. Soc.* **2009,** *131*, 7917-7927.
(43) Freidinger, R. M., Synthesis of γ-lactam-constrained tryptophyl-lysine derivatives. *J. Org. Chem.* **1985,** *50*, 3631-3633.
(44) Freidinger, R. M.; Perlow, D. S.; Veber, D. F., Protected lactam-bridged dipeptides for use as conformational constraints in peptides. *J. Org. Chem.* **1982,** *47*, 104-109.
(45) Freidinger, R. M.; Veber, D. F.; Perlow, D. S.; Saperstein, R., Bioactive conformation of luteinizing hormone-releasing hormone: evidence from a conformationally constrained analog. *Science* **1980,** *210*, 656-658.
(46) Hata, M.; Marshall, G. R., Do benzodiazepines mimic reverse-turn structures? *J. Comput.-Aided Mol. Des.* **2006,** *20*, 321-331.
(47) Genin, M. J.; Gleason, W. B.; Johnson, R. L., Design, synthesis, and x-ray crystallographic analysis of two novel spirolactam systems as β-turn mimics. *J. Org. Chem.* **1993,** *58*, 860-866.
(48) Hinds, M. G.; Welsh, J. H.; Brennand, D. M.; Fisher, J.; Glennie, M. J.; Richards, N. G.; Turner, D. L.; Robinson, J. A., Synthesis, conformational properties, and antibody recognition of peptides containing β-turn mimetics based on α-alkylproline derivatives. *J. Med. Chem.* **1991,** *34*, 1777-1789.
(49) Nigel, G., Design and synthesis of a novel peptide β-turn mimetic. *J. Chem. Soc., Chem. Commun.* **1988**, 1447-1449.
(50) Atmuri, N. P.; Lubell, W. D., Insight into transannular cyclization reactions to synthesize azabicyclo [XYZ] alkanone amino acid derivatives from 8-, 9-and 10-member macrocyclic dipeptide lactams. *J. Org. Chem.* **2015**, Accepted, DOI: 10.1021/acs.joc.5b00237.
(51) Cluzeau, J.; Lubell, W. D., Design, synthesis, and application of azabicyclo [XY0] alkanone amino acids as constrained dipeptide surrogates and peptide mimics. *Biopolymers (Pept. Sci.)* **2005,** *80*, 98-150.

(52) Bourguet, C. B.; Claing, A.; Laporte, S. A.; Hébert, T. E.; Chemtob, S.; Lubell, W. D., Synthesis of azabicycloalkanone amino acid and azapeptide mimics and their application as modulators of the prostaglandin F2α receptor for delaying preterm birth. *Can. J. Chem.* **2014,** *92*, 1031-1040.
(53) Bourguet, C. B.; Goupil, E.; Tassy, D.; Hou, X.; Thouin, E.; Polyak, F.; Hébert, T. E.; Claing, A.; Laporte, S. A.; Chemtob, S., Targeting the prostaglandin F2α receptor for preventing preterm labor with azapeptide tocolytics. *J. Med. Chem.* **2011,** *54*, 6085-6097.
(54) Hanessian, S.; McNaughton-Smith, G.; Lombart, H.-G.; Lubell, W. D., Design and synthesis of conformationally constrained amino acids as versatile scaffolds and peptide mimetics. *Tetrahedron* **1997,** *53*, 12789-12854.
(55) Bisang, C.; Weber, C.; Inglis, J.; Schiffer, C. A.; van Gunsteren, W. F.; Jelesarov, I.; Bosshard, H. R.; Robinson, J. A., Stabilization of Type-I β-turn conformations in peptides containing the NPNA-repeat motif of the Plasmodium falciparum Circumsporozoite protein by substituting proline for (*S*)-α-methylproline. *J. Am. Chem. Soc.* **1995,** *117*, 7904-7915.
(56) Halab, L.; Lubell, W. D., Use of steric interactions to control peptide turn geometry. Synthesis of type VI β-turn mimics with 5-tert-butylproline. *J. Org. Chem.* **1999,** *64*, 3312-3321.
(57) Halab, L., Influence of *N*-terminal residue stereochemistry on the prolyl amide geometry and the conformation of 5-tert-butylproline type VI β-turn mimics. *J. Pept. Sci.* **2001,** *7*, 92-104.
(58) Proulx, C.; Lubell, W. D., *N*-Amino-imidazolin-2-one peptide mimic synthesis and conformational analysis. *Org. Lett.* **2012,** *14*, 4552-4555.
(59) Proulx, C.; Lubell, W. D., Analysis of *N*-amino-imidazolin-2-one peptide turn mimic 4-position substituent effects on conformation by X-ray crystallography. *Biopolymers (Pept. Sci.)* **2014,** *102*, 7-15.
(60) Doan, N. D.; Lubell, W. D., X-Ray structure analysis reveals β-turn mimicry by *N*-amino-imidazolidin-2-ones. *Biopolymers (Pept. Sci.)* **2015**, Accepted, DOI: 10.1002/bip.22646.
(61) Rose, G. D.; Glerasch, L. M.; Smith, J. A., Turns in peptides and proteins. *Adv. Protein Chem.* **1985,** *37*, 1-109.
(62) Iden, H. S.; Lubell, W. D., 1, 3, 5-Tri-and 1, 3, 4, 5-tetra-substituted 1, 4-diazepin-2-one solid-phase synthesis. *J. Comb. Chem.* **2008,** *10*, 691-699.
(63) Rosenström, U.; Sköld, C.; Plouffe, B.; Beaudry, H.; Lindeberg, G.; Botros, M.; Nyberg, F.; Wolf, G.; Karlén, A.; Gallo-Payet, N., New selective AT2 receptor ligands encompassing a γ-turn mimetic replacing the amino acid residues 4-5 of angiotensin II act as agonists. *J. Med. Chem.* **2005,** *48*, 4009-4024.
(64) Ramanathan, S. K.; Keeler, J.; Lee, H.-L.; Reddy, D. S.; Lushington, G.; Aubé, J., Modular synthesis of cyclic peptidomimetics inspired by γ-turns. *Org. Lett.* **2005,** *7*, 1059-1062.
(65) Boutard, N.; Dufour-Gallant, J.; Deaudelin, P.; Lubell, W. D., Pyrrolo [3, 2-e][1, 4] diazepin-2-one synthesis: A head-to-head comparison of soluble versus insoluble supports. *J. Org. Chem.* **2011,** *76*, 4533-4545.
(66) Yuan, Z.; Blomberg, D.; Sethson, I.; Brickmann, K.; Ekholm, K.; Johansson, B.; Nilsson, A.; Kihlberg, J., Synthesis and pharmacological evaluation of an analogue of the peptide hormone oxytocin that contains a mimetic of an inverse γ-turn. *J. Med. Chem.* **2002,** *45*, 2512-2519.
(67) Baeza, J. L.; Gerona-Navarro, G.; Thompson, K.; Pérez de Vega, M. J. s.; Infantes, L.; García-López, M. T.; González-Muñiz, R.; Martín-Martínez, M., Further evidence for 2-Alkyl-2-carboxyazetidines as γ-turn inducers. *J. Org. Chem.* **2009,** *74*, 8203-8211.

(68) Curran, T. P.; Chandler, N. M.; Kennedy, R. J.; Keaney, M. T., *N*-α-benzoyl-cis-4-amino-L-proline: A γ-turn mimetic. *Tetrahedron Lett.* **1996,** *37*, 1933-1936.
(69) Kemp, D.; Carter, J. S., Amino acid derivatives that stabilize secondary structures of polypeptides—IV. Practical synthesis of 4-alkyamino-3-cyano-azabicyclo [3.2. 1.] oct-3-enes (Ben derivatives) as γ-turn templates. *Tetrahedron Lett.* **1987,** *28*, 4645-4648.
(70) Cheeseright, T. J.; Edwards, A. J.; Elmore, D. T.; Jones, J. H.; Raissi, M.; Lewis, E. C., Azasulfonamidopeptides as peptide bond hydrolysis transition state analogues. Part 1. Synthetic approaches. *J. Chem. Soc., Perkin Trans. 1* **1994**, 1595-1600.
(71) Cheeseright, T. J.; Daenke, S.; Elmore, D. T.; Jones, J. H., Azasulfonamidopeptides as peptide bond hydrolysis transition state analogues. Part 2. Potential HIV-1 proteinase inhibitor. *J. Chem. Soc., Perkin Trans. 1* **1994**, 1953-1955.
(72) Baldauf, C.; Günther, R.; Hofmann, H. J., Conformational properties of sulfonamido peptides. *J. Mol. Struc.-Theochem* **2004,** *675*, 19-28.
(73) Bharatam, P. V.; Gupta, A.; Kaur, D., Theoretical studies on S–N interactions in sulfonamides. *Tetrahedron* **2002,** *58*, 1759-1764.
(74) Mó, O.; Paz, J. L. D.; Yáñez, M.; Alkorta, I.; Elguero, J.; Goya, P.; Rozas, I., A molecular orbital study of the conformation (inversion and rotational barriers) and electronic properties of sulfamide. *Can. J. Chem.* **1989,** *67*, 2227-2236.
(75) Adsmond, D. A.; Grant, D. J., Hydrogen bonding in sulfonamides. *J. Pharm. Sci.* **2001,** *90*, 2058-2077.
(76) Gennari, C.; Gude, M.; Potenza, D.; Piarulli, U., Hydrogen-bonding donor/acceptor scales in β-sulfonamidopeptides. *Chem. Eur. J.* **1998,** *4*, 1924-1931.
(77) Langenhan, J. M.; Fisk, J. D.; Gellman, S. H., Evaluation of hydrogen bonding complementarity between a secondary sulfonamide and an α-amino acid residue. *Org. Lett.* **2001,** *3*, 2559-2562.
(78) Bourguet, C. B.; Sabatino, D.; Lubell, W. D., Benzophenone semicarbazone protection strategy for synthesis of aza-glycine containing aza-peptides. *Biopolymers (Pept. Sci.)* **2008,** *90*, 824-831.
(79) Sabatino, D.; Proulx, C.; Klocek, S.; Bourguet, C. B.; Boeglin, D.; Ong, H.; Lubell, W. D., Exploring side-chain diversity by submonomer solid-phase azapeptide synthesis. *Org. Lett.* **2009,** *11*, 3650-3653.
(80) Bourguet, C. B.; Proulx, C.; Klocek, S.; Sabatino, D.; Lubell, W. D., Solution-phase submonomer diversification of aza-dipeptide building blocks and their application in aza-peptide and aza-DKP synthesis. *J. Pept. Sci.* **2010,** *16*, 284-296.
(81) Sabatino, D.; Proulx, C.; Pohankova, P.; Ong, H.; Lubell, W. D., Structure–activity relationships of GHRP-6 azapeptide ligands of the CD36 scavenger receptor by solid-phase submonomer azapeptide synthesis. *J. Am. Chem. Soc.* **2011,** *133*, 12493-12506.
(82) Garcia-Ramos, Y.; Proulx, C.; Lubell, W. D., Synthesis of hydrazine and azapeptide derivatives by alkylation of carbazates and semicarbazones. *Can. J. Chem.* **2012,** *90*, 985-993.
(83) Zhang, J.; Proulx, C.; Tomberg, A.; Lubell, W. D., Multicomponent diversity-oriented synthesis of azalysine peptide mimics. *Org. Lett.* **2013,** *16*, 298-301.
(84) Nicolaou, K.; Mathison, C. J.; Montagnon, T., *o*-Iodoxybenzoic acid (IBX) as a viable reagent in the manipulation of nitrogen-and sulfur-containing substrates: scope, generality, and mechanism of IBX-mediated amine oxidations and dithiane deprotections. *J. Am. Chem. Soc.* **2004,** *126*, 5192-5201.

(85) Powell, J.; Whiting, M., The decomposition of sulphonyl-hydrazone salts. I: Mechanism and stereochemistry. *Tetrahedron* **1959,** *7*, 305-310.
(86) Powell, J.; Whiting, M., The decomposition of sulphonylhydrazone salts: Mechanism and stereochemistry. II: The pyrolysis of the diazodecalins. *Tetrahedron* **1961,** *12*, 168-172.
(87) Buncel, E.; Raoult, A., Bond scission in sulfur compounds. V. A kinetic study of Sulfur-Oxygen and Sulfur-Chlorine bond scission in the methanolysis of *p*-nitrophenyl chlorosulfate. *Can. J. Chem.* **1972,** *50*, 1907-1911.
(88) Armarego, W. L.; Chai, C., *Purification of laboratory chemicals*. Seventh Edition ed.; Butterworth-Heinemann **2012**.
(89) Fettes, K. J.; Howard, N.; Hickman, D. T.; Adah, S. A.; Player, M. R.; Torrence, P. F.; Micklefield, J., Replacement of the phosphodiester linkage in DNA with sulfamide and 3′-*N*-sulfamate groups. *Chem. Commun.* **2000**, 765-766.
(90) Fettes, K. J.; Howard, N.; Hickman, D. T.; Adah, S.; Player, M. R.; Torrence, P. F.; Micklefield, J., Synthesis and nucleic-acid-binding properties of sulfamide-and 3′-*N*-sulfamate-modified DNA. *J. Chem. Soc., Perkin Trans. 1* **2002**, 485-495.
(91) Turcotte, S.; Bouayad-Gervais, S. H.; Lubell, W. D., *N*-Aminosulfamide peptide mimic synthesis by alkylation of azasulfurylglycinyl peptides. *Org. Lett.* **2012,** *14*, 1318-1321.
(92) Boutard, N.; Turcotte, S.; Beauregard, K.; Quiniou, C.; Chemtob, S.; Lubell, W. D., Examination of the active secondary structure of the peptide 101.10, an allosteric modulator of the interleukin-1 receptor, by positional scanning using β-amino γ-lactams. *J. Pept. Sci.* **2011,** *17*, 288-296.
(93) Movassaghi, M.; Ahmad, O. K., *N*-isopropylidene-*N*'-2-nitrobenzenesulfonyl hydrazine, a reagent for reduction of alcohols via the corresponding monoalkyl diazenes. *J. Org. Chem.* **2007,** *72*, 1838-1841.
(94) Kurian, L. A.; Silva, T. A.; Sabatino, D., Submonomer synthesis of azapeptide ligands of the Insulin Receptor Tyrosine Kinase domain. *Bioorg. Med. Chem. Lett.* **2014,** *24*, 4176-4180.
(95) Garcia-Ramos, Y.; Lubell, W. D., Synthesis and alkylation of aza-glycinyl dipeptide building blocks. *J. Pept. Sci.* **2013,** *19*, 725-729.
(96) Milletti, F.; Storchi, L.; Goracci, L.; Bendels, S.; Wagner, B.; Kansy, M.; Cruciani, G., Extending pKa prediction accuracy: high-throughput pKa measurements to understand pKa modulation of new chemical series. *Eur. J. Med. Chem.* **2010,** *45*, 4270-4279.
(97) Turcotte, S.; Havard, T.; Lubell, W. D., Mild chemoslective alkylation of azasulfurylglycinyl peptides. In *Proceedings to the 32nd European Peptide Symposium*, Kokotos, G.; Constantinou-Kokotou, V.; Matsoukas, J., Eds.: Athens, Grece, **2012**; pp 140-141.
(98) Hirschmann, R.; Yager, K. M.; Taylor, C. M.; Witherington, J.; Sprengeler, P. A.; Phillips, B. W.; Moore, W.; Smith III, A. B., Phosphonate diester and phosphonamide synthesis. Reaction coordinate analysis by ^{31}P NMR spectroscopy: identification of pyrophosphonate anhydrides and highly reactive phosphonylammonium salts. *J. Am. Chem. Soc.* **1997,** *119*, 8177-8190 and refs 1-18 cited therein.
(99) Chen, C. A.; Sieburth, S. M. N.; Glekas, A.; Hewitt, G. W.; Trainor, G. L.; Erickson-Viitanen, S.; Garber, S. S.; Cordova, B.; Jeffry, S.; Klabe, R. M., Drug design with a new transition state analog of the hydrated carbonyl: silicon-based inhibitors of the HIV protease. *Chem. Biol.* **2001,** *8*, 1161-1166.
(100) Hamilton, W. C., The crystal structure of orthorhombic acetamide. *Acta Crystallogr.* **1965,** *18*, 866-870.

(101) Wei, L.; Lubell, W. D., Scope and limitations in the use of *N*-(PhF) serine-derived cyclic sulfamidates for amino acid synthesis. *Can. J. Chem.* **2001,** *79*, 94-104.
(102) Atfani, M.; Wei, L.; Lubell, W. D., N-(9-(9-Phenylfluorenyl)) homoserine-derived cyclic sulfamidates: novel chiral educts for the synthesis of enantiopure γ-substituted α-amino acids. *Org. Lett.* **2001,** *3*, 2965-2968.
(103) The presence of <10% diastereomeric azasulfurylglycinyl tripeptide **101** may likely be caused by racemization during formation of the *N*-(Boc)-L-Ala hydrazide. See: Benoiton, N.; Kuroda, K.; Chen, F. M. F., Examination of chiral stability during the preparation of hydrazides and coupling by the azide procedure using a series of model peptides. *Int. J. Pept. Protein Res.* **1982,** *20*, 81-86.
(104) Camp, N. P.; Perrey, D. A.; Kinchington, D.; Hawkins, P. C.; Gani, D., Synthesis of peptide analogues containing phosphonamidate methyl ester functionality: HIV-1 proteinase inhibitors possessing unique cell uptake properties. *Biorg. Med. Chem.* **1995,** *3*, 297-312.
(105) Elliott, R.; Marks, N.; Berg, M.; Portoghese, P., Synthesis and biological evaluation of phosphonamidate peptide inhibitors of enkephalinase and angiotensin-converting enzyme. *J. Med. Chem.* **1985,** *28*, 1208-1216.
(106) Amodeo, P.; Naider, F.; Picone, D.; Tancredi, T.; Temussi, P. A., Conformational sampling of bioactive conformers: a low-temperature NMR study of ^{15}N-Leu–enkephalin. *J. Pept. Sci.* **1998,** *4*, 253-265.
(107) Schwyzer, R.; Moutevelis-Minakakis, P.; Kimura, S.; Gremlich, H. U., Lipid-induced secondary structures and orientations of [Leu^5]-enkephalin: helical and crystallographic double-bend conformers revealed by IRATR and molecular modelling. *J. Pept. Sci.* **1997,** *3*, 65-81.
(108) Zhan, L.; Chen, J. Z.; Liu, W.-K., Conformational study of met-enkephalin based on the ECEPP force fields. *Biophys. J.* **2006,** *91*, 2399-2404.
(109) Bleich, H. E.; Galardy, R. E.; Printz, M. P., Conformation of angiotensin II in aqueous solution. Evidence for the γ-turn model. *J. Am. Chem. Soc.* **1973,** *95*, 2041-2042.
(110) Cann, J. R.; London, R. E.; Stewart, J. M.; Matwiyoff, N. A., Effect of temperature upon the circular dichroism of bradykinin. *Int. J. Pept. Protein Res.* **1979,** *14*, 388-392.
(111) Sato, M.; Lee, J. Y.; Nakanishi, H.; Johnson, M. E.; Chrusciel, R. A.; Kahn, M., Design, synthesis and conformational analysis of γ-turn peptide mimetics of bradykinin. *Biochem. Biophys. Res. Commun.* **1992,** *187*, 999-1006.
(112) Hedenström, M.; Yuan, Z.; Brickmann, K.; Carlsson, J.; Ekholm, K.; Johansson, B.; Kreutz, E.; Nilsson, A.; Sethson, I.; Kihlberg, J., Conformations and receptor activity of desmopressin analogues, which contain γ-turn mimetics or a Ψ [CH_2O] isostere. *J. Med. Chem.* **2002,** *45*, 2501-2511.
(113) Levian-Teitelbaum, D.; Kolodny, N.; Chorev, M.; Selinger, Z.; Gilon, C., ^{1}H-NMR studies of receptor-selective substance P analogues reveal distinct predominant conformations in DMSO-d_6. *Biopolymers* **1989,** *28*, 51-64.
(114) Wynants, C.; Sugg, E.; Hruby, V.; Binst, G., Conformational study of a somatostatin analogue by high-field nmr spectroscopy, in aqueous solution. *Int. J. Pept. Protein Res.* **1987,** *30*, 541-547.
(115) Callahan, J. F.; Bean, J. W.; Burgess, J. L.; Eggleston, D. S.; Hwang, S. M.; Kopple, K. D.; Koster, P. F.; Nichols, A.; Peishoff, C. E., Design and synthesis of a C_7 mimetic for the predicted γ-turn conformation found in several constrained RGD antagonists. *J. Med. Chem.* **1992,** *35*, 3970-3972.

(116) Newlander, K. A.; Callahan, J. F.; Moore, M. L.; Tomaszek Jr, T. A.; Huffman, W. F., A novel constrained reduced-amide inhibitor of HIV-1 protease derived from the sequential incorporation of γ-turn mimetics into a model substrate. *J. Med. Chem.* **1993,** *36*, 2321-2331.
(117) Callahan, J. F.; Newlander, K. A.; Burgess, J. L.; Eggleston, D. S.; Nichols, A.; Wong, A.; Huffman, W. F., The use of γ-turn mimetics to define peptide secondary structure. *Tetrahedron* **1993,** *49*, 3479-3488.
(118) Hoog, S. S.; Zhao, B.; Winborne, E.; Fisher, S.; Green, D. W.; DesJarlais, R. L.; Newlander, K. A.; Callahan, J. F.; Abdel-Meguid, S. S.; Moore, M. L., A check on rational drug design: crystal structure of a complex of Human Immunodeficiency Virus Type 1 protease with a novel γ-Turn mimetic inhibitor. *J. Med. Chem.* **1995,** *38*, 3246-3252.
(119) Brickmann, K.; Somfai, P.; Kihlberg, J., An approach to enantiomerically pure inverse γ-turn mimetics for use in solid-phase synthesis. *Tetrahedron Lett.* **1997,** *38*, 3651-3654.
(120) Raghothama, S.; Awasthi, S., β-Hairpin nucleation by Pro-Gly β-turns. Comparison of D-Pro-Gly and L-Pro-Gly sequences in an apolar octapeptide. *J. Chem. Soc., Perkin Trans. 2* **1998**, 137-144.
(121) Senior, R. M.; Griffin, G. L.; Mecham, R. P.; Wrenn, D. S.; Prasad, K. U.; Urry, D. W., Val-Gly-Val-Ala-Pro-Gly, a repeating peptide in elastin, is chemotactic for fibroblasts and monocytes. *J. Cell Biol.* **1984,** *99*, 870-874.
(122) Chopra, R.; Ananthanarayanan, V., Conformational implications of enzymatic proline hydroxylation in collagen. *Proc. Natl. Acad. Sci. U. S. A.* **1982,** *79*, 7180-7184.
(123) Proulx, C.; Picard, E. m.; Boeglin, D.; Pohankova, P.; Chemtob, S.; Ong, H.; Lubell, W. D., Azapeptide analogues of the growth hormone releasing peptide 6 as cluster of differentiation 36 receptor ligands with reduced affinity for the growth hormone secretagogue receptor 1a. *J. Med. Chem.* **2012,** *55*, 6502-6511.
(124) André, F.; Boussard, G.; Bayeul, D.; Didierjean, C.; Aubry, A.; Marraud, M., Aza-peptides II. X-Ray structures of aza-alanine and aza-asparagine-containing peptides. *J. Pept. Res.* **1997,** *49*, 556-562.
(125) André, F.; Vicherat, A.; Boussard, G.; Aubry, A.; Marraud, M., Aza-peptides. III. Experimental structural analysis of aza-alanine and aza-asparagine-containing peptides. *J. Pept. Res.* **1997,** *50*, 372-381.
(126) Marraud, M.; Dupont, V.; Grand, V.; Zerkout, S.; Lecoq, A.; Boussard, G.; Vidal, J.; Collet, A.; Aubry, A., Modifications of the amide bond and conformational constraints in pseudopeptide analogues. *Biopolymers* **1993,** *33*, 1135-1148.
(127) Marraud, M.; Aubry, A., Crystal structures of peptides and modified peptides. *Biopolymers (Pept. Sci.)* **1996,** *40*, 45-83.
(128) Benatalah, Z.; Aubry, A.; Boussard, G.; Marraud, M., Evidence for a β-turn in an azadipeptide sequence. *Int. J. Pept. Protein Res.* **1991,** *38*, 603-605.
(129) Reynolds, C. H.; Hormann, R. E., Theoretical study of the structure and rotational flexibility of diacylhydrazines: implications for the structure of nonsteroidal ecdysone agonists and azapeptides. *J. Am. Chem. Soc.* **1996,** *118*, 9395-9401.
(130) James, M. N.; Sielecki, A. R., Stereochemical analysis of peptide bond hydrolysis catalyzed by the aspartic proteinase penicillopepsin. *Biochemistry* **1985,** *24*, 3701-3713.
(131) Turcotte, S.; Lubell, W. D., Crystal structure analyses of azasulfuryltripeptides reveal potential for γ-turn mimicry. *Biopolymers (Pept. Sci.)* **2015**, Accepted, DOI: 10.1002/bip.22632.

(132) Picard, E.; Houssier, M.; Bujold, K.; Sapieha, P.; Lubell, W.; Dorfman, A.; Racine, J.; Hardy, P.; Febbraio, M.; Lachapelle, P., CD36 plays an important role in the clearance of oxLDL and associated age-dependent sub-retinal deposits. *Aging* **2010,** *2*, 981.
(133) For a library of sulfahydantoins, see: Albericio, F.; Bryman, L. M.; Garcia, J.; Michelotti, E. L.; Nicolás, E.; Tice, C. M., Synthesis of a sulfahydantoin library. *J. Comb. Chem.* **2001,** *3*, 290-300.
(134) The formation of a sulfonyldiazene intermediate may be responsible for the formation of the deletion sequence. See: Gölz, H.; Glatz, B.; Haas, G.; Helmchen, G.; Muxfeldt, H., *N*-Acyl-*N*′-arylsulfonyldiazenes; detection and use in the synthesis of amides. *Angew. Chem. Int. Ed.* **1977,** *16*, 728-729.
(135) Akira, S.; Uematsu, S.; Takeuchi, O., Pathogen recognition and innate immunity. *Cell* **2006,** *124*, 783-801.
(136) Kawai, T.; Akira, S., The role of pattern-recognition receptors in innate immunity: update on Toll-like receptors. *Nat. Immunol.* **2010,** *11*, 373-384.
(137) Piccinini, A.; Midwood, K., DAMPening inflammation by modulating TLR signalling. *Mediators Inflamm.* **2010,** *2010*, 1-21.
(138) Connolly, D. J.; O'Neill, L. A., New developments in Toll-like receptor targeted therapeutics. *Curr. Opin. Pharm.* **2012,** *12*, 510-518.
(139) Keogh, B.; Parker, A. E., Toll-like receptors as targets for immune disorders. *Trends Pharmacol. Sci.* **2011,** *32*, 435-442.
(140) Dunne, A.; Marshall, N. A.; Mills, K. H., TLR based therapeutics. *Curr. Opin. Pharm.* **2011,** *11*, 404-411.
(141) Schneider, A. R.; Sari, Y., Therapeutic perspectives of drugs targeting Toll-Like receptors based on immune physiopathology theory of Alzheimer's disease. *CNS Neurol. Disord. Drug Targets* **2014,** *13*, 909.
(142) Arslan, F.; Smeets, M. B.; O'Neill, L. A.; Keogh, B.; McGuirk, P.; Timmers, L.; Tersteeg, C.; Hoefer, I. E.; Doevendans, P. A.; Pasterkamp, G., Myocardial ischemia/reperfusion injury is mediated by leukocytic Toll-like receptor-2 and reduced by systemic administration of a novel anti–Toll-like receptor-2 antibody. *Circulation* **2010,** *121*, 80-90.
(143) Placebo-controlled study to evaluate the safety and efficacy of OPN-305 in preventing delayed renal graft function. http://www.clinicaltrials.gov/ct2/show/NCT01794663?term=opsona&rank=1
(144) Triantafilou, M.; Gamper, F. G.; Lepper, P. M.; Mouratis, M. A.; Schumann, C.; Harokopakis, E.; Schifferle, R. E.; Hajishengallis, G.; Triantafilou, K., Lipopolysaccharides from atherosclerosis-associated bacteria antagonize TLR4, induce formation of TLR2/1/CD36 complexes in lipid rafts and trigger TLR2-induced inflammatory responses in human vascular endothelial cells. *Cell. Microbiol.* **2007,** *9*, 2030-2039.
(145) Canton, J.; Neculai, D.; Grinstein, S., Scavenger receptors in homeostasis and immunity. *Nat. Rev. Immunol.* **2013,** *13*, 621-634.
(146) Bolduc, O. R.; Lambert-Lanteigne, P.; Colin, D. Y.; Zhao, S. S.; Proulx, C.; Boeglin, D.; Lubell, W. D.; Pelletier, J. N.; Féthière, J.; Ong, H., Modified peptide monolayer binding His-tagged biomolecules for small ligand screening with SPR biosensors. *Analyst* **2011,** *136*, 3142-3148.
(147) Lubell, W. D.; Huy, O.; Turcotte, S.; Mella, K.; Mukandila, M.; Dif-Yaiche, L. Azasulfurylpeptide-based CD36 modulators and uses thereof. No. 13/257,592, 2014.

(148) Dégénérescence maculaire liée à l'âge (DMLA). http://www.inserm.fr/thematiques/neurosciences-sciences-cognitives-neurologie-psychiatrie/dossiers-d-information/degenerescence-maculaire-liee-a-l-age-dmla
(149) Demers, A.; McNICOLL, N.; Febbraio, M.; Servant, M.; Marleau, S.; Silverstein, R.; Ong, H., Identification of the growth hormone-releasing peptide binding site in CD36: a photoaffinity cross-linking study. *Biochem. J* **2004,** *382*, 417-424.
(150) Page, M. I., The mechanisms of reactions of β-lactam antibiotics. *Acc. Chem. Res.* **1984,** *17*, 144-151.
(151) King, D. T.; Worrall, L. J.; Gruninger, R.; Strynadka, N. C., New Delhi metallo-β-lactamase: structural insights into β-lactam recognition and inhibition. *J. Am. Chem. Soc.* **2012,** *134*, 11362-11365.
(152) King, D.; Strynadka, N., Crystal structure of New Delhi metallo-β-lactamase reveals molecular basis for antibiotic resistance. *Protein Sci.* **2011,** *20*, 1484-1491.
(153) Yong, D.; Toleman, M. A.; Giske, C. G.; Cho, H. S.; Sundman, K.; Lee, K.; Walsh, T. R., Characterization of a new metallo-β-lactamase gene, blaNDM-1, and a novel erythromycin esterase gene carried on a unique genetic structure in Klebsiella pneumoniae sequence type 14 from India. *Antimicrob. Agents Chemother.* **2009,** *53*, 5046-5054.
(154) Cain, R.; Narramore, S.; McPhillie, M.; Simmons, K.; Fishwick, C. W., Applications of structure-based design to antibacterial drug discovery. *Bioorg. Chem.* **2014,** *55*, 69-76.
(155) Jansen, M.; Rabe, H.; Strehle, A.; Dieler, S.; Debus, F.; Dannhardt, G.; Akabas, M. H.; Lüddens, H., Synthesis of GABAA receptor agonists and evaluation of their α-subunit selectivity and orientation in the GABA binding Site. *J. Med. Chem.* **2008,** *51*, 4430-4448.
(156) Šink, R.; Zega, A., Simple and effective preparation of amino sulfonylureas from amino acids: application to the synthesis of amino sulfonylurea-containing peptidomimetics. *Tetrahedron Lett.* **2008,** *49*, 3943-3945.
(157) Harju, K.; Manevski, N.; Yli-Kauhaluoma, J., Microwave-assisted synthesis of pyridylpyrroles from *N*-acylated amino acids. *Tetrahedron* **2009,** *65*, 9702-9706.
(158) Still, W. C.; Kahn, M.; Mitra, A., Rapid chromatographic technique for preparative separations with moderate resolution. *J. Org. Chem.* **1978,** *43*, 2923-2925.
(159) Long, Y.-Q.; Xue, T.; Song, Y.-L.; Liu, Z.-L.; Huang, S.-X.; Yu, Q., Synthesis and utilization of chiral α-methylated α-amino acids with a carboxyalkyl side chain in the design of novel Grb2-SH_2 peptide inhibitors free of phosphotyrosine. *J. Med. Chem.* **2008,** *51*, 6371-6380.
(160) Barthel, B. L.; Rudnicki, D. L.; Kirby, T. P.; Colvin, S. M.; Burkhart, D. J.; Koch, T. H., Synthesis and biological characterization of protease-activated prodrugs of doxazolidine. *J. Med. Chem.* **2012,** *55*, 6595-6607.
(161) Galaud, F.; Lubell, W. D., Homoserine-derived cyclic sulfamidate as chiral educt for the diversity-oriented synthesis of lactam-bridged dipeptides. *Biopolymers (Pept. Sci.)* **2005,** *80*, 665-674.
(162) Feng, L.; Lv, K.; Liu, M.; Wang, S.; Zhao, J.; You, X.; Li, S.; Cao, J.; Guo, H., Synthesis and *in vitro* antibacterial activity of gemifloxacin derivatives containing a substituted benzyloxime moiety. *Eur. J. Med. Chem.* **2012,** *55*, 125-136.

Annexe 1 : Partie expérimentale du chapitre 2

General Methods

Unless specified otherwise, 4-nitrophenyl chlorosulfate **51**,[90] as well as *N*-(Boc)-L-alanine, L-phenylalanine and L-proline hydrazides **93**-**95**,[155] all were synthesized according to literature methods. L-Alanine and L-valine methyl ester hydrochlorides, **83** and **86**, were respectively synthesized from their corresponding amino acids using methanol (MeOH) and thionyl chloride.[156] L-Alanine and L-leucine benzyl esters, **82** and **84**, were synthesized from their corresponding amino acids using benzyl alcohol and *p*-toluenesulfonic acid in toluene[157] and free-based by partitioning between 1M aq. Na_2CO_3 and chloroform. Benzyl carbazate **92**, *tert*-butyl carbazate **81**, iodomethane, 4-nitrophenol, D- and L-phenylalanine *tert*-butyl esters [(*R*)- and (*S*)-**85**], propargyl bromide (80 wt.% in toluene) and triethylamine, all were purchased from Aldrich and used as received. Allyl and benzyl bromides were purchased from Aldrich and filtered through a small plug of silica gel prior to use. 1,2-Dichloroethane (DCE) was purchased from Anachemia and fractionally distilled prior to use. Phosphazene base, *tert*-butylimino-tri(pyrrolidino)phosphorane (BTPP) was purchased from Fluka and used as received. Anhydrous solvents [tetrahydrofuran (THF) and dichloromethane (DCM)] were obtained by passage through a solvent filtration system (GlassContour, Irvine, CA). Microwave irradiation was accomplished on a 300 MW Biotage apparatus on the high absorption level; temperature was monitored automatically. Flash chromatography[158] was performed on 230–400 mesh silica gel, and thin-layer chromatography was performed on silica gel 60 F254 plates from Merck™. Melting points were made on a Gallankamp apparatus and are uncorrected. Specific rotations, $[\alpha]_D$ values, were calculated from optical rotations measured at 20 °C in $CHCl_3$ or THF at the specified concentrations (*c* in g/100 mL) using a 1-dm cell (*l*) on a PerkinElmer Polarimeter 341, using the general formula: $[\alpha]^{20}_D = (100 \times \alpha)/(l \times c)$. Accurate mass measurements were performed on a LC-MSD instrument from Agilent technologies in positive electrospray ionisation (ESI) mode at the Université de Montréal Mass Spectrometry facility. Sodium adducts $[M + Na]^+$ were used for empirical formula confirmation. ^1H NMR spectra were measured in $CDCl_3$ (7.26 ppm), CD_3OD (3.34 ppm) or DMSO-d_6 (2.54 ppm). ^{13}C NMR spectra were measured in $CDCl_3$ (77.36 ppm) or DMSO-d_6 (40.45 ppm). Coupling constant *J* values are measured in Hertz (Hz) and chemical shift values in parts per million (ppm). Infrared spectra

were recorded in the neat on an ATR Bruker apparatus or in a KBr pellet using a FT-IR Perkin Elmer apparatus.

4-Nitrophenyl L-alanine benzyl ester sulfamidate 87

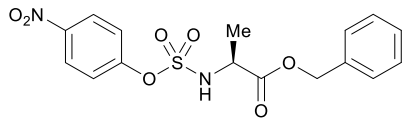

87

A solution of L-alanine benzyl ester (1.29 g, 3.50 mmol), 4-nitrophenol (0.97 g, 7.00 mmol) and NEt_3 (2.91 mL, 21.0 mmol) in dry DCM (25 mL) was added drop-wise to a solution of 4-nitrophenyl chlorosulfate (1.66 g, 7.00 mmol) in dry DCM (5 mL) at –78 °C under argon. After stirring at –78 °C for 1.5 h, the mixture was allowed to warm to room temperature. The volatiles were evaporated to a residue, which was purified by flash chromatography eluting with a solution of MeOH:DCM 1:99. The collected fractions were noticeably contaminated with 4-nitrophenol, and evaporated to a residue, which was dissolved in DCM (100 mL), washed with sat. $NaHCO_3$ (3 x 50 mL), dried over $MgSO_4$, filtered and evaporated. The resulting oil was dissolved in DCM and precipitated using hexane to afford sulfamidate **87** as a solid (0.500 g, 38%): R_f 0.72 (MeOH:DCM 1:99); mp 76 °C; $[\alpha]^{20}_D$ 26.0° ($CHCl_3$, *c* 1.04); ^{1}H NMR ($CDCl_3$, 400 MHz) δ 1.53 (3H, d, *J* = 7.2), 4.33 (1H, q, *J* = 7.1), 5.19 (1H, d, *J* = 12.0), 5.25 (1H, d, *J* = 12.1), 5.70-5.80 (1H, br), 7.30-7.40 (7H, m), 8.19 (2H d, *J* = 9.2); ^{13}C NMR ($CDCl_3$, 100 MHz) δ 19.7, 53.2, 68.4, 122.7, 125.8, 128.8, 129.1, 129.2, 135.0, 146.3, 154.6, 171.8; IR (neat) ν_{max}/cm^{-1} 1149, 1171, 1211, 1350, 1530, 1727, 3229; HRMS *m/z* calculated for $C_{16}H_{16}N_2NaO_7S$ $[M+Na]^+$ 403.0570; found 403.0576.

4-Nitrophenyl L-alanine methyl ester sulfamidate 88

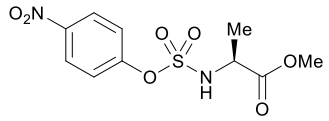

88

Employing the protocol for the synthesis of sulfamidate **87**, L-alanine methyl ester hydrochloride (0.558 g, 4.00 mmol) was transformed to sulfamidate **88**, which was isolated as a solid (0.389 g, 32%) contaminated with 5% of 4-nitrophenol, and used without further

purification: R_f 0.55 (MeOH:DCM 1:99); mp 62 °C; $[\alpha]^{20}_D$ 17.1° ($CHCl_3$, *c* 1.22); ^1H NMR ($CDCl_3$, 400 MHz) δ 1.51 (3H, d, *J* = 7.2), 3.79 (3H, s), 4.29 (1H, q, *J* = 7.2), 5.90-6.10 (1H, br), 7.43 (2H, d, *J* = 9.1), 8.24 (2H, d, *J* = 9.1); ^{13}C NMR ($CDCl_3$, 100 MHz) δ 19.6, 53.0, 53.5, 122.7, 125.8, 146.2, 154.7, 172.5; IR (neat) ν_{max}/cm^{-1} 1149, 1172, 1227, 1343, 1519, 1731, 3220; HRMS *m/z* calculated for $C_{10}H_{12}N_2NaO_7S$ $[M+Na]^+$ 327.0257; found 327.0257.

4-Nitrophenyl L-leucine benzyl ester sulfamidate 89

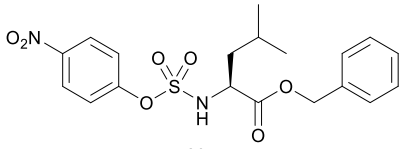

89

Employing the protocol for the synthesis of sulfamidate **87**, L-leucine benzyl ester (1.11 g, 5.00 mmol) was transformed to sulfamidate **89**, which was isolated as a solid (1.327 g, 63%): R_f 0.56 (MeOH:DCM 1:99); mp 59 °C; $[\alpha]^{20}_D$ 27.4° ($CHCl_3$, *c* 0.98); ^1H NMR ($CDCl_3$, 400 MHz) δ 0.96 (3H, d, *J* = 6.3), 0.98 (3H, d, *J* = 5.6), 1.60-1.70 (2H, m), 1.80-1.90 (1H, m), 4.25-4.35 (1H, m), 5.18 (1H, d, *J* = 12.0), 5.28 (1H, d, *J* = 12.0), 5.72 (1H, s), 7.31 (2H, d, *J* = 9.2), 7.35-7.40 (5H, m), 8.20 (2H, d, *J* = 9.2); ^{13}C NMR ($CDCl_3$, 100 MHz) δ 21.9, 22.9, 24.7, 42.4, 56.1, 68.2, 122.5, 125.8, 128.9, 129.1, 129.2, 135.0, 146.2, 154.7, 172.2; IR (neat) ν_{max}/cm^{-1} 1141, 1188, 1209, 1352, 1519, 1736, 3271; HRMS *m/z* calculated for $C_{19}H_{22}N_2NaO_7S$ $[M+Na]^+$ 445.1040; found 445.1048.

4-Nitrophenyl D-phenylalanine *tert*-butyl ester sulfamidate (*R*)-90

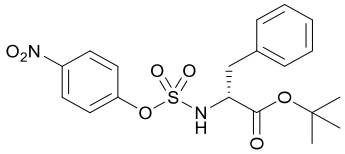

(*R*)-**90**

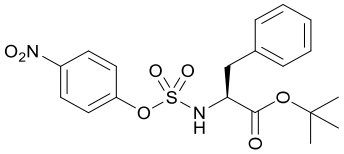

(*S*)-**90**

Employing the protocol for the synthesis of sulfamidate **87**, D-phenylalanine *tert*-butyl ester hydrochloride (1.29 g, 5.00 mmol) was transformed to sulfamidate (*R*)-**90**, which did not precipitate and was isolated as an oil (1.564 g, 72%): R_f 0.74 (MeOH:DCM 1:99); $[\alpha]^{20}_D$ –28.2° ($CHCl_3$, *c* 1.02); ^1H NMR ($CDCl_3$, 400 MHz) δ 1.42 (9H, s), 3.08 (1H, dd, *J* = 6.4, 14.0), 3.13 (1H, dd, *J* = 6.2, 14.0), 4.36 (1H, t, *J* = 6.3), 5.75 (1H, s), 7.19 (2H, d, *J* = 9.4), 7.25-7.35 (5H,

m), 8.18 (2H, d, J = 9.3); ^{13}C NMR ($CDCl_3$, 100 MHz) δ 28.2, 39.2, 58.7, 84.1, 122.7, 125.8, 127.8, 129.0, 129.9, 135.2, 146.2, 154.7, 169.9; IR (KBr) ν_{max}/cm^{-1} 1153, 1177, 1208, 1349, 1530, 1732, 3269; HRMS (ESI) *m/z* calculated for $C_{19}H_{22}N_2NaO_7S$ $[M+Na]^+$ 445.1040; found 445.1044. **4-Nitrophenyl L-phenylalanine *tert*-butyl ester sulfamidate (*S*)-90** was prepared in an identical manner from L-phenylalanine *tert*-butyl ester (0.64 g, 2.50 mmol) using the protocol described for (*R*)-**90** and isolated as an oil (0.764 g, 72%): $[\alpha]^{20}_D$ 28.4° (*c* 0.98); HRMS (ESI) *m/z* calculated for $C_{19}H_{22}N_2NaO_7S$ $[M+Na]^+$ 445.1040; found 445.1059.

4-Nitrophenyl L-valine methyl ester sulfamidate 91

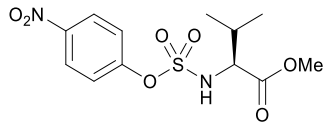

91

Employing the protocol for the synthesis of sulfamidate **87**, L-valine methyl ester hydrochloride (0.50 g, 3.00 mmol) was transformed to sulfamidate **91**, which was isolated as a solid (0.635 g, 64%), which was recrystallized from EtOAc on diffusion of hexane vapors: R_f 0.61 (MeOH:DCM 1:99); mp 73 °C; $[\alpha]^{20}_D$ 35.3° ($CHCl_3$, *c* 1.03); ^{1}H NMR ($CDCl_3$, 400 MHz) δ 0.94 (3H, d, J = 6.8), 1.04 (3H, d, J = 6.8), 2.17 (1H, dsept, J = 4.8, 6.8), 3.81 (3H, s), 4.10 (1H, dd, J = 4.8, 9.2), 5.49 (1H, d, J = 9.2), 7.43 (2H, d, J = 9.3), 8.28 (2H, d, J = 9.3); ^{13}C NMR ($CDCl_3$, 100 MHz) δ 17.6, 19.1, 32.0, 53.2, 62.6, 122.6, 125.9, 146.3, 154.8, 171.8; IR (KBr) ν_{max}/cm^{-1} 1145, 1161, 1216, 1353, 1521, 1710, 3209; HRMS *m/z* calculated for $C_{12}H_{16}N_2NaO_7S$ $[M+Na]^+$ 355.0570; found 355.0577.

***N*-(Benzhydrylidene)-azasulfurylglycinyl-L-phenylalanine *tert*-butyl ester 96**

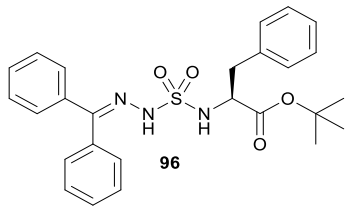

96

Benzophenone hydrazone (51 mg, 0.26 mmol) was added to a microwave vessel containing a solution of sulfamidate (*S*)-**90** (100 mg, 0.24 mmol) in DCE (1 mL). The mixture was treated with NEt_3 (36.1 μL, 0.26 mmol), at which point the solution turned yellow. The

vessel was sealed and heated to 60 °C using microwave irradiation for 2.5 h. The volatiles were evaporated. The residue was purified by flash chromatography eluting with a solution of MeOH:DCM 1:99 to afford azasulfurylglycinyl dipeptide **96** as a solid (90 mg; 80%): R_f 0.48 (hexane:EtOAc:TFA 85:5:10); mp 50 °C; $[\alpha]^{20}_D$ 28.2° ($CHCl_3$, *c* 1.00); ^{1}H NMR ($CDCl_3$, 300 MHz) δ 1.26 (9H, m), 3.13 (2H, d, *J* = 5.9), 4.44 (1H, dt, *J* = 5.9, 7.9), 5.41 (1H, d, *J* = 7.9), 7.20-7.40 (10H, m), 7.45-7.60 (6H, m); ^{13}C NMR ($CDCl_3$, 75 MHz) δ 28.1, 39.9, 58.1, 83.4, 127.5, 128.0, 128.55, 128.59, 128.62, 128.71, 130.14, 130.16, 130.4, 131.5, 135.7, 136.7, 153.9, 170.3; IR (KBr) ν_{max}/cm^{-1} 1151, 1256, 1320, 1368, 1393, 1445, 1728, 3273; HRMS *m/z* calculated for $C_{26}H_{29}N_3NaO_4S$ $[M+Na]^+$ 502.1771; found 502.1769.

_N_-(Boc)-azasulfurylglycinyl-L-alanine methyl ester 97

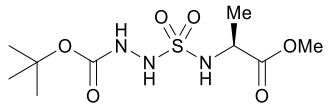

97

Employing the procedure described for azasulfuryl dipeptide **96**, *tert*-butyl carbazate (73 mg, 0.55 mmol) was reacted with sulfamidate **88** (152 mg, 0.50 mmol). The residue was purified by flash chromatography eluting with a 58:40:2 mixture of hexane:EtOAc:NEt_3 to afford azasulfurylglycinyl dipeptide **97** as a solid (131 mg, 88%): R_f 0.61 (hexane:EtOAc 1:1); mp 123 °C; $[\alpha]^{20}_D$ 21.5° ($CHCl_3$, *c* 1.01); ^{1}H NMR ($CDCl_3$, 400 MHz) δ 1.35-1.45 (12H, m), 3.74 (3H, s), 4.15-4.25 (1H, m), 5.70-5.80 (1H, br), 5.80-5.90 (1H, br), 5.90-6.00 (1H, br); ^{13}C NMR ($CDCl_3$, 100 MHz) δ 19.6, 28.4, 52.2, 53.1, 82.6, 155.6, 173.9; IR (KBr) ν_{max}/cm^{-1} 1163, 1206, 1343, 1370, 1447, 1727, 1746, 3347; HRMS *m/z* calculated for $C_9H_{19}N_3NaO_6S$ $[M+Na]^+$ 320.0887; found 320.0903.

_N_-(Cbz)-azasulfurylglycinyl-L-alanine methyl ester 98

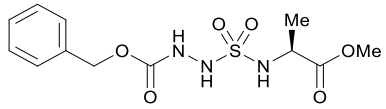

98

Employing the procedure described for azasulfuryl dipeptide **96**, benzyl carbazate (91 mg, 0.55 mmol) was reacted with sulfamidate **88** (152 mg, 0.50 mmol). The residue was purified by flash chromatography eluting with a 58:40:2 mixture of hexane:EtOAc:NEt_3 to

afford azasulfurylglycinyl dipeptide **98** as an oil (135 mg, 81%): R_f 0.47 (hexane:EtOAc 1:1); $[\alpha]^{20}_D$ 27.0° ($CHCl_3$, *c* 0.68); ^1H NMR ($CDCl_3$, 400 MHz) δ 1.38 (3H, d, *J* = 7.2), 3.71 (3H, s), 4.15-4.25 (1H, m), 5.11 (1H, d, *J* = 12.4), 5.13 (1H, d, *J* = 12.4), 7.25-7.40 (5H, m) ^{13}C NMR ($CDCl_3$, 100 MHz) δ 19.3, 52.3, 53.1, 68.3, 128.5, 128.7, 128.8, 135.6, 156.6, 174.1; IR (KBr) ν_{max}/cm^{-1} 1167, 1216, 1267, 1350, 1455, 1515, 1732, 3286; HRMS *m/z* calculated for $C_{12}H_{17}N_3NaO_6S$ $[M+Na]^+$ 354.0730; found 354.0741.

_N_-(Boc)-L-alaninyl-azasulfurylglycinyl-L-alanine methyl ester 99

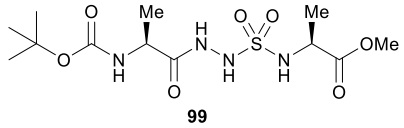

99

Employing the procedure described for azasulfuryl dipeptide **96**, *N*-(Boc)-L-alanine hydrazide (112 mg, 0.55 mmol) was reacted with sulfamidate **88** (152 mg, 0.50 mmol). The residue was purified by flash chromatography eluting initially with a 45:53:2 mixture of hexanes:EtOAc:NEt_3 (100 mL), followed by 2:3 hexanes:EtOAc. Evaporation of the collected fractions afforded azasulfurylglycinyl tripeptide **99** as a solid (155 mg; 84%): R_f 0.38 (hexanes:EtOAc 2:3); mp 52 °C; $[\alpha]^{20}_D$ –8.4° ($CHCl_3$, *c* 0.97); ^1H NMR ($CDCl_3$, 400 MHz) δ 1.37 (3H, d, *J* = 7.0), 1.40-1.45 (12H, m), 3.76 (3H, s), 4.10-4.20 (1H, m), 4.20-4.30 (1H, m), 5.30-5.35 (1H, br), 6.01 (1H, d, *J* = 7.6), 7.35-7.40 (1H, br), 8.90-9.00 (1H, br); ^{13}C NMR ($CDCl_3$, 100 MHz) δ 18.0, 19.5, 28.6, 49.1, 52.3, 53.2, 81.0, 156.1, 173.0, 174.0; IR (neat) ν_{max}/cm^{-1} 1143, 1163, 1247, 1351, 1450, 1507, 1678, 3243; HRMS *m/z* calculated for $C_{12}H_{24}N_4NaO_7S$ $[M+Na]^+$ 391.1258; found 391.1242.

_N_-(Boc)-L-alaninyl-azasulfurylglycinyl-L-leucine benzyl ester 100

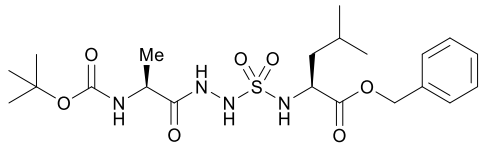

100

Employing the procedure described for azasulfuryl dipeptide **96**, *N*-(Boc)-L-alanine hydrazide (112 mg, 0.55 mmol) was reacted with sulfamidate **88** (211 mg, 0.50 mmol). The residue was purified by flash chromatography eluting initially with a 55:43:2 mixture of

hexane:EtOAc:NEt_3 (100 mL), followed by 3:2 hexane:EtOAc. Evaporation of the collected fractions gave azasulfurylglycinyl tripeptide **100** as a solid (203 mg, 84%): R_f 0.61 (hexane:EtOAc:NEt_3 45:53:2); mp 54 °C; $[\alpha]^{20}_D$ 17.0° ($CHCl_3$, *c* 0.98); ^{1}H NMR ($CDCl_3$, 400 MHz) δ 0.90 (3H, d, *J* = 6.6), 0.91 (3H, d, *J* = 6.5), 1.36 (3H, d, *J* = 7.0), 1.45 (9H, s), 1.50-1.65 (2H, m), 1.70-1.85 (1H, m), 4.15 (1H, dd, *J* = 5.8, 8.6), 4.20-4.30 (1H, m), 5.19 (2H, s), 5.20-5.30 (1H, br), 7.30-7.40 (5H, m); ^{13}C NMR ($CDCl_3$, 100 MHz) δ 17.7, 22.0, 22.9, 24.7, 28.7, 42.0, 49.1, 55.4, 68.0, 80.9, 128.7, 128.89, 128.96, 135.3, 156.1, 172.6, 174.0; IR (neat) ν_{max}/cm^{-1} 1144, 1164, 1246, 1351, 1455, 1499, 1681, 3262; HRMS *m/z* calculated for $C_{21}H_{34}N_4NaO_7S$ $[M+Na]^+$ 509.2040; found 509.2024.

_N_-(Boc)-L-alaninyl-azasulfurylglycinyl-D-phenylalanine *tert*-butyl ester (*S*,*R*)-101

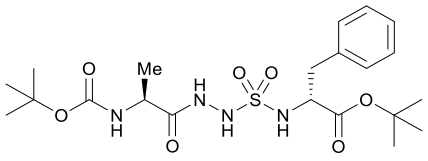
(*S*,*R*)-**101**

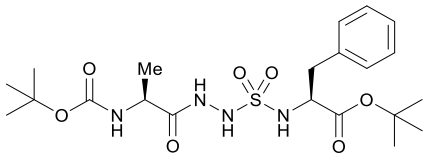
(*S*,*S*)-**101**

Employing the protocol described for azasulfuryl dipeptide **96**, *N*-(Boc)-L-alanine hydrazide (112 mg, 0.55 mmol) was reacted with sulfamidate (*R*)-**90** (211 mg, 0.50 mmol). The residue was purified by flash chromatography eluting initially with a 58:40:2 mixture of hexane:EtOAc:NEt_3 (100 mL), followed by 3:2 hexane:EtOAc. Evaporation of the collected fractions gave azasulfurylglycinyl tripeptide (*S*,*R*)-**101** as a solid (194 mg, 80%, 49:1 d.r.): R_f 0.34 (hexane:EtOAc 3:2); mp 70 °C; $[\alpha]^{20}_D$ –68.1° ($CHCl_3$, *c* 1.02); ^{1}H NMR (CD_3OD, 400 MHz) δ 1.32 (9H, s), 1.37 (3H, d, *J* = 7.2), 1.48 (9H, s), 2.89 (1H, dd, *J* = 9.1, 13.3), 3.10 (1H, dd, *J* = 5.4, 13.1), 4.10-4.20 (1H, m), 4.27 (1H, q, *J* = 5.5), 7.20-7.35 (5H, m), 7.93 (1H, s); ^{13}C NMR ($CDCl_3$, 100 MHz) δ 17.9, 28.2, 28.6, 39.1, 49.1, 57.6, 81.0, 83.4, 127.4, 128.7, 130.1, 135.9, 156.0, 171.1, 172.7; IR (KBr) ν_{max}/cm^{-1} 1152, 1249, 1365, 1454, 1498, 1679, 3231; HRMS (ESI) *m/z* calculated for $C_{21}H_{34}N_4NaO_7S$ $[M+Na]^+$ 509.2040; found 509.2029. ***N*-(Boc)-L-alaninyl-azasulfurylglycinyl-L-phenylalanine *tert*-butyl ester** (*S*,*S*)-**101** was prepared in an identical manner from sulfamidate (*S*)-**90** (211 mg, 0.50 mmol) using the protocol described for (*S*,*R*)-**101** and isolated as a solid (0.190 g, 78%, 23:2 d.r.): R_f 0.34 (hexane:EtOAc 3:2); mp 70 °C; $[\alpha]^{20}_D$ 16.8° ($CHCl_3$, *c* 1.08); ^{1}H NMR (CD_3OD, 400 MHz) δ 1.32 (9H, s), 1.35 (3H, d, *J* = 7.2), 1.42 (9H, s), 2.86 (1H, dd, *J* = 9.2, 12.9), 3.09 (1H, dd, *J* = 5.6, 13.3), 4.05-

4.15 (1H, m), 4.30 (1H, q, 5.6), 7.20-7.35 (5H, m), 7.92 (1H, s); ^{13}C NMR ($CDCl_3$, 100 MHz) δ 18.1, 28.2, 28.6, 39.1, 49.0, 57.6, 80.8, 83.4, 127.4, 128.7, 130.1, 135.9, 155.9, 171.2, 172.7; IR (KBr) ν_{max}/cm^{-1} 1152, 1250, 1366, 1454, 1498, 1682, 3231; HRMS (ESI) *m/z* calculated for $C_{21}H_{34}N_4NaO_7S$ $[M+Na]^+$ 509.2040; found 509.2024.

_N_-(Boc)-L-alaninyl-azasulfurylglycinyl-L-valine methyl ester 102

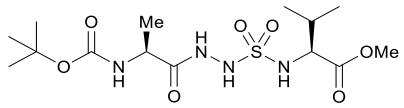

102

Employing the procedure described for azasulfuryl dipeptide **96**, *N*-(Boc)-L-alanine hydrazide (67 mg; 0.33 mmol) was reacted with sulfamidate **91** (100 mg; 0.30 mmol). The residue was purified by flash chromatography eluting with a 45:50:5 mixture of hexane:EtOAc:NEt_3 to afford azasulfurylglycinyl tripeptide **102** as a solid (109 mg; 92%): R_f 0.19 (hexane:EtOAc:NEt_3 55:40:5); mp 44 °C; $[\alpha]^{20}_D$ 21.0° ($CHCl_3$, *c* 0.83); ^{1}H NMR ($CDCl_3$, 400 MHz) δ 0.90 (3H, d, *J* = 6.9), 1.02 (3H, d, *J* = 6.8), 1.39 (3H, d, *J* = 7.1), 1.46 (9H, s), 2.15-2.25 (1H, m), 3.79 (3H, s), 3.95-4.00 (1H, m), 4.15-4.25 (1H, m), 4.97 (1H, d, *J* = 7.4), 5.57 (1H, d, *J* = 8.9), 6.90-7.00 (1H, br), 8.50-8.60 (1H, br); ^{13}C NMR ($CDCl_3$, 100 MHz) δ 17.6, 17.7, 19.1, 28.6, 31.7, 49.1, 53.0, 61.8, 80.9, 156.1, 172.6, 173.4; IR (KBr) ν_{max}/cm^{-1} 1149, 1169, 1266, 1367, 1453, 1520, 1693, 3291; HRMS *m/z* calculated for $C_{14}H_{28}N_4NaO_7S$ $[M+Na]^+$ 419.1571; found 419.1586.

_N_-(Boc)-L-phenylalaninyl-azasulfurylglycinyl-L-leucine benzyl ester 103

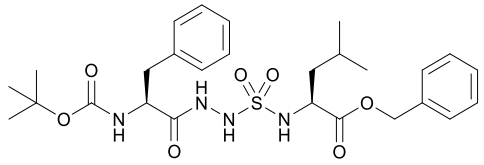

103

Employing the procedure described for azasulfuryl dipeptide **96**, *N*-(Boc)-L-phenylalanine hydrazide (154 mg, 0.55 mmol) was reacted with sulfamidate **89** (211 mg, 0.50 mmol). The residue was purified by flash chromatography eluting initially with a 60:38:2 mixture of hexane:EtOAc:NEt_3 (100 mL), followed by 13:7 hexane:EtOAc. Evaporation of the collected fractions afforded azasulfurylglycinyl tripeptide **103** as a solid (233 mg; 83%): R_f 0.28

(hexane:EtOAc 13:7); mp 57 °C; $[\alpha]^{20}_D$ 38.1° ($CHCl_3$, *c* 1.03); ^{1}H NMR ($CDCl_3$, 400 MHz) δ 0.93 (6H, d, *J* = 6.6), 1.40 (9H, s), 1.50-1.70 (2H, m), 1.70-1.85 (1H, m), 2.95-3.10 (1H, m), 3.10-3.20 (1H, m), 4.10-4.20 (1H, m), 4.40-4.50 (1H, m), 5.19 (2H, s), 5.30-5.40 (1H, br), 7.20-7.45 (10H, m); ^{13}C NMR ($CDCl_3$, 100 MHz) δ 22.0, 22.9, 24.7, 28.6, 38.0, 41.8, 54.8, 55.3, 67.9, 80.9, 127.3, 128.67, 128.85, 128.93, 128.95, 129.7, 135.3, 136.6, 156.1, 171.4, 174.1; IR (neat) ν_{max}/cm^{-1} 1144, 1162, 1269, 1366, 1454, 1497, 1677, 3229; HRMS *m/z* calculated for $C_{27}H_{38}N_4NaO_7S$ $[M+Na]^+$ 585.2353; found 585.2354.

_N_-(Boc)-L-prolyl-azasulfurylglycinyl-L-alanine methyl ester 104

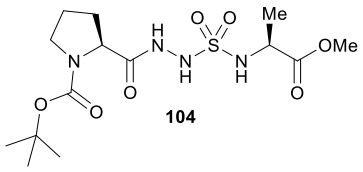

Employing the procedure described for azasulfuryl dipeptide **96**, *N*-(Boc)-L-proline hydrazide (126 mg, 0.55 mmol) was reacted with sulfamidate **88** (152 mg, 0.50 mmol). The residue was purified by flash chromatography eluting initially with a 45:53:2 mixture of hexane:EtOAc:NEt_3 followed by 2:3 hexane:EtOAc to afford azasulfurylglycinyl tripeptide **104** as a solid (162 mg, 82%): R_f 0.26 (hexane:EtOAc 2:3); mp 60 °C; $[\alpha]^{20}_D$ –47.4° ($CHCl_3$, *c* 1.03); ^{1}H NMR ($CDCl_3$, 400 MHz) δ 1.35-1.50 (12H, m), 1.80-2.10 (3H, m), 2.10-2.25 (1H, m), 3.30-3.55 (2H, m), 3.76 (3H, s), 4.10-4.20 (1H, m), 4.20-4.30 (1H, m), 5.75-5.85 (1H, br), 7.10-7.25 (1H, br), 8.90-9.00 (1H, br); ^{13}C NMR ($CDCl_3$, 75 MHz) δ 19.7, 24.9, 28.7, 28.9, 47.5, 52.4, 53.2, 58.9, 81.3, 155.9, 172.3, 173.9; IR (neat) ν_{max}/cm^{-1} 1133, 1163, 1287, 1365, 1511, 1670, 1735, 3247; HRMS *m/z* calculated for $C_{14}H_{26}N_4NaO_7S$ $[M+Na]^+$ 417.1414; found 417.1404.

_N_-(Boc)-L-prolyl-azasulfurylglycinyl-L-valine methyl ester 105

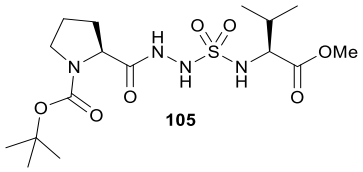

Employing the procedure described for azasulfuryl dipeptide **96**, Boc-L-proline hydrazide (76 mg, 0.33 mmol) was reacted with sulfamidate **91** (100 mg, 0.30 mmol). The residue was purified by flash chromatography eluting with a 45:50:5 mixture of

hexane:EtOAc:NEt_3 to afford azasulfurylglycinyl tripeptide **105** as a solid (115 mg, 91%): R_f 0.44 (hexane:EtOAc:NEt_3 45:50:5); mp 57 °C; $[\alpha]^{20}_D$ –13.7° ($CHCl_3$, *c* 1.05); ^{1}H NMR ($CDCl_3$, 300 MHz) δ 0.88 (3H, d, *J* = 6.9), 0.98 (3H, d, *J* = 6.8), 1.45 (9H, s), 1.80-1.90 (1H, m), 1.90-2.10 (2H, m), 2.20-2.30 (2H, m), 3.45-3.55 (2H, m), 3.76 (3H, s), 3.95 (1H, dd, *J* = 4.2, 9.1), 4.20-4.30 (1H, m), 5.80-5.90 (1H, br), 7.15-7.25 (1H, br), 8.90-9.00 (1H, br); ^{13}C NMR ($CDCl_3$, 75 MHz) δ 17.7, 19.0, 19.5, 24.8, 28.7, 31.7, 47.4, 52.9, 58.8, 61.7, 81.1, 155.9, 172.0, 173.2; IR (KBr) ν_{max}/cm^{-1} 1136, 1169, 1256, 1368, 1449, 1541, 1660, 1677, 1738, 3227; HRMS *m/z* calculated for $C_{16}H_{30}N_4NaO_7S$ $[M+Na]^+$ 445.1727; found 445.1742.

_N_-(Boc)-L-alaninyl-azapropargylsulfurylglycinyl-L-alanine methyl ester 106

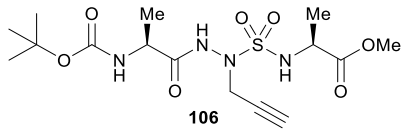

106

A solution of azasulfurylglycinyl tripeptide **99** (50 mg, 0.136 mmol) in dry THF (2.5 mL) at 0 °C was treated with BTPP (45.6 μL, 0.149 mmol), stirred for 0.5 h, treated with propargyl bromide (80 wt% in PhMe, 22.2 μL, 0.149 mmol), and stirred at 0 °C for 3 h. The volatiles were evaporated. The residue was purified by flash chromatography eluting with 3:2 hexane:EtOAc to afford aza-propargylsulfurylglycinyl tripeptide **106** as a solid (40 mg, 73%): R_f 0.59 (hexane:EtOAc 2:3); mp 52 °C; $[\alpha]^{20}_D$ –16.4° ($CHCl_3$, *c* 0.97); ^{1}H NMR (DMSO-d_6, 500 MHz) δ 1.23 (3H, d, *J* = 7.1), 1.27 (3H, d, *J* = 7.0), 1.41 (9H, s), 3.31 (1H, t, *J* = 2.4), 3.68 (3H, s), 4.00-4.15 (4H, m), 6.97 (1H, d, *J* = 7.6), 8.25 (1H, d, *J* = 7.6), 9.90 (1H, s); ^{13}C NMR (DMSO-d_6, 125 MHz) δ 18.7, 19.1, 29.1, 40.7, 41.3, 49.3, 52.2, 52.9, 77.0, 79.0, 155.9, 173.1, 173.9; IR (neat) ν_{max}/cm^{-1} 1144, 1164, 1255, 1354, 1451, 1508, 1685, 3278; HRMS *m/z* calculated for $C_{15}H_{26}N_4NaO_7S$ $[M+Na]^+$ 429.1414; found 429.1419.

***N*-(Boc)-L-alaninyl-aza-allylsulfurylglycinyl-D-phenylalanine *tert*-butyl ester (*S*,*R*)-107**

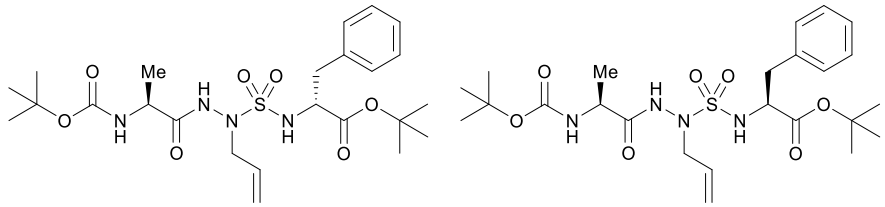

(*S*,*R*)-**107** (*S*,*S*)-**107**

Employing the protocol described for aza-propargylsulfurylglycinyl tripeptide **106**, allyl bromide (19.0 μL, 0.22 mmol) was reacted with azasulfurylglycinyl tripeptide (*S,R*)**-101** (97 mg, 0.20 mmol). The residue was purified by flash chromatography eluting with 7:3 hexane:EtOAc to afford aza-allylsulfurylglycinyl tripeptide (*S*,*R*)-**107** as a solid (75 mg, 71%, 97:3 d.r.): R_f 0.54 (hexane:EtOAc 3:2); mp 55 °C; $[\alpha]^{20}_D$ –12.7° (THF, *c* 0.61); ^{1}H NMR (CD_3OD, 400 MHz) δ 1.33 (3H, d, *J* = 7.1), 1.36 (9H, s), 1.47 (9H, s), 2.95 (1H, dd, *J* = 7.9, 12.8), 3.08 (1H, dd, *J* = 5.9, 13.4), 3.80-3.95 (2H, m), 4.10 (1H, q, *J* = 7.2), 4.32 (1H, q, *J* = 6.2), 5.20 (1H, d, *J* = 10.1), 5.28 (1H, d, *J* = 17.1), 5.80-5.90 (1H, m), 7.20-7.35 (5H, m); ^{13}C NMR ($CDCl_3$, 100 MHz) δ 17.8, 28.3, 28.6, 38.9, 49.3, 54.9, 57.5, 81.1, 83.3, 121.2, 127.3, 128.6, 130.3, 131.4, 136.1, 156.0, 170.4, 172.0; IR (KBr) ν_{max}/cm^{-1} 1152, 1248, 1365, 1454, 1497, 1686, 3281; HRMS (ESI) *m/z* calculated for $C_{24}H_{38}N_4NaO_7S$ $[M+Na]^+$ 549.2353; found 549.2367. ***N*-(Boc)-L-alaninyl-aza-allylsulfurylglycinyl-L-phenylalanine *tert*-butyl ester (*S*,*S*)-107** was prepared in an identical manner from azasulfurylglycinyl tripeptide (*S,S*)**-101** (97 mg, 0.20 mmol) using the protocol described for (*S*,*R*)-**107** and isolated as a solid (88 mg, 84%, 89:11 d.r.): R_f 0.54 (hexane:EtOAc 3:2); mp 43 °C; $[\alpha]^{20}_D$ –22.0° (THF, *c* 0.61); ^{1}H NMR (CD_3OD, 400 MHz) δ 1.31-1.33 (12H, m), 1.41 (9H, s), 2.80-2.90 (1H, m), 3.07 (1H, dd, *J* = 6.0, 13.2), 3.82 (1H, dd, *J* = 6.4, 13.5), 3.90-4.00 (1H, m), 4.09 (1H, q, *J* = 7.2), 4.32 (1H, q, *J* = 6.1), 5.22 (1H, d, *J* = 10.3), 5.28 (1H, d, *J* = 17.1), 5.80-5.90 (1H, m), 7.20-7.35 (5H, m); ^{13}C NMR ($CDCl_3$, 100 MHz) δ 17.8, 28.2, 28.6, 39.1, 49.0, 54.7, 57.5, 80.8, 83.2, 121.1, 127.3, 128.6, 130.2, 131.5, 136.1, 155.8, 170.5, 172.2; IR (KBr) ν_{max}/cm^{-1} 1151, 1249, 1365, 1454, 1498, 1686, 3296; HRMS (ESI) *m/z* calculated for $C_{24}H_{38}N_4NaO_7S$ $[M+Na]^+$ 549.2353; found 549.2367.

_N_-(Boc)-L-alaninyl-azasulfurylphenylalaninyl-L-alanine methyl ester 108

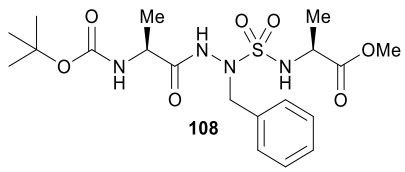

108

Employing the protocol for the synthesis of aza-propargylsulfurylglycinyl tripeptide **106**, azasulfurylglycinyl tripeptide **99** (45 mg, 0.122 mmol) was reacted with benzyl bromide (15.9 μL, 0.134 mmol). The residue was purified by flash chromatography eluting with 13:7 hexane:EtOAc to afford azasulfurylphenylalaninyl tripeptide **108** as a solid (36 mg, 64%): R_f 0.32 (hexane:EtOAc 3:2); mp 52 °C; $[\alpha]^{20}_D$ –20.5° ($CHCl_3$, *c* 0.72); ^{1}H NMR ($CDCl_3$, 400 MHz) δ 1.16 (3H, d, *J* = 7.0), 1.40 (9H, s), 1.45 (3H, d, *J* = 7.2), 3.74 (3H, s), 3.95-4.05 (1H, m), 4.25-4.40 (1H, m), 4.58 (2H, s), 4.80-4.95 (1H, br), 5.90-6.00 (1H, br), 7.25-7.40 (5H, m), 8.00-8.10 (1H, br); ^{13}C NMR ($CDCl_3$, 100 MHz) δ 17.6, 19.7, 28.6, 49.3, 52.3, 53.1, 55.2, 81.0, 128.5, 128.9, 129.6, 134.8, 155.9, 172.2, 173.7; IR (neat) ν_{max}/cm^{-1} 1143, 1163, 1248, 1349, 1453, 1509, 1685, 3293; HRMS *m/z* calculated for $C_{19}H_{30}N_4NaO_7S$ $[M+Na]^+$ 481.1727; found 481.1724.

_N_-(Boc)-L-alaninyl-azasulfurylphenylalaninyl-L-leucine benzyl ester 109

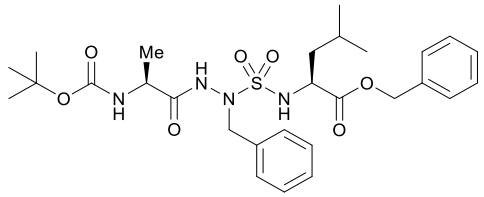

109

Employing the protocol for the synthesis of aza-propargylsulfurylglycinyl tripeptide **106**, azasulfurylglycinyl tripeptide **100** (85 mg, 0.175 mmol) was reacted with benzyl bromide (23.0 μL, 0.192 mmol). The residue was purified by flash chromatography eluting with 7:3 hexane:EtOAc to afford azasulfurylphenylalaninyl tripeptide **109** as a solid (76 mg, 75%): R_f 0.47 (hexane:EtOAc 17:3); mp 43 °C; $[\alpha]^{20}_D$ –13.4° ($CHCl_3$, *c* 1.00); ^{1}H NMR ($CDCl_3$, 400 MHz) δ 0.91 (3H, d, *J* =6.4), 0.93 (3H, d, *J* = 6.3), 1.19 (3H, d, *J* = 7.0), 1.40 (9H, s), 1.55-1.60 (1H, m), 1.60-1.65 (1H, m), 1.75-1.85 (1H, m), 4.00 (1H, t, *J* = 7.2), 4.27 (1H, q, *J* = 8.0), 4.53 (1H, d, *J* = 14.0), 4.58 (1H, d, *J* = 14.0), 4.90-5.00 (1H, br), 5.10 (1H, d, *J* = 12.2), 5.17 (1H, d,

J = 12.2), 5.90-6.00 (1H, br), 7.20-7.30 (5H, m), 7.30-7.40 (5H, m), 8.18 (1H, s); ^{13}C NMR ($CDCl_3$, 100 MHz) δ 17.6, 22.3, 22.9, 24.7, 28.6, 42.4, 49.1, 54.8, 55.3, 67.8, 80.8, 128.4, 128.6, 128.80, 128.82, 128.92, 129.5, 135.1, 135.4, 155.9, 172.3, 173.5; IR (neat) ν_{max}/cm^{-1} 1142, 1161, 1246, 1354, 1454, 1497, 1684, 3294; HRMS *m/z* calculated for $C_{28}H_{40}N_4NaO_7S$ $[M+Na]^+$ 599.2510; found 599.2516.

_N_-(Boc)-L-phenylalaninyl-aza-allylsulfurylglycinyl-L-leucine benzyl ester 110

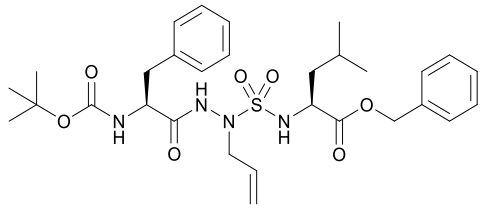

110

Employing the protocol for the synthesis of aza-propargylsulfurylglycinyl tripeptide **106**, azasulfurylglycinyl tripeptide **103** (50 mg, 0.089 mmol) was reacted with allyl bromide (8.46 μL, 0.098 mmol). The residue was purified by flash chromatography eluting with 3:1 Hex:EtOAc to afford aza-allylsulfurylglycinyl tripeptide **110** as a solid (44 mg, 83%): R_f 0.61 (Hex:EtOAc 13:7); mp 43 °C; $[\alpha]^{20}_D$ –12.5° (THF, *c* 1.25); ^{1}H NMR ($CDCl_3$, 500 MHz) δ 0.94 (3H, d, *J* = 6.6), 0.95 (3H, d, *J* = 6.5), 1.43 (9H, s), 1.50-1.70 (2H, m), 1.75-1.85 (1H, m), 3.00 (1H, dd, *J* = 7.6, 14.0), 3.14 (1H, dd, *J* = 6.7, 14.0), 3.85-3.90 (1H, dd, *J* = 6.2, 13.9), 3.96 (1H, dd, *J* = 6.7, 14.3), 4.20-4.25 (1H, m), 4.31 (1H, q, *J* = 7.6), 5.01 (1H, d, *J* = 7.7), 5.12 (1H, d, *J* = 16.2), 5.14 (1H, d, *J* = 10.8), 5.22 (2H, s) 5.65-5.75 (1H, m), 5.75-5.85 (1H, br), 7.20-7.40 (10H, m), 8.07 (1H, s); ^{13}C NMR ($CDCl_3$, 125 MHz) δ 22.3, 22.9, 24.7, 28.6, 37.5, 42.4, 54.6, 55.0, 55.3, 67.9, 81.1, 120.8, 127.4, 128.74, 128.84, 128.94, 129.04, 129.7, 131.5, 135.5, 136.6, 156.1, 171.0, 173.6; IR (neat) ν_{max}/cm^{-1} 1142, 1162, 1249, 1352, 1455, 1497, 1685, 3288; HRMS *m/z* calculated for $C_{30}H_{42}N_4NaO_7S$ $[M+Na]^+$ 625.2666; found 625.2643.

***N*-(Boc)-L-phenylalaninyl-aza-propargylsulfurylglycinyl-L-leucine benzyl ester 111**

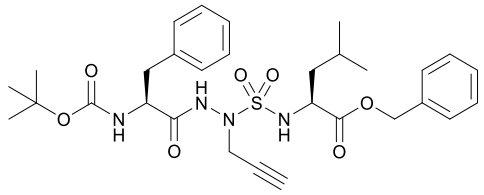

111

Employing the protocol for the synthesis of aza-propargylsulfurylglycinyl tripeptide **106**, azasulfurylglycinyl tripeptide **103** (100 mg, 0.178 mmol) was reacted with propargyl bromide (80 wt% in PhMe, 29.1 μL; 0.195 mmol). The residue was purified by flash chromatography eluting with a solution of hexane:EtOAc 3:1 to afford aza-propargylsulfurylglycinyl tripeptide **111** as a solid (72 mg, 67%): R_f 0.55 (hexane:EtOAc 13:7); mp 47 °C; $[\alpha]^{20}_D$ –1.8° ($CHCl_3$, *c* 0.97); ^{1}H NMR ($CDCl_3$, 400 MHz) δ 0.93 (3H, d, *J* = 6.6), 0.94 (3H, d, *J* = 6.5), 1.43 (9H, s), 1.50-1.60 (1H, m), 1.60-1.70 (1H, m), 1.70-1.80 (1H, m), 2.23 (1H, s), 3.02 (1H, dd, *J* = 7.8, 14.0), 3.16 (1H, dd, *J* = 6.4, 14.0), 4.10-4.15 (1H, m), 4.17 (1H, d, *J* = 8.2), 4.21 (1H, d, *J* = 6.5), 4.37 (1H, q, *J* = 7.4), 5.00-5.10 (1H, br), 5.18 (1H, d, *J* = 12.3), 5.23 (1H, d, *J* = 12.2), 5.65-5.75 (1H, br), 7.20-7.40 (10H, m), 8.33 (1H, s); ^{13}C NMR ($CDCl_3$, 100 MHz) δ 22.3, 22.8, 24.7, 28.6, 37.7, 41.9, 42.3, 55.0, 55.3, 67.9, 74.8, 76.8, 81.0, 127.4, 128.7, 128.84, 128.93, 129.1, 129.7, 135.4, 136.5, 156.0, 170.8, 173.4; IR (neat) ν_{max}/cm^{-1} 1145, 1163, 1248, 1365, 1455, 1497, 1684, 3275; HRMS *m/z* calculated for $C_{30}H_{40}N_4NaO_7S$ $[M+Na]^+$ 623.2510; found 623.2510.

***N*-(Boc)-L-phenylalaninyl-azasulfurylalaninyl-L-leucine benzyl ester 112**

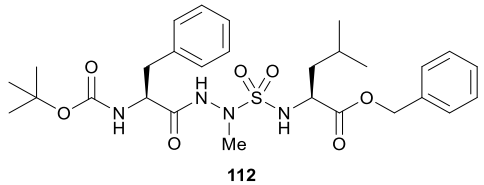

112

Employing the protocol for the synthesis of aza-propargylsulfurylglycinyl tripeptide **106**, azasulfuryl tripeptide **103** (50 mg, 0.089 mmol) was reacted with iodomethane (6.09 μL, 0.098 mmol). The residue was purified by flash chromatography eluting with 7:3 hexane:EtOAc to afford azasulfurylalaninyl tripeptide **112** as a solid (35 mg, 68%): R_f 0.55 (hexane:EtOAc 13:7); mp 52 °C; $[\alpha]^{20}_D$ 10.6° ($CHCl_3$, *c* 1.74); ^{1}H NMR ($CDCl_3$, 500 MHz)

δ 0.93 (3H, d, *J* = 6.4), 0.94 (3H, d, *J* = 6.6), 1.42 (9H, s), 1.50-1.60 (1H, m), 1.60-1.70 (1H, m), 1.70-1.80 (1H, m), 2.86, (3H, s), 2.95-3.05 (1H, m), 3.05-3.15 (1H, m), 4.10-4.20 (1H, m), 4.31 (1H, q, *J* = 7.5), 5.17 (1H, d, *J* = 12.6), 5.19 (1H, d, J = 12.1), 5.75-5.85 (1H, br), 5.98 (1H, d, *J* = 8.55), 7.20-7.40 (10H, m), 8.25 (1H, s); ^{13}C NMR ($CDCl_3$, 125 MHz) δ 22.1, 22.9, 24.6, 28.6, 37.8, 39.4, 42.1, 55.0, 55.2, 67.9, 81.1, 127.4, 128.77, 128.85, 128.91, 129.02, 129.7, 135.3, 136.4, 156.0, 170.7, 173.9; IR (neat) ν_{max}/cm^{-1} 1142, 1161, 1249, 1365, 1455, 1497, 1682, 3267; HRMS *m/z* calculated for $C_{28}H_{40}N_4NaO_7S$ $[M+Na]^+$ 599.2510; found 599.2494.

Université de Montréal

CRYSTAL AND MOLECULAR STRUCTURE OF

C12 H16 N2 O7 S (COMPOUND 91)

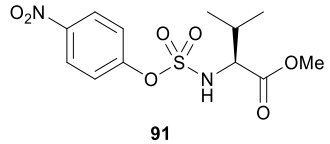

91

Equipe Lubell

Département de chimie, Université de Montréal,

C.P. 6128, Succ. Centre-Ville, Montréal, Québec, H3C 3J7 (Canada)

Structure solved and refined in the laboratory of X-ray diffraction Université de Montréal by Francine Bélanger.

Table 1. Crystal data and structure refinement for C12 H16 N2 O7 S.

Identification code	lube49
Empirical formula	C12 H16 N2 O7 S
Formula weight	332.33
Temperature	150K
Wavelength	1.54178 Å
Crystal system	Orthorhombic
Space group	P212121
Unit cell dimensions	a = 5.2757(1) Å α = 90° b = 9.3605(2) Å β = 90° c = 31.0792(6) Å γ = 90°
Volume	1534.79(5)Å^3
Z	4
Density (calculated)	1.438 g/cm^3
Absorption coefficient	2.224 mm^{-1}
F(000)	696
Crystal size	0.10 x 0.05 x 0.02 mm
Theta range for data collection	2.84 to 69.66°
Index ranges	$-5 \leq h \leq 6$, $-11 \leq k \leq 11$, $-37 \leq \ell \leq 37$
Reflections collected	25343
Independent reflections	2872 [R_{int} = 0.043]
Absorption correction	Semi-empirical from equivalents
Max. and min. transmission	0.9565 and 0.7907
Refinement method	Full-matrix least-squares on F^2
Data / restraints / parameters	2872 / 0 / 203
Goodness-of-fit on F^2	1.074
Final R indices [I>2sigma(I)]	R_1 = 0.0290, wR_2 = 0.0805

R indices (all data)	R_1 = 0.0292, wR_2 = 0.0807
Absolute structure parameter	0.061(16)
Largest diff. peak and hole	0.353 and -0.321 e/Å^3

Table 2. Atomic coordinates (x 10^4) and equivalent isotropic displacement parameters (Å^2 x 10^3) for C12 H16 N2 O7 S.

U_{eq} is defined as one third of the trace of the orthogonalized Uij tensor.

	x	y	z	U_{eq}
C(1)	3352(4)	-2060(2)	1771(1)	35(1)
O(1)	2428(2)	-620(1)	1705(1)	29(1)
C(2)	4125(3)	416(2)	1736(1)	24(1)
O(2)	6318(2)	233(1)	1841(1)	34(1)
C(3)	3046(3)	1888(2)	1643(1)	23(1)
N(4)	453(2)	1845(1)	1470(1)	24(1)
S(5)	9(1)	1897(1)	963(1)	24(1)
O(51)	1352(2)	3051(1)	776(1)	32(1)
O(52)	-2630(2)	1733(2)	885(1)	33(1)
O(6)	1424(2)	456(1)	817(1)	29(1)
C(7)	1936(3)	165(2)	387(1)	26(1)
C(8)	464(3)	650(2)	48(1)	33(1)
C(9)	1082(4)	240(2)	-369(1)	35(1)
C(10)	3136(4)	-642(2)	-428(1)	34(1)
C(11)	4632(4)	-1124(2)	-94(1)	37(1)
C(12)	4023(4)	-710(2)	321(1)	31(1)
N(10)	3806(5)	-1063(2)	-869(1)	49(1)
O(13)	5721(6)	-1806(3)	-914(1)	106(1)
O(14)	2529(3)	-626(2)	-1167(1)	60(1)
C(31)	3163(3)	2820(2)	2053(1)	30(1)
C(32)	1439(4)	2261(2)	2407(1)	40(1)
C(33)	2596(5)	4372(2)	1946(1)	48(1)

Table 3. Hydrogen coordinates (x 10^4) and isotropic displacement parameters (Å^2 x 10^3) for C12 H16 N2 O7 S.

	x	y	z	U_{eq}
H(1A)	4788	-2240	1579	52
H(1B)	1993	-2743	1709	52
H(1C)	3901	-2170	2071	52
H(3)	4152	2347	1421	28
H(4)	-850	1790	1646	29
H(8)	-949	1255	100	39
H(9)	109	562	-607	42
H(11)	6047	-1726	-148	44
H(12)	5021	-1021	557	37
H(31)	4941	2777	2163	36
H(32A)	1653	2846	2666	59
H(32B)	1882	1268	2472	59
H(32C)	-329	2309	2311	59
H(33A)	854	4454	1839	72
H(33B)	3776	4706	1724	72
H(33C)	2791	4957	2205	72

Table 4. Anisotropic parameters ($Å^2$ x 10^3) for C12 H16 N2 O7 S.

The anisotropic displacement factor exponent takes the form:

$$-2\pi^2 [h^2 a^{*2} U_{11} + ... + 2 h k a^* b^* U_{12}]$$

	U11	U22	U33	U23	U13	U12
C(1)	43(1)	24(1)	38(1)	1(1)	-6(1)	4(1)
O(1)	26(1)	24(1)	36(1)	0(1)	-4(1)	-2(1)
C(2)	20(1)	28(1)	24(1)	1(1)	3(1)	-1(1)
O(2)	20(1)	39(1)	44(1)	11(1)	-3(1)	0(1)
C(3)	16(1)	26(1)	28(1)	1(1)	0(1)	-2(1)
N(4)	17(1)	29(1)	26(1)	-2(1)	2(1)	0(1)
S(5)	20(1)	27(1)	25(1)	1(1)	1(1)	3(1)
O(51)	31(1)	32(1)	34(1)	8(1)	3(1)	2(1)
O(52)	19(1)	48(1)	31(1)	0(1)	-1(1)	3(1)
O(6)	32(1)	31(1)	24(1)	1(1)	2(1)	8(1)
C(7)	25(1)	28(1)	26(1)	-2(1)	4(1)	-1(1)
C(8)	28(1)	41(1)	29(1)	-1(1)	1(1)	5(1)
C(9)	33(1)	42(1)	28(1)	3(1)	-1(1)	-2(1)
C(10)	42(1)	32(1)	27(1)	-2(1)	8(1)	-8(1)
C(11)	41(1)	32(1)	37(1)	-2(1)	9(1)	5(1)
C(12)	30(1)	31(1)	31(1)	-2(1)	1(1)	4(1)
N(10)	72(1)	44(1)	32(1)	-6(1)	13(1)	-2(1)
O(13)	164(2)	109(2)	44(1)	-3(1)	31(1)	80(2)
O(14)	62(1)	87(1)	29(1)	-9(1)	0(1)	-16(1)
C(31)	24(1)	34(1)	31(1)	-6(1)	-2(1)	-2(1)
C(32)	34(1)	57(1)	29(1)	-8(1)	2(1)	-7(1)
C(33)	63(1)	32(1)	51(1)	-7(1)	0(1)	2(1)

Table 5. Bond lengths [Å] and angles [°] for C12 H16 N2 O7 S

C(1)-O(1)	1.448(2)	N(4)-C(3)-C(31)	110.72(13)
O(1)-C(2)	1.323(2)	C(2)-C(3)-C(31)	109.79(13)
C(2)-O(2)	1.213(2)	C(3)-N(4)-S(5)	119.79(10)
C(2)-C(3)	1.520(2)	O(51)-S(5)-O(52)	120.13(8)
C(3)-N(4)	1.4700(19)	O(51)-S(5)-N(4)	110.86(7)
C(3)-C(31)	1.546(2)	O(52)-S(5)-N(4)	108.04(7)
N(4)-S(5)	1.5930(13)	O(51)-S(5)-O(6)	106.95(7)
S(5)-O(51)	1.4168(13)	O(52)-S(5)-O(6)	108.41(7)
S(5)-O(52)	1.4219(12)	N(4)-S(5)-O(6)	100.67(7)
S(5)-O(6)	1.6071(12)	C(7)-O(6)-S(5)	121.71(11)
O(6)-C(7)	1.392(2)	C(8)-C(7)-C(12)	121.80(16)
C(7)-C(8)	1.383(2)	C(8)-C(7)-O(6)	123.88(15)
C(7)-C(12)	1.387(3)	C(12)-C(7)-O(6)	114.29(15)
C(8)-C(9)	1.390(3)	C(7)-C(8)-C(9)	119.07(17)
C(9)-C(10)	1.375(3)	C(10)-C(9)-C(8)	118.41(17)
C(10)-C(11)	1.378(3)	C(9)-C(10)-C(11)	123.14(17)
C(10)-N(10)	1.470(2)	C(9)-C(10)-N(10)	118.40(18)
C(11)-C(12)	1.384(3)	C(11)-C(10)-N(10)	118.44(18)
N(10)-O(14)	1.216(3)	C(10)-C(11)-C(12)	118.43(18)
N(10)-O(13)	1.234(3)	C(11)-C(12)-C(7)	119.13(18)
C(31)-C(33)	1.520(3)	O(14)-N(10)-O(13)	123.79(19)
C(31)-C(32)	1.521(3)	O(14)-N(10)-C(10)	119.1(2)
		O(13)-N(10)-C(10)	117.0(2)
C(2)-O(1)-C(1)	116.29(14)	C(33)-C(31)-C(32)	111.69(17)
O(2)-C(2)-O(1)	124.20(16)	C(33)-C(31)-C(3)	110.53(15)
O(2)-C(2)-C(3)	122.42(16)	C(32)-C(31)-C(3)	112.27(15)
O(1)-C(2)-C(3)	113.36(13)		
N(4)-C(3)-C(2)	113.17(13)		

Table 6. Torsion angles [°] for C12 H16 N2 O7 S.

C(1)-O(1)-C(2)-O(2)	-4.4(2)
C(1)-O(1)-C(2)-C(3)	177.38(14)
O(2)-C(2)-C(3)-N(4)	172.69(15)
O(1)-C(2)-C(3)-N(4)	-9.06(19)
O(2)-C(2)-C(3)-C(31)	-63.0(2)
O(1)-C(2)-C(3)-C(31)	115.21(15)
C(2)-C(3)-N(4)-S(5)	-95.54(14)
C(31)-C(3)-N(4)-S(5)	140.70(12)
C(3)-N(4)-S(5)-O(51)	-50.72(14)
C(3)-N(4)-S(5)-O(52)	175.73(12)
C(3)-N(4)-S(5)-O(6)	62.19(13)
O(51)-S(5)-O(6)-C(7)	-52.43(14)
O(52)-S(5)-O(6)-C(7)	78.45(14)
N(4)-S(5)-O(6)-C(7)	-168.29(13)
S(5)-O(6)-C(7)-C(8)	-29.5(2)
S(5)-O(6)-C(7)-C(12)	152.78(13)
C(12)-C(7)-C(8)-C(9)	0.5(3)
O(6)-C(7)-C(8)-C(9)	-177.00(17)
C(7)-C(8)-C(9)-C(10)	0.3(3)
C(8)-C(9)-C(10)-C(11)	-0.9(3)
C(8)-C(9)-C(10)-N(10)	-179.32(18)
C(9)-C(10)-C(11)-C(12)	0.6(3)
N(10)-C(10)-C(11)-C(12)	179.02(18)
C(10)-C(11)-C(12)-C(7)	0.3(3)
C(8)-C(7)-C(12)-C(11)	-0.8(3)
O(6)-C(7)-C(12)-C(11)	176.92(16)
C(9)-C(10)-N(10)-O(14)	-0.3(3)
C(11)-C(10)-N(10)-O(14)	-178.8(2)
C(9)-C(10)-N(10)-O(13)	177.0(2)
C(11)-C(10)-N(10)-O(13)	-1.5(3)
N(4)-C(3)-C(31)-C(33)	-65.69(19)
C(2)-C(3)-C(31)-C(33)	168.64(16)
N(4)-C(3)-C(31)-C(32)	59.76(19)
C(2)-C(3)-C(31)-C(32)	-65.92(18)

Table 7. Bond lengths [Å] and angles [°] related to the hydrogen bonding for C12 H16 N2 O7 S.

D-H	..A	d(D-H)	d(H..A)	d(D..A)	<DHA
N(4)-H(4)	O(2)#1	0.88	2.17	2.8917(18)	138.5

Symmetry transformations used to generate equivalent atoms:

#1 x-1,y,z

ORTEP view of the C12 H16 N2 O7 S compound with the numbering scheme adopted. Ellipsoids drawn at 30% probability level. Hydrogen atoms are represented by sphere of arbitrary size.

REFERENCES

Flack, H.D. (1983). Acta Cryst. A39, 876-881.

Flack, H.D. and Schwarzenbach, D. (1988). Acta Cryst. A44, 499-506.

SAINT (2006) Release 7.34A; Integration Software for Single Crystal Data. Bruker AXS Inc., Madison, WI 53719-1173.

Sheldrick, G.M. (2008). SADABS, Bruker Area Detector Absorption Corrections.
Bruker AXS Inc., Madison, WI 53719-1173.

Sheldrick, G.M. (2008). Acta Cryst. A64, 112-122.

SHELXTL (2001) version 6.12; Bruker Analytical X-ray Systems Inc., Madison, WI 53719-1173.

APEX2 (2009) ; Bruker Molecular Analysis Research Tool.
Bruker AXS Inc., Madison, WI 53719-1173.

Spek, A.L. (2008). PLATON, A Multipurpose Crystallographic Tool, Utrecht University, Utrecht, The Netherlands.

Maris, T. (2004). UdMX, University of Montréal, Montréal, QC, Canada.

XPREP (2008) Version 2008/2; X-ray data Preparation and Reciprocal space Exploration Program. Bruker AXS Inc., Madison, WI 53719-1173.

Annexe 2 : Partie expérimentale du chapitre 3

General Methods

Literature methods were employed to synthesize *N*-(Boc)proline hydrazide (**95**),[91] *N*-(Cbz)alanine (**120**),[159] and 4-nitrophenyl sulfamidates of valine methyl ester (**91**) and D-phenylalanine *tert*-butyl ester [(*R*)**-90**].[91] *Iso*-butyl chloroformate, 4-methylmorpholine, *tert*-butyl carbazate (**81**), triethylamine and 1,2-dichloroethane (DCE) were purchased from Aldrich® and used as received. Trifluoroacetic acid (TFA) was purchased from A&C Chemicals® and used as received. Anhydrous tetrahydrofuran (THF) and dichloromethane (DCM) were obtained by passage through a solvent filtration system (GlassContour®, Irvine, CA). Ethyl acetate (EtOAc) and hexanes were purchased from Fisher Chemicals® and fractionally distilled prior to use. Microwave irradiation was accomplished using a 300 MW Biotage® apparatus on the high-absorption level; temperature was monitored automatically. Flash chromatography[158] was performed on 230–400 mesh silica gel, and thin-layer chromatography was performed on silica gel 60 F254 plates from Merck®. Melting points were measured using a Gallankamp® apparatus and are uncorrected. Specific rotations, $[\alpha]_D$ values, were calculated from optical rotations measured at 20 °C in $CHCl_3$ or MeOH at the specified concentrations (*c* in g/100 mL) using a 1-dm cell (*l*) on a PerkinElmer Polarimeter 341, using the general formula: $[\alpha]^{20}_D = (100 \times \alpha)/(l \times c)$. Accurate mass measurements were performed on a LC-MSD instrument from Agilent technologies in positive electrospray ionisation (ESI) mode at the Université de Montréal Mass Spectrometry facility. Sodium and proton adducts ($[M+Na]^+$ and $[M+H]^+$) were used for empirical formula confirmation. ^1H NMR spectra were measured in $CDCl_3$ (7.26 ppm) or CD_3OD (3.34 ppm). ^{13}C NMR spectra were measured in $CDCl_3$ (77.36 ppm) or CD_3OD (49.86 ppm). Coupling constant *J* values are measured in Hertz (Hz) and chemical shift values are reported in parts per million (ppm). Infrared spectra were recorded in the neat on an ATR Bruker® apparatus.

***N*-(Boc)-prolyl-azasulfurylglycinyl-valine methyl ester (105)**

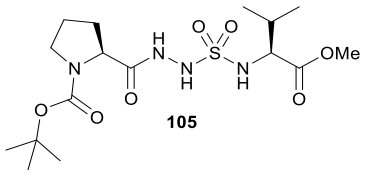

105

Azasulfurylglycine peptide **105** was prepared according to reference 91. Crystals were grown from mixtures of hexanes in ethyl acetate.

_N_-(Cbz)-alanine _N_-(Boc)-hydrazide (121)

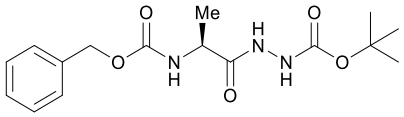

121

_N_-(Cbz)Alanine (**120**, 6.70 g, 30.0 mmol, prepared according to reference 159) was dissolved in dry THF (100 mL), cooled to −15 °C, treated with *iso*-butyl chloroformate (3.92 mL, 30.0 mmol) and 4-methylmorpholine (4.13 mL, 37.5 mmol), stirred for 15 min, and treated with a solution of *tert*-butyl carbazate (**81**, 3.30 g, 25.0 mmol) in dry THF (5 mL). After stirring at −15 °C for 2h, the volatiles were evaporated and the residue was dissolved in DCM (100 mL), washed with water (2 x 100 mL), dried over $MgSO_4$, filtered and evaporated. The residue was purified by flash chromatography eluting with 1:1 hexane/EtOAc to afford hydrazide **121** as a solid (8.22 g, 97%): R_f 0.29 (hexane:EtOAc 1:1); mp 58 °C; $[\alpha]^{20}_D$ –31.8° ($CHCl_3$, *c* 0.99); ^{1}H NMR ($CDCl_3$, 400 MHz) δ 1.37 (3H, d, *J* = 7.0), 1.43 (9H, s), 4.25-4.35 (1H, m), 5.01 (1H, d, *J* = 12.2), 5.10 (1H, d, *J* = 12.2), 5.70-5.80 (1H, br), 6.80-6.90 (1H, br), 7.20-7.30 (5H, m), 8.60-8.75 (1H, br); ^{13}C NMR ($CDCl_3$, 100 MHz) δ 18.6, 28.4, 49.3, 67.4, 82.0, 128.4, 128.5, 128.8, 136.4, 155.7, 156.5, 172.6; IR (neat) ν_{max}/cm^{-1} 1155, 1235, 1367, 1453, 1498, 1675, 2979, 3281; HRMS (ESI) m/z calculated for $C_{16}H_{23}N_3NaO_5$ $[M+Na]^+$ 360.1530; found 360.1534.

_N_-(Cbz)-alanine hydrazidium trifluoroacetate (122)

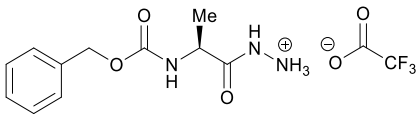

122

Hydrazide **121** (1.01 g, 3.0 mmol) was treated with TFA:DCM 1:1 (5 mL) for 2h at room temperature. The volatiles were evaporated to afford hydrazide salt **122** as an oil (1.04 g, 99%): $[\alpha]^{20}_D$ 8.0° (MeOH, *c* 1.01); ^{1}H NMR (CD_3OD, 400 MHz) δ 1.40 (3H, d, *J* = 7.1), 4.20-4.30 (1H, m), 5.00-5.20 (2H, m), 7.20-7.40 (5H, m); ^{13}C NMR (CD_3OD, 100 MHz) δ 18.7, 51.5,

68.6, 118.8 (q, J-^{19}F = 290.5), 129.7, 129.9, 130.3, 138.8, 159.1, 163.5 (q, J-^{19}F = 36.0), 175.1; IR (neat) ν_{max}/cm^{-1} 1135, 1185, 1359, 1420, 1656, 2981; HRMS (ESI) m/z calculated for $C_{11}H_{16}N_3O_3$ $[M]^+$ 238.1186; found 238.1191.

_N_-(Cbz)-alaninyl-azasulfurylglycinyl-D-phenylalanine _tert_-butyl ester (119)

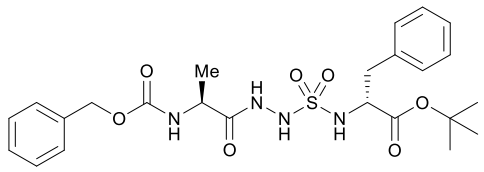

119

Hydrazide salt **122** (1.05 g, 3.00 mmol) was added to a microwave vessel containing a solution of D-phenylalanine-derived 4-nitrophenyl sulfamidate (*R*)-**90** (0.94 g, 2.00 mmol, prepared according to reference 91) in $CHCl_3$ (15 mL). The mixture was treated with NEt_3 (834 μL, 6.00 mmol), at which point the solution turned yellow. The vessel was sealed and heated to 60 °C using microwave irradiation for 2.5 h. After completion of the reaction, $CHCl_3$ (100 mL) was added and the organic phase was washed with 5% citric acid (2 x 100 mL) and H_2O (1 x 100 mL), dried over $MgSO_4$, filtered, and evaporated. The residue was purified by flash chromatography eluting with 11:9 hexane/EtOAc to afford sulfamide **119** as a solid (575 mg, 55%). Crystals were grown from hexanes in ethyl acetate: R_f 0.30 (hexane:EtOAc 3:2); mp 61 °C; $[\alpha]^{20}_D$ –59.4° ($CHCl_3$, *c* 0.98); ^{1}H NMR ($CDCl_3$, 400 MHz) δ 1.36 (3H, d, J = 7.0), 1.40 (9H, s), 3.00-3.20 (2H, m), 4.25-4.40 (2H, m), 5.04 (1H, d, J = 12.0), 5.14 (1H, d, J = 12.0), 5.60 (1H, br), 5.74 (1H, br), 7.20-7.40 (11H, m), 8.66 (1H, s); ^{13}C NMR ($CDCl_3$, 100 MHz) δ 18.2, 28.2, 39.1, 49.5, 57.6, 67.6, 83.4, 127.4, 128.45, 128.49, 128.7, 128.8, 130.1, 135.9, 136.3, 156.5, 171.1, 172.4; IR (neat) ν_{max}/cm^{-1} 1153, 1253, 1368, 1457, 1509, 1687, 2989, 3248; HRMS (ESI) m/z calculated for $C_{24}H_{32}N_4NaO_7S$ $[M+Na]^+$ 543.1884; found 543.1876.

Université de Montréal

CRYSTAL AND MOLECULAR STRUCTURE OF

C16 H30 N4 O7 S (COMPOUND 105)

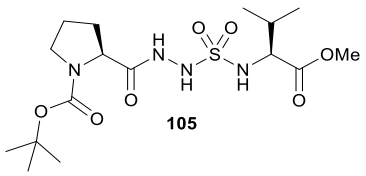

105

Equipe Lubell

Département de chimie, Université de Montréal,

C.P. 6128, Succ. Centre-Ville, Montréal, Québec, H3C 3J7 (Canada)

Structure solved and refined in the laboratory of X-ray diffraction Université de Montréal by Francine Bélanger.

Table 1. Crystal data and structure refinement for C16 H30 N4 O7 S.

Identification code	lube50
Empirical formula	C16 H30 N4 O7 S
Formula weight	422.50
Temperature	150K
Wavelength	1.54178 Å
Crystal system	Monoclinic
Space group	P21
Unit cell dimensions	a = 13.1965(15) Å α = 90° b = 6.0370(9) Å β = 113.093(7)° c = 14.3152(19) Å γ = 90°
Volume	1049.1(2)Å^3
Z	2
Density (calculated)	1.338 g/cm^3
Absorption coefficient	1.763 mm^{-1}
F(000)	452
Crystal size	0.20 x 0.02 x 0.01 mm
Theta range for data collection	3.36 to 70.68°
Index ranges	$-16 \leq h \leq 16$, $-6 \leq k \leq 6$, $-17 \leq \ell \leq 16$
Reflections collected	17220
Independent reflections	3312 [R_{int} = 0.069]
Absorption correction	Semi-empirical from equivalents
Max. and min. transmission	0.9825 and 0.7467
Refinement method	Full-matrix least-squares on F^2
Data / restraints / parameters	3312 / 4 / 272
Goodness-of-fit on F^2	1.026
Final R indices [I>2sigma(I)]	R_1 = 0.0590, wR_2 = 0.1390

R indices (all data)	R_1 = 0.0875, wR_2 = 0.1544
Absolute structure parameter	0.01(3)
Largest diff. peak and hole	0.406 and -0.318 e/Å^3

Table 2. Atomic coordinates (x 10^4) and equivalent isotropic displacement parameters (Å^2 x 10^3) for C16 H30 N4 O7 S.

U_{eq} is defined as one third of the trace of the orthogonalized Uij tensor.

	x	y	z	U_{eq}
C(1)	-447(6)	5578(13)	4092(5)	78(2)
O(1)	-595(3)	4938(6)	3075(3)	50(1)
C(2)	43(4)	3324(9)	2987(4)	41(1)
O(2)	695(4)	2378(9)	3703(3)	84(2)
C(3)	-188(4)	2826(8)	1882(3)	32(1)
N(4)	755(3)	1634(5)	1852(3)	35(1)
S(5)	1176(1)	1978(3)	953(1)	33(1)
O(51)	294(2)	2207(6)	-19(2)	38(1)
O(52)	2023(3)	392(6)	1109(3)	39(1)
N(6)	1778(3)	4478(6)	1121(3)	33(1)
N(7)	2566(3)	4862(7)	2089(3)	35(1)
C(8)	2372(4)	6269(8)	2738(3)	32(1)
O(8)	1465(2)	7086(6)	2543(2)	38(1)
C(9)	3377(3)	6786(8)	3696(3)	34(1)
N(10)	3693(3)	9110(7)	3675(3)	35(1)
C(11)	3347(4)	10548(9)	4326(4)	42(1)
C(12)	2762(5)	8942(10)	4775(4)	53(2)
C(13)	3133(4)	6658(9)	4658(4)	44(1)
C(14)	4241(4)	9898(8)	3137(4)	34(1)
O(14)	4471(2)	11883(6)	3104(2)	38(1)
O(15)	4529(3)	8261(6)	2648(2)	38(1)
C(16)	5225(4)	8680(9)	2087(4)	38(1)
C(17)	4659(5)	10259(9)	1201(4)	50(1)
C(18)	6339(4)	9521(11)	2803(4)	50(1)
C(19)	5307(5)	6361(9)	1686(4)	56(2)
C(31)	-1278(4)	1599(9)	1340(4)	46(1)
C(32)	-2278(4)	2996(10)	1190(4)	53(2)
C(33)	-1290(5)	-570(10)	1865(7)	83(2)

Table 3. Hydrogen coordinates (x 10^4) and isotropic displacement parameters (Å^2 x 10^3) for C16 H30 N4 O7 S.

	x	y	z	U_{eq}
H(1A)	-640	4332	4430	117
H(1B)	-924	6844	4062	117
H(1C)	324	5992	4476	117
H(3)	-238	4272	1526	38
H(4)	970(50)	370(60)	2180(40)	90(20)
H(6)	1220(30)	5400(70)	970(40)	55(18)
H(7)	3218(16)	4270(70)	2230(30)	21(11)
H(9)	4002	5781	3754	41
H(11A)	2839	11722	3923	50
H(11B)	3990	11246	4866	50
H(12A)	2955	9280	5501	63
H(12B)	1953	9071	4411	63
H(13A)	2548	5559	4577	52
H(13B)	3803	6246	5255	52
H(17A)	3900	9767	820	75
H(17B)	5061	10266	752	75
H(17C)	4653	11757	1462	75
H(18A)	6262	11030	3020	75
H(18B)	6847	9528	2454	75
H(18C)	6629	8551	3399	75
H(19A)	5613	5331	2257	83
H(19B)	5787	6411	1310	83
H(19C)	4571	5859	1233	83
H(31)	-1316	1216	647	55
H(32A)	-2307	3311	1850	80
H(32B)	-2944	2194	762	80
H(32C)	-2232	4392	859	80
H(33A)	-642	-1447	1928	125
H(33B)	-1960	-1397	1465	125
H(33C)	-1277	-272	2543	125

Table 4. Anisotropic parameters ($Å^2$ x 10^3) for C16 H30 N4 O7 S.

The anisotropic displacement factor exponent takes the form:

$$-2\pi^2 [h^2 a^{*2} U_{11} + ... + 2 h k a^* b^* U_{12}]$$

	U11	U22	U33	U23	U13	U12
C(1)	90(5)	88(6)	57(4)	-11(3)	31(4)	33(4)
O(1)	63(2)	40(2)	50(2)	-1(2)	26(2)	19(2)
C(2)	47(3)	33(3)	48(3)	0(2)	22(3)	8(2)
O(2)	103(3)	98(4)	50(2)	19(2)	28(2)	63(3)
C(3)	37(3)	20(2)	42(3)	3(2)	20(2)	3(2)
N(4)	35(2)	22(2)	50(2)	5(2)	18(2)	9(2)
S(5)	34(1)	26(1)	38(1)	-3(1)	13(1)	0(1)
O(51)	40(2)	31(2)	37(2)	-4(2)	10(1)	-1(2)
O(52)	38(2)	30(2)	49(2)	0(2)	18(2)	9(2)
N(6)	35(2)	25(2)	33(2)	-2(2)	9(2)	-5(2)
N(7)	32(2)	31(2)	38(2)	-3(2)	9(2)	1(2)
C(8)	39(3)	22(2)	36(3)	4(2)	14(2)	-6(2)
O(8)	34(2)	24(2)	51(2)	-4(2)	12(1)	3(2)
C(9)	35(2)	28(3)	36(2)	1(2)	10(2)	-2(2)
N(10)	41(2)	25(2)	41(2)	-5(2)	18(2)	-2(2)
C(11)	38(3)	28(3)	59(3)	-6(2)	18(2)	0(2)
C(12)	65(4)	47(4)	50(3)	6(3)	27(3)	14(3)
C(13)	52(3)	37(3)	39(3)	0(2)	15(2)	3(3)
C(14)	30(2)	30(3)	40(3)	-8(2)	11(2)	3(2)
O(14)	38(2)	20(2)	54(2)	-5(2)	16(1)	-3(2)
O(15)	48(2)	23(2)	51(2)	-8(1)	27(2)	-2(2)
C(16)	44(3)	32(3)	43(3)	-3(2)	22(2)	1(2)
C(17)	67(4)	35(3)	44(3)	4(2)	17(3)	-2(3)
C(18)	42(3)	57(4)	53(3)	-6(3)	21(3)	-3(3)
C(19)	80(4)	40(4)	63(4)	-5(3)	46(3)	4(3)
C(31)	51(3)	38(3)	56(3)	-13(2)	28(3)	-13(2)
C(32)	45(3)	44(3)	62(4)	9(3)	10(3)	-3(3)
C(33)	69(4)	24(3)	182(8)	11(4)	76(5)	5(3)

Table 5. Bond lengths [Å] and angles [°] for C16 H30 N4 O7 S

C(1)-O(1)	1.444(7)	C(3)-N(4)-S(5)	122.0(3)
O(1)-C(2)	1.325(6)	O(52)-S(5)-O(51)	120.6(2)
C(2)-O(2)	1.194(6)	O(52)-S(5)-N(4)	106.6(2)
C(2)-C(3)	1.520(7)	O(51)-S(5)-N(4)	112.80(19)
C(3)-N(4)	1.453(5)	O(52)-S(5)-N(6)	106.5(2)
C(3)-C(31)	1.531(6)	O(51)-S(5)-N(6)	102.2(2)
N(4)-S(5)	1.603(4)	N(4)-S(5)-N(6)	107.2(2)
S(5)-O(52)	1.421(3)	N(7)-N(6)-S(5)	114.9(3)
S(5)-O(51)	1.428(3)	C(8)-N(7)-N(6)	121.3(4)
S(5)-N(6)	1.678(4)	O(8)-C(8)-N(7)	121.9(4)
N(6)-N(7)	1.387(5)	O(8)-C(8)-C(9)	123.7(4)
N(7)-C(8)	1.356(6)	N(7)-C(8)-C(9)	114.4(4)
C(8)-O(8)	1.221(5)	N(10)-C(9)-C(8)	109.4(4)
C(8)-C(9)	1.520(6)	N(10)-C(9)-C(13)	103.1(4)
C(9)-N(10)	1.467(6)	C(8)-C(9)-C(13)	112.5(4)
C(9)-C(13)	1.535(6)	C(14)-N(10)-C(9)	125.1(4)
N(10)-C(14)	1.334(6)	C(14)-N(10)-C(11)	121.9(4)
N(10)-C(11)	1.471(6)	C(9)-N(10)-C(11)	113.0(4)
C(11)-C(12)	1.529(7)	N(10)-C(11)-C(12)	103.0(4)
C(12)-C(13)	1.495(8)	C(13)-C(12)-C(11)	107.2(4)
C(14)-O(14)	1.242(6)	C(12)-C(13)-C(9)	104.3(4)
C(14)-O(15)	1.348(5)	O(14)-C(14)-N(10)	124.2(4)
O(15)-C(16)	1.460(6)	O(14)-C(14)-O(15)	124.4(4)
C(16)-C(18)	1.512(7)	N(10)-C(14)-O(15)	111.4(4)
C(16)-C(17)	1.528(7)	C(14)-O(15)-C(16)	121.6(4)
C(16)-C(19)	1.533(7)	O(15)-C(16)-C(18)	109.8(4)
C(31)-C(32)	1.509(7)	O(15)-C(16)-C(17)	110.9(4)
C(31)-C(33)	1.513(8)	C(18)-C(16)-C(17)	112.5(5)
		O(15)-C(16)-C(19)	101.5(4)
C(2)-O(1)-C(1)	116.9(4)	C(18)-C(16)-C(19)	111.6(5)
O(2)-C(2)-O(1)	122.7(5)	C(17)-C(16)-C(19)	110.0(4)
O(2)-C(2)-C(3)	125.6(5)	C(32)-C(31)-C(33)	112.1(4)
O(1)-C(2)-C(3)	111.7(4)	C(32)-C(31)-C(3)	113.4(4)
N(4)-C(3)-C(2)	107.8(4)	C(33)-C(31)-C(3)	111.0(5)
N(4)-C(3)-C(31)	113.0(4)		
C(2)-C(3)-C(31)	112.8(4)		

Table 6. Torsion angles [°] for C16 H30 N4 O7 S.

C(1)-O(1)-C(2)-O(2)	1.9(9)
C(1)-O(1)-C(2)-C(3)	-179.5(5)
O(2)-C(2)-C(3)-N(4)	-20.3(7)
O(1)-C(2)-C(3)-N(4)	161.1(4)
O(2)-C(2)-C(3)-C(31)	105.1(7)
O(1)-C(2)-C(3)-C(31)	-73.4(5)
C(2)-C(3)-N(4)-S(5)	-144.5(4)
C(31)-C(3)-N(4)-S(5)	90.1(5)
C(3)-N(4)-S(5)-O(52)	-173.8(4)
C(3)-N(4)-S(5)-O(51)	-39.2(4)
C(3)-N(4)-S(5)-N(6)	72.5(4)
O(52)-S(5)-N(6)-N(7)	-62.6(4)
O(51)-S(5)-N(6)-N(7)	170.0(3)
N(4)-S(5)-N(6)-N(7)	51.2(4)
S(5)-N(6)-N(7)-C(8)	-107.8(4)
N(6)-N(7)-C(8)-O(8)	7.4(7)
N(6)-N(7)-C(8)-C(9)	-170.6(4)
O(8)-C(8)-C(9)-N(10)	-66.4(6)
N(7)-C(8)-C(9)-N(10)	111.6(4)
O(8)-C(8)-C(9)-C(13)	47.6(6)
N(7)-C(8)-C(9)-C(13)	-134.4(4)
C(8)-C(9)-N(10)-C(14)	-78.0(5)
C(13)-C(9)-N(10)-C(14)	162.1(4)
C(8)-C(9)-N(10)-C(11)	102.2(5)
C(13)-C(9)-N(10)-C(11)	-17.7(5)
C(14)-N(10)-C(11)-C(12)	179.9(4)
C(9)-N(10)-C(11)-C(12)	-0.3(5)
N(10)-C(11)-C(12)-C(13)	19.2(5)
C(11)-C(12)-C(13)-C(9)	-30.1(5)
N(10)-C(9)-C(13)-C(12)	28.7(5)
C(8)-C(9)-C(13)-C(12)	-89.1(5)
C(9)-N(10)-C(14)-O(14)	177.6(4)
C(11)-N(10)-C(14)-O(14)	-2.6(7)
C(9)-N(10)-C(14)-O(15)	-3.5(6)
C(11)-N(10)-C(14)-O(15)	176.2(4)
O(14)-C(14)-O(15)-C(16)	4.7(7)
N(10)-C(14)-O(15)-C(16)	-174.1(4)
C(14)-O(15)-C(16)-C(18)	61.8(6)
C(14)-O(15)-C(16)-C(17)	-63.1(6)
C(14)-O(15)-C(16)-C(19)	-179.9(4)
N(4)-C(3)-C(31)-C(32)	-168.9(4)
C(2)-C(3)-C(31)-C(32)	68.6(6)
N(4)-C(3)-C(31)-C(33)	63.9(6)
C(2)-C(3)-C(31)-C(33)	-58.6(6)

Table 7. Bond lengths [Å] and angles [°] related to the hydrogen bonding for C16 H30 N4 O7 S.

D-H	..A	d(D-H)	d(H..A)	d(D..A)	<DHA
N(4)-H(4)	O(8)#1	0.8800(1)	2.09(2)	2.944(5)	164(6)
N(6)-H(6)	O(51)#2	0.8800(1)	2.21(2)	3.049(5)	158(5)
N(7)-H(7)	O(14)#1	0.8801(1)	2.18(2)	2.966(5)	149(4)

Symmetry transformations used to generate equivalent atoms:

#1 x,y-1,z #2 -x,y+1/2,-z

ORTEP view of the C16 H30 N4 O7 S compound with the numbering scheme adopted. Ellipsoids drawn at 30% probability level. Hydrogen atoms are represented by sphere of arbitrary size.

REFERENCES

Flack, H.D. (1983). Acta Cryst. A39, 876-881.

Flack, H.D. and Schwarzenbach, D. (1988). Acta Cryst. A44, 499-506.

SAINT (2006) Release 7.34A; Integration Software for Single Crystal Data. Bruker AXS Inc., Madison, WI 53719-1173.

Sheldrick, G.M. (2008). SADABS, Bruker Area Detector Absorption Corrections. Bruker AXS Inc., Madison, WI 53719-1173.

Sheldrick, G.M. (2008). Acta Cryst. A64, 112-122.

SHELXTL (2001) version 6.12; Bruker Analytical X-ray Systems Inc., Madison, WI 53719-1173.

APEX2 (2009) ; Bruker Molecular Analysis Research Tool. Bruker AXS Inc., Madison, WI 53719-1173.

Spek, A.L. (2008). PLATON, A Multipurpose Crystallographic Tool, Utrecht University, Utrecht, The Netherlands.

Maris, T. (2004). UdMX, University of Montréal, Montréal, QC, Canada.

XPREP (2008) Version 2008/2; X-ray data Preparation and Reciprocal space Exploration Program. Bruker AXS Inc., Madison, WI 53719-1173.

Université de Montréal

CRYSTAL AND MOLECULAR STRUCTURE OF

C24 H32 N4 O7 S (COMPOUND 119)

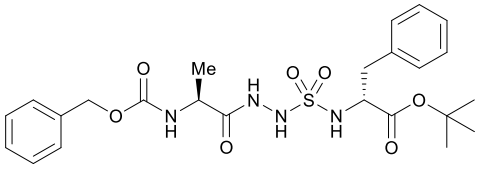

119

Equipe Lubell

Département de chimie, Université de Montréal,

C.P. 6128, Succ. Centre-Ville, Montréal, Québec, H3C 3J7 (Canada)

Structure solved and refined in the laboratory of X-ray diffraction Université de Montréal by Francine Bélanger.

Table 1. Crystal data and structure refinement for C24 H32 N4 O7 S.

Identification code	lube60
Empirical formula	C24 H32 N4 O7 S
Formula weight	520.60
Temperature	100K
Wavelength	1.54178 Å
Crystal system	Monoclinic
Space group	P21
Unit cell dimensions	a = 5.8703(1) Å α = 90° b = 33.4244(6) Å β = 90.907(1)° c = 13.3371(3) Å γ = 90°
Volume	2616.56(9)Å^3
Z	4
Density (calculated)	1.322 g/cm^3
Absorption coefficient	1.524 mm^{-1}
F(000)	1104
Crystal size	0.25 x 0.06 x 0.03 mm
Theta range for data collection	3.57 to 70.90°
Index ranges	$-7 \leq h \leq 7$, $-40 \leq k \leq 40$, $-16 \leq \ell \leq 15$
Reflections collected	50758
Independent reflections	9710 [R_{int} = 0.032]
Absorption correction	Semi-empirical from equivalents
Max. and min. transmission	0.9553 and 0.7897
Refinement method	Full-matrix least-squares on F^2
Data / restraints / parameters	9710 / 1 / 690
Goodness-of-fit on F^2	1.053
Final R indices [I>2sigma(I)]	R_1 = 0.0264, wR_2 = 0.0684
R indices (all data)	R_1 = 0.0269, wR_2 = 0.0722

Absolute structure parameter 0.025(7)

Largest diff. peak and hole 0.238 and -0.228 e/Å^3

Table 2. Atomic coordinates (x 10^4) and equivalent isotropic displacement parameters (Å^2 x 10^3) for C24 H32 N4 O7 S.

U_{eq} is defined as one third of the trace of the orthogonalized Uij tensor.

	x	y	z	U_{eq}
C(1)	1478(3)	-817(1)	10662(1)	32(1)
O(1)	2977(2)	-875(1)	9790(1)	25(1)
C(2)	2497(3)	-726(1)	8891(1)	22(1)
O(2)	774(2)	-554(1)	8634(1)	27(1)
C(3)	4501(3)	-803(1)	8214(1)	22(1)
N(4)	3986(2)	-610(1)	7246(1)	23(1)
S(5)	6033(1)	-396(1)	6649(1)	24(1)
O(5)	4938(2)	-181(1)	5846(1)	30(1)
O(6)	7769(2)	-682(1)	6470(1)	34(1)
N(6)	7353(2)	-56(1)	7356(1)	24(1)
N(7)	5959(2)	257(1)	7662(1)	23(1)
C(8)	5207(2)	281(1)	8610(1)	22(1)
O(8)	5585(2)	23(1)	9239(1)	26(1)
C(9)	3749(3)	648(1)	8839(1)	24(1)
N(10)	3909(2)	965(1)	8099(1)	25(1)
C(11)	5547(3)	1247(1)	8148(1)	24(1)
O(11)	7100(2)	1259(1)	8751(1)	30(1)
O(12)	5190(2)	1520(1)	7405(1)	30(1)
C(13)	6736(3)	1858(1)	7419(1)	34(1)
C(14)	6169(3)	2148(1)	8239(1)	28(1)
C(15)	7659(3)	2214(1)	9042(1)	32(1)
C(16)	7130(3)	2484(1)	9787(2)	37(1)
C(17)	5094(3)	2689(1)	9755(1)	36(1)
C(18)	3581(3)	2623(1)	8964(2)	39(1)
C(19)	4119(3)	2357(1)	8211(1)	36(1)
C(20)	-673(3)	-1066(1)	10526(2)	39(1)
C(21)	2968(3)	-976(1)	11506(1)	49(1)
C(22)	957(4)	-376(1)	10809(2)	47(1)
C(23)	5069(3)	-1252(1)	8100(1)	26(1)
C(24)	3093(3)	-1505(1)	7748(1)	24(1)
C(25)	1672(3)	-1693(1)	8429(1)	29(1)
C(26)	-159(3)	-1923(1)	8103(1)	33(1)
C(27)	-621(3)	-1968(1)	7091(2)	34(1)
C(28)	778(3)	-1783(1)	6402(1)	34(1)
C(29)	2616(3)	-1555(1)	6728(1)	30(1)
C(30)	1267(3)	514(1)	8908(1)	32(1)
C(31)	12226(3)	1542(1)	1598(1)	25(1)
O(31)	12640(2)	1351(1)	2594(1)	20(1)
C(32)	10965(2)	1294(1)	3225(1)	19(1)
O(32)	8982(2)	1383(1)	3104(1)	26(1)
C(33)	11878(2)	1096(1)	4184(1)	19(1)
N(34)	9940(2)	1062(1)	4855(1)	20(1)

S(35)	9717(1)	697(1)	5631(1)	19(1)
O(35)	7535(2)	748(1)	6071(1)	26(1)
O(36)	11735(2)	673(1)	6238(1)	26(1)
N(36)	9781(3)	280(1)	4983(1)	30(1)
N(37)	7892(2)	202(1)	4370(1)	24(1)
C(38)	8108(2)	218(1)	3365(1)	21(1)
O(38)	9838(2)	334(1)	2952(1)	26(1)
C(39)	6052(2)	82(1)	2740(1)	20(1)
N(40)	4103(2)	-38(1)	3322(1)	20(1)
C(41)	4000(2)	-413(1)	3720(1)	20(1)
O(41)	5600(2)	-639(1)	3776(1)	26(1)
O(42)	1889(2)	-489(1)	4053(1)	25(1)
C(43)	1685(3)	-856(1)	4652(1)	29(1)
C(44)	1437(3)	-1227(1)	4013(1)	23(1)
C(45)	-613(3)	-1305(1)	3509(1)	29(1)
C(46)	-857(3)	-1645(1)	2922(2)	32(1)
C(47)	937(3)	-1911(1)	2830(1)	28(1)
C(48)	2955(3)	-1841(1)	3345(1)	26(1)
C(49)	3213(3)	-1498(1)	3930(1)	24(1)
C(50)	11315(3)	1963(1)	1750(1)	34(1)
C(51)	14601(3)	1551(1)	1164(1)	34(1)
C(52)	10663(3)	1277(1)	973(1)	31(1)
C(53)	13913(2)	1325(1)	4645(1)	21(1)
C(54)	13572(3)	1769(1)	4806(1)	23(1)
C(55)	15127(3)	2036(1)	4410(1)	34(1)
C(56)	14911(4)	2446(1)	4583(2)	45(1)
C(57)	13120(4)	2591(1)	5116(2)	42(1)
C(58)	11550(3)	2330(1)	5500(2)	41(1)
C(59)	11776(3)	1921(1)	5358(1)	34(1)
C(60)	5390(3)	419(1)	2014(1)	28(1)

Table 3. Hydrogen coordinates (x 10^4) and isotropic displacement parameters (Å^2 x 10^3) for C24 H32 N4 O7 S.

	x	y	z	U_{eq}
H(3)	5865	-667	8516	27
H(4)	2600(30)	-482(6)	7207(14)	21(4)
H(6)	8030(40)	-162(6)	7844(16)	26(5)
H(7)	5930(30)	458(7)	7281(15)	26(5)
H(9)	4242	758	9506	29
H(10)	2910(30)	970(6)	7630(16)	25(5)
H(13A)	6651	1997	6764	40
H(13B)	8316	1760	7521	40
H(15)	9060	2072	9079	38
H(16)	8176	2528	10326	44
H(17)	4732	2874	10269	43
H(18)	2168	2762	8938	47
H(19)	3078	2316	7668	43
H(20A)	-1519	-973	9931	59
H(20B)	-1625	-1037	11119	59
H(20C)	-262	-1347	10441	59
H(21A)	3406	-1253	11360	73
H(21B)	2125	-968	12135	73
H(21C)	4339	-810	11573	73
H(22A)	2331	-218	10687	70
H(22B)	455	-331	11497	70
H(22C)	-253	-294	10337	70
H(23A)	6323	-1280	7618	31
H(23B)	5624	-1355	8755	31
H(25)	1963	-1663	9128	35
H(26)	-1104	-2050	8579	39
H(27)	-1881	-2125	6869	41
H(28)	472	-1812	5705	41
H(29)	3566	-1431	6249	36
H(30A)	320	743	9097	47
H(30B)	1143	304	9415	47
H(30C)	748	411	8255	47
H(33)	12397	820	4012	23
H(34)	8710(30)	1120(6)	4591(14)	18(4)
H(36)	10790(40)	102(8)	5069(18)	44(6)
H(37)	6890(40)	81(7)	4630(16)	27(5)
H(39)	6530	-153	2331	24
H(40)	2920(30)	100(6)	3271(14)	20(4)
H(43A)	343	-832	5089	35
H(43B)	3053	-883	5091	35
H(45)	-1850	-1124	3568	35
H(46)	-2260	-1695	2580	38
H(47)	778	-2141	2416	34
H(48)	4173	-2026	3300	31
H(49)	4615	-1450	4274	28
H(50A)	9742	1949	1982	51
H(50B)	11356	2109	1113	51
H(50C)	12261	2102	2251	51

H(51A)	15609	1710	1603	51
H(51B)	14537	1673	496	51
H(51C)	15191	1278	1114	51
H(52A)	11322	1008	928	47
H(52B)	10488	1390	299	47
H(52C)	9170	1261	1289	47
H(53A)	14304	1201	5300	25
H(53B)	15238	1288	4205	25
H(55)	16347	1939	4018	41
H(56)	16018	2625	4329	54
H(57)	12962	2871	5219	50
H(58)	10297	2430	5866	49
H(59)	10698	1743	5641	41
H(60A)	4087	334	1598	41
H(60B)	6682	480	1584	41
H(60C)	4976	658	2396	41

Table 4. Anisotropic parameters ($Å^2$ x 10^3) for C24 H32 N4 O7 S.

The anisotropic displacement factor exponent takes the form:

$$-2\pi^2 [h^2 a^{*2} U_{11} + ... + 2 h k a^* b^* U_{12}]$$

	U11	U22	U33	U23	U13	U12
C(1)	28(1)	51(1)	17(1)	0(1)	4(1)	-10(1)
O(1)	27(1)	32(1)	16(1)	3(1)	1(1)	-3(1)
C(2)	28(1)	20(1)	17(1)	-1(1)	-2(1)	-5(1)
O(2)	27(1)	32(1)	23(1)	0(1)	0(1)	2(1)
C(3)	28(1)	22(1)	16(1)	2(1)	-2(1)	-2(1)
N(4)	31(1)	21(1)	16(1)	1(1)	0(1)	0(1)
S(5)	36(1)	21(1)	15(1)	-1(1)	5(1)	0(1)
O(5)	49(1)	26(1)	16(1)	0(1)	2(1)	-3(1)
O(6)	46(1)	28(1)	27(1)	-2(1)	13(1)	4(1)
N(6)	29(1)	23(1)	20(1)	1(1)	3(1)	0(1)
N(7)	30(1)	21(1)	18(1)	0(1)	3(1)	-2(1)
C(8)	20(1)	24(1)	21(1)	-3(1)	-2(1)	-5(1)
O(8)	34(1)	28(1)	18(1)	2(1)	3(1)	2(1)
C(9)	28(1)	24(1)	20(1)	-3(1)	0(1)	-2(1)
N(10)	28(1)	22(1)	25(1)	-2(1)	-7(1)	-2(1)
C(11)	28(1)	22(1)	22(1)	-3(1)	0(1)	1(1)
O(11)	29(1)	29(1)	32(1)	-1(1)	-6(1)	-4(1)
O(12)	40(1)	23(1)	28(1)	1(1)	-5(1)	-5(1)
C(13)	41(1)	30(1)	30(1)	2(1)	4(1)	-8(1)
C(14)	33(1)	21(1)	29(1)	6(1)	0(1)	-8(1)
C(15)	31(1)	26(1)	39(1)	1(1)	-6(1)	-1(1)
C(16)	40(1)	34(1)	37(1)	-3(1)	-10(1)	-1(1)
C(17)	39(1)	32(1)	37(1)	-5(1)	1(1)	-2(1)
C(18)	30(1)	39(1)	48(1)	-1(1)	-4(1)	4(1)
C(19)	34(1)	37(1)	36(1)	1(1)	-9(1)	-2(1)
C(20)	29(1)	58(1)	30(1)	4(1)	2(1)	-12(1)
C(21)	35(1)	92(2)	19(1)	14(1)	-1(1)	-16(1)
C(22)	54(1)	54(1)	33(1)	-16(1)	17(1)	-12(1)
C(23)	30(1)	23(1)	25(1)	3(1)	0(1)	2(1)
C(24)	33(1)	17(1)	23(1)	2(1)	2(1)	3(1)
C(25)	38(1)	25(1)	24(1)	3(1)	4(1)	1(1)
C(26)	36(1)	26(1)	36(1)	5(1)	5(1)	-2(1)
C(27)	37(1)	26(1)	40(1)	0(1)	-4(1)	-3(1)
C(28)	48(1)	27(1)	27(1)	-2(1)	-4(1)	-2(1)
C(29)	41(1)	24(1)	24(1)	2(1)	5(1)	-2(1)
C(30)	26(1)	31(1)	38(1)	-3(1)	3(1)	0(1)
C(31)	23(1)	32(1)	19(1)	6(1)	2(1)	3(1)
O(31)	16(1)	26(1)	19(1)	3(1)	2(1)	1(1)
C(32)	18(1)	19(1)	20(1)	-2(1)	1(1)	-1(1)
O(32)	18(1)	34(1)	26(1)	3(1)	0(1)	3(1)
C(33)	16(1)	20(1)	21(1)	1(1)	3(1)	0(1)
N(34)	16(1)	22(1)	23(1)	2(1)	1(1)	2(1)
S(35)	19(1)	20(1)	17(1)	1(1)	0(1)	0(1)
O(35)	26(1)	26(1)	25(1)	4(1)	6(1)	2(1)
O(36)	27(1)	28(1)	24(1)	1(1)	-7(1)	-1(1)

N(36)	28(1)	27(1)	35(1)	-8(1)	-13(1)	8(1)
N(37)	23(1)	25(1)	24(1)	-2(1)	-4(1)	-3(1)
C(38)	18(1)	16(1)	28(1)	-1(1)	-1(1)	3(1)
O(38)	16(1)	29(1)	35(1)	3(1)	1(1)	0(1)
C(39)	16(1)	22(1)	22(1)	-2(1)	3(1)	0(1)
N(40)	14(1)	18(1)	27(1)	0(1)	2(1)	2(1)
C(41)	20(1)	21(1)	19(1)	-4(1)	3(1)	0(1)
O(41)	25(1)	21(1)	31(1)	0(1)	3(1)	6(1)
O(42)	24(1)	19(1)	31(1)	1(1)	10(1)	-1(1)
C(43)	42(1)	21(1)	25(1)	2(1)	15(1)	-3(1)
C(44)	29(1)	19(1)	21(1)	5(1)	11(1)	-2(1)
C(45)	21(1)	23(1)	44(1)	7(1)	10(1)	2(1)
C(46)	22(1)	30(1)	43(1)	4(1)	0(1)	-5(1)
C(47)	32(1)	21(1)	32(1)	-1(1)	1(1)	-3(1)
C(48)	27(1)	23(1)	29(1)	2(1)	4(1)	5(1)
C(49)	25(1)	24(1)	22(1)	5(1)	0(1)	-1(1)
C(50)	36(1)	30(1)	36(1)	9(1)	1(1)	6(1)
C(51)	28(1)	48(1)	28(1)	11(1)	5(1)	0(1)
C(52)	26(1)	45(1)	23(1)	-3(1)	-2(1)	3(1)
C(53)	15(1)	26(1)	22(1)	1(1)	-1(1)	0(1)
C(54)	22(1)	25(1)	23(1)	0(1)	-8(1)	-2(1)
C(55)	31(1)	31(1)	40(1)	3(1)	-2(1)	-4(1)
C(56)	51(1)	31(1)	54(1)	8(1)	-11(1)	-14(1)
C(57)	49(1)	24(1)	51(1)	-5(1)	-24(1)	2(1)
C(58)	40(1)	36(1)	48(1)	-15(1)	-8(1)	4(1)
C(59)	33(1)	32(1)	39(1)	-8(1)	3(1)	-2(1)
C(60)	24(1)	34(1)	25(1)	6(1)	-3(1)	-5(1)

Table 5. Bond lengths [Å] and angles [°] for C24 H32 N4 O7 S

C(1)-O(1)	1.483(2)	C(39)-N(40)	1.4501(19)
C(1)-C(21)	1.511(3)	C(39)-C(60)	1.529(2)
C(1)-C(22)	1.519(3)	N(40)-C(41)	1.361(2)
C(1)-C(20)	1.520(2)	C(41)-O(41)	1.2085(19)
O(1)-C(2)	1.3238(19)	C(41)-O(42)	1.3477(18)
C(2)-O(2)	1.209(2)	O(42)-C(43)	1.4686(19)
C(2)-C(3)	1.516(2)	C(43)-C(44)	1.512(2)
C(3)-N(4)	1.4704(18)	C(44)-C(49)	1.387(2)
C(3)-C(23)	1.545(2)	C(44)-C(45)	1.394(2)
N(4)-S(5)	1.6183(14)	C(45)-C(46)	1.385(3)
S(5)-O(6)	1.4211(13)	C(46)-C(47)	1.386(2)
S(5)-O(5)	1.4327(12)	C(47)-C(48)	1.380(2)
S(5)-N(6)	1.6620(14)	C(48)-C(49)	1.392(2)
N(6)-N(7)	1.3929(19)	C(53)-C(54)	1.513(2)
N(7)-C(8)	1.349(2)	C(54)-C(55)	1.387(2)
C(8)-O(8)	1.221(2)	C(54)-C(59)	1.392(2)
C(8)-C(9)	1.530(2)	C(55)-C(56)	1.396(3)
C(9)-N(10)	1.452(2)	C(56)-C(57)	1.368(3)
C(9)-C(30)	1.528(2)	C(57)-C(58)	1.375(3)
N(10)-C(11)	1.347(2)	C(58)-C(59)	1.386(3)
C(11)-O(11)	1.208(2)		
C(11)-O(12)	1.360(2)	O(1)-C(1)-C(21)	101.26(15)
O(12)-C(13)	1.449(2)	O(1)-C(1)-C(22)	110.57(15)
C(13)-C(14)	1.502(2)	C(21)-C(1)-C(22)	111.16(18)
C(14)-C(15)	1.390(2)	O(1)-C(1)-C(20)	109.68(14)
C(14)-C(19)	1.392(3)	C(21)-C(1)-C(20)	111.53(16)
C(15)-C(16)	1.380(3)	C(22)-C(1)-C(20)	112.13(17)
C(16)-C(17)	1.379(3)	C(2)-O(1)-C(1)	122.74(13)
C(17)-C(18)	1.386(3)	O(2)-C(2)-O(1)	126.99(15)
C(18)-C(19)	1.382(3)	O(2)-C(2)-C(3)	124.37(14)
C(23)-C(24)	1.505(2)	O(1)-C(2)-C(3)	108.65(13)
C(24)-C(25)	1.393(2)	N(4)-C(3)-C(2)	107.36(12)
C(24)-C(29)	1.395(2)	N(4)-C(3)-C(23)	112.42(13)
C(25)-C(26)	1.385(3)	C(2)-C(3)-C(23)	113.18(13)
C(26)-C(27)	1.381(3)	C(3)-N(4)-S(5)	118.82(11)
C(27)-C(28)	1.388(3)	O(6)-S(5)-O(5)	121.77(7)
C(28)-C(29)	1.385(3)	O(6)-S(5)-N(4)	109.01(7)
C(31)-O(31)	1.4898(18)	O(5)-S(5)-N(4)	105.14(7)
C(31)-C(52)	1.515(2)	O(6)-S(5)-N(6)	103.13(8)
C(31)-C(51)	1.519(2)	O(5)-S(5)-N(6)	106.28(7)
C(31)-C(50)	1.521(2)	N(4)-S(5)-N(6)	111.47(7)
O(31)-C(32)	1.3176(18)	N(7)-N(6)-S(5)	114.16(11)
C(32)-O(32)	1.2094(18)	C(8)-N(7)-N(6)	121.41(14)
C(32)-C(33)	1.531(2)	O(8)-C(8)-N(7)	122.99(15)
C(33)-N(34)	1.4627(19)	O(8)-C(8)-C(9)	121.71(14)
C(33)-C(53)	1.538(2)	N(7)-C(8)-C(9)	115.26(13)
N(34)-S(35)	1.6076(13)	N(10)-C(9)-C(30)	109.04(13)
S(35)-O(36)	1.4262(10)	N(10)-C(9)-C(8)	114.07(13)
S(35)-O(35)	1.4275(11)	C(30)-C(9)-C(8)	108.30(13)
S(35)-N(36)	1.6416(14)	C(11)-N(10)-C(9)	122.14(13)
N(36)-N(37)	1.3919(19)	O(11)-C(11)-N(10)	125.89(15)
N(37)-C(38)	1.350(2)	O(11)-C(11)-O(12)	124.71(15)
C(38)-O(38)	1.2255(19)	N(10)-C(11)-O(12)	109.40(13)
C(38)-C(39)	1.5244(19)	C(11)-O(12)-C(13)	115.03(13)

O(12)-C(13)-C(14)	111.52(14)	O(35)-S(35)-N(36)	110.28(8)
C(15)-C(14)-C(19)	118.27(17)	N(34)-S(35)-N(36)	107.68(7)
C(15)-C(14)-C(13)	121.33(16)	N(37)-N(36)-S(35)	116.36(11)
C(19)-C(14)-C(13)	120.40(16)	C(38)-N(37)-N(36)	119.28(14)
C(16)-C(15)-C(14)	120.87(17)	O(38)-C(38)-N(37)	123.36(14)
C(17)-C(16)-C(15)	120.53(17)	O(38)-C(38)-C(39)	120.20(14)
C(16)-C(17)-C(18)	119.26(18)	N(37)-C(38)-C(39)	116.44(13)
C(19)-C(18)-C(17)	120.28(18)	N(40)-C(39)-C(38)	114.47(13)
C(18)-C(19)-C(14)	120.78(17)	N(40)-C(39)-C(60)	110.38(12)
C(24)-C(23)-C(3)	114.22(13)	C(38)-C(39)-C(60)	108.64(12)
C(25)-C(24)-C(29)	117.97(15)	C(41)-N(40)-C(39)	120.29(12)
C(25)-C(24)-C(23)	121.11(15)	O(41)-C(41)-O(42)	125.29(15)
C(29)-C(24)-C(23)	120.91(15)	O(41)-C(41)-N(40)	124.19(14)
C(26)-C(25)-C(24)	120.99(16)	O(42)-C(41)-N(40)	110.51(12)
C(27)-C(26)-C(25)	120.52(17)	C(41)-O(42)-C(43)	114.96(12)
C(26)-C(27)-C(28)	119.23(17)	O(42)-C(43)-C(44)	112.67(13)
C(29)-C(28)-C(27)	120.29(16)	C(49)-C(44)-C(45)	118.96(15)
C(28)-C(29)-C(24)	121.00(16)	C(49)-C(44)-C(43)	121.05(15)
O(31)-C(31)-C(52)	109.21(13)	C(45)-C(44)-C(43)	119.97(15)
O(31)-C(31)-C(51)	102.19(12)	C(46)-C(45)-C(44)	120.40(15)
C(52)-C(31)-C(51)	110.76(14)	C(45)-C(46)-C(47)	120.32(16)
O(31)-C(31)-C(50)	109.34(13)	C(48)-C(47)-C(46)	119.55(16)
C(52)-C(31)-C(50)	113.75(14)	C(47)-C(48)-C(49)	120.32(15)
C(51)-C(31)-C(50)	110.94(15)	C(44)-C(49)-C(48)	120.43(15)
C(32)-O(31)-C(31)	121.15(11)	C(54)-C(53)-C(33)	116.10(12)
O(32)-C(32)-O(31)	127.31(14)	C(55)-C(54)-C(59)	118.33(16)
O(32)-C(32)-C(33)	122.77(14)	C(55)-C(54)-C(53)	119.20(15)
O(31)-C(32)-C(33)	109.92(12)	C(59)-C(54)-C(53)	122.45(15)
N(34)-C(33)-C(32)	106.23(11)	C(54)-C(55)-C(56)	120.43(19)
N(34)-C(33)-C(53)	113.58(12)	C(57)-C(56)-C(55)	120.5(2)
C(32)-C(33)-C(53)	112.21(12)	C(56)-C(57)-C(58)	119.52(18)
C(33)-N(34)-S(35)	121.61(10)	C(57)-C(58)-C(59)	120.62(19)
O(36)-S(35)-O(35)	121.08(7)	C(58)-C(59)-C(54)	120.51(18)
O(36)-S(35)-N(34)	109.42(7)		
O(35)-S(35)-N(34)	104.83(7)		
O(36)-S(35)-N(36)	103.02(7)		

Table 6. Torsion angles [°] for C24 H32 N4 O7 S.

C(21)-C(1)-O(1)-C(2)	-170.37(16)	C(51)-C(31)-O(31)-C(32)	178.57(14)
C(22)-C(1)-O(1)-C(2)	-52.5(2)	C(50)-C(31)-O(31)-C(32)	60.97(18)
C(20)-C(1)-O(1)-C(2)	71.7(2)	C(31)-O(31)-C(32)-O(32)	0.0(2)
C(1)-O(1)-C(2)-O(2)	-5.7(2)	C(31)-O(31)-C(32)-C(33)	-179.68(12)
C(1)-O(1)-C(2)-C(3)	173.82(13)	O(32)-C(32)-C(33)-N(34)	-2.24(19)
O(2)-C(2)-C(3)-N(4)	3.4(2)	O(31)-C(32)-C(33)-N(34)	177.43(12)
O(1)-C(2)-C(3)-N(4)	-176.12(12)	O(32)-C(32)-C(33)-C(53)	-126.92(15)
O(2)-C(2)-C(3)-C(23)	-121.23(16)	O(31)-C(32)-C(33)-C(53)	52.75(16)
O(1)-C(2)-C(3)-C(23)	59.22(16)	C(32)-C(33)-N(34)-S(35)	147.56(11)
C(2)-C(3)-N(4)-S(5)	142.55(11)	C(53)-C(33)-N(34)-S(35)	-88.62(14)
C(23)-C(3)-N(4)-S(5)	-92.34(14)	C(33)-N(34)-S(35)-O(36)	54.20(13)
C(3)-N(4)-S(5)-O(6)	57.68(13)	C(33)-N(34)-S(35)-O(35)	-174.52(11)
C(3)-N(4)-S(5)-O(5)	-170.24(11)	C(33)-N(34)-S(35)-N(36)	-57.09(13)
C(3)-N(4)-S(5)-N(6)	-55.50(13)	O(36)-S(35)-N(36)-N(37)	174.83(12)
O(6)-S(5)-N(6)-N(7)	-178.19(11)	O(35)-S(35)-N(36)-N(37)	44.26(15)
O(5)-S(5)-N(6)-N(7)	52.66(12)	N(34)-S(35)-N(36)-N(37)	-69.57(14)
N(4)-S(5)-N(6)-N(7)	-61.37(13)	S(35)-N(36)-N(37)-C(38)	110.67(15)
S(5)-N(6)-N(7)-C(8)	105.09(14)	N(36)-N(37)-C(38)-O(38)	-7.0(2)
N(6)-N(7)-C(8)-O(8)	-4.1(2)	N(36)-N(37)-C(38)-C(39)	173.23(13)
N(6)-N(7)-C(8)-C(9)	178.27(13)	O(38)-C(38)-C(39)-N(40)	-178.52(13)
O(8)-C(8)-C(9)-N(10)	166.40(14)	N(37)-C(38)-C(39)-N(40)	1.25(19)
N(7)-C(8)-C(9)-N(10)	-15.98(19)	O(38)-C(38)-C(39)-C(60)	-54.65(18)
O(8)-C(8)-C(9)-C(30)	-71.98(18)	N(37)-C(38)-C(39)-C(60)	125.12(14)
N(7)-C(8)-C(9)-C(30)	105.64(15)	C(38)-C(39)-N(40)-C(41)	-81.93(17)
C(30)-C(9)-N(10)-C(11)	152.29(15)	C(60)-C(39)-N(40)-C(41)	155.14(13)
C(8)-C(9)-N(10)-C(11)	-86.51(18)	C(39)-N(40)-C(41)-O(41)	13.4(2)
C(9)-N(10)-C(11)-O(11)	4.3(3)	C(39)-N(40)-C(41)-O(42)	-167.71(12)
C(9)-N(10)-C(11)-O(12)	-175.78(13)	O(41)-C(41)-O(42)-C(43)	9.1(2)
O(11)-C(11)-O(12)-C(13)	-4.7(2)	N(40)-C(41)-O(42)-C(43)	-169.77(12)
N(10)-C(11)-O(12)-C(13)	175.43(14)	C(41)-O(42)-C(43)-C(44)	-82.36(18)
C(11)-O(12)-C(13)-C(14)	-74.89(18)	O(42)-C(43)-C(44)-C(49)	107.22(17)
O(12)-C(13)-C(14)-C(15)	114.60(17)	O(42)-C(43)-C(44)-C(45)	-73.80(19)
O(12)-C(13)-C(14)-C(19)	-65.3(2)	C(49)-C(44)-C(45)-C(46)	-0.9(2)
C(19)-C(14)-C(15)-C(16)	-0.6(3)	C(43)-C(44)-C(45)-C(46)	-179.95(15)
C(13)-C(14)-C(15)-C(16)	179.49(17)	C(44)-C(45)-C(46)-C(47)	0.0(3)
C(14)-C(15)-C(16)-C(17)	0.7(3)	C(45)-C(46)-C(47)-C(48)	1.4(3)
C(15)-C(16)-C(17)-C(18)	-0.1(3)	C(46)-C(47)-C(48)-C(49)	-1.8(2)
C(16)-C(17)-C(18)-C(19)	-0.6(3)	C(45)-C(44)-C(49)-C(48)	0.5(2)
C(17)-C(18)-C(19)-C(14)	0.7(3)	C(43)-C(44)-C(49)-C(48)	179.47(14)
C(15)-C(14)-C(19)-C(18)	-0.1(3)	C(47)-C(48)-C(49)-C(44)	0.9(2)
C(13)-C(14)-C(19)-C(18)	179.79(17)	N(34)-C(33)-C(53)-C(54)	-69.13(17)
N(4)-C(3)-C(23)-C(24)	-66.92(18)	C(32)-C(33)-C(53)-C(54)	51.38(17)
C(2)-C(3)-C(23)-C(24)	54.94(18)	C(33)-C(53)-C(54)-C(55)	-126.35(15)
C(3)-C(23)-C(24)-C(25)	-92.16(18)	C(33)-C(53)-C(54)-C(59)	55.2(2)
C(3)-C(23)-C(24)-C(29)	87.13(19)	C(59)-C(54)-C(55)-C(56)	1.3(3)
C(29)-C(24)-C(25)-C(26)	0.0(2)	C(53)-C(54)-C(55)-C(56)	-177.18(16)
C(23)-C(24)-C(25)-C(26)	179.33(15)	C(54)-C(55)-C(56)-C(57)	-2.3(3)
C(24)-C(25)-C(26)-C(27)	-0.3(3)	C(55)-C(56)-C(57)-C(58)	1.4(3)
C(25)-C(26)-C(27)-C(28)	0.3(3)	C(56)-C(57)-C(58)-C(59)	0.5(3)
C(26)-C(27)-C(28)-C(29)	0.1(3)	C(57)-C(58)-C(59)-C(54)	-1.4(3)
C(27)-C(28)-C(29)-C(24)	-0.4(3)	C(55)-C(54)-C(59)-C(58)	0.5(3)
C(25)-C(24)-C(29)-C(28)	0.3(2)	C(53)-C(54)-C(59)-C(58)	178.96(16)
C(23)-C(24)-C(29)-C(28)	-178.97(16)		
C(52)-C(31)-O(31)-C(32)	-64.08(17)		

Table 7. Bond lengths [Å] and angles [°] related to the hydrogen bonding for C24 H32 N4 O7 S.

D-H	..A	d(D-H)	d(H..A)	d(D..A)	<DHA
N(6)-H(6)	O(2)#1	0.84(2)	2.32(2)	3.0987(18)	155.8(19)
N(7)-H(7)	O(35)	0.84(2)	2.12(2)	2.8484(18)	145.1(18)
N(10)-H(10)	O(36)#2	0.85(2)	2.21(2)	2.9407(17)	144.6(18)
N(36)-H(36)	O(42)#1	0.84(3)	2.49(3)	3.1187(18)	132(2)
N(37)-H(37)	O(5)	0.80(2)	2.18(2)	2.9375(19)	158(2)
N(40)-H(40)	O(38)#2	0.84(2)	2.01(2)	2.8314(17)	167.3(18)

Symmetry transformations used to generate equivalent atoms:

#1 x+1,y,z #2 x-1,y,z

ORTEP view of the C24 H32 N4 O7 S compound with the numbering scheme adopted. Ellipsoids drawn at 30% probability level. Hydrogen atoms are represented by sphere of arbitrary size.

REFERENCES

Flack, H.D. (1983). Acta Cryst. A39, 876-881.

Flack, H.D. and Schwarzenbach, D. (1988). Acta Cryst. A44, 499-506.

SAINT (2006) Release 7.34A; Integration Software for Single Crystal Data. Bruker AXS Inc., Madison, WI 53719-1173.

Sheldrick, G.M. (2008). SADABS, Bruker Area Detector Absorption Corrections.
Bruker AXS Inc., Madison, WI 53719-1173.

Sheldrick, G.M. (2008). Acta Cryst. A64, 112-122.

SHELXTL (2001) version 6.12; Bruker Analytical X-ray Systems Inc., Madison, WI 53719-1173.

APEX2 (2009) ; Bruker Molecular Analysis Research Tool.
Bruker AXS Inc., Madison, WI 53719-1173.

Spek, A.L. (2008). PLATON, A Multipurpose Crystallographic Tool, Utrecht University, Utrecht, The Netherlands.

Maris, T. (2004). UdMX, University of Montréal, Montréal, QC, Canada.

XPREP (2008) Version 2008/2; X-ray data Preparation and Reciprocal space Exploration Program. Bruker AXS Inc., Madison, WI 53719-1173.

Annexe 3 : Partie expérimentale du chapitre 4

Solution Phase Synthesis

General Methods

The 4-nitrophenyl sulfamidate of D-phenylalanine *tert*-butyl ester [(*R*)-**90**],[91] *N*-(Boc)-alaninyl-azasulfurylglycinyl-D-phenylalanine *tert*-butyl ester [(S,R)-**101**],[91] *tert*-butyl 3-fluorenylidene carbazate (**161**),[82] alloc-alanine (**164**),[160] 2-phenyl-2-propanol (**174**),[161] 2,4-Dimethoxybenzyl alcohol (**176**),[162] and 4-nitrophenyl chlorosulfate (**51**),[90] all were synthesized according to literature methods. *Iso*-butyl chloroformate, 4-methylmorpholine, *tert*-butyl carbazate (**81**), potassium carbonate, 4-fluorobenzyl bromide, triethylamine, 40% tetraethylammonium hydroxide in water, *N*,*N*-*di*-*iso*-propylethylamine, allyl and benzyl chloroformates (**173** and **175** respectively), hydrazine hydrate, sodium hydroxide (NaOH, pellets), dicyclohexylcarbodiimide (DCC), 4-hydroxybenzaldehyde (**179**), imidazole, *tert*-butyldimethylsilyl chloride (TBDMSCl), and sodium borohydride ($NaBH_4$), all were purchased from Aldrich® and used as received. Benzyl bromide was purchased from Aldrich® and filtered through a small plug of silica gel prior to use. Phosphorus tribromide (PBr_3) was purchased from Aldrich® and vacuum distilled prior to use. Fmoc-alanine (**166**), Fmoc-D- (*R*)-**172** and L-Trp(Boc) (*S*)-**172**, and hydroxybenzotriazole (HOBt), all were purchased from GL Biochem® (Shanghai, China) Ltd. *O*-(Benzotriazol-1-yl)-*N*,*N*,*N'*,*N'*-tetramethyluronium tetrafluoroborate (TBTU) was purchased from Albatross®. 1,2-Dichloroethane (DCE), trifluoroacetic acid (TFA), 1,4-dioxane, Fmoc-OSu, sulfuric acid and *tert*-butyl acetate were respectively purchased from Aldrich®, A&C Chemicals®, J. T. Baker®, GenScript® Corporation, A&C Chemicals® and Aldrich®, and used as received. Anhydrous solvents [tetrahydrofuran (THF) and dichloromethane (DCM)] were obtained by passage through a solvent filtration system (GlassContour®, Irvine, CA). Ethyl acetate (EtOAc) and hexanes were purchased from Fisher Chemical® and fractionally distilled prior to use. Microwave irradiation was accomplished using a 300 MW Biotage® apparatus on the high-absorption level; temperature was monitored automatically. Flash chromatography[158] was performed on 230–400 mesh silica gel, and thin-layer chromatography was performed on silica gel 60 F254 plates from Merck®. Melting points were measured using a Gallankamp® apparatus and are uncorrected. Specific rotations, $[\alpha]_D$ values, were calculated from optical rotations measured at 20 °C in $CHCl_3$ or MeOH at the

specified concentrations (*c* in g/100 mL) using a 1-dm cell (*l*) on a PerkinElmer Polarimeter 341, using the general formula: $[\alpha]^{20}_{D} = (100 \times \alpha)/(l \times c)$. Accurate mass measurements were performed on a LC-MS instrument from Agilent technologies in positive electrospray ionisation (ESI) mode at the Université de Montréal Mass Spectrometry facility. Sodium and proton adducts ($[M+Na]^+$ and $[M+H]^+$) were used for empirical formula confirmation. ^{1}H NMR spectra were measured in $CDCl_3$ (7.26 ppm) or CD_3OD (3.34 ppm). ^{13}C NMR spectra were measured in $CDCl_3$ (77.36 ppm) or CD_3OD (49.86 ppm). Coupling constant *J* values are measured in Hertz (Hz) and chemical shift values are reported in parts per million (ppm). When distinguishable, the proton and carbon resonances for the minor isomer are respectively reported in brackets and parentheses. Infrared spectra were recorded in the neat on an ATR Bruker® apparatus.

Scheme 1. Synthesis of *N*-(Alloc)-Alaninyl-azasulfuryl-4-fluorophenylalaninyl-D-phenylalanine (127)

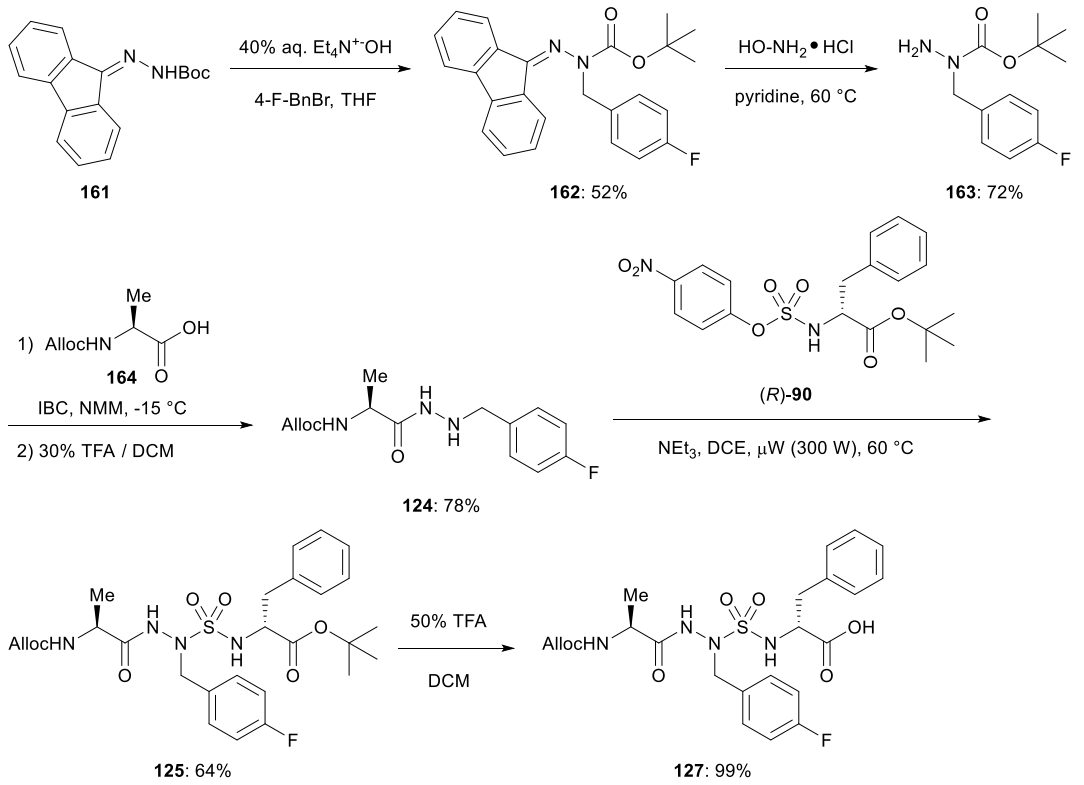

***tert*-Butyl *N*-(4-fluorobenzyl)fluorenylidene carbazate (162)**

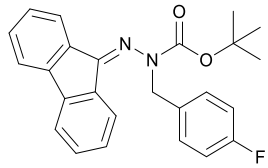

162

tert-Butyl 3-fluorenylidene carbazate (**161**; 3 g, 10.2 mmol, prepared according to reference 82) was dissolved in 40 mL of anhydrous THF at 0 °C, treated with 40% tetraethylammonium hydroxide in H_2O (5.49 mL, 15.3 mmol), stirred for 30 min, and treated with 4-fluorobenzyl bromide (3.26 mL, 15.3 mmol). The ice bath was removed, and the mixture was allowed to warm to room temperature, stirred for 16 h, treated with CH_2Cl_2, extracted twice with H_2O, dried with $MgSO_4$, filtered, and evaporated. The residue was purified by flash chromatography using EtOAc:hexane 1:4 as the solvent system. Evaporation of the collected fractions gave carbazate **162** as a yellow solid (2.56 g, 52% yield): *Rf* 0.61 (4:1 hexane/EtOAc); mp 140 °C; ^{1}H NMR ($CDCl_3$, 400 MHz) δ 1.31 (9H, s), 4.99 (2H, s), 7.10-7.30 (4H, m), 7.30-7.45 (4H, m), 7.51 (1H, d, *J* = 11.0), 7.54 (1H, d, *J* = 11.1), 7.73 (1H, d, *J* = 10.2), 7.84 (1H, d, *J* = 10.0); ^{13}C NMR ($CDCl_3$, 75 MHz) δ: 28.5, 56.3, 82.1, 120.1 (d, J-^{19}F = 22.5) 123.4, 127.8 (d, J-^{19}F = 41.0), 128.43, 128.45, 128.6, 131.58, 131.85 (d, J-^{19}F = 41.1), 137.1, 139.9 (d, J-^{19}F = 214.5), 142.9, 152.9; HRMS (ESI) m/z calculated for $C_{25}H_{24}FN_2O_2$ $[M+H]^+$ 403.1744; found 403.1816.

***tert*-Butyl *N*-(4-fluorobenzyl)carbazate (163)**

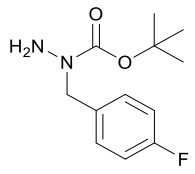

163

tert-Butyl *N*-(4-fluorobenzyl)fluorenylidene carbazate (**162**, 2.52 g, 6.27 mmol) was treated with a solution of hydroxylamine hydrochloride (1.7 g, 25.11 mmol) in pyridine (17 mL) at 60 °C for 12 h. The volatiles were evaporated and the residue was purified by flash chromatography eluting with EtOAc:Hexane 1:9. Carbazate **163** was obtained as an oil (1.08 g,

72% yield): *Rf* 0.1 (hexane:EtOAc 4:1); ^{1}H NMR ($CDCl_3$, 400 MHz) δ 1.46 (9H, s), 3.96 (2H, br), 4.48 (2H, s), 6.90-7.05 (2H, m), 7.15-7.30 (2H, m); ^{13}C NMR ($CDCl_3$, 75 MHz) δ 29.0, 54.0, 81.2, 115.6 (d, J-^{19}F = 21.2), 129.9 (d, J-^{19}F = 8.0), 134.1 (d, J-^{19}F = 3.2), 157.0, 162.5 (d, J-^{19}F = 243.8); HRMS (ESI) m/z calculated for $C_{12}H_{18}FN_2O_2$ $[M+H]^+$ 241.1274; found 241.1346.

_N_-(Alloc)-alanine-_N_'-4-fluorobenzylhydrazide (124)

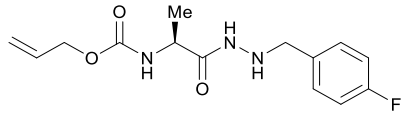

124

A solution of *N*-(Alloc)-alanine (**164**, 945 mg, 5.42 mmol, prepared according to reference 160) in THF (25 mL) was cooled to –15°C, treated slowly with *iso*-butyl chloroformate (700 μL, 5.42 mmol) and *N*-methylmorpholine (750 μL, 6.75 mmol), stirred for 15 min and treated slowly with a solution of *tert*-butyl *N*-(4-fluorobenzyl)carbazate (**163**, 1.08 g, 4.42 mmol) in THF (25 mL). After stirring for 3 h at –15°C, the volatiles were evaporated to a residue, which was used without further purification. The residue (450 mg, 1.14 mmol) in DCM (7 mL) was treated with trifluoroacetic acid (3 mL) and stirred for 3 h. The volatiles were evaporated, the residue was dissolved in DCM (20 mL), evaporated and dissolved in DCM (20 mL) and evaporated twice more. The residue was dissolved in EtOAc (30 mL), treated with K_2CO_3 (15 mL) and H_2O (10 mL), dried over $MgSO_4$, filtered and evaporated to afford **124** as a white powder (321 mg, 78%): mp 96 °C; $[\alpha]^{20}_D$ −36.8° ($CHCl_3$, *c* 1.5); ^{1}H NMR ($CDCl_3$, 500 MHz) δ 1.29 (3H, d, J = 7.0), 3.87 (2H, s), 4.10-4.20 (1H, m), 4.30-4.40 (1H, br), 4.40-4.55 (2H, m), 5.17 (1H, dd, J = 1.5, 10.5), 5.25 (1H, dd, J = 1.5, 17.0), 5.54 (1H, d, J = 7.5), 5.80-5.90 (1H, m), 6.90-7.00 (2H, m), 7.20-7.30 (2H, m), 8.10 (1H, br); ^{13}C NMR ($CDCl_3$, 125 MHz) δ 18.7, 49.4, 55.2, 66.3, 115.6 (d, J-^{19}F = 21.2), 118.4, 131.0 (d, J-^{19}F = 8.0), 132.7, 133.3 (d, J-^{19}F = 2.6), 156.2, 162.6 (d, J-^{19}F = 244.4), 172.4; HRMS (ESI) m/z calculated for $C_{14}H_{19}FN_3O_3$ $[M+H]^+$ 296,1332; found 296,1405.

_N_-(Alloc)-alaninyl-azasulfuryl-4-fluorophenylalaninyl-D-phenylalanine _tert_-butyl ester (125)

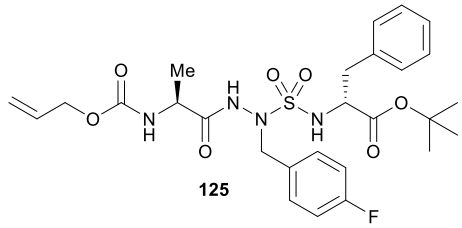

125

_N_-(Alloc)-alanine _N_'-4-fluorobenzylhydrazide (**124**, 267 mg, 0.91 mmol) was added to a microwave vessel containing a solution of sulfamidate (_R_)-**90** (340 mg, 0.72 mmol, prepared according to reference 91) in DCE (1 mL). The mixture was treated with NEt_3 (126 μL, 0.91 mmol), at which point the solution turned yellow. The vessel was sealed and heated to 60 °C using microwave irradiation for 2.5 h. The volatiles were evaporated. The residue was purified by flash chromatography eluting with a solution of 7:3 Et_2O:petroleum ether. The collected fractions were evaporated to a residue, which was dissolved in DCM (25 mL), washed with sat. $NaHCO_3$ (3 x 25 mL), dried over $MgSO_4$, filtered and evaporated to afford azasulfuryl tripeptide **125** as a solid (268 mg; 64%): R_f_ 0.38 (7:3 Et_2O:petroleum ether); mp 56 °C; $[\alpha]^{20}_D$ −56.5° ($CHCl_3$, _c_ 0.42); ^{1}H NMR ($CDCl_3$, 400 MHz) δ 1.16 (3H, d, _J_ = 6.9), 1.39 (9H, s), 3.11 (2H, d, _J_ = 5.6), 4.00-4.10 (1H, m), 4.35-4.50 (5H, m), 5.15-5.17 (1H, br), 5.18 (1H, dd, _J_ = 1.3, 10.4), 5.25 (1H, dd, _J_ = 1.3, 17.2), 5.65-5.75 (1H, br), 6.30-6.40 (1H, m), 6.95-7.05 (2H, m), 7.20-7.35 (7H, m), 8.07 (1H, s); ^{13}C NMR ($CDCl_3$, 100 MHz) δ 18.1, 28.2, 39.0, 49.4, 54.6, 57.6, 66.5, 83.3, 115.7 (d, J-^{19}F = 21.4), 118.4, 127.3, 128.6, 130.3, 130.6 (d, J-^{19}F = 3.2), 131.5 (d, J-^{19}F = 8.1), 132.7, 136.2, 156.2, 163.0 (d, J-^{19}F = 245.4), 170.4, 171.8; IR (neat) ν_{max}/cm^{-1} 1150, 1222, 1365, 1454, 1510, 1690, 2979, 3278; HRMS (ESI) m/z calculated for $C_{27}H_{35}FN_4NaO_7S$ $[M+Na]^+$ 601.2103; found 601.2115.

***N*-(Alloc)-alaninyl-azasulfuryl-4-fluorophenylalaninyl-D-phenylalanine (127)**

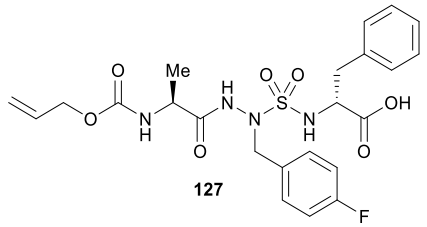

127

tert-Butyl ester **125** (100 mg, 0.17 mmol) was treated with TFA:DCM 1:1 (1 mL) for 1.5 h at room temperature. The volatiles were then evaporated to afford acid **127** as a solid (89 mg, 99%): mp 66 °C; $[\alpha]^{20}_{D}$ −42.2° ($CHCl_3$, *c* 0.65); ^{1}H NMR ($CDCl_3$, 400 MHz) δ 0.80-0.90 (3H, br), 3.19 (1H, dd, *J* = 4.1, 13.9), 3.26 (1H, dd, *J* = 5.0, 14.0), 3.85-3.95 (1H, m), 4.15-4.25 (1H, dd, *J* = 4.8, 12.4), 4.27 (1H, d, *J* = 13.6), 4.39 (1H, dd, *J* = 4.9, 13.1), 4.60-4.70 (2H, m), 5.03 (1H, d, *J* = 9.9), 5.12 (1H, d, *J* = 17.2), 5.60-5.70 (1H, m), 5.82 (1H, d, *J* = 5.8), 5.90-6.00 (1H, br), 6.95-7.05 (2H, m), 7.15-7.30 (5H, m), 7.30-7.40 (2H, m), 8.60 (1H, s), 9.30-9.60 (1H, br); ^{13}C NMR ($CDCl_3$, 100 MHz) δ 16.4, 39.2, 49.4, 54.9, 57.0, 66.6, 115.6 (d, J-^{19}F = 21.7), 118.5, 127.3, 128.5, 130.1 (d, J-^{19}F = 2.5), 130.3, 131.8 (d, J-^{19}F = 8.0), 132.6, 135.7, 157.2, 163.1 (d, J-^{19}F = 245.6), 172.7, 173.7; IR (neat) ν_{max}/cm^{-1} 1155, 1221, 1346, 1455, 1510, 1676, 2972, 3707; HRMS (ESI) m/z calculated for $C_{23}H_{27}FN_4O_7S$ $[M+Na]^+$ 545.1477; found 545.1489.

Scheme 2. Synthesis of *N*-(Fmoc)-alaninyl-azasulfurylphenylalaninyl-D-phenylalanine (128)

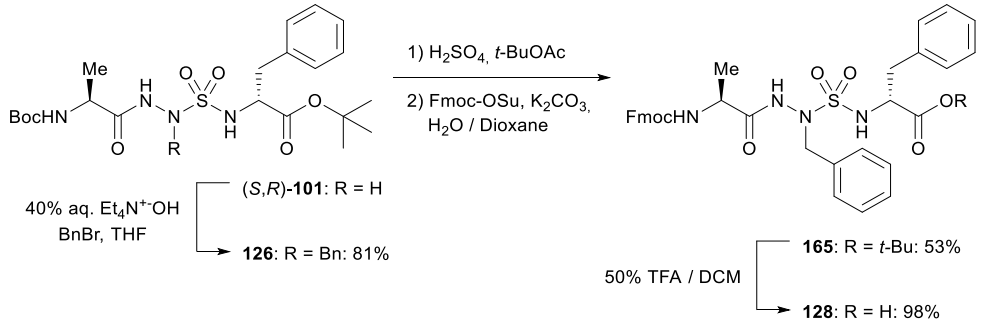

_N_-(Boc)-alaninyl-azasulfurylphenylalaninyl-D-phenylalanine _tert_-butyl ester (126)

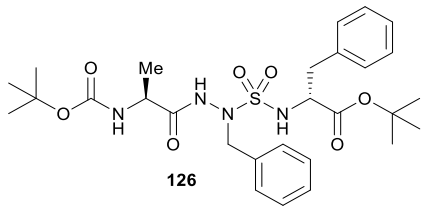

126

_N_-(Boc)-alaninyl-azasulfurylglycinyl-D-phenylalanine _tert_-butyl ester [(_S_,_R_)-**101**, 243 mg, 0.50 mmol, prepared according to reference 91] was dissolved in THF (5 mL), treated at room temperature with tetraethylammonium hydroxide (40% in H_2O, 202 μL, 0.55 mmol) and benzyl bromide (66 μL, 0.55 mmol), stirred at room temperature for 3h, and the volatiles were evaporated to a residue, which was dissolved in DCM (10 mL), washed with 5% citric acid (1 x 10 mL), water (1 x 10 mL) and brine (1 x 10 mL), dried over $MgSO_4$, filtered and evaporated. The residue was purified by flash chromatography eluting with hexane:EtOAc 3:1 to afford **126** as a solid (235 mg, 81%): R_f 0.42 (hexane:EtOAc 7:3); mp 60 °C; $[\alpha]^{20}_D$ –57.6° ($CHCl_3$, _c_ 0.96); ^{1}H NMR ($CDCl_3$, 400 MHz) δ 1.14 (3H, d, _J_ = 7.0), 1.39 (9H, s), 1.40 (9H, s), 3.14 (2H, d, _J_ = 5.7), 3.95-4.05 (1H, m), 4.46 (1H, q, _J_ = 5.8), 4.50 (1H, d, _J_ = 14.2), 4.55 (1H, d, _J_ = 14.1), 4.90 (1H, d, _J_ = 7.2), 5.61 (1H, d, _J_ = 6.8), 7.20-7.35 (10H, m), 7.88 (1H, s); ^{13}C NMR ($CDCl_3$, 100 MHz) δ 18.0, 28.3, 28.6, 39.0, 49.2, 55.2, 57.7, 80.9, 83.2, 127.3, 128.5, 128.6, 128.9, 129.6, 130.3, 134.8, 136.2, 156.0, 170.5, 172.1; IR (neat) ν_{max}/cm^{-1} 1155, 1253, 1369, 1460, 1501, 1693, 2989; HRMS (ESI) m/z calculated for $C_{28}H_{40}N_4NaO_7S$ $[M+Na]^+$ 599.2510; found 599.2526.

_N_-(Fmoc)-alaninyl-azasulfurylphenylalaninyl-D-phenylalanine _tert_-butyl ester (165)

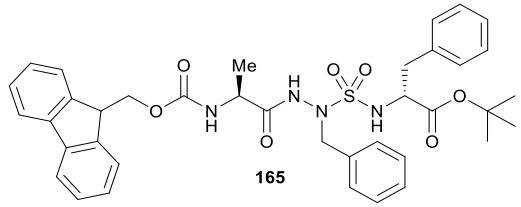

165

Azasulfuryl tripeptide **126** (202 mg, 0.35 mmol) was dissolved in _t_-BuOAc, treated with conc. H_2SO_4 (77.8 μL, 1.40 mmol), stirred at room temperature for 3 h, and the mixture was quenched with saturated $NaHCO_3$ (10 mL). The mixture was extracted with EtOAc (4 x 15 mL).

The organic layers were combined and evaporated to a residue, which was dissolved in water (3.5 mL), cooled in an ice bath, and treated with potassium carbonate (65 mg, 0.47 mmol) followed drop-wise with a solution of Fmoc-OSu (138 mg, 0.14 mmol) in 1,4-dioxane (6.5 mL). After stirring at 0 °C for 1h and at room temperature for 4h, brine was added (25 mL) to the mixture. The layers were separated and the resulting aqueous phase was extracted with EtOAc (3 x 40 mL). The organic phases were combined, dried over $MgSO_4$, filtered and evaporated. The residue was purified by flash chromatography eluting with hexane:EtOAc 7:3 to afford carbamate **165** as a solid (123 mg, 53%): R_f 0.33 (hexane:EtOAc 7:3); mp 77 °C; $[\alpha]^{20}_D$ −38.5° ($CHCl_3$, *c* 1.00); ^{1}H NMR ($CDCl_3$, 400 MHz) δ 1.16 (3H, d, *J* = 6.2), 1.41 (9H, s), 3.10-3.15 (1H, m), 3.15-3.20 (1H, m), 4.05-4.10 (1H, m), 4.15 (1H, t, *J* = 6.4), 4.25-4.35 (2H, m), 4.45-4.65 (3H, m), 5.29 (1H, d, *J* = 6.9), 5.75 (1H, d, *J* = 6.6), 7.20-7.35 (12H, m), 7.40 (2H, t, *J* = 7.2), 7.50-7.60 (2H, m), 7.76 (2H, d, *J* = 7.6), 8.00 (1H, s); ^{13}C NMR ($CDCl_3$, 100 MHz) δ 18.3, 28.2, 39.1, 47.3, 49.4, 55.3, 57.6, 67.6, 83.3, 120.3, 125.4, 127.28, 127.38, 127.41, 128.02, 128.05, 128.56, 128.59, 128.8, 129.7, 130.3, 134.7, 136.2, 141.6, 143.9, 144.2, 156.3, 170.5, 171.7; IR (neat) ν_{max}/cm^{-1} 1155, 1252, 1369, 1454, 1502, 1703, 3263; HRMS (ESI) m/z calculated for $C_{38}H_{43}N_4O_7S$ $[M+H]^+$ 699.2847; found 699.2861.

_N_-(Fmoc)-alaninyl-azasulfurylphenylalaninyl-D-phenylalanine (128)

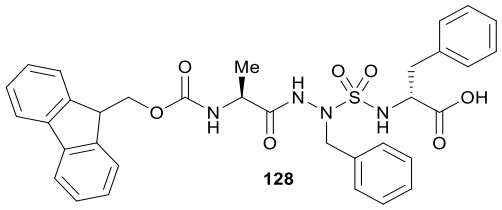

128

Starting from *tert*-butyl ester **165** (95 mg, 0.14 mmol), acid **128** was synthesized as described for **127**. The volatiles were evaporated to afford **128** as a white powder (86 mg, 98%): mp 98 °C; $[\alpha]^{20}_D$ –31.7° ($CHCl_3$, *c* 1.05); ^{1}H NMR ($CDCl_3$, 400 MHz) δ 0.70-0.90 (3H, m), 3.10-3.30 (2H, m) 3.90-4.15 (3H, m), 4.15-4.25 (1H, m), 4.25-4.35 (1H, m), 4.55-4.65 (1H, m), 4.65-4.75 (1H, m), 5.75-5.85 (1H, br), 5.85-6.00 (1H, br), 6.70-7.50 (17H, m), 7.60-7.75 (2H, m), 8.48 (1H, br); ^{13}C NMR ($CDCl_3$, 100 MHz) δ 17.2, 39.0, 47.1, 49.4, 55.5, 57.2, 67.8, 120.2, 125.4, 127.32, 127.39, 128.1, 128.6, 128.7, 129.8, 130.3, 134.2, 135.7, 141.5, 143.7, 144.1,

157.0, 172.9, 173.5; IR (neat) ν_{max}/cm^{-1} 1165, 1252, 1353, 1454, 1520, 1694, 3299; HRMS (ESI) m/z calculated for $C_{34}H_{35}N_4O_7S$ $[M+H]^+$ 643.2221; found 643.2231.

Scheme 3. Synthesis of *N*-(Fmoc)-alaninyl-azasulfurylglycinyl-D-phenylalanine (136)

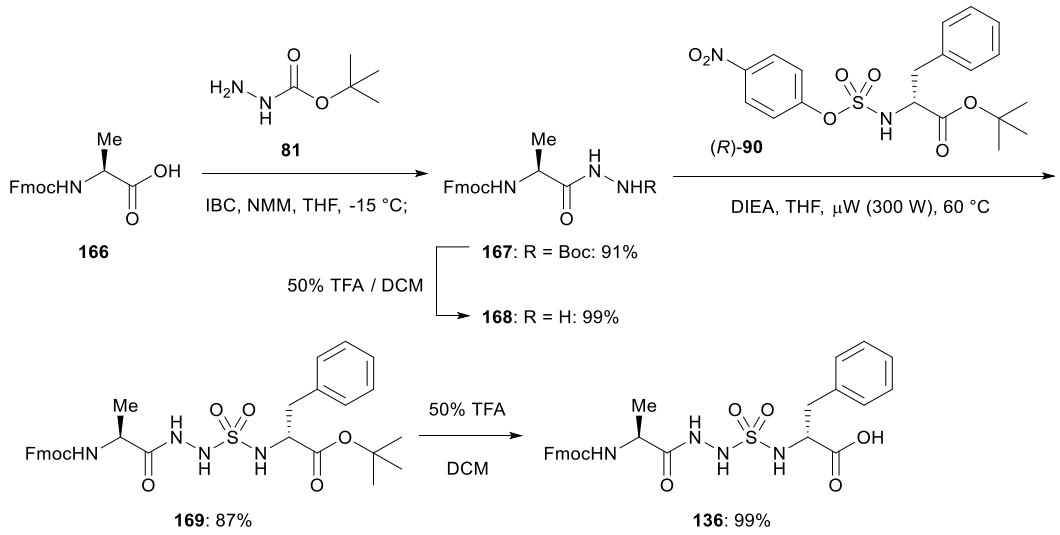

***N*-(Fmoc)-alanine *N*-(Boc)-hydrazide (167)**

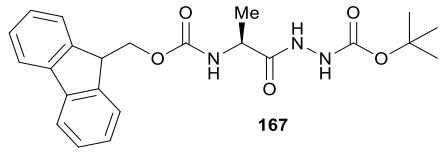

Starting from Fmoc-alanine (**166**, 1.87 g, 6.00 mmol), *iso*-butyl chloroformate (780 μL, 6.00 mmol), 4-methylmorpholine (825 μL, 7.50 mmol) and *tert*-butyl carbazate (**81**, 0.66 g, 5.00 mmol) in dry THF (35 mL), hydrazide **167** was synthesized as described for **124**. The volatiles were evaporated and the residue was dissolved in DCM (100 mL), washed with water (2 x 100 mL), dried over $MgSO_4$, filtered and evaporated. The residue was purified by flash chromatography eluting with hexane:EtOAc 1:1 to afford azadipeptide **167** as a solid (1.94 g, 91%): R_f 0.32 (hexane:EtOAc 1:1); mp 73 °C; $[\alpha]^{20}_D$ –23.9° ($CHCl_3$, *c* 1.04); ^{1}H NMR ($CDCl_3$, 400 MHz) δ 1.35-1.50 (12H, m), 4.10-4.20 (1H, m), 4.30-4.40 (3H, m), 5.79 (1H, br), 6.82 (1H, br), 7.20-7.30 (2H, m), 7.30-7.40 (2H, m), 7.50-7.60 (2H, m), 7.70-7.80 (2H, m), 8.64 (1H, br); ^{13}C NMR ($CDCl_3$, 100 MHz) δ 18.7, 28.4, 47.3, 49.3, 67.5, 82.1, 120.3, 125.4, 127.4, 128.0,

141.6, 144.0, 155.7, 156.5, 172.6; IR (neat) ν_{max}/cm^{-1} 1161, 1245, 1368, 1450, 1531, 1695, 2979, 3290; HRMS (ESI) m/z calculated for $C_{23}H_{27}N_3NaO_5$ $[M+Na]^+$ 448.1842; found 448.1836.

_N_-(Fmoc)-alanine hydrazide (168)

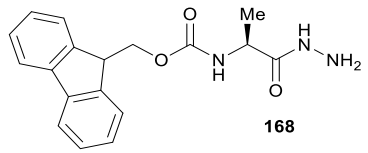

168

_N_-(Boc)-hydrazide **168** (399 mg, 0.94 mmol) was treated with TFA:DCM 1:1 (1 mL) at room temperature for 1h. The volatiles were evaporated, the residue was dissolved in DCM and co-evaporated several times to remove TFA. The residue was partitioned between sat. $NaHCO_3$ (20 mL) and $CHCl_3$ (20 mL), and the aqueous phase was extracted with $CHCl_3$ (4 x 20 mL). The combined organic layers were dried over $MgSO_4$, filtered and evaporated to afford **168** as a solid (302 mg, 99%), that was used for the next step without further purification: R_f 0.20 (hexane:EtOAc 3:7); mp 141 °C; $[\alpha]^{20}_D$ –15.3° (THF, _c_ 0.68); ^{1}H NMR (DMSO-d_6, 400 MHz) δ 1.24 (3H, d, _J_ = 7.1), 4.00-4.10 (1H, m), 4.20-4.35 (5H, m), 7.30-7.40 (2H, m), 7.45 (2H, t, _J_ = 7.2), 7.53 (1H, d, _J_ = 7.8), 7.77 (2H, d, _J_ = 6.8), 7.92 (2H, d, _J_ = 7.5), 9.11 (1H, s); ^{13}C NMR (DMSO-d_6, 100 MHz) δ 18.4, 46.6, 48.8, 65.6, 120.1, 125.3, 127.1, 127.6, 140.7, 143.8, 143.9, 155.6, 171.8. IR (neat) ν_{max}/cm^{-1} 1104, 1251, 1323, 1381, 1537, 1660, 1655, 1688, 2974, 3303; HRMS (ESI) m/z calculated for $C_{18}H_{19}N_3NaO_3$ $[M+Na]^+$ 348.1319; found 348.1318.

_N_-(Fmoc)-alaninyl-azasulfurylglycinyl-D-phenylalanine _tert_-butyl ester (169)

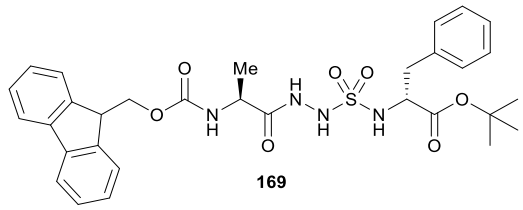

169

Starting from hydrazide **168** (976 mg, 3.00 mmol), sulfamidate (_R_)-**90** (976 mg, 2.31 mmol) and DIEA (517 μL, 3.00 mmol) in THF (10 mL), sulfamide **169** was synthesized as described for **125**. The volatiles were then evaporated and the residue was purified by flash chromatography eluting with hexane:EtOAc 3:2. The collected fractions were combined, and

evaporated to a residue that was dissolved in DCM (25 mL). The organic phase was washed with sat. $NaHCO_3$ (3 x 25 mL), dried over $MgSO_4$, filtered and evaporated to afford **169** as a solid (1.22 g, 87%): R_f 0.24 (hexane:EtOAc 3:2); mp 82 °C; $[\alpha]^{20}_D$ 48.9° ($CHCl_3$, *c* 0.79); ^{1}H NMR ($CDCl_3$, 400 MHz) δ 1.35-1.45 (12H, m), 3.09 (1H, dd, *J* = 7.4, 13.9), 3.15 (1H, dd, *J* = 5.6, 14.0), 4.15-4.25 (1H, m), 4.30-4.45 (4H, m), 5.65 (1H, d, *J* = 7.4), 5.77 (1H, d, *J* = 6.9), 7.20-7.35 (8H, m), 7.42 (2H, t, *J* = 7.4), 7.61 (2H, t, *J* = 7.5), 7.78 (2H, d, *J* = 7.5), 8.64 (1H, s); ^{13}C NMR ($CDCl_3$, 100 MHz) δ 18.2, 28.2, 39.1, 47.3, 49.4, 57.6, 67.6, 83.5, 120.2, 125.4, 127.4, 128.0, 128.7, 130.1, 135.9, 141.6, 143.9, 144.1, 156.5, 171.2, 172.3; IR (neat) ν_{max}/cm^{-1} 1105, 1154, 1251, 1367, 1451, 1523, 1709, 2979, 3065, 3275; HRMS (ESI) m/z calculated for $C_{31}H_{36}N_4NaO_7S$ $[M+Na]^+$ 631.2197; found 631.2187.

_N_-(Fmoc)-alaninyl-azasulfurylglycinyl-D-phenylalanine (136)

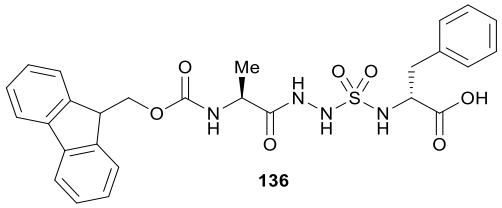

136

Starting from *tert*-butyl ester **169** (150 mg, 0.25 mmol), acid **136** was synthesized as described for **127**. The volatiles were evaporated to afford **136** as a solid (135 mg, 99%): R_f 0.17 (hexane:EtOAc 3:7); mp 185 °C; $[\alpha]^{20}_D$ –15.3° ($CHCl_3$, *c* 0.84); ^{1}H NMR ($CDCl_3$, 400 MHz) δ 1.24 (3H, d, *J* = 6.3), 3.00-3.15 (2H, m), 4.05-4.15 (1H, m), 4.20-4.25 (1H, m), 4.25-4.35 (2H, m), 4.41 (1H, t, *J* = 5.1), 5.78 (1H, br), 5.89 (1H, br), 7.00-7.15 (6H, m), 7.21 (2H, t, *J* = 7.4), 7.32 (2H, t, *J* = 7.4), 7.45-7.60 (2H, m), 7.68 (2H, d, *J* = 7.6), 8.76 (1H, br); ^{13}C NMR ($CDCl_3$, 100 MHz) δ 18.2, 38.8, 47.2, 49.4, 56.9, 67.9, 120.3, 125.4, 127.4, 128.1, 128.9, 130.0, 135.3, 141.5, 143.7, 144.0, 157.0, 173.4, 174.3; IR (neat) ν_{max}/cm^{-1} 1161, 1239, 1261, 1353, 1457, 1525, 1689, 3221; HRMS (ESI) m/z calculated for $C_{27}H_{29}N_4O_7S$ $[M+H]^+$ 553.1752; found 553.1750.

Scheme 4. Synthesis of *N*-(Alloc)-alaninyl-aza(Fmoc)-sulfurylglycinyl-D-phenylalanine (141)

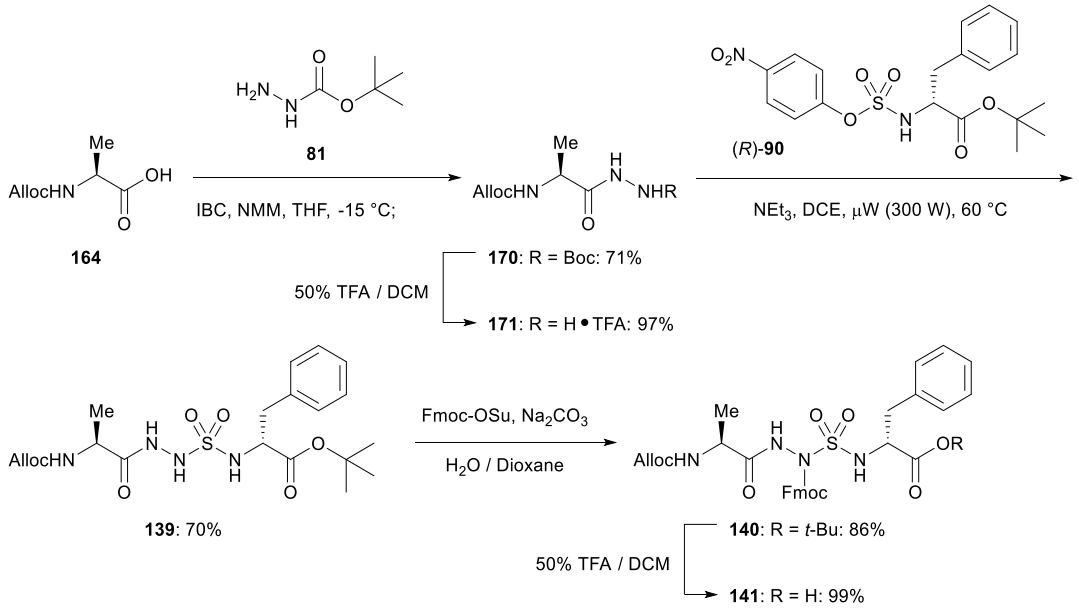

***N*-(Alloc)-alanine *N*-(Boc)-hydrazide (170)**

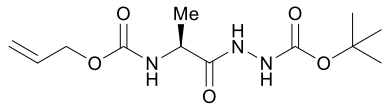

170

Starting from *N*-(Alloc)-alanine (**164**, 2.08 g, 12.0 mmol), *iso*-butyl chloroformate (1.57 mL, 12.0 mmol), 4-methylmorpholine (1.65 mL, 15.0 mmol) and *tert*-butyl carbazate (**81**, 1.32 g, 10.00 mmol) in dry THF (70 mL), hydrazide **170** was synthesized as described for **124**. The volatiles were evaporated and the residue was purified by flash chromatography eluting with hexane:EtOAc 11:9 to afford hydrazide **170** as a solid (2.04 g, 71%): R_f 0.19 (hexane:EtOAc 3:2); mp 54 °C; $[\alpha]^{20}_D$ –36.8° ($CHCl_3$, *c* 1.06); ^{1}H NMR ($CDCl_3$, 400 MHz) δ 1.41 (3H, d, *J* = 7.1), 1.45 (9H, s), 4.25-4.35 (1H, m), 4.50-4.60 (2H, m), 5.21 (1H, dq, *J* = 1.2, 10.4), 5.30 (1H, dq, *J* = 1.5, 17.2), 5.53 (1H, br), 5.80-5.95 (1H, m), 6.69 (1H, br), 8.42 (1H, br); ^{13}C NMR ($CDCl_3$, 100 MHz) δ 18.7, 28.4, 49.2, 66.2, 81.9, 118.2, 132.7, 155.8, 156.4, 172.8; IR (neat) ν_{max}/cm^{-1} 1156, 1236, 1367, 1452, 1501, 1679, 2978, 3279; HRMS (ESI) m/z calculated for $C_{12}H_{21}N_3NaO_5$ $[M+Na]^+$ 310.1373; found 310.1377.

_N_-(Alloc)-alanine hydrazidium trifluoroacetate (171)

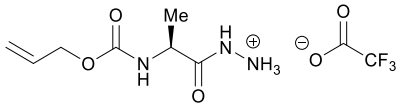

171

_N_-(Boc)-hydrazide **170** (1.44 g, 5.0 mmol) was treated with TFA:DCM 1:1 (5 mL) for 2h at room temperature. The volatiles were evaporated to afford hydrazide salt **171** as an oil (1.49 g, 99%): $[\alpha]^{20}_D$ –66.5° (MeOH, *c* 0.92); ^{1}H NMR (CD_3OD, 400 MHz) showed an 1:1 mixture of hydrazide salt isomers: δ 1.417 (3H, d, *J* = 7.2) [1.419 (3H, d, *J* = 7.2)], 4.20-4.30 (1H, m), 4.50-4.60 (2H, m), 5.20 (1H, dq, *J* = 1.3, 10.5), 5.33 (1H, dq, *J* = 1.4, 17.2), 5.90-6.00 (1H, m); ^{13}C NMR (CD_3OD, 100 MHz) δ 19.2 (18.6) 51.5, 67.5 (67.6), 118.2 (q, J-^{19}F = 287.9), 118.54 (118.60), 135.05 (134.95), 158.9 (159.0), 162.5 (q, J-^{19}F = 36.9), 175.1 (172.2). IR (neat) ν_{max}/cm^{-1} 1129, 1179, 1201, 1249, 1450, 1521, 1655, 3270; HRMS (ESI) m/z calculated for $C_7H_{14}N_3O_3$ $[M]^+$ 188.1030; found 188.1033.

_N_-(Alloc)-alaninyl-azasulfurylglycinyl-D-phenylalanine *tert*-butyl ester (139)

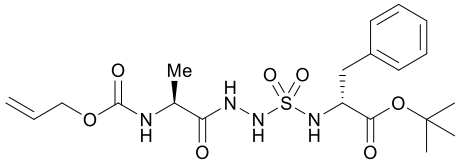

139

Starting from hydrazide salt **171** (563 mg, 1.87 mmol), sulfamidate (*R*)-**90** (718 mg, 1.70 mmol) and NEt_3 (496 µL, 3.57 mmol) in DCE (7.5 mL), sulfamide **139** was synthesized as described for **125**. The residue was purified by flash chromatography eluting with hexane:EtOAc 3:2. The collected fractions were evaporated to a residue, which was dissolved in DCM (25 mL), washed with sat. $NaHCO_3$ (3 x 25 mL), dried over $MgSO_4$, filtered and evaporated to afford sulfamide **139** as a solid (557 mg, 70%): R_f 0.33 (hexane:EtOAc 3:2); mp 52 °C; $[\alpha]^{20}_D$ –70.9° ($CHCl_3$, *c* 1.00); ^{1}H NMR ($CDCl_3$, 400 MHz) δ 1.36 (3H, d, *J* = 7.1), 1.39 (9H, s), 3.06 (1H, dd, *J* = 6.6, 13.9), 3.11 (1H, dd, *J* = 5.5, 13.9), 4.20-4.30 (2H, m), 4.45-4.60 (2H, m), 5.19 (1H, dd, *J* = 1.2, 10.4), 5.27 (1H, dd, *J* = 1.2, 17.2), 5.51 (1H, d, *J* = 6.9), 5.64 (1H, d, *J* = 7.8), 5.80-5.95 (1H, m), 7.20-7.30 (6H, m), 8.56 (1H, s); ^{13}C NMR ($CDCl_3$,

100 MHz) δ 18.2, 28.2, 39.1, 49.5, 57.6, 66.5, 83.5, 118.4, 127.4, 128.7, 130.1, 132.7, 135.9, 156.4, 171.2, 172.4; IR (neat) ν_{max}/cm^{-1} 1150, 1249, 1364, 1454, 1515, 1688, 2977, 3219; HRMS (ESI) m/z calculated for $C_{20}H_{30}N_4NaO_7S$ $[M+Na]^+$ 493.1727; found 493.1728.

_N_-(Alloc)-alaninyl-aza(Fmoc)-sulfurylglycinyl-D-phenylalanine *tert*-butyl ester (140)

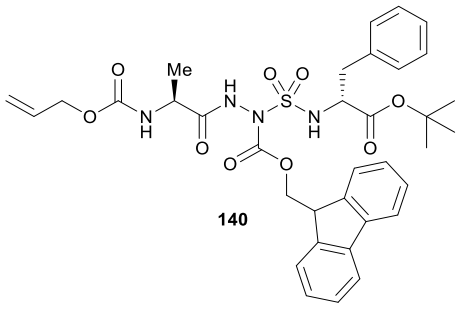

Sodium carbonate (286 mg, 2.70 mmol) and sulfamide **139** (725 mg, 1.54 mmol) were dissolved in a 1:1 mixture of water and 1,4-dioxane (25 mL) and then cooled down to 0 °C. The mixture was treated with a solution of Fmoc-OSu (780 mg, 2.31 mmol) in dioxane (12.5 mL), stirred at 0 °C for 1 h, and allowed to warm to room temperature with stirring for 18 h. Brine (50 mL) was added to the mixture. The aqueous phase was extracted with EtOAc (3 x 100 mL). The organic phases were combined, dried over $MgSO_4$, filtered and evaporated to a residue, which was purified by two separate flash chromatography columns eluting first with hexane:EtOAc 3:1 and then with DCM:EtOAc 19:1. Evaporation of the collected fractions afforded fluorenyl carbazate **140** (913 mg, 86%) as a solid: R_f 0.27 (hexane:EtOAc 3:1), mp 83 °C; $[\alpha]^{20}_D$ –14.6° (MeOH, c 0.98); ^{1}H NMR (CD_3OD, 300 MHz) showed an 7:50 mixture of carbazate isomers: δ 1.32 (9H, s), [1.36, (9H, s)], 1.34 (3H, d, *J* = 7.1), [1.43 (3H, d, *J* = 7.1)], 2.90-3.10 (2H, m), 4.20-4.40 (3H, m), 4.40-4.60 (4H, m), 5.13 (1H, d, *J* = 10.7), [5.19 (1H, d, *J* = 10.7)] 5.26 (1H, d, *J* = 16.4), [5.32 (1H, d, *J* = 16.4)], 5.80-6.00 (1H, m), 7.15-7.35 (7H, m), 7.40 (2H, t, *J* = 7.4), 7.60-7.70 (2H, m), 7.81 (2H, d, *J* = 7.4); ^{13}C NMR (CD_3OD, 75 MHz): δ 19.1, 28.97 (29.01), 40.6 (40.8), 48.6, 51.2, 60.2 (60.4), 67.5, 71.3 (71.8), 83.9 (84.3), 118.6, 121.8 (121.9), 127.10 (127.17), 127.3 (127.4), 128.7, 129.2, 129.8, 130.2, 131.6 (131.7), 135.04 (135.10), 138.4 (138.5), 143.31 (143.37), 145.5 (145.6), 145.6 (145.7), 154.2, 172.4 (172.7), 175.0; IR (neat) ν_{max}/cm^{-1} 1152, 1178, 1226, 1316, 1369, 1384, 1450, 1498, 1695, 2978, 3292; HRMS (ESI) m/z calculated for $C_{35}H_{40}N_4NaO_9S$ $[M+Na]^+$ 715.2408; found 715.2424.

_N_-(Alloc)-alaninyl-aza(Fmoc)-sulfurylglycinyl-D-phenylalanine (141)

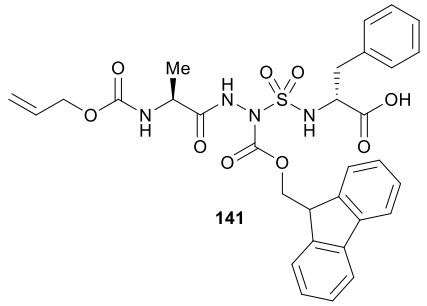

141

Starting from *tert*-butyl ester **140** (0.750 g, 1.1 mmol), acid **141** was synthesized as described for **127**. The volatiles were evaporated to afford **141** as a solid (0.682 g, 99%): $[\alpha]^{20}_{D}$ –36.8° (MeOH, *c* 0.98); ^{1}H NMR (CD_3OD, 300 MHz) showed an 9:20 mixture of carbazate isomers: δ 1.34 (3H, d, *J* = 7.1) [1.42 (3H, d, *J* = 7.1)], 3.00-3.20 (2H, m), 4.20-4.40 (3H, m), 4.40-4.55 (3H, m), 4.55-4.70 (1H, m), 5.13 (1H, d, *J* = 10.8) [5.18 (1H, d, *J* = 10.8)], 5.32 (1H, d, *J* = 15.7) [5.37 (1H, d, *J* = 15.7)], 5.80-6.00 (1H, m), 7.15-7.35 (7H, m), 7.40 (2H, t, *J* = 7.4), 7.60-7.70 (2H, m), 7.80 (2H, d, *J* = 7.4); ^{13}C NMR (CD_3OD, 75 MHz): δ 19.1 (19.2), 40.4, 48.54 (48.63), 51.17 (51.41), 59.9, 67.5, 71.4 (71.8), 118.6, 121.8 (121.9), 127.2 (127.4), 128.7, 129.2, 129.8, 130.2, 131.6, 135.1, 138.4 (138.5), 143.3 (143.4), 145.6 (145.7), 154.1, 158.7, 174.8, 175.0. IR (neat) ν_{max}/cm^{-1} 1178, 1220, 1315, 1384, 1449, 1519, 1543, 1643, 1688, 1737, 3071, 3289; HRMS (ESI) m/z calculated for $C_{31}H_{33}N_4O_9S$ $[M+H]^+$ 637.1963; found 637.1970.

Scheme 5. Synthesis of *N*-(Alloc)-*N*^{in}-(Boc)-D-tryptophan hydrazide (150)

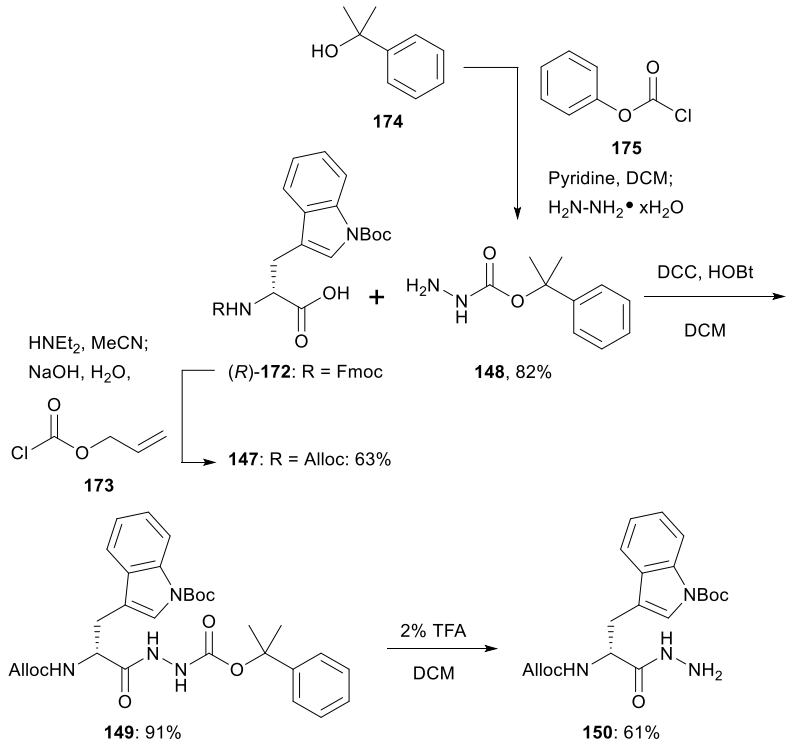

***N*-(Alloc)-*N*^{in}-(Boc)-D-tryptophan (147)**

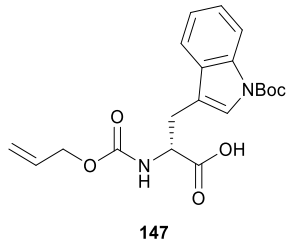

N-(Fmoc)-*N*^{in}-(Boc)-D-tryptophan [(*R*)-**172**, 1.00 g, 1.9 mmol] was dissolved in MeCN (20 mL) and treated with diethylamine (5.87 mL, 57 mmol) for 1.5 h. The volatiles were evaporated and water (25 mL) was added. The product in the aqueous phase was washed with Et_2O (2 x 25 mL). Sodium hydroxide (1 M, 2 mL) was then added to the aqueous phase. Next, allyl chloroformate (**173**, 0.301 mL, 2.82 mmol) and sodium hydroxide (2 M, 1 mL) were added while stirring in 4 portions every 30 min (ie. 0.075 mL for allyl chloroformate and 0.250 mL for 2M sodium hydroxide). After the last addition, the reaction mixture was allowed to stir for an additional 30 min. After completion, the aqueous phase was washed with Et_2O (2 x 25 mL) and

then acidified using 1M HCl until pH is approx. 1. The product was finally extracted with Et_2O (3 x 50 mL). The organic layers were combined, dried over $MgSO_4$, filtered and evaporated to afford acid **147** (0.46 g, 63 %) as a solid: *Rf* 0.21 (MeOH:DCM 1:19); mp 73 °C; $[\alpha]^{20}_D$ –42.0° ($CHCl_3$, *c* 1.00); ^{1}H NMR ($CDCl_3$, 400 MHz) δ 1.66 (9H, s), 3.21 (1H, dd, *J* = 6.4, 14.8), 3.33 (1H, dd, *J* = 5.1, 14.9), 4.50-4.60 (2H, m), 4.70-4.80 (1H, m), 5.19 (1H, d, *J* = 10.2), 5.27 (1H, d, *J* = 17.4), 5.38 (1H, d, *J* = 7.9), 5.80-5.90 (1H, m), 7.22 (1H, dt, *J* = 0.8, 7.5), 7.31 (1H, dt, *J* = 1.0, 7.7), 7.48 (1H, s), 7.54 (1H, d, *J* = 7.8), 8.09 (1H, d, *J* = 7.3), 9.89 (1H, br); ^{13}C NMR ($CDCl_3$, 100 MHz) δ 27.9, 28.5, 54.1, 66.3, 84.2, 115.1, 115.6, 118.3, 119.2, 123.0, 124.6, 124.9, 130.7, 132.7, 135.6, 150.0, 156.2, 176.2; IR (neat) ν_{max}/cm^{-1} 1149, 1253, 1368, 1452, 1521, 1712, 2981; HRMS (ESI) m/z calculated for $C_{20}H_{24}N_2NaO_6$ $[M+Na]^+$ 411.1527; found 411.1532.

Cumyl carbazate (148)

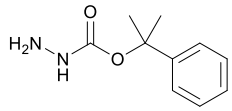

148

2-phenyl-2-propanol (**174**, 408 mg, 3 mmol, prepared according to reference 161) was dissolved in DCM (5 mL) and pyridine (0.36 mL, 4.5 mmol) was added. A solution of phenyl chloroformate (**172**, 0.51 mL, 4.06 mmol) in DCM (5 mL) was then added drop-wise at 0 °C. The cold water bath was allowed to slowly warm at room temperature and let stirring at room temperature for 18 h. The reaction mixture was then diluted with DCM (50 mL) and washed with 1M HCl (50 mL), 1M NaOH (50 mL) and water (50 mL). The organic phase was dried with $MgSO_4$, filtered and evaporated to a residue. Hydrazine hydrate (2 mL) was added and it was stirred at room temperature for 18 h. After completion, the mixture was diluted with water (25 mL) and the product was extracted with EtOAc (3 x 25 mL). The organic layers were combined and washed with 1M NaOH (50 mL) and water (50 mL). It was then dried over $MgSO_4$, filtered and evaporated. The crude was finally purified by flash chromatography eluting with EtOAc:Hexane 3:2 + 1% NEt_3 to afford carbazate **148** (479 mg, 82 %) as an oil: *Rf* 0.19 (EtOAc:Hexane 3:2 + 1% NEt_3); ^{1}H NMR ($CDCl_3$, 400 MHz) δ 1.82 (6H, s), 3.69 (2H, br), 6.17 (1H, br), 7.25-7.30 (1H, m), 7.35-7.45 (4H, m); ^{13}C NMR ($CDCl_3$, 100 MHz) δ 29.2, 82.0,

124.6, 127.4, 128.5, 146.2, 157.7; IR (neat) ν_{max}/cm^{-1} 1139, 1266, 1365, 1495, 1632, 1707, 2981, 3326; HRMS (ESI) m/z calculated for $C_{10}H_{14}N_2NaO_2$ $[M+Na]^+$ 217.0948; found 217.0945.

_N_-(Alloc)-N^{in}-(Boc)-D-tryptophan _N_-(Coc)-hydrazide (149)

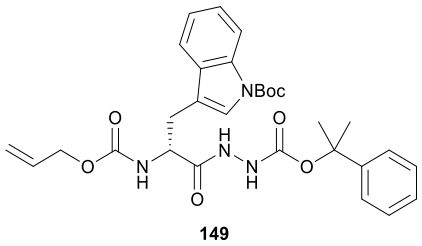

149

HOBt (172 mg, 1.27 mmol) followed by DCC (262 mg, 1.27 mmol) were added to a solution of acid **147** (450 mg, 1.16 mmol) in DCM (5 mL) and stirred for 30 min. Cumyl carbazate (**148**, 225 mg, 1.16 mmol) in DCM (1 mL) was then added. The reaction mixture was stirred at room temperature for 18 h. After completion, the mixture was filtered and the filtrate was evaporated. Cold EtOAc (15 mL) was added and the mixture was let standing for 15 min, filtered again and evaporated to a residue. The crude was finally purified by flash chromatography eluting with 3:7 EtOAc/hexane + 1% NEt_3 to afford *N*-(Coc) hydrazide **149** (595 mg, 91 %) as a solid: *Rf* 0.27 (3:7 EtOAc/hexane + 1% NEt_3); mp 84 °C; $[\alpha]^{20}_D$ –0.3° ($CHCl_3$, *c* 1.03); ^1H NMR ($CDCl_3$, 400 MHz) δ 1.64 (9H, s), 1.77 (6H, s), 3.00-3.10 (1H, m), 3.18 (1H, dd, *J* = 6.4, 14.9), 4.40-4.50 (2H, m), 4.50-4.60 (1H, m), 5.13 (1H, d, *J* = 10.2), 5.19 (1H, d, *J* = 17.5), 5.54 (1H, d, *J* = 8.0), 5.75-5.85 (1H, m), 6.70-6.80 (1H, br), 7.15-7.25 (2H, m), 7.25-7.40 (5H, m), 7.45 (1H, s), 7.53 (1H, d, *J* =7.7), 8.05-8.15 (1H, br), 8.09 (1H, d, *J* = 7.9); ^{13}C NMR ($CDCl_3$, 100 MHz) δ 28.1, 28.5, 29.0, 53.6, 66.4, 83.3, 84.0, 115.4, 115.6, 118.3, 119.2, 123.0, 124.6, 124.9, 127.4, 128.6, 130.5, 132.6, 135.8, 145.7, 149.9, 154.8, 156.4, 171.0; IR (neat) ν_{max}/cm^{-1} 1152, 1227, 1252, 1367, 1451, 1695, 3268; HRMS (ESI) m/z calculated for $C_{30}H_{36}N_4NaO_7$ $[M+Na]^+$ 587.2476; found 587.2484.

_N_-(Alloc)-N^{in}-(Boc)-D-tryptophan hydrazide (150)

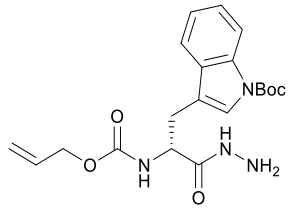

150

N-(Coc)-hydrazide **149** (510 mg, 0.90 mmol) was treated with 2% of TFA in DCM (5 mL) for 1.5 h. The volatiles were then evaporated to a residue. The crude was purified by flash chromatography eluting with a gradient of 50-80% EtOAc:Hexanes + 2% NEt_3 to afford hydrazide **150** (220 mg, 61 %) as a solid: *Rf* 0.13 (EtOAc:Hexane 3:2 + 2% NEt_3); mp 79 °C; $[\alpha]^{20}_D$ –7.8° ($CHCl_3$, *c* 1.03); ^{1}H NMR ($CDCl_3$, 400 MHz) δ 1.65 (9H, s), 3.14 (2H, d, *J* = 6.8), 3.78 (2H, br), 4.40-4.50 (1H, m), 4.51 (2H, d, *J* = 5.7), 5.18 (1H, d, *J* = 10.4), 5.25 (1H, d, *J* = 17.2), 5.66 (1H, d, *J* = 7.2), 5.80-5.90 (1H, m), 7.20 (1H, t, *J* = 7.5), 7.30 (1H, t, *J* = 7.4), 7.45 (1H, s), 7.54 (1H, d, *J* = 8.2), 7.55 (1H, s), 8.09 (1H, d, *J* = 7.8); ^{13}C NMR ($CDCl_3$, 100 MHz) δ 28.5, 28.6, 54.0, 664, 84.2, 115.5, 115.7, 118.4, 119.1, 123.0, 124.6, 125.0, 130.4, 132.7, 135.8, 149.9, 156.2, 172.1; IR (neat) ν_{max}/cm^{-1} 1149, 1252, 1367, 1453, 1524, 1722, 2983, 3570; HRMS (ESI) m/z calculated for $C_{20}H_{26}N_4NaO_5$ $[M+Na]^+$ 425.1795; found 425.1799.

Scheme 6. Synthesis of *N*-(Alloc)-*N*^{in}-(Boc)-D-tryptophanyl-aza(Fmoc)-sulfurylglycinyl-*N*^{in}-(Boc)-tryptophane 2,4-dimethoxybenzyl ester (153)

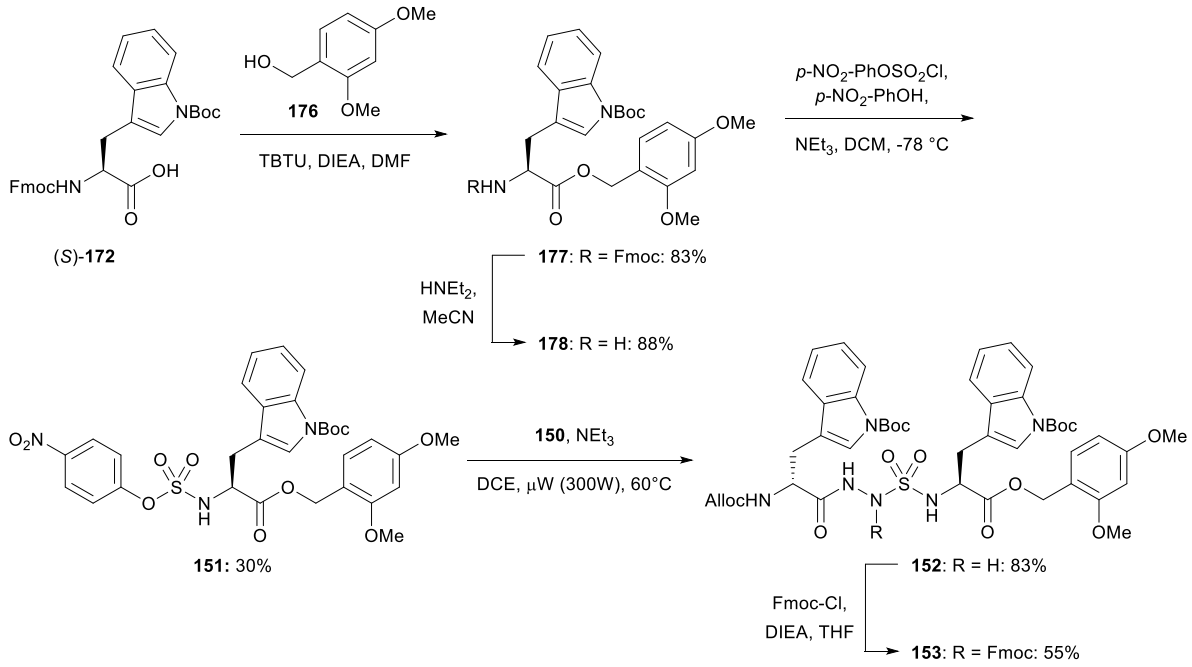

***N*-(Fmoc)-*N*^{in}-(Boc)-tryptophan 2,4-dimethoxybenzyl ester (177)**

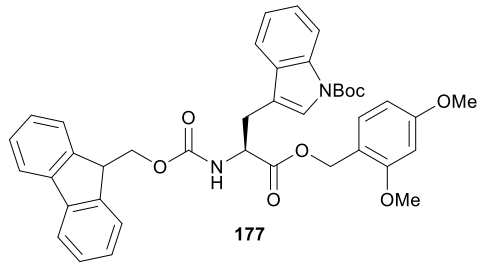

In an flamed-dried round-bottomed flask equipped with a magnetic stir bar, *N*-(Fmoc)-*N*^{in}-(Boc)-L-tryptophan [(*S*)-**172**, (2.05 g, 3.89 mmol), TBTU (1.25 g, 3.89 mmol) and DIEA (1.29 mL, 7.78 mmol) were dissolved in DMF (8 mL) and the resulting mixture was stirred at rt for 30 min under argon atmosphere. 2,4-dimethoxybenzyl alcohol (**176**, 0.72 g, 4.2 mmol, prepared according to reference 162) in DMF (2 mL) was then injected into the reaction mixture via syringe and stirring was continued at room temperature for 4h. The reaction mixture was diluted with DCM (250 mL) and the resulting mixture was washed with water (2 x 100 mL). The organic phase was dried over $MgSO_4$, filtered and evaporated to a residue. It was then

purified by flash chromatography eluting with EtOAc:Hexane 1:4 to afford ester **177** (2.2 g, 83 %) as a solid: *Rf* 0.29 (EtOAc:Hexane 1:4); mp 73 °C; $[\alpha]^{20}_{D}$ –2.1° ($CHCl_3$, *c* 1.00); ^{1}H NMR ($CDCl_3$, 400 MHz) δ 1.66 (9H, s), 3.26 (1H, dd, *J* = 5.9, 15.1), 3.31 (1H, dd, *J* = 5.6, 14.8), 3.804 (3H, s), 3.810 (3H, s), 4.21 (1H, t, *J* = 7.2), 4.20-4.30 (2H, m), 4.75-4.85 (1H, m), 5.14 (2H, s), 5.47 (1H, d, *J* = 8.1), 6.43 (1H, s), 6.45 (1H, s), 7.12 (1H, d, *J* = 8.0), 7.24 (1H, t, *J* = 7.3), 7.25-7.45 (5H, m), 7.46 (1H, s), 7.55-7.60 (3H, m), 7.76 (2H, d, *J* = 7.4), 8.12 (1H, d, *J* = 7.2); ^{13}C NMR ($CDCl_3$, 100 MHz) δ 28.2, 28.5, 47.4, 54.6, 55.67, 55.70, 63.5, 67.5, 83.9, 98.9, 104.4, 115.3, 115.6, 116.0, 119.2, 120.3, 123.0, 124.6, 124.8, 125.5, 127.4, 128.0, 131.0, 131.9, 135.6, 141.6, 144.1, 144.2, 149.9, 156.0, 159.4, 161.9, 171.9; IR (neat) ν_{max}/cm^{-1} 1152, 1252, 1369, 1451, 1509, 1616, 1722, 2937; HRMS (ESI) m/z calculated for $C_{40}H_{40}N_2NaO_8$ $[M+Na]^+$ 699.2677; found 699.2676.

N^{in}-(Boc)-tryptophan 2,4-dimethoxybenzyl ester (178)

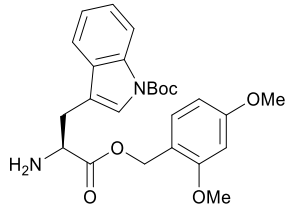

178

Ester **177** (0.92 g, 1.36 mmol) was dissolved in MeCN (16 mL) and diethylamine (4 mL, 38.8 mmol) was added to the solution. It was stirred at room temperature for 1.5 h. After completion of the reaction, the volatiles were evaporated to a residue and the crude was purified by flash chromatography eluting with EtOAc:Hexane 2:3 + 2% NEt_3 to afford amine **178** (542 mg, 88 %) as an oil: *Rf* 0.26 (EtOAc:Hexane 2:3 + 2% NEt_3); $[\alpha]^{20}_{D}$ –9.5° ($CHCl_3$, *c* 1.31); ^{1}H NMR ($CDCl_3$, 400 MHz) δ 1.60 (2H, s), 1.66 (9H, s), 2.97 (1H, dd, *J* = 7.7, 14.4), 3.18 (1H, dd, *J* = 5.0, 14.5), 3.807 (3H, s), 3.814 (3H, s), 3.81-3.90 (1H, m), 5.12 (2H, s), 6.40-6.50 (2H, m), 7.13 (1H, d, *J* = 7.9), 7.22 (1H, t, *J* = 7.4), 7.29 (1H, t, *J* = 7.3), 7.46 (1H, s), 7.55 (1H, d, *J* = 7.8), 8.12 (1H, d, *J* = 6.7); ^{13}C NMR ($CDCl_3$, 100 MHz) δ 28.5, 30.8, 54.9, 55.71, 55.75, 62.8, 83.8, 98.9, 104.4, 115.6, 116.5, 116.6, 119.3, 122.8, 124.5, 124.8, 130.9, 131.8, 135.8, 149.9, 159.4, 161.7, 175.5; IR (neat) ν_{max}/cm^{-1} 1158, 1256, 1369, 1452, 1510, 1615, 1725, 3057, 3556; HRMS (ESI) m/z calculated for $C_{25}H_{31}N_2O_6$ $[M+H]^+$ 455.2177; found 455.2168.

4-nitrophenyl sulfamidate of *N*^{in}-(Boc)-tryptophan 2,4-dimethoxybenzyl ester (151)

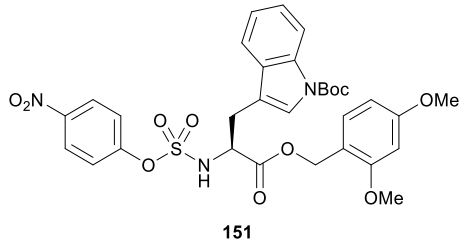

151

4-Nitrophenyl chlorosulfate (475 mg, 2.00 mmol, prepared according to reference 91) was dissolved in dry DCM (5 mL) and treated drop-wise with a solution of amine **178** (454 mg, 1.00 mmol), 4-nitrophenol (417 mg, 3.00 mmol) and triethylamine (0.83 mL, 6.00 mmol) in dry DCM (25 mL) at –78 °C. It was stirred at –78 °C for 1.5 h. The reaction mixture was then allowed to warm at room temperature and stirring was continued for 1 h. The reaction mixture was evaporated to a residue and the crude was purified by flash chromatography eluting with Et_2O:petroleum ether 2:3 to afford fractions contaminated with 4-nitrophenol. The necessary fractions containing the product were evaporated and redissolved in DCM (25 mL), washed with sat. $NaHCO_3$ (aq.) (3 x 25 mL), dried over $MgSO_4$, filtered and evaporated to afford sulfamidate **151** (197 mg, 30 %) as a solid: *Rf* 0.30 (Et_2O:petroleum ether 2:3); mp 70 °C; $[\alpha]^{20}_D$ 19.1° ($CHCl_3$, *c* 0.97); ^{1}H NMR ($CDCl_3$, 400 MHz) δ 1.69 (9H, s), 3.26 (1H, dd, *J* = 5.4, 14.8), 3.32 (1H, dd, *J* = 5.0, 14.8), 3.82 (3H, s), 3.84 (3H, s), 4.55-4.65 (1H, m), 5.12 (1H, d, *J* = 11.6), 5.17 (1H, d, *J* = 11.6), 5.60-5.70 (1H, br), 6.40-6.50 (2H, m), 7.12 (1H, d, *J* = 8.0), 7.20-7.30 (3H, m), 7.34 (1H, dt, *J* = 1.1, 7.2), 7.48 (1H, s), 7.52 (1H, d, *J* = 7.8), 8.05-8.15 (3H, m); ^{13}C NMR ($CDCl_3$, 100 MHz) δ 28.5, 29.0, 55.73, 55.79, 57.4, 64.4, 84.4, 98.94, 104.5, 113.9, 115.4, 115.7, 119.1, 122.5, 123.1, 125.1, 125.7, 130.4, 132.4, 135.6, 146.2, 149.8, 154.6, 159.6, 162.2, 170.7; IR (neat) ν_{max}/cm^{-1} 1149, 1257, 1346, 1369, 1451, 1525, 1589, 1615, 1729; HRMS (ESI) m/z calculated for $C_{31}H_{33}N_3NaO_{11}S$ $[M+Na]^+$ 678.1728; found 678.1711.

N-(Alloc)-N^{in}-(Boc)-D-tryptophanyl-azasulfurylglycinyl-N^{in}-(Boc)-tryptophan 2,4-dimethoxybenzyl ester (152)

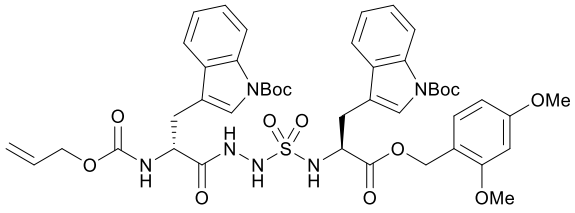

152

Starting from hydrazide **150** (167 mg, 0.42 mmol), sulfamidate **151** (210 mg, 0.32 mmol) and NEt_3 (57.9 μL, 0.42 mmol) in DCE (3.5 mL), sulfamide **152** was synthesized as described for **125**. The crude was purified by flash chromatography eluting first with EtOAc:Hexane 1:4 to remove 4-nitrophenol and then with EtOAc:Hexane 7:13 to afford sulfamide **152** (166 mg, 56%) as a solid: *Rf* 0.21 (EtOAc:Hexane 3:7); mp 109 °C; $[\alpha]^{20}_D$ 35.5° ($CHCl_3$, *c* 1.10); ^{1}H NMR ($CDCl_3$, 500 MHz) δ 1.62 (9H, s), 1.65 (9H, s), 3.10-3.20 (4H, m), 3.74 (3H, s), 3.77 (3H, s), 4.35-4.40 (1H, m), 4.45-4.50 (1H, m), 4.50-4.55 (2H, m), 5.01 (2H, s), 5.15 (1H, d, *J* = 10.5), 5.23 (1H, d, *J* = 17.2), 5.54 (1H, br), 5.62 (1H, d, *J* = 7.7), 5.80-5.90 (1H, m), 6.30-6.40 (2H, m), 6.92 (1H, s), 6.97 (1H, d, *J* = 7.8), 7.20-7.25 (2H, m), 7.25-7.30 (2H, m), 7.49 (1H, s), 7.52 (1H, d, *J* = 7.8), 7.55 (1H, s), 7.62 (1H, d, *J* = 7.3), 7.97 (1H, br), 8.05-8.10 (2H, m); ^{13}C NMR ($CDCl_3$, 125 MHz) δ 28.40, 28.49, 28.50, 28.7, 53.9, 55.67, 55.75, 56.5, 64.0, 66.4, 84.0, 84.3, 98.8, 104.4, 114.7, 115.3, 115.55, 115.58, 115.63, 118.4, 119.3, 119.4, 122.9, 123.1, 124.8, 124.9, 125.0, 125.3, 130.5, 130.7, 132.0, 132.7, 135.7, 149.9, 150.2, 156.3, 159.4, 162.0, 170.8, 172.6; IR (neat) ν_{max}/cm^{-1} 1152, 1255, 1368, 1452, 1511, 1615, 1717, 2941, 3296; HRMS (ESI) m/z calculated for $C_{45}H_{54}N_6NaO_{13}S$ $[M+Na]^+$ 941.3362; found 941.3373.

_N_-(Alloc)-_N^in^_-(Boc)-D-tryptophanyl-aza(Fmoc)-sulfurylglycinyl-_N^in^_-(Boc)-tryptophan 2,4-dimethoxybenzyl ester (153)

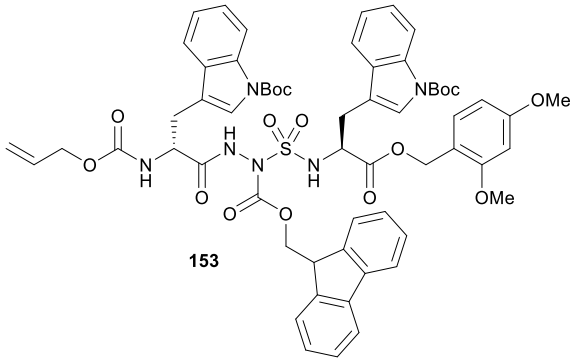

Sulfamide **152** (50 mg, 0.054 mmol) was dissolved in THF (1 mL). DIEA (9.89 µL, 0.060 mmol) and Fmoc chloride (15.5 mg, 0.060 mmol) were added and the mixture was stirred at room temperature for 24 h. The THF was evaporated and the crude was purified by flash chromatography eluting with a gradient of 50-75% Et2O:petroleum ether to afford carbazate **153** (34 mg, 0.0298 mmol, 55 %) as a solid: *Rf* 0.54 (3:1 Et_2O:petroleum ether); mp 104 °C; $[\alpha]^{20}_D$ 13.1° ($CHCl_3$, *c* 0.88); ^1H NMR ($CDCl_3$, 500 MHz) showed an 3:7 mixture of carbazate isomers: δ 1.63 (9H, s) [1.59 (9H, s)], 1.65 (9H, s), 3.10-3.25 (4H, m), 3.74 (3H, s) [3.70 (3H, s)], 3.75 (3H, s), 4.15-4.20 (1H, m) [4.10-4.15 (1H, m)], 4.25-4.35 (1H, m), 4.45-4.55 (2H, m), 4.55-4.65 (2H, m), 4.75-4.85 (1H, m), 5.05-5.15 (2H, m) [5.00-5.05 (2H, m)] 5.17 (1H, d, *J* = 10.4), 5.23 (1H, d, *J* = 17.1), 5.41 (1H, br) [5.31 (1H , d, *J* = 7.7)], 5.75-5.90 (1H, m), 6.05-6.10 (1H, br) [6.00-6.05 (1H, br)], 6.30-6.40 (2H, m), 7.09 (1H, d, *J* = 8.4) [6.95-7.00 (1H, m)], 7.15-7.40 (7H, m), 7.40-7.60 (6H, m), 7.60-7.70 (2H,m), 7.70-7.75 (1H, m), 8.00-8.10 (2H, m), 8.10-8.20 (1H, br) [8.65-8.70 (1H, br)]; ^{13}C NMR ($CDCl_3$, 125 MHz): δ 28.45, 28.52, 29.0, 30.0, 30.7, 46.9, 53.5 (53.2), 55.7, 57.0 (57.7), 63.9 (63.8), 66.7 (66.5), 70.1, 83.9, 84.2, 98.8, 104.3, 114.7, 114.9, 115.5, 115.7, 115.9, 118.5, 119.4, 119.5, 120.3, 120.4, 122.9, 123.1, 123.2, 124.7, 124.9, 125.0, 125.1, 125.34, 125.30, 125.6, 125.9, 127.54, 127.47, 128.2, 130.9, 131.8, 132.6, 135.7, 135.9, 141.6, 143.3, 143.6, 149.9, 151.6, 159.4, 161.8, 170.2, 170.9, 170.96, 171.05; IR (neat) ν_{max}/cm^{-1} 1152, 1208, 1255, 1368, 1451, 1510, 1614, 1727, 2935, 3295; HRMS (ESI) m/z calculated for $C_{60}H_{64}N_6NaO_{15}S$ $[M+Na]^+$ 1163.4043; found 1163.4040.

Scheme 7. Synthesis of 4-(TBDMSO)benzyl bromide (64)

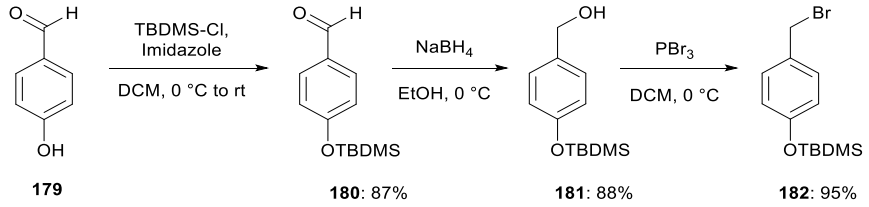

4-(TBDMSO)benzaldehyde (180)

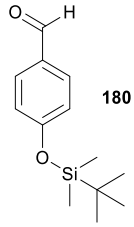

Imidazole (5.11 g, 75.0 mmol) was dissolved in dry DCM (250 mL) in a 500 mL flamed dried flask under argon, cooled to 0 °C, treated with 4-hydroxybenzaldehyde (**179**, 5.00 g, 40.9 mmol), followed by tert-butyldimethylsilyl chloride (6.78 g, 45.0 mmol), and allowed to warm to room temperature. After stirring for 18 h, the mixture was washed with water (3 x 100 mL). The organic layer was dried over $MgSO_4$, filtered and evaporated to a residue, that was purified by flash chromatography eluting with hexane:EtOAc 19:1 to afford aldehyde **180** as an oil (8.38 g, 87%): R_f 0.68 (hexane:EtOAc 4:1); ^{1}H NMR ($CDCl_3$, 400 MHz) δ 0.27 (6H, s), 1.02 (9H, s), 6.97 (2H, d, J = 8.3), 7.81 (2H, d, J = 8.3), 9.91 (1H, s); ^{13}C NMR ($CDCl_3$, 100 MHz) δ −4.0, 18.6, 25.9, 120.8, 130.7, 132.2, 161.8, 191.2; IR (neat) ν_{max}/cm^{-1} 1157, 1212, 1275, 1473, 1508, 1599, 1698, 2859, 2933; HRMS (ESI) m/z calculated for $C_{13}H_{21}O_2Si$ $[M+H]^+$ 237.1305; found 237.1314.

4-(TBDMSO)benzyl alcohol (181)

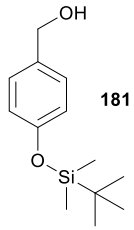

Aldehyde **180** (3.00 g, 12.7 mmol) was dissolved in EtOH (25 mL), cooled to 0 °C, and treated with $NaBH_4$ (0.96 g, 25.4 mmol). After stirring for 2 h, the solution was poured slowly into 150 mL of 1 N HCl at 0 °C. The aqueous solution was then extracted with Et_2O (4 x 150 mL) and the organic phase was dried over $MgSO_4$, filtered and evaporated to a residue. The residue was purified by flash chromatography eluting with hexane: EtOAc 4:1 to afford alcohol **181** as an oil (2.68 g, 88%): R_f 0.32 (Hexane:EtOAc 4:1); ^{1}H NMR ($CDCl_3$, 400MHz) δ 0.24 (6H, s), 1.03 (9H, s), 2.43 (1H, br) 4.58 (2H, s), 6.86 (2H, d, *J* = 8.1), 7.23 (2H, d, *J* = 8.1); ^{13}C NMR ($CDCl_3$, 100 MHz) δ −4.1, 18.5, 26.0, 65.2, 120.4, 128.8, 134.0, 155.5; IR (neat) ν_{max}/cm^{-1} 1254, 1472, 1510, 1610, 2857, 2930, 3339; HRMS (ESI) m/z calculated for $C_{13}H_{23}O_2Si$ $[M+H]^+$ 239.1462; found 239.1457.

4-(TBDMSO)benzyl bromide (182)

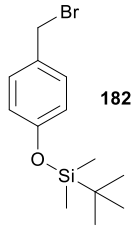

182

Phosphorus tribromide (35 μL, 0.38 mmol) was dissolved in dry DCM (30 mL), cooled to 0 °C, and treated drop-wise with a solution of alcohol **181** (180 mg, 0.76 mmol) in dry DCM (40 mL). After stirring at 0 °C for 30 min, the mixture was filtered through a small plug of silica gel to afford benzyl bromide **182** as an oil (215 mg, 95%: R_f 0.77 (hexane: EtOAc, 9:1); ^{1}H NMR ($CDCl_3$, 400 MHz) δ 0.26 (6H, s), 1.04 (9H, s), 4.53 (2H, s), 6.85 (2H, d, *J* = 8.5), 7.31 (2H, d, *J* = 8.5); ^{13}C NMR ($CDCl_3$, 100 MHz) δ −4.1, 18.5, 26.0, 34.3, 120.6, 130.7, 130.8, 156.2; IR (neat) ν_{max}/cm^{-1} 1269, 1511, 1608, 2859, 2929, 2953.

Solid Phase Synthesis

General Methods

Fmoc-Rink resins (**183**, 100–200 mesh, 0.64 and 1.00 mmol / g loading) were purchased respectively from NovaBiochem® (EMD Bioscience Inc., San Diego, CA, USA) and Advanced ChemTech® (Louisville, Kentucky, USA). Amino acids [*e.g.*, Fmoc-Lys(Boc), Fmoc-D-Phe, Fmoc-D-Trp(Boc), Fmoc-Ala, Fmoc- and Boc-His(Trt)] were purchased from GL Biochem® (Shanghai, China) Ltd. *O*-Benzotriazole-*N*,*N*,*N*',*N*'-tetramethyl-uronium-hexafluoro-phosphate (HBTU) and hydroxybenzotriazole (HOBt) were purchased from GL Biochem®. Tetrakis(triphenylphosphine)palladium(0) [$Pd(PPh_3)_4$], 1,3-Dimethylbarbituric acid (DMBA), sodium diethyldithiocarbamate (Et_2NCS_2Na), Di-*iso*-propylethylamine (DIEA), di-*iso*-propylcarbodiimide (DIC), triethylsilane (TES), 4-fluorobenzyl bromide, 4-methoxybenzyl bromide, and 2-(bromomethyl)-naphthalene (**184**), all were purchased from Aldrich® and used as received. Unless stated otherwise, all alkylations and coupling reactions were monitored by reverse phase high performance liquid chromatography-mass spectrometry (RP-HPLC-MS) on either a Sunfire™ C18 3.5 micron, 2.1 x 50 mm column or on a Gemini C18 5.0 micron, 4.6 x 150 mm column using UV detection at $\lambda = 214$ nm, a flow rate of 0.4 mL / min for the Sunfire™ column or 0.5 mL / min for the Gemini® column and an eluent containing solvent A [H_2O containing 0.1% formic acid (FA)] and solvent B (MeOH containing 0.1% FA). RP-HPLC analyses of crude and purified peptides were performed on the same columns using the specified gradient. Peptides were purified with a Gemini® 5 micron C18 110A column (Phenomenex® Inc., 250×21.2 mm, 5 μm) using the specified linear gradient of MeOH (0.1% FA) in water (0.1% FA), with a flow rate of 10.0 mL / min.

General protocol for Fmoc deprotection and washings

The Fmoc protecting group was removed by treating the resin with a solution of 20% piperidine in DMF for 30 min. The resin was filtered, washed and filtered successively using 15 sec agitations with DMF (3 times), MeOH (3 times) and DCM (3 times), sequentially.

General protocol for the HBTU couplings

The resin was swollen in DMF (1.5 mL) for 30 min. Meanwhile, a solution of the desired Fmoc-amino acid (3.0 eq.) and HBTU (3.0 eq.) in DMF (1.5 mL) was stirred for 1 min, treated with DIEA (6.0 eq.), stirred for 5 min and then added to the swollen resin. The reaction mixture was shaken for 18 h at room temperature. The resin was then filtered and washed as described above, and dried *in vacuo*.

General protocol for cleavage of aliquots of resin-bound peptide for analysis by LC-MS

Fmoc-Protected resin (5 mg) in a 1 mL plastic filtration tube with a polyethylene filter was treated with 20% piperidine in DMF as described above. The resin was swollen and cleaved with 0.5 mL of a cocktail of TFA:H_2O:TES (95:2.5:2.5) for 1 h at room temperature. The resin was filtered. The filtrate was collected in a 1.5 mL Eppendorf® tube and its volume was concentrated by bubbling air through the solution. A precipitate was then produced on addition of Et_2O (1 mL), and collected with a centrifuge for 2 min. After decantation of the ethereal solvent, the precipitate was dissolved in H_2O (1 mL) and analyzed by LC-MS. Resin without Fmoc-protection (5 mg) was directly cleaved and treated as described above in a 1 mL plastic filtration tube with a polyethylene filter.

General protocol for peptide cleavage

Peptide was cleaved from the resin (100 mg) using a cocktail of TFA:H_2O:TES (95:2.5:2.5, 2 mL) for 3 h in a cold room (4 °C). The resin was filtered and washed with TFA (2 x 2 mL). The filtrate was collected in a 50 mL Eppendorf tube and concentrated by bubbling air. A precipitate was produced by adding Et_2O (50 mL) to the concentrate, and collected with a centrifuge for 5 min. The ethereal solvent was decanted. The precipitate was dissolved in H_2O (5 mL) and freeze-dried to a solid.

Lys(Boc)-NH-Rink resin (129)

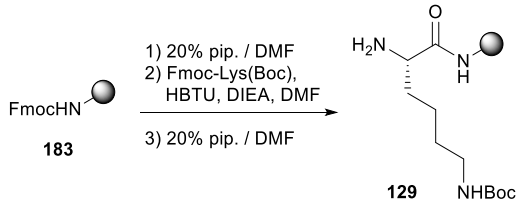

Fmoc-Rink resin (**183**, 1.25 g, 0.64 mmol / g, 0.80 mmol or 1.00 g, 1.00 mmol / g, 1.00 mmol) was swollen in DMF (8 mL) in a 12 mL plastic filtration tube with a polyethylene filter, treated with 20% piperidine in DMF (8 mL) to remove the Fmoc group as described above, and coupled to Fmoc-Lys(Boc) (respectively 1.12 g, 2.40 mmol or 1.41 g, 3.00 mmol) using HBTU (respectively 0.91 g, 2.40 mmol or 1.14 g, 3.00 mmol) and DIEA (respectively 0.83 mL, 4.80 mmol or 1.00 mL, 6.00 mL) as described in the general protocol. After washing the resin with DMF (3 x 8 mL), MeOH (3 x 8 mL) and DCM (3 x 8 mL), the resin was treated with 20% piperidine in DMF (8 mL) to remove the Fmoc group, which afforded resin **129**.

D-Phe-Lys(Boc)-NH-Rink resin (155)

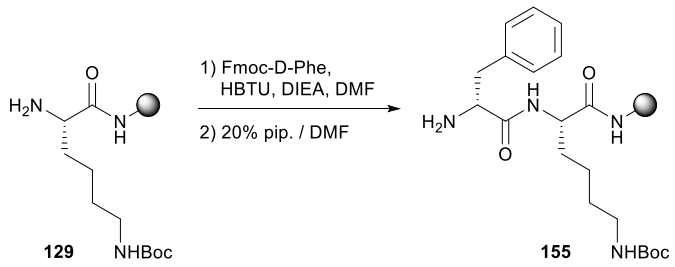

Starting from resin **129** (500 mg, 0.45 mmol / g, 0.22 mmol), Fmoc-D-Phe (261 mg, 0.673 mmol), DIEA (223 µL, 1.35 mmol) and HBTU (255 mg, 0.673 mmol) in DMF (4 mL), the coupling was accomplished as described for resin **129**. After washing the resin with DMF (3 x 8 mL), MeOH (3 x 8 mL) and DCM (3 x 8 mL), the resin was treated with 20% piperidine in DMF (8 mL) to remove the Fmoc group, which afforded resin **155**.

Building block approach (Method A)

***N*-(Alloc)-Ala-AsF(4-F)-D-Phe-Lys(Boc)-NH-Rink resin (130)**

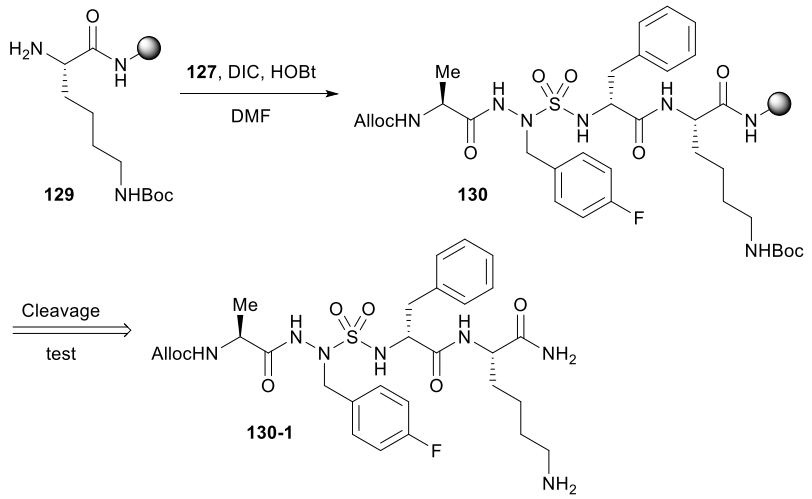

Resin **29** (264 mg, 0.42 mmol / g, 0.111 mmol) was swollen in DMF (3 mL) in a 6 mL plastic filtration tube with a polyethylene filter. Meanwhile, a solution of tripeptide **127** (87 mg, 0.166 mmol) and HOBT (23 mg, 0.166 mmol) in DMF (3 mL) was stirred for 1 min, treated with DIC (25.9 μL, 0.166 mmol), stirred for 5 min and then added to the resin. The resin mixture was shaken for 18 h at room temperature. The resin was filtered and washed as described above to afford resin **130**: [**130-1**, R*t* 6.86 min: Sunfire™ column; gradient: 5%-80% MeOH (0.1% FA) for 7.5 min + 90% MeOH (0.1% FA) for 2.0 min]. The unreacted amine was capped after treatment of the resin with acetic anhydride (57 μL, 0.6 mmol) and DIEA (100 μL, 0.6 mmol) in DMF (2 mL), shaking for 0.5 h, washing, and drying *in vacuo*.

***N*-(Fmoc)-Ala-AsF-D-Phe-Lys(Boc)-NH-Rink resin (131)**

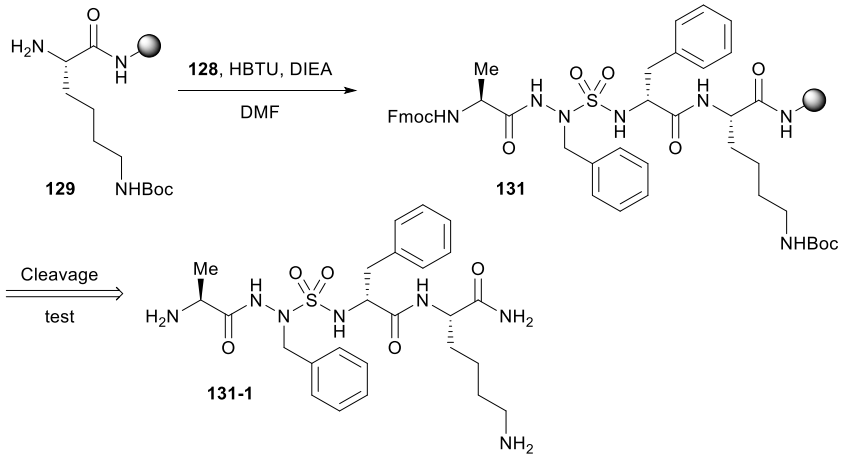

Resin **129** (188 mg, 0.64 mmol / g, 0.12 mmol) was swollen in DMF (2 mL) in a 3 mL plastic filtration tube with a polyethylene filter. Meanwhile, a solution of tripeptide **128** (77 mg, 0.12 mmol) and HBTU (46 mg, 0.12 mmol) in DMF (2 mL) was stirred for 1 min, treated with DIEA (42 μL, 0.24 mmol), stirred for 5 min and then added to the resin. The resin mixture was shaken for 18 h at room temperature. The resin was filtered and washed as described above to afford resin **131**: [**131-1**, R*t* 4.97 min: Sunfire™ column; gradient: 5%-80% MeOH (0.1% FA) for 7.5 min + 90% MeOH (0.1% FA) for 2.0 min]. The unreacted amine was capped after treatment of the resin with acetic anhydride (57 μL, 0.6 mmol) and DIEA (100 μL, 0.6 mmol) in DMF (2 mL), shaking for 0.5 h, washing, and drying *in vacuo*.

Ala-AsF(4-F)-D-Phe-Lys(Boc)-NH-Rink resin (132)

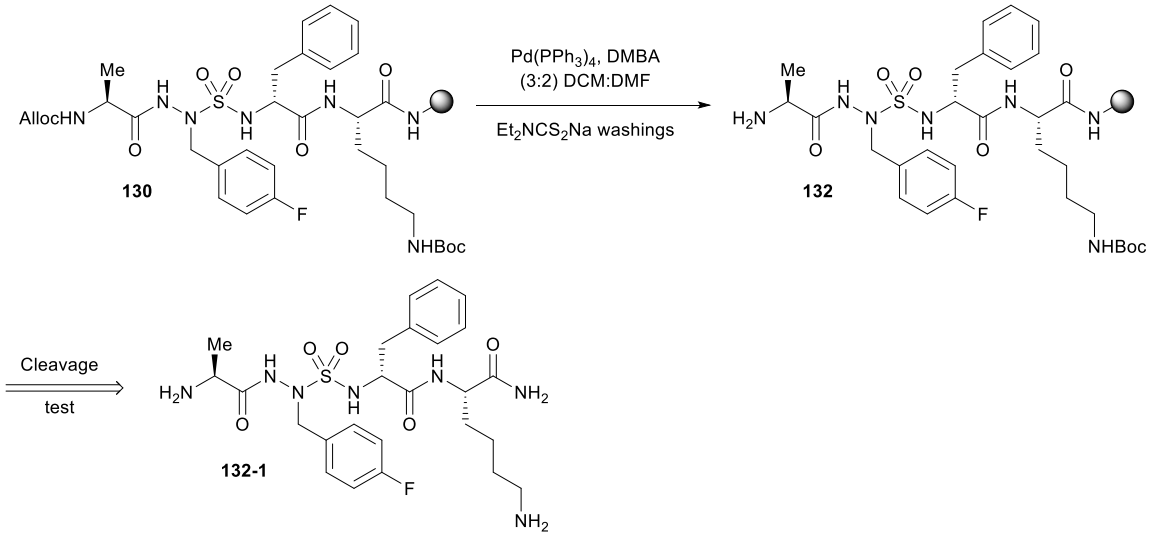

Resin **130** was swollen in DMF (2 mL) for 30 min, filtered, and treated with a solution of $Pd(PPh_3)_4$ (16 mg, 0.014 mmol, freshly washed with EtOH) and 1,3-dimethylbarbituric acid (111 mg, 0.47 mmol, 7.0 eq.) in 2 mL of 3:2 DCM:DMF. After shaking at room temperature for 2 h, the resin was filtered and retreated with the same conditions for a second time for 2 h. The resin was filtered, washed, treated with 0.5% sodium diethyldithiocarbamate (2 mL) for 30 min, filtered and washed two more times with 0.5% sodium diethyldithiocarbamate (2 mL) for 15 sec. The resin was washed as described above to afford resin **132**: [**132-1**, R*t* 4.28 min: Sunfire™ column; gradient: 5%-80% MeOH (0.1% FA) for 7.5 min + 90% MeOH (0.1% FA) for 2.0 min].

Ala-D-Trp-Ala-AsF(4-F)-D-Phe-Lys-NH$_2$ (134)

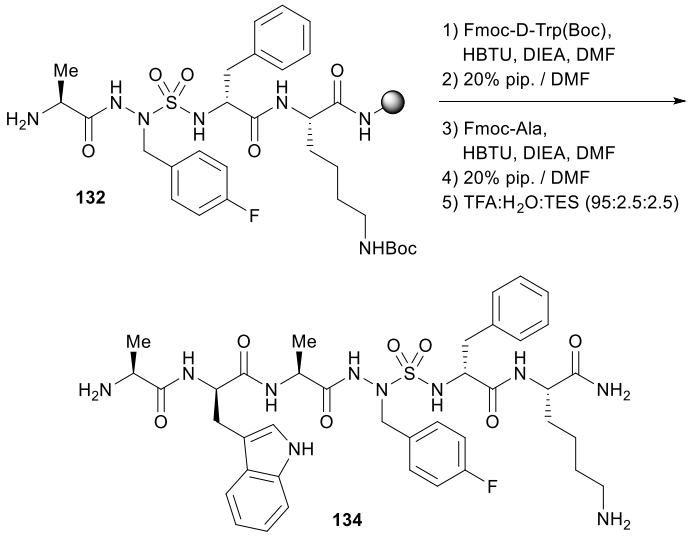

Azasulfurypeptide **134** was synthesized from resin **132** by sequential Fmoc group removals, HBTU couplings of Fmoc-D-Trp(Boc), followed by Fmoc-Ala and resin cleavage using the respective general protocols described above. Analysis of a resin aliquot as described above indicated peptide **134** to be of 59% purity: R*t* 8.82 min using a Sunfire column and a gradient of 20%-80% MeOH (0.1% FA) in water (0.1% FA) for 14 min. The TFA salt was purified by preparative RP-HPLC using a Gemini 5 micron C18 110A column (Phenomenex® Inc., 250×21.2 mm, 5 µm) with a gradient of 35%-50% MeOH (0.1% FA) in water (0.1% FA), with a flow rate of 10.0 mL/min, to afford the desired FA salt **134** (6.5 mg, 23%). The purified product was analyzed by analytical RP-HPLC using the Sunfire column and revealed to be of >99% purity: gradient 1: R*t* 6.79 min [20%-80% MeOH (0.1% FA) in water (0.1% FA) for 7.5 min followed by 90% MeOH (0.1% FA) in water (0.1% FA) for 2.0 min]; Gradient 2: R*t* 7.65 min [10%-80% MeCN (0.1% FA) in water (0.1% FA) for 7.5 min followed by 90% MeCN (0.1% FA) in water (0.1% FA) for 2.0 min]. HRMS (ESI) m/z calculated for $C_{39}H_{51}FN_{10}O_7S$ $[M+Na]^+$ 845.3647; found 845.3539.

His-D-Trp-Ala-AsF-D-Phe-Lys-NH_2 (135)

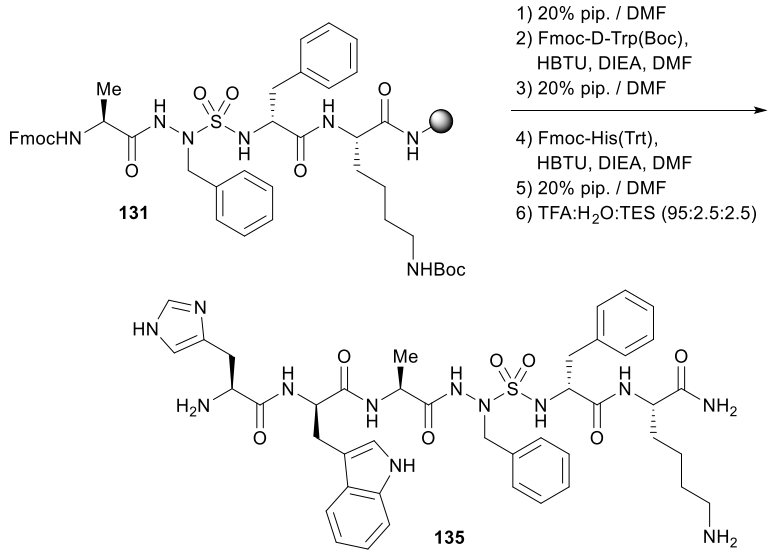

Azasulfurypeptide **135** was synthesized from resin **131** by sequential Fmoc group removals, HBTU couplings with Fmoc-D-Trp(Boc), followed by Fmoc-His(Trt) and resin cleavage using the respective general protocols described above. Analysis of a resin aliquot as described above indicated peptide **135** to be of 73% purity: R*t* 13.08 min on a Gemini C18 column with a gradient of 0%-80% MeOH (0.1% FA) in water (0.1% FA) for 30.0 min, followed by 90% MeOH (0.1% FA) in water (0.1% FA) for 10.0 min. The TFA salt was purified by preparative RP-HPLC using a Gemini® 5 micron C18 110A column (Phenomenex® Inc., 250×21.2 mm, 5 μm) with a gradient of 30%-55% MeOH (0.1% FA) in water (0.1% FA), with a flow rate of 10.0 mL / min, to afford the desired formic acid (FA) salt **135** (11.0 mg, 12%). The purified product was analyzed by analytical RP-HPLC using a Gemini® 5 micron C18 110A column (Phenomenex® Inc., 150 × 4.6 mm, 5 μm) and revealed to be of 99% purity: Gradient 1: R*t* 18.95 min [5%-80% MeOH (0.1% FA) in water (0.1% FA) for 30.0 min + 90% MeOH (0.1% FA) in water (0.1% FA) for 10.0 min]; Gradient 2: R*t* 13.55 min [5%-80% MeCN (0.1% FA) in water (0.1% FA) for 30.0 min + 90% MeCN (0.1% FA) in water (0.1% FA) for 10.0 min]. HRMS (ESI) m/z calculated for $C_{42}H_{54}N_{12}NaO_7S$ $[M+Na]^+$ 893.3851; found 893.3832.

Diversity-oriented approach (Method B)

***N*-(Alloc)-Ala-AsG(Fmoc)-D-Phe-Lys(Boc)-NH-Rink resin (142)**

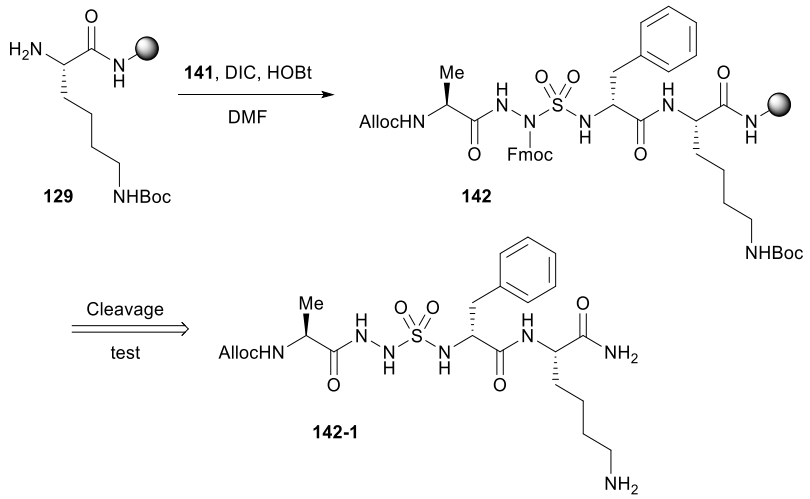

Starting from resin **129** (497 mg, 1.00 mmol / g, 0.497 mmol), tripeptide **141** (396 mg, 0.621 mmol), DIC (97 µL, 0.621 mmol) and HOBt (84 mg, 0.621 mmol) in DMF (2 mL), resin **142** was synthesized as described for resin **130**. The resin mixture was filtered and washed as described above to afford resin **142**. Analysis of a resin aliquot as described above indicated peptide **142-1** (R*t* 4.53 min) to be of 78% purity**:** Sunfire™ column using a gradient of 5%-80% MeOH (0.1% FA) in water (0.1% FA) for 7.5 min + 90% MeOH (0.1% FA) in water (0.1% FA) for 2.0 min at 0.5 mL/min. The resin was then dried *in vacuo*.

***N*-(Alloc)-D-Trp(Boc)-AsG(Fmoc)-Trp(Boc)-D-Phe-Lys(Boc)-NH-Rink resin (156)**

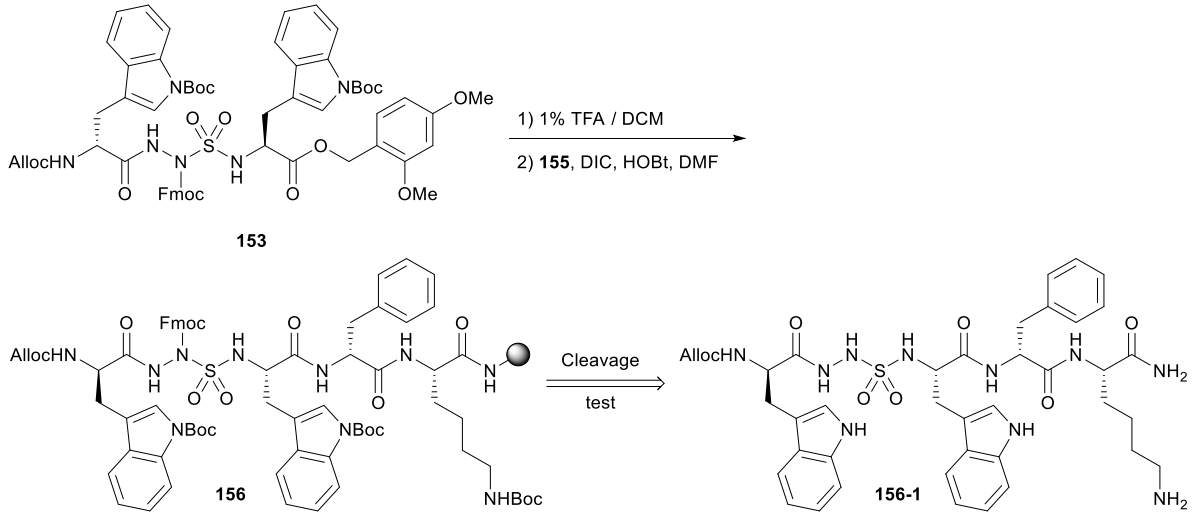

2,4-Dimethoxybenzyl ester **153** (100 mg, 0.088 mmol) was treated with 1% of TFA in DCM (2.5 mL) for 1 h at room temperature. The volatiles were evaporated and Et_2O (5 mL) was added. The precipitate was filtered and the filtrate was evaporated to afford acid **154**. Then, starting from resin **155** (116 mg, 0.42 mmol / g, 0.049 mmol), tripeptide **154** (85 mg, 0.086 mmol), DIC (13.4 μL, 0.086 mmol) and HOBt (12 mg, 0.086 mmol) in DMF (2 mL), resin **156** was synthesized as described for resin **130**. Unreacted starting material was capped by adding acetic anhydride (24 μL, 0.25 mmol) and DIEA (41 μL, 0.25 mmol) in DMF (2 mL) to the resin, and shaking for 0.5 h, followed by the washing procedure. The resin was then dried *in vacuo*. Analysis of a resin aliquot as described above indicated peptide **156-1** (R*t* 12.1 min) to be of 40% purity contaminated with 31% of unreacted starting material (R*t* 2.89 min): Sunfire™ column using a gradient of 5%-90% MeOH (0.1% FA) in water (0.1% FA) for 12.0 min followed by 90% MeOH (0.1% FA) in water (0.1% FA) for 3.0 min.

Representative protocol for the alkylation of aryl halides on resin 142

Resin **142** (100 mg, 0.071 mmol) was swollen in DMF, the Fmoc protection was removed, and the resin was washed as described above. A solution of 40% tetraethylammonium hydroxide in water (3.0 eq.) and alkyl halide (3.0 eq.) in DMF (2 mL) was added to the swollen resin, which was shaken at room temperature for 18 h, filtered, washed and dried *in vacuo*.

_N_-(Alloc)-Ala-AsF-D-Phe-Lys(Boc)-NH-Rink resin (144a)

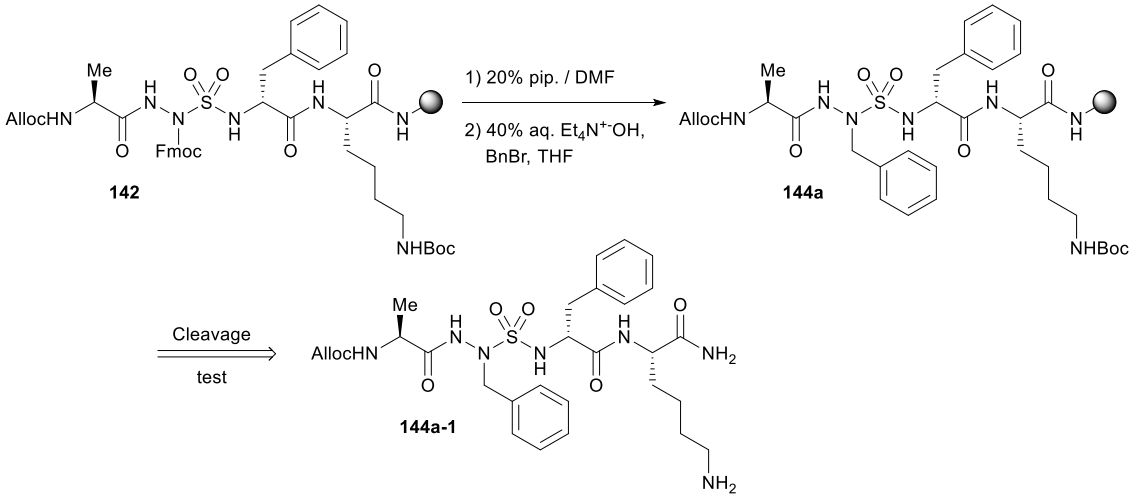

Employing resin **142** (100 mg, 0.071 mmol), 40% tetraethylammonium hydroxide in water (79 μL, 0.214 mmol) and benzyl bromide (26 μL, 0.214 mmol) in DMF (2 mL), resin **144a** was synthesized as described above. Analysis of a resin aliquot as described above indicated azasulfurylphenylalanine peptide **144a-1** to be of 75% purity: R*t* 5.89 min on a Sunfire™ column with a gradient of 20%-80% MeOH (0.1% FA) in water (0.1% FA) for 6 min, followed by 90% MeOH (0.1% FA) in water (0.1% FA) for 2.0 min.

_N_-(Alloc)-Ala-AsF(4-F)-D-Phe-Lys(Boc)-NH-Rink resin (144b) and _N_-(Alloc)-Ala-AsF(4-F)-_N_-(4-F-Bn)-D-Phe-Lys(Boc)-NH-Rink resin (145b)

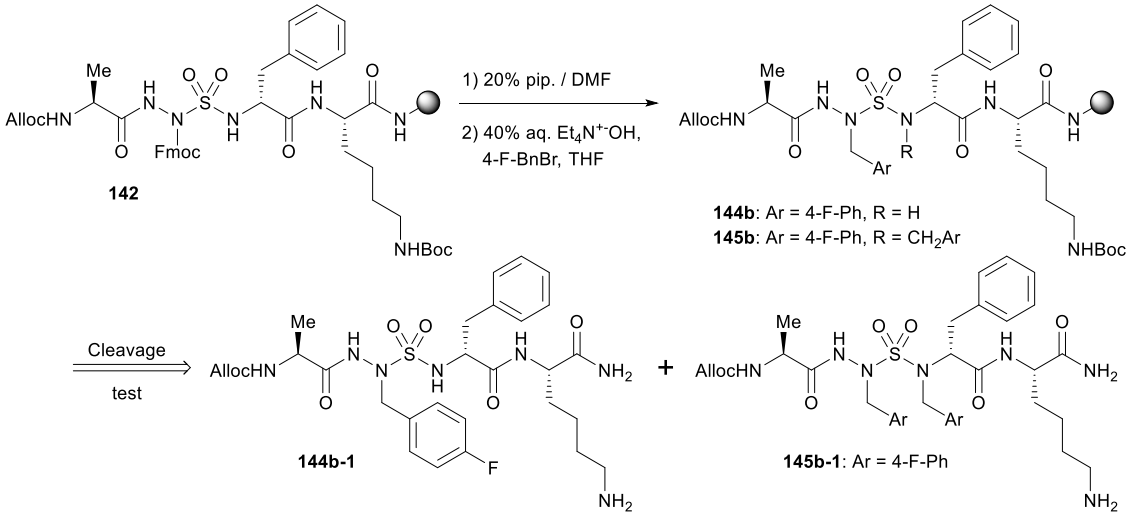

Employing resin **142** (100 mg, 0.071 mmol), 40% tetraethylammonium hydroxide in water (79 µL, 0.214 mmol) and 4-fluorobenzyl bromide (27 µL, 0.214 mmol) in DMF (2 mL), resin **144b** was synthesized as described above. Cleavage of an aliquot of the resin as described above and analysis by LC-MS indicated azasulfuryl-4-fluorophenylalanine peptide **144b-1** was of 75% purity (R*t* 6.86 min) contaminated with bis-alkylation product peptide **145b-1** of 8% purity (R*t* 8.33 min) using a Sunfire™ column with a gradient of 5%-80% MeOH (0.1% FA) for 7.5 min followed by 90% MeOH (0.1% FA) for 2.0 min.

***N*-(Alloc)-Ala-AsF-(4-MeO)-D-Phe-Lys(Boc)-NH-Rink resin (144c) and *N*-(Alloc)-Ala-AsF(4-MeO)-*N*-(4-MeO-Bn)-D-Phe-Lys(Boc)-NH-Rink resin (145c)**

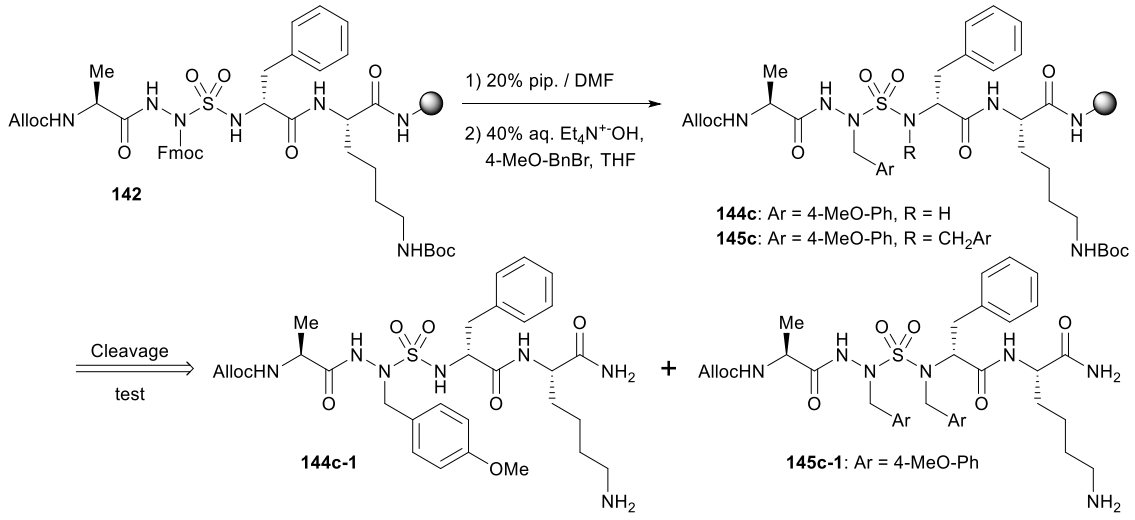

Employing resin **142** (100 mg, 0.071 mmol), 40% tetraethylammonium hydroxide in water (79 µL, 0.214 mmol) and 4-methoxybenzyl bromide (32 µL, 0.214 mmol), resin **144c** was synthesized as described above. Cleavage of an aliquot of the resin as described above and analysis by LC-MS indicated azasulfuryl-4-methoxyphenylalanine peptide **144c-1** was of 66% purity (R*t* 6.71 min) contaminated with bis-alkylation product peptide **145c-1** of 11% purity (R*t* 8.07 min): Sunfire™ column with a gradient of 5%-80% MeOH (0.1% FA) in water (0.1% FA) for 7.5 min followed by 90% MeOH (0.1% FA) in water (0.1% FA) for 2.0 min.

_N_-(Alloc)-Ala-AsA(2-naphthyl)-D-Phe-Lys(Boc)-NH-Rink resin (144d) and _N_-(Alloc)-Ala-AsA(2-naphthyl)-_N_-(2-naphthylmethyl)-D-Phe-Lys(Boc)-NH-Rink resin (145d)

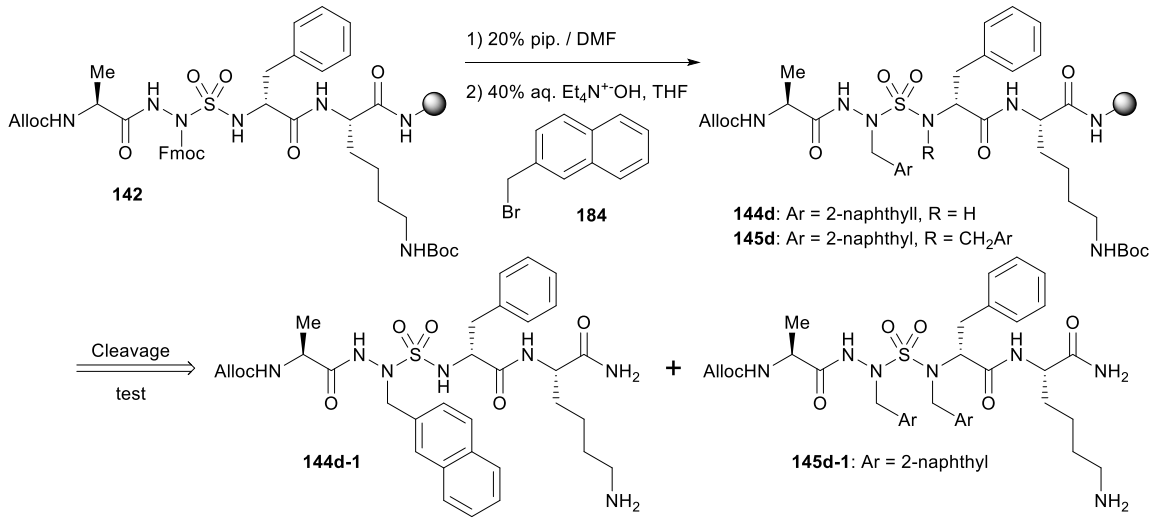

Employing resin **142** (100 mg, 0.071 mmol), 40% tetraethylammonium hydroxide in water (79 µL, 0.214 mmol) and 2-bromomethylnaphthalene (**184**, 47 mg, 0.214 mmol), resin **144d** was synthesized as described above. Cleavage of an aliquot of the resin as described above and analysis by LC-MS indicated azasulfuryl-2-naphthylalanine peptide **145d-1** was of 81% purity (R*t* 7.71 min) contaminated with bis-alkylation product peptide **145d-1** of 7% purity (R*t* 7.71 min): Sunfire™ column with a gradient of 5%-80% MeOH (0.1% FA) in water (0.1% FA) for 7.5 min followed by 90% MeOH (0.1% FA) in water (0.1% FA) for 2.0 min.

_N_-(Alloc)-Ala-AsF(4-TBDMSO)-D-Phe-Lys(Boc)-NH-Rink resin (144e) and _N_-(Alloc)-Ala-AsF(4-TBDMSO)-_N_-(4-TBDMSO-Bn)-D-Phe-Lys(Boc)-NH-Rink resin (145e)

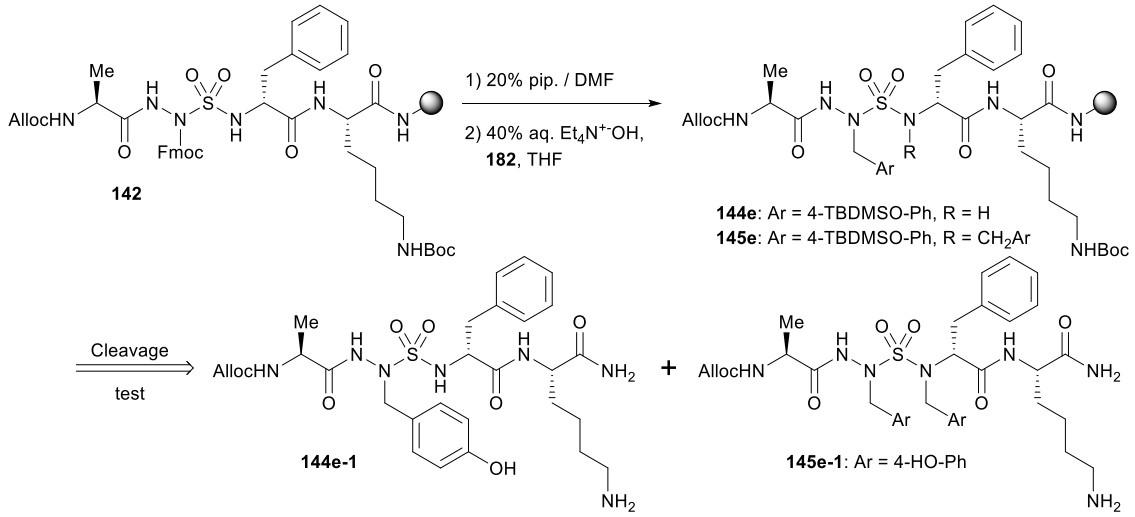

Employing resin **142** (100 mg, 0.071 mmol), 40% tetraethylammonium hydroxide in water (79 μL, 0.214 mmol) and 4-(TBDMSO)benzyl bromide (**182**, 65 mg, 0.214 mmol), resin **144e** was synthesized as described above. Cleavage of an aliquot of the resin as described above and analysis by LC-MS indicated azasulfuryl-4-(TBDMSO)phenylalanine peptide **144e-1** was of 53% purity (R*t* 6.09 min) contaminated with bis-alkylation product peptide **145e-1** of 5% purity (R*t* 6.09 min): Sunfire™ column with a gradient of 5%-80% MeOH (0.1% FA) in water (0.1% FA) for 7.5 min followed by 90% MeOH (0.1% FA) in water (0.1% FA) for 2.0 min.

_N_-(Alloc)-D-Trp(Boc)-AsA-Trp(Boc)-D-Phe-Lys(Boc)-NH-Rink resin (158)

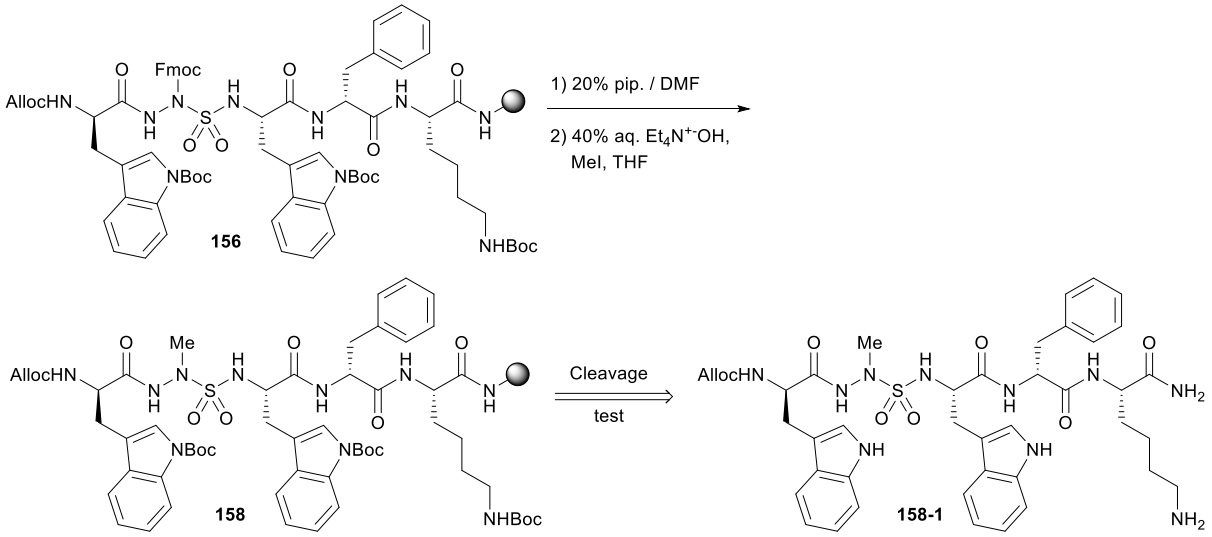

Treating resin **156** (91 mg, 0.015 mmol) with 40% tetraethylammonium hydroxide in water (18.7 µL, 0.045 mmol) and iodomethane (2.78 µL, 0.045 mmol) in DMF (2 mL) for 5 h, resin **158** was synthesized as described above. Analysis of a resin aliquot as described above indicated that the alkylation for azasulfurylalanine peptide **158-1** (R*t* 7.74 min) to be of 60% conversion based on unalkylated starting material (R*t* 7.65 min): Sunfire™ column with a gradient of 20%-80% MeOH (0.1% FA) in water (0.1% FA) for 12.0 min, followed by 90% MeOH (0.1% FA) in water (0.1% FA) for 3.0 min.

Ala-AsF-D-Phe-Lys(Boc)-NH-Rink resin (185a)

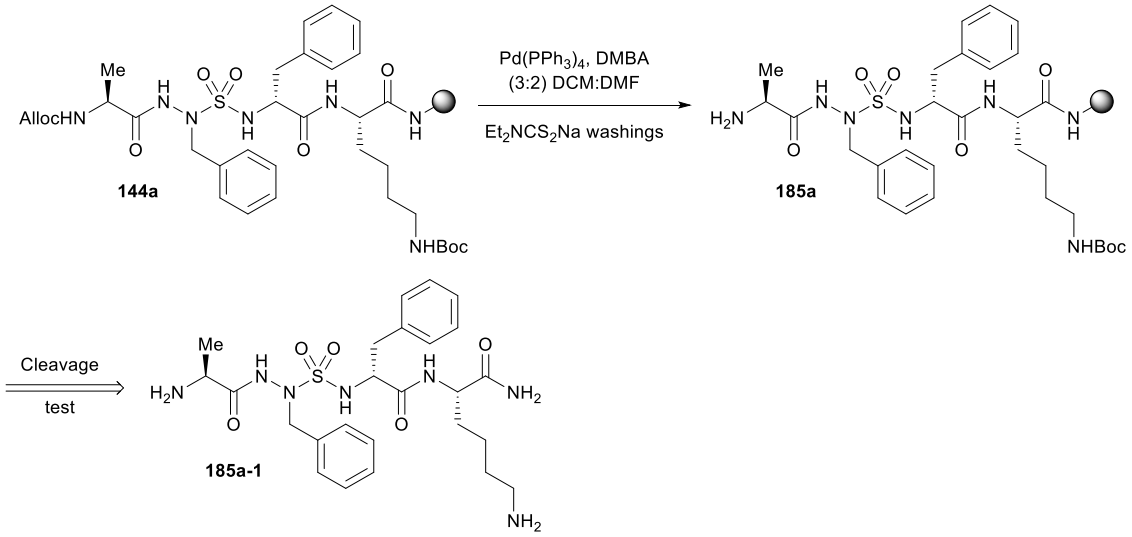

Starting from resin **144a** (100 mg, 0.067 mmol), the Alloc was cleaved as described for resin **132** to afford resin **185a**. Analysis of an aliquot as described indicated peptide **185a-1** to be of 70% purity: R*t* 4.58 min using a Sunfire™ column and a gradient of 5%-80% MeOH (0.1% FA) in water (0.1% FA) for 6 min followed by 90% MeOH (0.1% FA) in water (0.1% FA) for 2.0 min.

Ala-AsF(4-F)-D-Phe-Lys(Boc)-NH-Rink resin (185b)

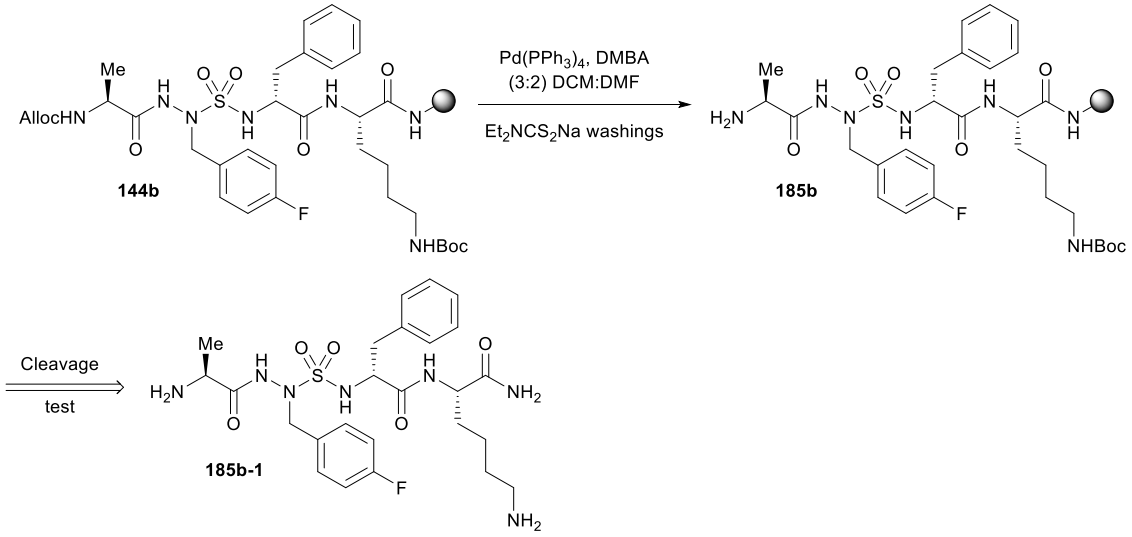

Starting from resin **144b** (100 mg, 0.066 mmol), the Alloc was cleaved as described for resin **132** to afford resin **185b**. Analysis of an aliquot as described indicated peptide **185b-1** to be of 54% purity: R*t* 4.28 min using a Sunfire column and a gradient of 5%-80% MeOH (0.1% FA) in water (0.1% FA) for 7.5 min followed by 90% MeOH (0.1% FA) in water (0.1% FA) for 2.0 min.

Ala-AsF(4-MeO)-D-Phe-Lys(Boc)-NH-Rink resin (185c)

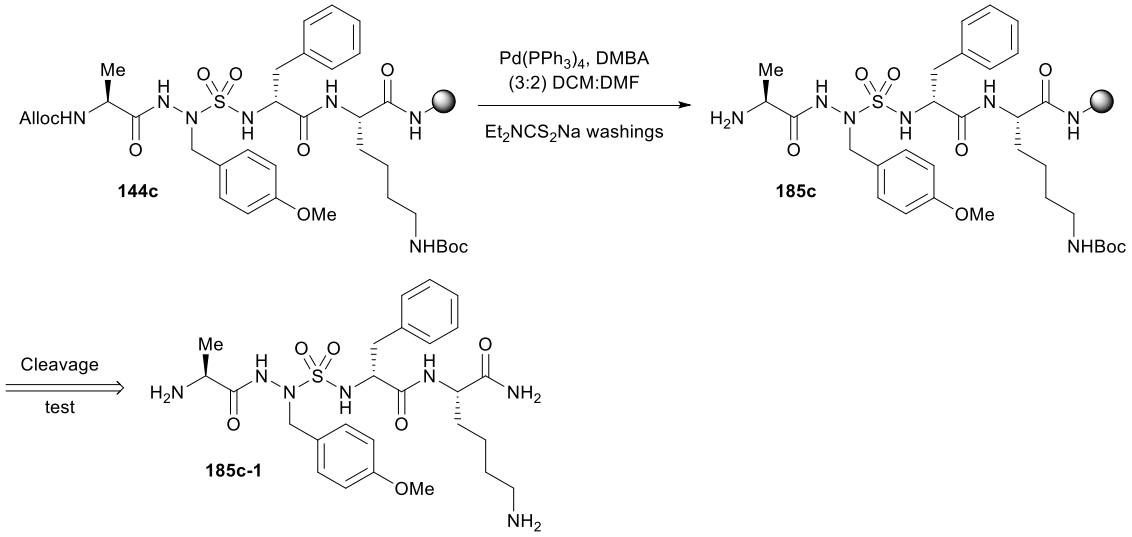

Starting from resin **144c** (100 mg, 0.066 mmol), the Alloc was cleaved as described for resin **132** to afford resin **185c**. Analysis of an aliquot as described indicated peptide **185c-1** to be of 61% purity: R*t* 4.46 min using a Sunfire™ column and a gradient of 5%-80% MeOH (0.1% FA) in water (0.1% FA) for 7.5 min followed by 90% MeOH (0.1% FA) in water (0.1% FA) for 2.0 min.

Ala-AsA(2-naphthyl)-D-Phe-Lys(Boc)-NH-Rink resin (185d)

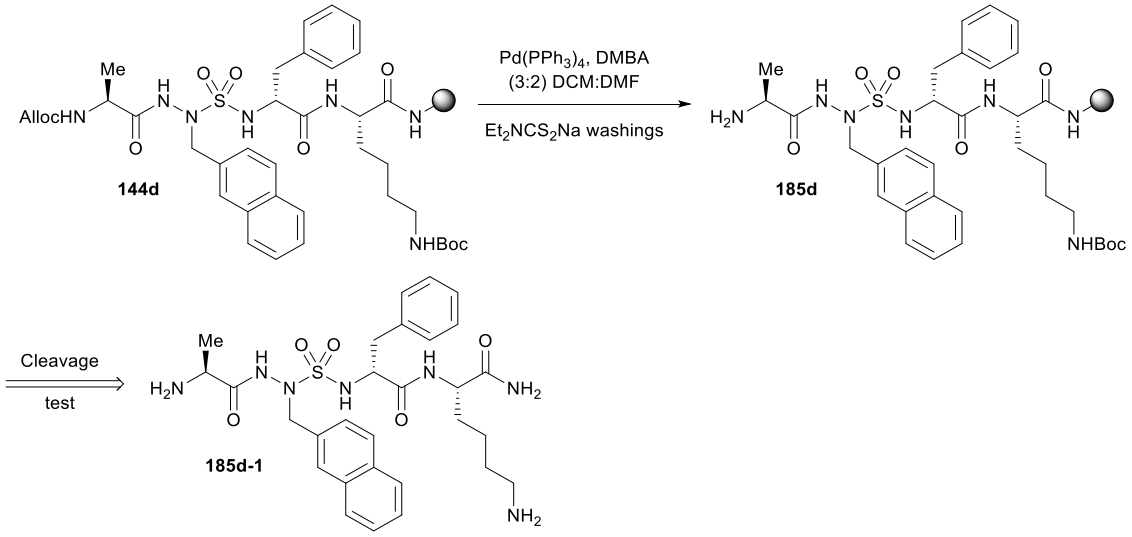

Starting from resin **144d** (100 mg, 0.065 mmol), the Alloc was cleaved as described for resin **132** to afford resin **185d**. Analysis of an aliquot as described indicated peptide **185d-1** to be of 51% purity: R*t* 5.38 min using a Sunfire™ column and a gradient of 5%-80% MeOH (0.1% FA) in water (0.1% FA) for 7.5 min followed by 90% MeOH (0.1% FA) in water (0.1% FA) for 2.0 min.

Ala-AsF(4-TBDMSO)-D-Phe-Lys(Boc)-NH-Rink resin (185e)

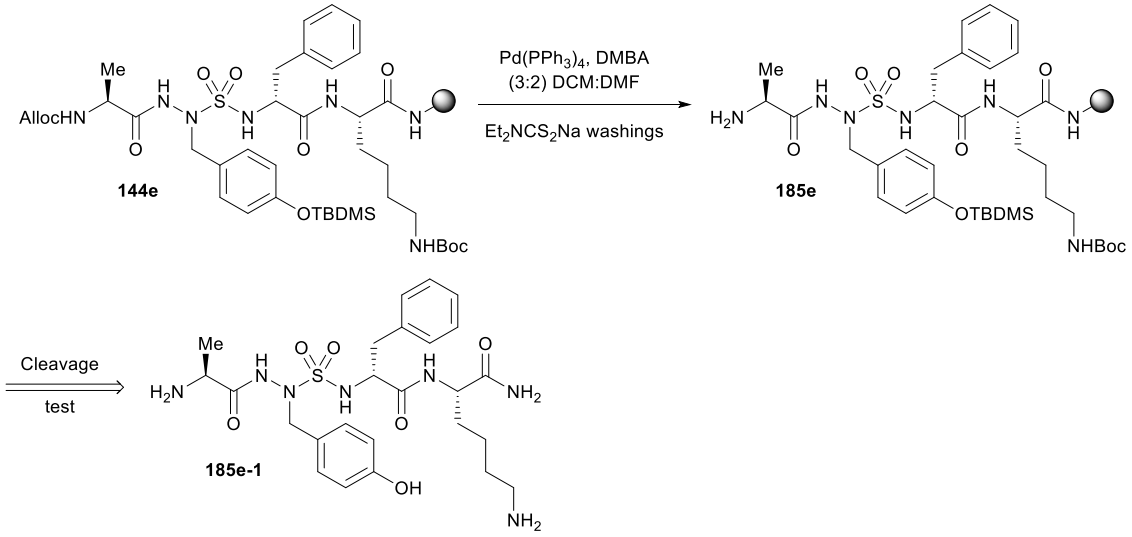

Starting from resin **185e** (100 mg, 0.065 mmol), the Alloc was cleaved as described for resin **132** to afford resin **185e**. Analysis of an aliquot as described indicated peptide **185e-1** to be of 53% purity: R*t* 4.14 min; Sunfire™ column using a gradient of 5%-80% MeOH (0.1% FA) in water (0.1% FA) for 7.5 min followed by 90% MeOH (0.1% FA) in water (0.1% FA) for 2.0 min.

D-Trp(Boc)-AsA-Trp(Boc)-D-Phe-Lys(Boc)-NH-Rink resin (186)

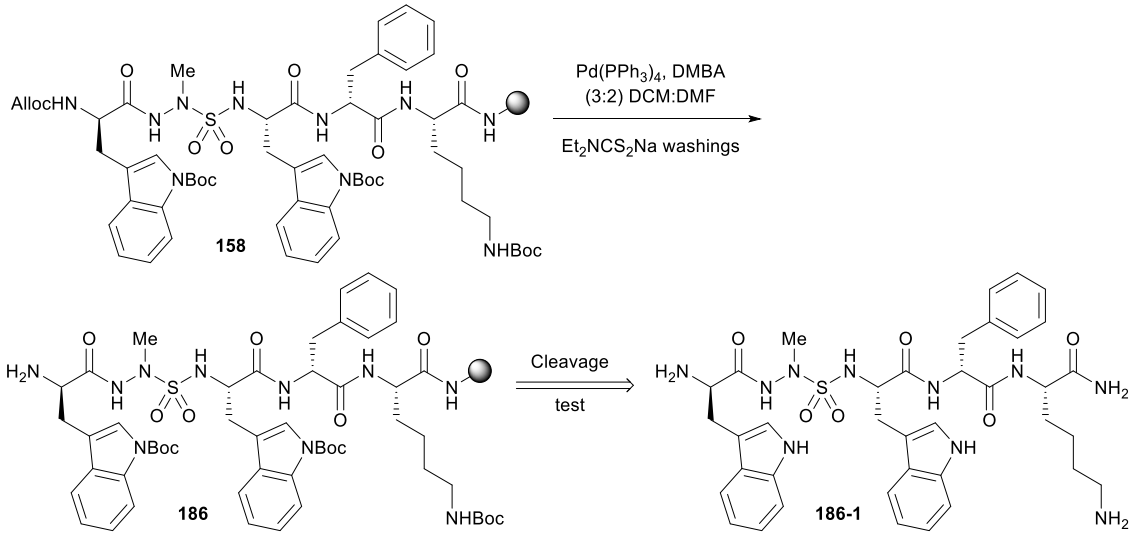

Starting from resin **158** (50 mg, 0.017 mmol), the Alloc was cleaved as described for resin **132** to afford resin **186**. Analysis of an aliquot as described indicated peptide **186-1** to be of 17% purity: R*t* 6.07 min; Sunfire™ column using a gradient of 10%-80% MeOH (0.1% FA) in water (0.1% FA) for 7.5 min followed by 90% MeOH (0.1% FA) in water (0.1% FA) for 2.0 min.

His-D-Trp-Ala-AsF-D-Phe-Lys-NH_2 (146a)

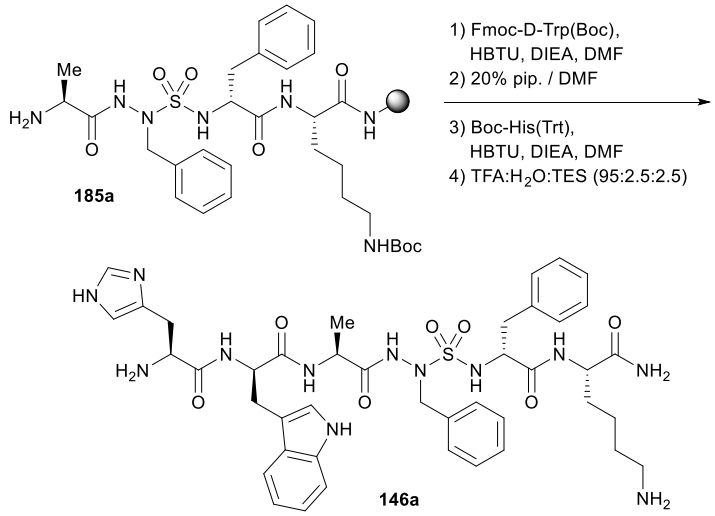

Azasulfurylpeptide **146a** was synthesized from resin **185a** by sequential Fmoc group removal, HBTU couplings of Fmoc-D-Trp(Boc), followed by Boc-His(Trt) and resin cleavage using the respective general protocols described above. Analysis of a resin aliquot as described above indicated that peptide **146a** exhibited identical retention time as material prepared from azasulfuryl tripeptide **134** and revealed to be of 78% purity: R*t* 5.61 min; Sunfire™ column using a gradient of 15%-45% MeOH (0.1% FA) in water (0.1% FA) for 7.5 min followed by 90% MeOH (0.1% FA) in water (0.1% FA) for 2.0 min. Analysis of a co-injection of peptide **146a** with the material prepared from azasulfuryl tripeptide **134** exhibited identical retention time.

His-D-Trp-Ala-AsF(4-F)-D-Phe-Lys-NH_2 (146b)

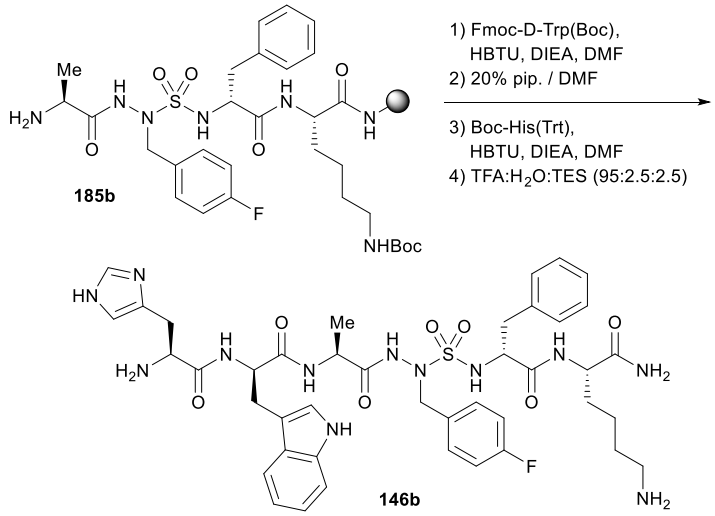

Azasulfurylpeptide **146b** was synthesized from resin **185b** by sequential Fmoc group removal, HBTU couplings of Fmoc-D-Trp(Boc), followed by Boc-His(Trt) and resin cleavage using the respective general protocols described above. Analysis of a resin aliquot as described above indicated peptide **146b** to be of 63% purity: R*t* 5.96 min using a Sunfire™ column and a gradient of 5%-80% MeOH (0.1% FA) in water (0.1% FA) for 7.5 min followed by 90% MeOH (0.1% FA) in water (0.1% FA) for 2.0 min. The TFA salt was purified by preparative RP-HPLC using a Gemini® 5 micron C18 110A column (Phenomenex® Inc., 250×21.2 mm, 5 μm) with a gradient of 20%-50% MeOH (0.1% FA) in water (0.1% FA), with a flow rate of 10.0 mL / min, to afford the desired FA salt of **146b** (1.0 mg, 3%). Analysis of the purified product by analytical RP-HPLC using the Sunfire™ column revealed >99% purity: Gradient 1: R*t* 5.23 min [5%-80% MeOH (0.1% FA) in water (0.1% FA) for 7.5 min + 90% MeOH (0.1% FA) in water (0.1% FA) for 2.0 min]; Gradient 2: R*t* 3.59 min [5%-80% MeCN (0.1% FA) for 7.5 min + 90% MeCN (0.1% FA) for 2.0 min]. HRMS (ESI) m/z calculated for $C_{42}H_{53}FN_{12}NaO_7S$ $[M+Na]^+$ 911.3757; found 911.3769.

His-D-Trp-Ala-AsF(4-MeO)-D-Phe-Lys-NH_2 (146c)

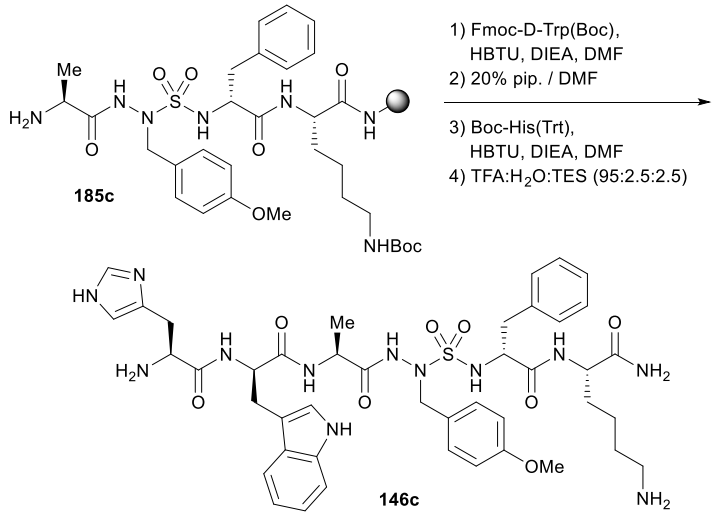

Azasulfurylpeptide **146c** was synthesized from resin **185c** by sequential Fmoc group removal, HBTU couplings with Fmoc-D-Trp(Boc), followed by Boc-His(Trt) and resin cleavage using the respective general protocols described above. Analysis of a resin aliquot as described above indicated peptide **146c** to be of 70% purity: R*t* 5.26 min using a Sunfire™ column on a gradient of 5%-80% MeOH (0.1% FA) in water (0.1% FA) for 7.5 min followed by 90% MeOH (0.1% FA) in water (0.1% FA) for 2.0 min. The TFA salt was purified by preparative RP-HPLC using a Gemini® 5 micron C18 110A column (Phenomenex® Inc., 250×21.2 mm, 5 μm) with a gradient of 15%-45% MeOH (0.1% FA) in water (0.1% FA), with a flow rate of 10.0 mL / min, to afford the desired FA salt of **146c** (4.1 mg; 10%). The purified product was analyzed by analytical RP-HPLC using the Sunfire™ column and revealed to be of >99% purity: Gradient 1: R*t* 5.40 min [15%-45% MeOH (0.1% FA) in water (0.1% FA) for 7.5 min + 90% MeOH (0.1% FA) in water (0.1% FA) for 2.0 min]; Gradient 2: R*t* 6.19 min [10%-30% MeCN (0.1% FA) for 7.5 min + 90% MeCN (0.1% FA) for 2.0 min]. HRMS (ESI) m/z calculated for $C_{43}H_{56}N_{12}NaO_8S$ $[M+Na]^+$ 923.3957; found 923.3936.

His-D-Trp-Ala-AsA(2-naphthyl)-D-Phe-Lys-NH_2 (146d)

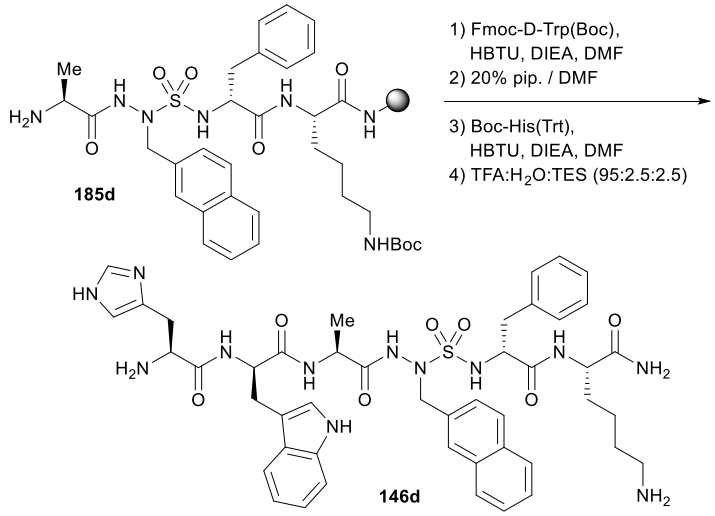

Azasulfurylpeptide **146d** was synthesized from resin **185d** by sequential Fmoc group removal, HBTU couplings with Fmoc-D-Trp(Boc), followed by Boc-His(Trt) and resin cleavage using the respective general protocols described above. Analysis of a resin aliquot as described above indicated peptide **146d** to be of 52% purity: R*t* 5.92 min using a Sunfire™ column and a gradient of 5%-80% MeOH (0.1% FA) in water (0.1% FA) for 7.5 min followed by 90% MeOH (0.1% FA) in water (0.1% FA) for 2.0 min. The TFA salt was purified by preparative RP-HPLC using a Gemini® 5 micron C18 110A column (Phenomenex® Inc., 250×21.2 mm, 5 μm) with a gradient of 20%-50% MeOH (0.1% FA) in water (0.1% FA), with a flow rate of 10.0 mL / min, to afford the desired FA salt of **146d** (4.2 mg, 10%). The purified product was analyzed by analytical RP-HPLC using the Sunfire™ column and revealed to be of 98% purity: Gradient 1: R*t* 3.89 min [25%-55% MeOH (0.1% FA) in water (0.1% FA) for 7.5 min + 90% MeOH (0.1% FA) in water (0.1% FA) for 2.0 min]; Gradient 2: R*t* 4.83 min [15%-35% MeCN (0.1% FA) in water (0.1% FA) for 7.5 min + 90% MeCN (0.1% FA) in water (0.1% FA) for 2.0 min]. HRMS (ESI) m/z calculated for $C_{46}H_{56}N_{12}NaO_7S$ $[M+Na]^+$ 943.4008; found 943.4007.

His-D-Trp-Ala-AsY-D-Phe-Lys-NH_2 (146e)

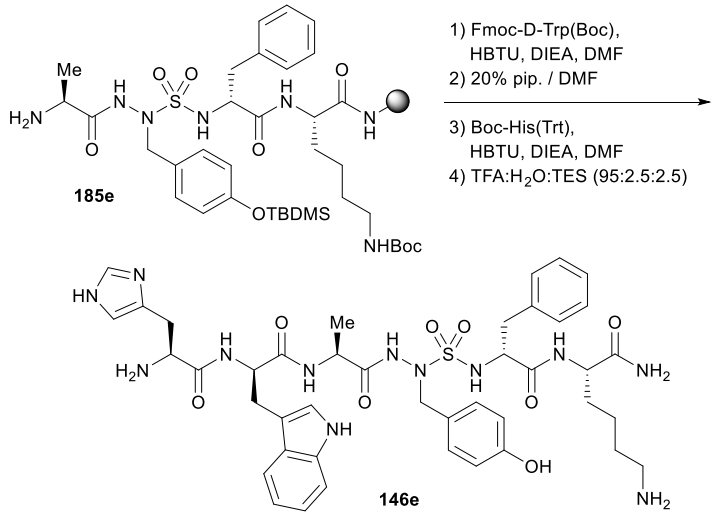

Azasulfurylpeptide **146e** was synthesized from resin **185e** by sequential Fmoc group removal, HBTU couplings with Fmoc-D-Trp(Boc), followed by Boc-His(Trt) and resin cleavage using the respective general protocols described above. Analysis of a resin aliquot as described above indicated peptide **146e** to be of 63% purity: R*t* 5.03 min using a Sunfire™ column and a gradient of 10%-40% MeOH (0.1% FA) in water (0.1% FA) for 7.5 min followed by 90% MeOH (0.1% FA) in water (0.1% FA) for 2.0 min. The TFA salt was purified by preparative RP-HPLC using a Gemini® 5 micron C18 110A column (Phenomenex® Inc., 250×21.2 mm, 5 μm) with a gradient of 20%-50% MeOH (0.1% FA) in water (0.1% FA), with a flow rate of 10.0 mL / min, to afford the desired FA salt of **146e** (3.4 mg, 9%). The purified product was analyzed by analytical RP-HPLC using the Sunfire™ column and revealed to be of >99% purity: Gradient 1: R*t* 5.03 min [15%-45% MeOH (0.1% FA) in water (0.1% FA) for 7.5 min + 90% MeOH (0.1% FA) in water (0.1% FA) for 2.0 min]; Gradient 2: R*t* 5.22 min [15%-40% MeCN (0.1% FA) in water (0.1% FA) for 7.5 min + 90% MeCN (0.1% FA) in water (0.1% FA) for 2.0 min]. HRMS (ESI) m/z calculated for $C_{42}H_{54}N_{12}NaO_8S$ $[M+Na]^+$ 909.3801; found 909.3805.

Annexe 4 : Partie expérimentale du chapitre 5

Measure of azasulfurylpeptide influence on the overproduction of nitric oxide (NO) induced by TLR2 agonist, R-FSL-1 in J774 macrophage cell line

The murine J774A.1 macrophage cell line was obtained from American Type Cell Collection (ATCC #TIB-67), seeded at 1.5 x 105 cells/well in DMEM containing 100U/mL of penicillin (Pen) and 100 μg/mL of streptomycin (Strep) on a 48-well plate (Costar® #3548), and incubated at 37 °C with 5% CO_2. After 2 h, the medium of adhered cells was changed to DMEM-Pen/Strep containing 0.2% of bovine serum albumin (BSA), and supplemented with either azasulfurylpeptide **134, 146b-e** or [azaLys^6]-GHRP-6 (**188**) as a negative control. After 2 h of pre-incubation, the cells were stimulated overnight with 300 ng/mL of fibroblast-stimulating lipopeptide (R-FSL-1). Supernatants were collected for fluorescence determination of nitrite using 2,3-diaminonaphtalene (DAN). Briefly, 25 μL of sample was incubated with 0.5 μg of DAN in a 100 μL final volume of phosphate buffer (50 mM, pH 7.5) at room temperature in the dark. After 15 min, the reaction was stopped with 20 μL of NaOH (2.8N) and the plate was read using a fluorescence plate reader (TECAN® Safire, λ_{exc} 365 nm and λ_{em} 430 nm).

Assessment of azasulfurylpeptides 146b-e on NF-κB activation and proinflammatory cytokine and chemokine production in macrophages

Peritoneal macrophages from C57BL/6 mice or CD36-deficient mice were harvested from sterile DMEM cell-culture medium (Wisent # 319-005-CL). Peritoneal cells were allowed to adhere for 1 h at 37°C in a 5% CO_2 atmosphere, and washed twice with PBS to remove non-adherent cells. Macrophages (0.5 x 10^6 cells/well) were plated in 48 well-culture plates with DMEM containing 0.2 % of bovine serum albumin (BSA). Macrophages were pretreated for 2 h with azasulfurylpeptides **146b-e** or **188** (1 μM), before stimulation with a TLR2 ligand:

fibroblast-stimulating lipopeptide (R-FSL-1, Invivogen® #L7022) at 300 ng/ml, lipoteichoic acid (LTA Invivogen® #TLRL-PSLTA) at 1 µg/ml or $Pam_3CysSerLys_4$ (PAM_3CSK_4 Invivogen® #TLRL-PMS) at 100 ng/ml and interferon gamma (IFNγ R&D Systems® # 172-5201) at 20 ng/ml for 4 or 24 hours. The supernatants were recovered, and ELISA (eBioscience® #88-7324; 88-7391) was performed to measure the amounts of proinflammatory cytokine and chemokine (TNFα, MCP-1). The effect on NF-κB activation was documented on cell lysates after 0, 5, 10, 15 and 30 minutes stimulation with R-FSL1, using NF-κB p65/RelA specific ELISA-based assay (eBioscience® #85-86083). The results were expressed as mean ± SEM and were analyzed statistically by a one-way ANOVA with a Dunnett as a post-test. Level of significance was set at $P < 0.05$.

Tyr-Ala-His-D-Trp-Ala-AsF(4-F)-D-Phe-Lys-NH_2 (189)

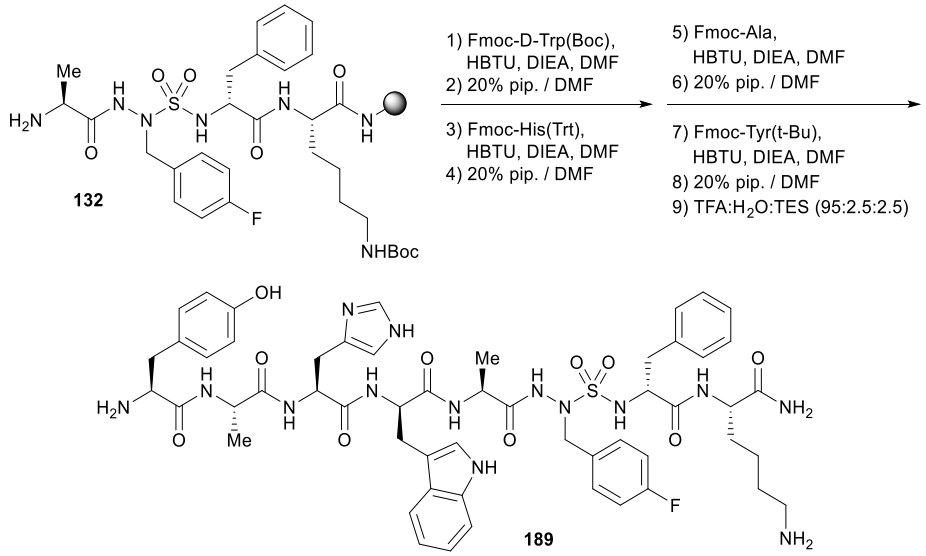

Azasulfurylpeptide **189** was synthesized from resin **132** by sequential Fmoc group removal, HBTU couplings of Fmoc-D-Trp(Boc), Fmoc-His(Trt), Fmoc-Ala, followed by Fmoc-Try(*t*-Bu) and resin (60 mg) cleavage using the respective general protocols described above. Analysis of a resin aliquot as described above indicated peptide **189** to be of 86% purity:

R*t* 4.98 min using a Sunfire™ column and a gradient of 10%-80% MeOH (0.1% FA) in water (0.1% FA) for 7.5 min followed by 90% MeOH (0.1% FA) in water (0.1% FA) for 2.0 min. The TFA salt was purified by preparative RP-HPLC using a Gemini® 5 micron C18 110A column (Phenomenex® Inc., 250×21.2 mm, 5 μm) with a gradient of 20%-50% MeOH (0.1% FA) in water (0.1% FA), with a flow rate of 10.0 mL / min, to afford the desired FA salt of **189** (2.5 mg, 13%). Analysis of the purified product by analytical RP-HPLC using the Sunfire™ column revealed >99% purity: Gradient 1: R*t* 5.95 min [5%-80% MeOH (0.1% FA) in water (0.1% FA) for 7.5 min + 90% MeOH (0.1% FA) in water (0.1% FA) for 2.0 min]; Gradient 2: R*t* 5.61 min [5%-80% MeCN (0.1% FA) for 7.5 min + 90% MeCN (0.1% FA) for 2.0 min]. HRMS (ESI) m/z calculated for $C_{54}H_{67}FN_{14}NaO_{10}S$ $[M+Na]^+$ 1145.4762; found 1145.4759.

Scheme 1. Synthesis of *N*-(Alloc)-alaninyl-azasulfurylglycinyl-D-phenylalanine methyl ester (193)

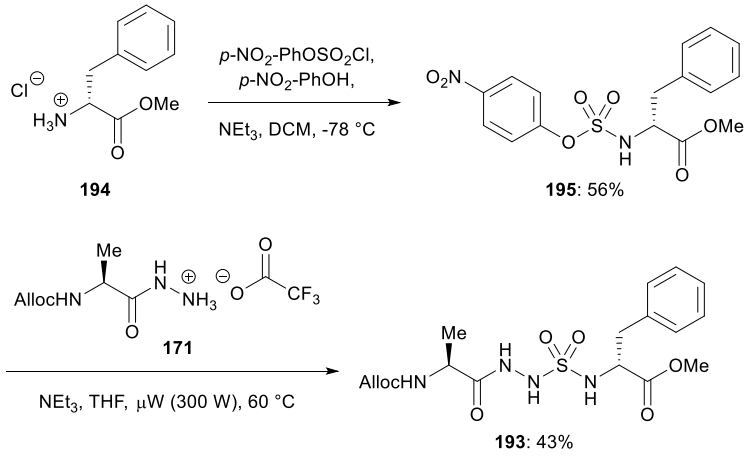

4-Nitrophenyl D-phenylalanine methyl ester sulfamidate 195

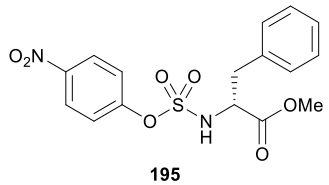

Employing the protocol for the synthesis of sulfamidate **87**, D-phenylalanine methyl ester hydrochloride (**194**, 2.157 g, 10.0 mmol) was transformed to sulfamidate **195**, which was

isolated as a solid (2.136 g, 56%): R_f 0.82 (MeOH:DCM 1:99); mp 77 °C; $[\alpha]^{20}_D$ −34.5° ($CHCl_3$, *c* 1.34); ^{1}H NMR ($CDCl_3$, 400 MHz) δ 3.09 (1H, dd, *J* = 6.6, 13.9), 3.20 (1H, dd, *J* = 5.4, 14.0), 3.78 (3H, s), 4.47-4.53 (1H, m), 5.76 (1H, d, *J* = 8.7), 7.14-7.18 (2H, m), 7.25 (2H, d *J* = 9.2), 7.27-7.33 (3H, m), 8.18 (2H, d *J* = 9.2); ^{13}C NMR ($CDCl_3$, 100 MHz) δ 39.0, 53.3, 58.4, 122.7, 125.8, 127.9, 129.1, 129.7, 134.9, 146.2, 154.5, 171.3; IR (neat) ν_{max}/cm^{-1} 1155, 1175, 1347, 1529, 1622, 1730, 3249; HRMS *m/z* calculated for $C_{16}H_{16}N_2NaO_7S$ $[M+Na]^+$ 398.1032; found 398.1017.

_N_-(Alloc)-alaninyl-azasulfurylglycinyl-D-phenylalanine methyl ester (193)

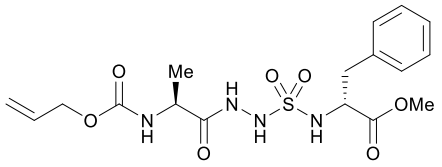

193

N-(Alloc)-alanine hydrazidium trifluoroacetate (**171**, 331 mg; 1.1 mmol) was neutralized by adding aq. sat. $NaHCO_3$ and extracting with EtOAc. It was then added to a solution of sulfamidate **195** (380 mg, 1.00 mmol) in THF (4.0 mL) in a microwave vessel. The mixture was treated with NEt_3 (153 μL, 1.10 mmol), at which point the solution turned yellow. Gentle heating with a heat gun may be required to facilitate dissolution. The vessel was sealed and heated to 60 °C using microwave irradiation for 2.5 h. The volatiles were then evaporated and the residue was purified by flash chromatography eluting with hexane:EtOAc 1:1. The necessary fractions were evaporated and redissolved in DCM (25 mL). The organic phase was washed with sat. $NaHCO_3$ (3 x 25 mL), dried over $MgSO_4$, filtered and evaporated to afford sulfamide **193** as a solid (184 mg; 43%): R_f 0.24 (hexane:EtOAc 1:1); mp 57 °C; $[\alpha]^{20}_D$ –65.4° ($CHCl_3$, *c* 0.66); ^{1}H NMR ($CDCl_3$, 400 MHz) δ 1.33 (3H, d, *J* = 7.1), 3.10 (2H, d, *J* = 5.8), 3.68 (3H, s), 4.20-4.30 (1H, m), 4.40-4.50 (1H, m), 4.50-4.60 (2H, m), 5.20 (1H, d, *J* = 10.4), 5.27 (1H, d, *J* = 17.2), 5.65 (1H, d, *J* = 7.5), 5.80-5.95 (2H, m), 7.10-7.15 (2H, m), 7.20-7.30 (3H, m), 7.40 (1H, br), 8.71 (1H, s); ^{13}C NMR ($CDCl_3$, 100 MHz) δ 18.2, 19.4, 30.9, 39.2, 49.5, 53.0,57.4, 66.5, 118.4, 127.5, 128.8, 129.9, 132.7, 135.6, 156.5, 172.4, 172.7; IR (neat) ν_{max}/cm^{-1} 1108, 1165, 1252,

1356, 1452, 1520, 1692, 3259; HRMS (ESI) m/z calculated for $C_{17}H_{25}N_4O_7S$ $[M+H]^+$ 429.1439; found 429.1458.

Annexe 5 : Spectres RMN

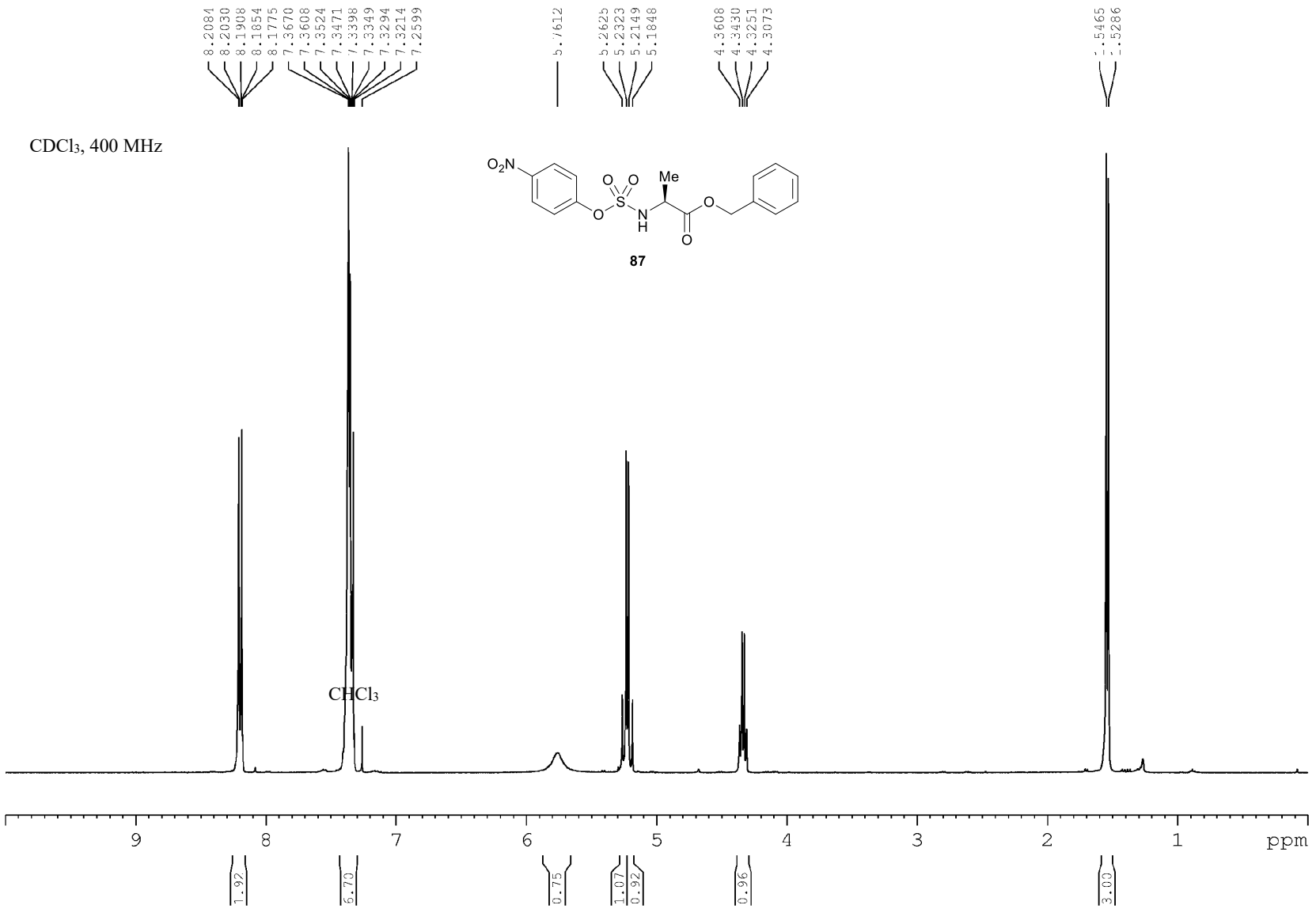
8.2084
8.2030
8.1908
8.1854
8.1775
7.3670
7.3608
7.3524
7.3471
7.3398
7.3349
7.3294
7.3214
7.2599
5.7612
5.2625
5.2323
5.2149
5.1848
4.3608
4.3430
4.3251
4.3073
1.5465
1.5286
CDCl3, 400 MHz
O2N
Me
87
CHCl3
9
8
7
6
5
4
3
2
1
ppm
1.92
5.70
0.75
1.07
0.92
0.96
3.00

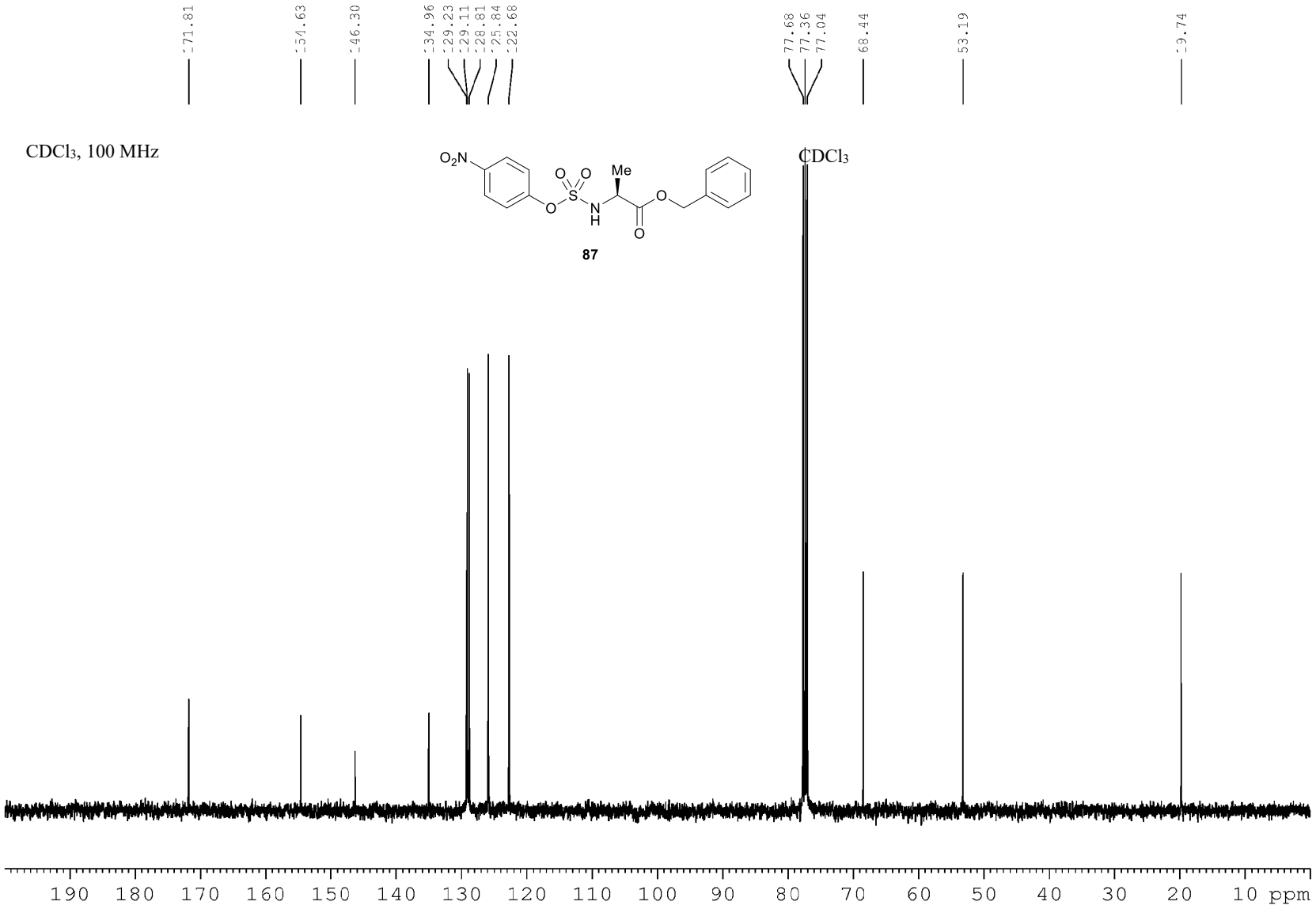
171.81
154.63
146.30
134.96
129.23
129.11
128.81
125.84
122.68
77.68
77.36
77.04
68.44
53.19
19.74
CDCl3, 100 MHz
O2N
O
O
S
O
N
H
Me
O
O
87
CDCl3
190 180 170 160 150 140 130 120 110 100 90 80 70 60 50 40 30 20 10 ppm

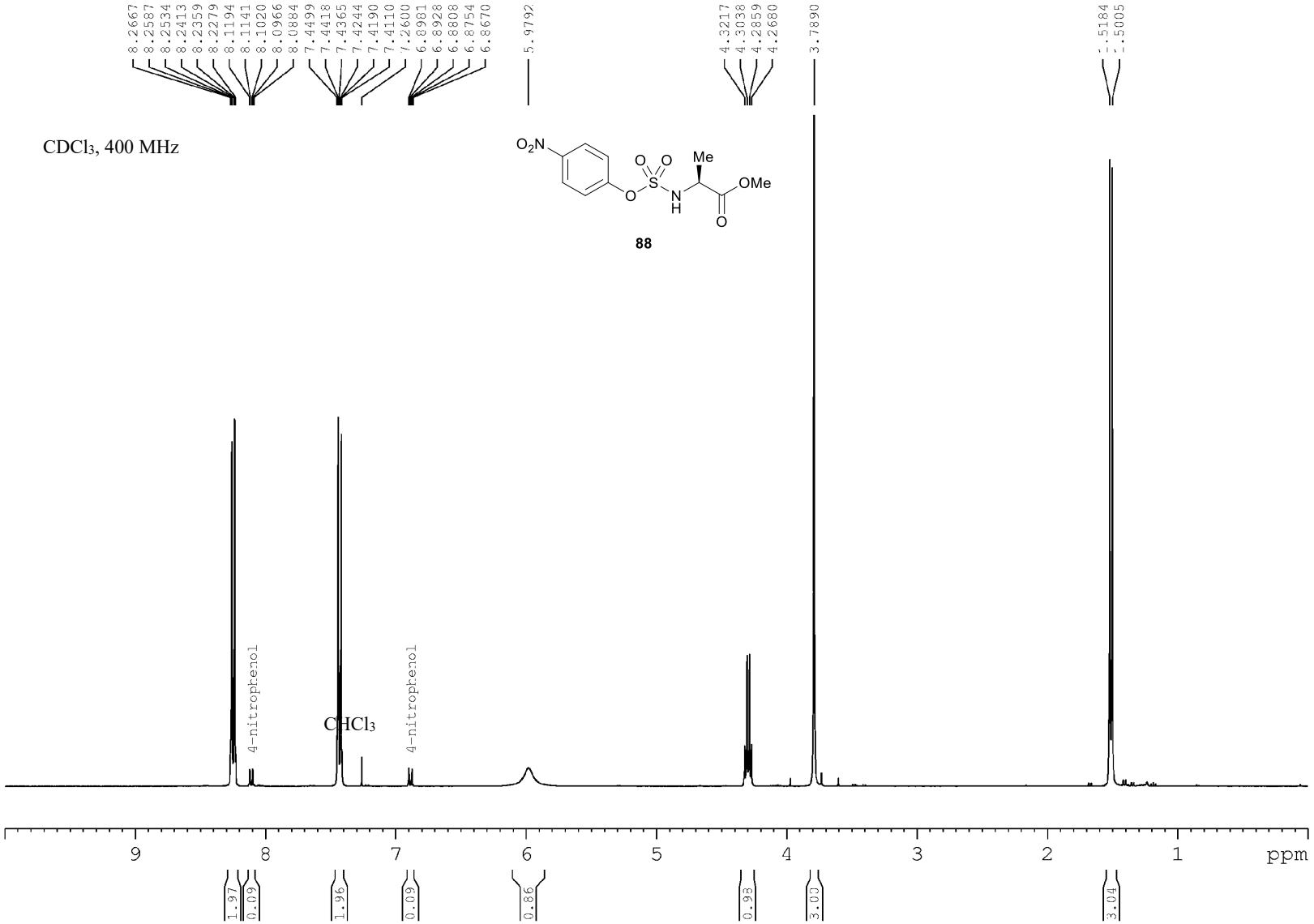
8.2667
8.2587
8.2534
8.2413
8.2359
8.2279
8.1194
8.1141
8.1020
8.0966
8.0884
7.4499
7.4418
7.4365
7.4244
7.4190
7.4110
7.2600
6.8981
6.8928
6.8808
6.8754
6.8670
5.9792
4.3217
4.3038
4.2859
4.2680
3.7890
1.5184
1.5005
CDCl3, 400 MHz
O2N
O
O
S
O
N
H
Me
OMe
O
88
4-nitrophenol
CHCl3
4-nitrophenol
9
8
7
6
5
4
3
2
1
ppm
1.97
0.09
1.96
0.09
0.86
0.93
3.03
3.04

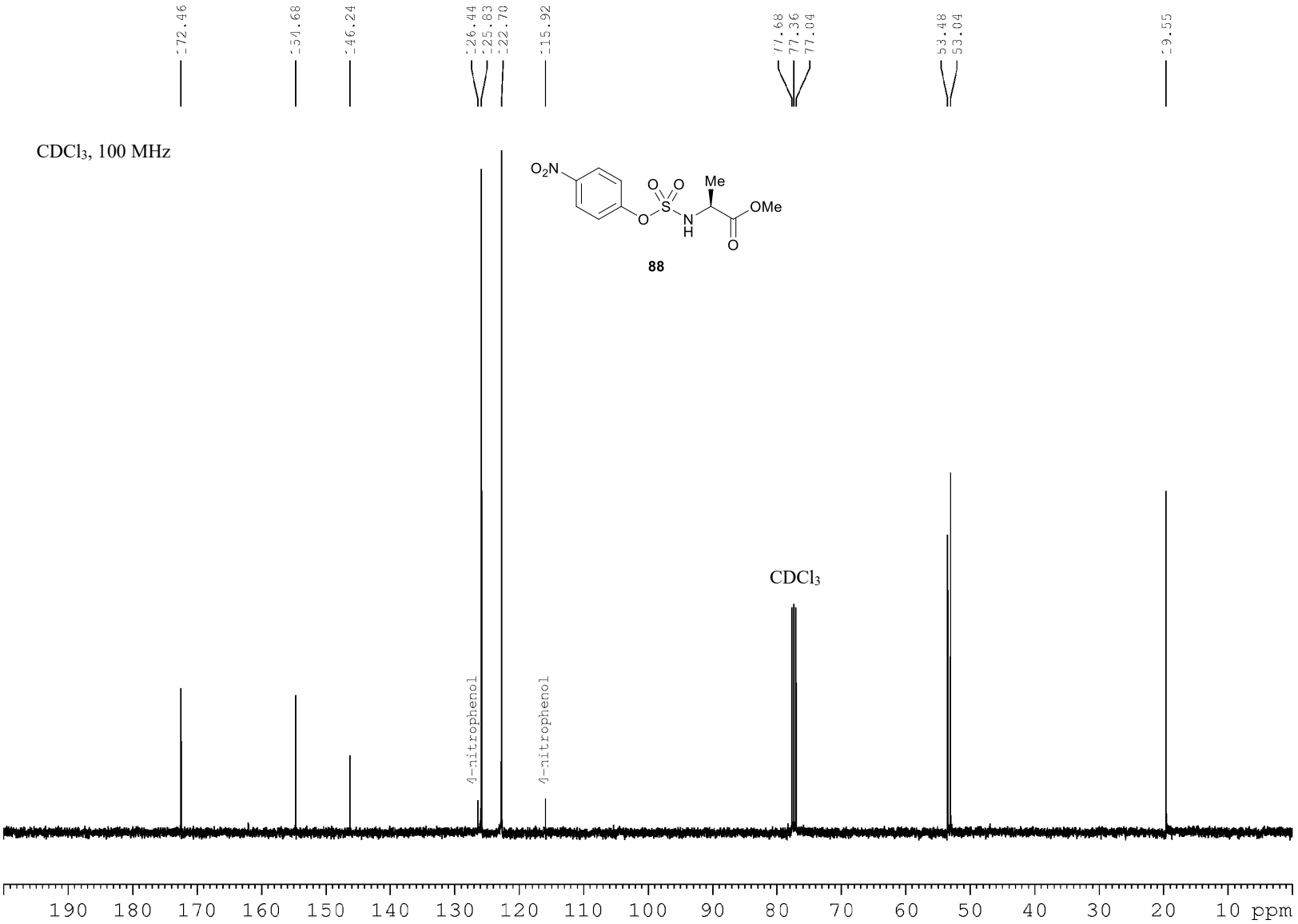
172.46
154.68
146.24
126.44
125.83
122.70
115.92
77.68
77.36
77.04
53.48
53.04
19.55
CDCl3, 100 MHz
O2N
O
O
S
O
N
H
Me
OMe
O
88
4-nitrophenol
4-nitrophenol
CDCl3
190 180 170 160 150 140 130 120 110 100 90 80 70 60 50 40 30 20 10 ppm

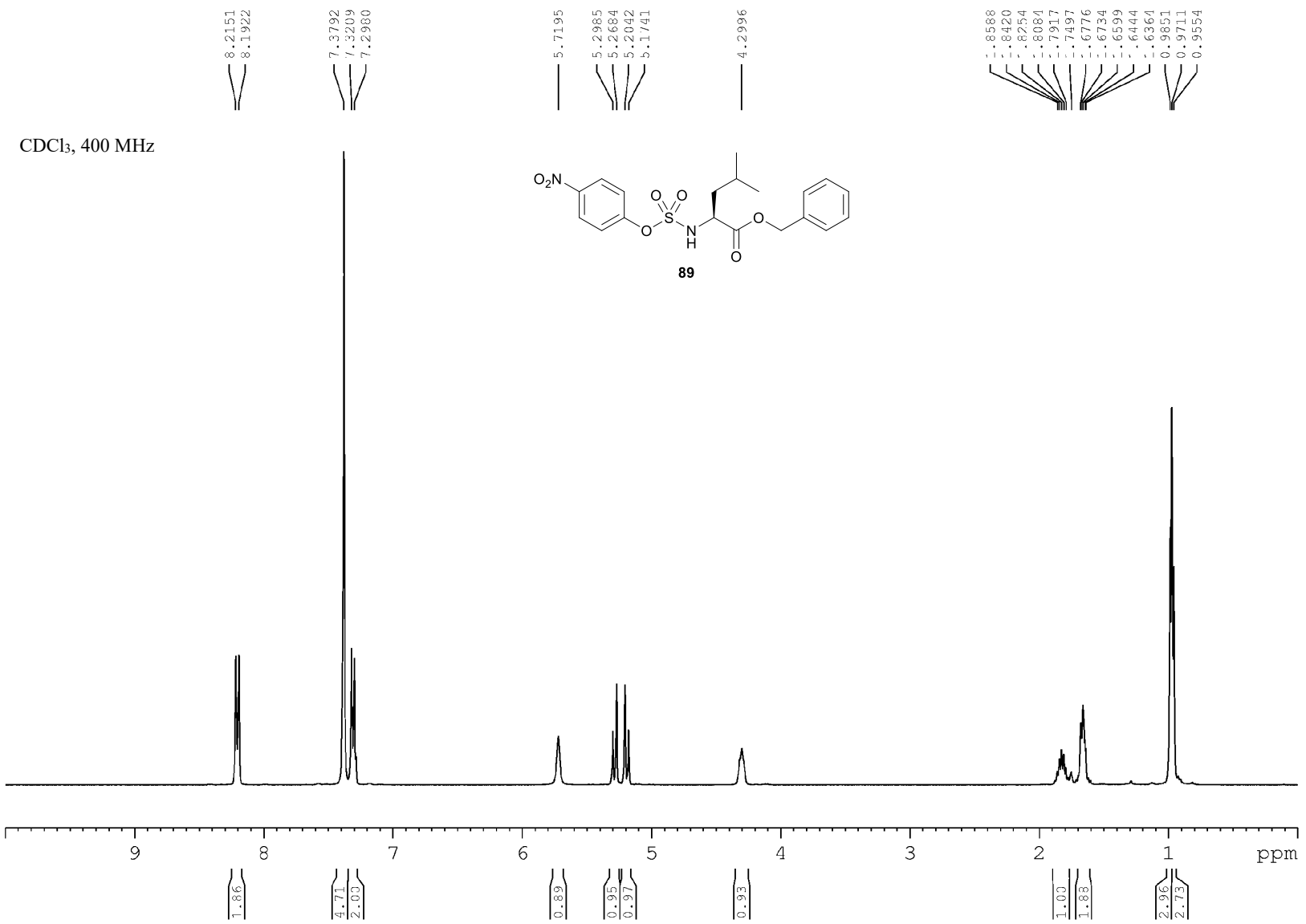
8.2151
8.1922
7.3792
7.3209
7.2980
5.7195
5.2985
5.2684
5.2042
5.1741
4.2996
1.8588
1.8420
1.8254
1.8084
1.7917
1.7497
1.6776
1.6734
1.6599
1.6444
1.6361
0.9851
0.9711
0.9554
CDCl3, 400 MHz
O2N
O
O
S
O
N
H
O
O
O
89
9
8
7
6
5
4
3
2
1
ppm
1.86
4.71
2.03
0.89
0.95
0.97
0.93
1.00
1.88
2.96
2.73

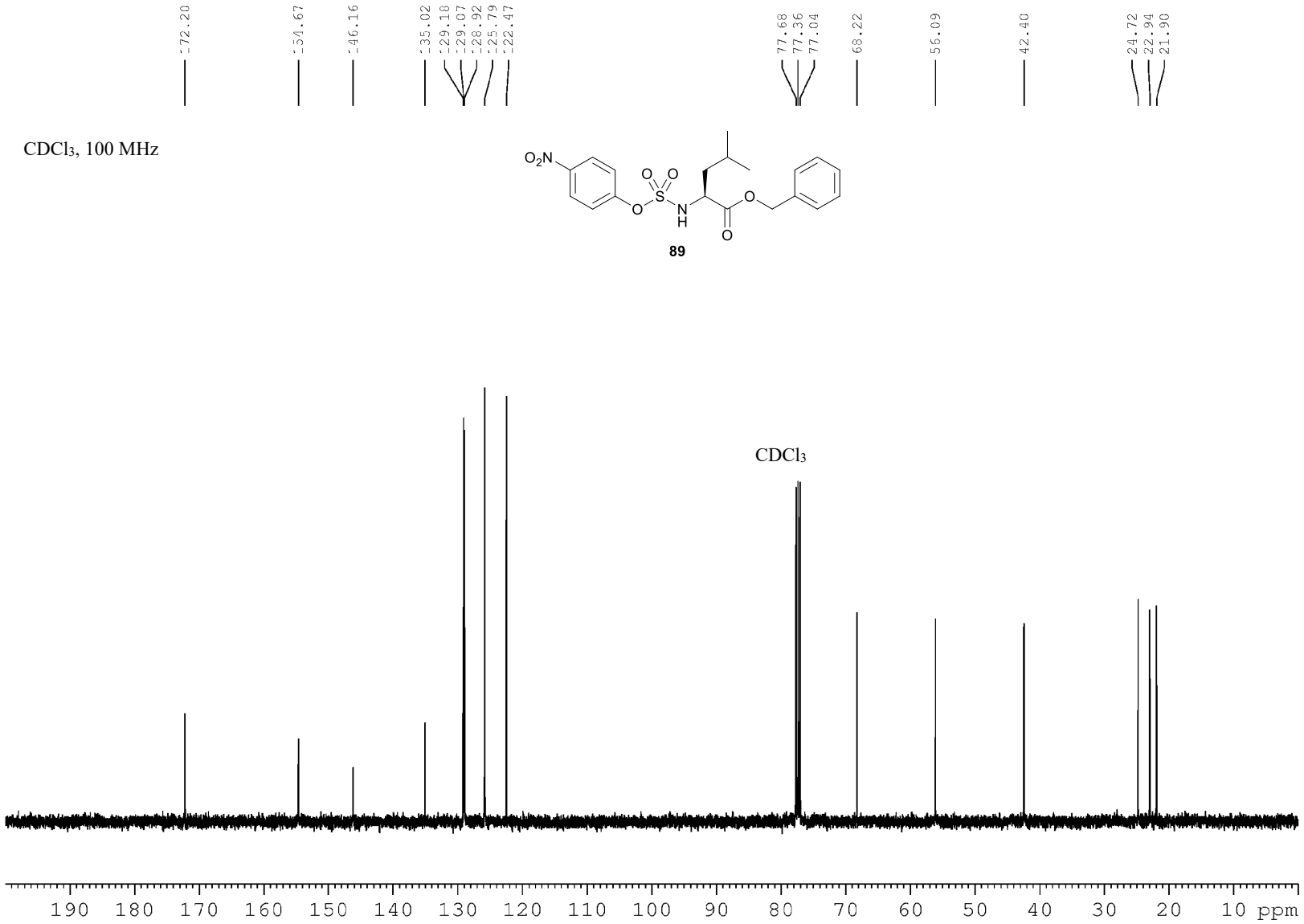
172.20
154.67
146.16
135.02
129.10
129.07
128.92
125.79
122.47
77.68
77.36
77.04
68.22
56.09
42.40
24.72
22.94
21.90
CDCl3, 100 MHz
O2N
O
O
S
O
N
H
O
O
O
89
CDCl3
190 180 170 160 150 140 130 120 110 100 90 80 70 60 50 40 30 20 10 ppm

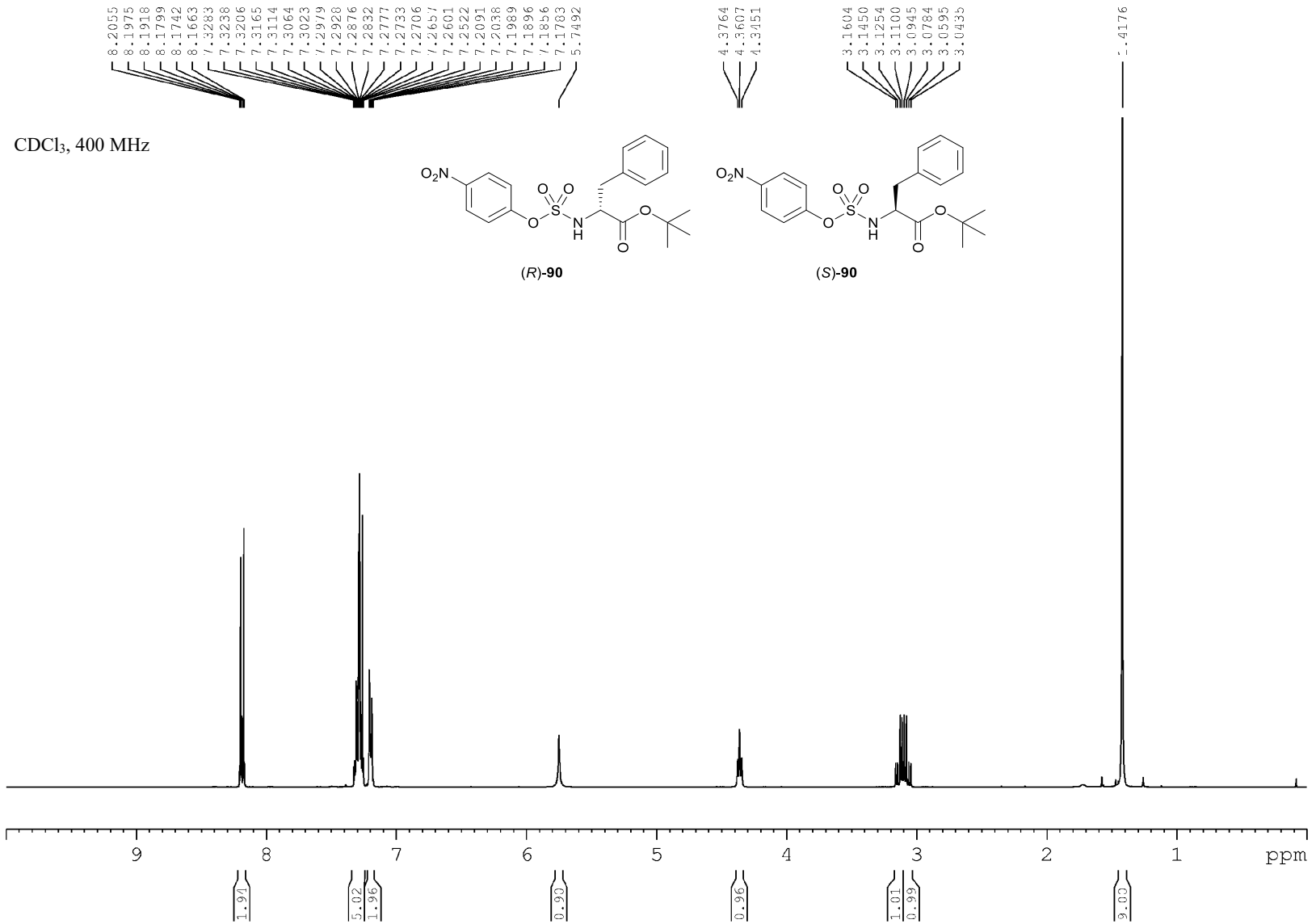
8.2055
8.1975
8.1918
8.1799
8.1742
8.1663
7.3283
7.3238
7.3206
7.3165
7.3114
7.3064
7.3023
7.2979
7.2928
7.2876
7.2832
7.2777
7.2733
7.2706
7.2657
7.2601
7.2522
7.2091
7.2038
7.1989
7.1896
7.1856
7.1783
5.7492
4.3764
4.3607
4.3451
3.1604
3.1450
3.1254
3.1100
3.0945
3.0784
3.0595
3.0435
1.4176
CDCl3, 400 MHz
(R)-90
(S)-90
9
8
7
6
5
4
3
2
1
ppm
1.94
5.02
1.96
0.90
0.96
1.01
0.99
9.00

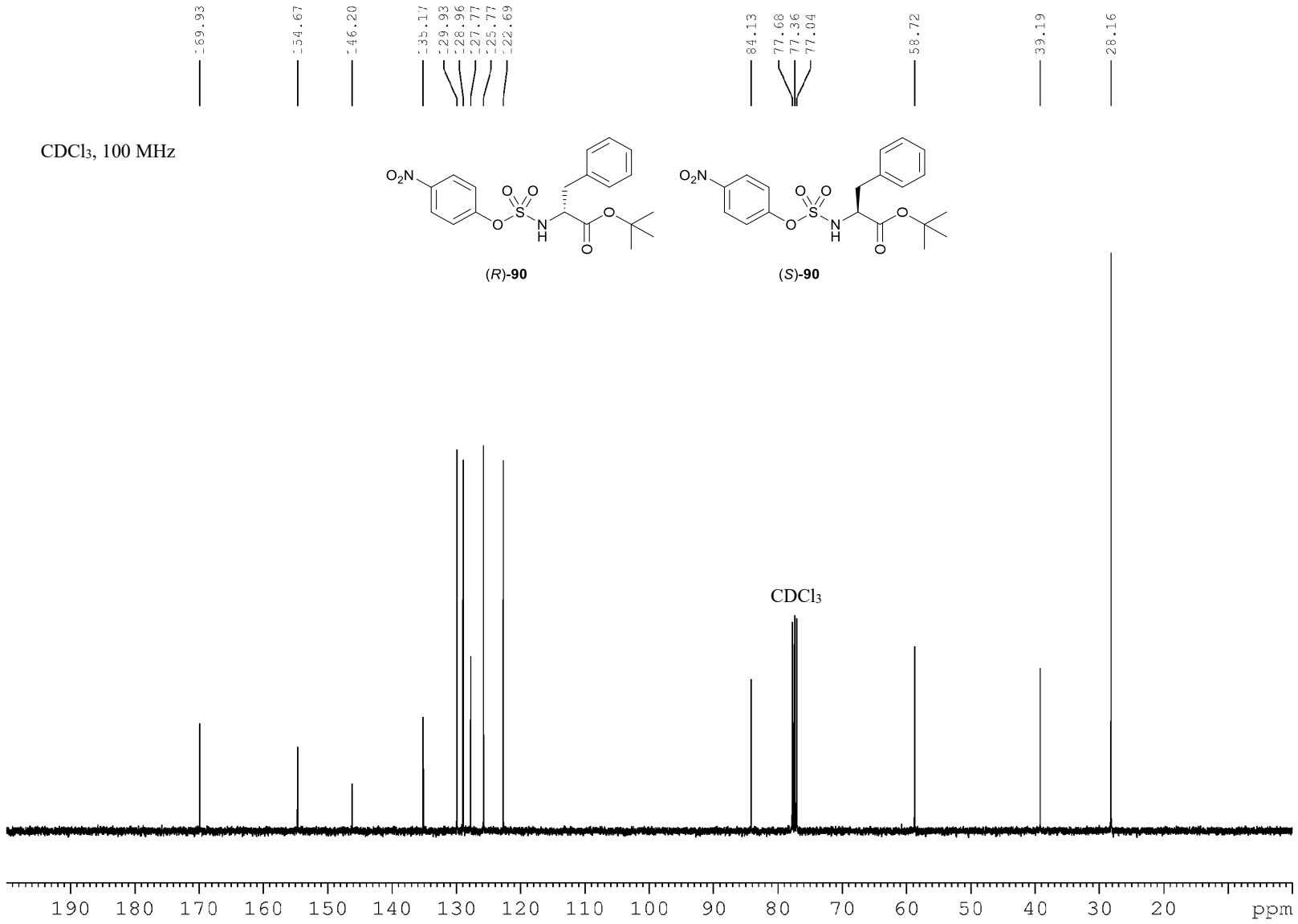
169.93
134.67
146.20
135.17
129.93
128.96
127.77
125.77
122.69
84.13
77.68
77.36
77.04
58.72
39.19
28.16
CDCl3, 100 MHz
(R)-90
(S)-90
CDCl3
190 180 170 160 150 140 130 120 110 100 90 80 70 60 50 40 30 20 ppm

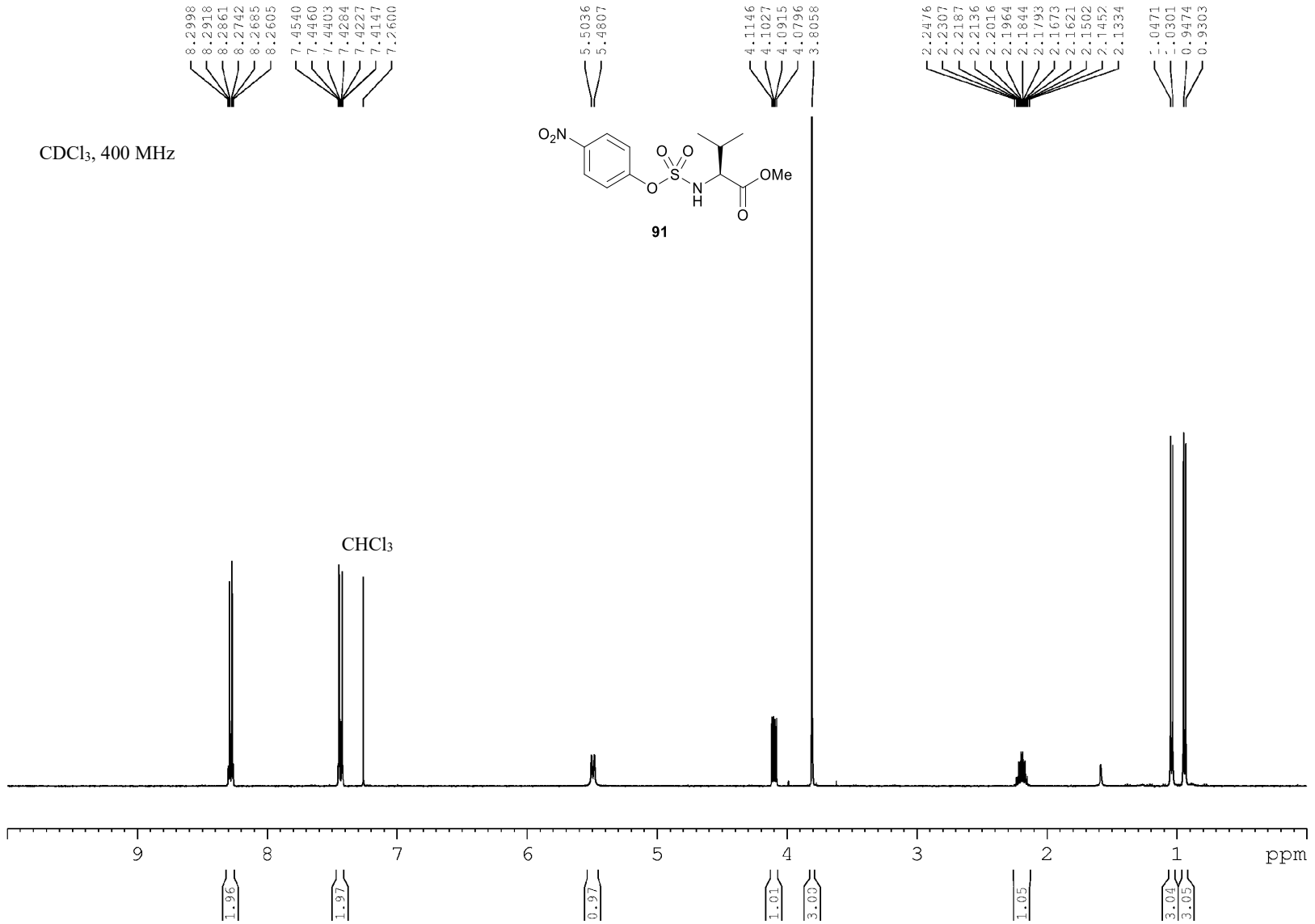
8.2998
8.2918
8.2861
8.2742
8.2685
8.2605
7.4540
7.4460
7.4403
7.4284
7.4227
7.4147
7.2600
5.5036
5.4807
4.1146
4.1027
4.0915
4.0796
3.8058
2.2476
2.2307
2.2187
2.2136
2.2016
2.1964
2.1844
2.1793
2.1673
2.1621
2.1502
2.1452
2.1334
1.0471
1.0301
0.9474
0.9303
CDCl3, 400 MHz
O2N
O
O
S
O
N
H
OMe
O
91
CHCl3
9
8
7
6
5
4
3
2
1
ppm
1.96
1.97
0.97
1.01
3.03
1.05
3.04
3.05

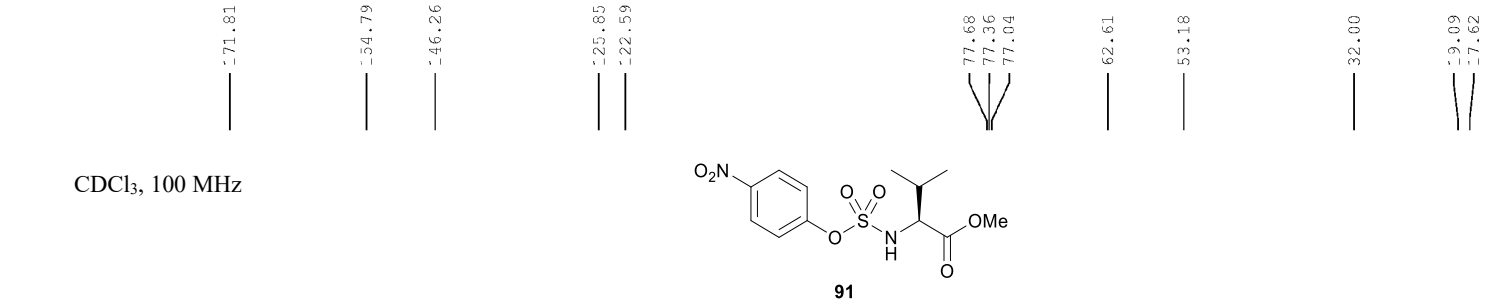

$CDCl_3$, 100 MHz

91

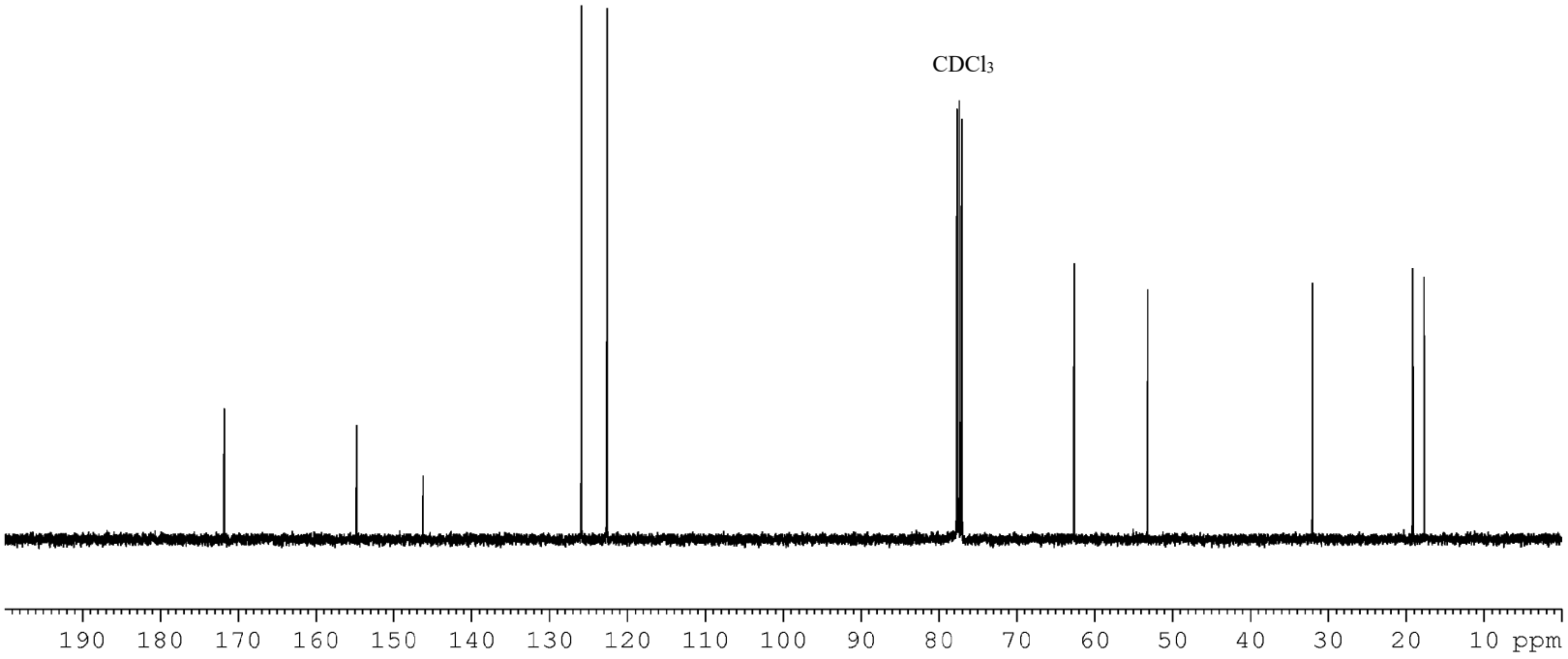

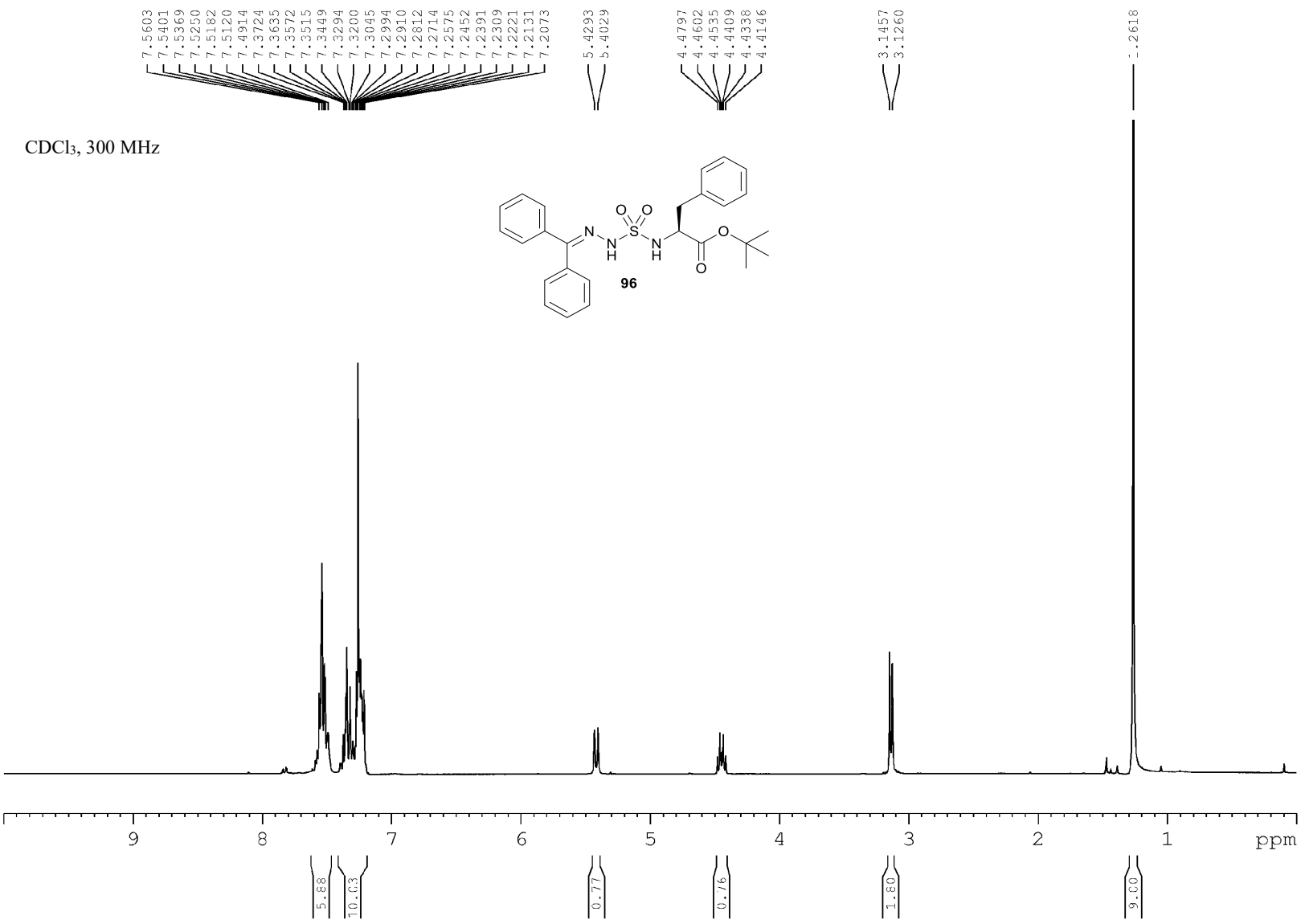
7.5603
7.5401
7.5369
7.5250
7.5182
7.5120
7.4914
7.3724
7.3635
7.3572
7.3515
7.3449
7.3294
7.3200
7.3045
7.2994
7.2910
7.2812
7.2714
7.2575
7.2452
7.2391
7.2309
7.2221
7.2131
7.2073
5.4293
5.4029
4.4797
4.4602
4.4535
4.4409
4.4338
4.4146
3.1457
3.1260
.2618
CDCl3, 300 MHz
96
9
8
7
6
5
4
3
2
1
ppm
5.88
10.03
0.77
0.76
1.80
9.00

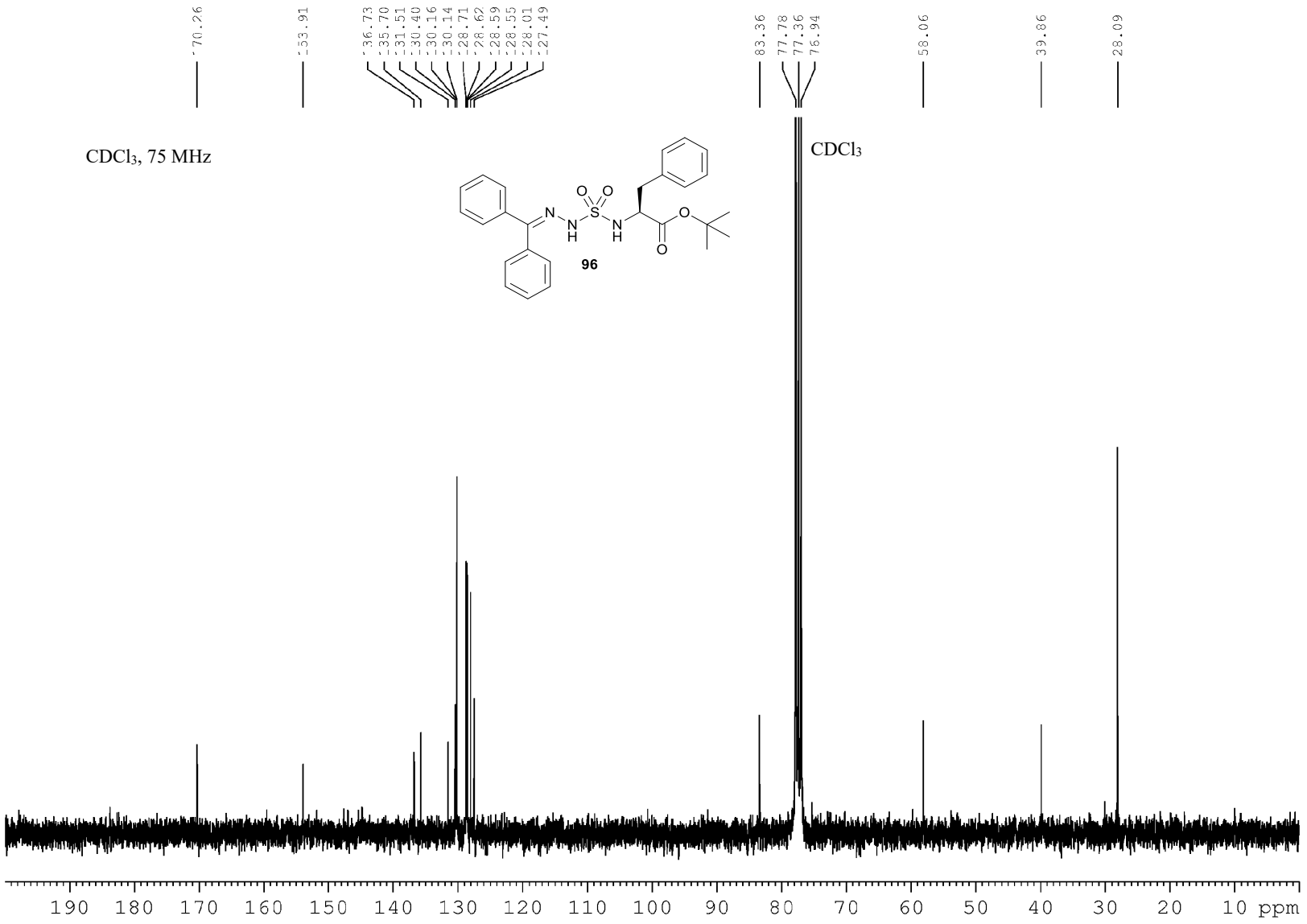
170.26
153.91
136.73
135.70
131.51
130.40
130.16
130.14
128.71
128.62
128.59
128.55
128.01
127.49
83.36
77.78
77.36
76.94
58.06
39.86
28.09
CDCl3, 75 MHz
CDCl3
96
190 180 170 160 150 140 130 120 110 100 90 80 70 60 50 40 30 20 10 ppm

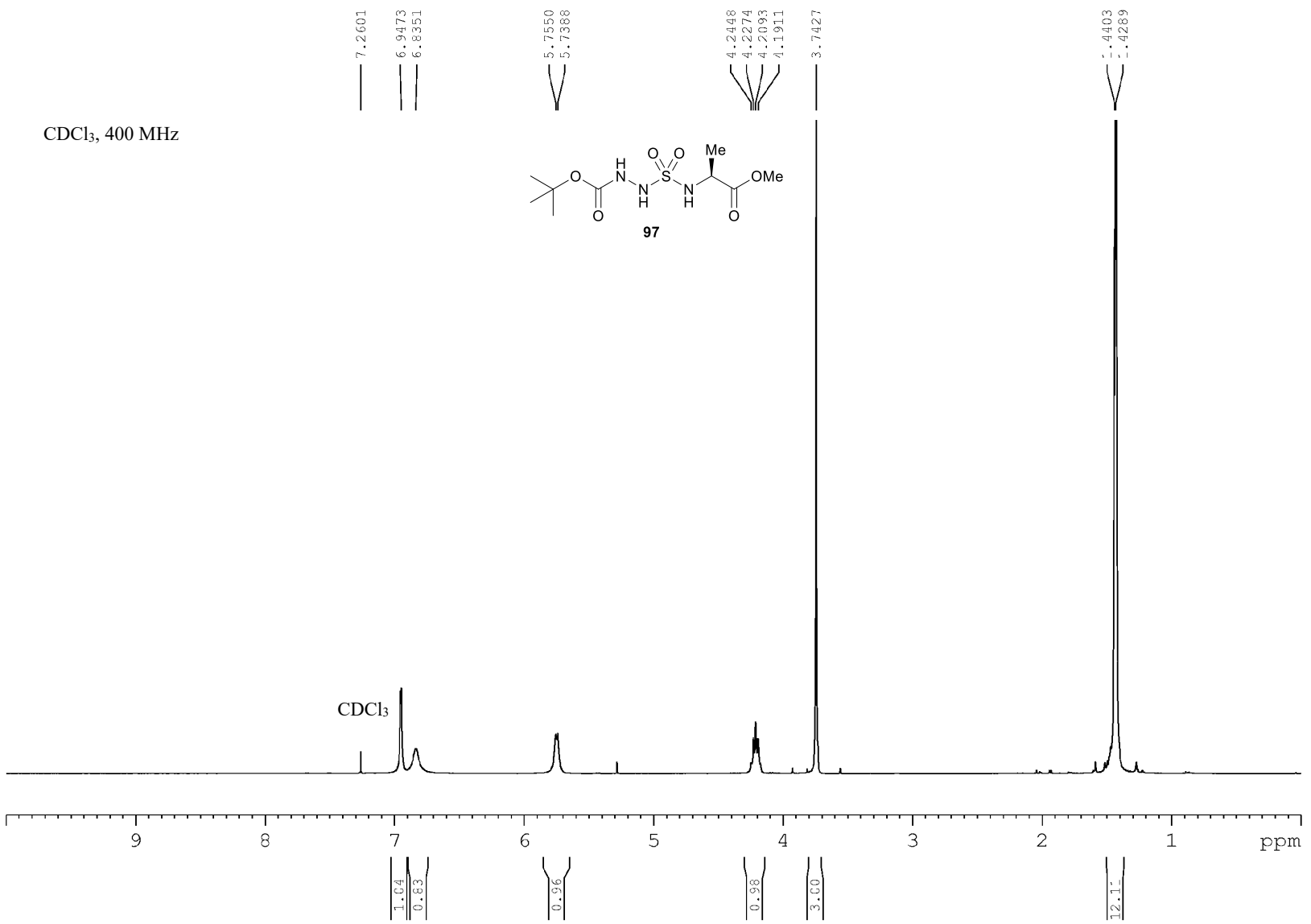
CDCl3, 400 MHz
7.2601
6.9473
6.8351
5.7550
5.7388
4.2448
4.2274
4.2093
4.1911
3.7427
1.4403
1.4289
CDCl3
9
8
7
6
5
4
3
2
1
ppm
1.64
0.83
0.96
0.98
3.60
12.1

97

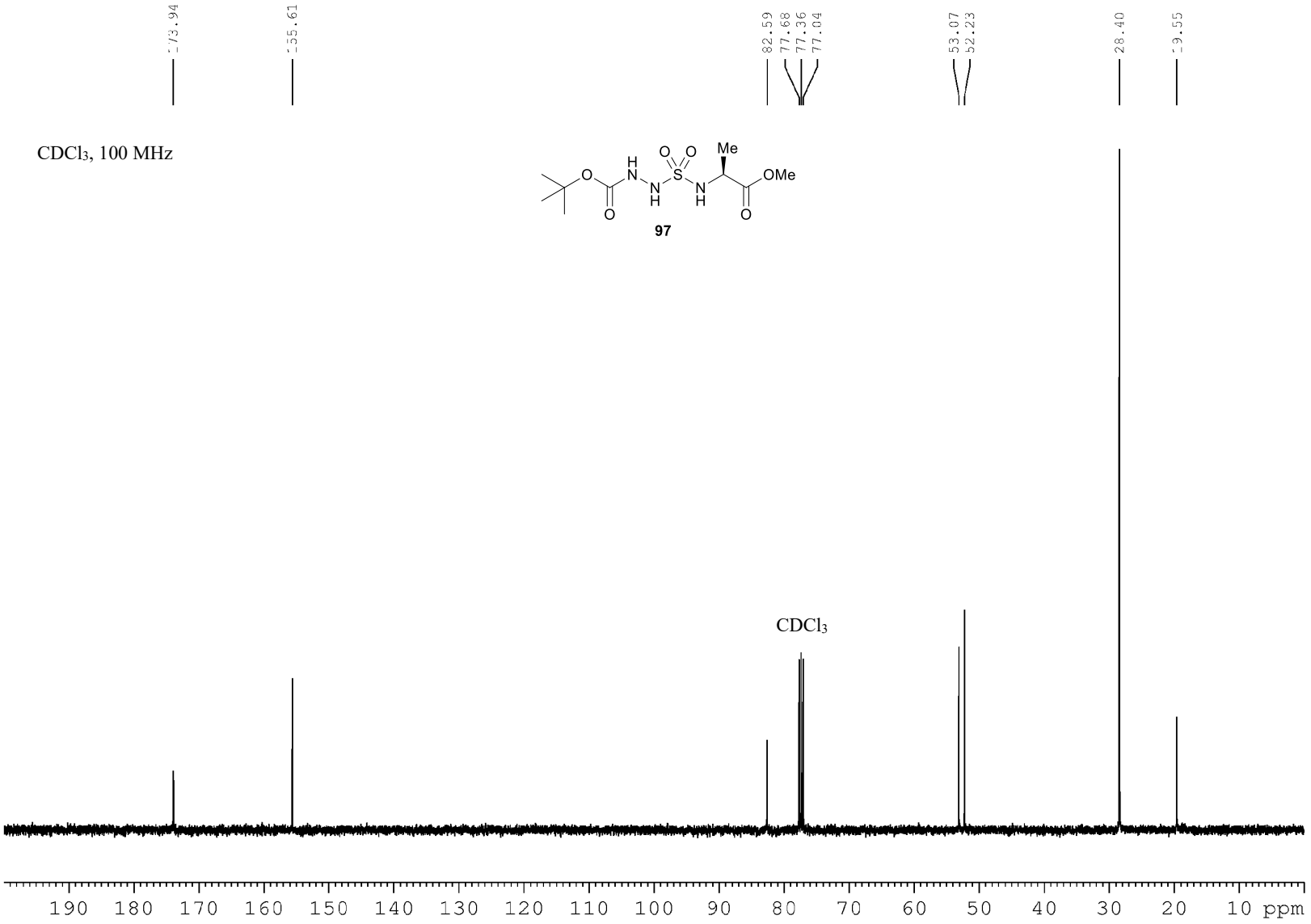
173.94
155.61
82.59
77.68
77.36
77.04
53.07
52.23
28.40
19.55
CDCl3, 100 MHz
CDCl3
190 180 170 160 150 140 130 120 110 100 90 80 70 60 50 40 30 20 10 ppm

Me
OMe

97

$CDCl_3$, 400 MHz

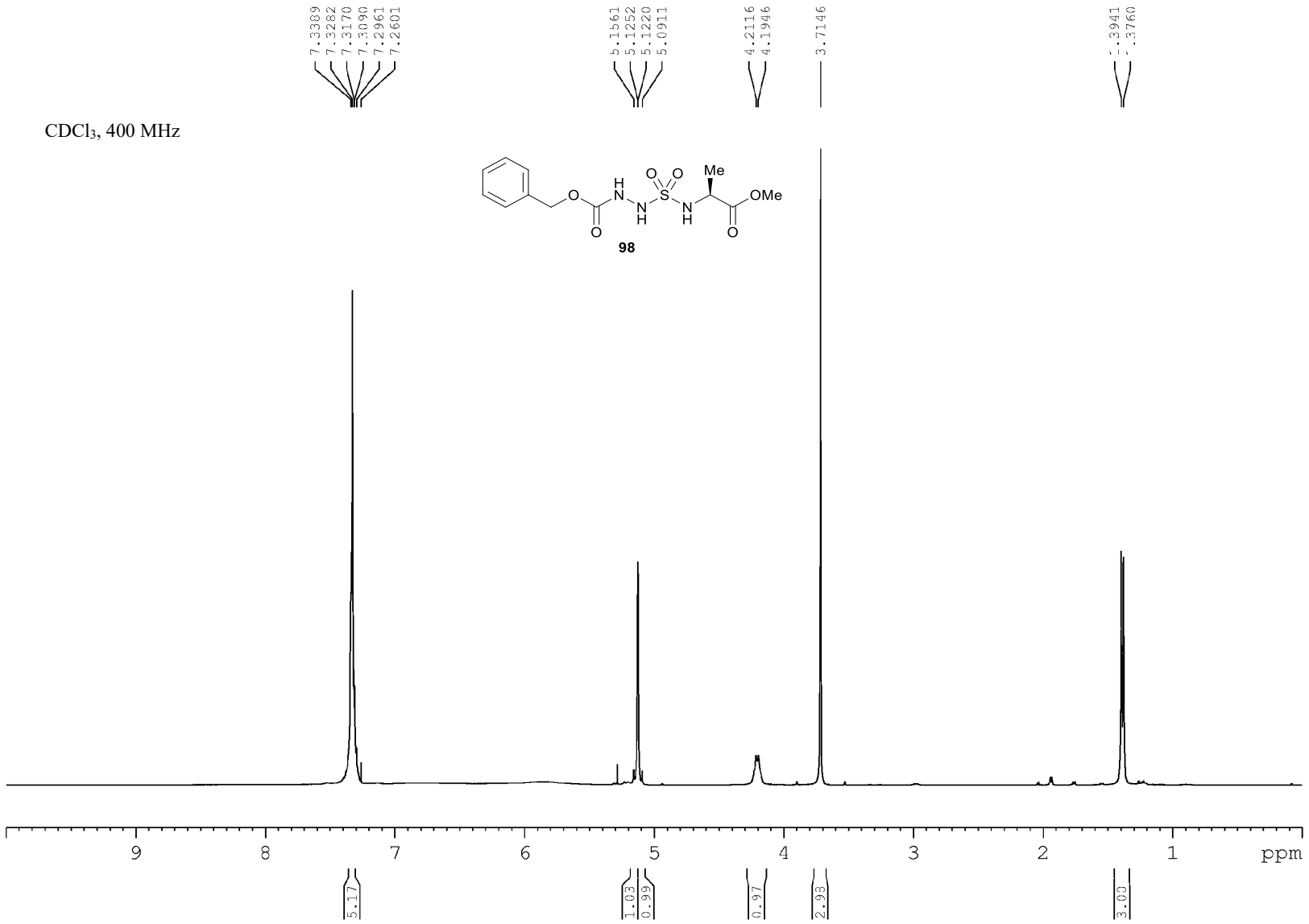

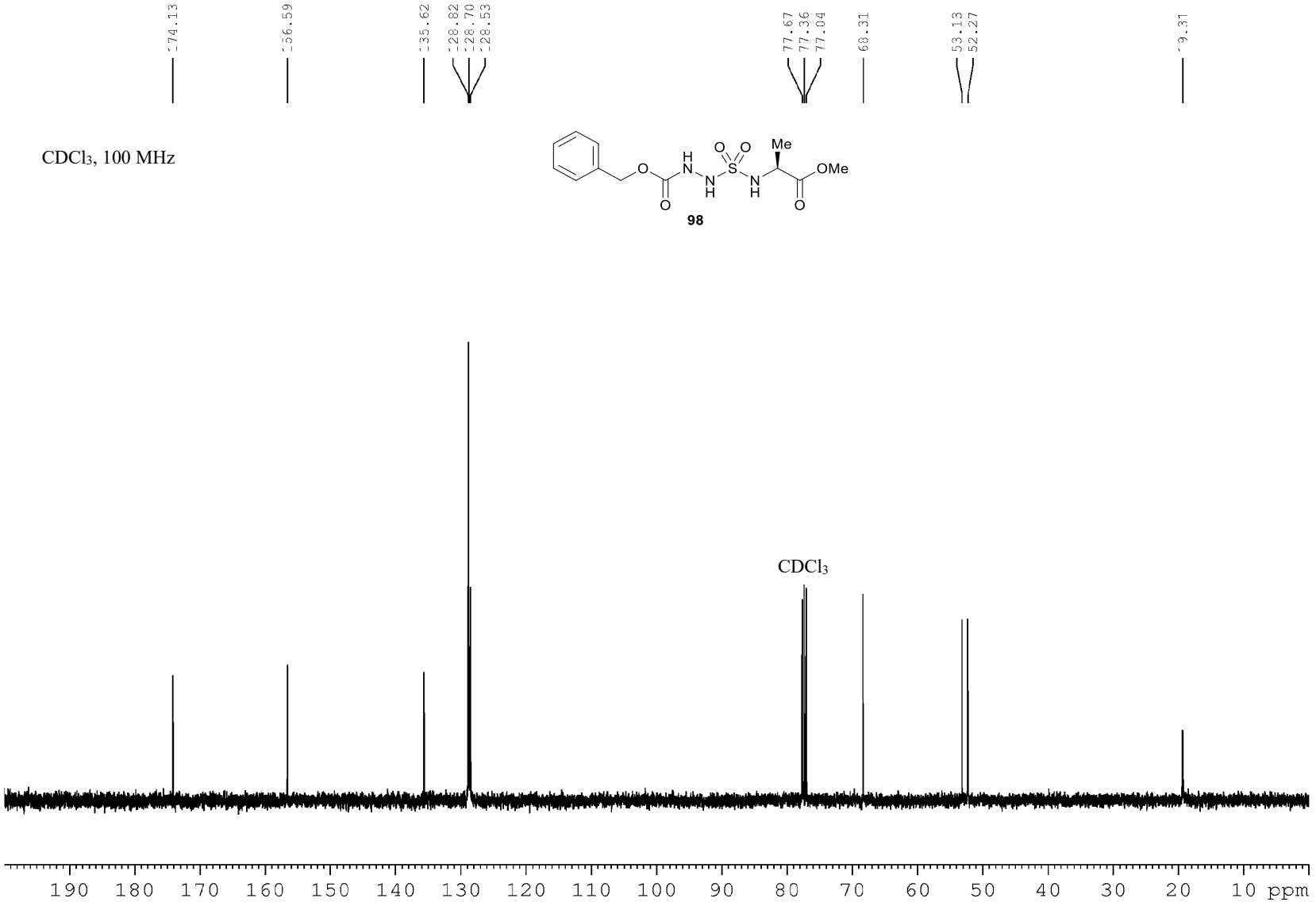
174.13
156.59
135.62
128.82
128.70
128.53
77.67
77.36
77.04
68.31
53.13
52.27
19.31
CDCl3, 100 MHz
98
CDCl3
190 180 170 160 150 140 130 120 110 100 90 80 70 60 50 40 30 20 10 ppm

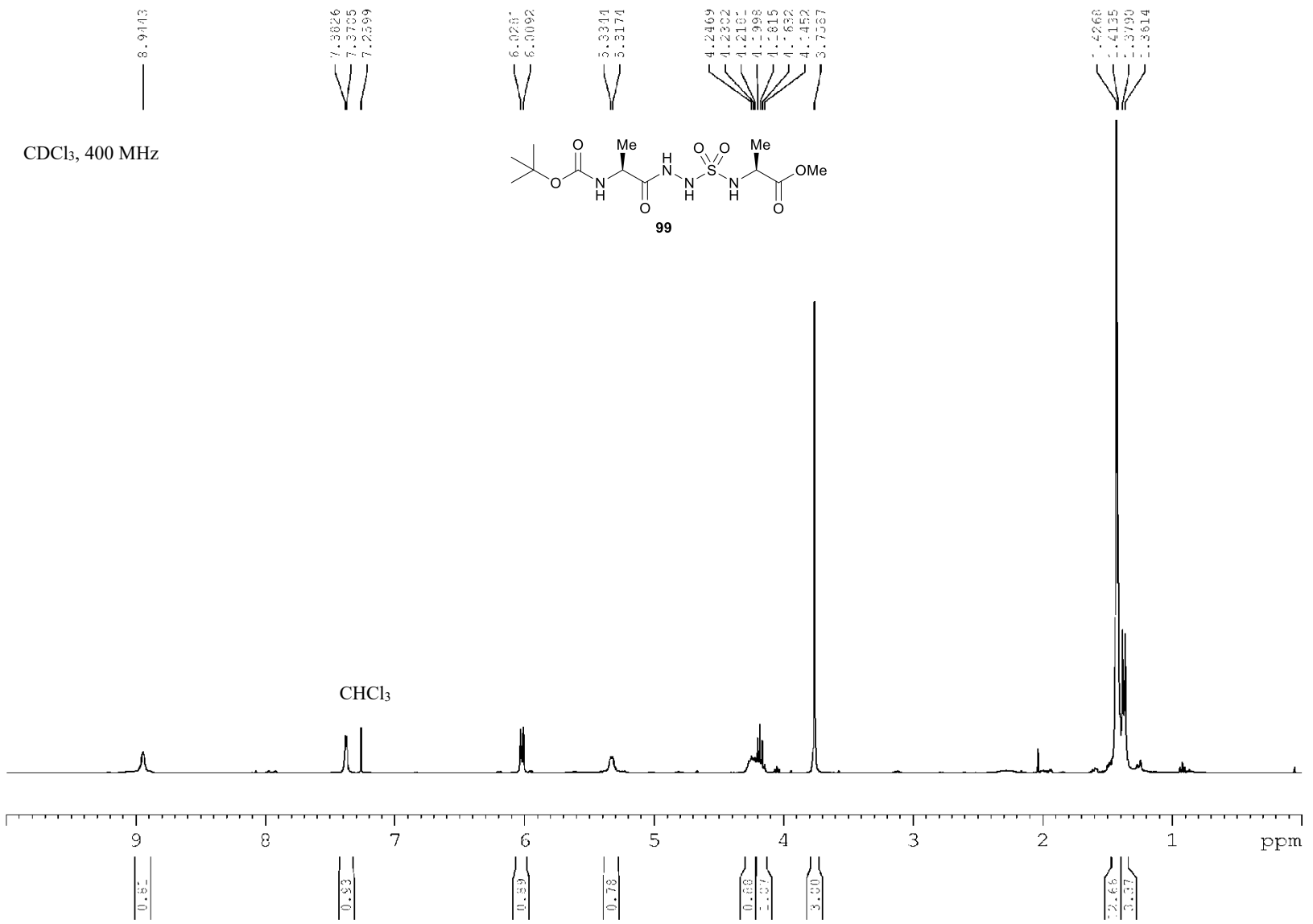
8.9443
7.3826
7.3755
7.2599
6.0283
6.0092
5.3341
5.3174
4.2469
4.2302
4.2103
4.1998
4.1815
4.1632
4.1452
3.7587
1.4268
1.4135
1.3790
1.3614
CDCl3, 400 MHz
CHCl3
99
9
8
7
6
5
4
3
2
1
ppm
0.85
0.93
0.89
0.78
0.68
3.00
2.66
3.37

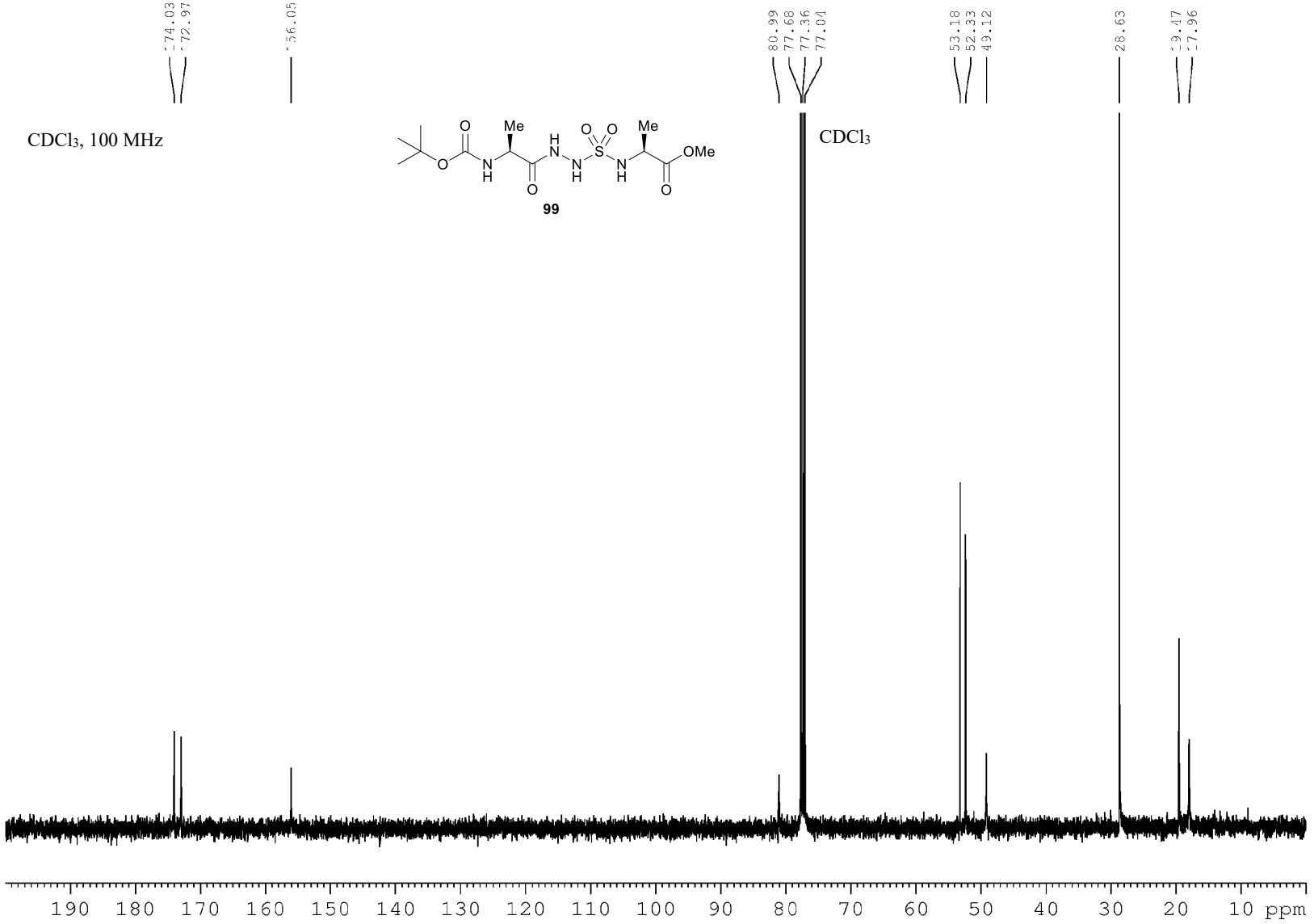
174.03
172.97
156.05
80.99
77.68
77.36
77.04
53.18
52.33
49.12
28.63
19.47
17.96
CDCl3, 100 MHz
CDCl3
99
190 180 170 160 150 140 130 120 110 100 90 80 70 60 50 40 30 20 10 ppm

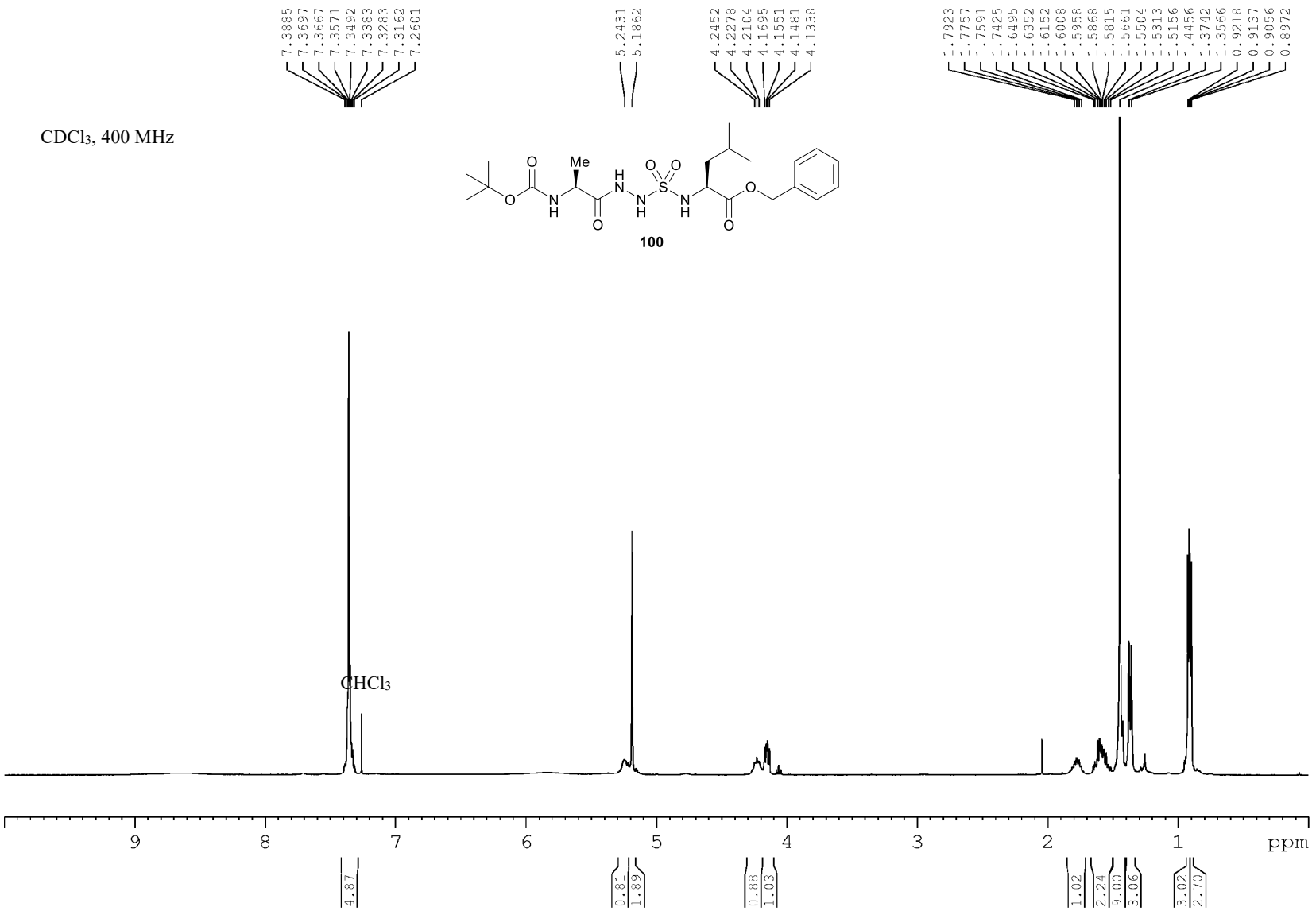
CDCl3, 400 MHz
7.3885
7.3697
7.3667
7.3571
7.3492
7.3383
7.3283
7.3162
7.2601
5.2431
5.1862
4.2452
4.2278
4.2104
4.1695
4.1551
4.1481
4.1338
1.7923
1.7757
1.7591
1.7425
1.6495
1.6352
1.6152
1.6008
1.5958
1.5868
1.5815
1.5661
1.5504
1.5313
1.5156
1.4456
1.3742
1.3566
0.9218
0.9137
0.9056
0.8972
Me
100
CHCl3
9
8
7
6
5
4
3
2
1
ppm
4.87
0.81
1.89
0.88
1.03
1.02
2.24
9.03
3.06
3.02
2.79

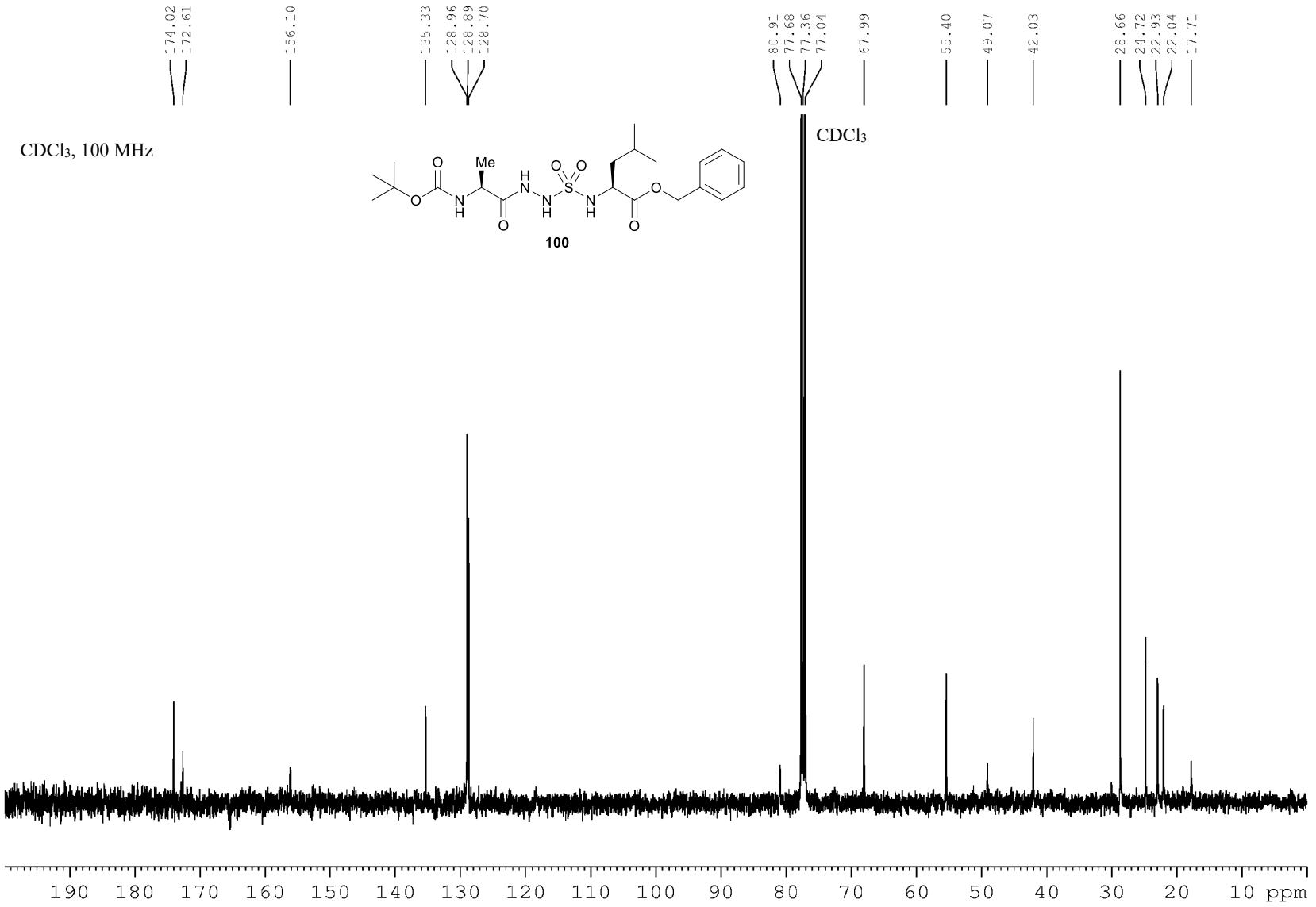
174.02
172.61
156.10
135.33
128.96
128.89
128.70
80.91
77.68
77.36
77.04
67.99
55.40
49.07
42.03
28.66
24.72
22.93
22.04
17.71
CDCl3, 100 MHz
CDCl3
100
190 180 170 160 150 140 130 120 110 100 90 80 70 60 50 40 30 20 10 ppm

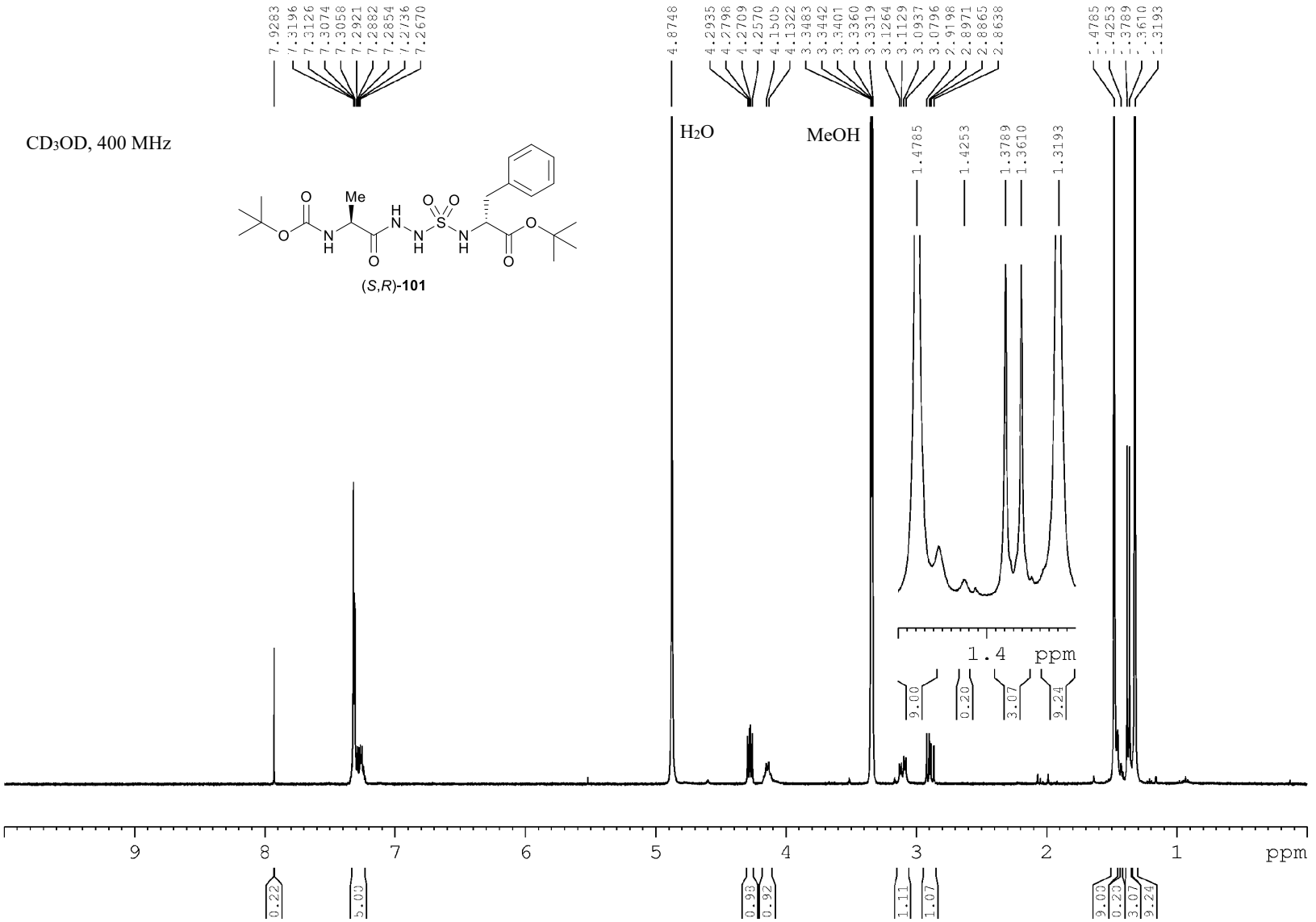
CD3OD, 400 MHz
(S,R)-101
H2O
MeOH
1.4 ppm
ppm

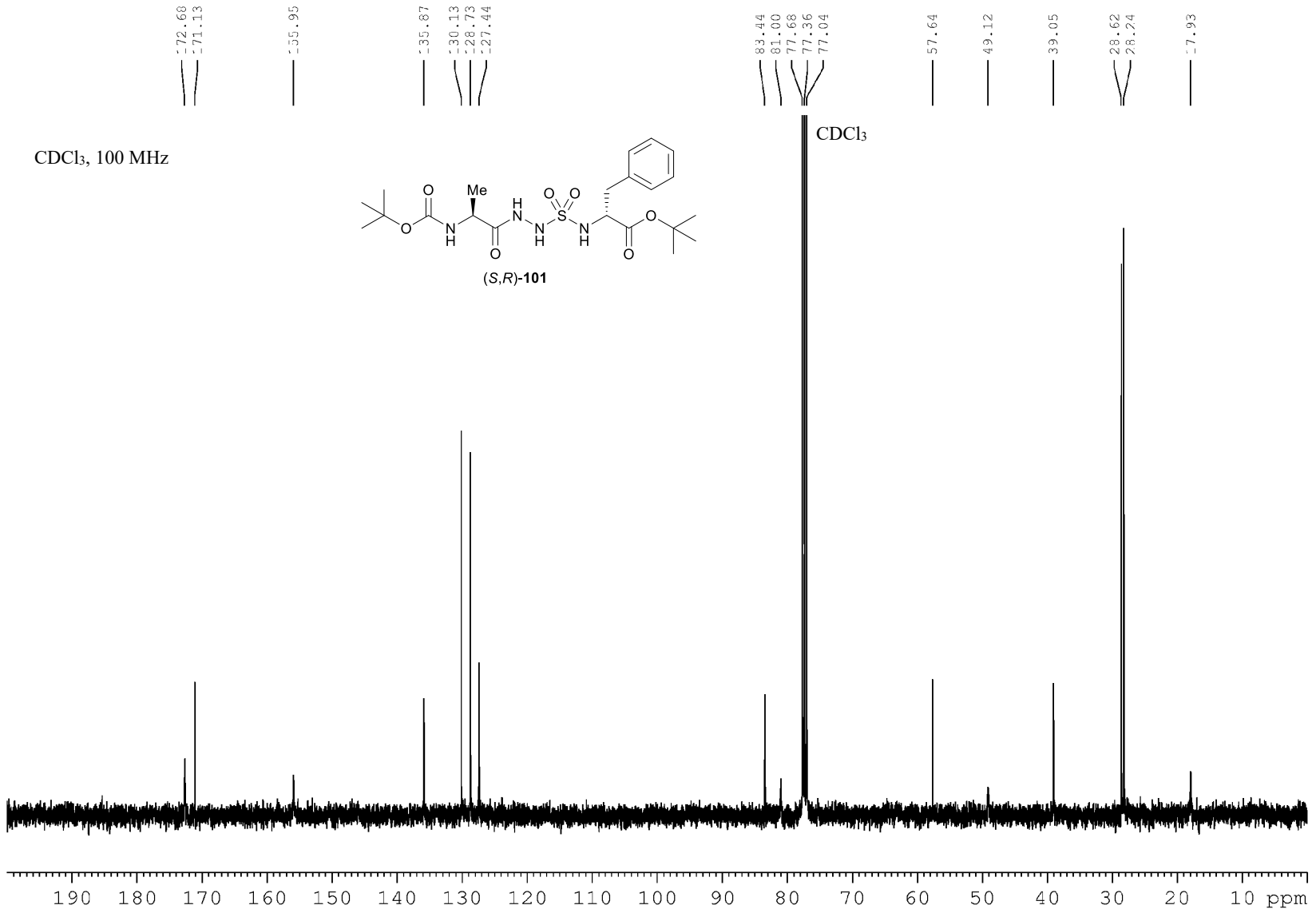
172.68
171.13
155.95
135.87
130.13
128.73
127.44
83.44
81.00
77.68
77.36
77.04
57.64
49.12
39.05
28.62
28.24
17.93
CDCl3
CDCl3, 100 MHz
(S,R)-101
190 180 170 160 150 140 130 120 110 100 90 80 70 60 50 40 30 20 10 ppm

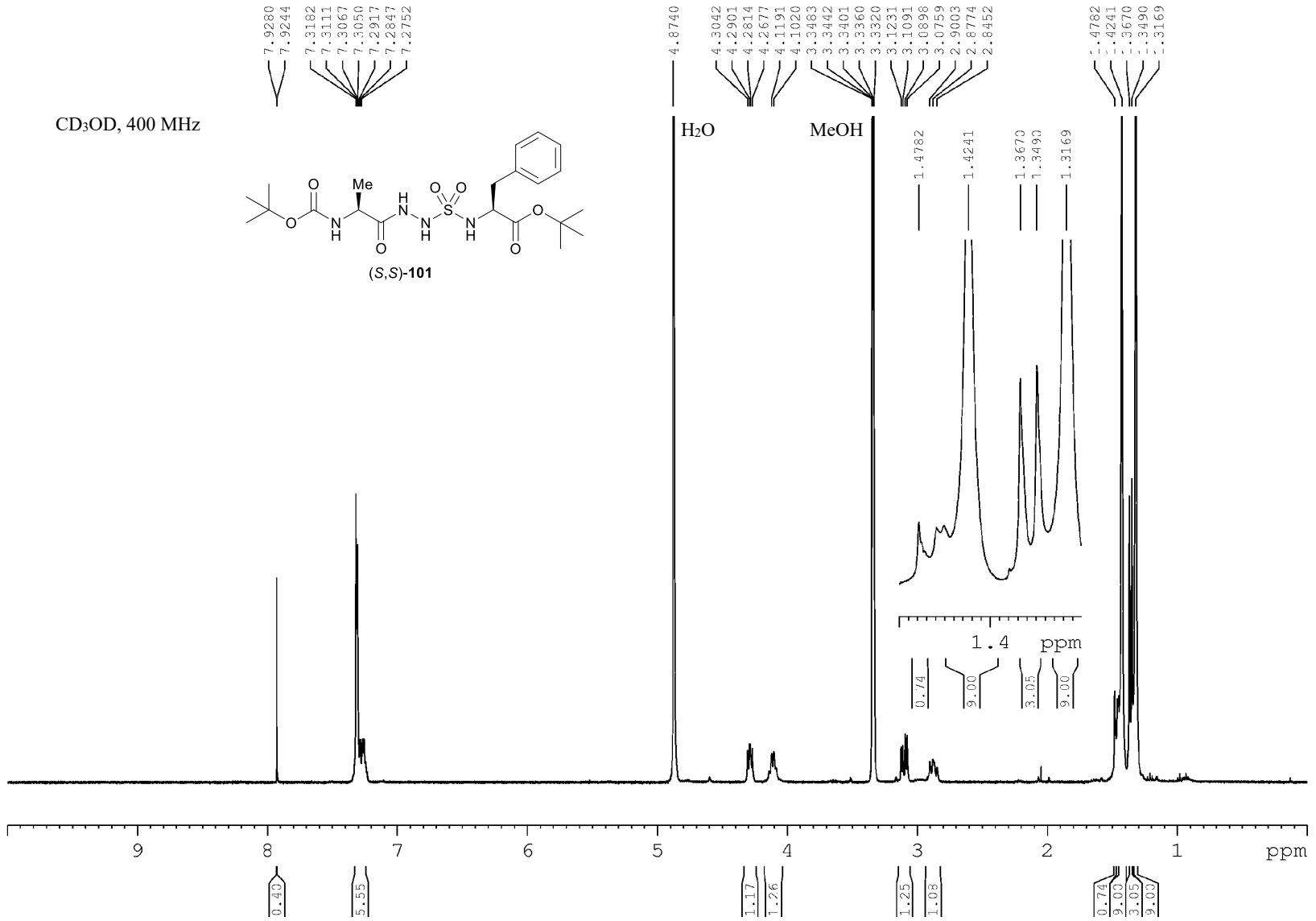
CD3OD, 400 MHz
H2O
MeOH
(S,S)-101
ppm

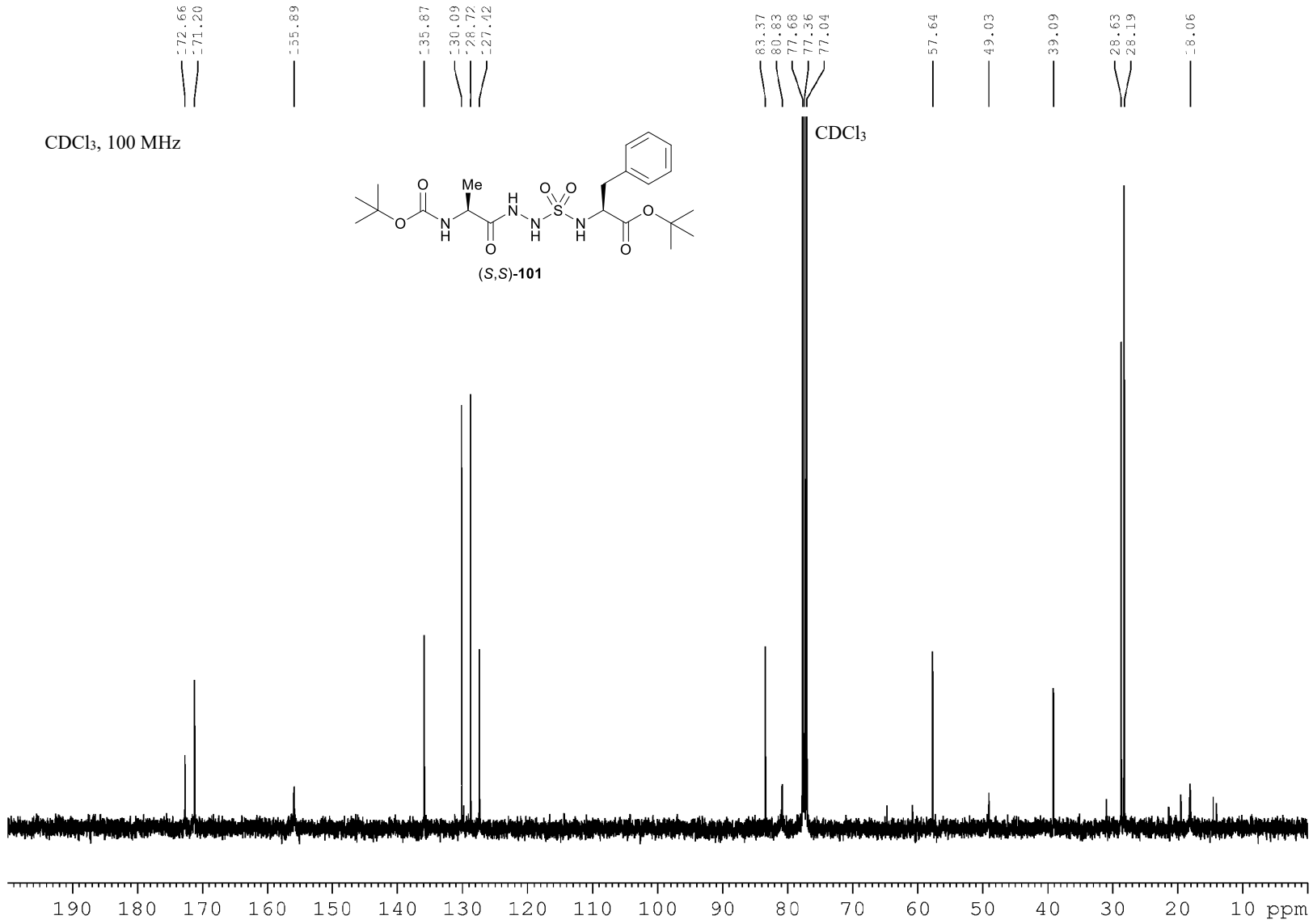
172.66
171.20
155.89
135.87
130.09
128.72
127.42
83.37
80.83
77.68
77.36
77.04
57.64
49.03
39.09
28.63
28.19
18.06
CDCl3, 100 MHz
CDCl3
(S,S)-101
190 180 170 160 150 140 130 120 110 100 90 80 70 60 50 40 30 20 10 ppm

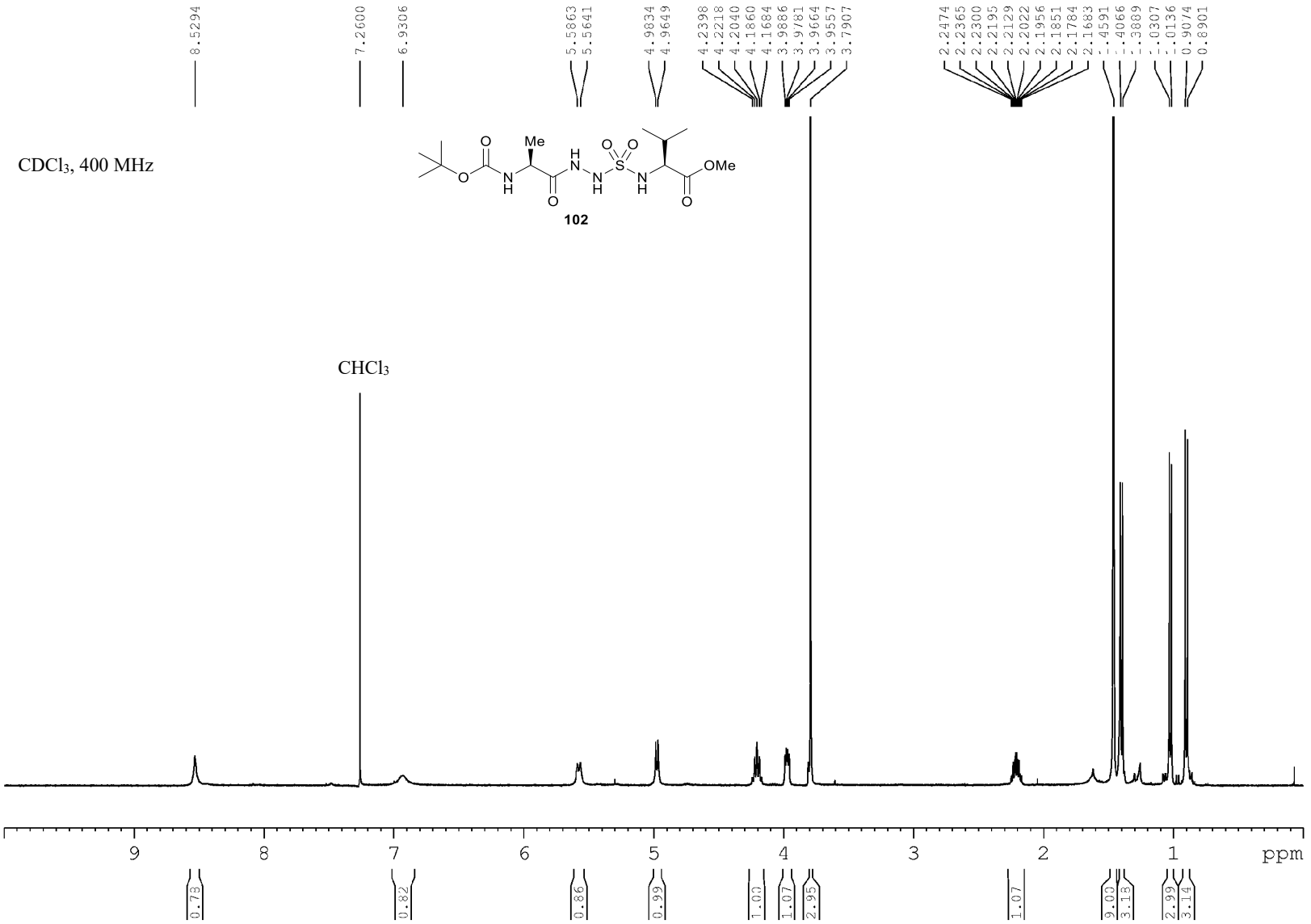
8.5294
7.2600
6.9306
5.5863
5.5641
4.9834
4.9649
4.2398
4.2218
4.2040
4.1860
4.1684
3.9886
3.9781
3.9664
3.9557
3.7907
2.2474
2.2365
2.2300
2.2195
2.2129
2.2022
2.1956
2.1851
2.1784
2.1683
1.4591
1.4066
1.3889
1.0307
1.0136
0.9074
0.8901
CDCl3, 400 MHz
CHCl3
102
9
8
7
6
5
4
3
2
1
ppm
0.78
0.82
0.86
0.99
1.00
1.07
2.95
1.07
9.00
3.18
2.99
3.14

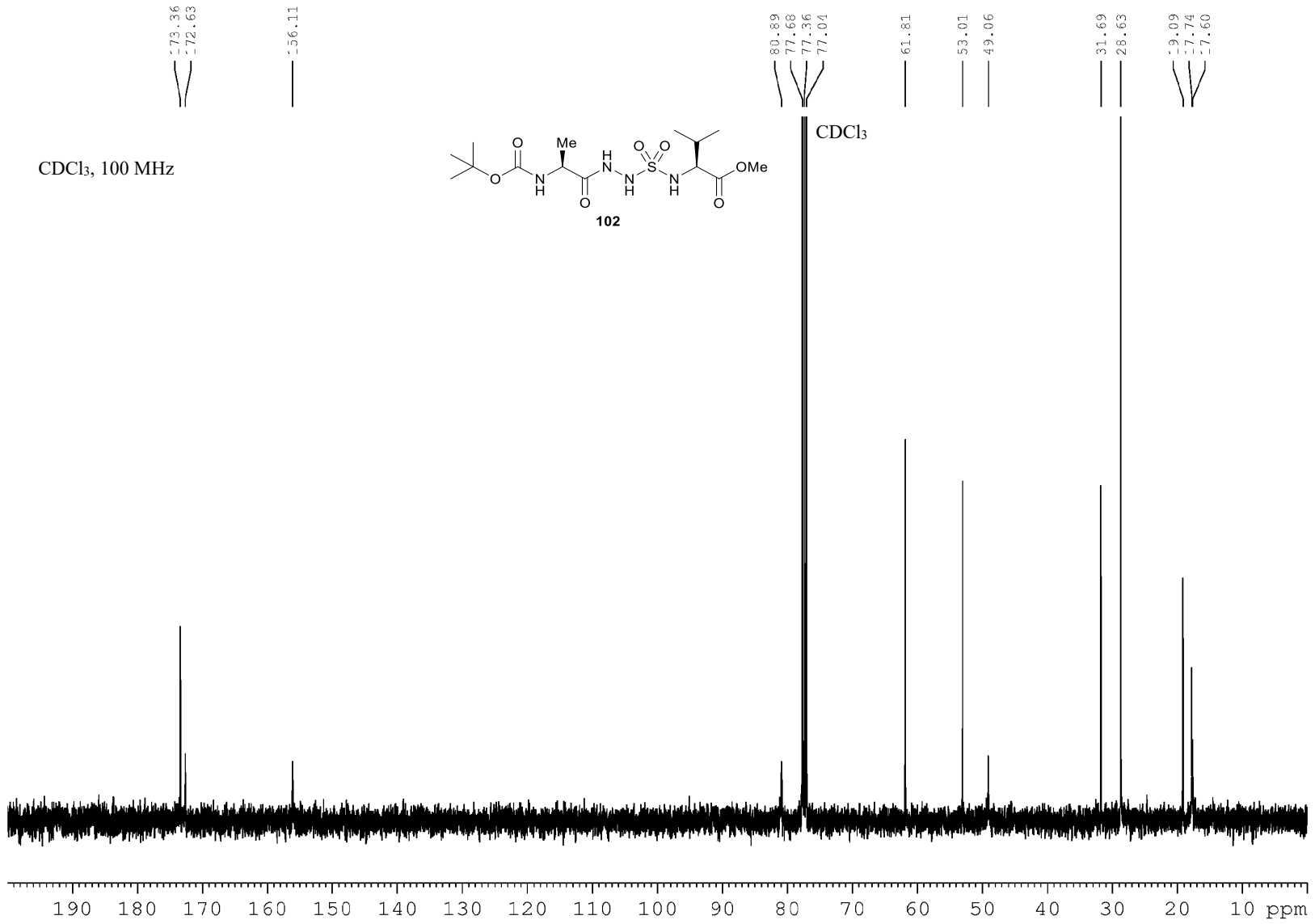
173.36
172.63
156.11
80.89
77.68
77.36
77.04
61.81
53.01
49.06
31.69
28.63
19.09
17.74
17.60
CDCl3
CDCl3, 100 MHz
102
190 180 170 160 150 140 130 120 110 100 90 80 70 60 50 40 30 20 10 ppm

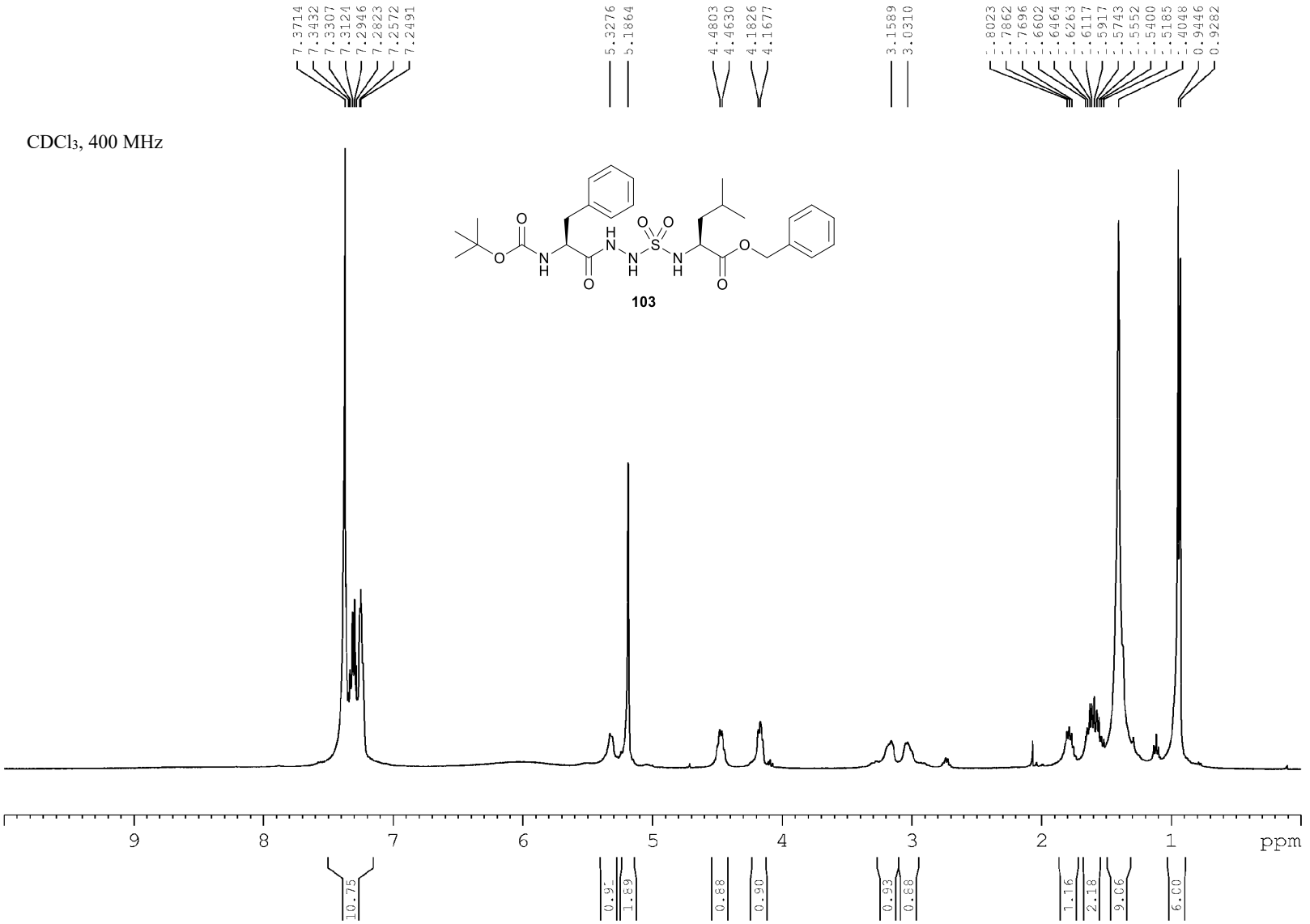
7.3714
7.3432
7.3307
7.3124
7.2946
7.2823
7.2572
7.2491
5.3276
5.1864
4.4803
4.4630
4.1826
4.1677
3.1589
3.0310
1.8023
1.7862
1.7696
1.6602
1.6464
1.6263
1.6117
1.5917
1.5743
1.5552
1.5400
1.5185
1.4048
0.9446
0.9282
CDCl3, 400 MHz
103
9
8
7
6
5
4
3
2
1
ppm
10.75
0.9
1.89
0.88
0.90
0.93
0.88
1.16
2.18
9.06
6.00

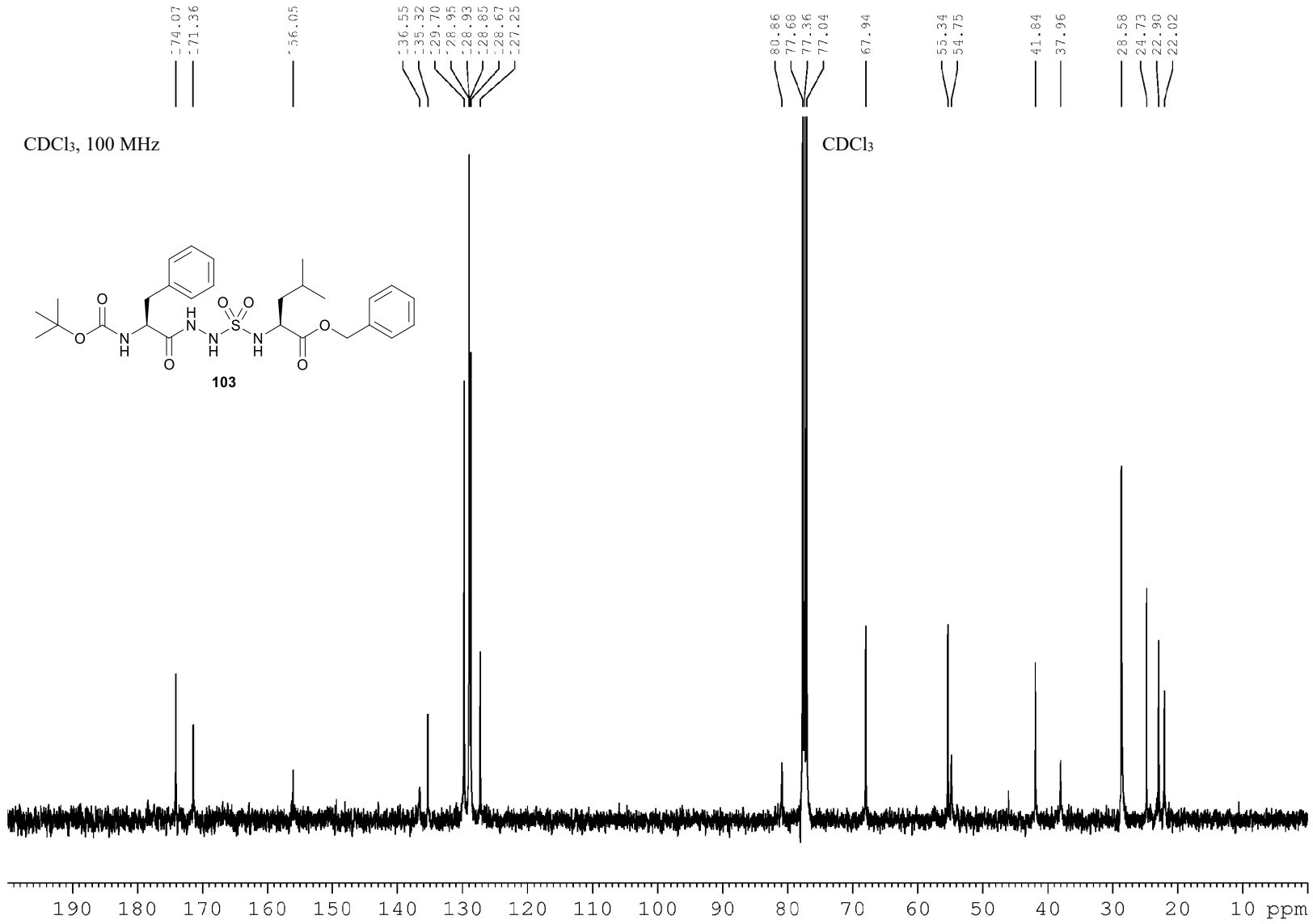
174.07
171.36
156.05
136.55
135.32
129.70
128.95
128.93
128.85
128.67
127.25
80.86
77.68
77.36
77.04
67.94
55.34
54.75
41.84
37.96
28.58
24.73
22.90
22.02
CDCl3, 100 MHz
CDCl3
103
190 180 170 160 150 140 130 120 110 100 90 80 70 60 50 40 30 20 10 ppm

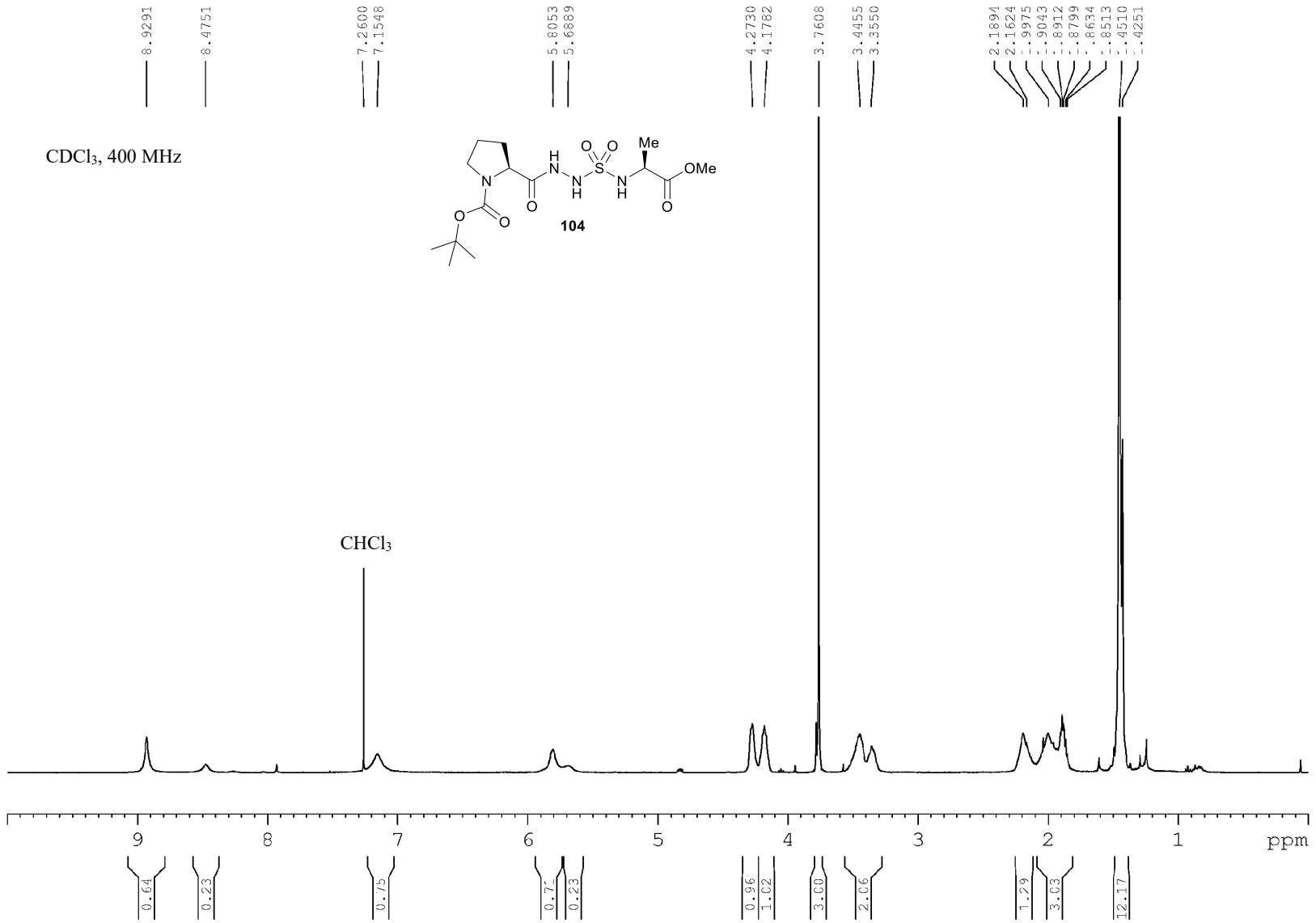
8.9291
8.4751
7.2600
7.1548
5.8053
5.6889
4.2730
4.1782
3.7608
3.4455
3.3550
2.1894
2.1624
1.9975
1.9043
1.8912
1.8799
1.8634
1.8513
1.4510
1.4251
CDCl3, 400 MHz
CHCl3
104
ppm
0.64
0.23
0.75
0.73
0.23
0.96
1.02
3.00
2.06
1.29
3.03
12.17

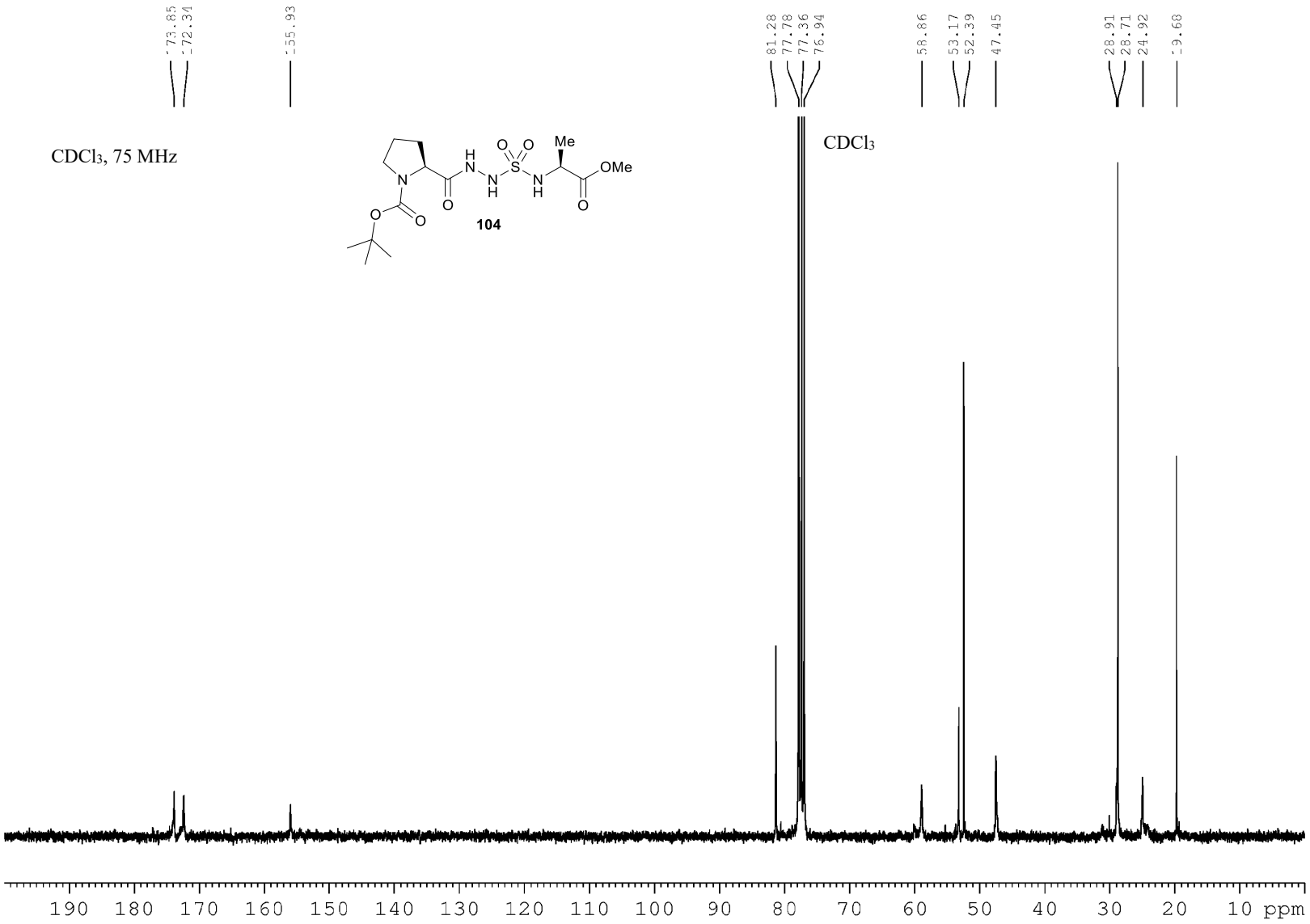
173.85
172.34
155.93
81.28
77.78
77.36
76.94
58.86
53.17
52.39
47.45
28.91
28.71
24.92
19.68
CDCl3, 75 MHz
CDCl3
104
190 180 170 160 150 140 130 120 110 100 90 80 70 60 50 40 30 20 10 ppm

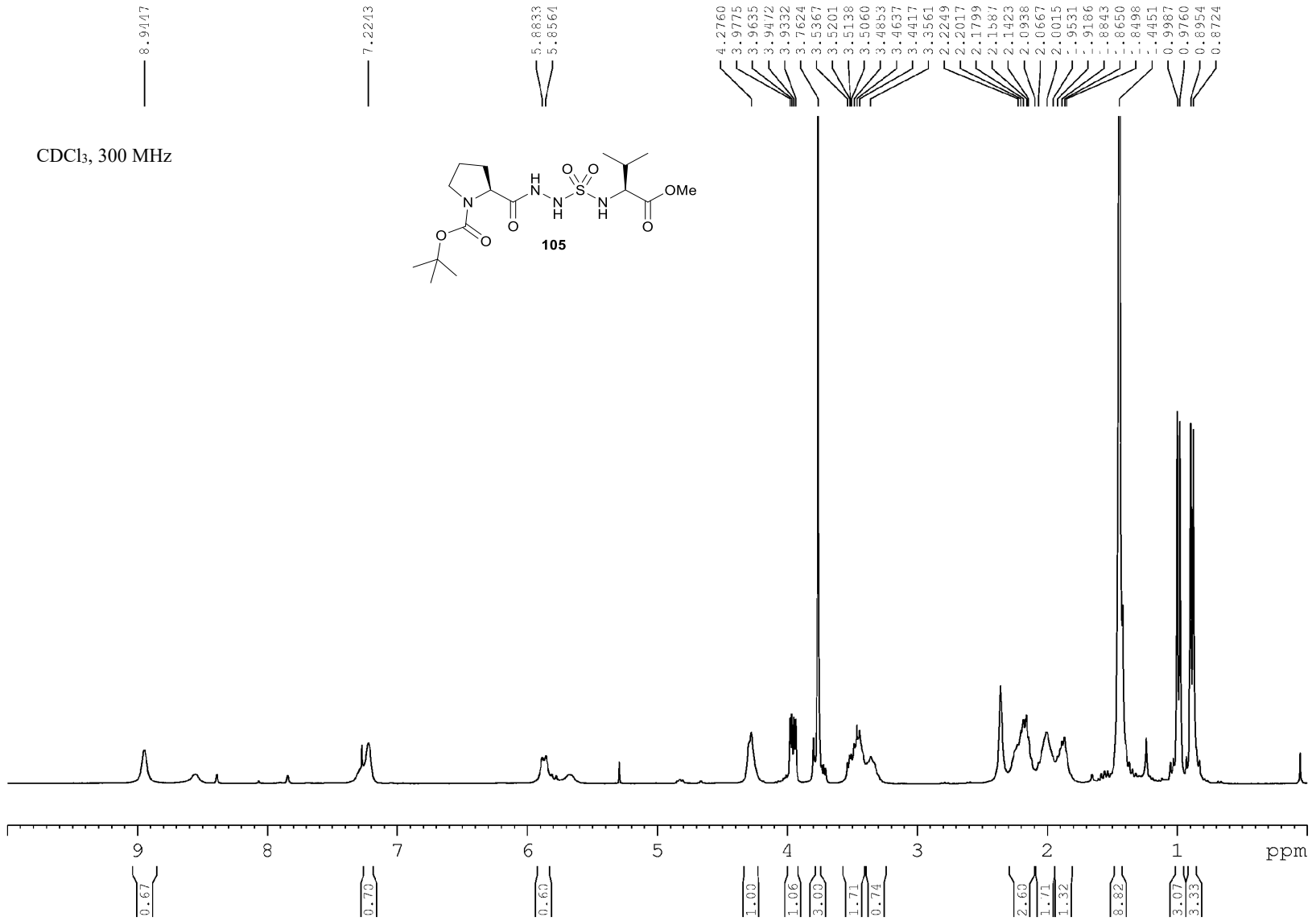
8.9417
7.2243
5.8833
5.8564
4.2760
3.9775
3.9635
3.9472
3.9332
3.7624
3.5367
3.5201
3.5138
3.5060
3.4853
3.4637
3.4417
3.3561
2.2249
2.2017
2.1799
2.1587
2.1423
2.0938
2.0667
2.0015
1.9531
1.9186
1.8843
1.8650
1.8498
1.4451
0.9987
0.9760
0.8954
0.8724
CDCl3, 300 MHz
105
9
8
7
6
5
4
3
2
1
ppm
0.67
0.70
0.60
1.00
1.06
3.00
1.71
0.74
2.60
1.71
1.32
8.82
3.07
3.33

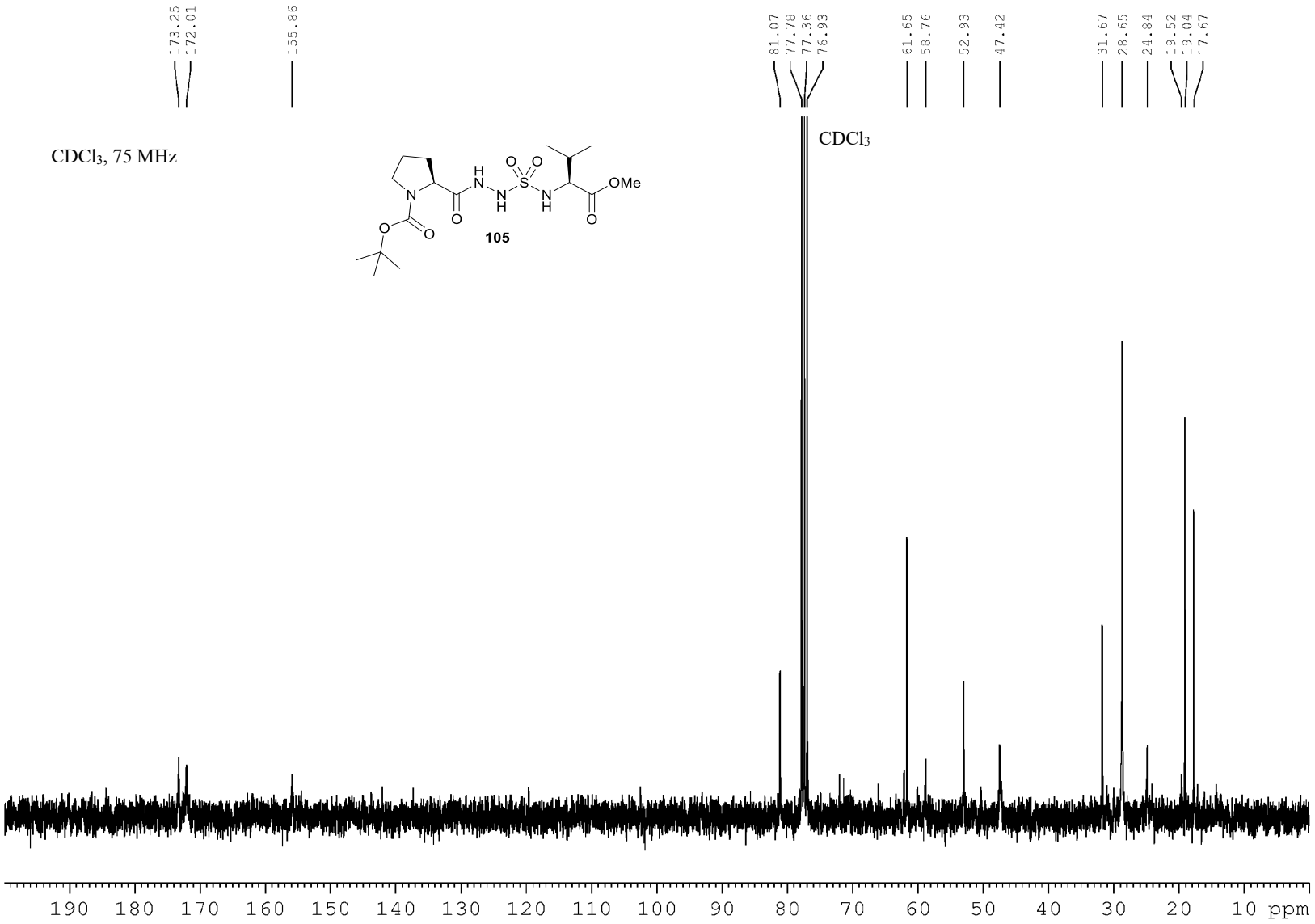
173.25
172.01
155.86
81.07
77.78
77.36
76.93
61.65
58.76
52.93
47.42
31.67
28.65
24.84
19.52
19.04
17.67
CDCl3
CDCl3, 75 MHz
105
190 180 170 160 150 140 130 120 110 100 90 80 70 60 50 40 30 20 10 ppm

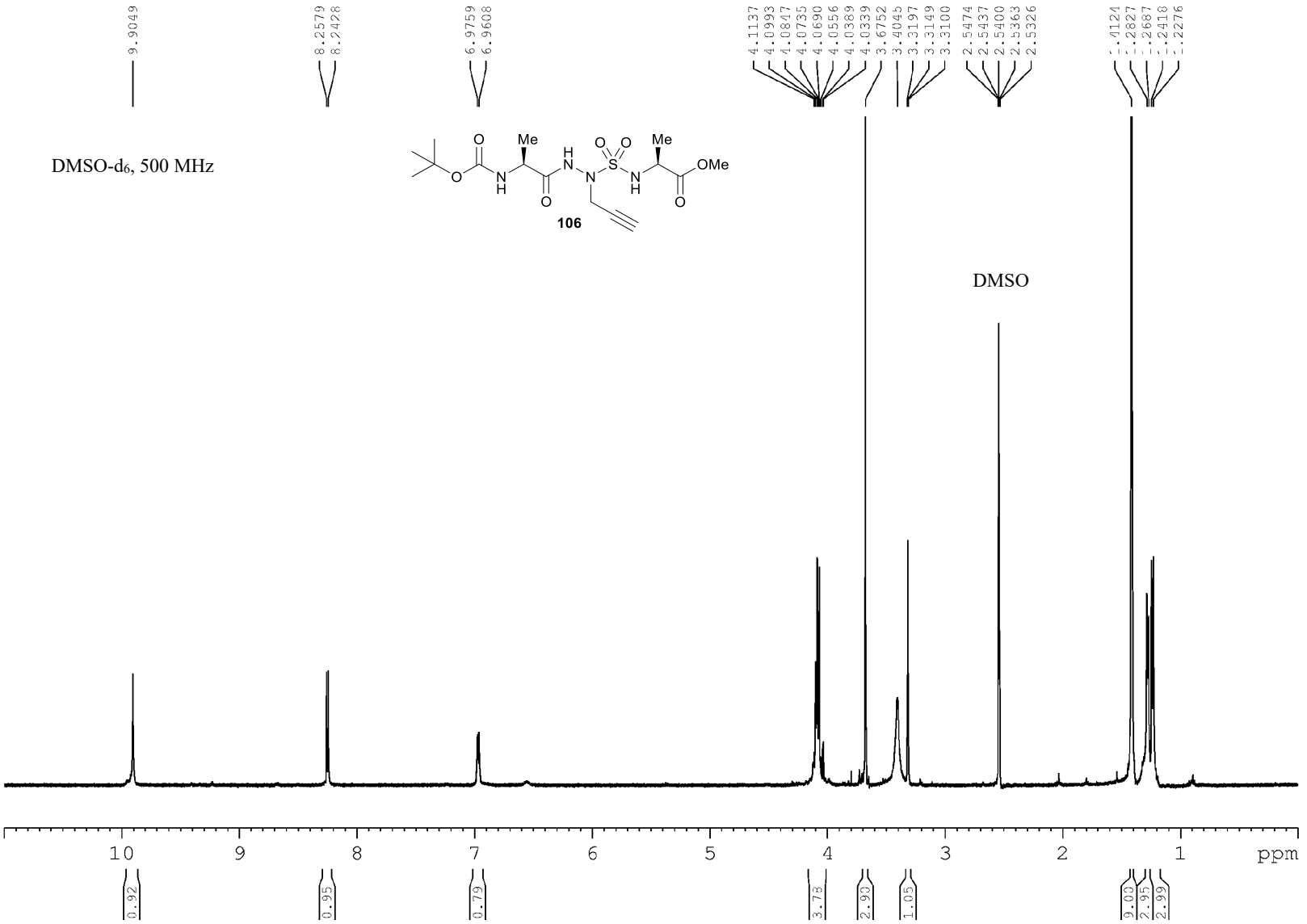
DMSO-d6, 500 MHz
106
DMSO
9.9049
8.2579
8.2428
6.9759
6.9608
4.1137
4.0993
4.0847
4.0735
4.0690
4.0556
4.0389
4.0339
3.6752
3.4045
3.3197
3.3149
3.3100
2.5474
2.5437
2.5400
2.5363
2.5326
1.4124
1.2827
1.2687
1.2418
1.2276
10
9
8
7
6
5
4
3
2
1
ppm
0.92
0.95
0.79
3.78
2.90
1.05
9.00
2.95
2.99

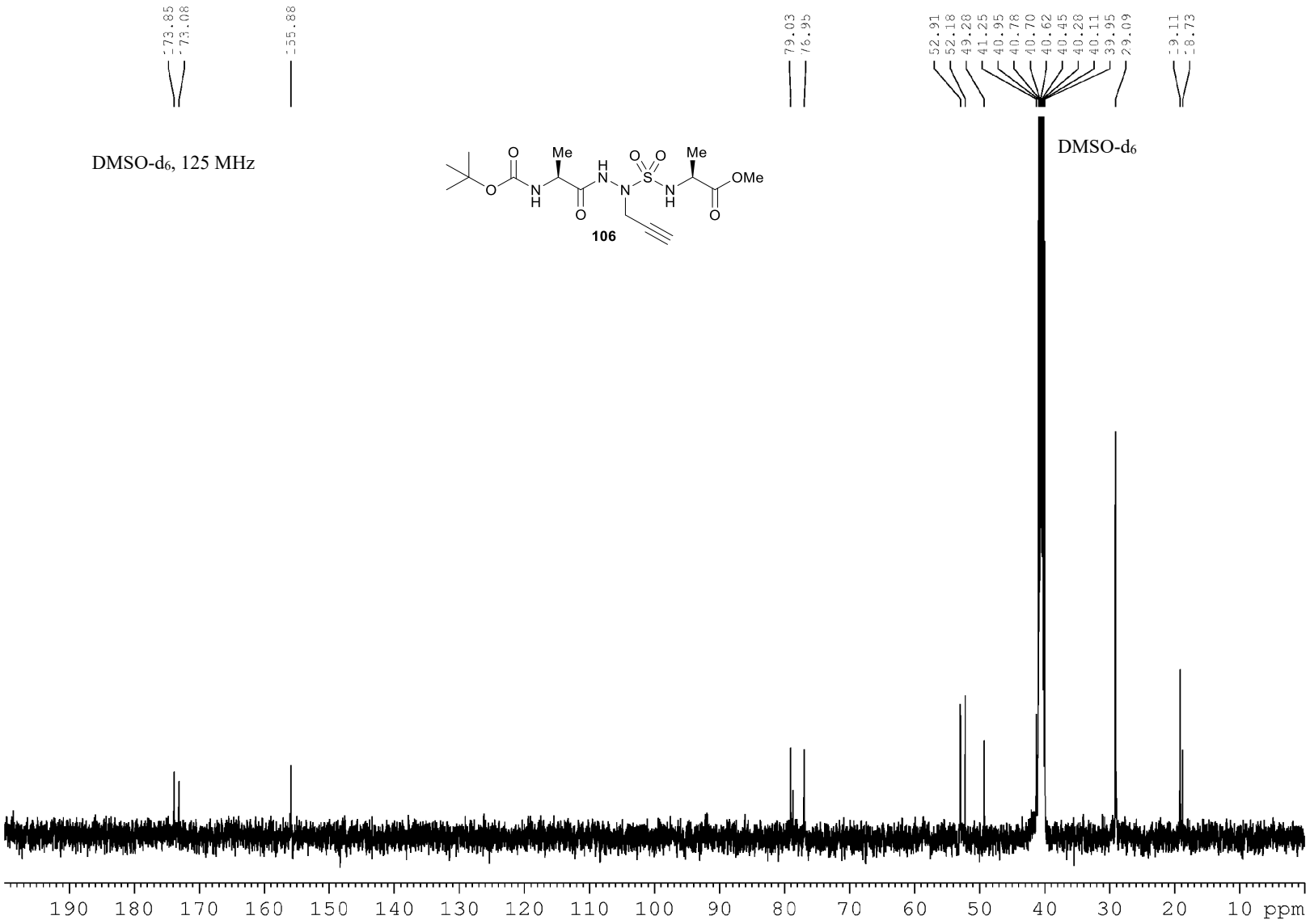
173.85
173.08
155.88
79.03
76.95
52.91
52.18
49.28
41.25
40.95
40.78
40.70
40.62
40.45
40.28
40.11
39.95
29.09
19.11
18.73
DMSO-d6, 125 MHz
DMSO-d6
106
190 180 170 160 150 140 130 120 110 100 90 80 70 60 50 40 30 20 10 ppm

DMSO-d_6, 500 MHz

COSY

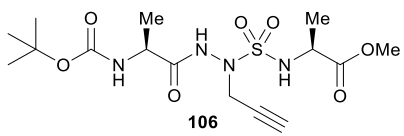

106

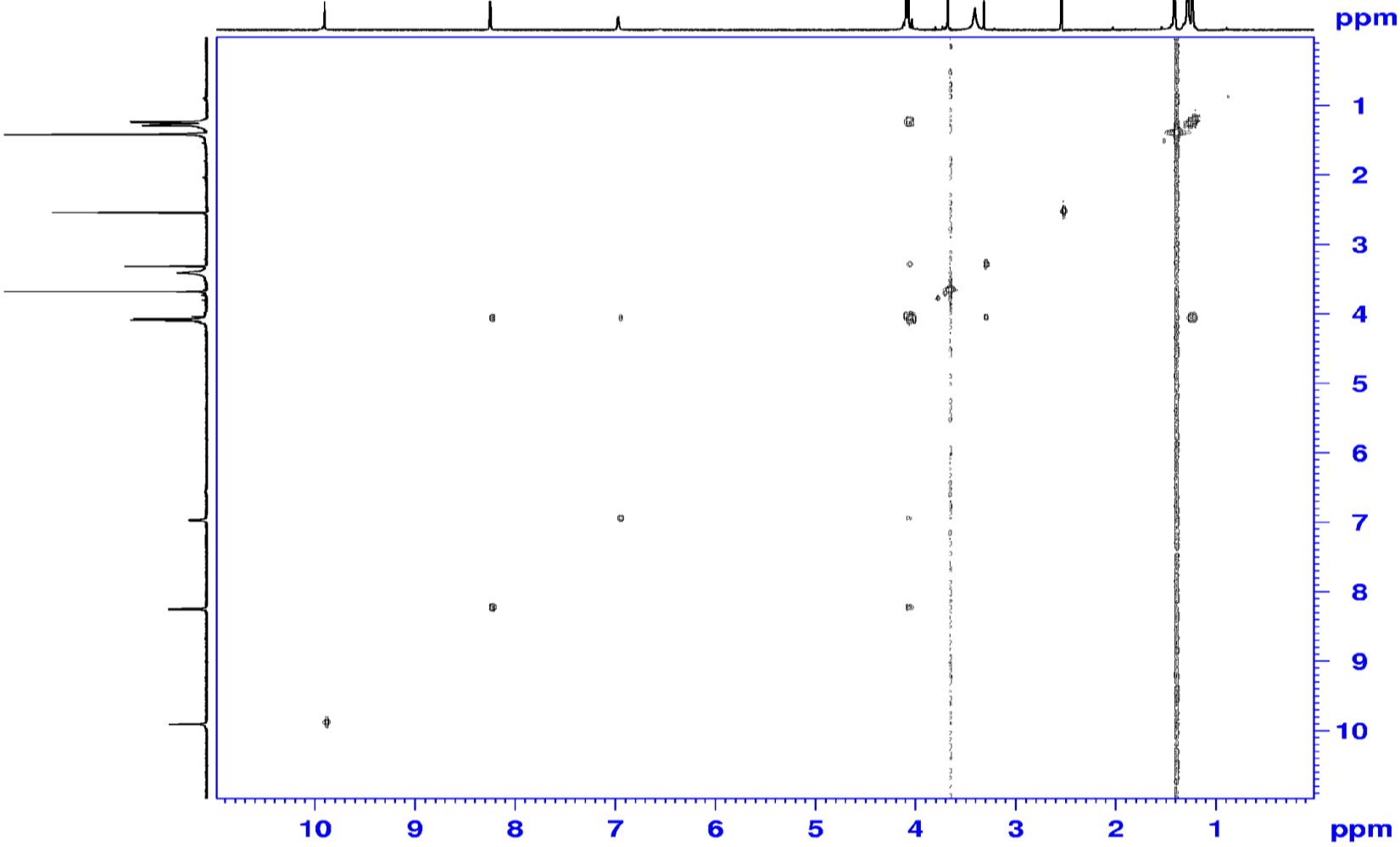

DMSO-d_6, 125 MHz

HMBC

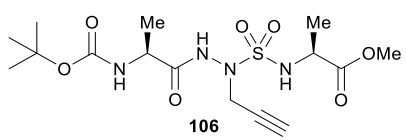

106

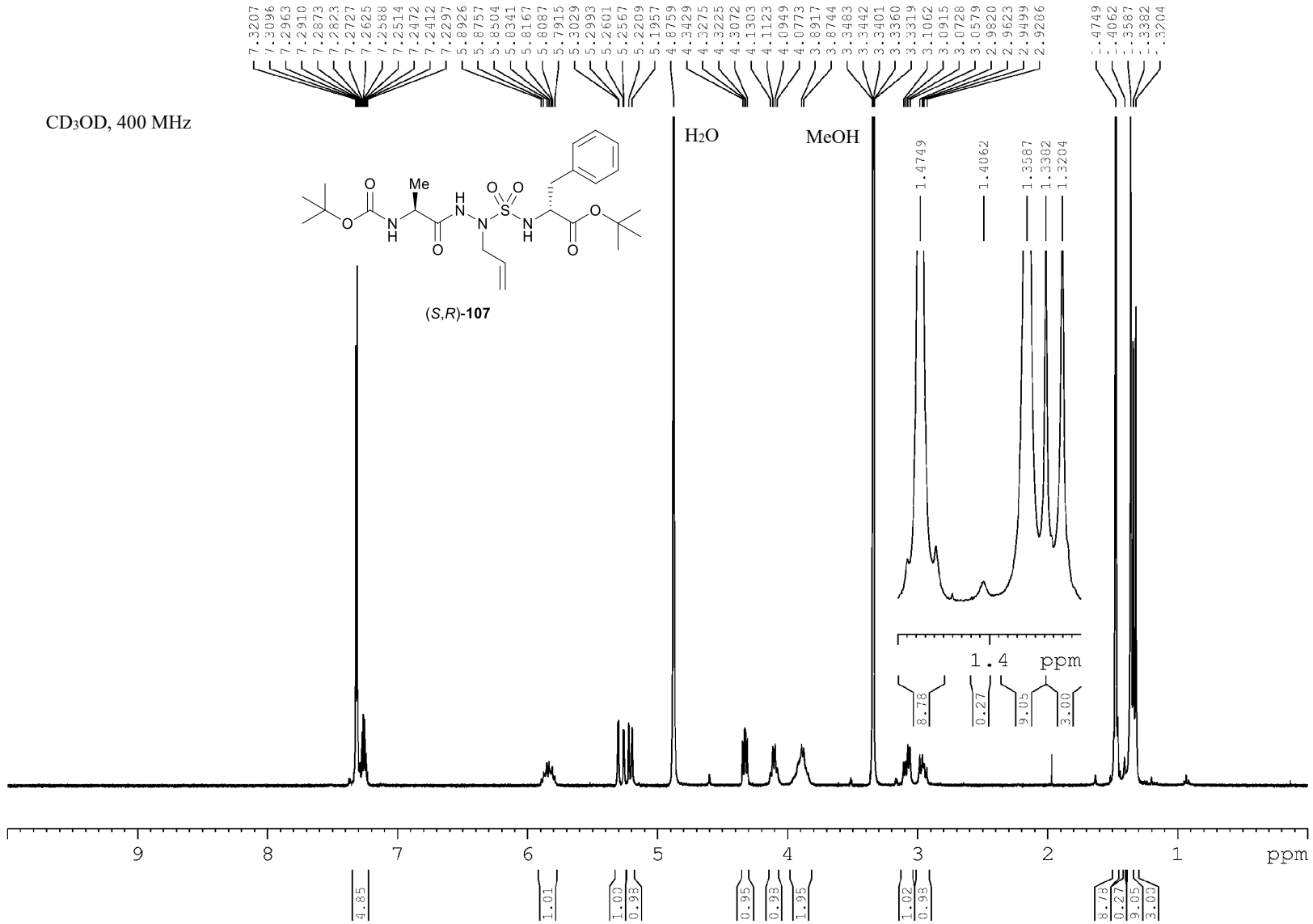
CD3OD, 400 MHz
H2O
MeOH
(S,R)-107
1.4749
1.4062
1.3587
1.3382
1.3204
1.4 ppm
ppm

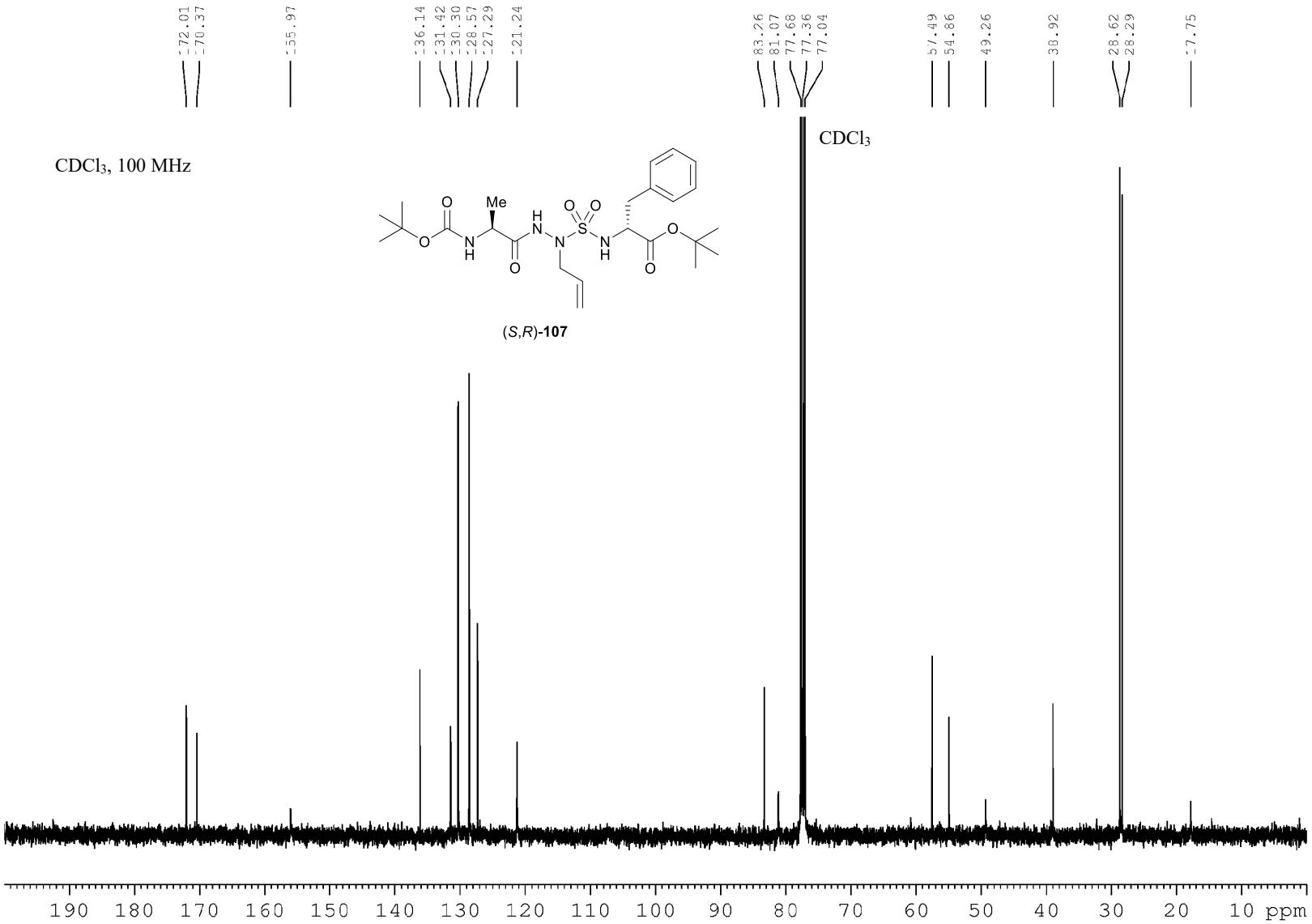
172.01
170.37
155.97
136.14
131.42
130.30
128.57
127.29
121.24
83.26
81.07
77.68
77.36
77.04
57.49
54.86
49.26
38.92
28.62
28.29
17.75
CDCl3
CDCl3, 100 MHz
(S,R)-107
190 180 170 160 150 140 130 120 110 100 90 80 70 60 50 40 30 20 10 ppm

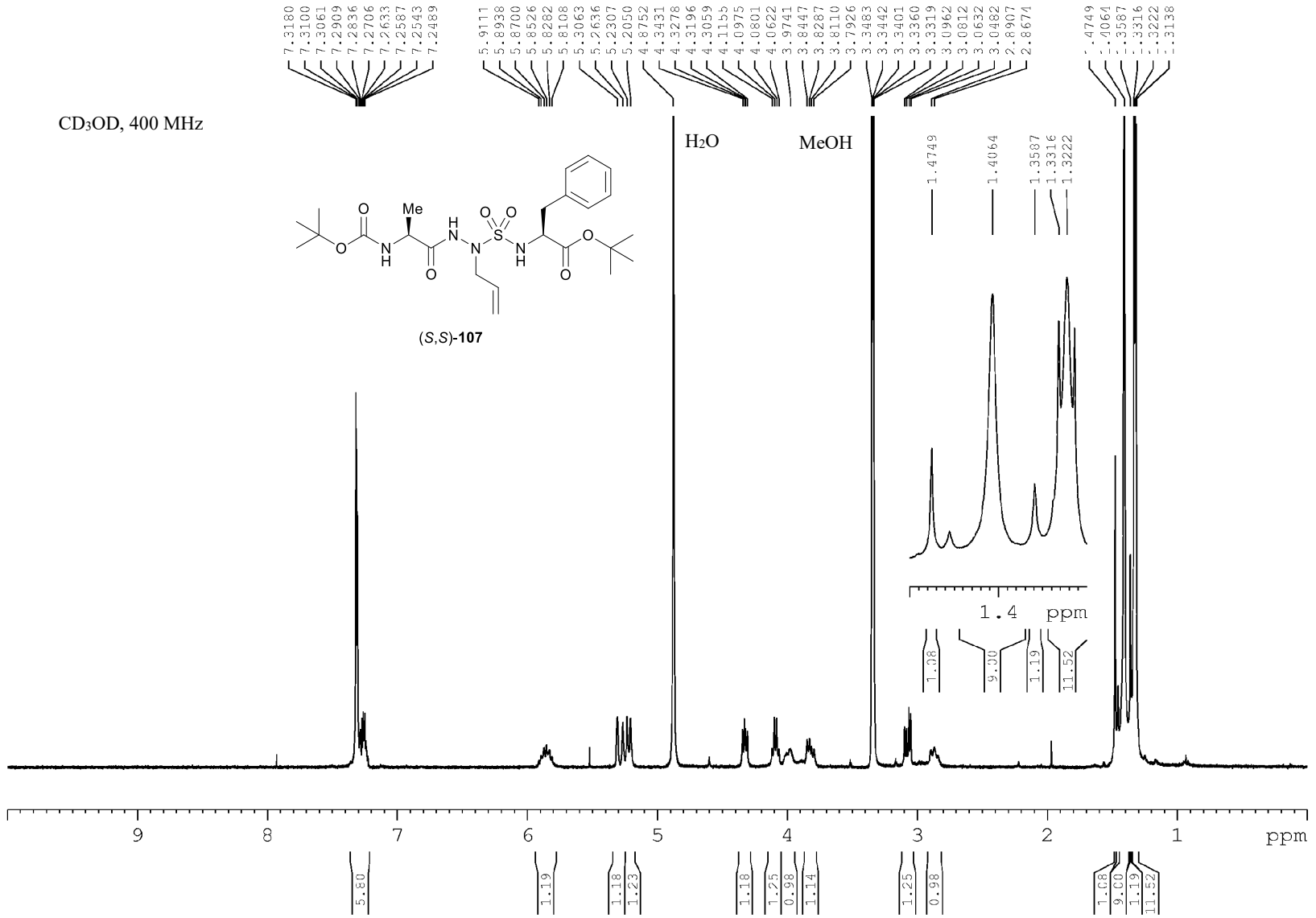
CD3OD, 400 MHz
H2O
MeOH
(S,S)-107
1.4 ppm
9 8 7 6 5 4 3 2 1 ppm

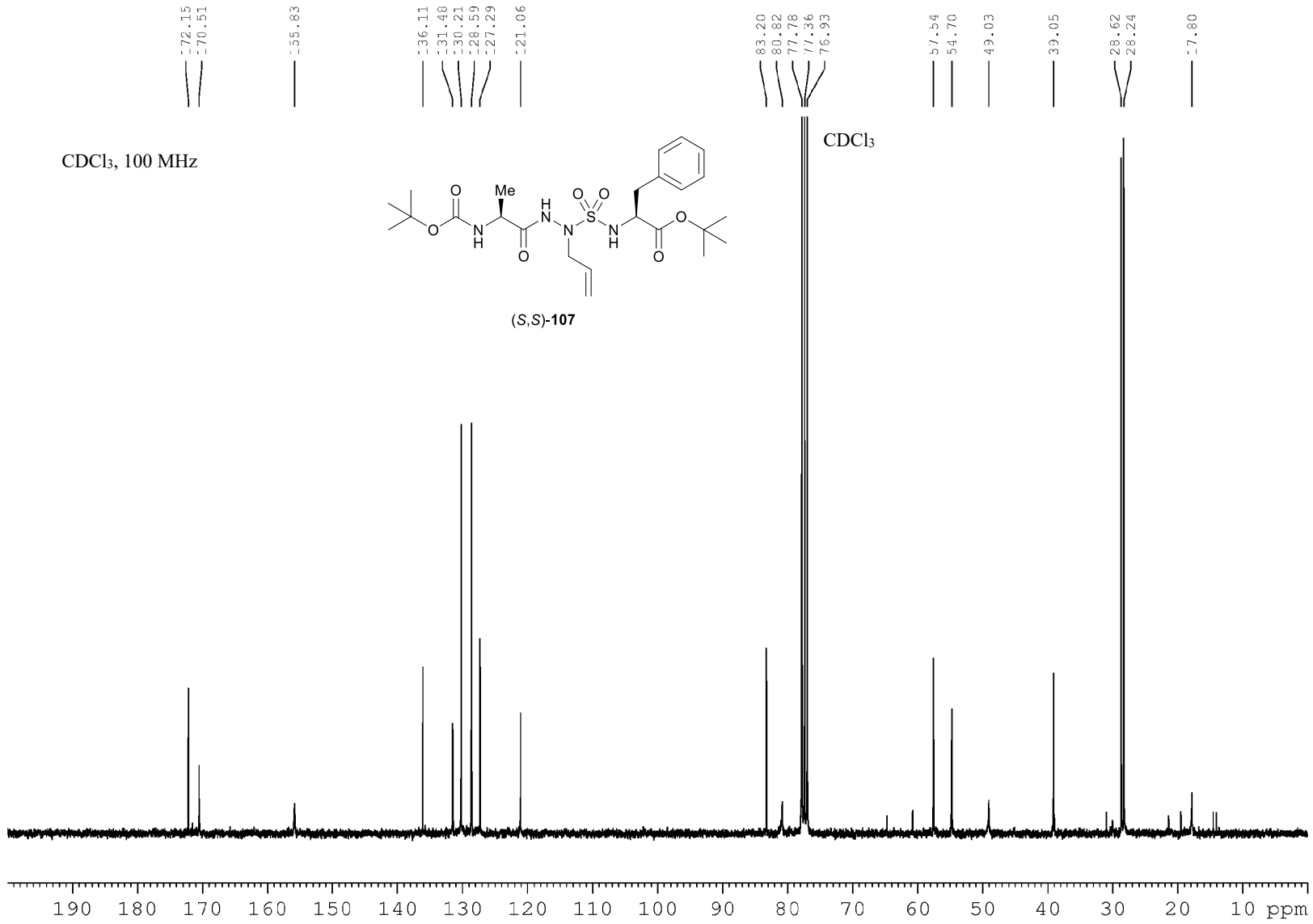
172.15
170.51
155.83
136.11
131.48
130.21
128.59
127.29
121.06
83.20
80.82
77.78
77.36
76.93
57.54
54.70
49.03
39.05
28.62
28.24
17.80
CDCl3
CDCl3, 100 MHz
(S,S)-107
190 180 170 160 150 140 130 120 110 100 90 80 70 60 50 40 30 20 10 ppm

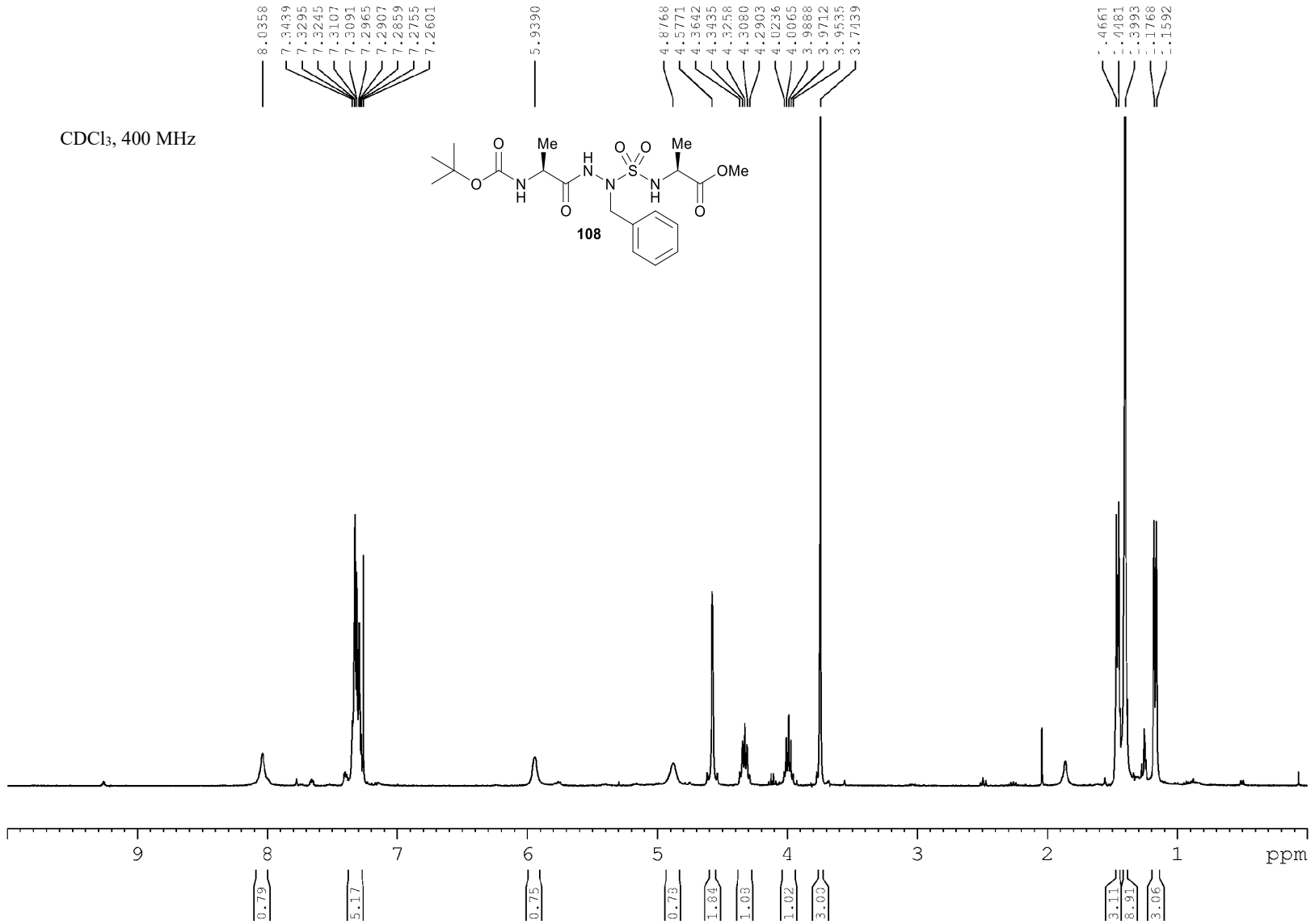
8.0358
7.3439
7.3295
7.3245
7.3107
7.3091
7.2965
7.2907
7.2859
7.2755
7.2601
5.9390
4.8768
4.5771
4.3642
4.3435
4.3258
4.3080
4.2903
4.0236
4.0065
3.9888
3.9712
3.9535
3.7439
1.4661
1.4481
1.3993
1.1768
1.1592
CDCl3, 400 MHz
108
9
8
7
6
5
4
3
2
1
ppm
0.79
5.17
0.75
0.78
1.84
1.03
1.02
3.03
3.11
8.91
3.06

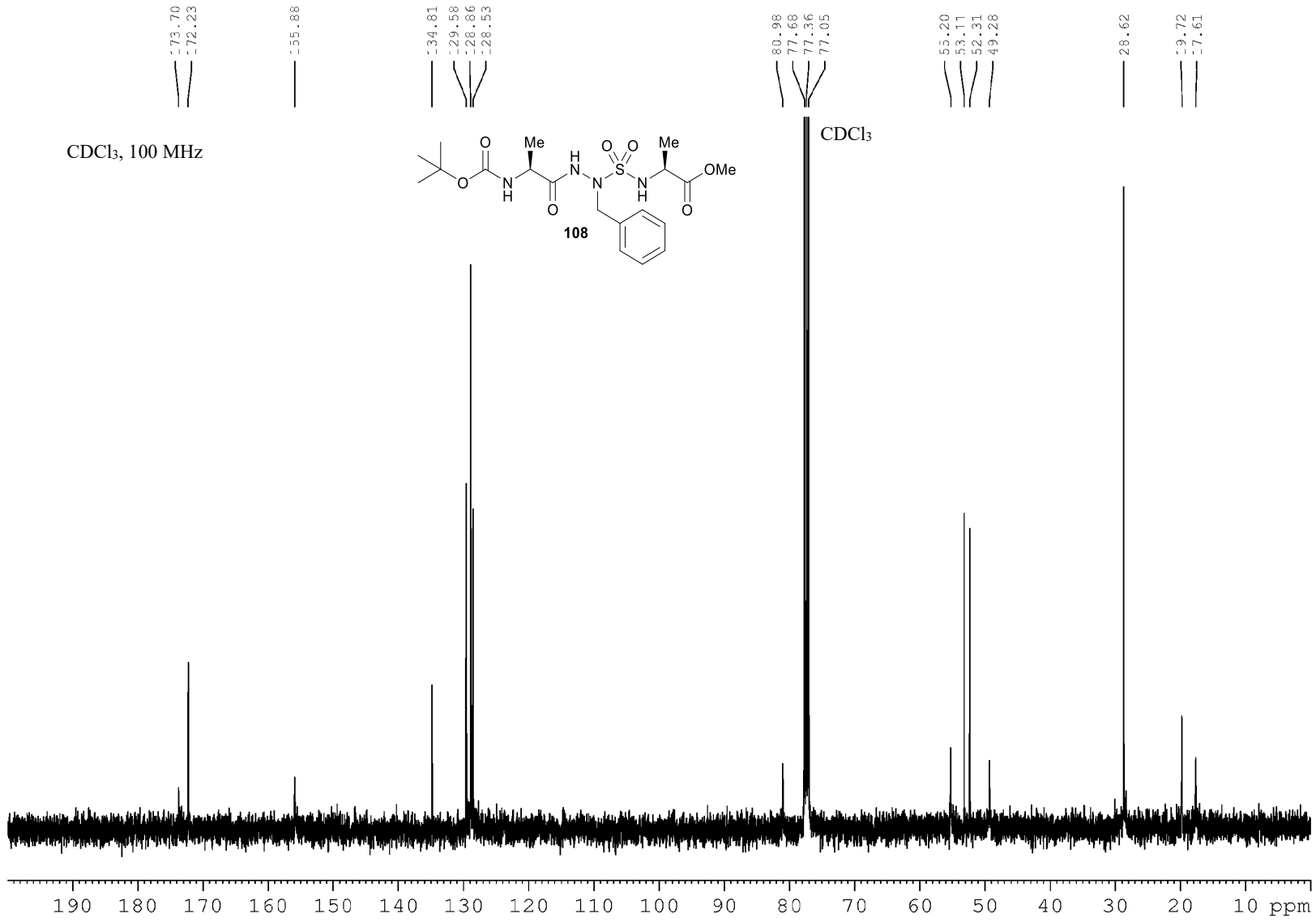
173.70
172.23
155.88
134.81
129.58
128.86
128.53
80.98
77.68
77.36
77.05
55.20
53.11
52.31
49.28
28.62
19.72
17.61
CDCl3, 100 MHz
CDCl3
108
190 180 170 160 150 140 130 120 110 100 90 80 70 60 50 40 30 20 10 ppm

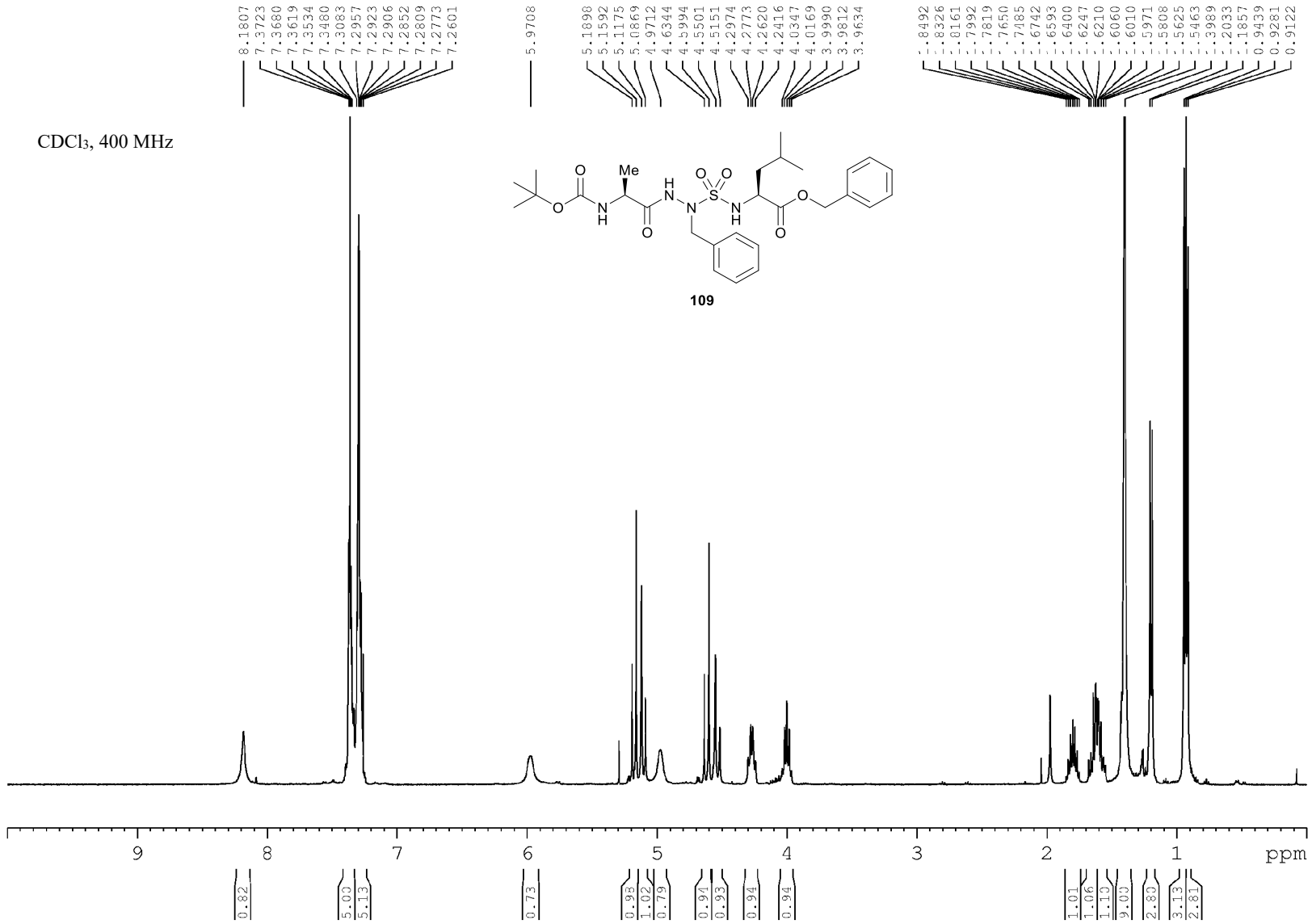
CDCl3, 400 MHz
8.1807
7.3723
7.3680
7.3619
7.3534
7.3480
7.3083
7.2957
7.2923
7.2906
7.2852
7.2809
7.2773
7.2601
5.9708
5.1098
5.1592
5.1175
5.0869
4.9712
4.6344
4.5994
4.5501
4.5151
4.2974
4.2773
4.2620
4.2416
4.0347
4.0169
3.9990
3.9812
3.9634
1.8492
1.8326
1.8161
1.7992
1.7819
1.7650
1.7485
1.6742
1.6593
1.6400
1.6247
1.6210
1.6060
1.6010
1.5971
1.5808
1.5625
1.5463
1.3989
1.2033
1.1857
0.9439
0.9281
0.9122
Me
109
9
8
7
6
5
4
3
2
1
ppm
0.82
5.00
5.13
0.73
0.93
1.02
0.79
0.94
0.93
0.94
0.94
1.01
1.06
1.10
9.00
2.80
3.13
2.81

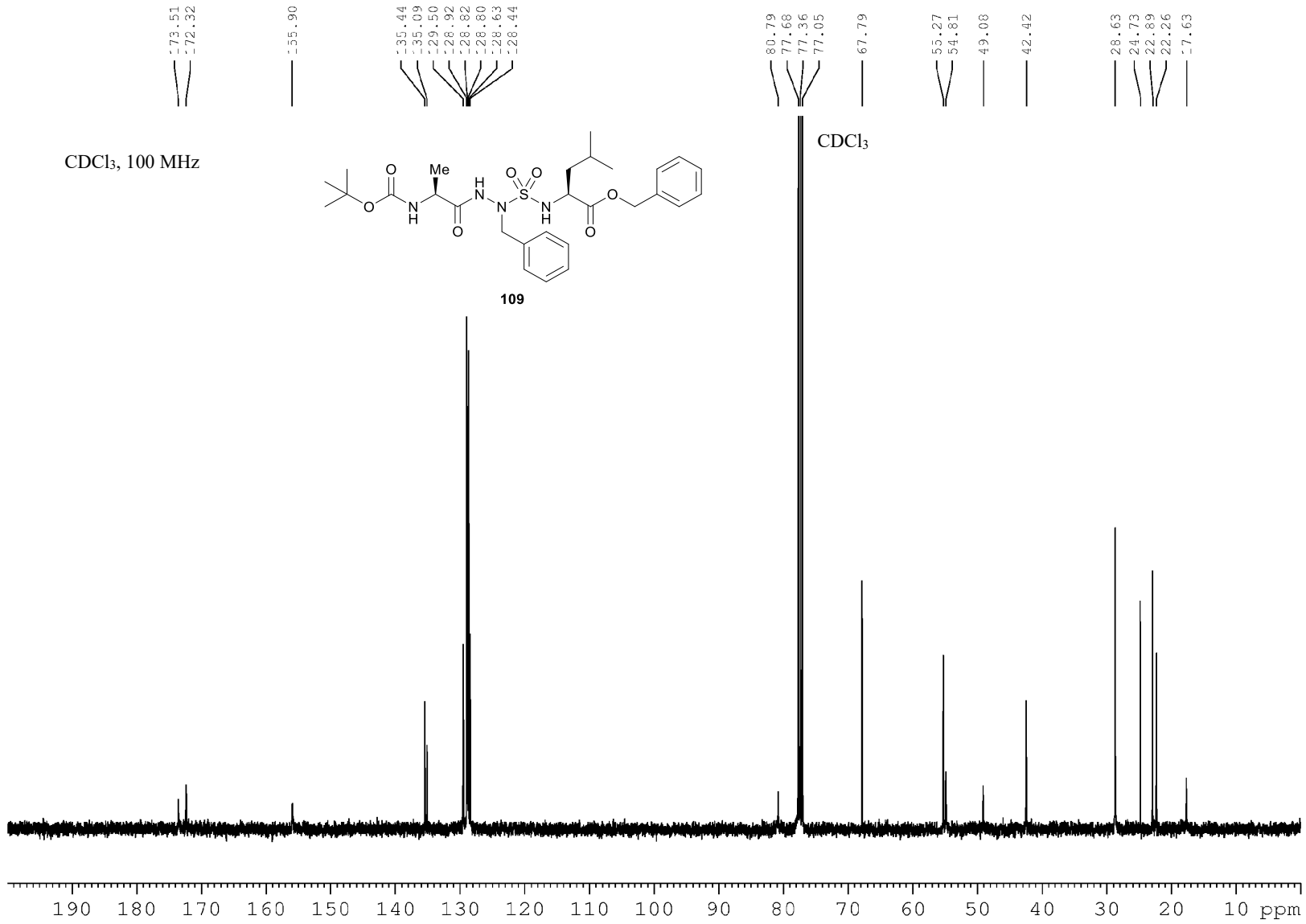
173.51
172.32
155.90
135.44
135.09
129.50
128.92
128.82
128.80
128.63
128.44
80.79
77.68
77.36
77.05
67.79
55.27
54.81
49.08
42.42
28.63
24.73
22.89
22.26
17.63
CDCl3, 100 MHz
CDCl3
109
190 180 170 160 150 140 130 120 110 100 90 80 70 60 50 40 30 20 10 ppm

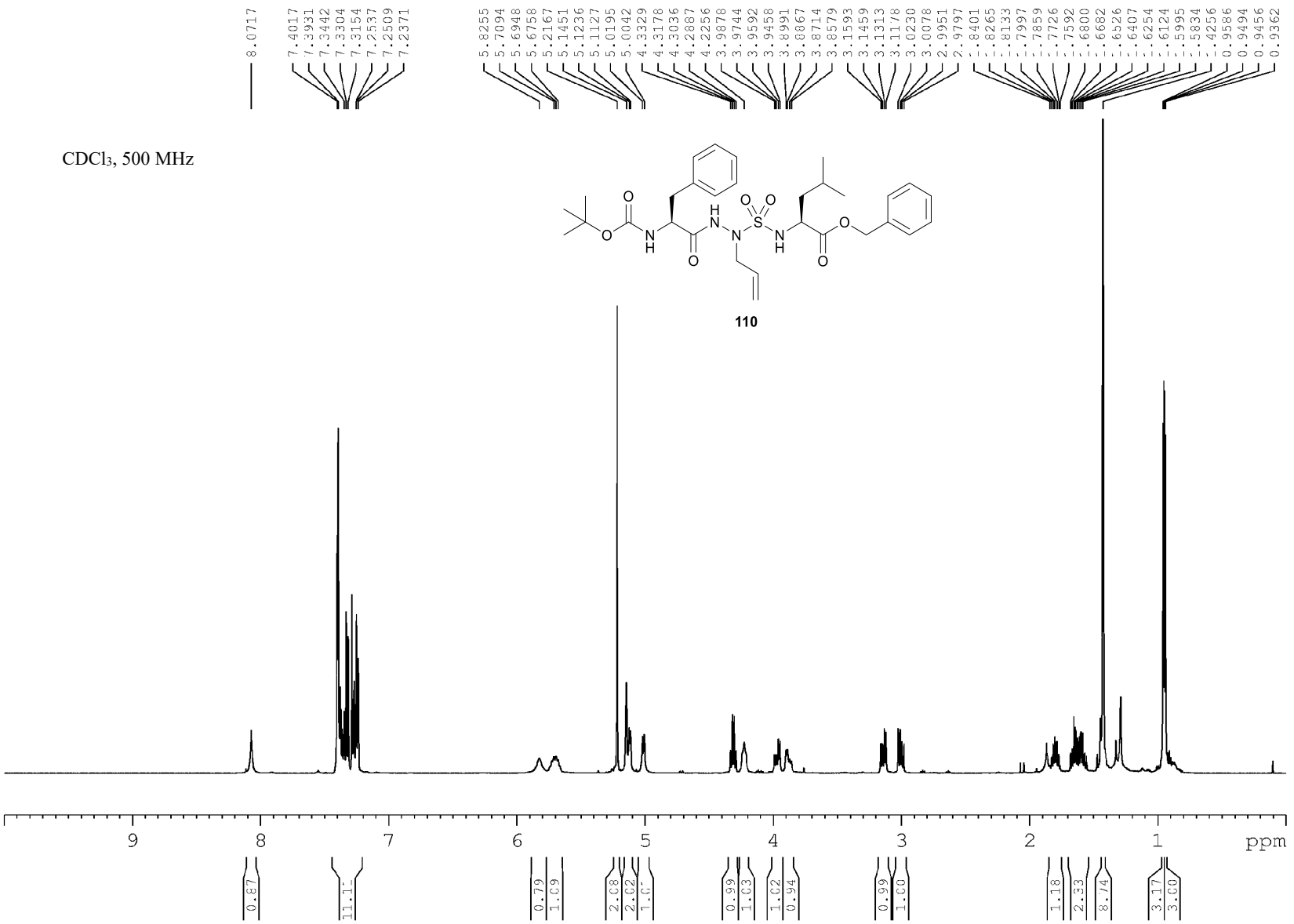
CDCl3, 500 MHz
110
ppm

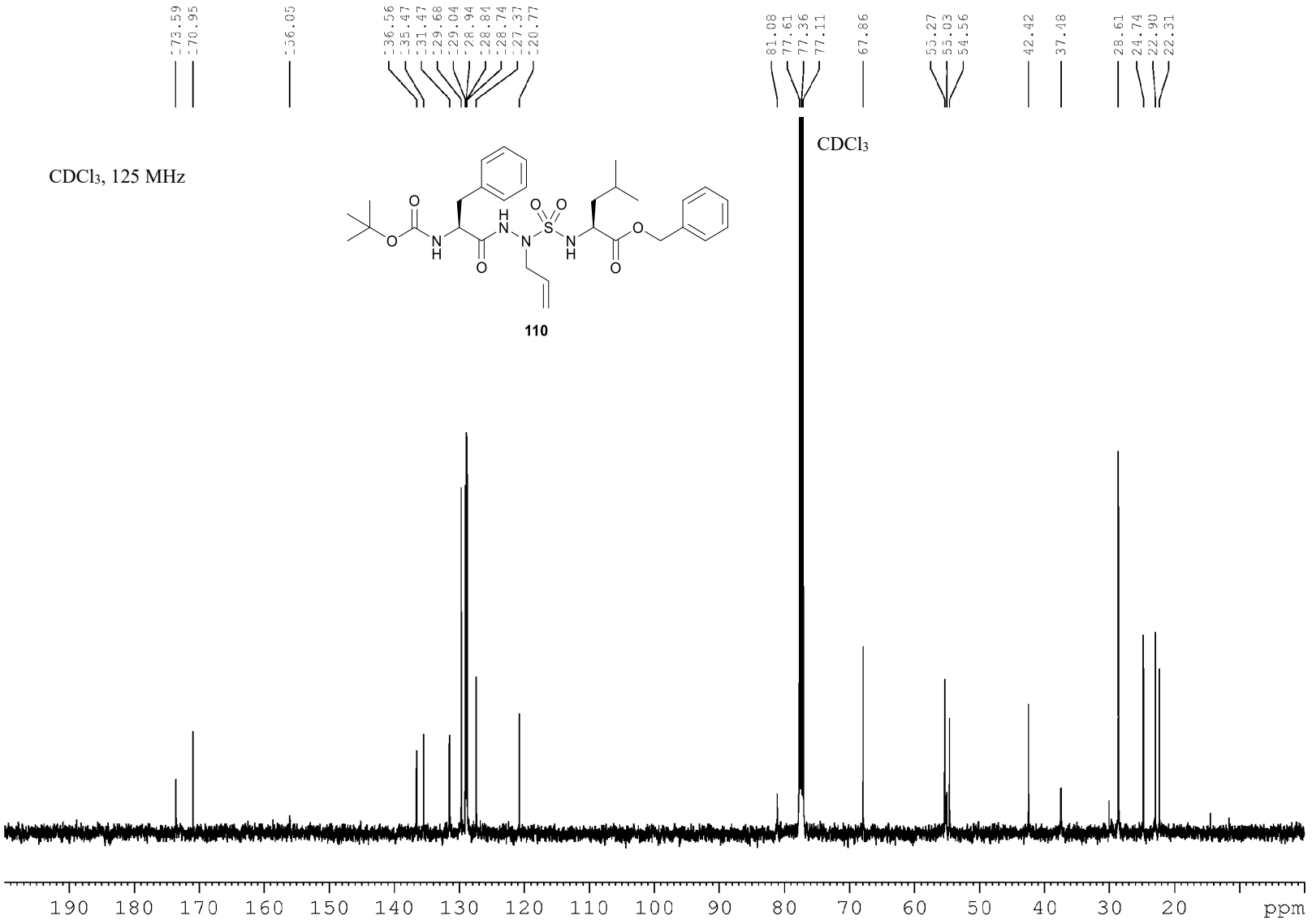
173.59
170.95
156.05
136.56
135.47
131.47
129.68
129.04
128.94
128.84
128.74
127.37
120.77
81.08
77.61
77.36
77.11
67.86
55.27
55.03
54.56
42.42
37.48
28.61
24.74
22.90
22.31
CDCl3
CDCl3, 125 MHz
110
190 180 170 160 150 140 130 120 110 100 90 80 70 60 50 40 30 20 ppm

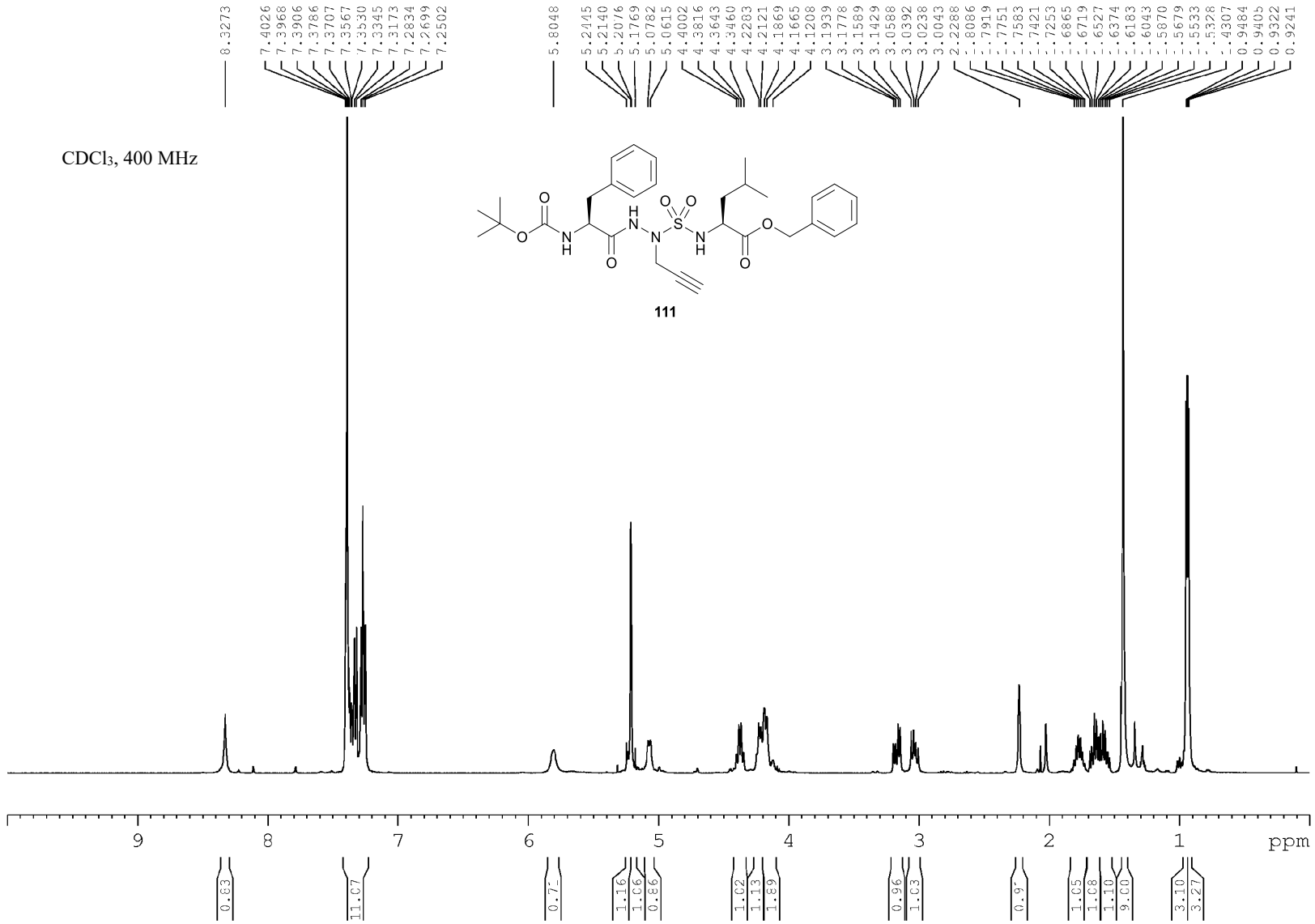
CDCl3, 400 MHz
111
ppm

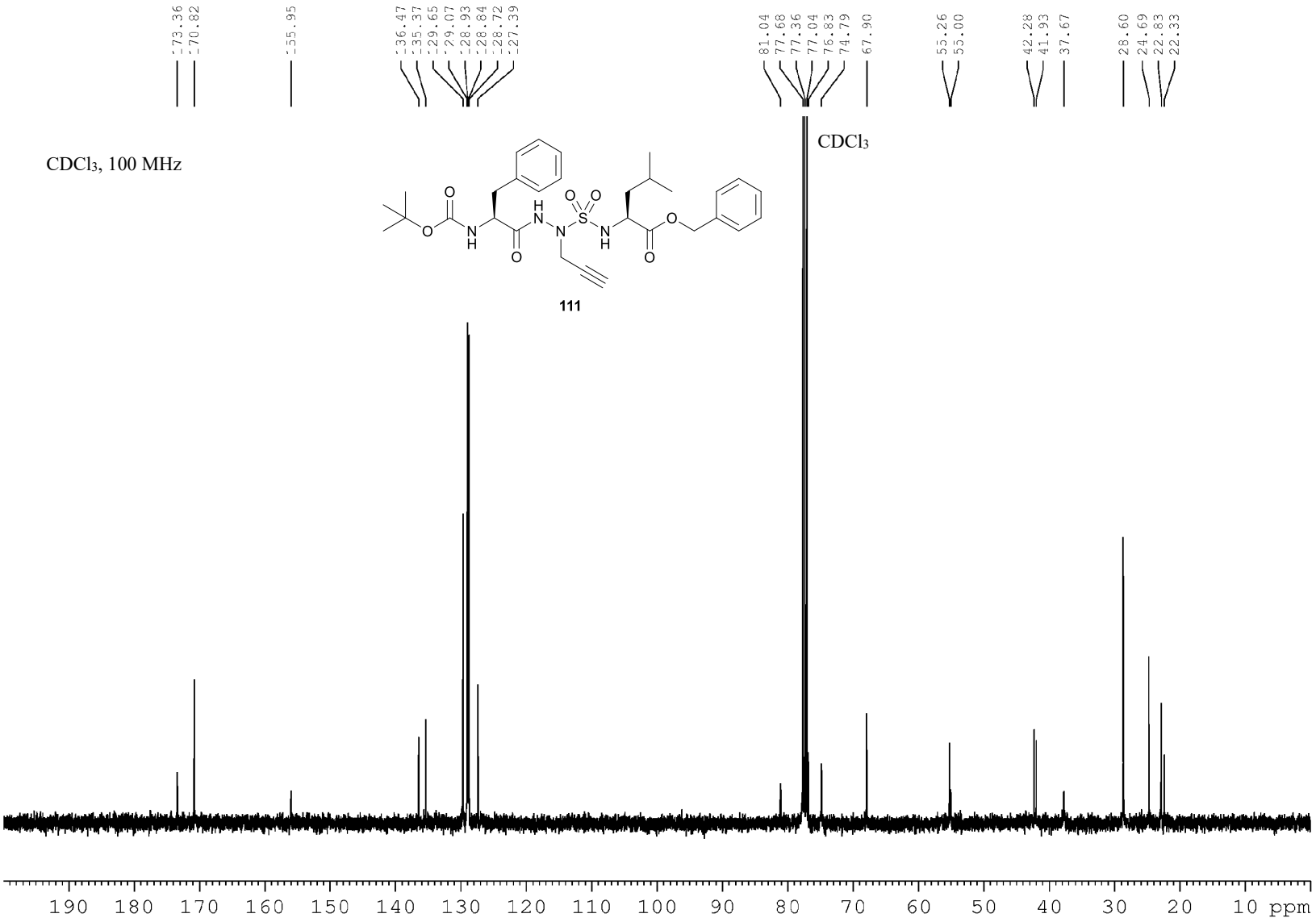
173.36
170.82
155.95
136.47
135.37
129.65
129.07
128.93
128.84
128.72
127.39
81.04
77.68
77.36
77.04
76.83
74.79
67.90
55.26
55.00
42.28
41.93
37.67
28.60
24.69
22.83
22.33
CDCl3
CDCl3, 100 MHz
111
190 180 170 160 150 140 130 120 110 100 90 80 70 60 50 40 30 20 10 ppm

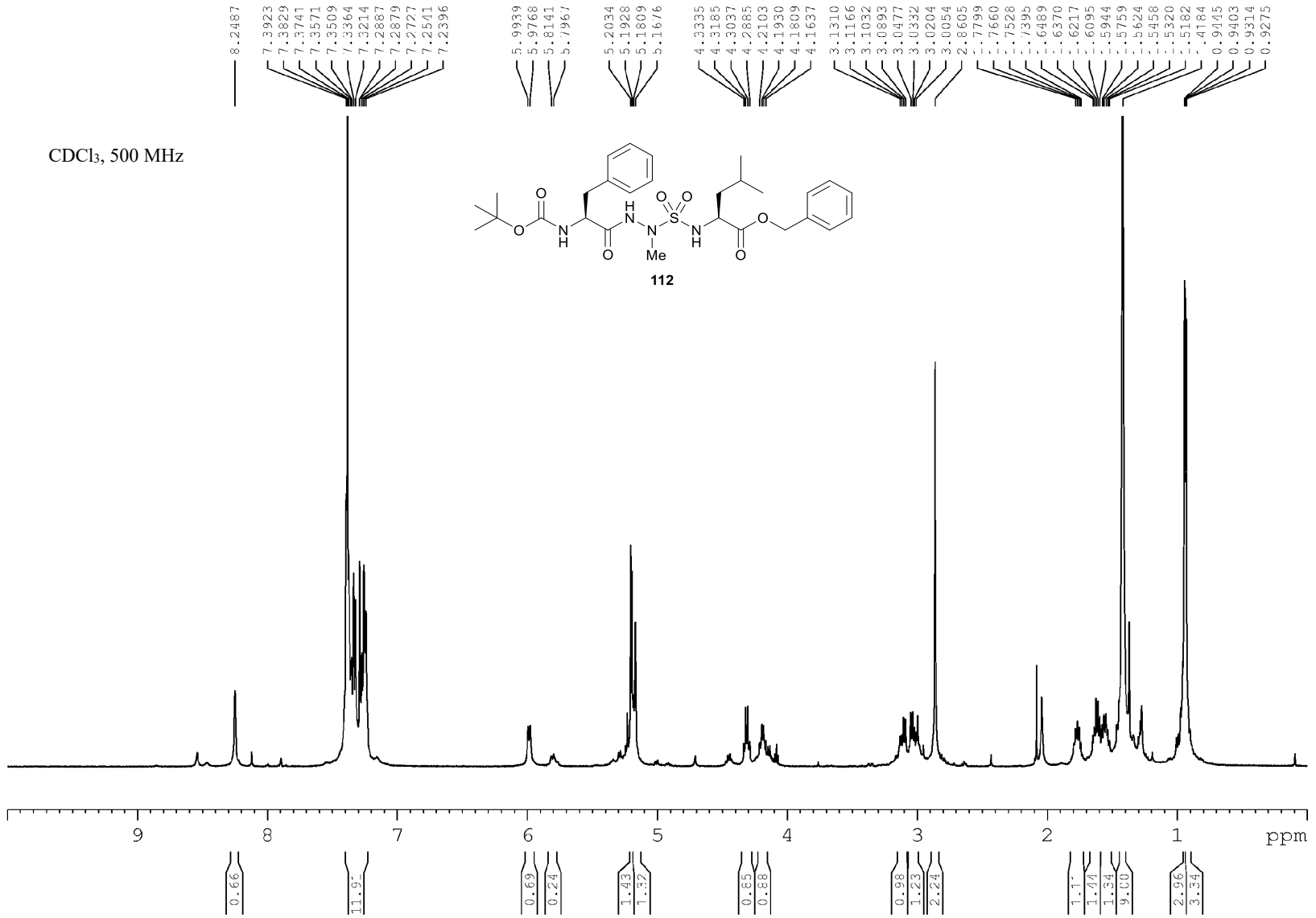
CDCl3, 500 MHz
8.2487
7.3923
7.3829
7.3741
7.3571
7.3509
7.3364
7.3214
7.2887
7.2879
7.2727
7.2541
7.2396
5.9939
5.9768
5.8141
5.1928
5.1809
5.1676
4.3335
4.3185
4.3037
4.2885
4.2103
4.1930
4.1809
4.1637
3.1310
3.1166
3.1032
3.0893
3.0477
3.0332
3.0204
3.0054
2.8605
9
8
7
6
5
4
3
2
1
ppm
0.66
11.9
0.69
0.24
1.43
1.32
0.85
0.88
0.98
1.23
2.24
1.1
1.44
1.34
9.00
2.96
3.34

112

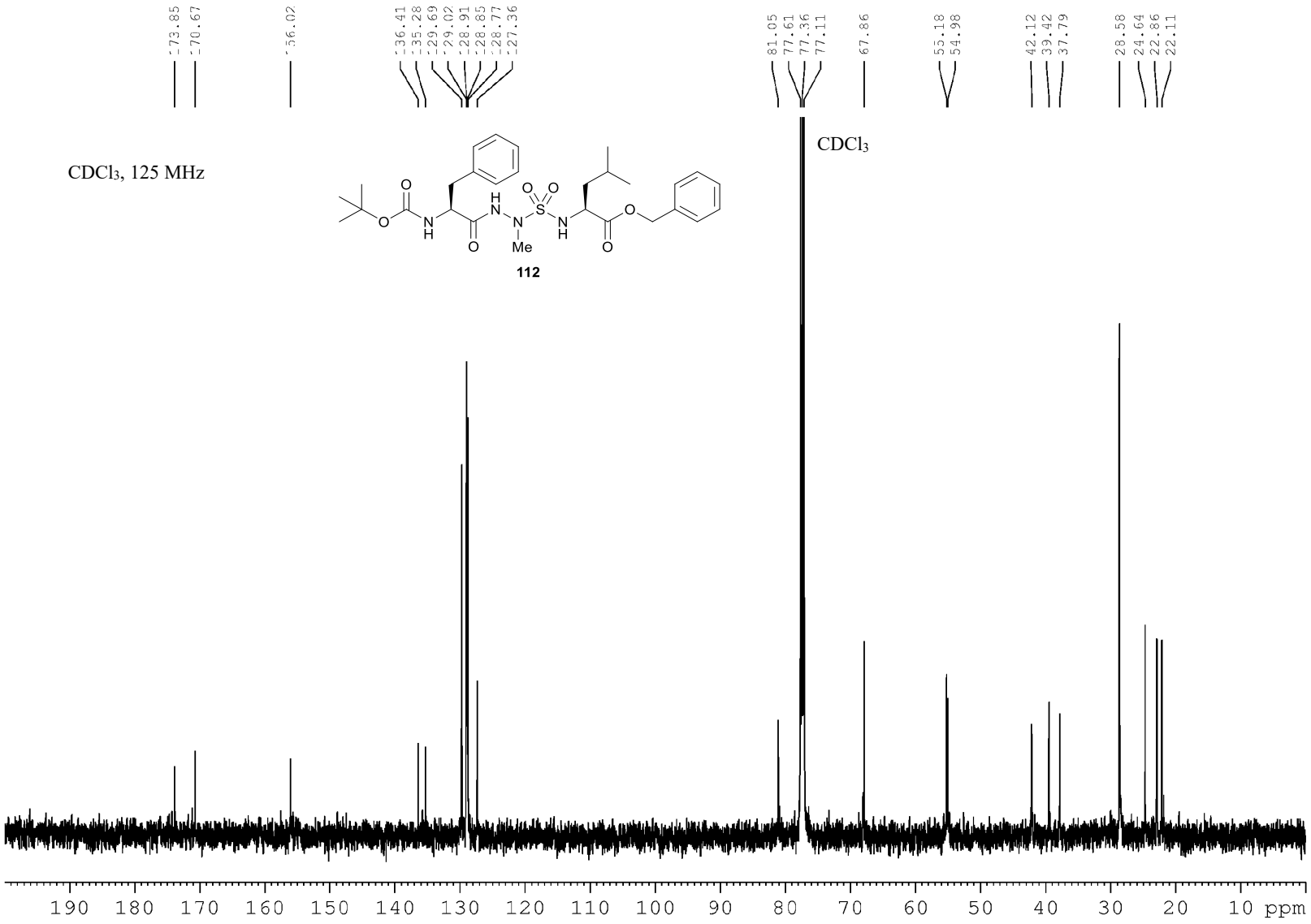
173.85
170.67
156.02
136.41
135.28
129.69
129.02
128.91
128.85
128.77
127.36
81.05
77.61
77.36
77.11
67.86
55.18
54.98
42.12
39.42
37.79
28.58
24.64
22.86
22.11
CDCl3
CDCl3, 125 MHz
112
190 180 170 160 150 140 130 120 110 100 90 80 70 60 50 40 30 20 10 ppm

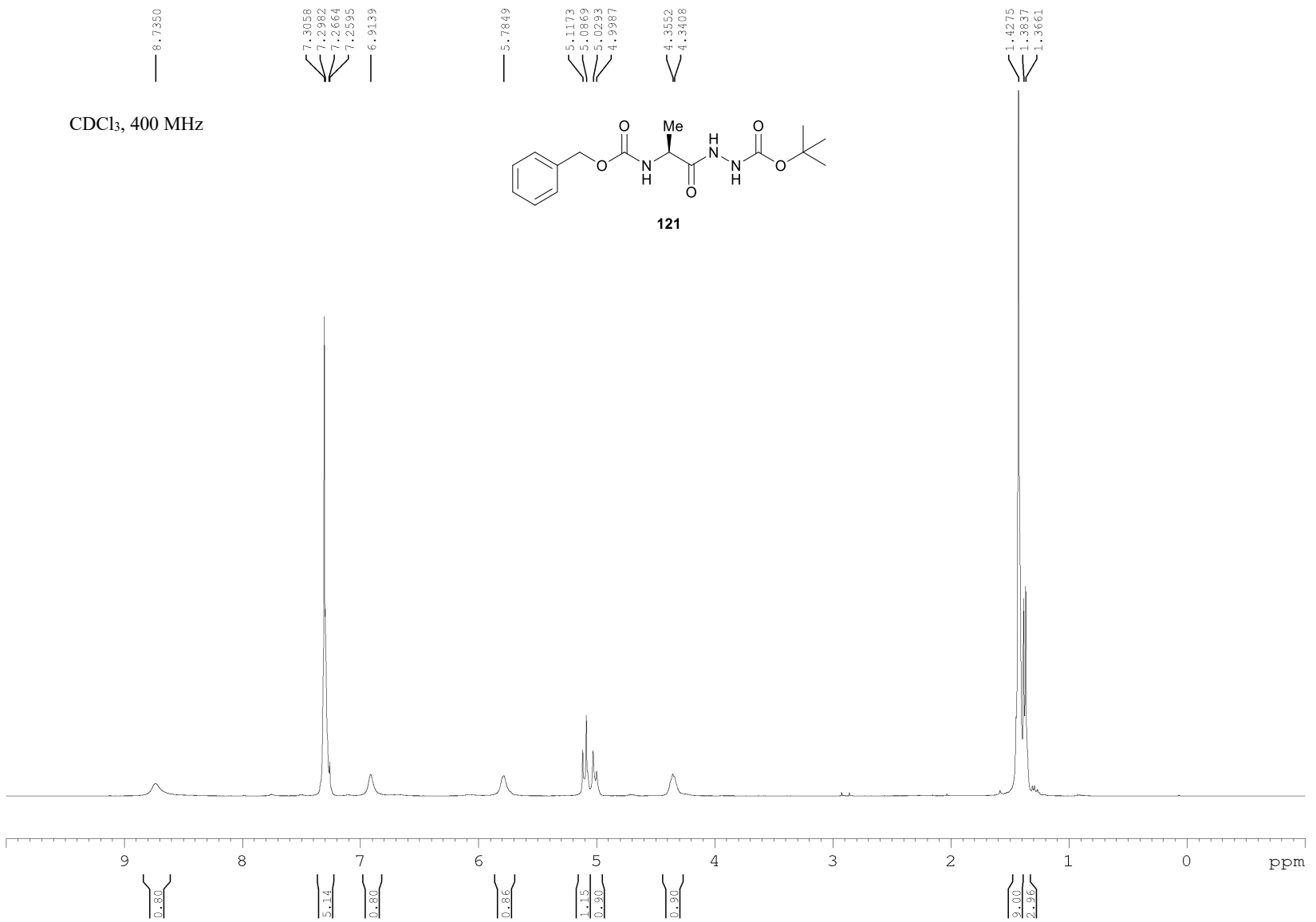
8.7350
7.3058
7.2982
7.2664
7.2595
6.9139
5.7849
5.1173
5.0869
5.0293
4.9987
4.3552
4.3408
1.4275
1.3837
1.3661
CDCl3, 400 MHz
Me
O
N
H
O
O
H
N
N
H
O
O
121
9
8
7
6
5
4
3
2
1
0
ppm
0.80
5.14
0.80
0.86
1.15
0.90
0.90
9.00
2.96

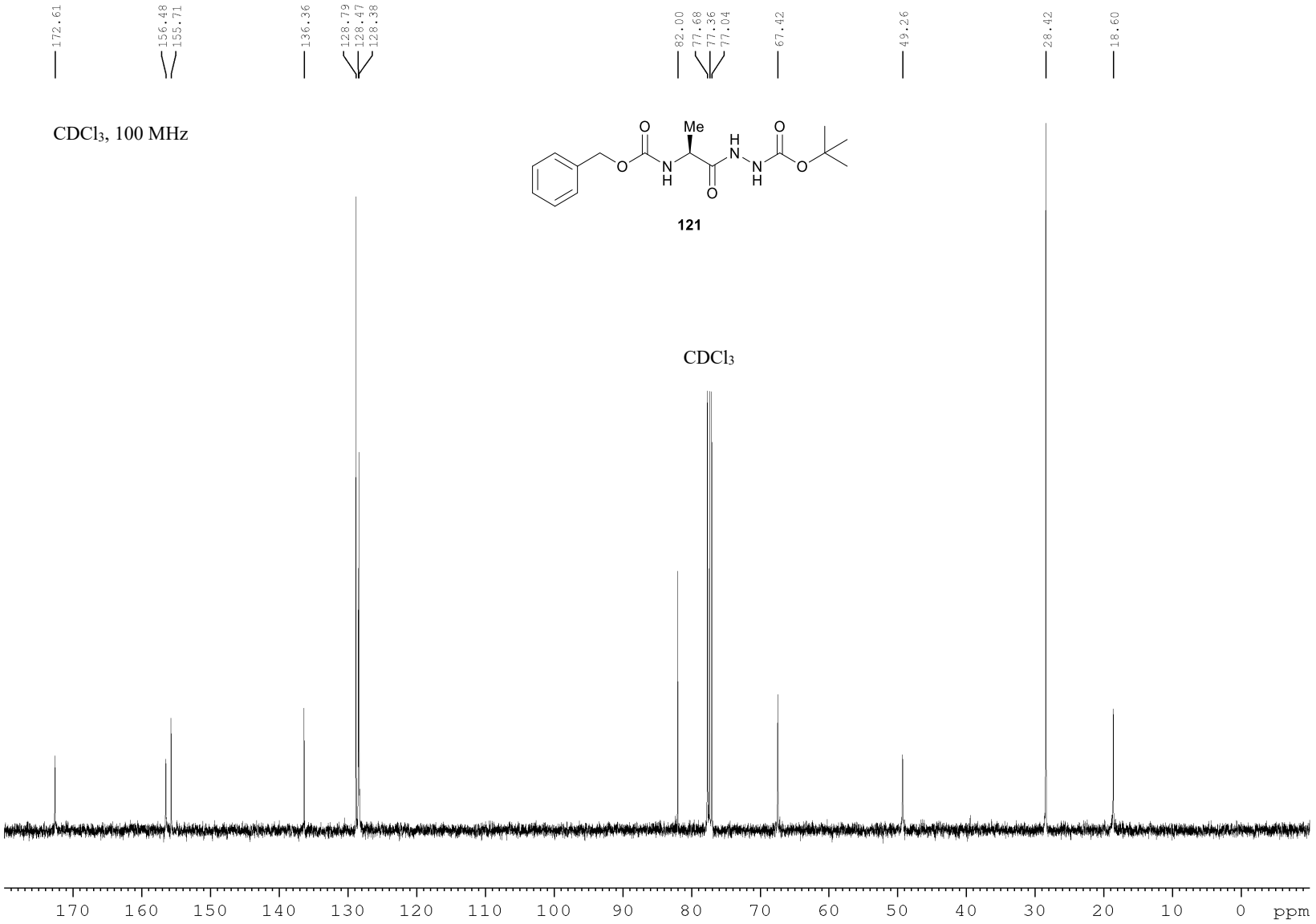
172.61
156.48
155.71
136.36
128.79
128.47
128.38
82.00
77.68
77.36
77.04
67.42
49.26
28.42
18.60
CDCl3, 100 MHz
Me
O
N
H
H
N
N
H
O
O
O
O
121
CDCl3
170
160
150
140
130
120
110
100
90
80
70
60
50
40
30
20
10
0
ppm

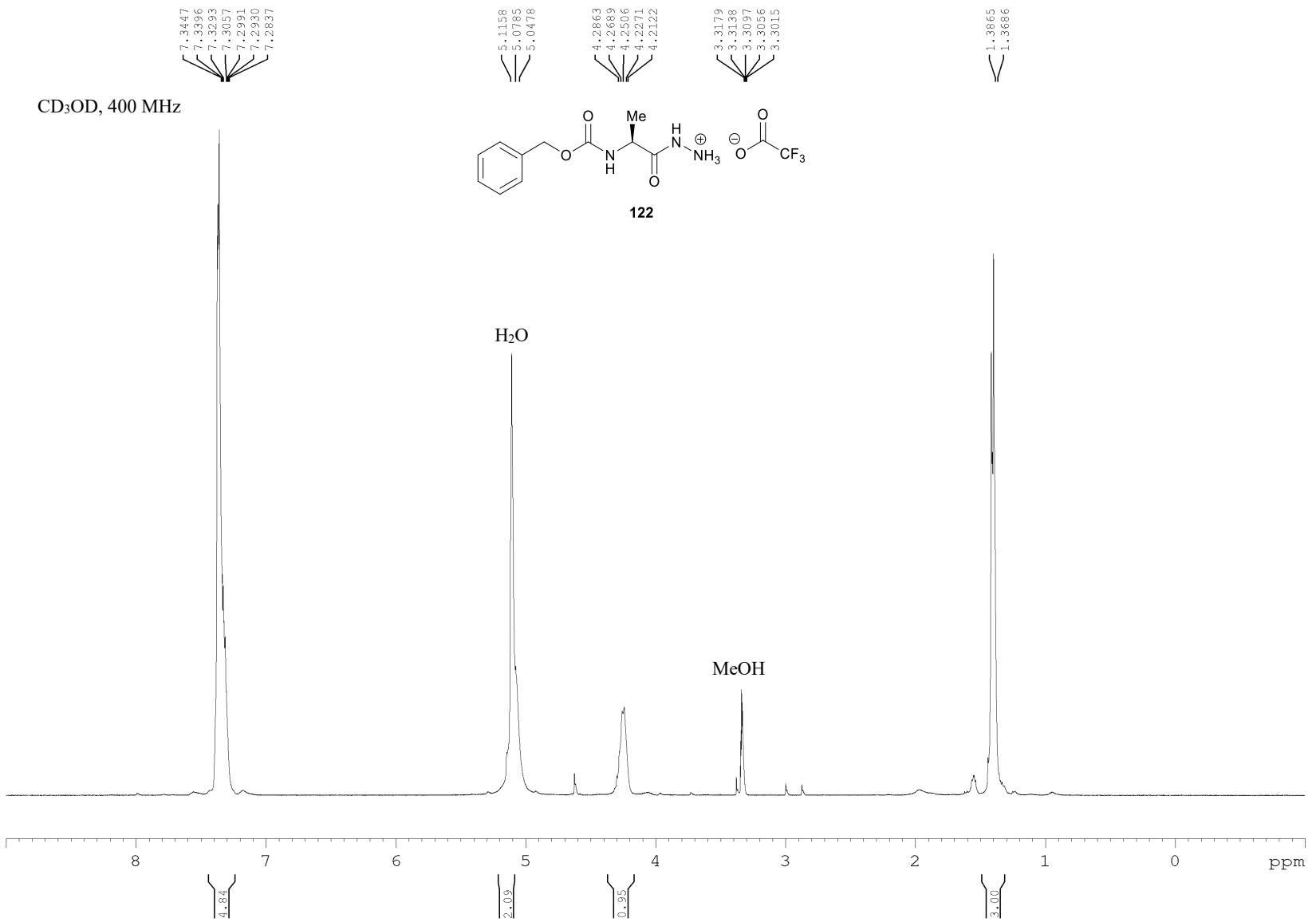
7.3447
7.3396
7.3293
7.3057
7.2991
7.2930
7.2837
5.1158
5.0785
5.0478
4.2863
4.2689
4.2506
4.2271
4.2122
3.3179
3.3138
3.3097
3.3056
3.3015
1.3865
1.3686
CD3OD, 400 MHz
122
H2O
MeOH
8
7
6
5
4
3
2
1
0
ppm
4.84
2.09
0.95
3.00

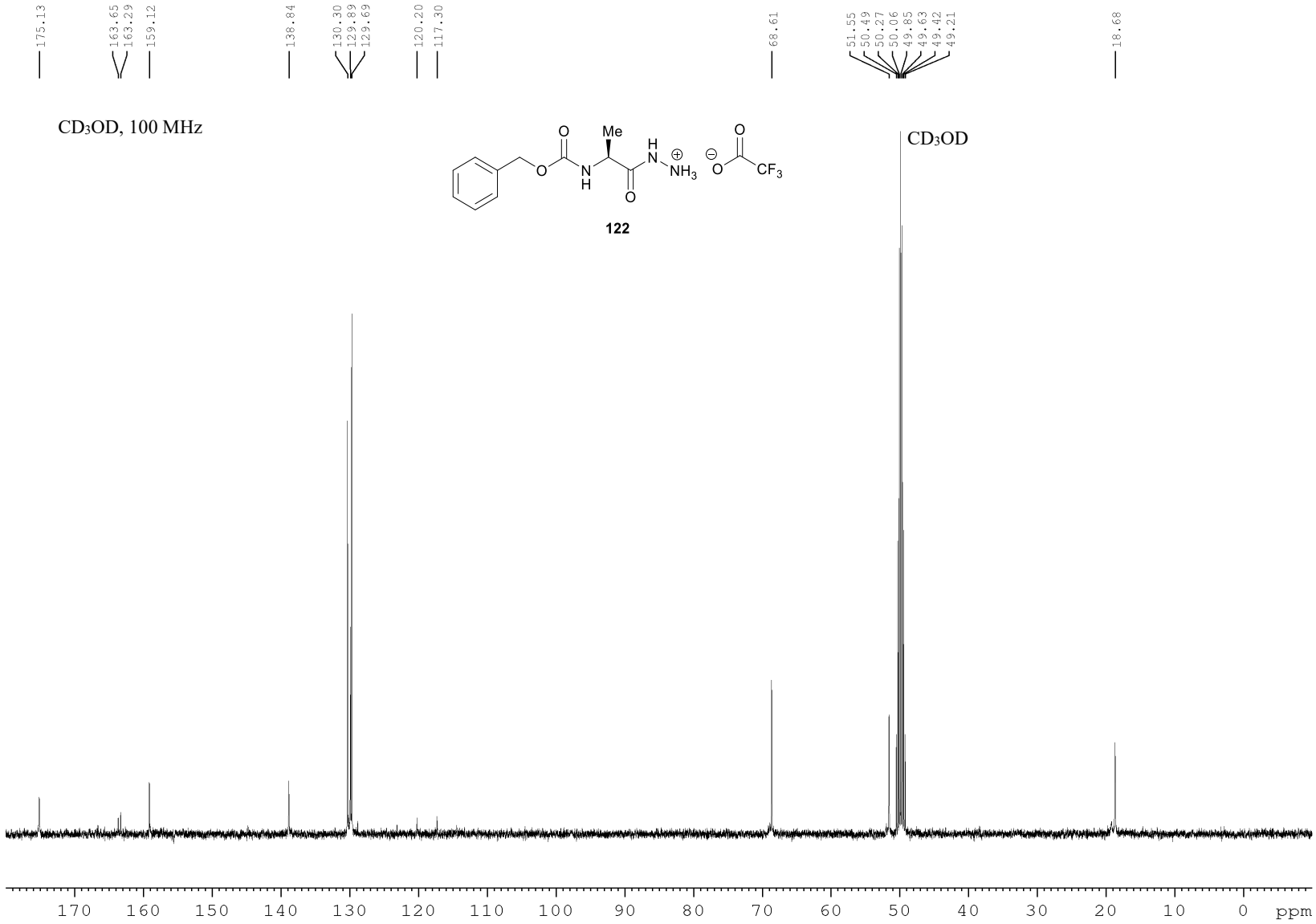
175.13
163.65
163.29
159.12
138.84
130.30
129.89
129.69
120.20
117.30
68.61
51.55
50.49
50.27
50.06
49.85
49.63
49.42
49.21
18.68
CD3OD, 100 MHz
CD3OD
122
170
160
150
140
130
120
110
100
90
80
70
60
50
40
30
20
10
0
ppm

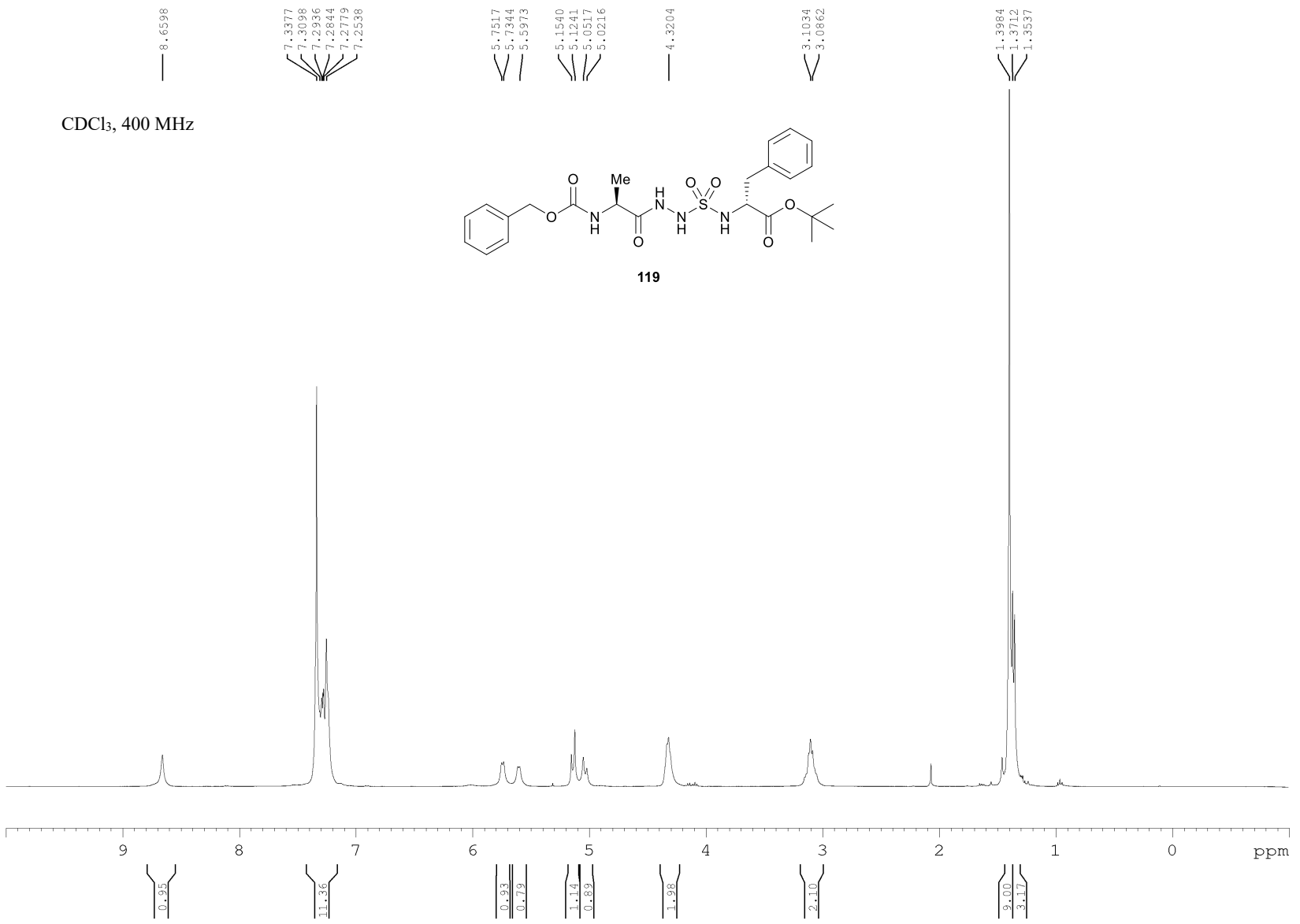
8.6598
7.3377
7.3098
7.2936
7.2844
7.2779
7.2538
5.7517
5.7344
5.5973
5.1540
5.1241
5.0517
5.0216
4.3204
3.1034
3.0862
1.3984
1.3712
1.3537
CDCl3, 400 MHz
119
9
8
7
6
5
4
3
2
1
0
ppm
0.95
11.36
0.93
0.79
1.14
0.89
1.98
2.10
9.00
3.17

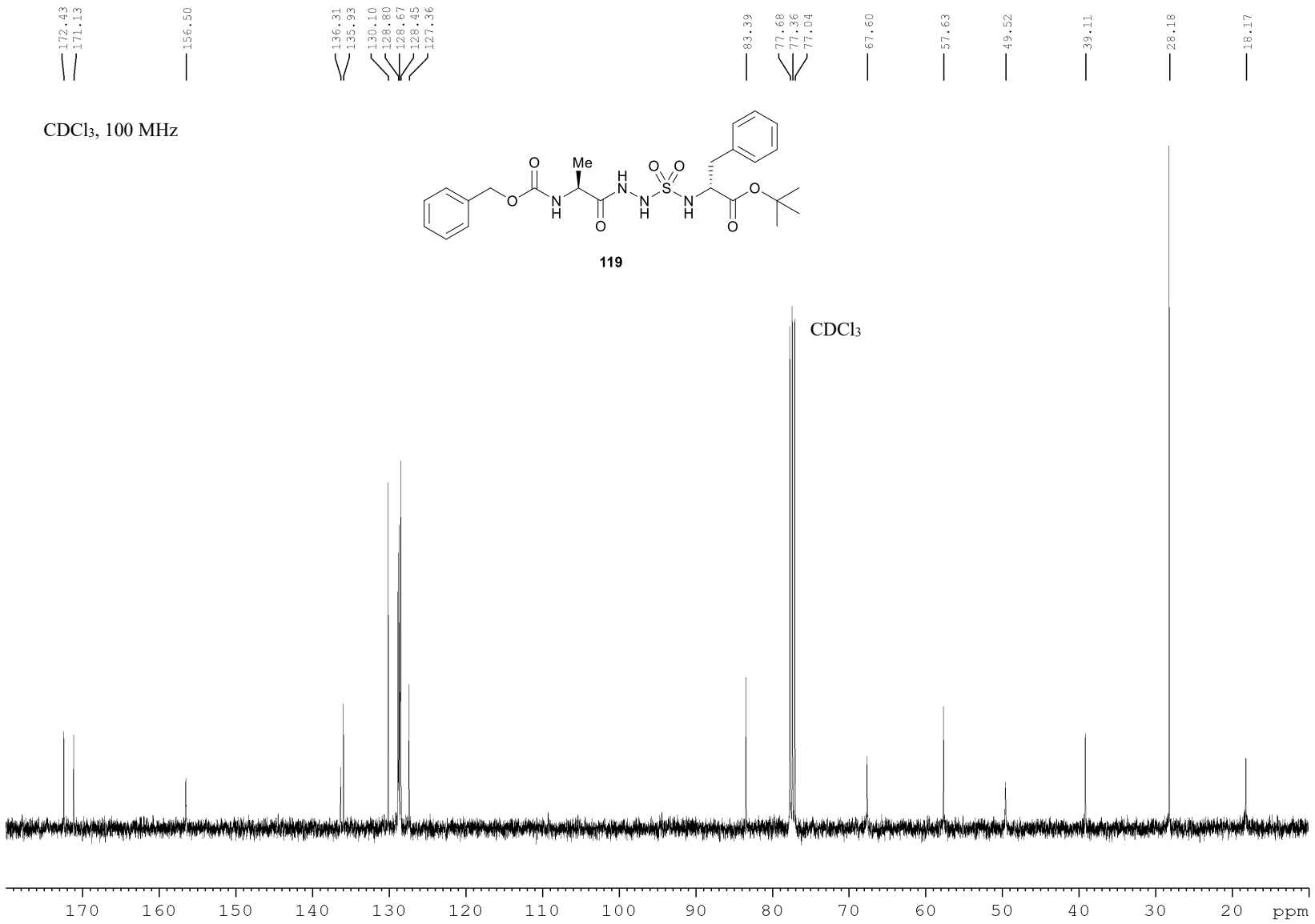
172.43
171.13
156.50
136.31
135.93
130.10
128.80
128.67
128.45
127.36
83.39
77.68
77.36
77.04
67.60
57.63
49.52
39.11
28.18
18.17
CDCl3, 100 MHz
119
CDCl3
170
160
150
140
130
120
110
100
90
80
70
60
50
40
30
20
ppm

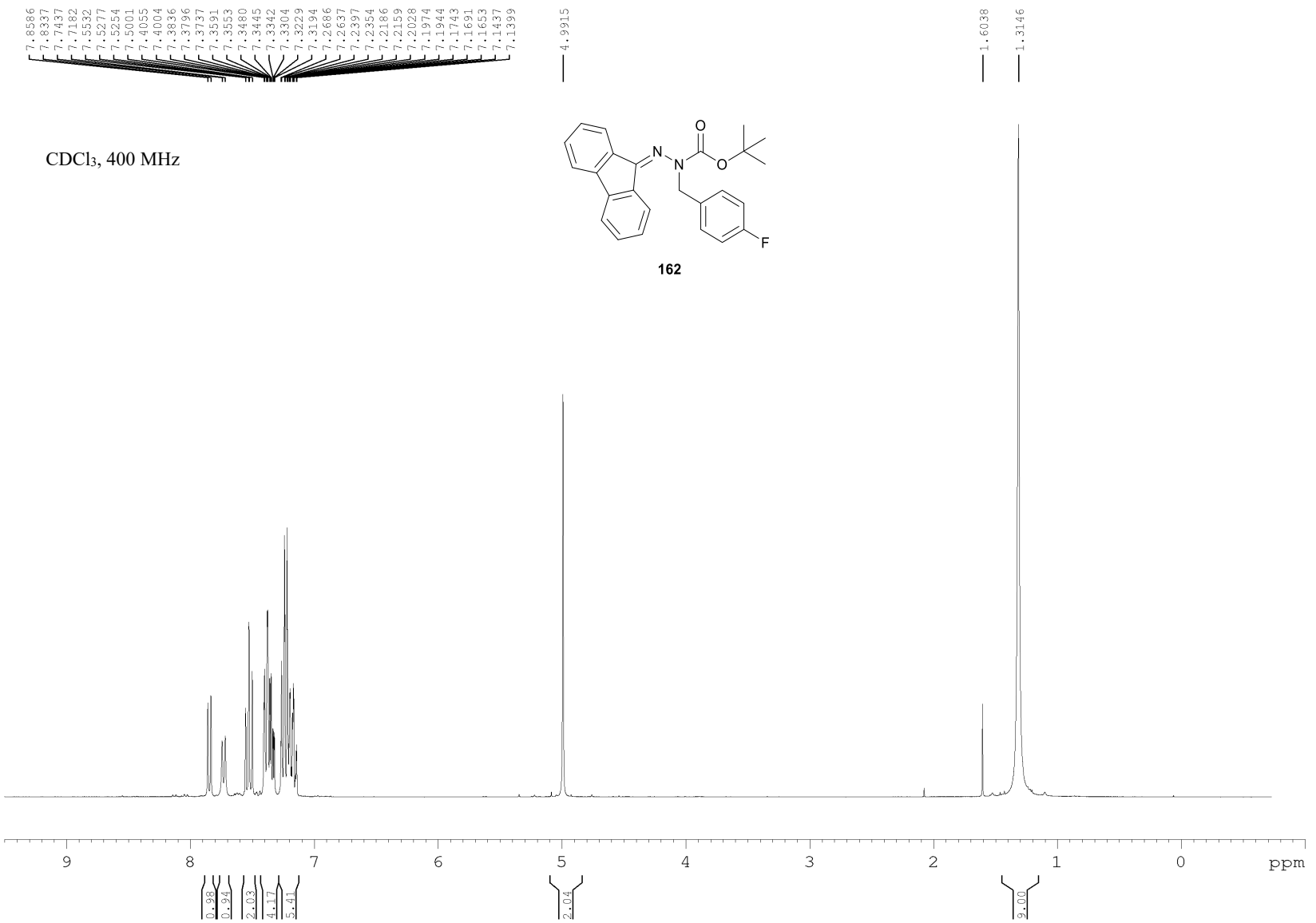
7.8586
7.8337
7.7437
7.7182
7.5532
7.5277
7.5254
7.5001
7.4055
7.4004
7.3836
7.3796
7.3737
7.3591
7.3553
7.3480
7.3445
7.3342
7.3304
7.3229
7.3194
7.2686
7.2637
7.2397
7.2354
7.2186
7.2159
7.2028
7.1974
7.1944
7.1743
7.1691
7.1653
7.1437
7.1399
4.9915
1.6038
1.3146
CDCl3, 400 MHz
N
N
O
O
F
162
9
8
7
6
5
4
3
2
1
0
ppm
0.98
0.94
2.03
4.17
5.41
2.04
9.00

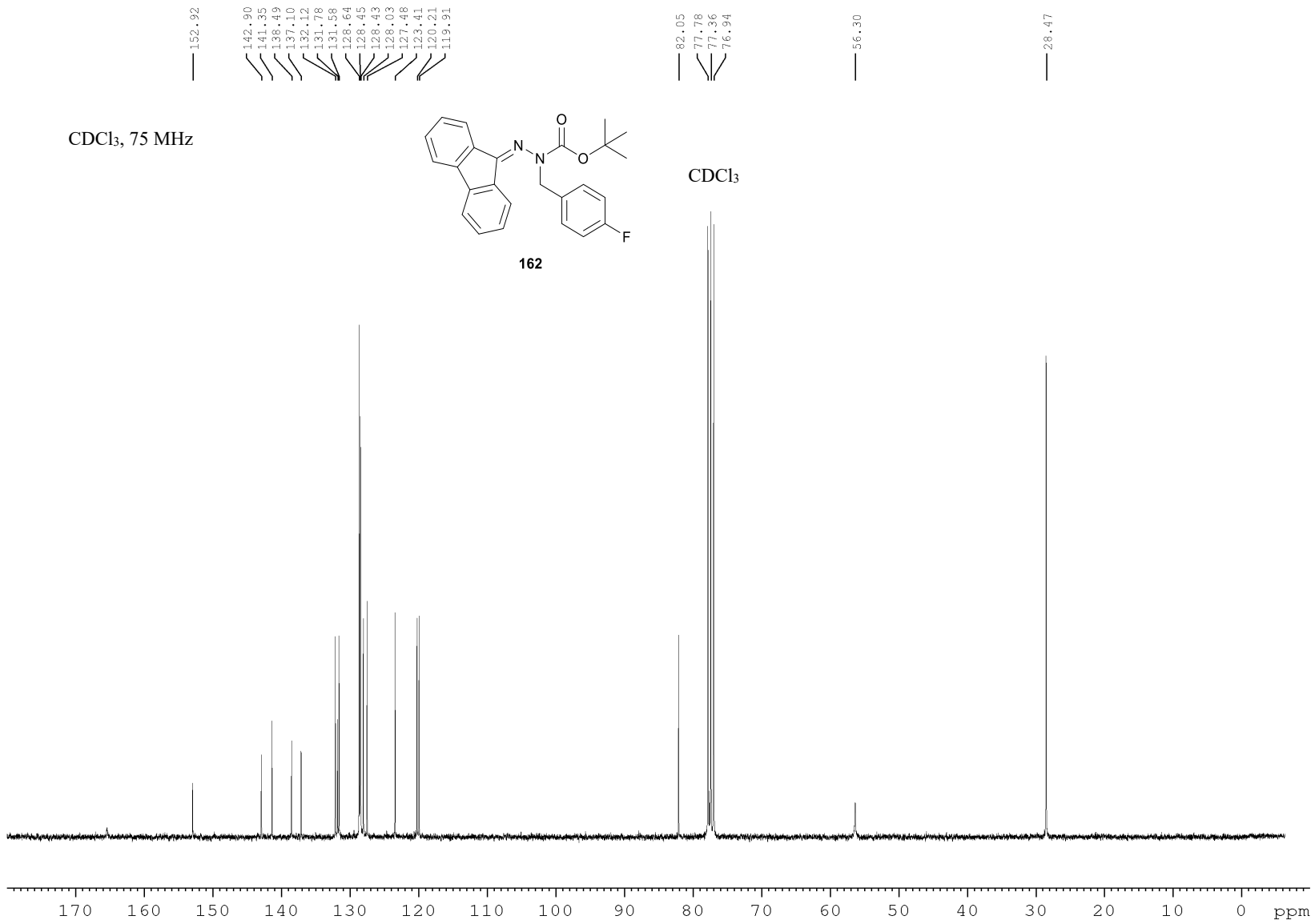
152.92
142.90
141.35
138.49
137.10
132.12
131.78
131.58
128.64
128.45
128.43
128.03
127.48
123.41
120.21
119.91
82.05
77.78
77.36
76.94
56.30
28.47
CDCl3, 75 MHz
CDCl3
N
N
O
O
F
162
170
160
150
140
130
120
110
100
90
80
70
60
50
40
30
20
10
0
ppm

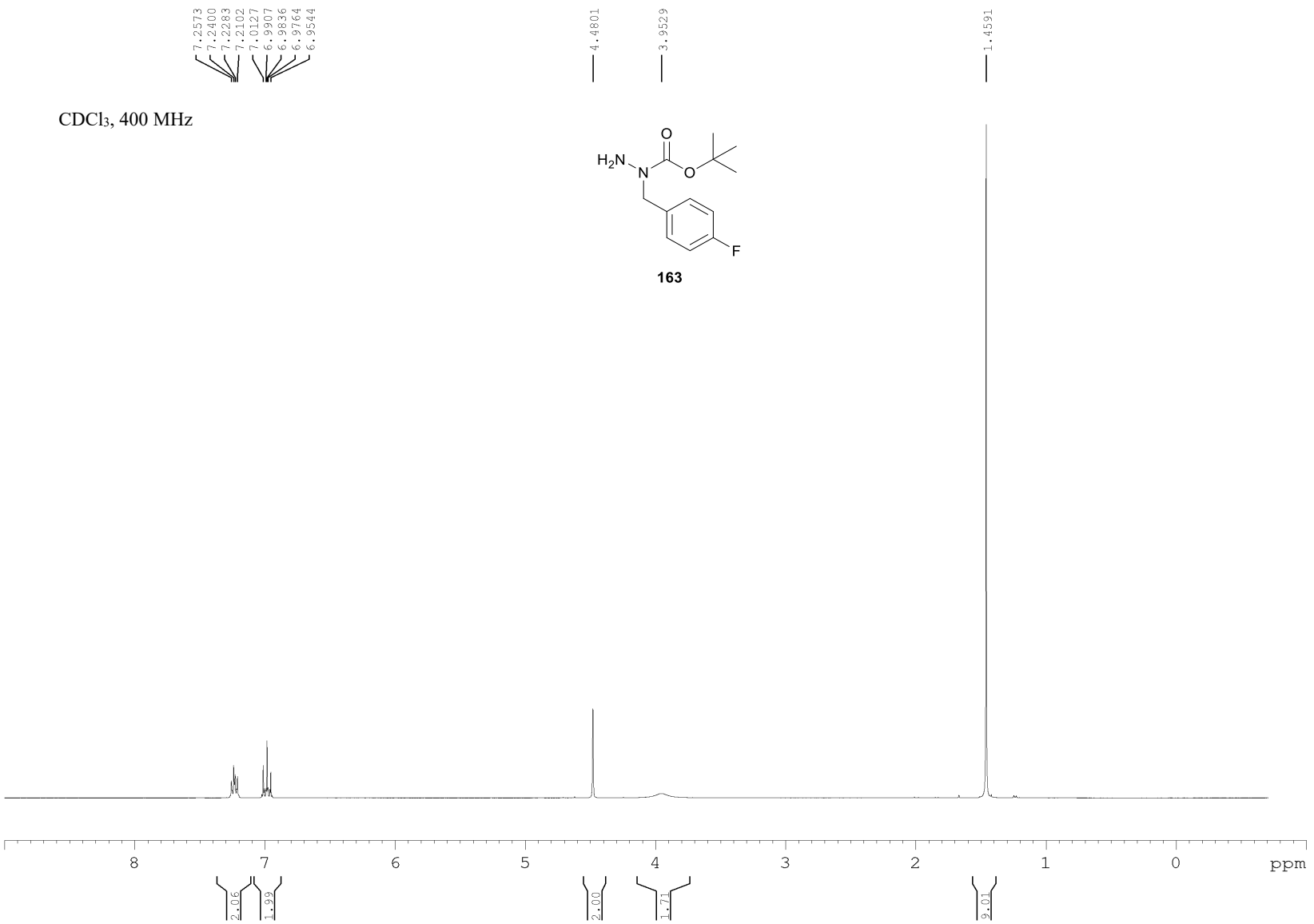
7.2573
7.2400
7.2283
7.2102
7.0127
6.9907
6.9836
6.9764
6.9544
4.4801
3.9529
1.4591
CDCl3, 400 MHz
O
H2N
N
O
F
163
8
7
6
5
4
3
2
1
0
ppm
2.06
1.99
2.00
1.71
9.01

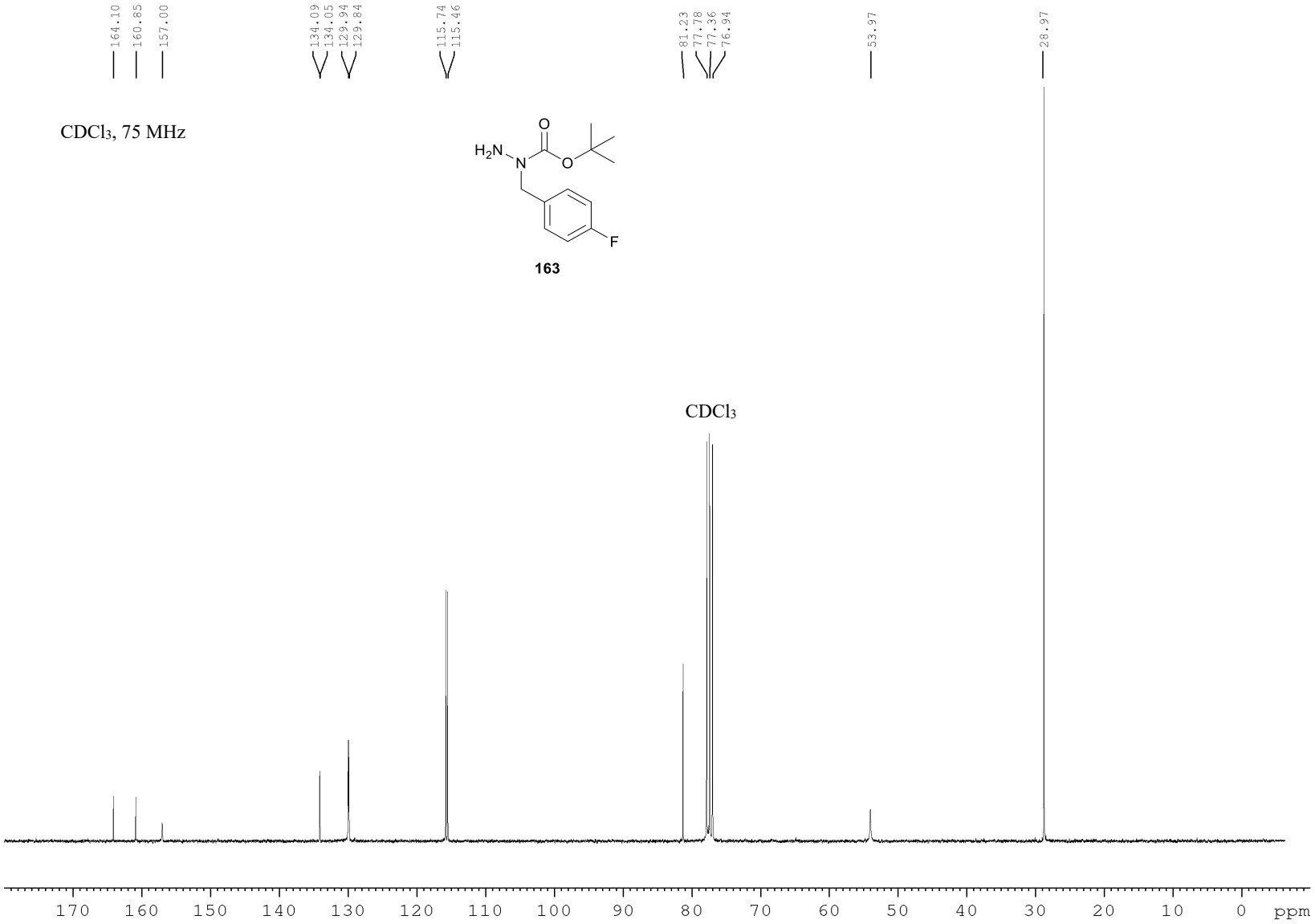
164.10
160.85
157.00
134.09
134.05
129.94
129.84
115.74
115.46
81.23
77.78
77.36
76.94
53.97
28.97
CDCl3, 75 MHz
O
H2N
N
O
F
163
CDCl3
170
160
150
140
130
120
110
100
90
80
70
60
50
40
30
20
10
0
ppm

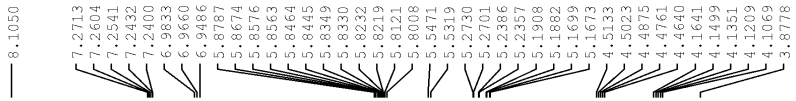

$CDCl_3$, 500 MHz

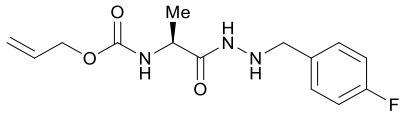

124

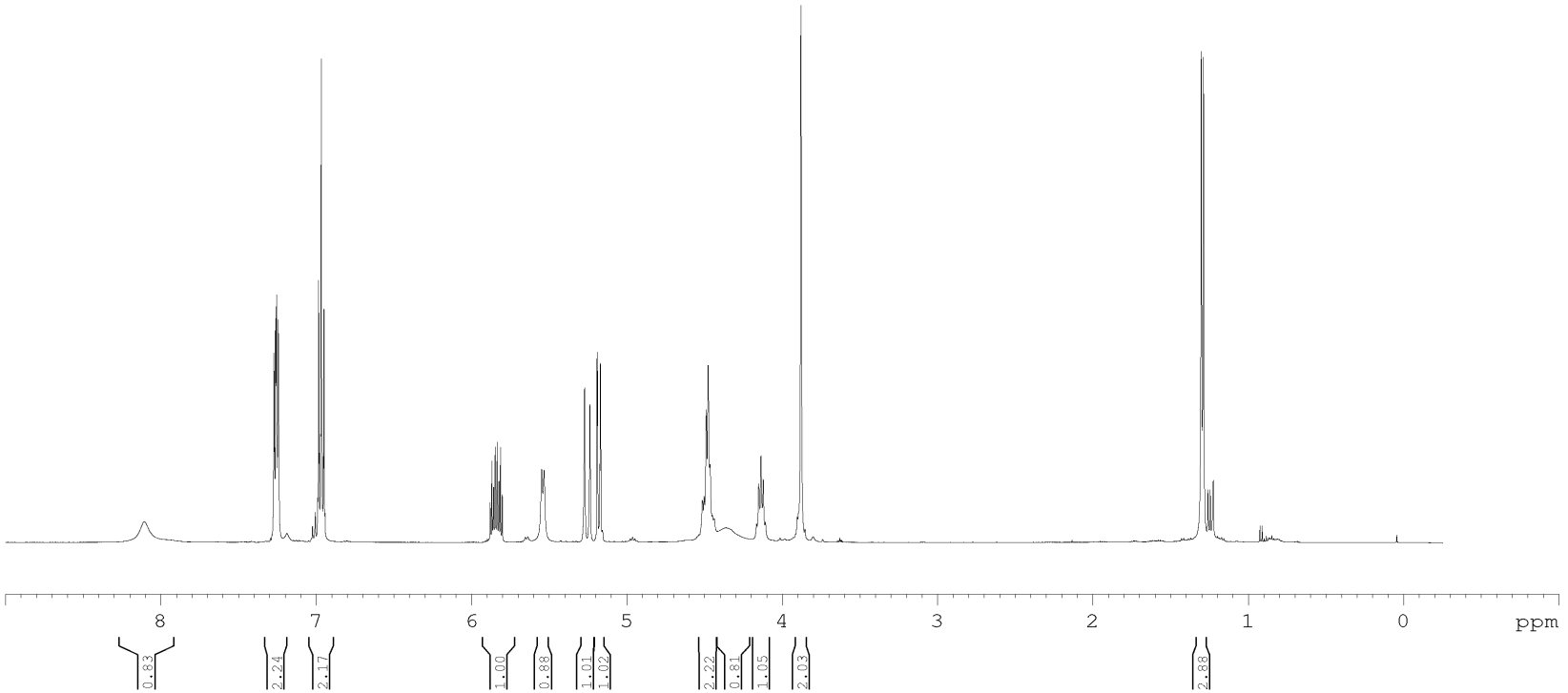

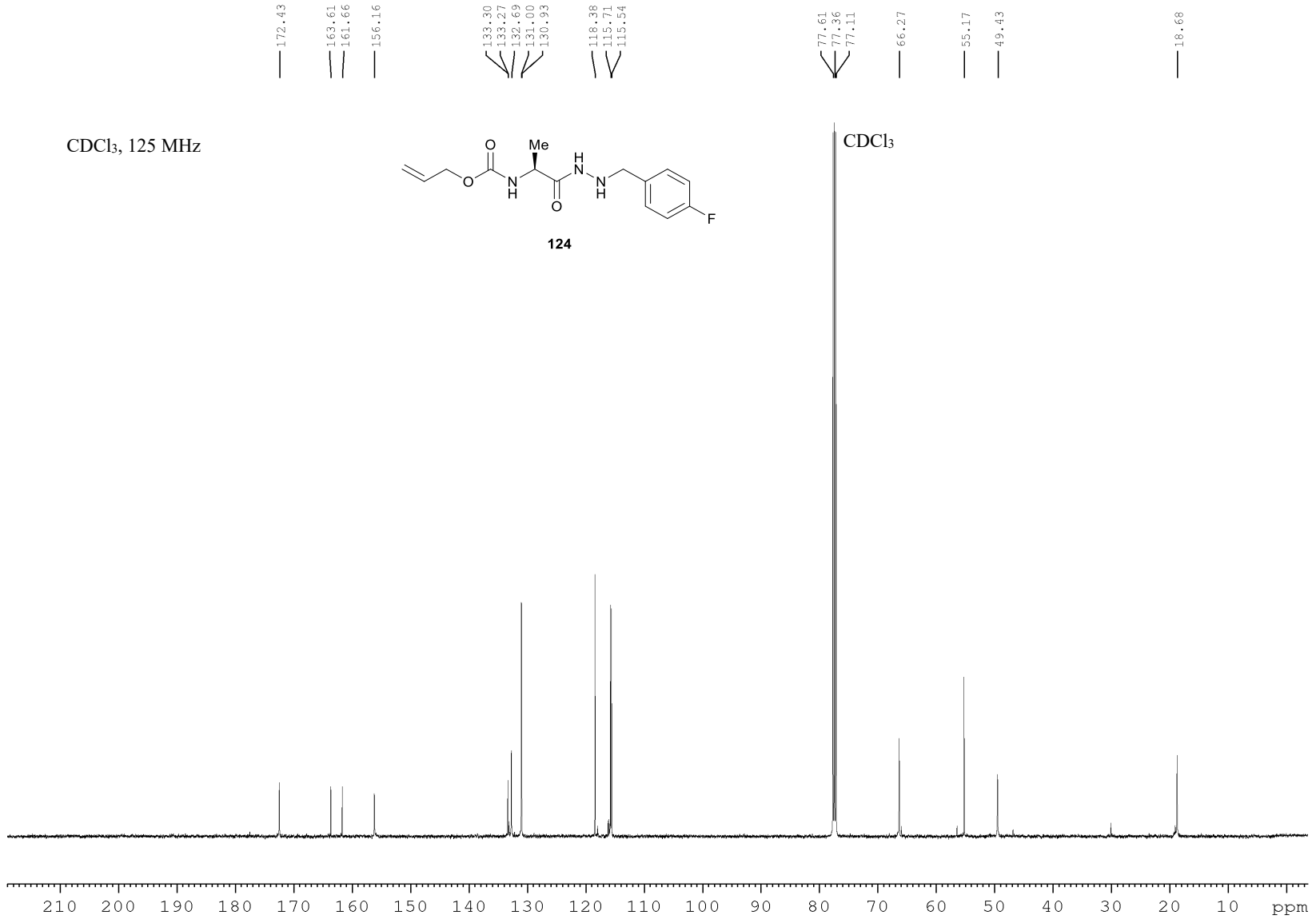
172.43
163.61
161.66
156.16
133.30
133.27
132.69
131.00
130.93
118.38
115.71
115.54
77.61
77.36
77.11
66.27
55.17
49.43
18.68
CDCl3, 125 MHz
CDCl3
O
Me
H
N
O
N
H
O
N
H
F
124
210 200 190 180 170 160 150 140 130 120 110 100 90 80 70 60 50 40 30 20 10 ppm

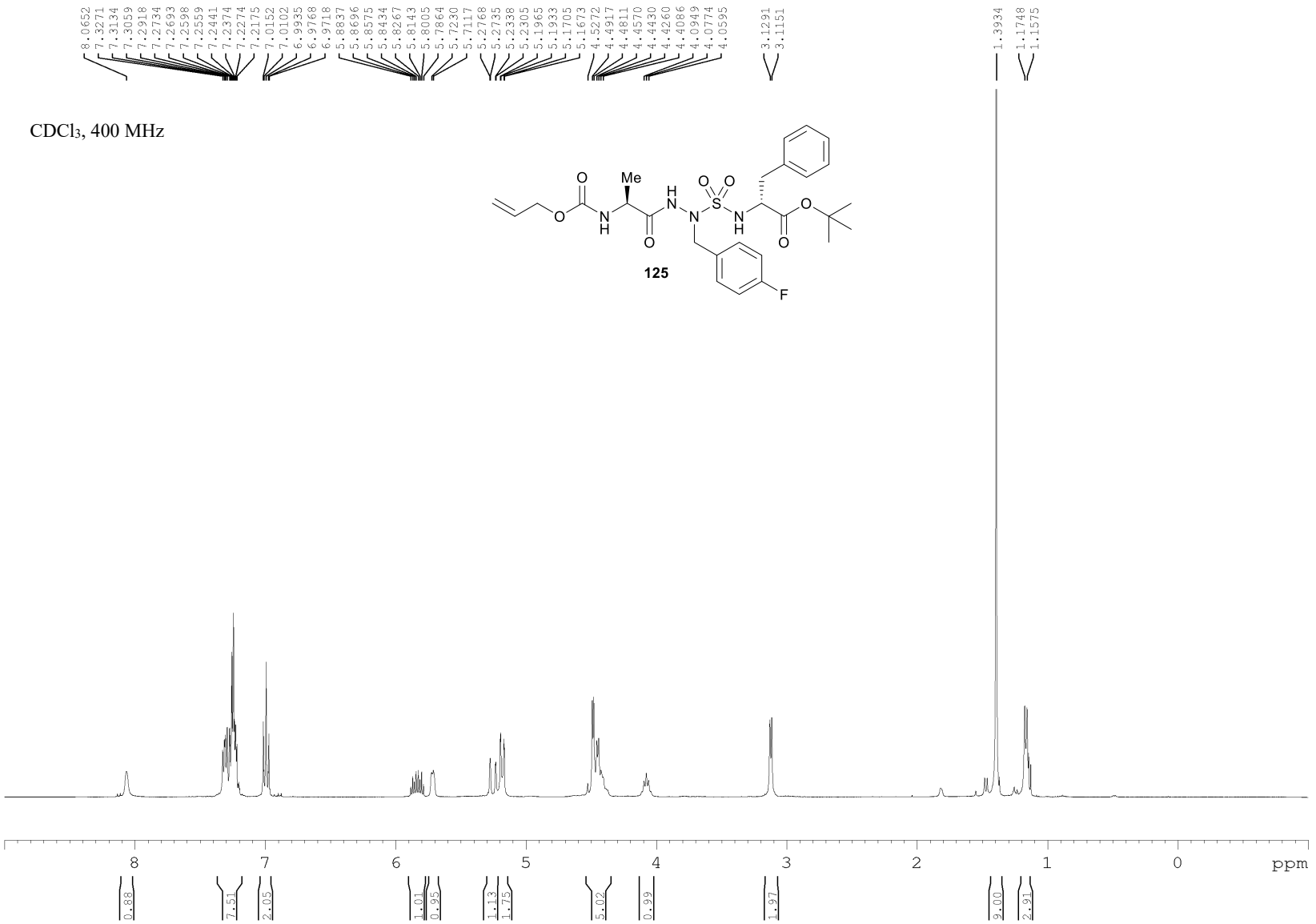
8.0652
7.3271
7.3134
7.3059
7.2918
7.2734
7.2693
7.2598
7.2559
7.2441
7.2374
7.2274
7.2175
7.0152
7.0102
6.9935
6.9768
6.9718
5.8837
5.8696
5.8575
5.8434
5.8267
5.8143
5.8005
5.7864
5.7230
5.7117
5.2768
5.2735
5.2338
5.2305
5.1965
5.1933
5.1705
5.1673
4.5272
4.4917
4.4811
4.4570
4.4430
4.4260
4.4086
4.0949
4.0774
4.0595
3.1291
3.1151
1.3934
1.1748
1.1575
CDCl3, 400 MHz
Me
125
F
8
7
6
5
4
3
2
1
0
ppm
0.88
7.51
2.05
1.01
0.95
1.13
1.75
5.02
0.99
1.97
9.00
2.91

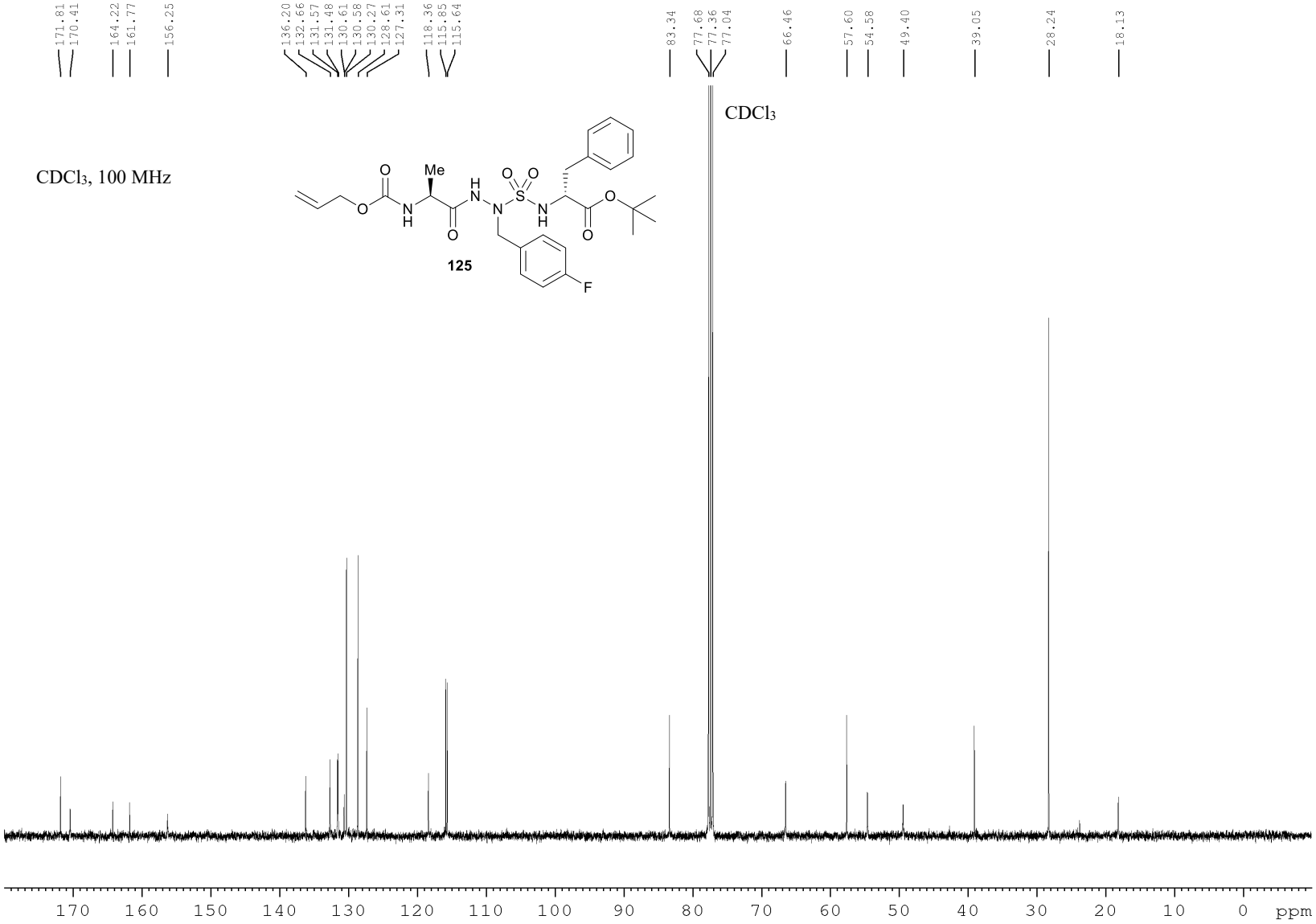
171.81
170.41
164.22
161.77
156.25
136.20
132.66
131.57
131.48
130.61
130.58
130.27
128.61
127.31
118.36
115.85
115.64
83.34
77.68
77.36
77.04
66.46
57.60
54.58
49.40
39.05
28.24
18.13
CDCl3
CDCl3, 100 MHz
125
170
160
150
140
130
120
110
100
90
80
70
60
50
40
30
20
10
0
ppm

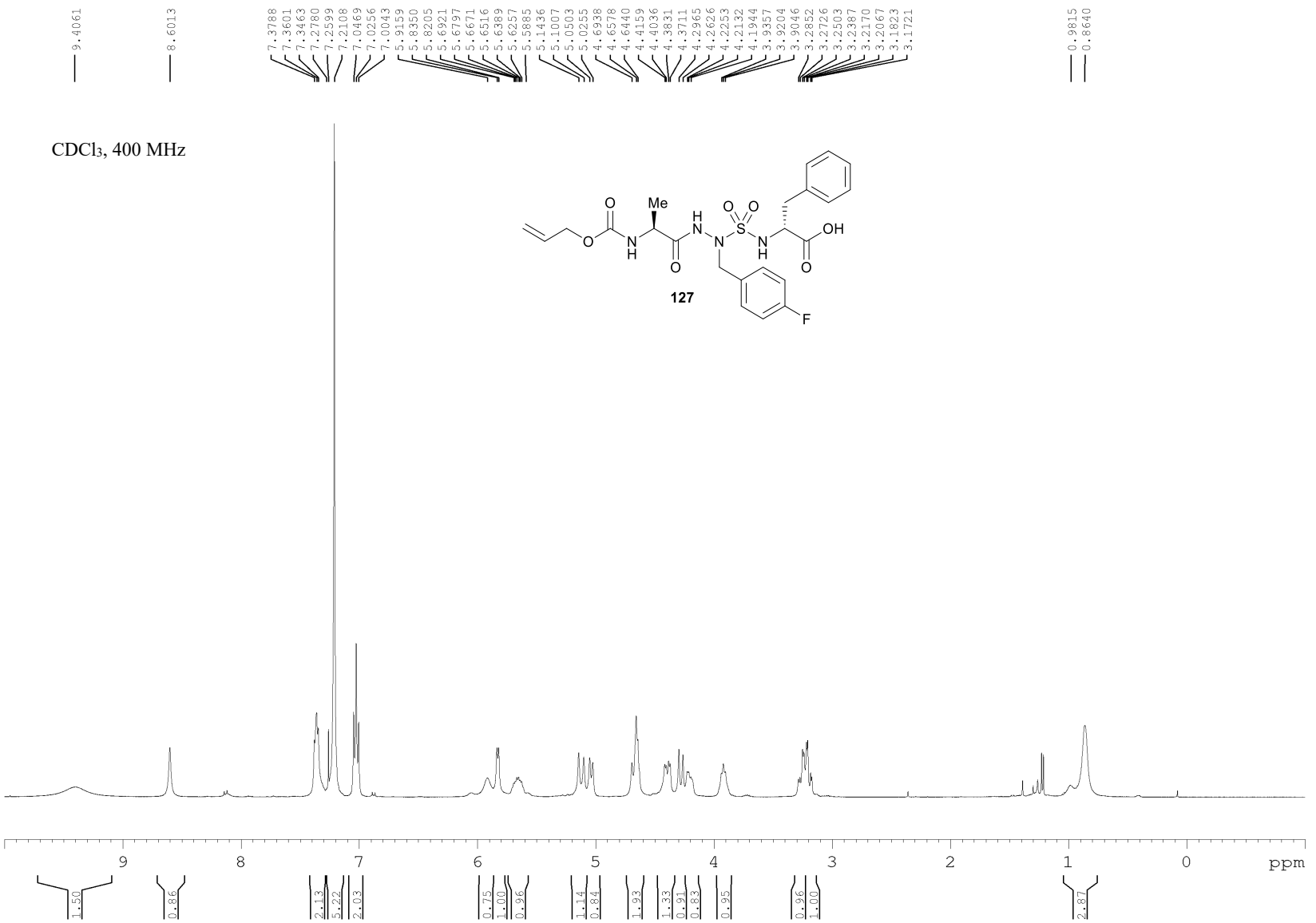
9.4061
8.6013
7.3788
7.3601
7.3463
7.2780
7.2599
7.2108
7.0469
7.0256
7.0043
5.9159
5.8350
5.8205
5.6921
5.6797
5.6671
5.6516
5.6389
5.6257
5.5885
5.1436
5.1007
5.0503
5.0255
4.6938
4.6578
4.6440
4.4159
4.4036
4.3831
4.3711
4.2965
4.2626
4.2253
4.2132
4.1944
3.9357
3.9204
3.9046
3.2852
3.2726
3.2503
3.2387
3.2170
3.2067
3.1823
3.1721
0.9815
0.8640
CDCl3, 400 MHz
Me
OH
F
127
9
8
7
6
5
4
3
2
1
0
ppm
1.50
0.86
2.13
5.22
2.03
0.75
1.00
0.96
1.14
0.84
1.93
1.33
0.91
0.83
0.95
0.96
1.00
2.87

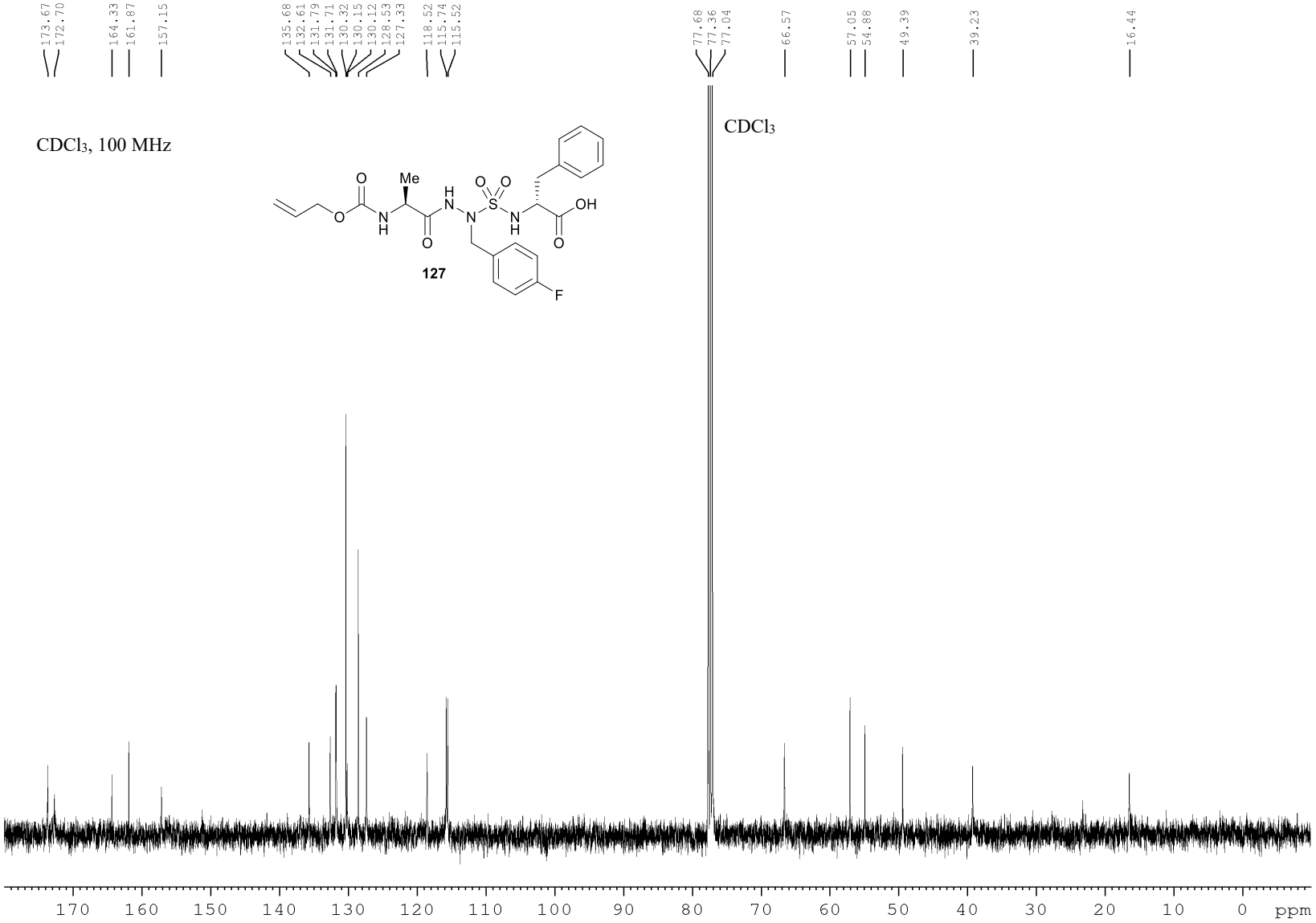
173.67
172.70
164.33
161.87
157.15
135.68
132.61
131.79
131.71
130.32
130.15
130.12
128.53
127.33
118.52
115.74
115.52
77.68
77.36
77.04
66.57
57.05
54.88
49.39
39.23
16.44
CDCl3, 100 MHz
CDCl3
127
170
160
150
140
130
120
110
100
90
80
70
60
50
40
30
20
10
0
ppm

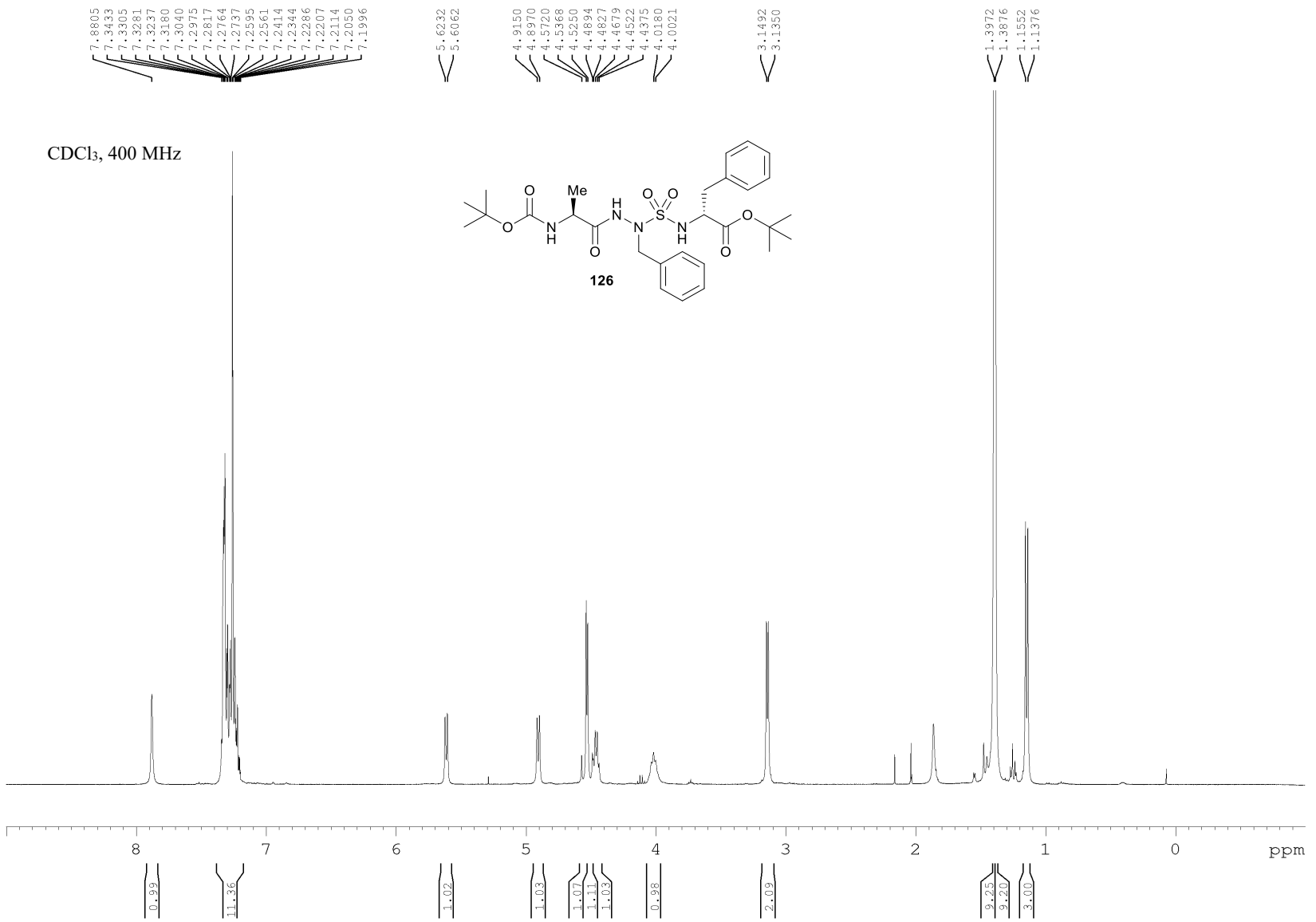
7.8805
7.3433
7.3305
7.3281
7.3237
7.3180
7.3040
7.2975
7.2817
7.2764
7.2737
7.2595
7.2561
7.2414
7.2344
7.2286
7.2207
7.2114
7.2050
7.1996
5.6232
5.6062
4.9150
4.8970
4.5720
4.5368
4.5250
4.4894
4.4827
4.4679
4.4522
4.4375
4.0180
4.0021
3.1492
3.1350
1.3972
1.3876
1.1552
1.1376
CDCl3, 400 MHz
126
8
7
6
5
4
3
2
1
0
ppm
0.99
11.36
1.02
1.03
1.07
1.11
1.03
0.98
2.09
9.25
3.20
3.00

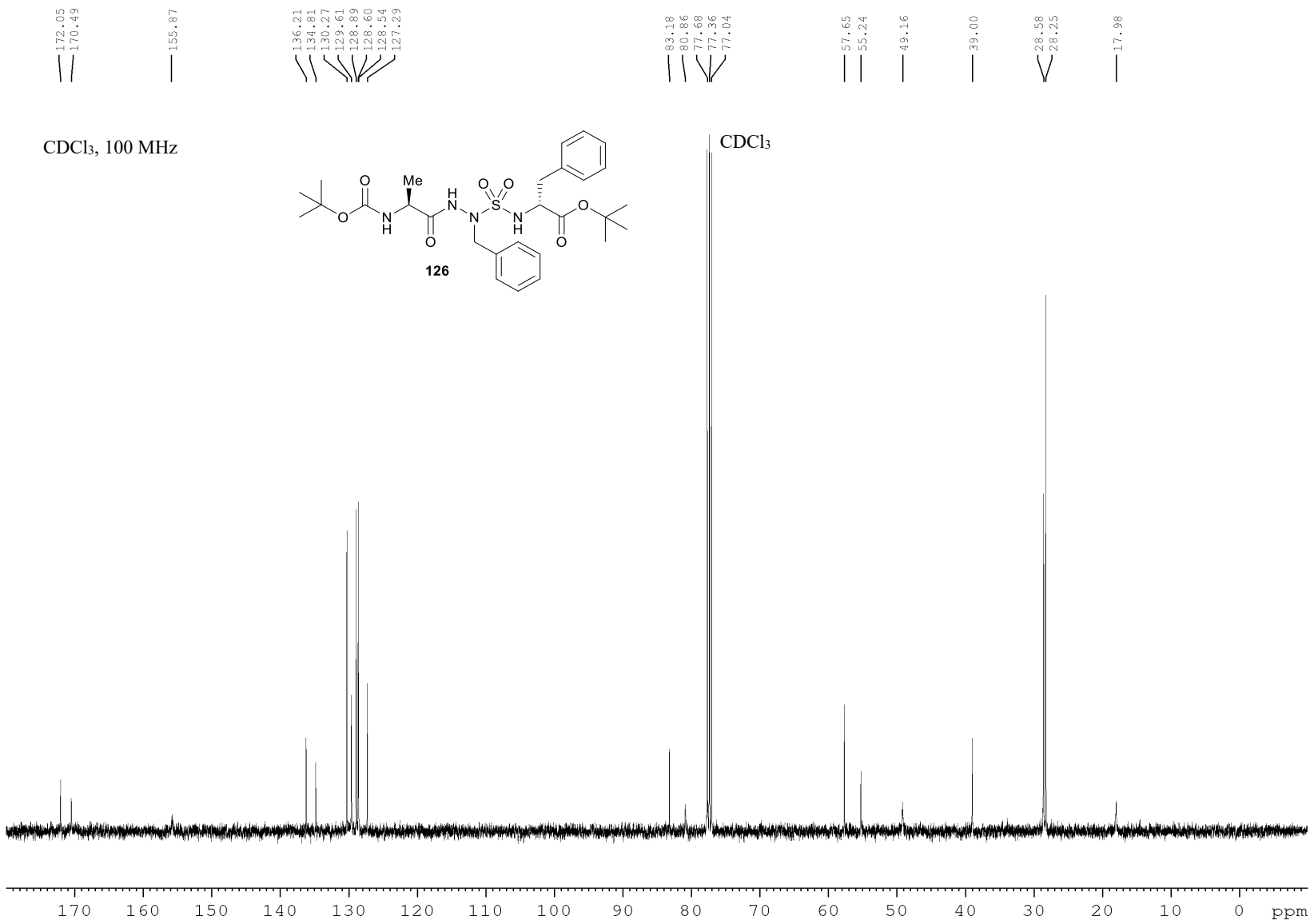
172.05
170.49
155.87
136.21
134.81
130.27
129.61
128.89
128.60
128.54
127.29
83.18
80.86
77.68
77.36
77.04
57.65
55.24
49.16
39.00
28.58
28.25
17.98
CDCl3, 100 MHz
CDCl3
Me
126
170
160
150
140
130
120
110
100
90
80
70
60
50
40
30
20
10
0
ppm

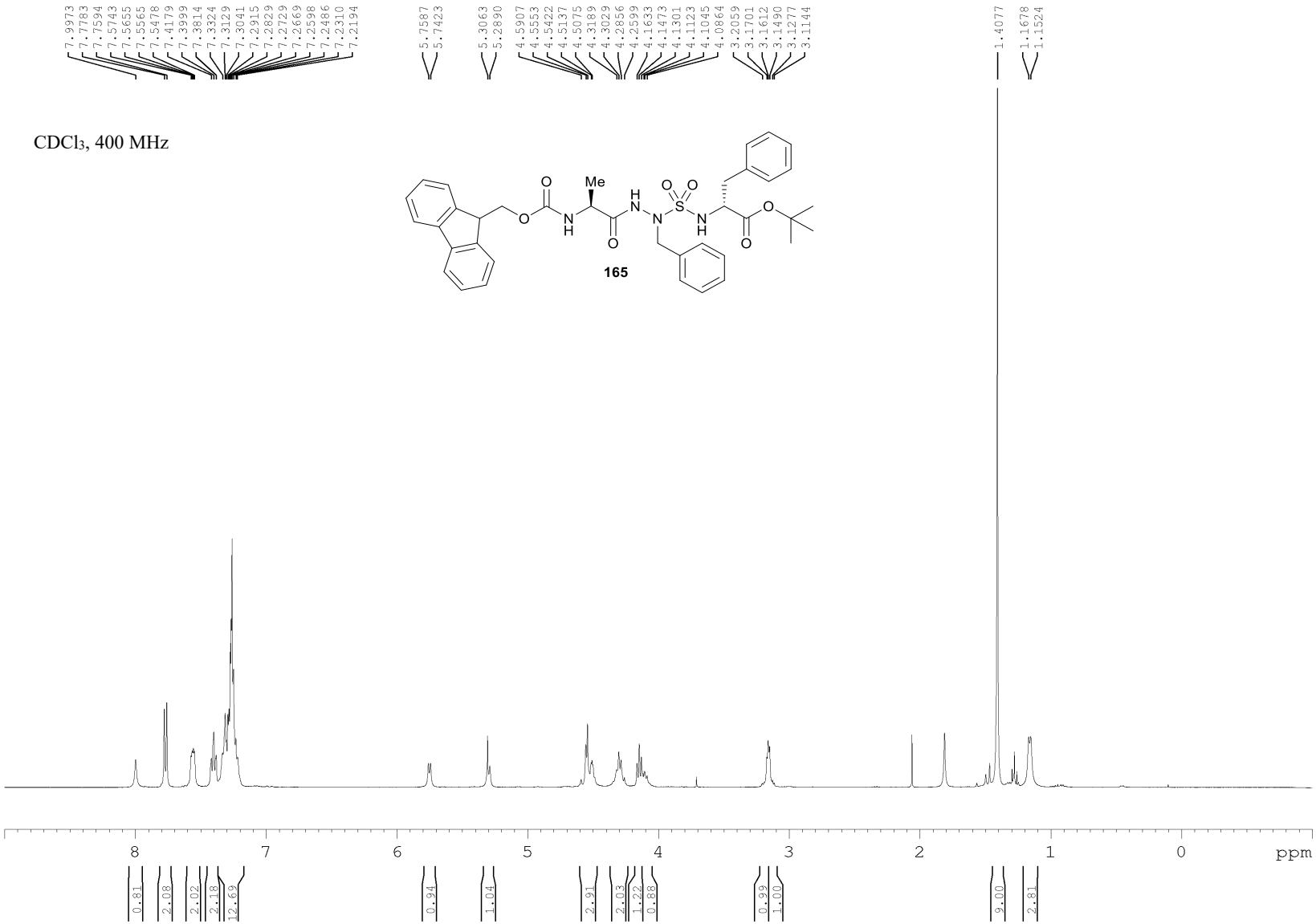
7.9973
7.7783
7.7594
7.5743
7.5655
7.5565
7.5478
7.4179
7.3999
7.3814
7.3324
7.3129
7.3041
7.2915
7.2829
7.2729
7.2669
7.2598
7.2486
7.2310
7.2194
5.7587
5.7423
5.3063
5.2890
4.5907
4.5553
4.5422
4.5137
4.5075
4.3189
4.3029
4.2856
4.2599
4.1633
4.1473
4.1301
4.1123
4.1045
4.0864
3.2059
3.1701
3.1612
3.1490
3.1277
3.1144
1.4077
1.1678
1.1524
CDCl3, 400 MHz
Me
H
N
O
S
165
8
7
6
5
4
3
2
1
0
ppm
0.81
2.08
2.02
2.18
12.69
0.94
1.04
2.91
2.03
1.22
0.88
0.99
1.00
9.00
2.81

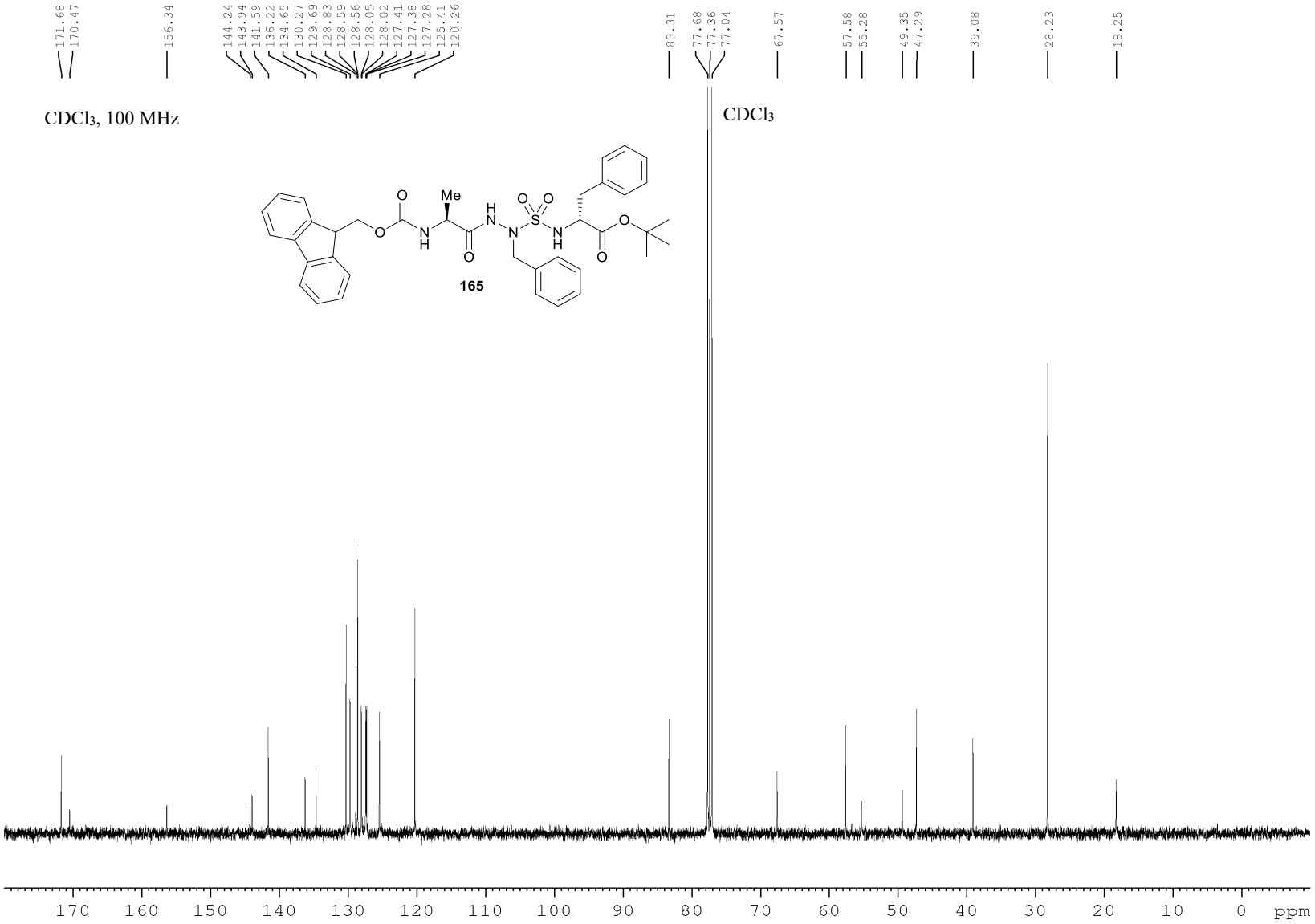
171.68
170.47
156.34
144.24
143.94
141.59
136.22
134.65
130.27
129.69
128.83
128.59
128.56
128.05
128.02
127.41
127.38
127.28
125.41
120.26
83.31
77.68
77.36
77.04
67.57
57.58
55.28
49.35
47.29
39.08
28.23
18.25
CDCl3, 100 MHz
CDCl3
Me
165
170
160
150
140
130
120
110
100
90
80
70
60
50
40
30
20
10
0
ppm

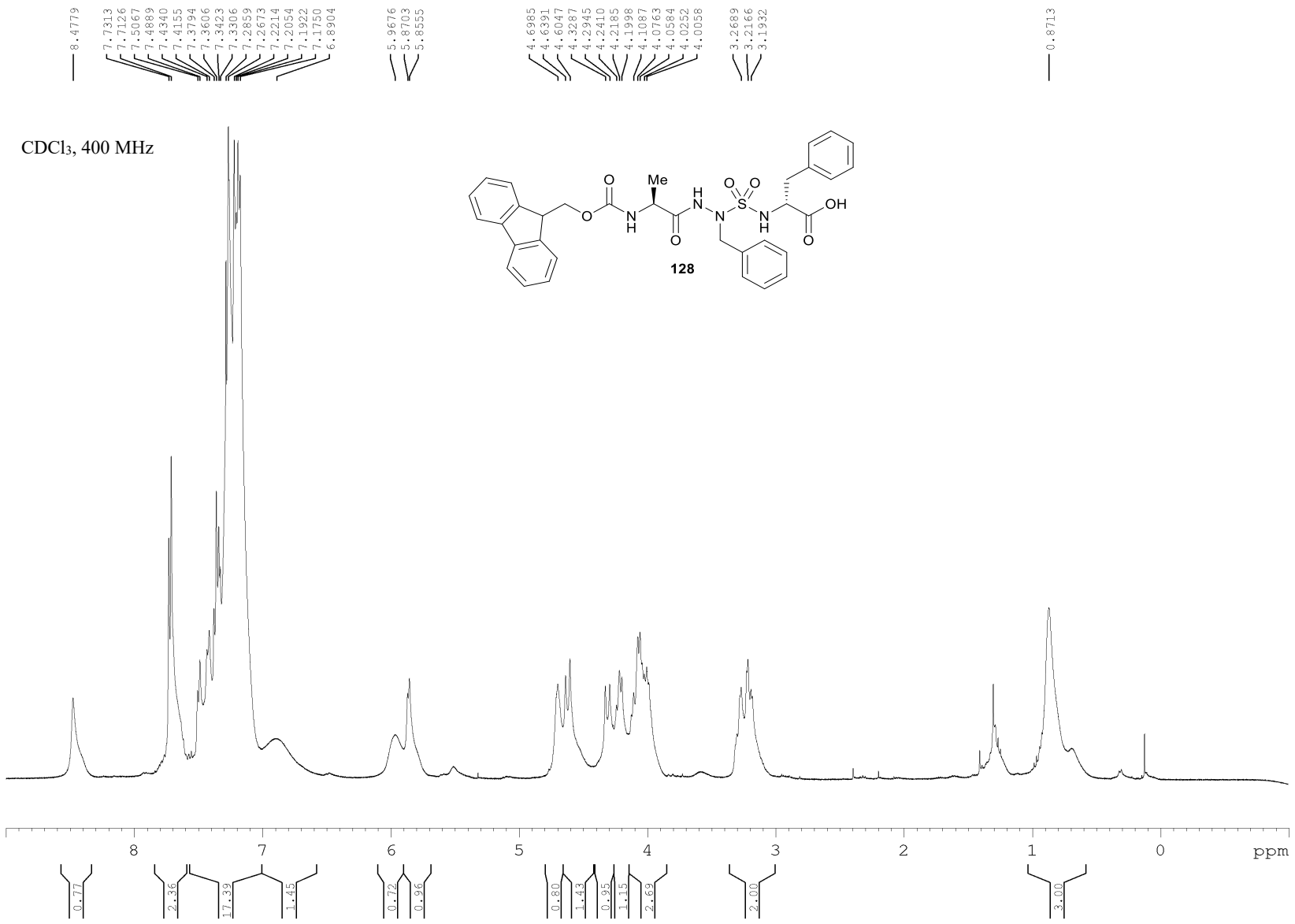
8.4779
7.7313
7.7126
7.5067
7.4889
7.4340
7.4155
7.3794
7.3606
7.3423
7.3306
7.2859
7.2673
7.2214
7.2054
7.1922
7.1750
6.8904
5.9676
5.8703
5.8555
4.6985
4.6391
4.6047
4.3287
4.2945
4.2410
4.2185
4.1998
4.1087
4.0763
4.0584
4.0252
4.0058
3.2689
3.2166
3.1932
0.8713
CDCl3, 400 MHz
Me
OH
128
8
7
6
5
4
3
2
1
0
ppm
0.77
2.36
17.39
1.45
0.72
0.96
0.80
1.43
0.95
1.15
2.69
2.00
3.00

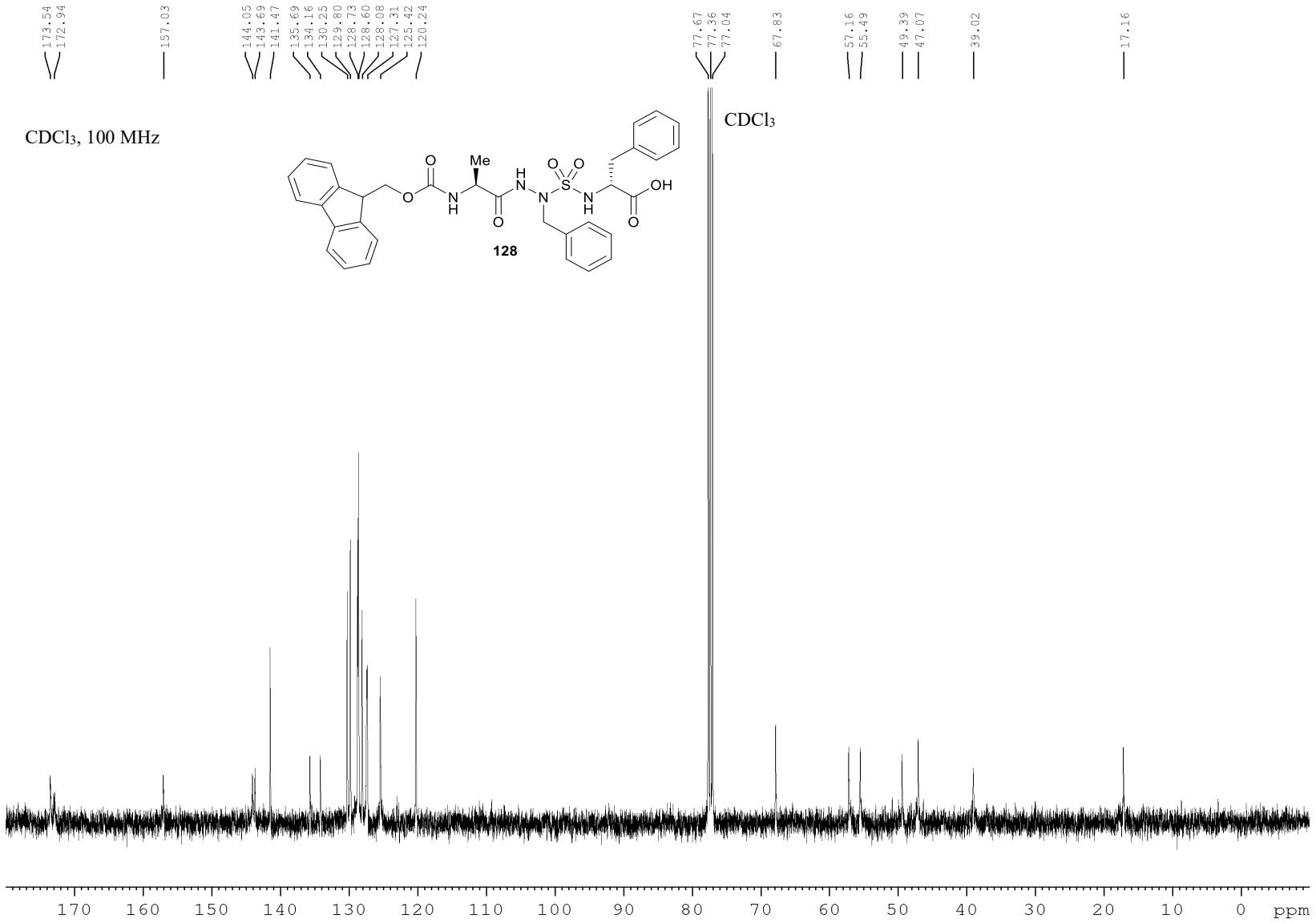
173.54
172.94
157.03
144.05
143.69
141.47
135.69
134.16
130.25
129.80
128.73
128.60
128.08
127.31
125.42
120.24
77.67
77.36
77.04
67.83
57.16
55.49
49.39
47.07
39.02
17.16
CDCl3, 100 MHz
CDCl3
Me
OH
128
170
160
150
140
130
120
110
100
90
80
70
60
50
40
30
20
10
0
ppm

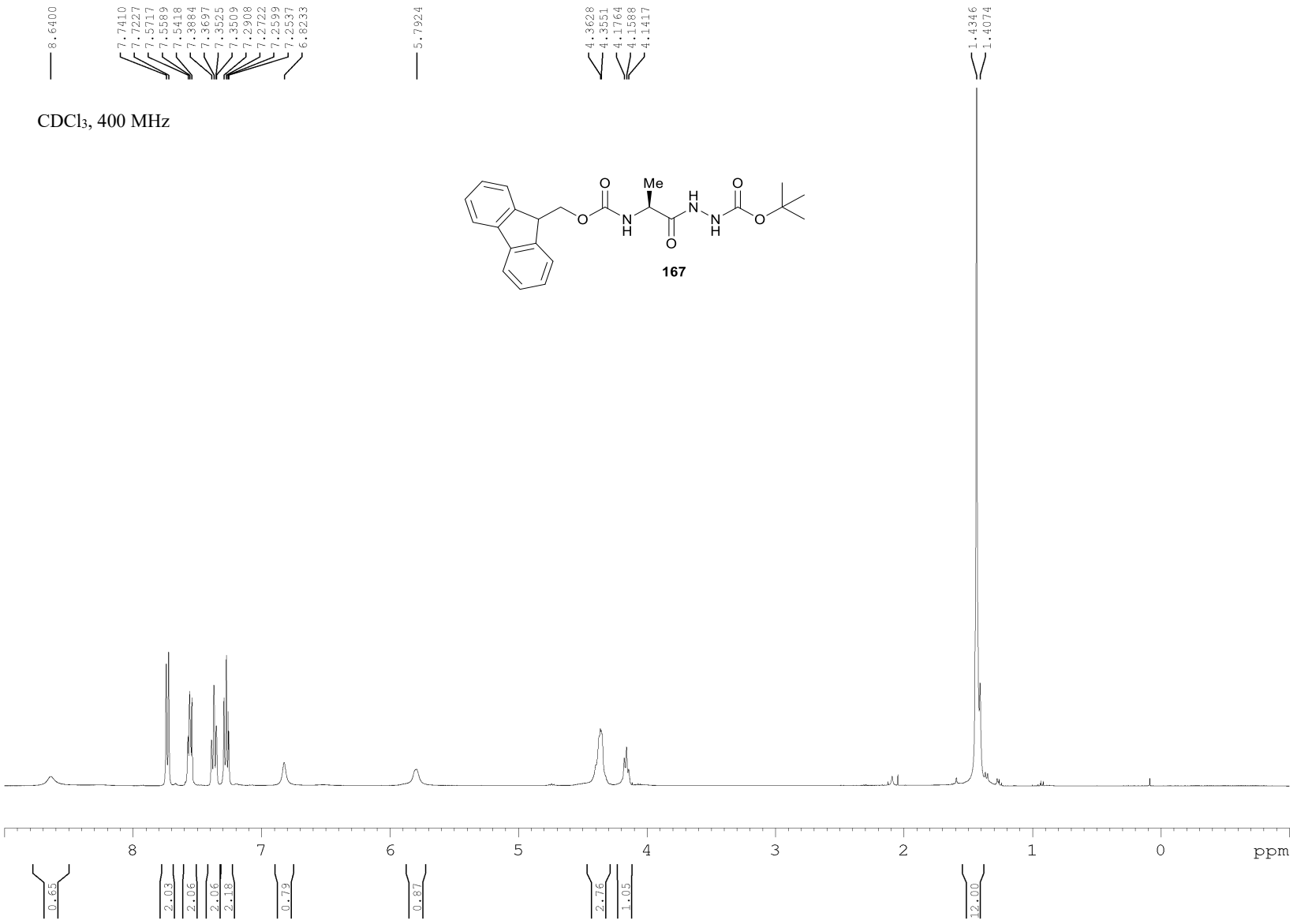
8.6400
7.7410
7.7227
7.5717
7.5589
7.5418
7.3884
7.3697
7.3525
7.3509
7.2908
7.2722
7.2599
7.2537
6.8233
5.7924
4.3628
4.3551
4.1764
4.1588
4.1417
1.4346
1.4074
CDCl3, 400 MHz
Me
O
N
H
H
N
N
H
O
O
O
O
167
8
7
6
5
4
3
2
1
0
ppm
0.65
2.03
2.06
2.06
2.18
0.79
0.87
2.76
1.05
12.00

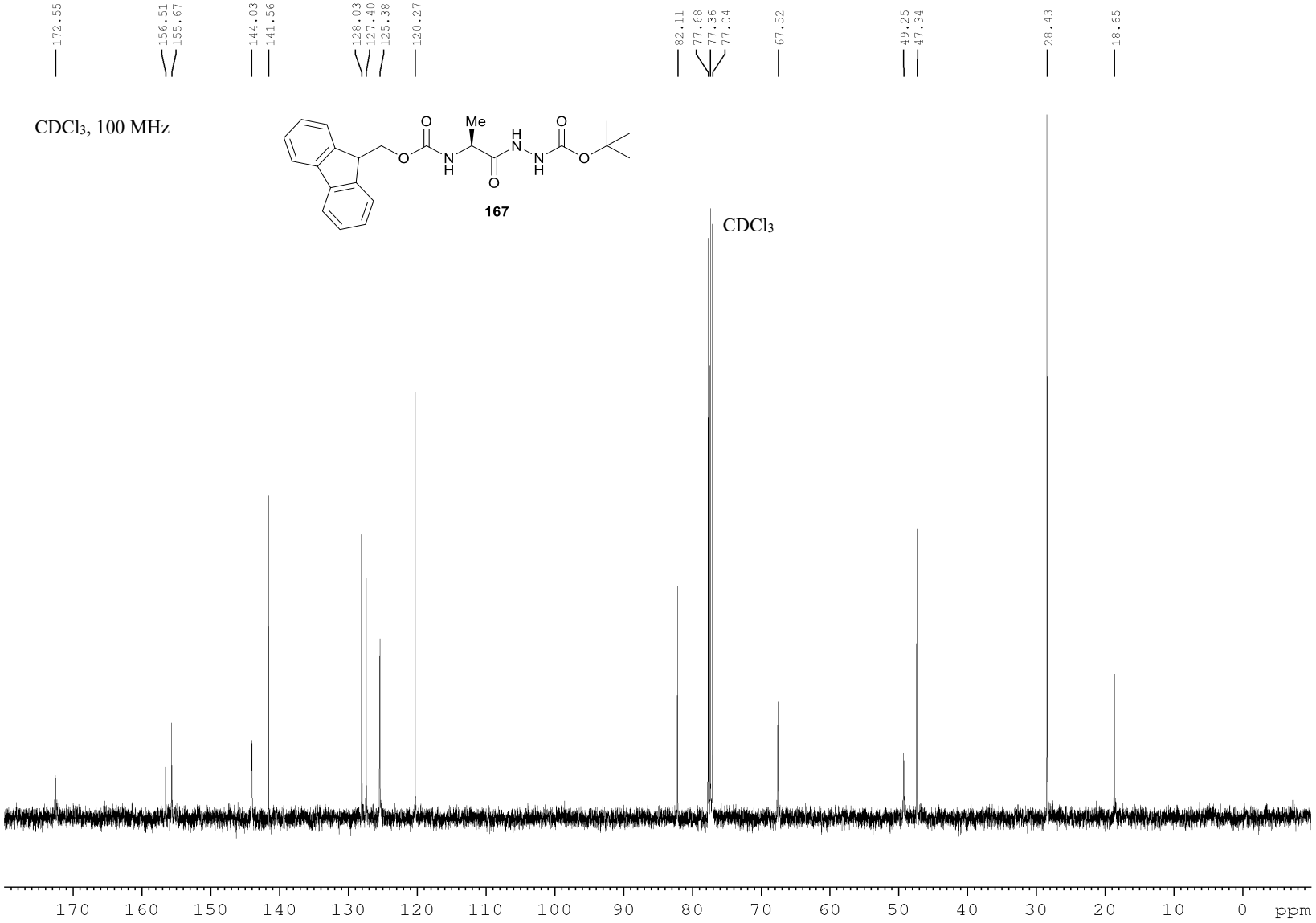
172.55
156.51
155.67
144.03
141.56
128.03
127.40
125.38
120.27
82.11
77.68
77.36
77.04
67.52
49.25
47.34
28.43
18.65
CDCl3, 100 MHz
Me
O
N
H
N
H
O
O
O
O
167
CDCl3
170
160
150
140
130
120
110
100
90
80
70
60
50
40
30
20
10
0
ppm

9.1120

7.9345
7.9158
7.7909
7.7740
7.7573
7.5491
7.5296
7.4726
7.4546
7.4366
7.4046
7.3893
7.3707
7.3600
7.3521

4.3014
4.2971
4.2820
4.2601
4.2461
4.2397
4.0916
4.0738
4.0554
4.0369
4.0188

3.3866

2.5489
2.5445
2.5399
2.5354
2.5310

1.2553
1.2375

DMSO-d_6, 400 MHz

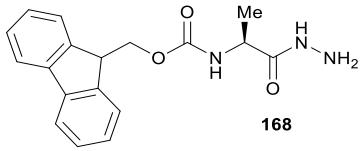

168

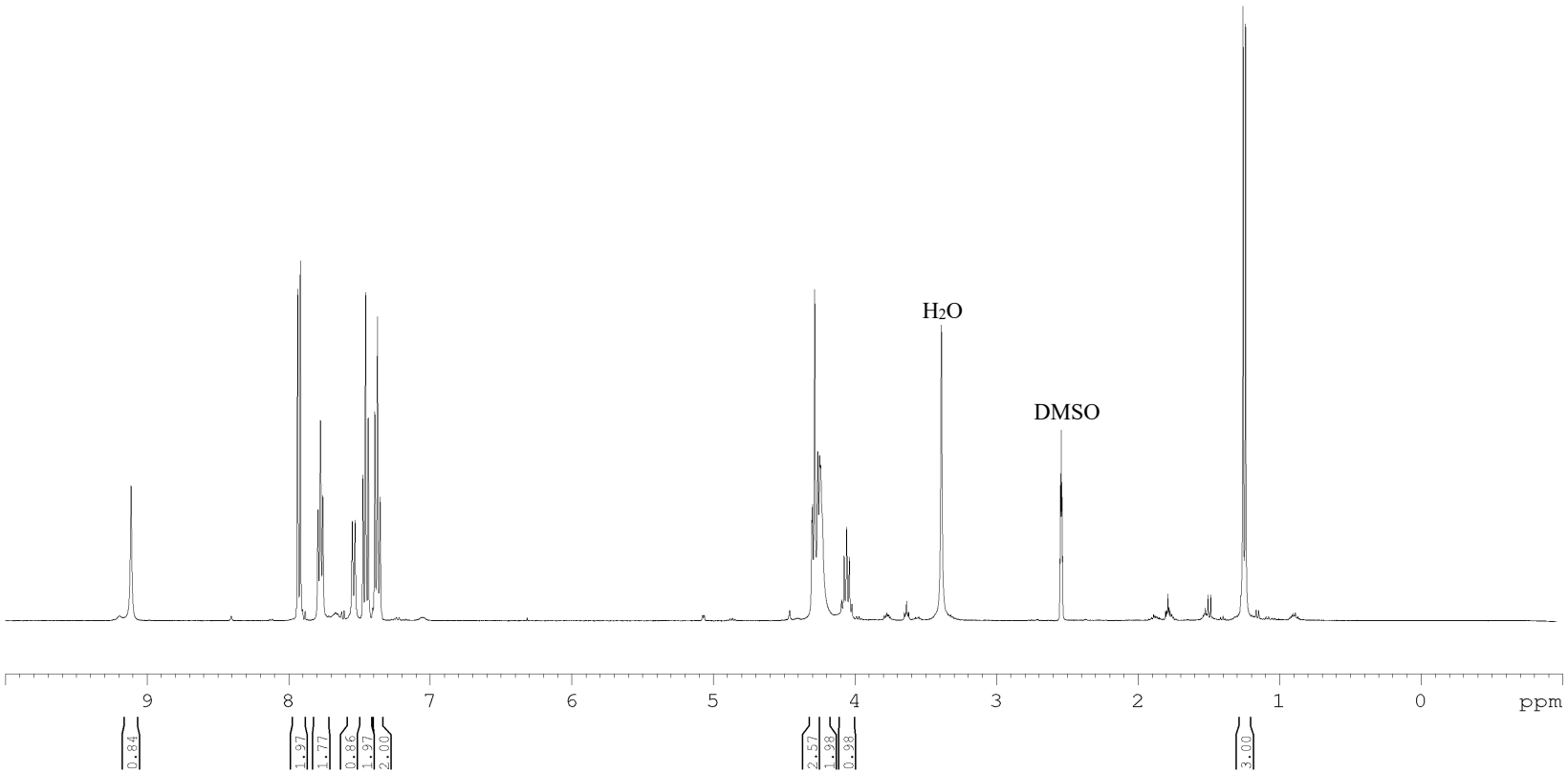

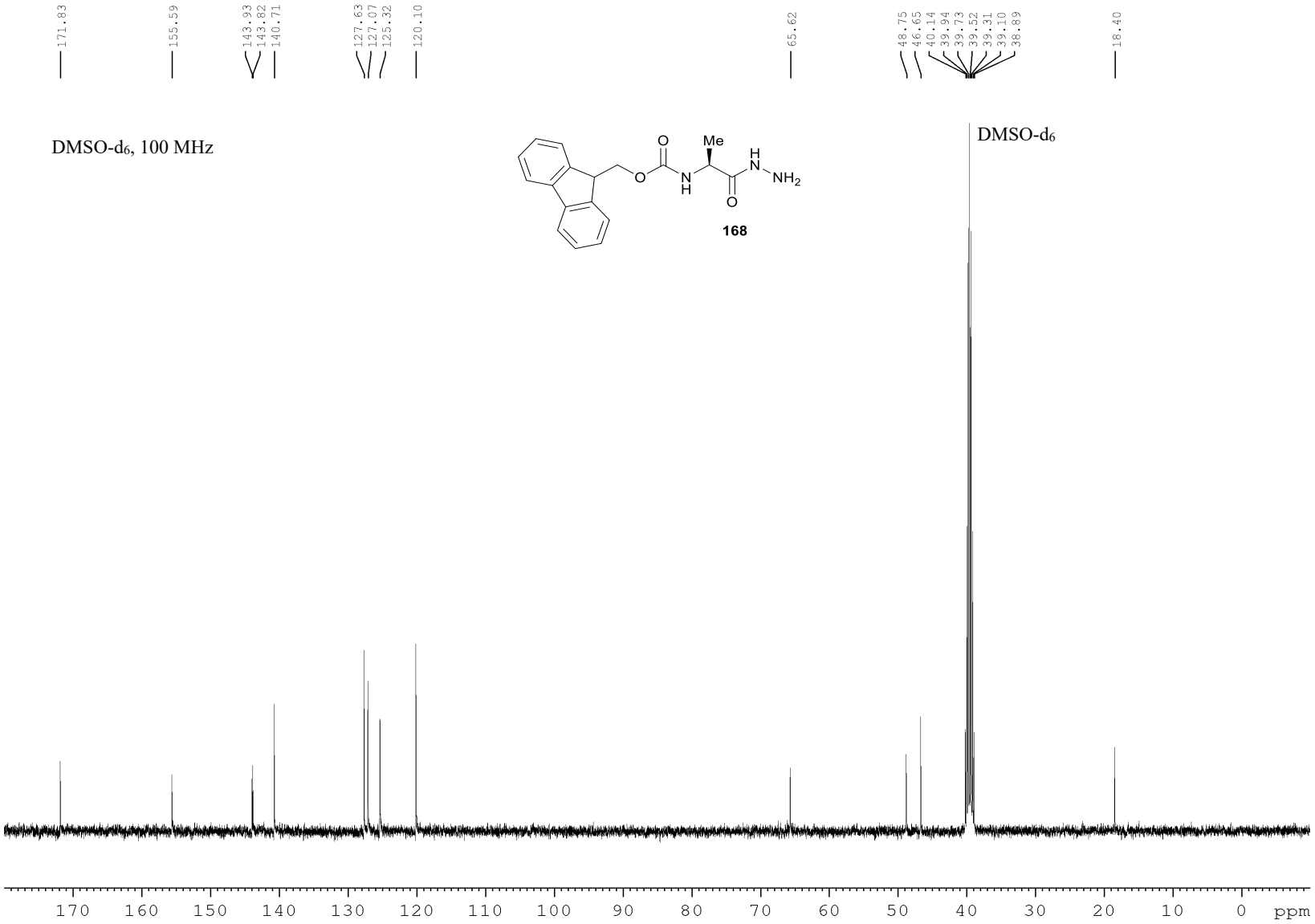
171.83
155.59
143.93
143.82
140.71
127.63
127.07
125.32
120.10
65.62
48.75
46.65
40.14
39.94
39.73
39.52
39.31
39.10
38.89
18.40
DMSO-d6, 100 MHz
DMSO-d6
O
Me
H
N
O
N
H
N
NH2
O
168
170
160
150
140
130
120
110
100
90
80
70
60
50
40
30
20
10
0
ppm

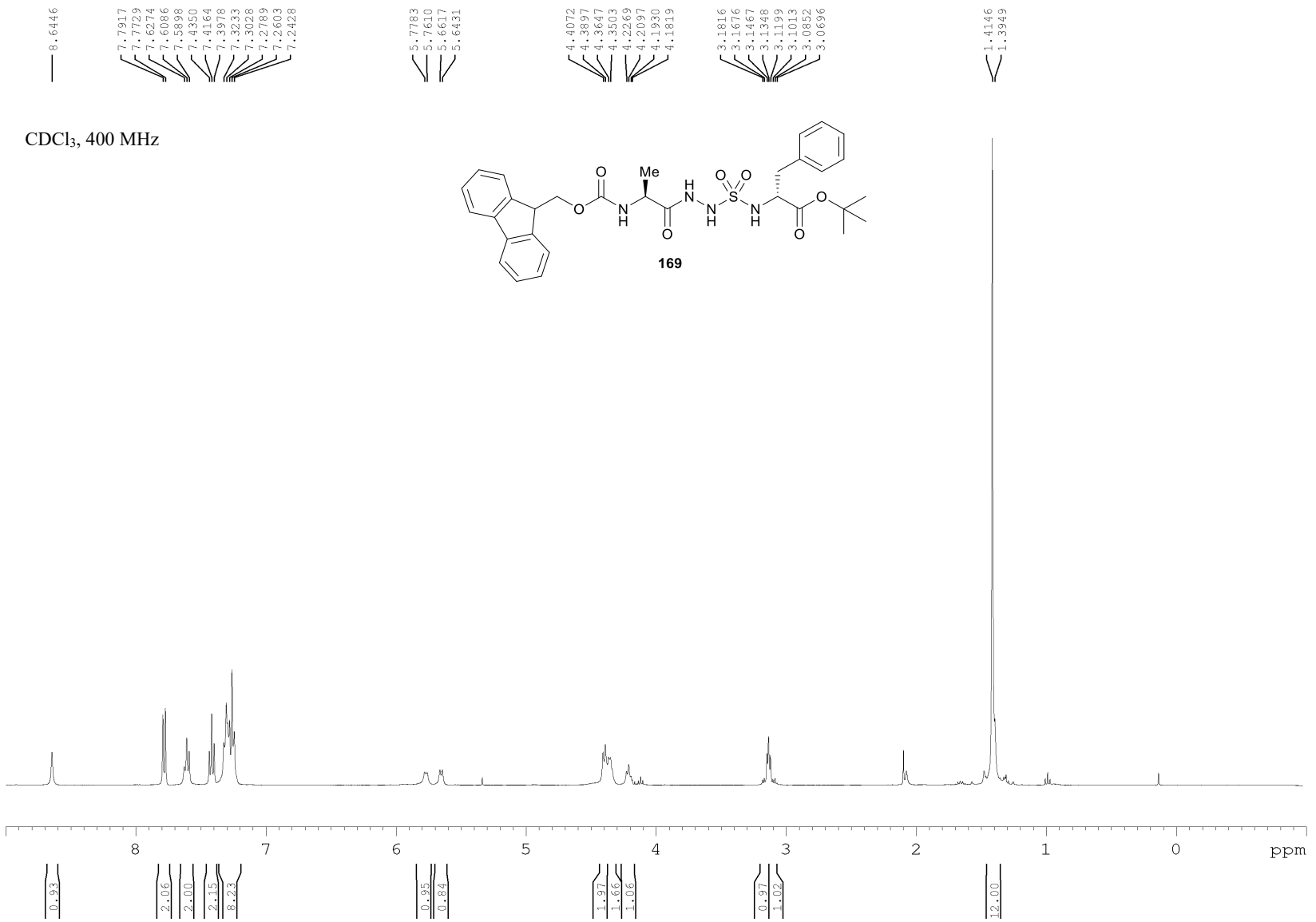
8.6446
7.7917
7.7729
7.6274
7.6086
7.5898
7.4350
7.4164
7.3978
7.3233
7.3028
7.2789
7.2603
7.2428
5.7783
5.7610
5.6617
5.6431
4.4072
4.3897
4.3647
4.3503
4.2269
4.2097
4.1930
4.1819
3.1816
3.1676
3.1467
3.1348
3.1199
3.1013
3.0852
3.0696
1.4146
1.3949
CDCl3, 400 MHz
169
8
7
6
5
4
3
2
1
0
ppm
0.93
2.06
2.00
2.15
8.23
0.95
0.84
1.97
1.66
1.06
0.97
1.02
12.00

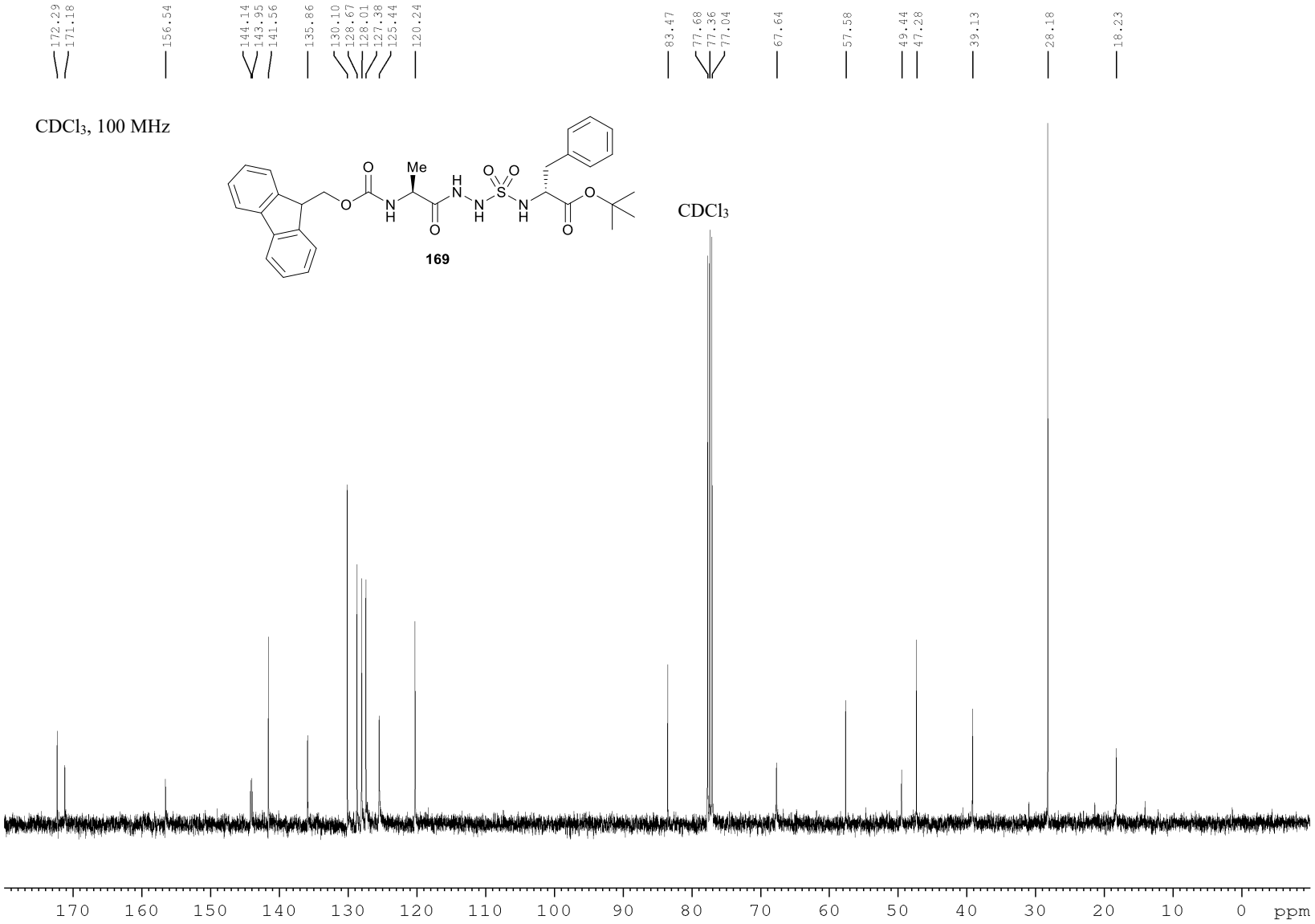
172.29
171.18
156.54
144.14
143.95
141.56
135.86
130.10
128.67
128.01
127.38
125.44
120.24
83.47
77.68
77.36
77.04
67.64
57.58
49.44
47.28
39.13
28.18
18.23
CDCl3, 100 MHz
CDCl3
169
170
160
150
140
130
120
110
100
90
80
70
60
50
40
30
20
10
0
ppm

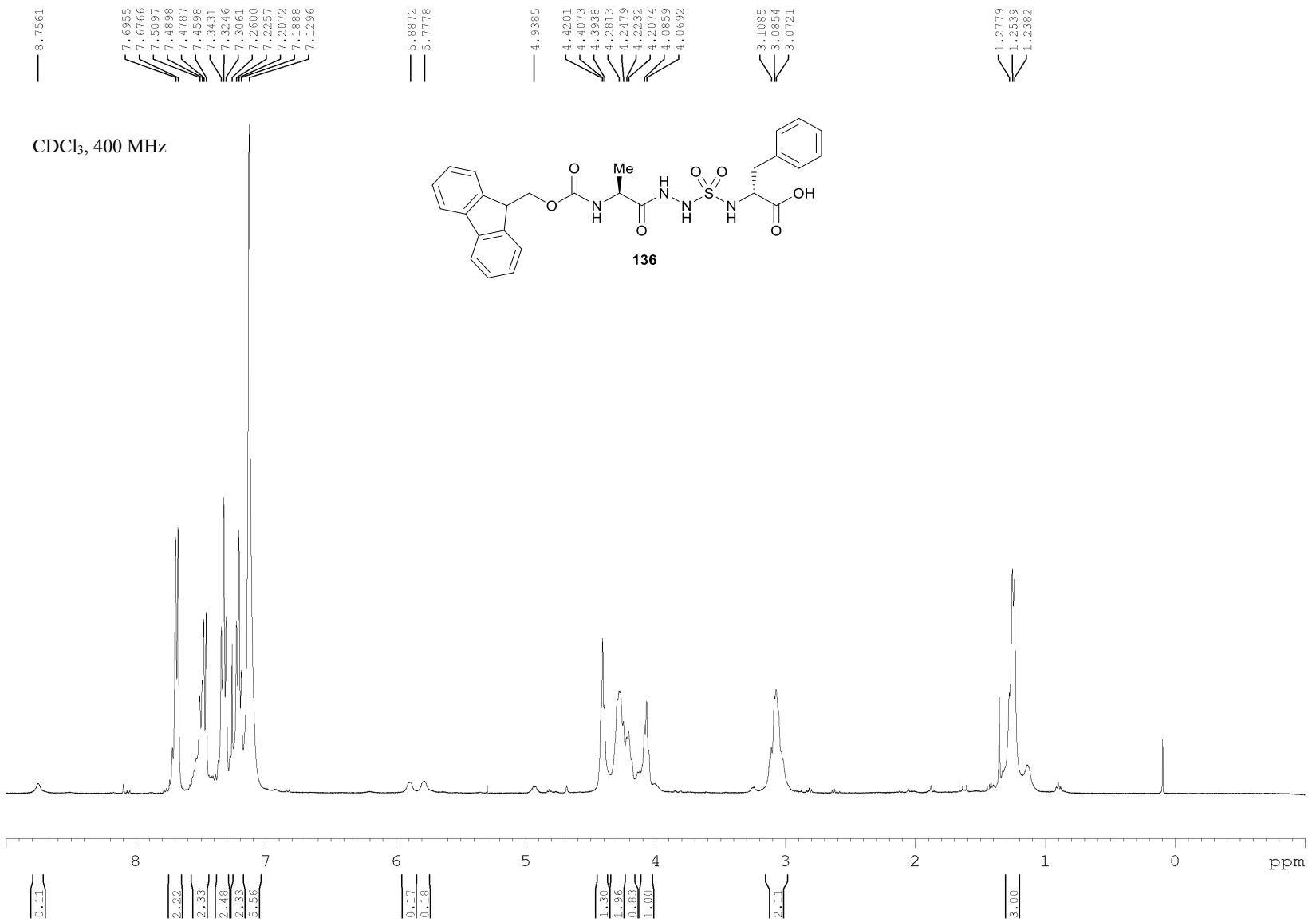
8.7561
7.6955
7.6766
7.5097
7.4898
7.4787
7.4598
7.3431
7.3246
7.3061
7.2600
7.2257
7.2072
7.1888
7.1296
5.8872
5.7778
4.9385
4.4201
4.4073
4.3938
4.2813
4.2479
4.2232
4.2074
4.0859
4.0692
3.1085
3.0854
3.0721
1.2779
1.2539
1.2382
CDCl3, 400 MHz
136
8
7
6
5
4
3
2
1
0
ppm
0.11
2.22
2.33
2.48
2.33
5.56
0.17
0.18
1.30
1.96
0.83
1.00
2.11
3.00

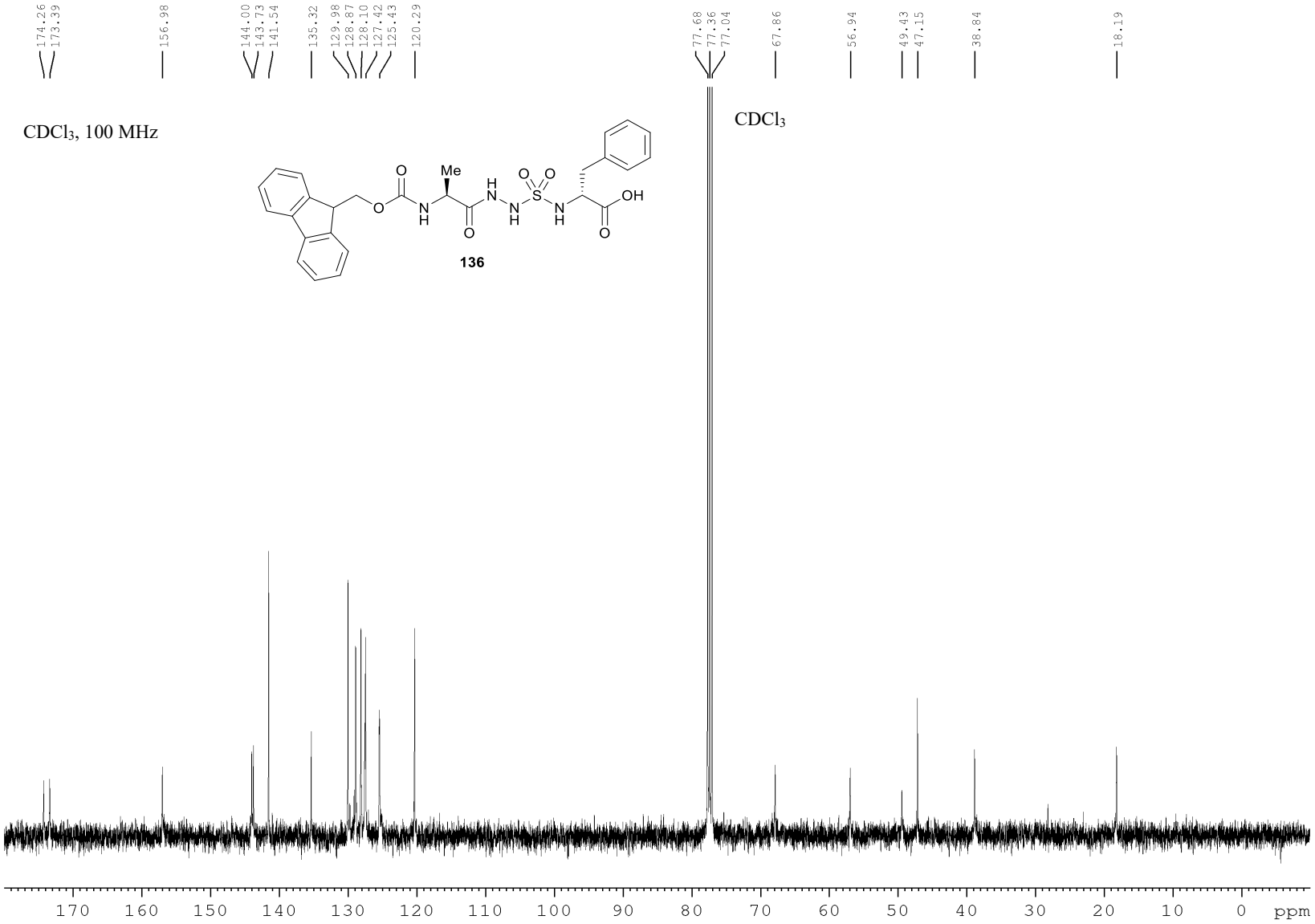
174.26
173.39
156.98
144.00
143.73
141.54
135.32
129.98
128.87
128.10
127.42
125.43
120.29
77.68
77.36
77.04
67.86
56.94
49.43
47.15
38.84
18.19
CDCl3, 100 MHz
CDCl3
Me
OH
136
170
160
150
140
130
120
110
100
90
80
70
60
50
40
30
20
10
0
ppm

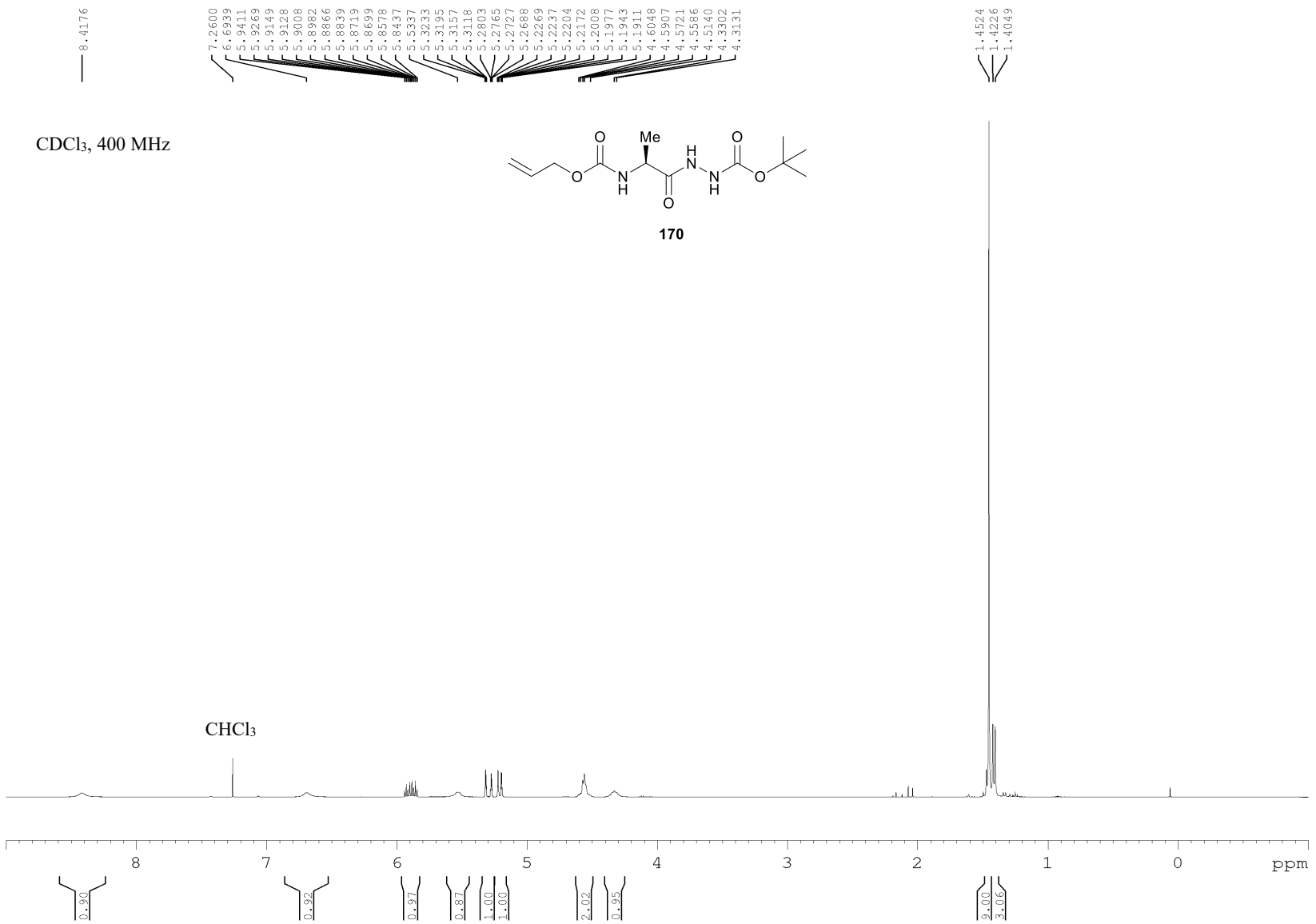
8.4176
7.2600
6.6939
5.9411
5.9269
5.9149
5.9128
5.9008
5.8982
5.8866
5.8839
5.8719
5.8699
5.8578
5.8437
5.5337
5.3233
5.3195
5.3157
5.3118
5.2803
5.2765
5.2727
5.2688
5.2269
5.2237
5.2204
5.2172
5.2008
5.1977
5.1943
5.1911
4.6048
4.5907
4.5721
4.5586
4.5140
4.3302
4.3131
1.4524
1.4226
1.4049
CDCl3, 400 MHz
CHCl3
ppm
0.90
0.92
0.97
0.87
1.00
1.00
2.02
0.95
9.00
3.06

170

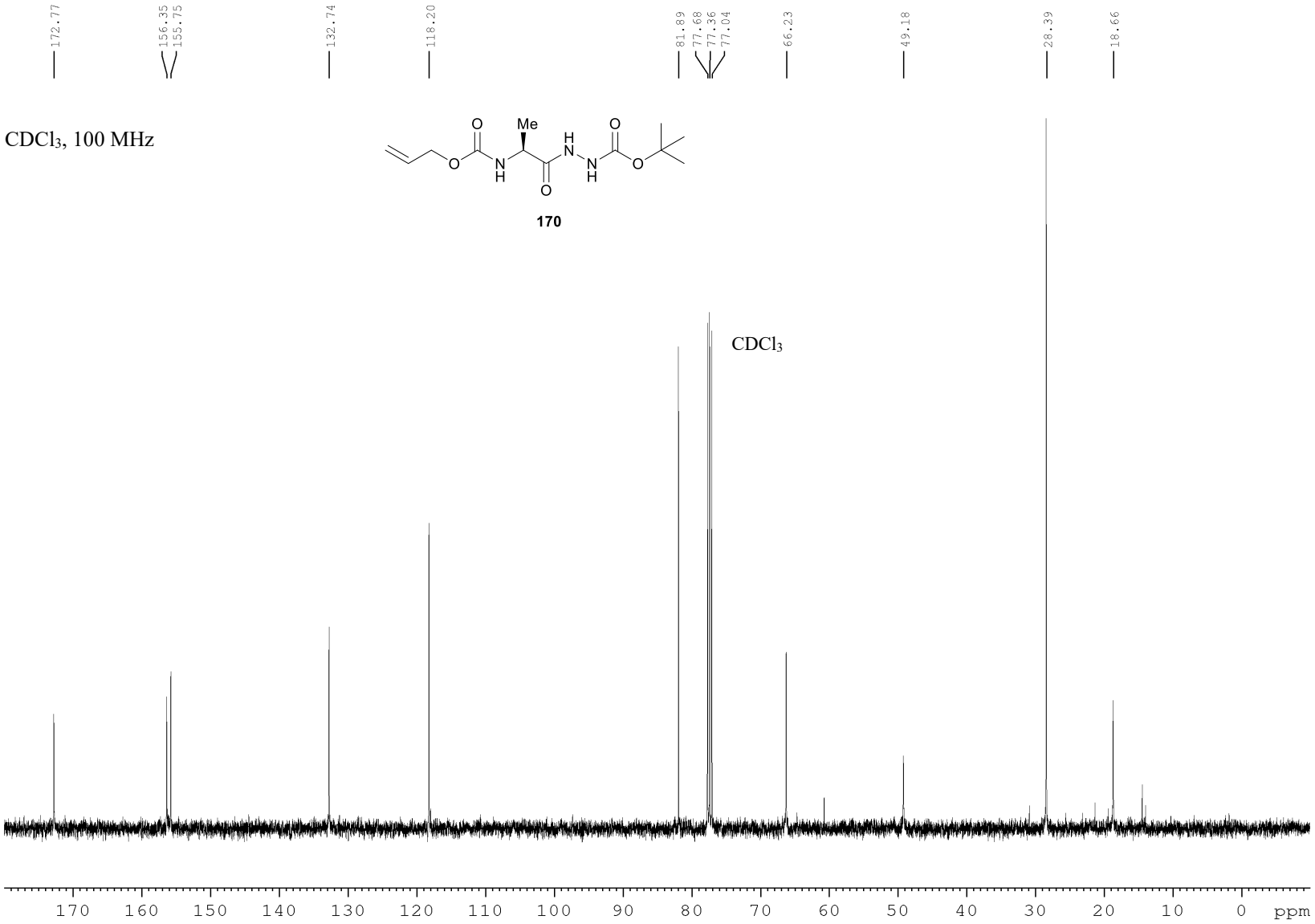
172.77
156.35
155.75
132.74
118.20
81.89
77.68
77.36
77.04
66.23
49.18
28.39
18.66
CDCl3, 100 MHz
Me
O
N
H
O
O
O
N
H
O
170
CDCl3
170 160 150 140 130 120 110 100 90 80 70 60 50 40 30 20 10 0 ppm

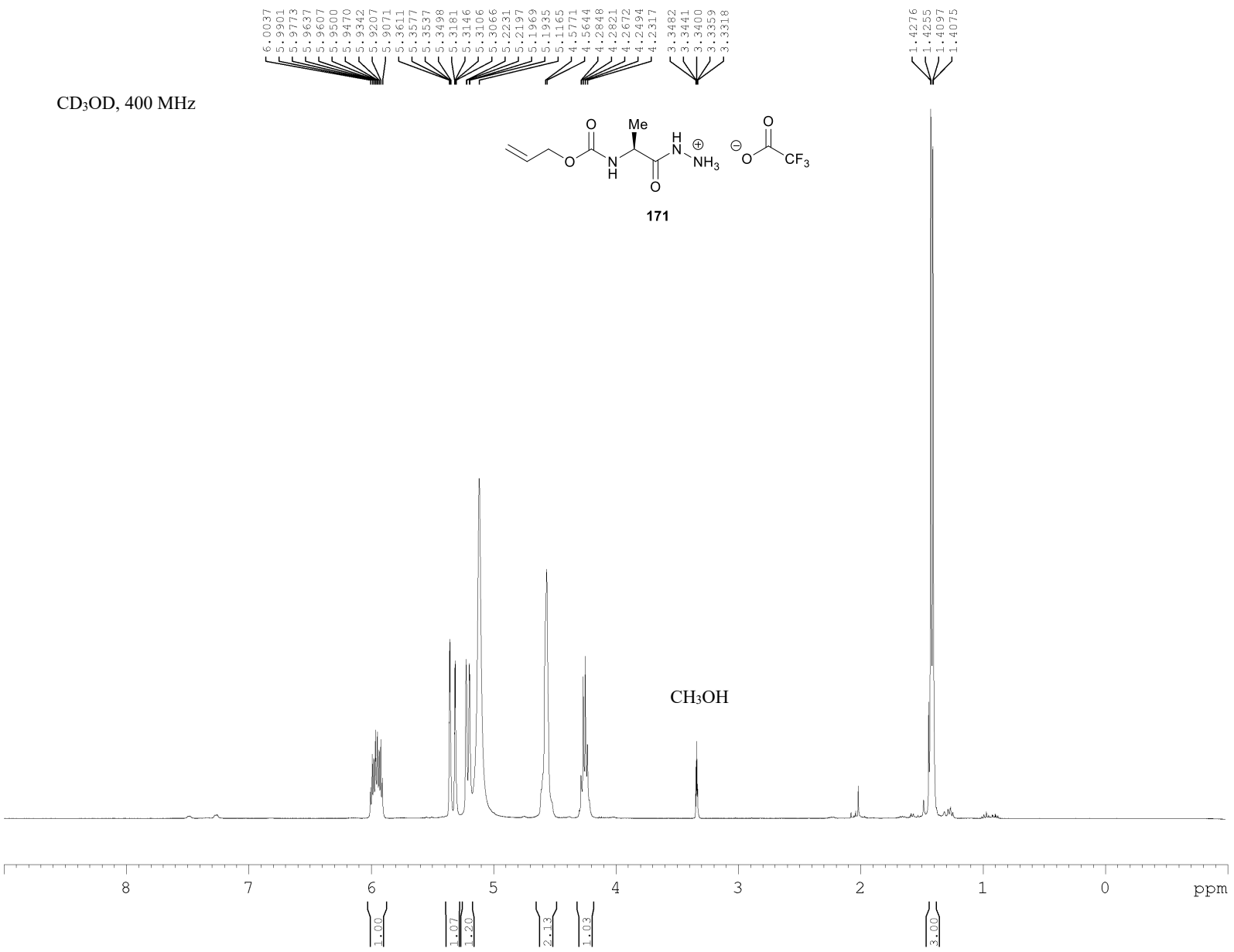
6.0037
5.9901
5.9773
5.9637
5.9607
5.9500
5.9470
5.9342
5.9207
5.9071
5.3611
5.3577
5.3537
5.3498
5.3181
5.3146
5.3106
5.3066
5.2231
5.2197
5.1969
5.1935
5.1165
4.5771
4.5644
4.2848
4.2821
4.2672
4.2494
4.2317
3.3482
3.3441
3.3400
3.3359
3.3318
1.4276
1.4255
1.4097
1.4075
CD3OD, 400 MHz
Me
H
N
NH3
O
N
H
O
O
O
CF3
171
CH3OH
8
7
6
5
4
3
2
1
0
ppm
1.00
1.07
1.20
2.13
1.03
3.00

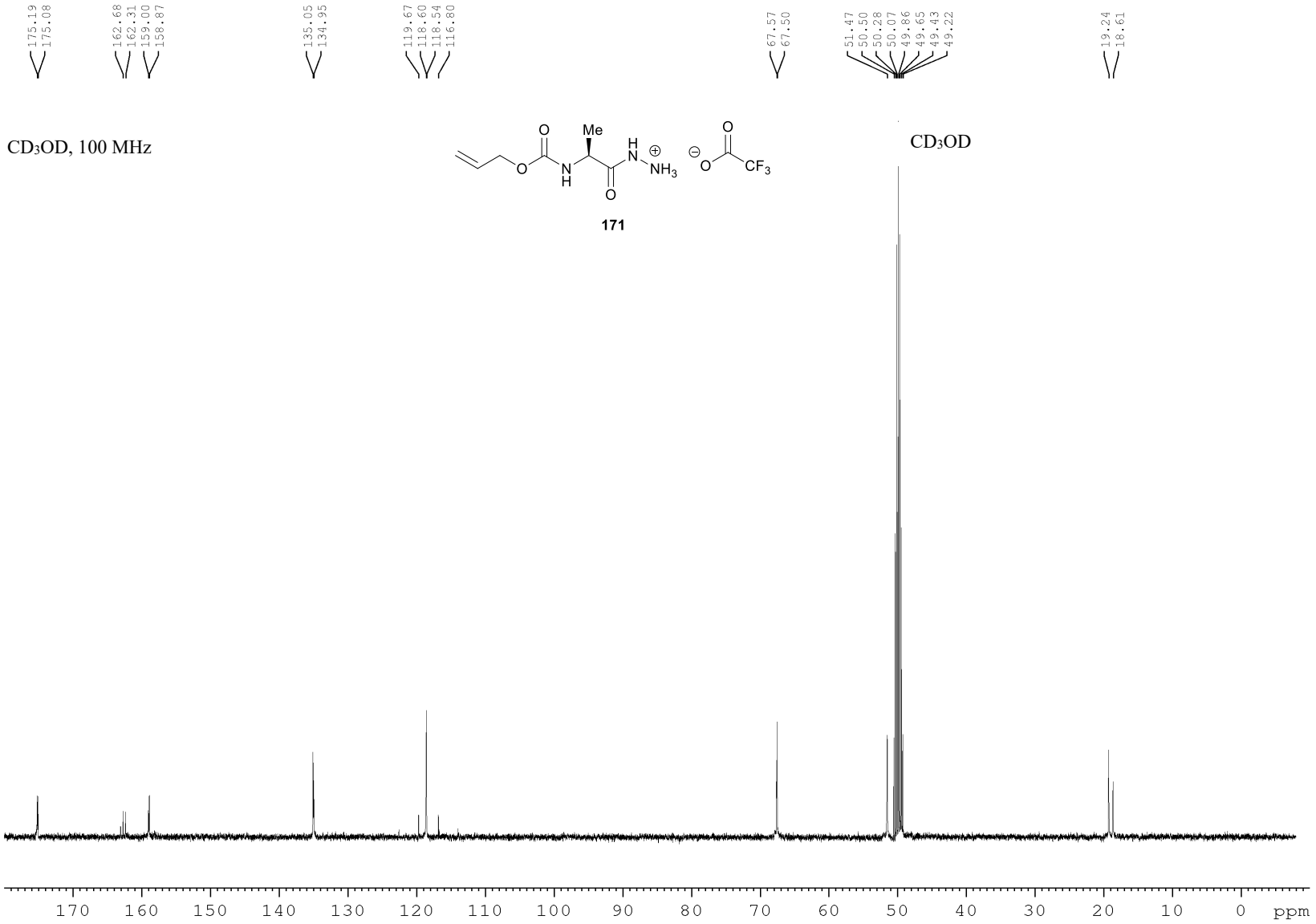
175.19
175.08
162.68
162.31
159.00
158.87
135.05
134.95
119.67
118.60
118.54
116.80
67.57
67.50
51.47
50.50
50.28
50.07
49.86
49.65
49.43
49.22
19.24
18.61
CD3OD, 100 MHz
CD3OD
Me
NH3
CF3
171
170
160
150
140
130
120
110
100
90
80
70
60
50
40
30
20
10
0
ppm

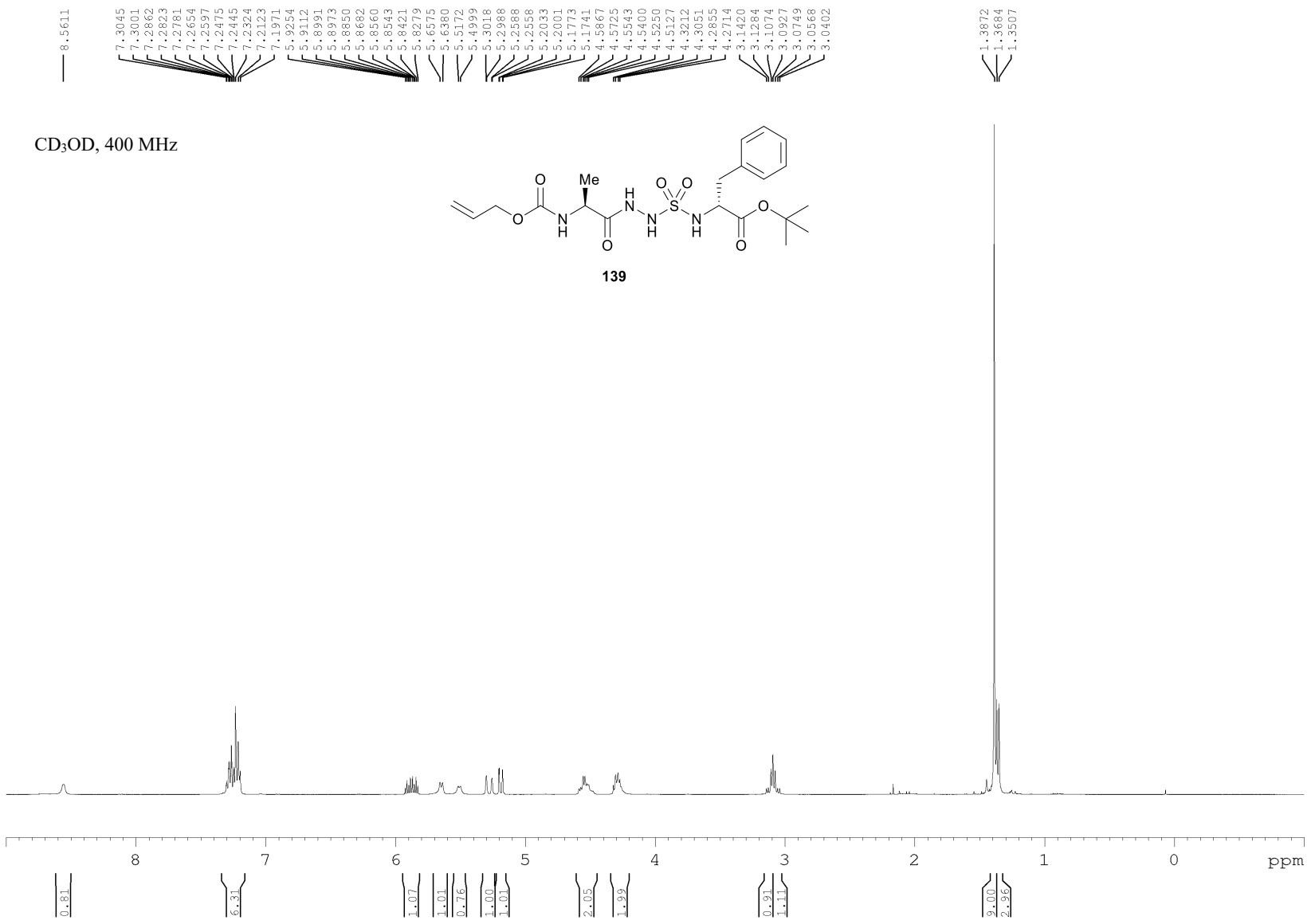
8.5611
7.3045
7.3001
7.2862
7.2823
7.2781
7.2654
7.2597
7.2475
7.2445
7.2324
7.2123
7.1971
5.9254
5.9112
5.8991
5.8973
5.8850
5.8682
5.8560
5.8543
5.8421
5.8279
5.6575
5.6380
5.5172
5.4999
5.3018
5.2988
5.2588
5.2558
5.2033
5.2001
5.1773
5.1741
4.5867
4.5725
4.5543
4.5400
4.5250
4.5127
4.3212
4.3051
4.2855
4.2714
3.1420
3.1284
3.1074
3.0927
3.0749
3.0568
3.0402
1.3872
1.3684
1.3507
CD3OD, 400 MHz
Me
139
8
7
6
5
4
3
2
1
0
ppm
0.81
6.31
1.07
1.01
0.76
1.00
1.01
2.05
1.99
0.91
1.11
9.00
2.96

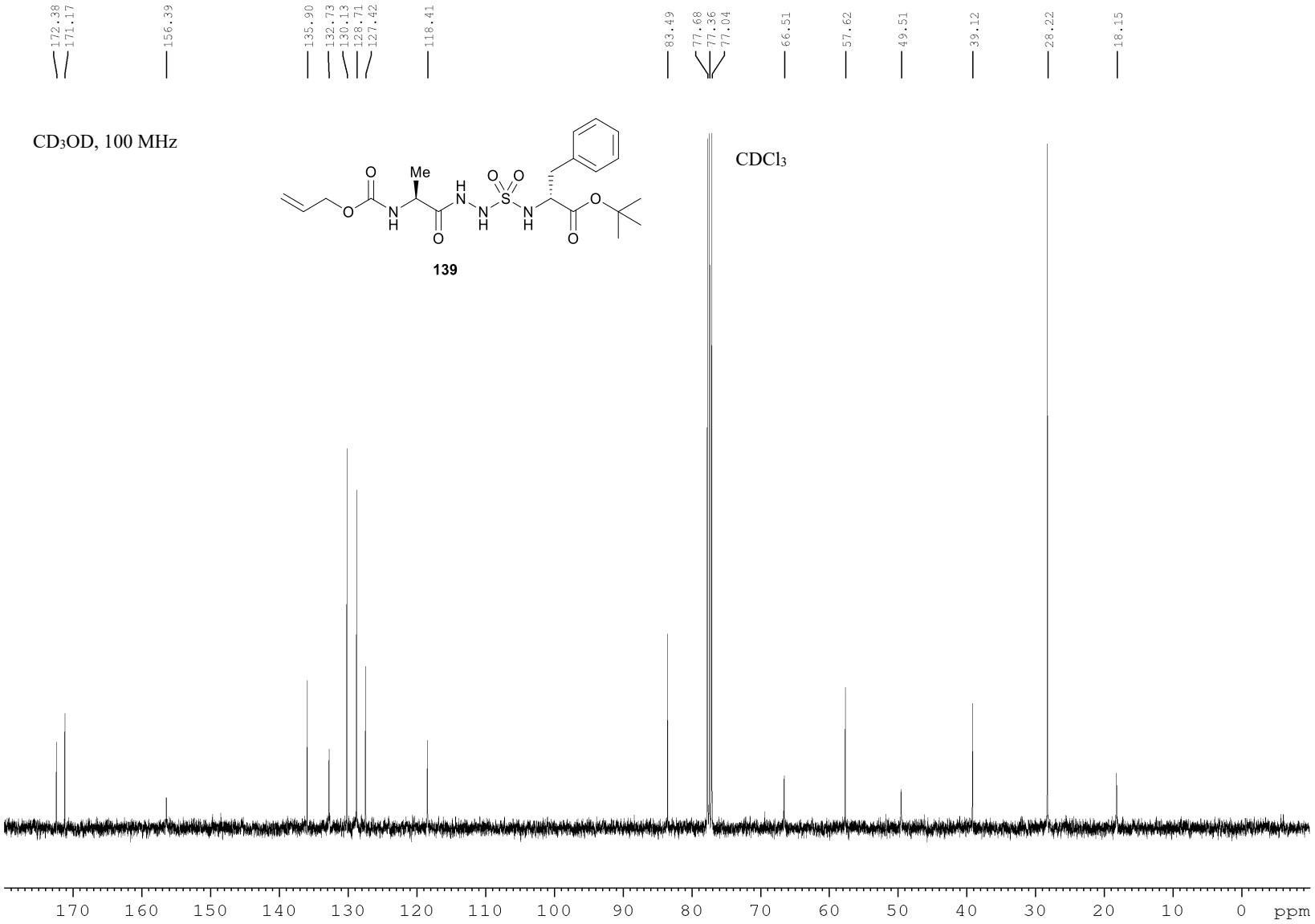
172.38
171.17
156.39
135.90
132.73
130.13
128.71
127.42
118.41
83.49
77.68
77.36
77.04
66.51
57.62
49.51
39.12
28.22
18.15
CD3OD, 100 MHz
CDCl3
139
170
160
150
140
130
120
110
100
90
80
70
60
50
40
30
20
10
0
ppm

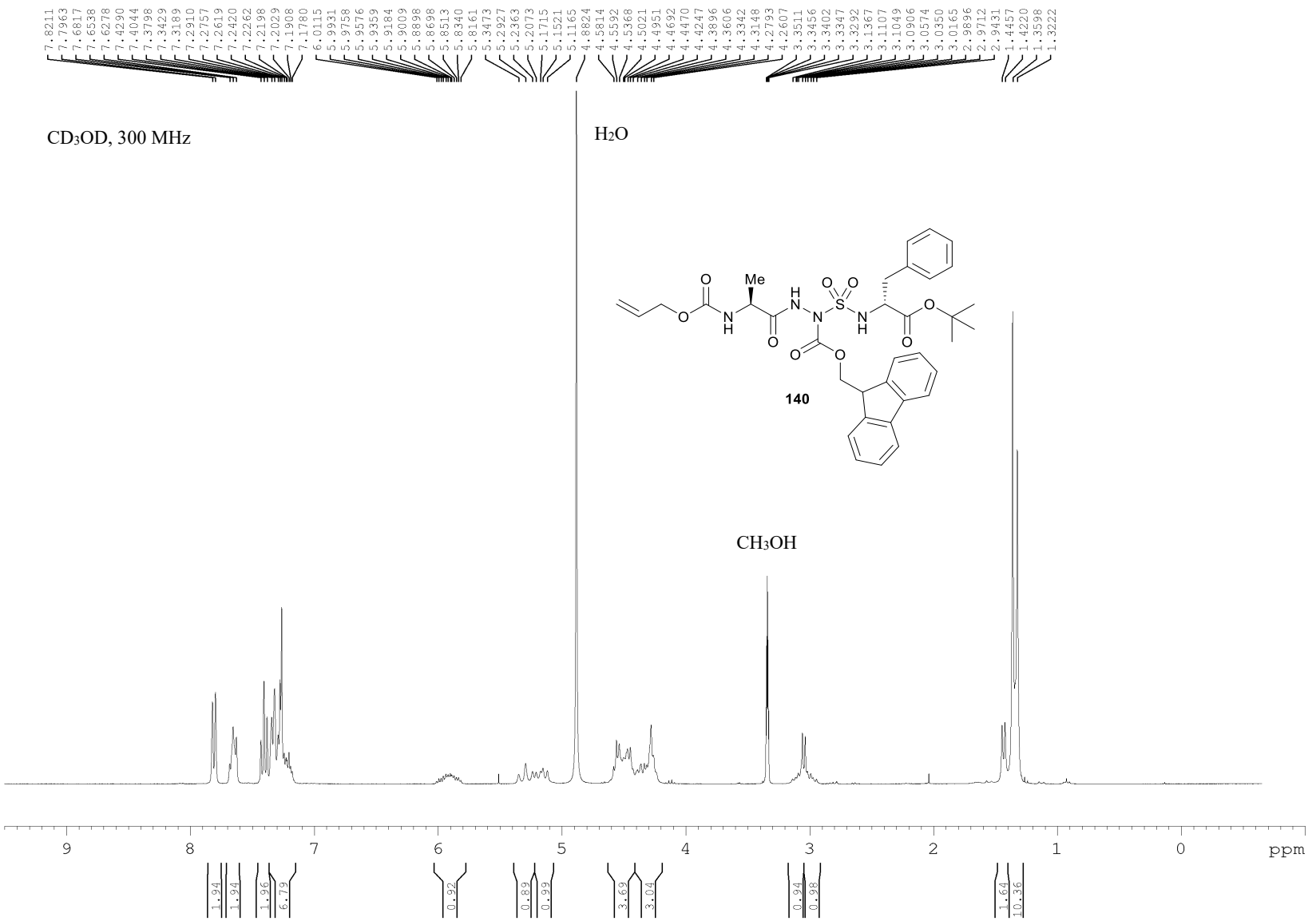
7.8211
7.7963
7.6617
7.6538
7.6278
7.4290
7.4044
7.3798
7.3429
7.3189
7.2910
7.2757
7.2619
7.2420
7.2262
7.2198
7.2029
7.1908
7.1780
6.0115
5.9931
5.9758
5.9576
5.9359
5.9184
5.9009
5.8898
5.8698
5.8513
5.8340
5.8161
5.3473
5.2927
5.2363
5.2073
5.1715
5.1521
5.1165
4.8824
4.5814
4.5592
4.5368
4.5021
4.4951
4.4692
4.4470
4.4247
4.3896
4.3606
4.3342
4.3148
4.2793
4.2607
3.3511
3.3456
3.3402
3.3347
3.3292
3.1367
3.1107
3.1049
3.0906
3.0574
3.0350
3.0165
2.9896
2.9712
2.9431
1.4457
1.4220
1.3598
1.3222
CD3OD, 300 MHz
H2O
Me
140
CH3OH
9
8
7
6
5
4
3
2
1
0
ppm
1.94
1.94
1.96
6.79
0.92
0.89
0.99
3.69
3.04
0.94
0.98
1.64
10.36

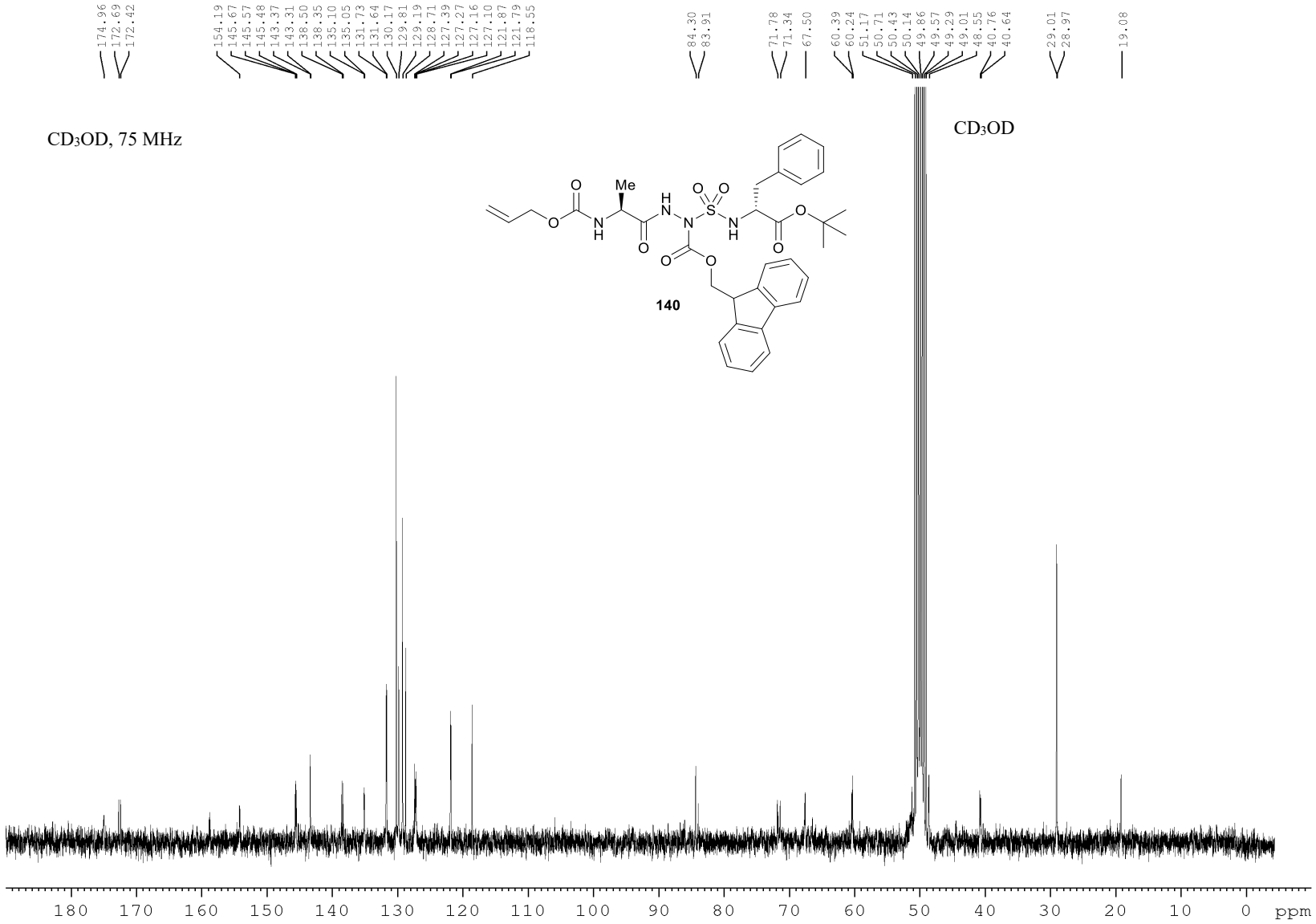
174.96
172.69
172.42
154.19
145.67
145.57
145.48
143.37
143.31
138.50
138.35
135.10
135.05
131.73
131.64
130.17
129.81
129.19
128.71
127.39
127.27
127.16
127.10
121.87
121.79
118.55
84.30
83.91
71.78
71.34
67.50
60.39
60.24
51.17
50.71
50.43
50.14
49.86
49.57
49.29
49.01
48.55
40.76
40.64
29.01
28.97
19.08
CD3OD, 75 MHz
CD3OD
140
180
170
160
150
140
130
120
110
100
90
80
70
60
50
40
30
20
10
0
ppm

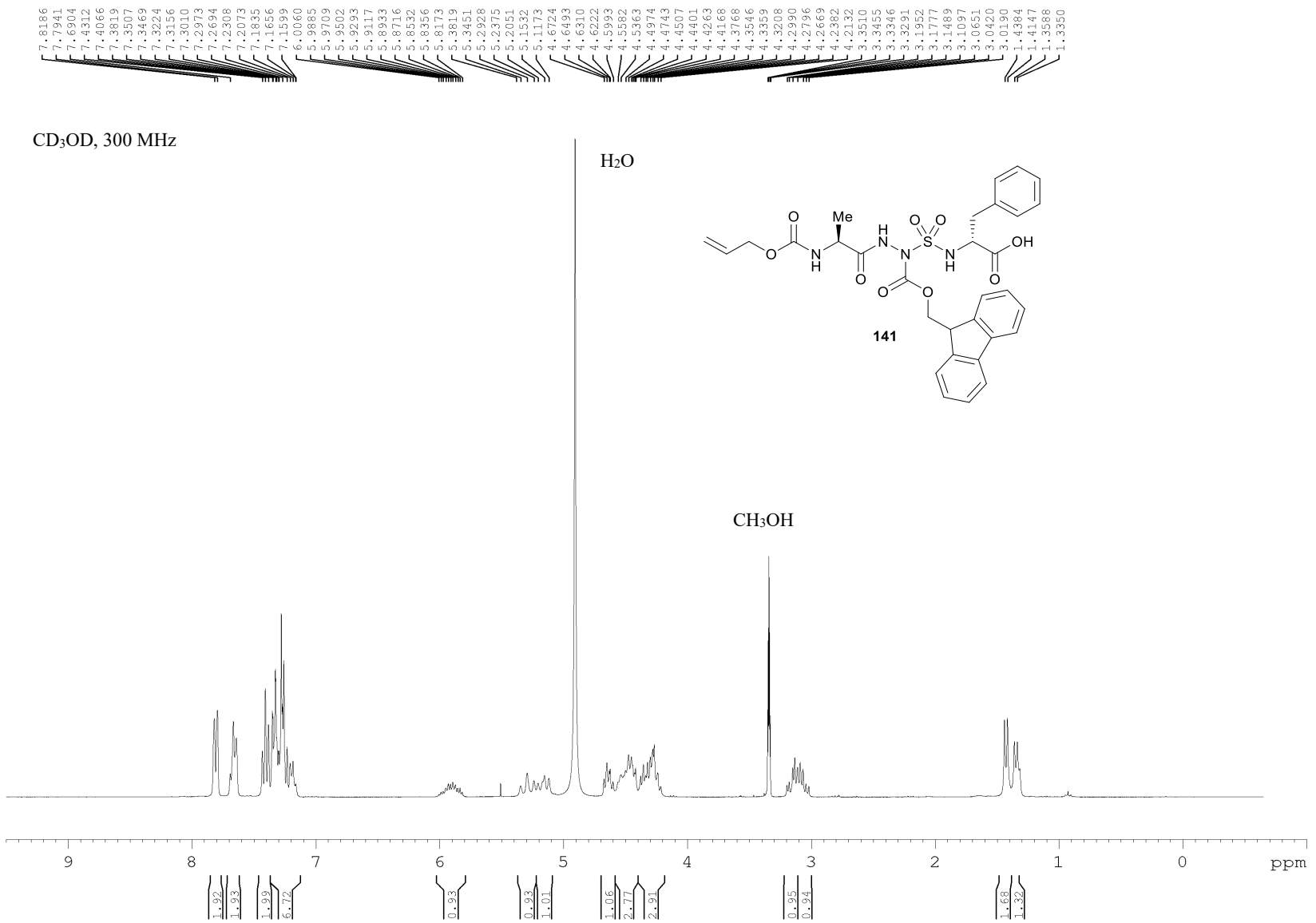
7.8186
7.7941
7.6904
7.4312
7.4066
7.3819
7.3507
7.3469
7.3224
7.3156
7.3010
7.2973
7.2694
7.2308
7.2073
7.1835
7.1656
7.1599
6.0060
5.9885
5.9709
5.9502
5.9293
5.9117
5.8933
5.8716
5.8532
5.8356
5.8173
5.3819
5.3451
5.2928
5.2375
5.2051
5.1532
5.1173
4.6724
4.6493
4.6310
4.6222
4.5993
4.5582
4.5363
4.4974
4.4743
4.4507
4.4401
4.4263
4.4168
4.3768
4.3546
4.3359
4.3208
4.2990
4.2796
4.2669
4.2382
4.2132
3.3510
3.3455
3.3346
3.3291
3.1952
3.1777
3.1489
3.1097
3.0651
3.0420
3.0190
1.4384
1.4147
1.3588
1.3350
CD3OD, 300 MHz
H2O
CH3OH
141
9
8
7
6
5
4
3
2
1
0
ppm
1.92
1.93
1.99
6.72
0.93
0.93
1.01
1.06
2.77
2.91
0.95
0.94
1.68
1.32

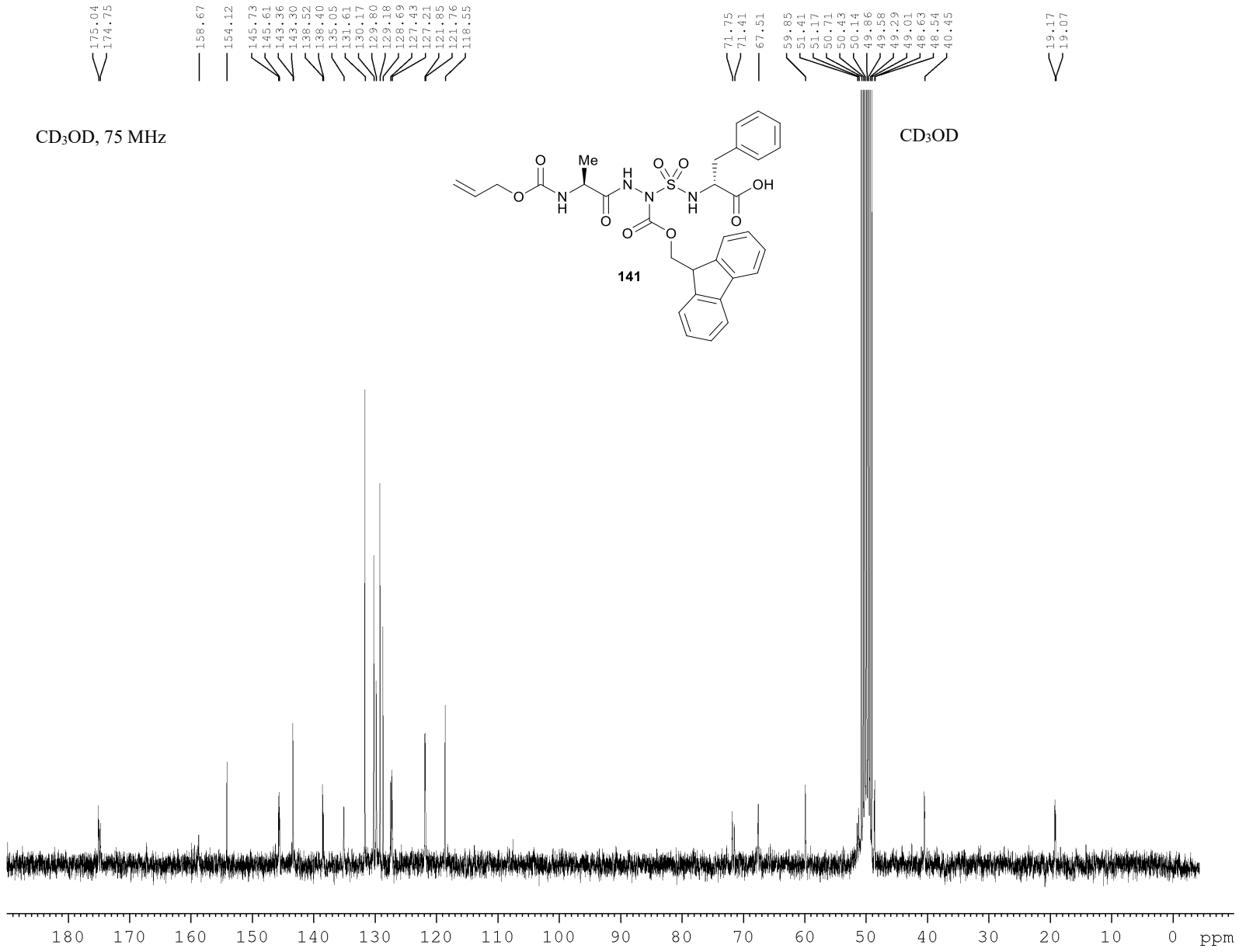
175.04
174.75
158.67
154.12
145.73
145.61
143.36
143.30
138.52
138.40
135.05
131.61
130.17
129.80
129.18
128.69
127.43
127.21
121.85
121.76
118.55
71.75
71.41
67.51
59.85
51.41
51.17
50.71
50.43
50.14
49.86
49.58
49.29
49.01
48.63
48.54
40.45
19.17
19.07
CD3OD, 75 MHz
CD3OD
141
180
170
160
150
140
130
120
110
100
90
80
70
60
50
40
30
20
10
0
ppm

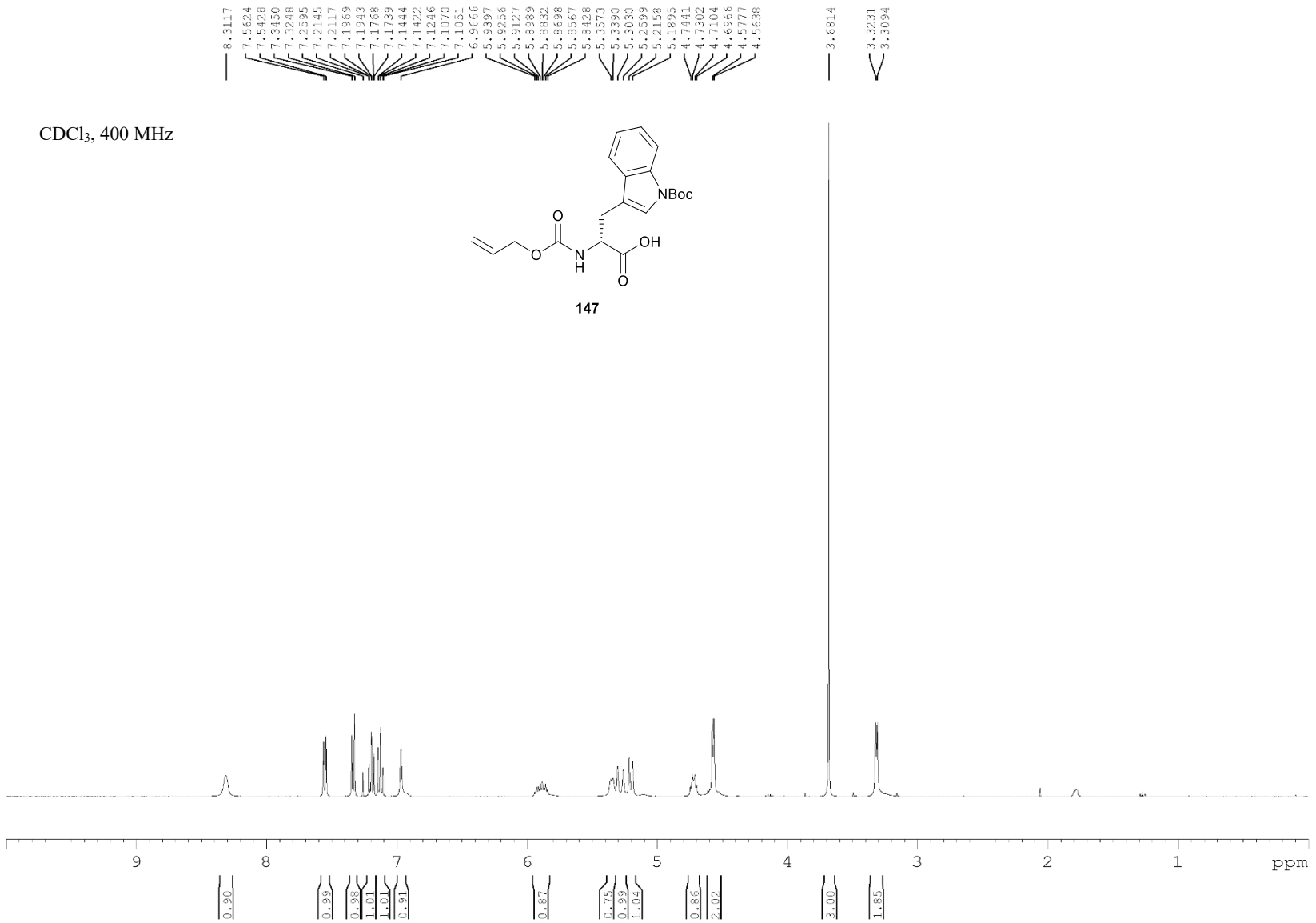
8.3117
7.5624
7.5428
7.3450
7.3248
7.2595
7.2145
7.2117
7.1969
7.1943
7.1768
7.1739
7.1444
7.1422
7.1246
7.1070
7.1051
6.9666
5.9397
5.9256
5.9127
5.8989
5.8832
5.8698
5.8567
5.8428
5.3573
5.3390
5.3030
5.2599
5.2158
5.1895
4.7441
4.7302
4.7104
4.6966
4.5777
4.5638
3.6814
3.3231
3.3094
CDCl3, 400 MHz
NBoc
O
O
N
H
OH
O
147
9
8
7
6
5
4
3
2
1
ppm
0.90
0.99
0.98
1.01
1.01
0.91
0.87
0.75
0.99
1.04
0.86
2.02
3.00
1.85

172.81
156.04
136.47
132.90
127.80
123.17
122.49
119.93
118.83
118.09
111.60
110.03
77.68
77.36
77.04
66.09
54.79
52.65
28.23

$CDCl_3$, 100 MHz

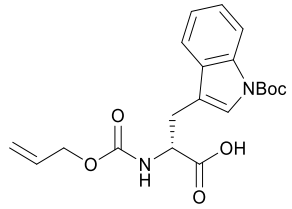

147

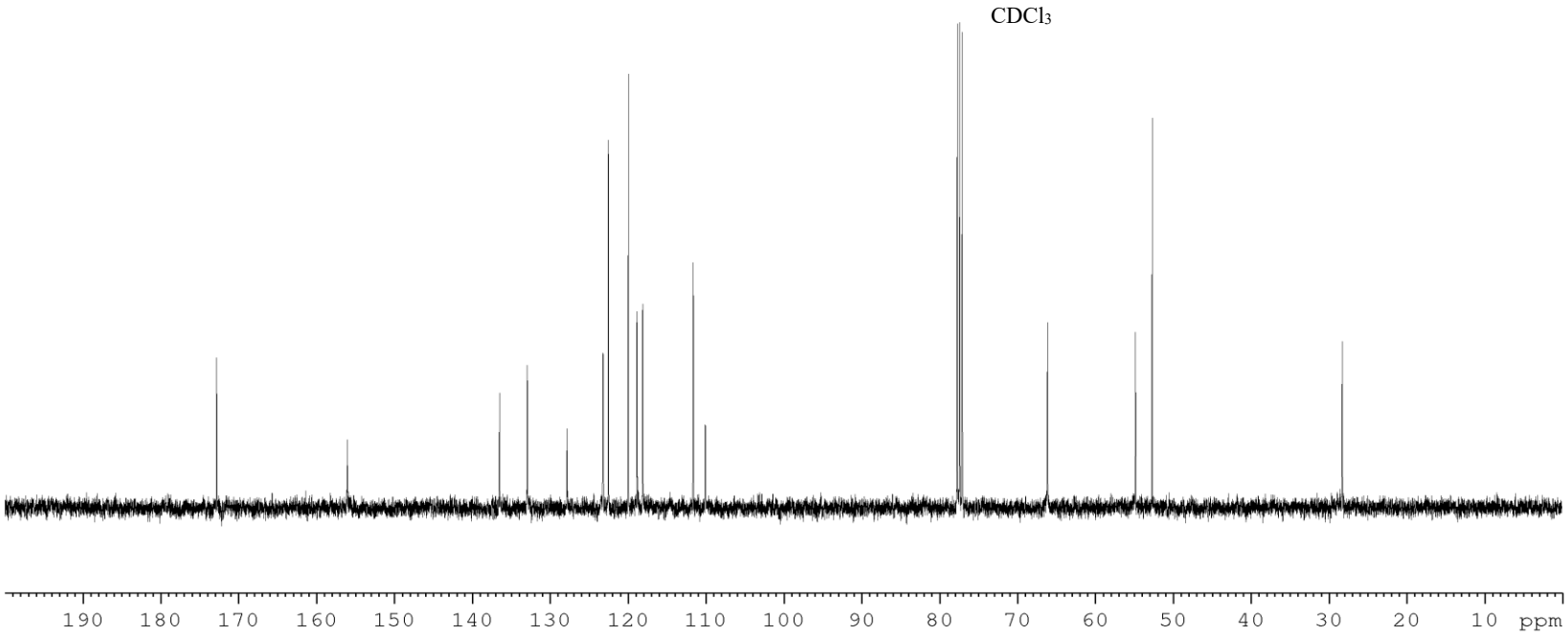

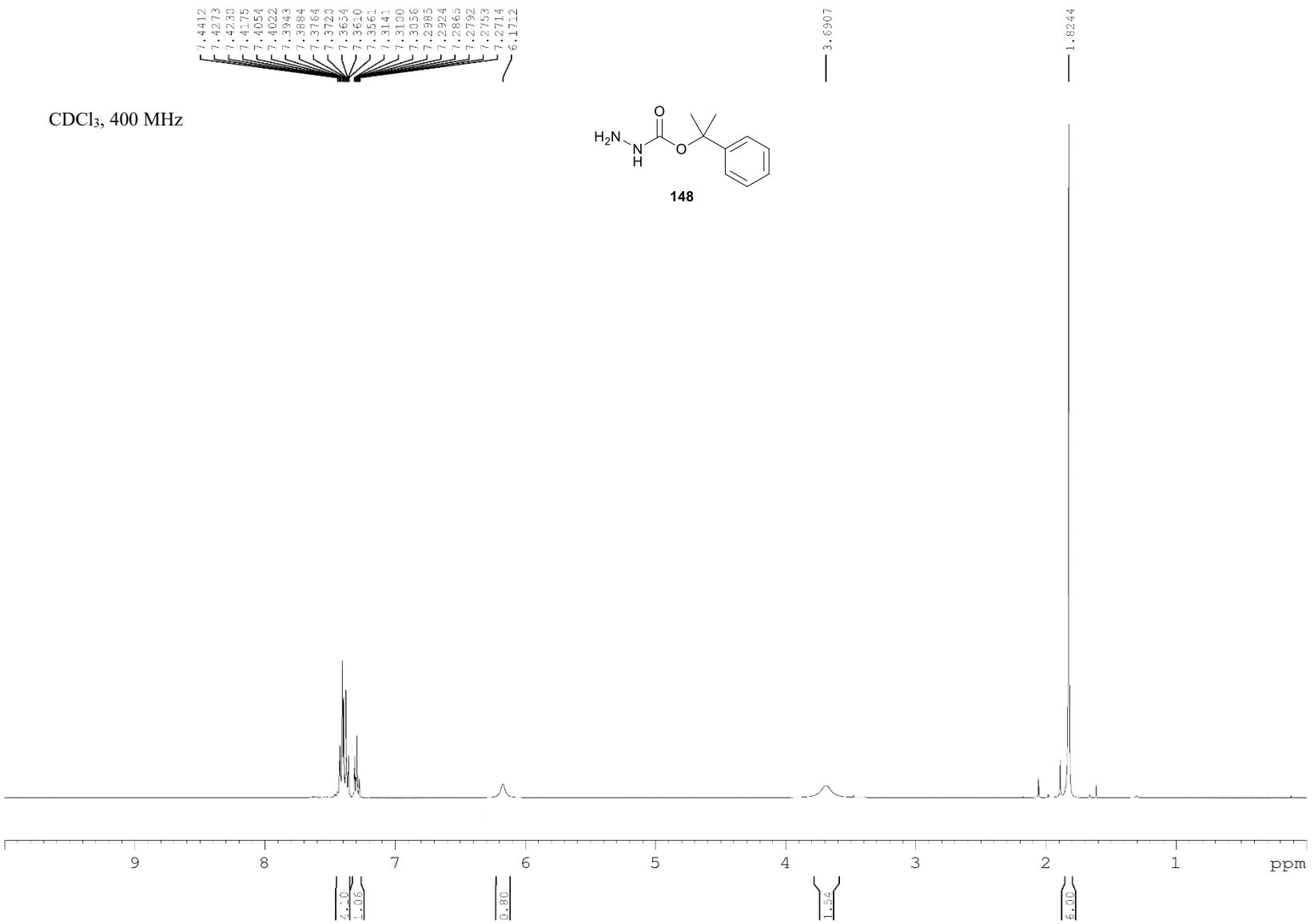
7.4412
7.4273
7.4230
7.4175
7.4054
7.4022
7.3943
7.3884
7.3764
7.3720
7.3654
7.3610
7.3561
7.3141
7.3100
7.3036
7.2985
7.2924
7.2865
7.2792
7.2753
7.2714
6.1712
3.6907
1.8244
CDCl3, 400 MHz
148
9
8
7
6
5
4
3
2
1
ppm
4.10
1.06
0.80
1.54
6.00

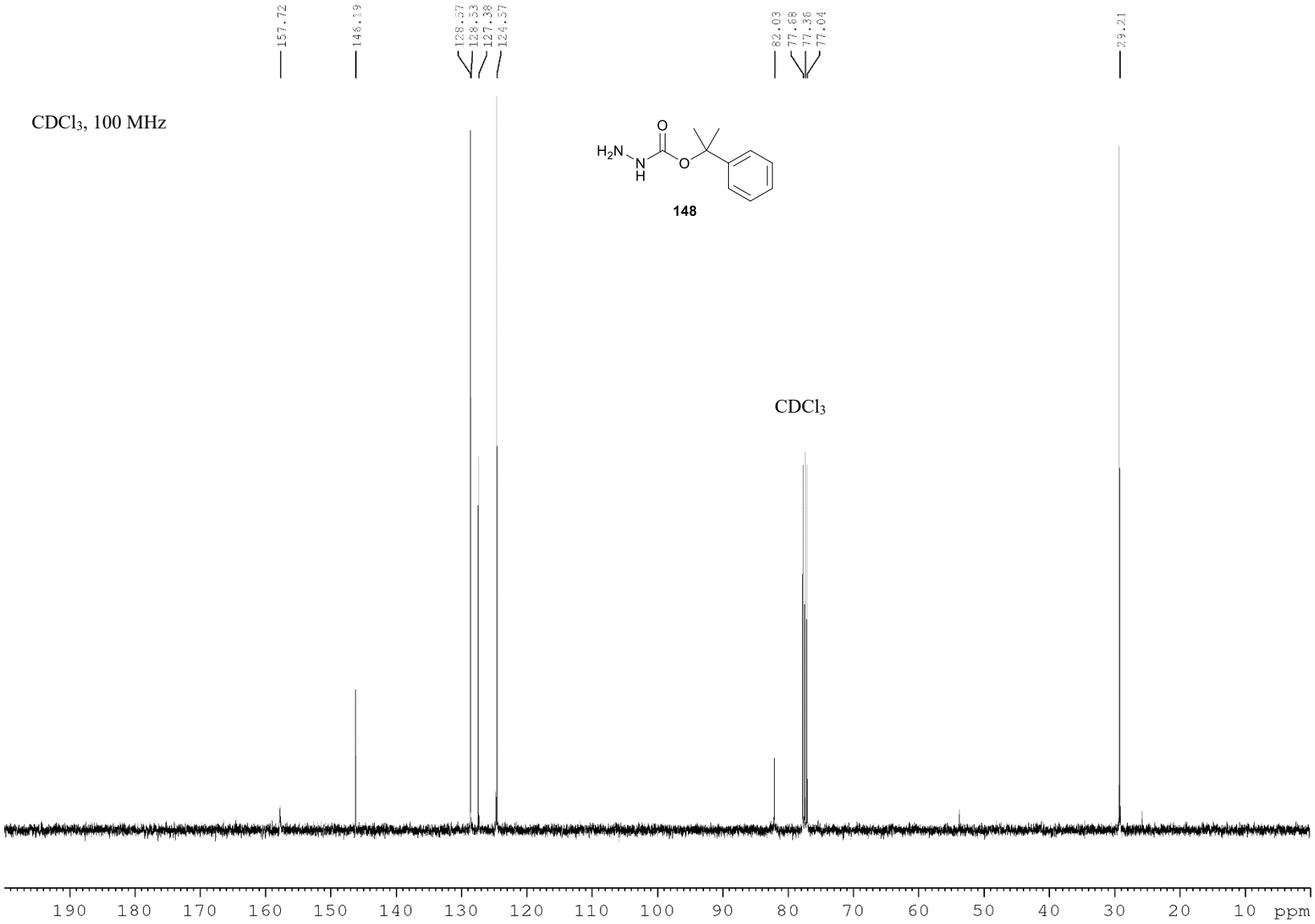
157.72
146.19
128.57
128.53
127.38
124.57
82.03
77.68
77.36
77.04
29.21
CDCl3, 100 MHz
148
CDCl3
190 180 170 160 150 140 130 120 110 100 90 80 70 60 50 40 30 20 10 ppm

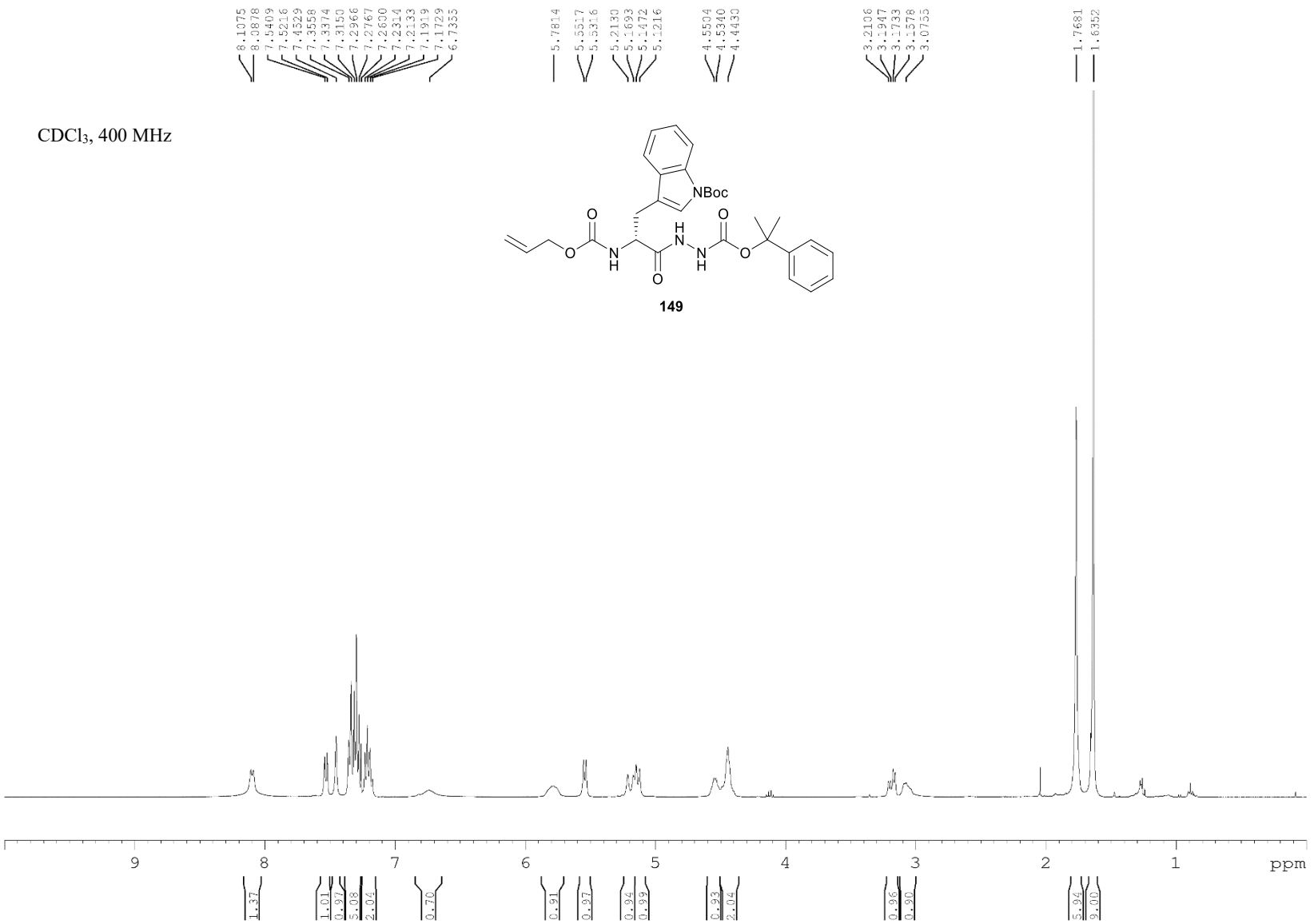
8.1075
8.0878
7.5409
7.5216
7.4529
7.3558
7.3374
7.3150
7.2966
7.2767
7.2600
7.2314
7.2133
7.1919
7.1729
6.7355
5.7814
5.5517
5.5316
5.2130
5.1693
5.1472
5.1216
4.5504
4.5340
4.4430
3.2106
3.1947
3.1733
3.1578
3.0755
1.7681
1.6852
CDCl3, 400 MHz
NBoc
149
9
8
7
6
5
4
3
2
1
ppm
1.37
1.01
0.97
3.08
2.04
0.70
0.91
0.97
0.94
0.99
0.93
2.04
0.96
0.90
5.94
9.00

171.01
156.35
154.80
149.91
145.72
135.75
132.63
130.52
128.61
127.44
124.88
124.63
123.01
119.24
118.26
115.60
115.39
84.01
83.32
77.68
77.36
77.04
66.39
53.57
29.03
28.50
28.11

$CDCl_3$, 100 MHz

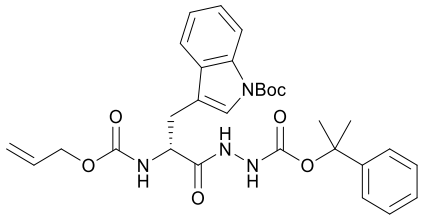

149

$CDCl_3$

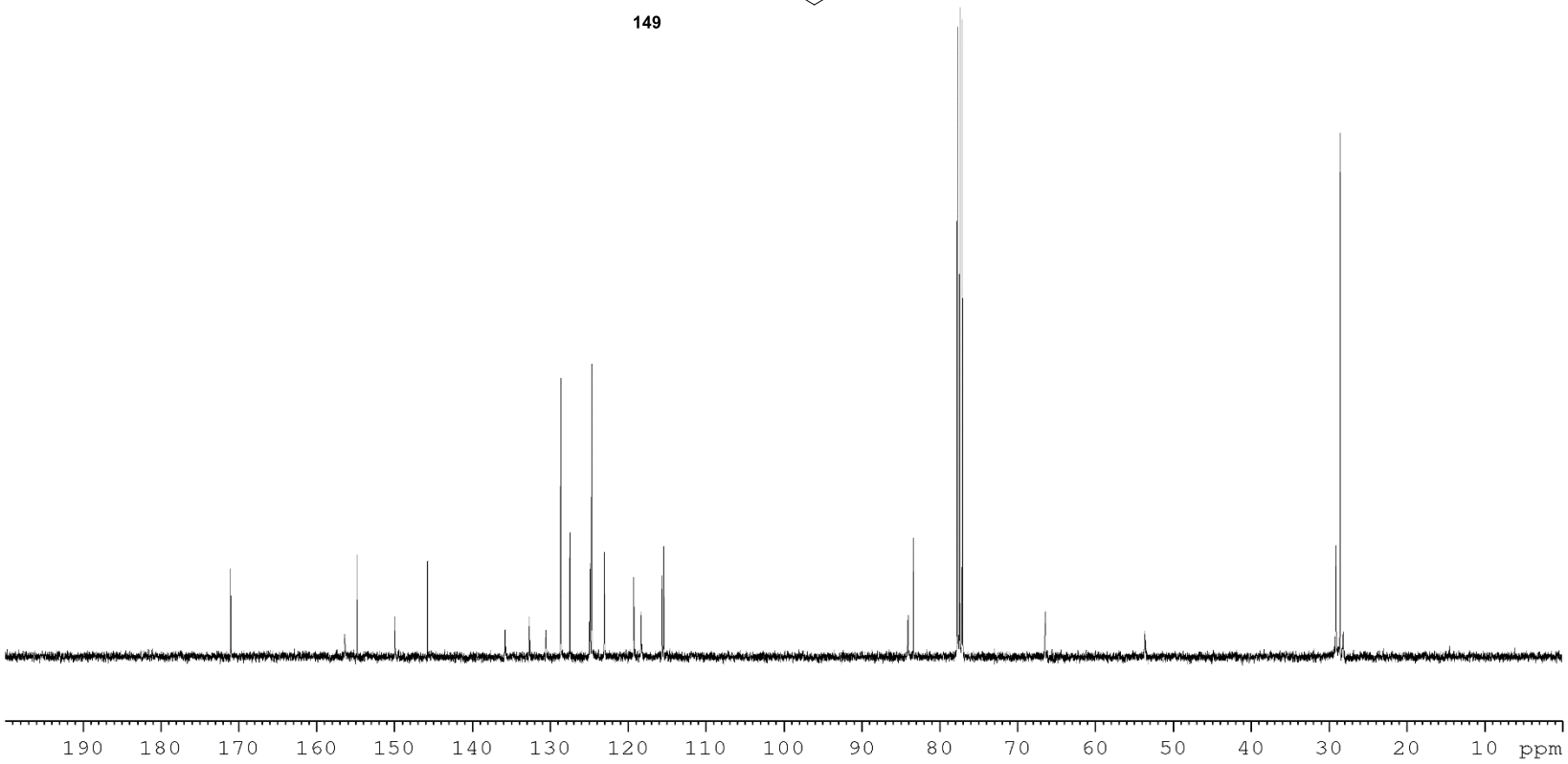

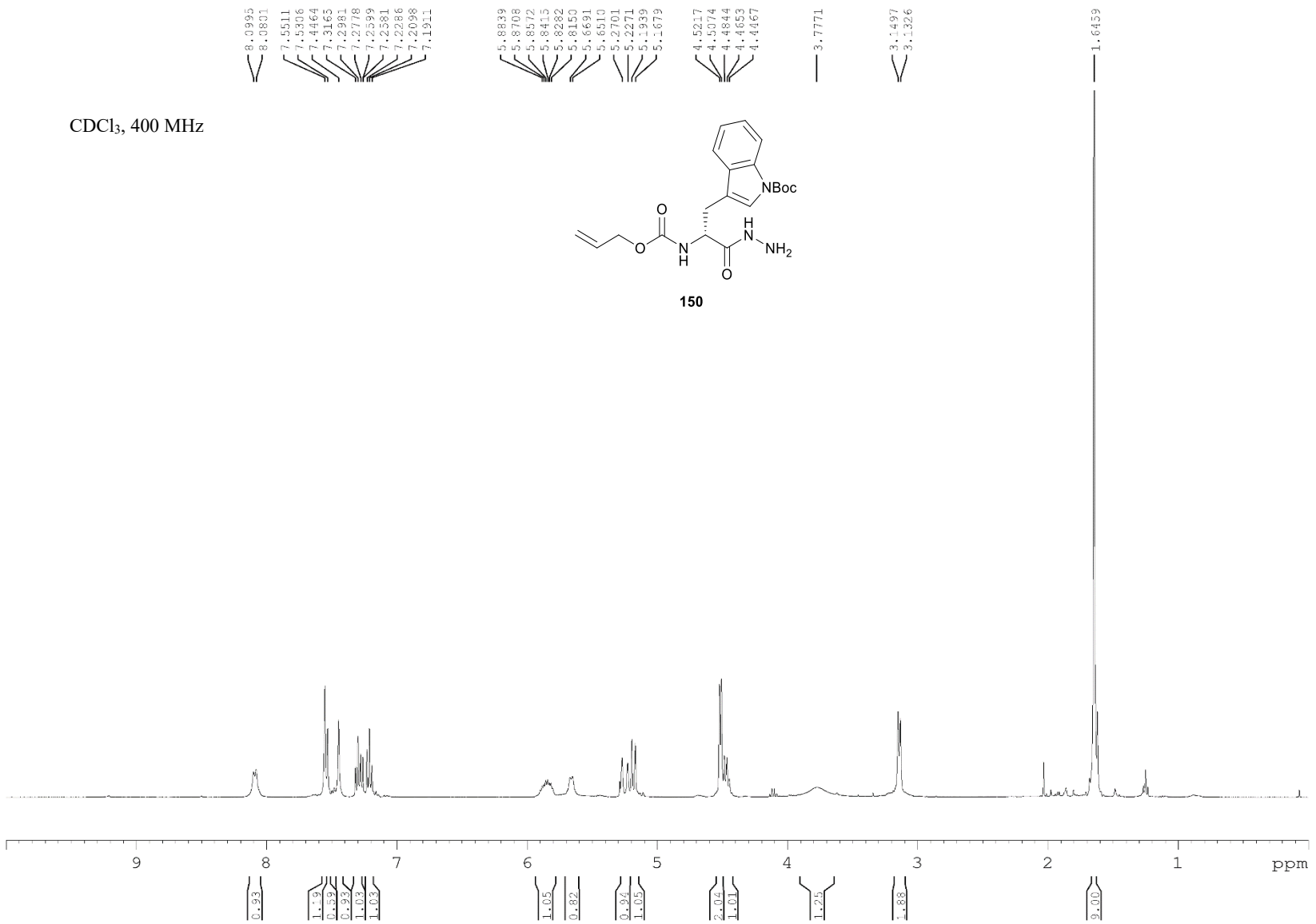

$CDCl_3$, 400 MHz

150

172.10
156.20
149.88
135.75
132.69
130.43
125.01
124.63
123.03
119.13
118.38
115.71
115.45
84.18
77.68
77.36
77.04
66.37
54.02
28.63
28.51

$CDCl_3$, 100 MHz

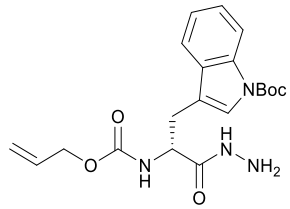

150

$CDCl_3$

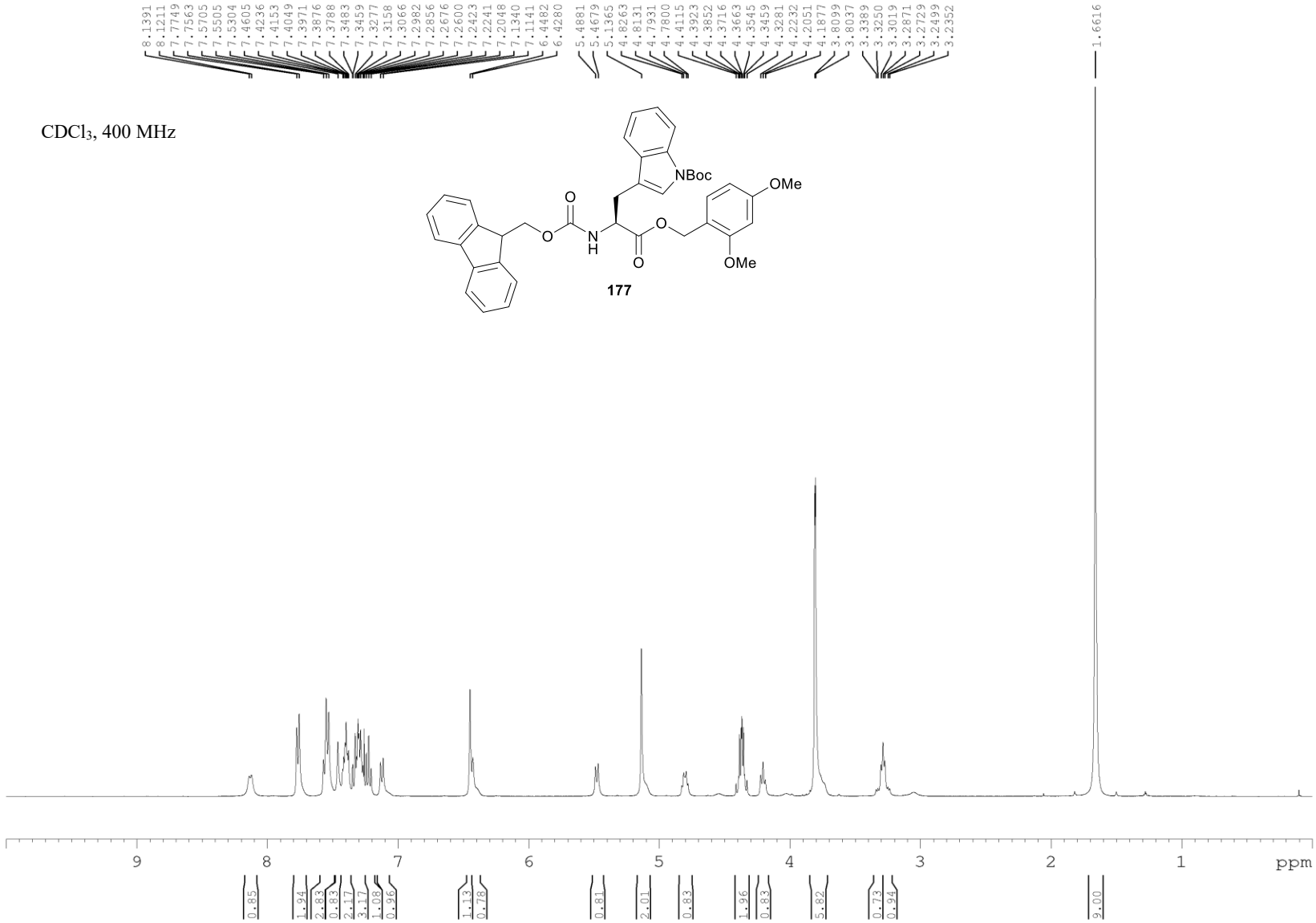
8.1391
8.1211
7.7749
7.7563
7.5705
7.5505
7.5304
7.4605
7.4236
7.4153
7.4049
7.3971
7.3876
7.3788
7.3483
7.3459
7.3277
7.3158
7.3066
7.2982
7.2856
7.2676
7.2600
7.2423
7.2241
7.2048
7.1340
7.1141
6.4482
6.4280
5.4881
5.4679
5.1365
4.8263
4.8131
4.7931
4.7800
4.4115
4.3923
4.3852
4.3716
4.3663
4.3545
4.3459
4.3281
4.2232
4.2051
4.1877
3.8099
3.8037
3.3389
3.3250
3.3019
3.2871
3.2729
3.2499
3.2352
1.6616
CDCl3, 400 MHz
NBoc
OMe
OMe
O
O
N
H
O
O
177
9
8
7
6
5
4
3
2
1
ppm
0.85
1.94
2.83
0.83
2.17
3.17
1.08
0.96
1.13
0.78
0.81
2.01
0.83
1.96
0.83
5.82
0.73
0.94
9.00

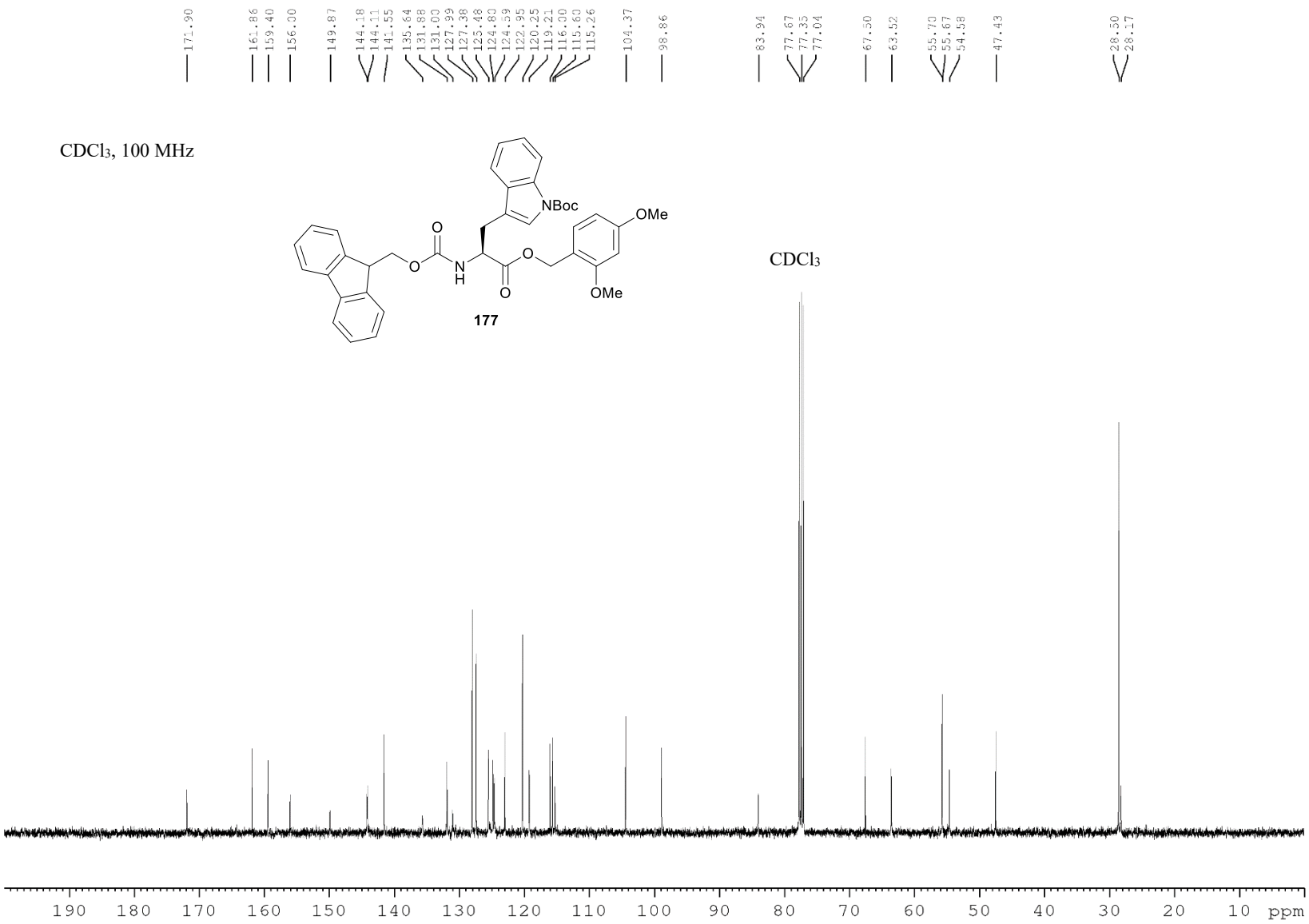
171.90
161.86
159.40
156.00
149.87
144.18
144.11
141.55
135.64
131.88
131.00
127.99
127.38
123.48
124.80
124.59
122.95
120.25
119.21
116.00
115.60
115.26
104.37
98.86
83.94
77.67
77.35
77.04
67.50
63.52
55.70
55.67
54.58
47.43
28.50
28.17
CDCl3, 100 MHz
NBoc
OMe
OMe
O
O
N
H
O
O
177
CDCl3
190
180
170
160
150
140
130
120
110
100
90
80
70
60
50
40
30
20
10
ppm

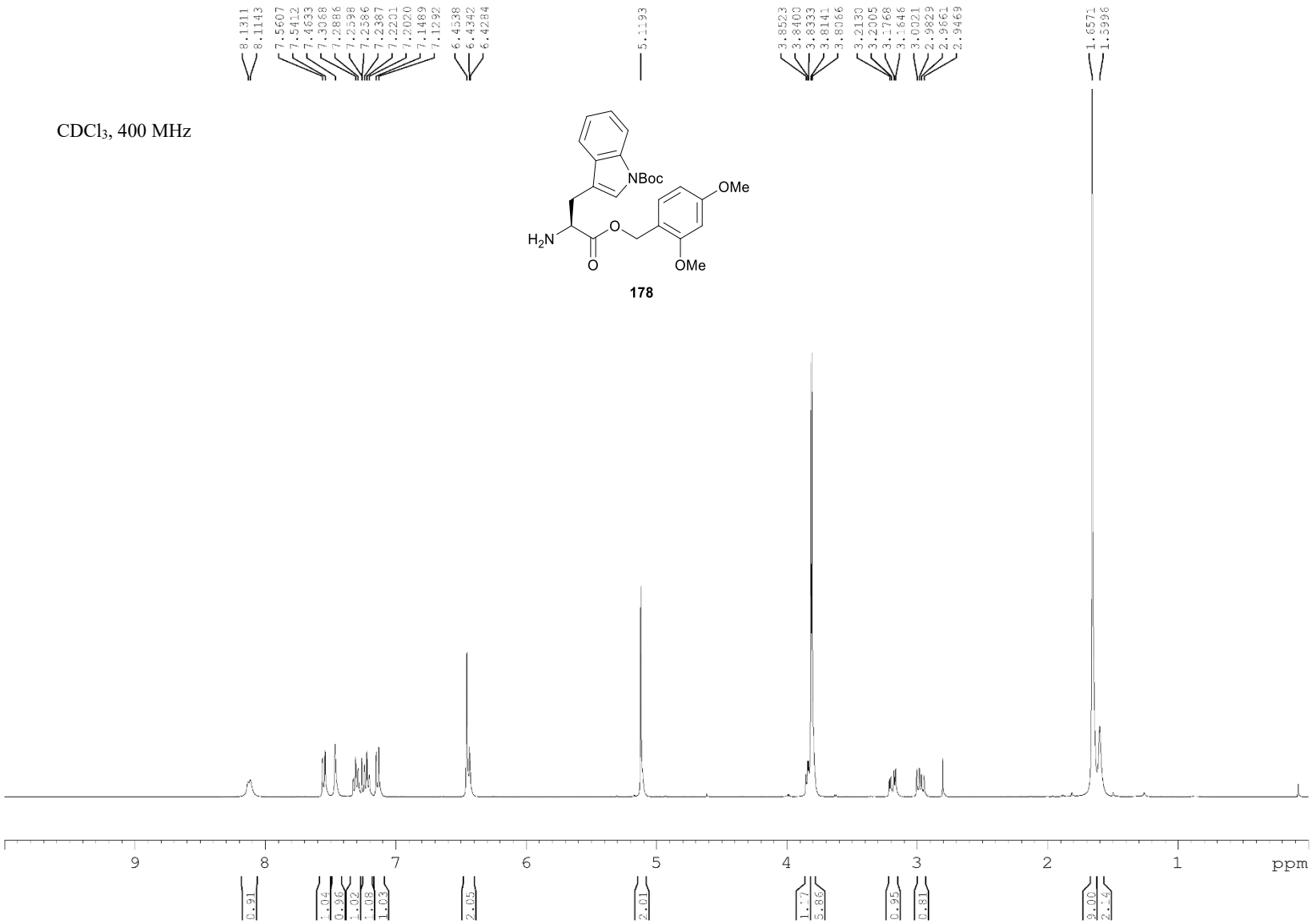
8.1311
8.1143
7.5607
7.5412
7.4633
7.3068
7.2886
7.2598
7.2586
7.2387
7.2201
7.2020
7.1489
7.1292
6.4538
6.4342
6.4284
5.1193
3.8523
3.8400
3.8333
3.8141
3.8066
3.2130
3.2005
3.1768
3.1646
3.0021
2.9829
2.9661
2.9469
1.6571
1.5996
CDCl3, 400 MHz
NBoc
OMe
OMe
H2N
O
O
178
9
8
7
6
5
4
3
2
1
ppm
0.91
1.04
0.96
1.02
1.08
1.03
2.05
2.01
1.17
5.86
0.95
0.81
9.00
2.14

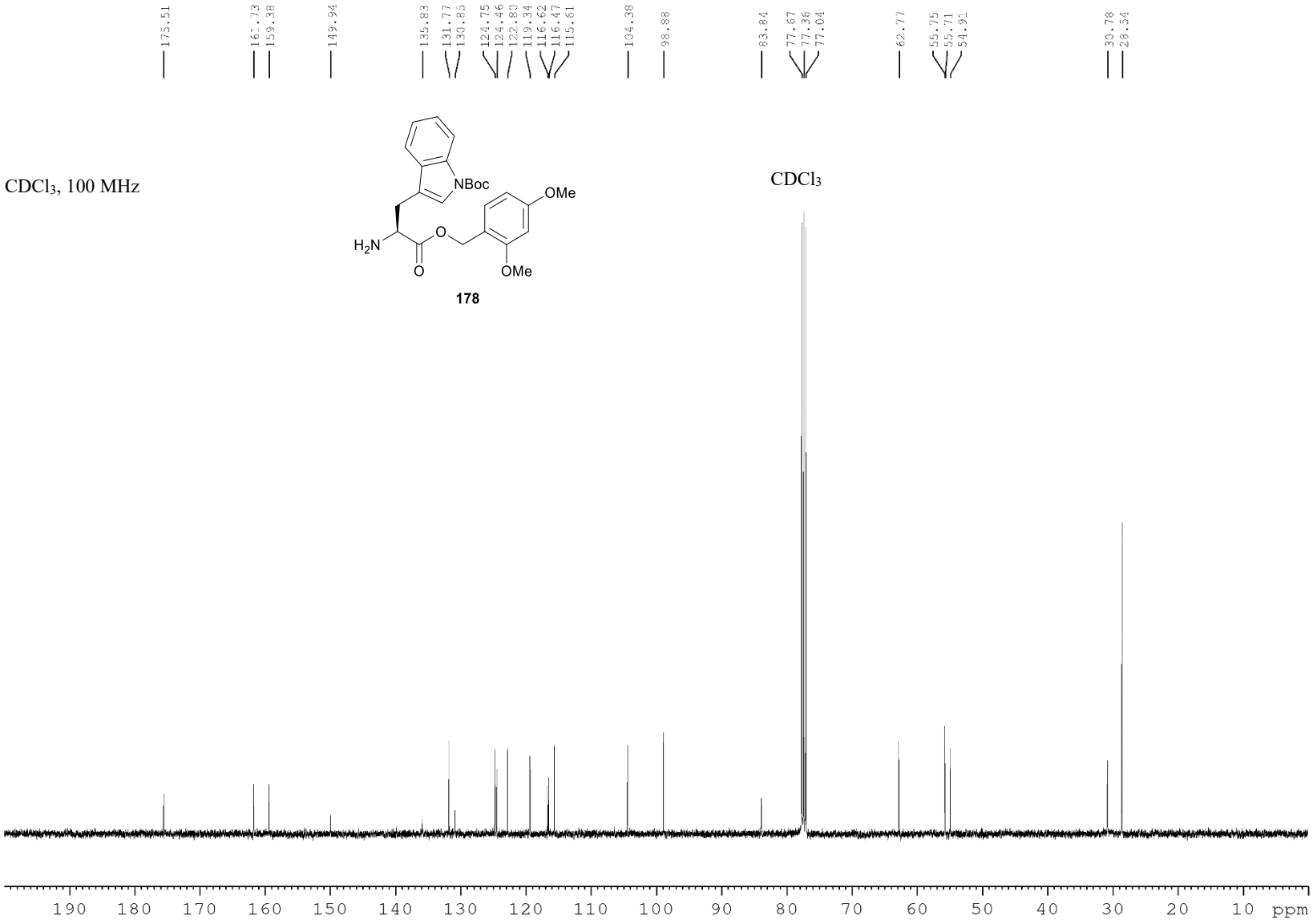
175.51
161.73
159.38
149.94
135.83
131.77
130.85
124.75
124.46
122.80
119.34
116.62
116.47
115.61
104.38
98.88
83.84
77.67
77.36
77.04
62.77
55.75
55.71
54.91
30.78
28.54
CDCl3, 100 MHz
NBoc
OMe
OMe
H2N
O
O
178
CDCl3
190
180
170
160
150
140
130
120
110
100
90
80
70
60
50
40
30
20
10
ppm

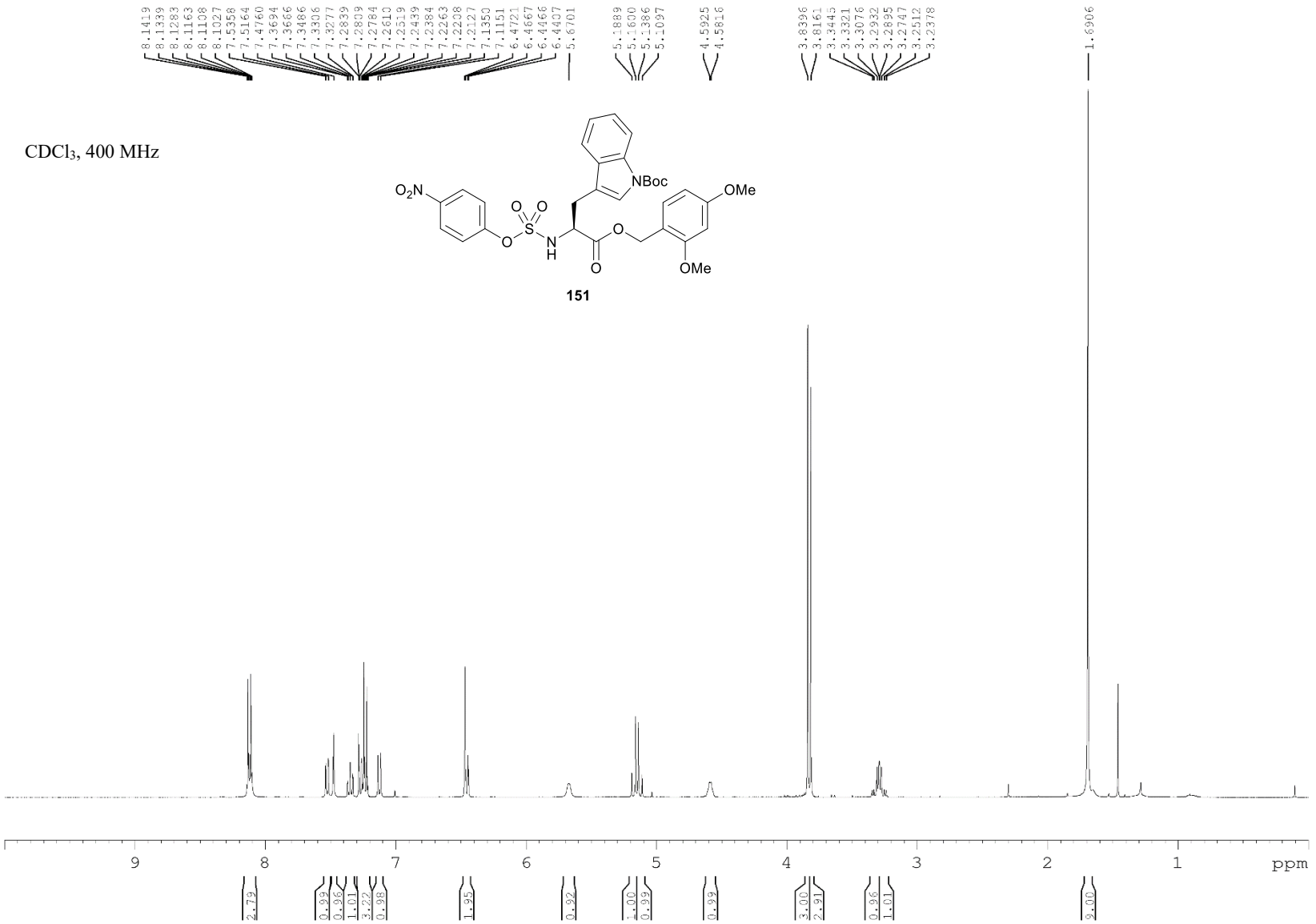
8.1419
8.1339
8.1283
8.1163
8.1108
8.1027
7.5358
7.5164
7.4760
7.3694
7.3666
7.3486
7.3306
7.3277
7.2839
7.2809
7.2784
7.2610
7.2519
7.2439
7.2384
7.2263
7.2208
7.2127
7.1350
7.1151
6.4721
6.4667
6.4466
6.4407
5.6701
5.1889
5.1600
5.1386
5.1097
4.5925
4.5816
3.8396
3.8161
3.3445
3.3321
3.3076
3.2932
3.2895
3.2747
3.2512
3.2378
1.6906
CDCl3, 400 MHz
O2N
NBoc
OMe
OMe
151
9
8
7
6
5
4
3
2
1
ppm
2.79
0.99
0.96
1.01
3.22
0.98
1.95
0.92
1.00
0.99
0.99
3.00
2.91
0.96
1.01
9.00

170.72
162.23
159.58
154.58
149.77
146.17
135.61
132.36
130.43
125.67
125.08
123.11
122.46
119.09
115.70
115.41
113.85
104.49
98.94
84.37
77.68
77.36
77.04
64.35
57.41
55.79
55.73
28.96
28.51

$CDCl_3$, 100 MHz

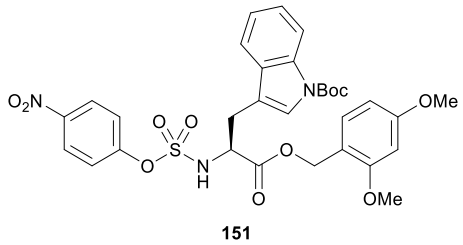

151

$CDCl_3$

CDCl$_3$, 500 MHz

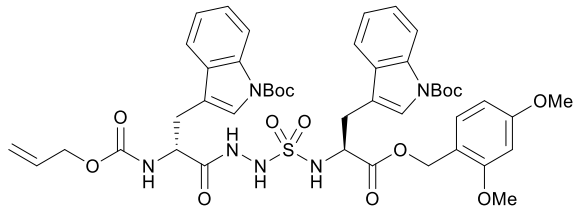

152

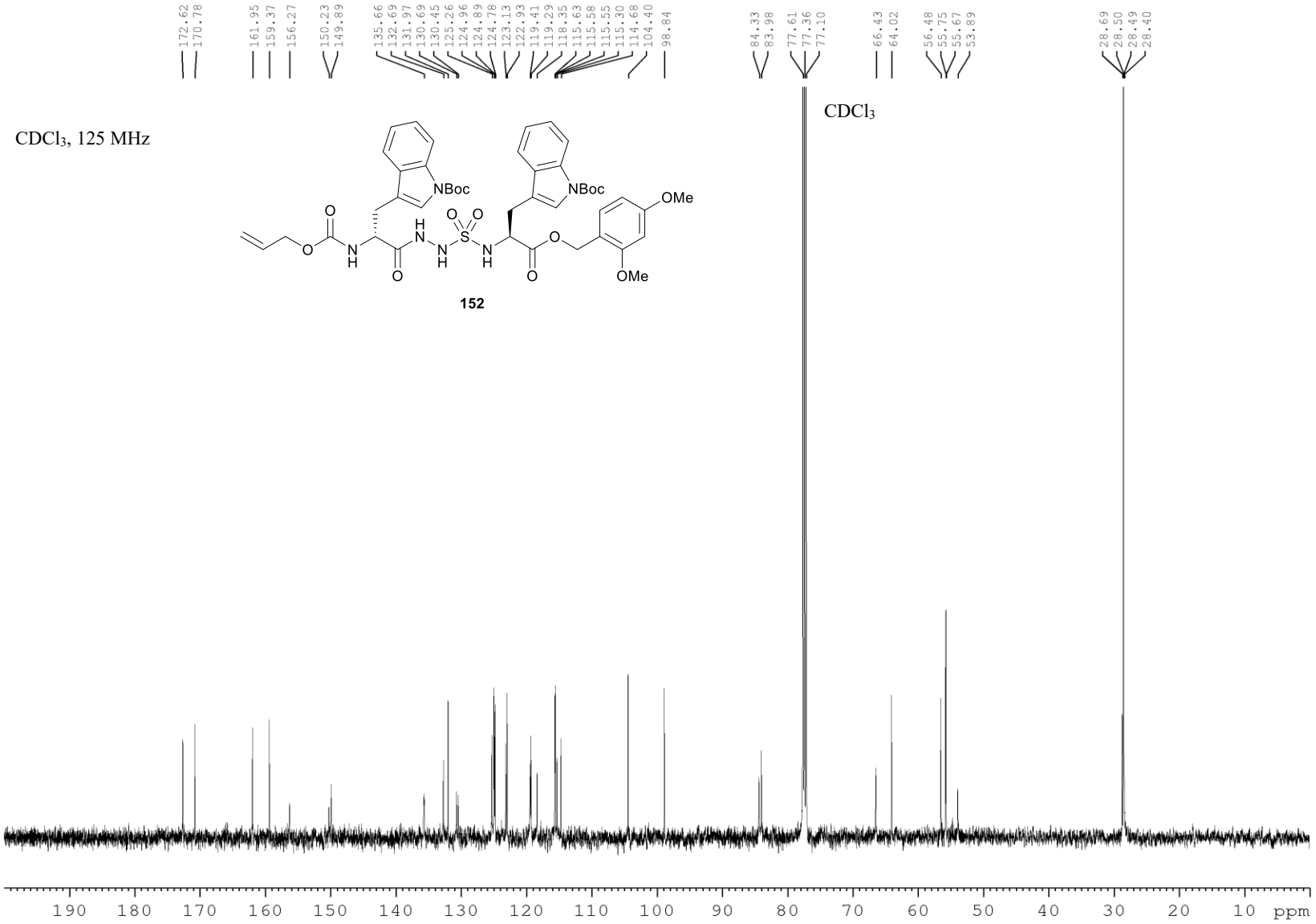
172.62
170.78
161.95
159.37
156.27
150.23
149.89
135.66
132.69
131.97
130.69
130.45
125.26
124.96
124.89
124.78
123.13
122.93
119.41
119.29
118.35
115.63
115.58
115.55
115.30
114.68
104.40
98.84
84.33
83.98
77.61
77.36
77.10
66.43
64.02
56.48
55.75
55.67
53.89
28.69
28.50
28.49
28.40
CDCl3
CDCl3, 125 MHz
NBoc
NBoc
OMe
OMe
152
190 180 170 160 150 140 130 120 110 100 90 80 70 60 50 40 30 20 10 ppm

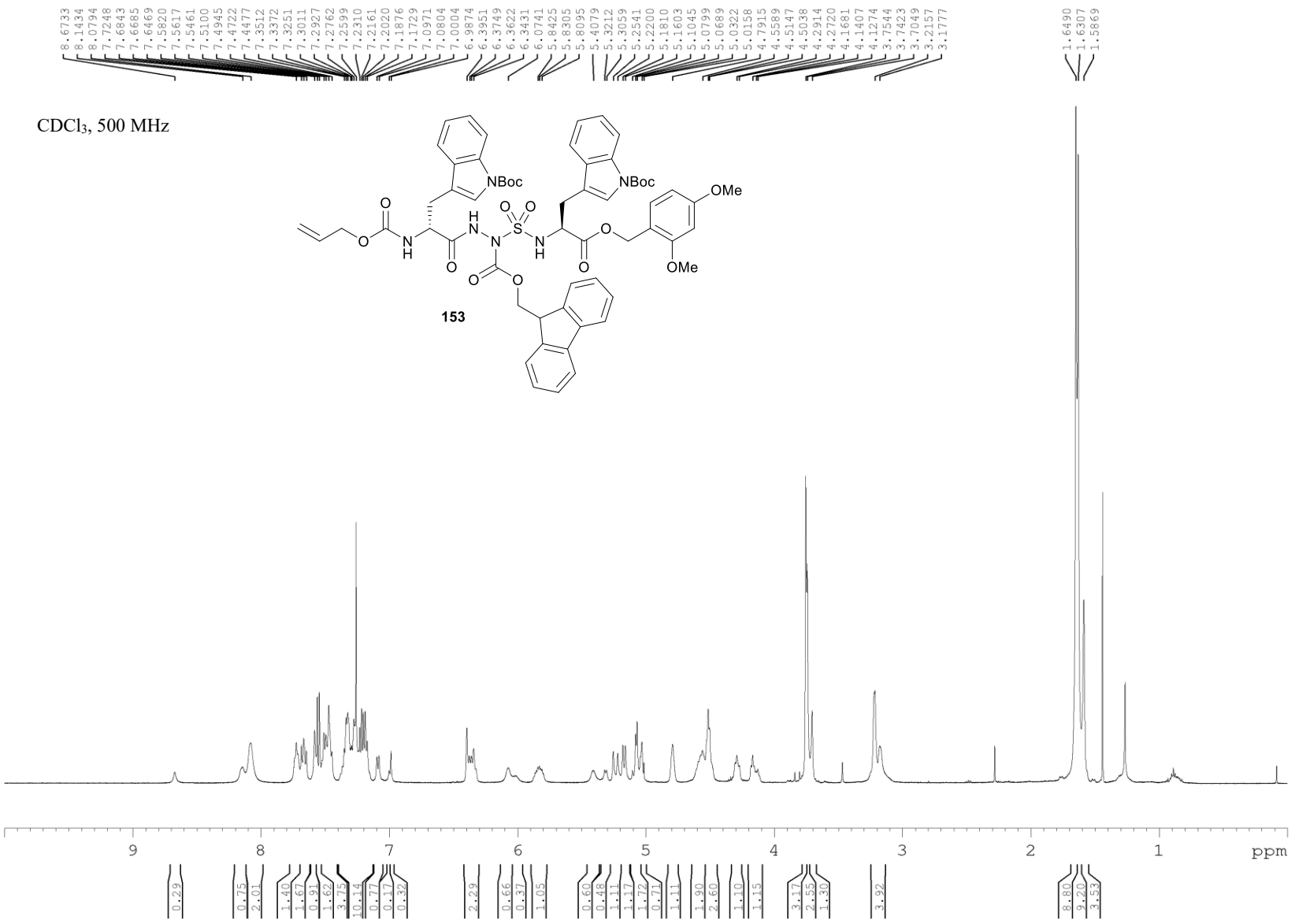
8.6733
8.1434
8.0794
7.7248
7.6843
7.6685
7.6469
7.5820
7.5617
7.5461
7.5100
7.4945
7.4722
7.4477
7.3512
7.3372
7.3251
7.3011
7.2927
7.2762
7.2599
7.2310
7.2161
7.2020
7.1876
7.1729
7.0971
7.0804
7.0004
6.9874
6.3951
6.3749
6.3622
6.3431
6.0741
5.8425
5.8305
5.8095
5.4079
5.3212
5.3059
5.2541
5.2200
5.1810
5.1603
5.1045
5.0799
5.0689
5.0322
5.0158
4.7915
4.5589
4.5147
4.5038
4.2914
4.2720
4.1681
4.1407
4.1274
3.7544
3.7423
3.7049
3.2157
3.1777
1.6490
1.6307
1.5869
CDCl3, 500 MHz
NBoc
NBoc
OMe
OMe
153
9
8
7
6
5
4
3
2
1
ppm
0.29
0.75
2.01
1.40
1.67
0.91
1.62
3.75
10.14
0.77
0.17
0.32
2.29
0.66
0.37
1.05
0.60
0.48
1.11
1.17
1.72
0.71
1.11
1.90
2.60
1.10
1.15
3.17
2.55
1.30
3.92
8.80
9.20
3.53

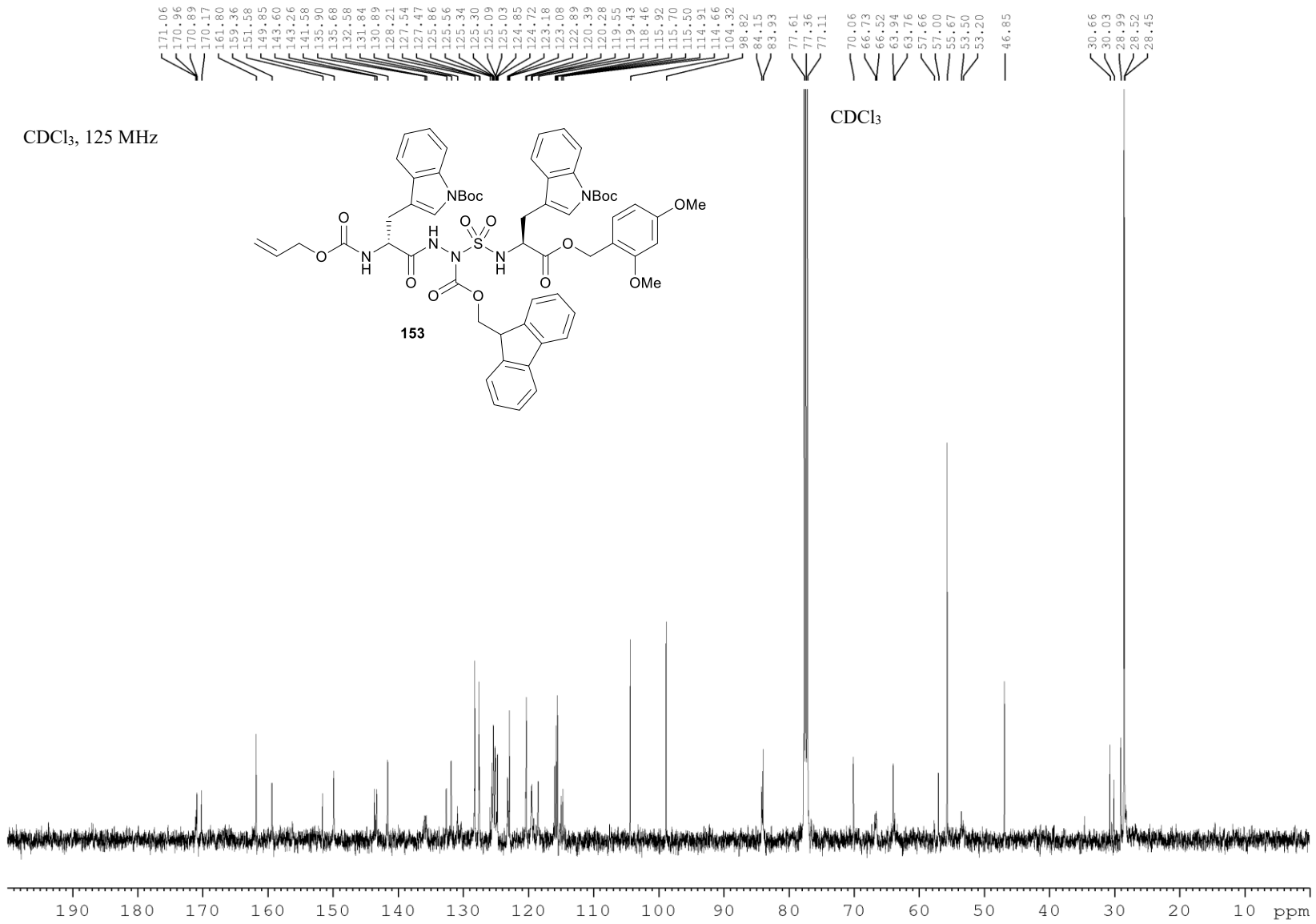
171.06
170.96
170.89
170.17
161.80
159.36
151.58
149.85
143.60
143.26
141.58
135.90
135.68
132.58
131.84
130.89
128.21
127.54
127.47
125.86
125.56
125.34
125.30
125.09
125.03
124.85
124.72
123.18
123.08
122.89
120.39
120.28
119.55
119.43
118.46
115.92
115.70
115.50
114.91
114.66
104.32
98.82
84.15
83.93
77.61
77.36
77.11
70.06
66.73
66.52
63.94
63.76
57.66
57.00
55.67
53.50
53.20
46.85
30.66
30.03
28.99
28.52
28.45
CDCl3, 125 MHz
CDCl3
NBoc
NBoc
OMe
OMe
153
190
180
170
160
150
140
130
120
110
100
90
80
70
60
50
40
30
20
10
ppm

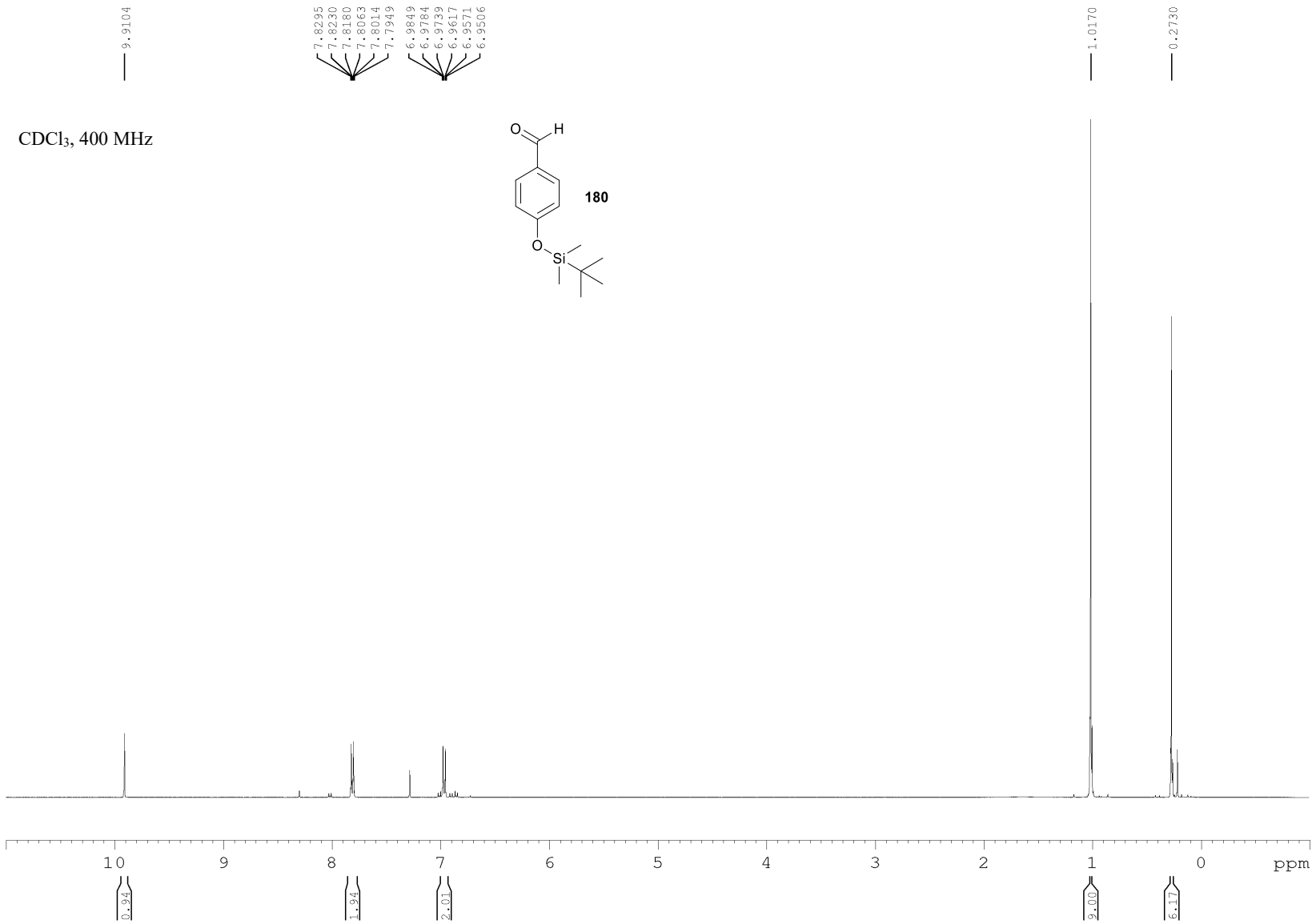
9.9104
7.8295
7.8230
7.8180
7.8063
7.8014
7.7949
6.9849
6.9784
6.9739
6.9617
6.9571
6.9506
1.0170
0.2730
CDCl3, 400 MHz
O
H
180
O
Si
10
9
8
7
6
5
4
3
2
1
0
ppm
0.94
1.94
2.01
9.00
6.17

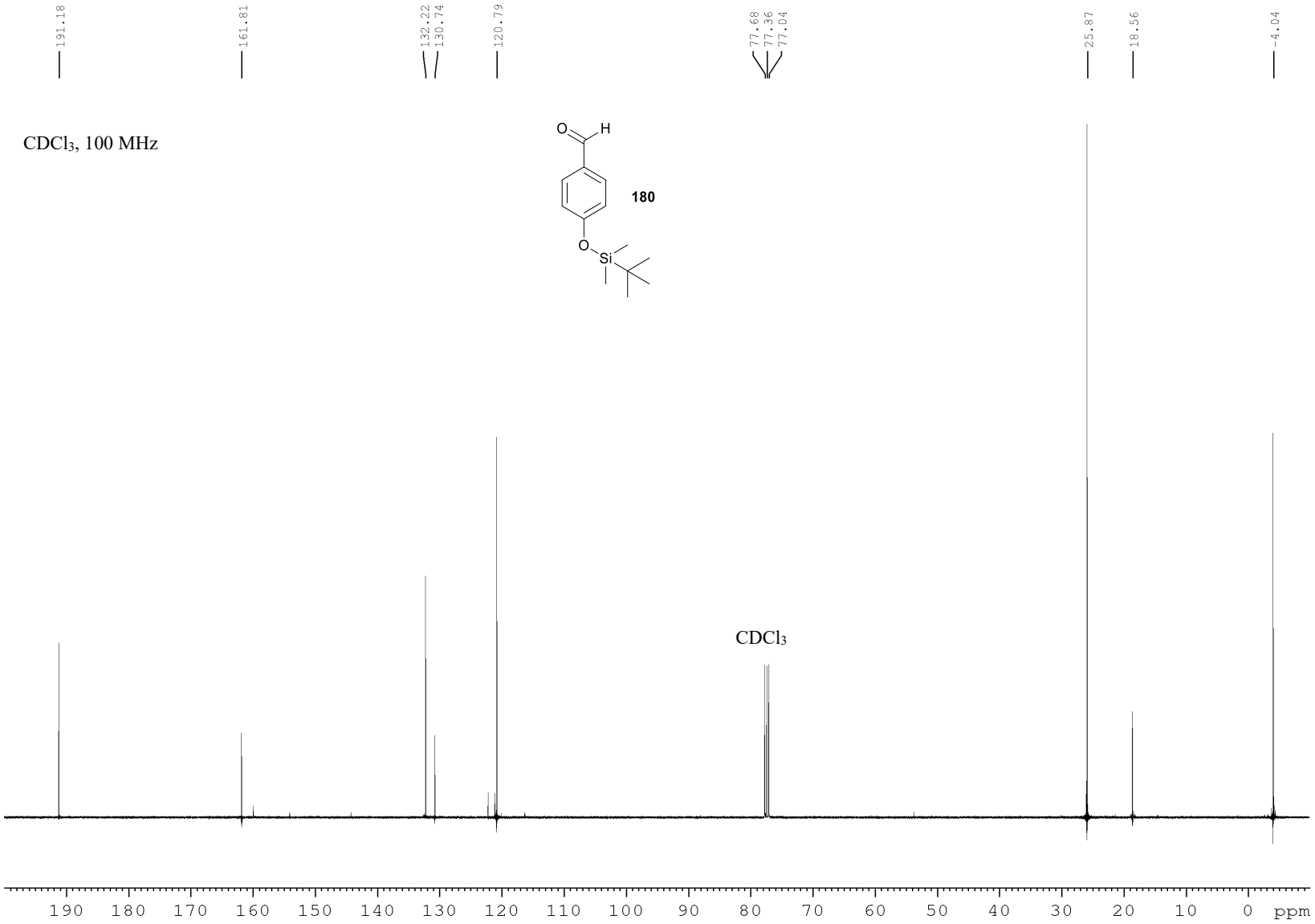
191.18
161.81
132.22
130.74
120.79
77.68
77.36
77.04
25.87
18.56
-4.04
CDCl3, 100 MHz
O
H
180
O
Si
CDCl3
190 180 170 160 150 140 130 120 110 100 90 80 70 60 50 40 30 20 10 0 ppm

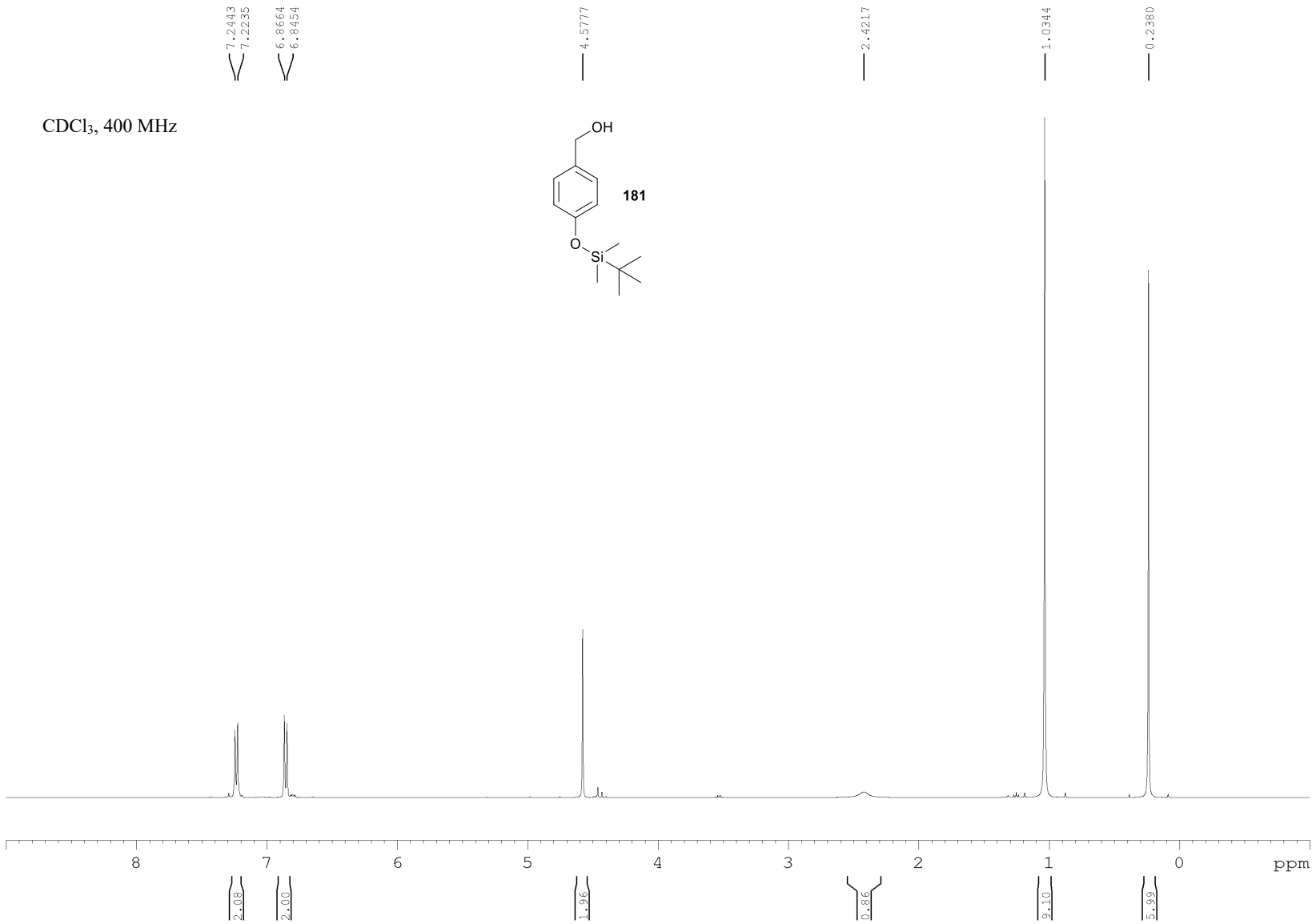
7.2443
7.2235
6.8664
6.8454
4.5777
2.4217
1.0344
0.2380
CDCl3, 400 MHz
OH
181
O
Si
8
7
6
5
4
3
2
1
0
ppm
2.08
2.00
1.96
0.86
9.10
5.99

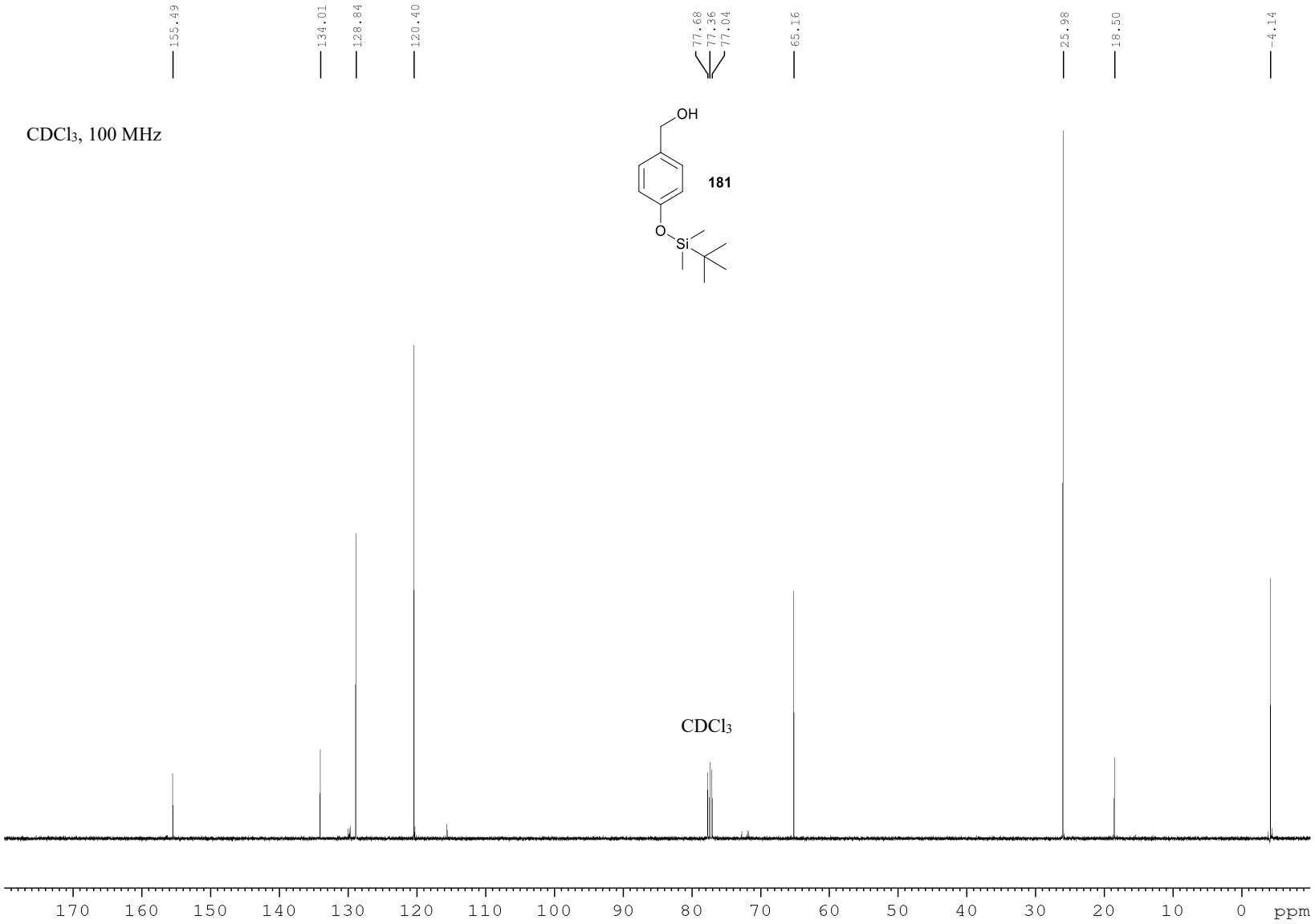
155.49
134.01
128.84
120.40
77.68
77.36
77.04
65.16
25.98
18.50
-4.14
CDCl3, 100 MHz
OH
181
O
Si
CDCl3
170
160
150
140
130
120
110
100
90
80
70
60
50
40
30
20
10
0
ppm

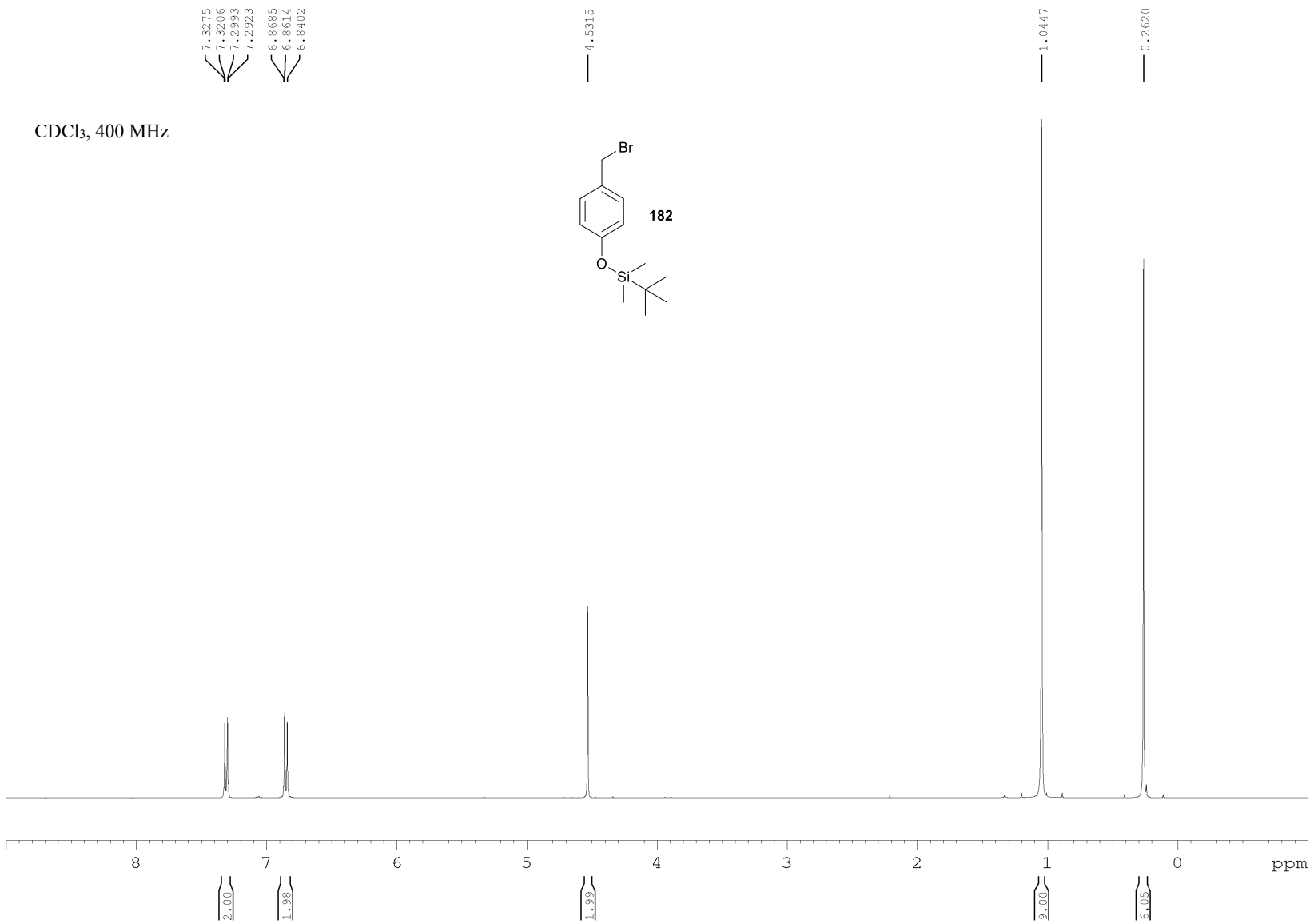
7.3275
7.3206
7.2993
7.2923
6.8685
6.8614
6.8402
4.5315
1.0447
0.2620
CDCl3, 400 MHz
Br
182
O
Si
8
7
6
5
4
3
2
1
0
ppm
2.00
1.98
1.99
9.00
6.05

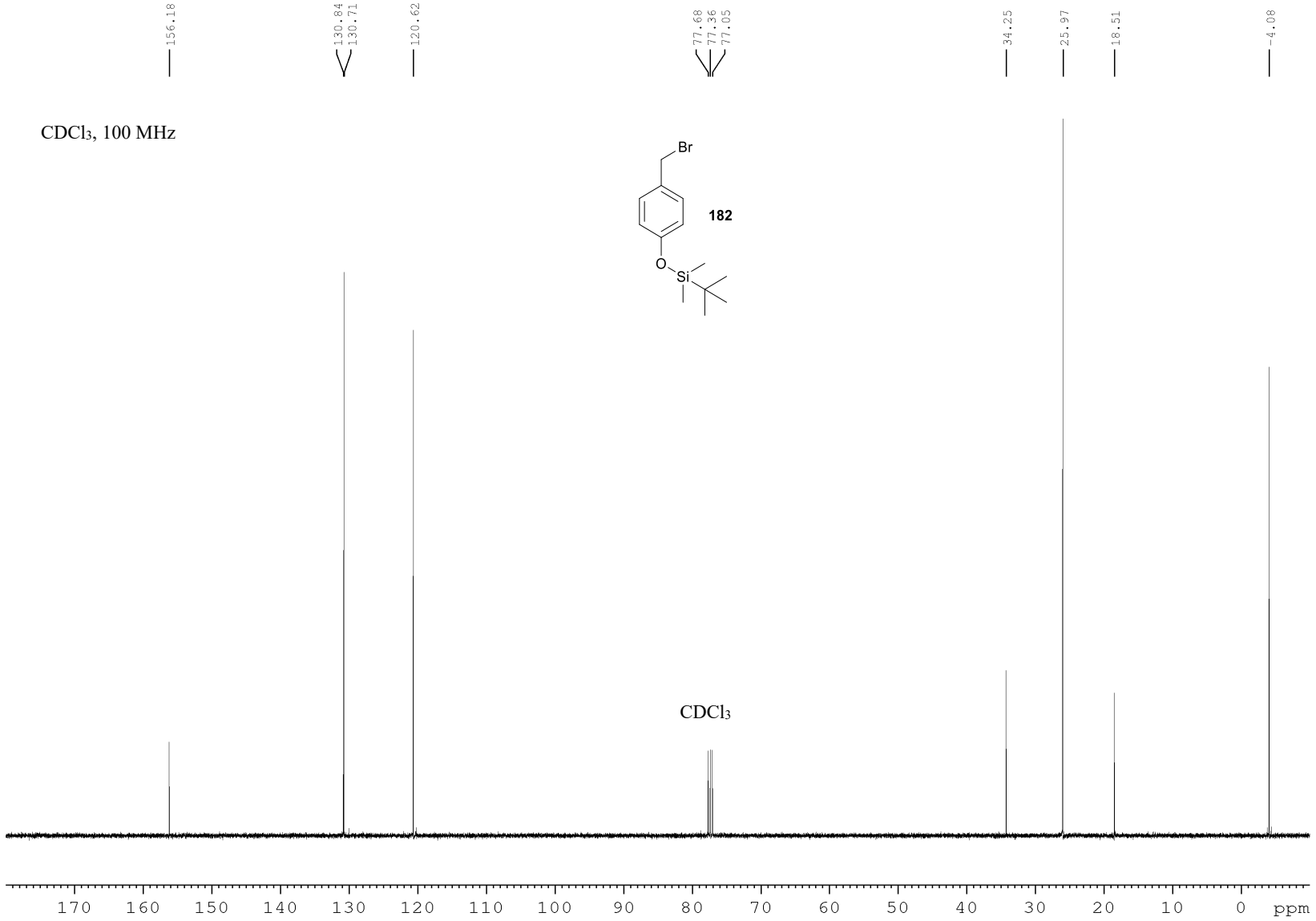
156.18
130.84
130.71
120.62
77.68
77.36
77.05
34.25
25.97
18.51
-4.08
CDCl3, 100 MHz
Br
182
O
Si
CDCl3
170
160
150
140
130
120
110
100
90
80
70
60
50
40
30
20
10
0
ppm

$CDCl_3$, 400 MHz

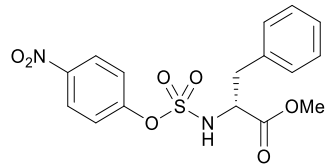

195

171.32
154.54
146.19
134.85
129.70
129.14
127.92
125.74
122.65
77.68
77.36
77.04
58.36
53.29
39.04

$CDCl_3$, 100 MHz

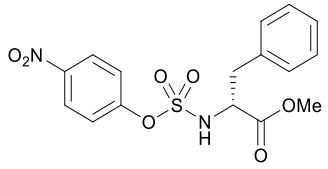

195

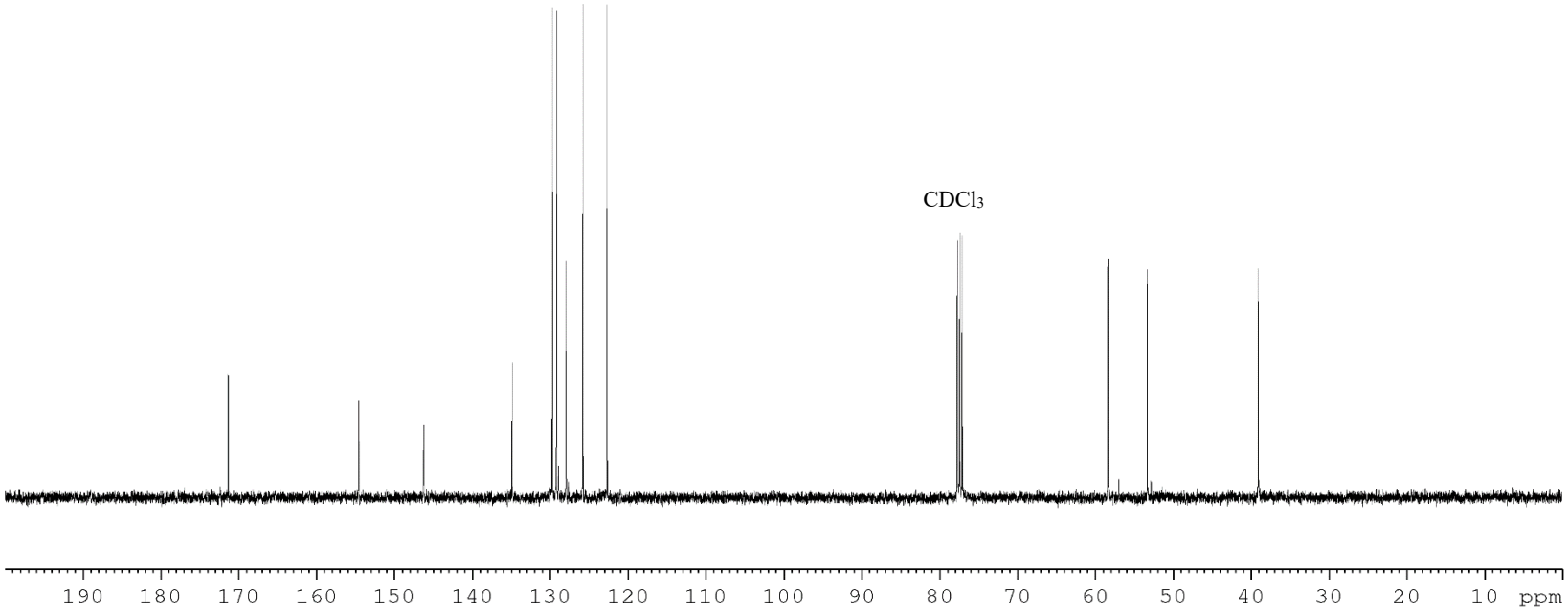

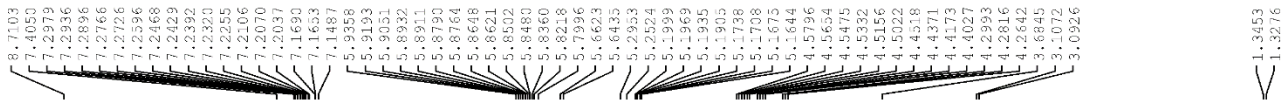

$CDCl_3$, 400 MHz

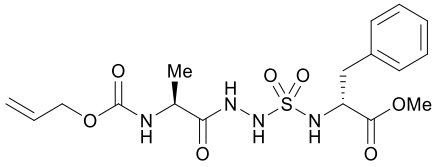

193

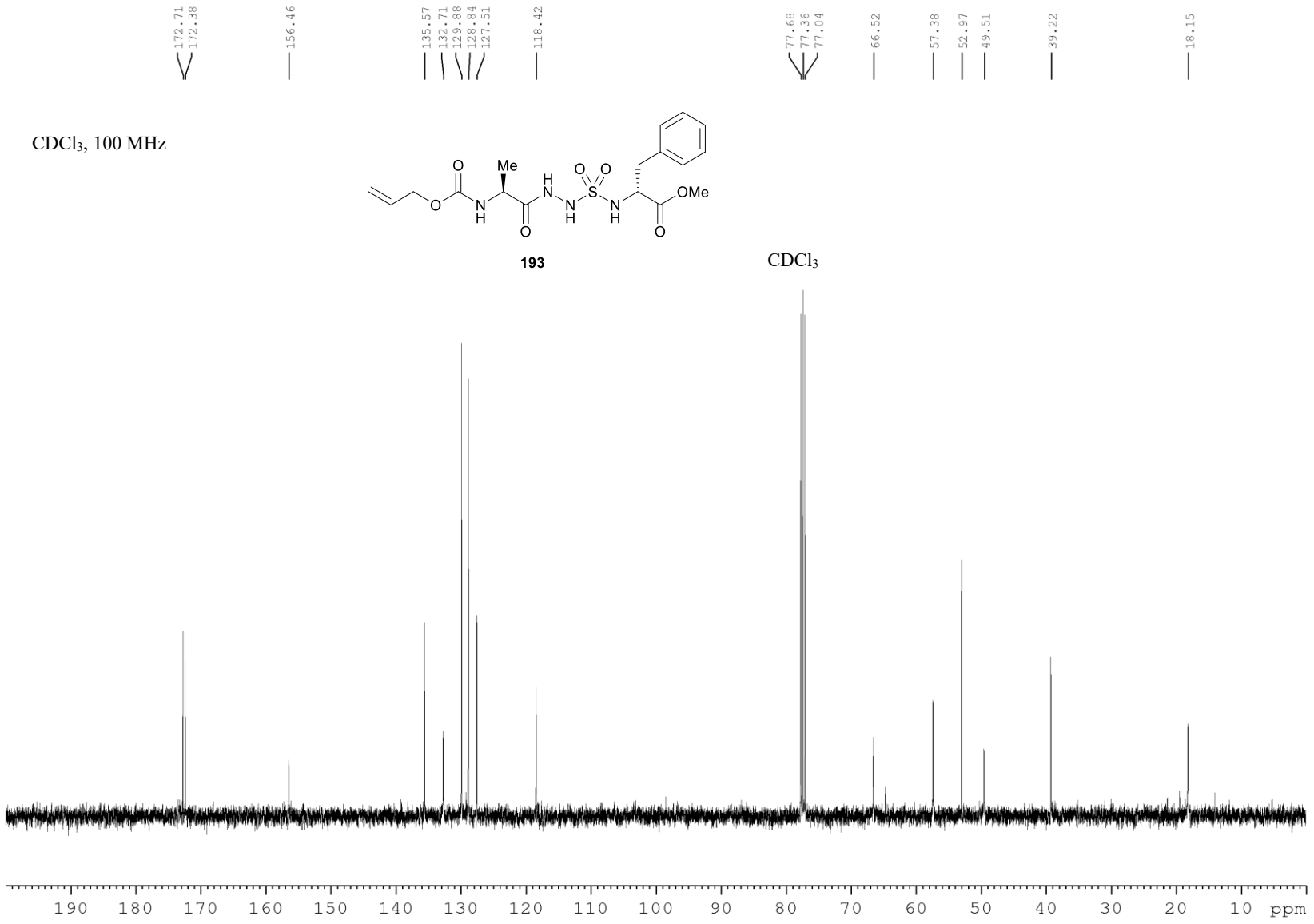
172.71
172.38
156.46
135.57
132.71
129.88
128.84
127.51
118.42
77.68
77.36
77.04
66.52
57.38
52.97
49.51
39.22
18.15
CDCl3, 100 MHz
Me
OMe
193
CDCl3
190 180 170 160 150 140 130 120 110 100 90 80 70 60 50 40 30 20 10 ppm

Annexe 6 : Spectres LC-MS

Data File name: C:\BACKUP_2013\2013SEPT18\ST0147_(5-80MEOHS).D
Date:18 September 2013
Acq method: C:\CHEM32\1\METHODS\LC_05_80_12MN_MEOH_

0.5mL/min

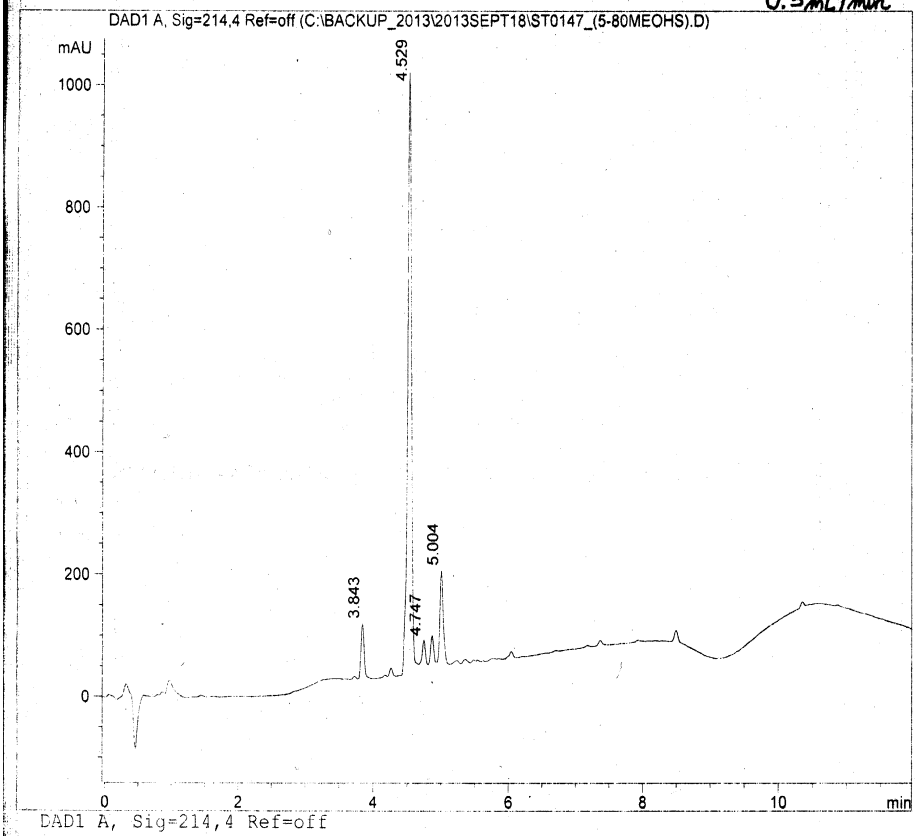

DAD1 A, Sig=214,4 Ref=off

Ret. Time	Height	Area	Area %	
3.843	91.254	282.471	5.863	
4.529	979.892	3762.439	78.096	Alloc-A-AoG-ϱ-K-NH2
4.747	39.288	114.151	2.369	
4.867	45.366	131.166	2.723	
5.004	152.331	527.454	10.948	

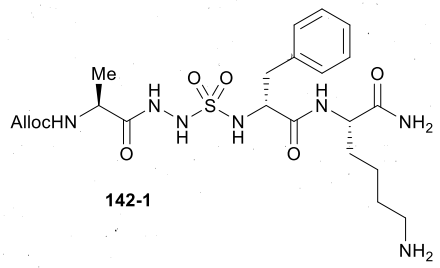

142-1

Data File name: C:\BACKUP_2013\2013NOV08\ST0180_(20-80MEOH).D
Date:8 November 2013
Acq method: C:\CHEM32\1\METHODS\LC_20_80_12MN_MEOH_

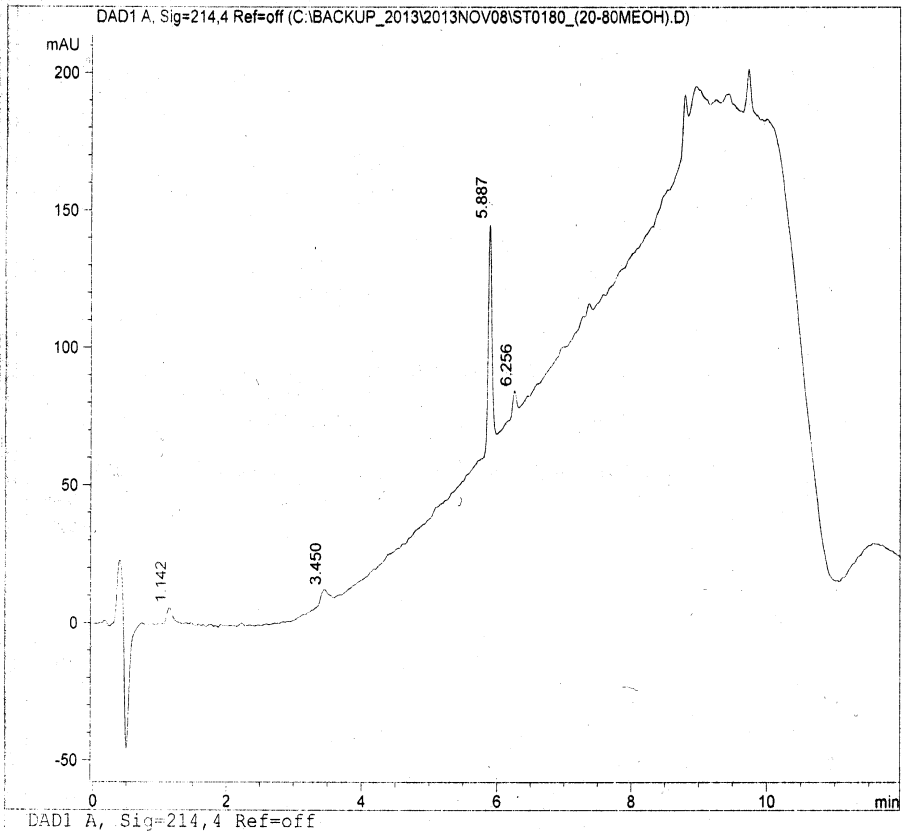

DAD1 A, Sig=214,4 Ref=off

Ret. Time	Height	Area	Area %
1.142	5.620	31.094	8.003
3.450	4.875	36.088	9.288
5.887	80.399	292.749	75.346
6.256	8.255	28.607	7.363

Alloc-A-AₒF-ƒ-K-NH₂

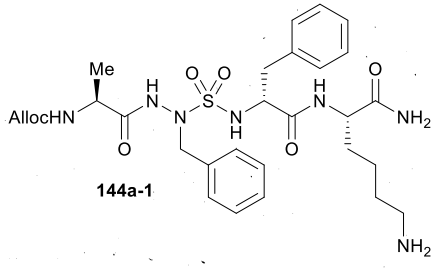

144a-1

Data File name: C:\BACKUP_2013\2013NOV11\ST0182_(5-80MEOH).D
Date:11 November 2013
Acq method: C:\CHEM32\1\METHODS\LC_05_80_12MN_MEOH_

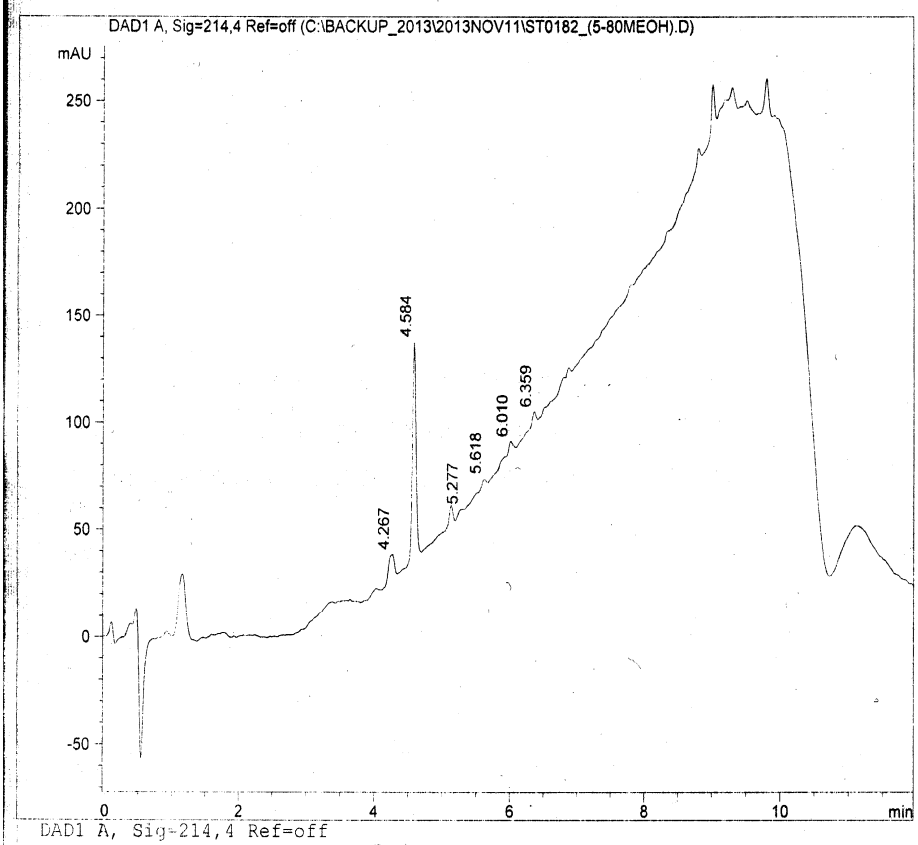

DAD1 A, Sig=214,4 Ref=off

Ret. Time	Height	Area	Area %
4.267	11.470	65.685	12.390
4.584	101.007	369.393	69.680
5.131	8.568	29.004	5.471
5.277	2.097	9.043	1.706
5.618	3.778	15.567	2.937
6.010	5.669	22.283	4.203
6.359	5.771	19.154	3.613

A-A-F-β-K-NH_2

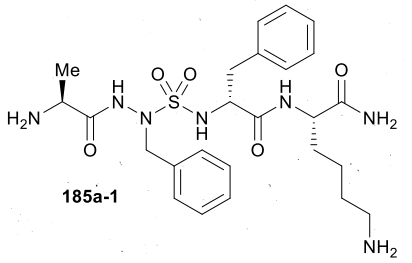

185a-1

Data File name: C:\BACKUP_2013\2013NOV18\ST0185_(15-45MEOH).D
Date:18 November 2013
Acq method: C:\CHEM32\1\METHODS\LC_15_45_12MN_MEOH_

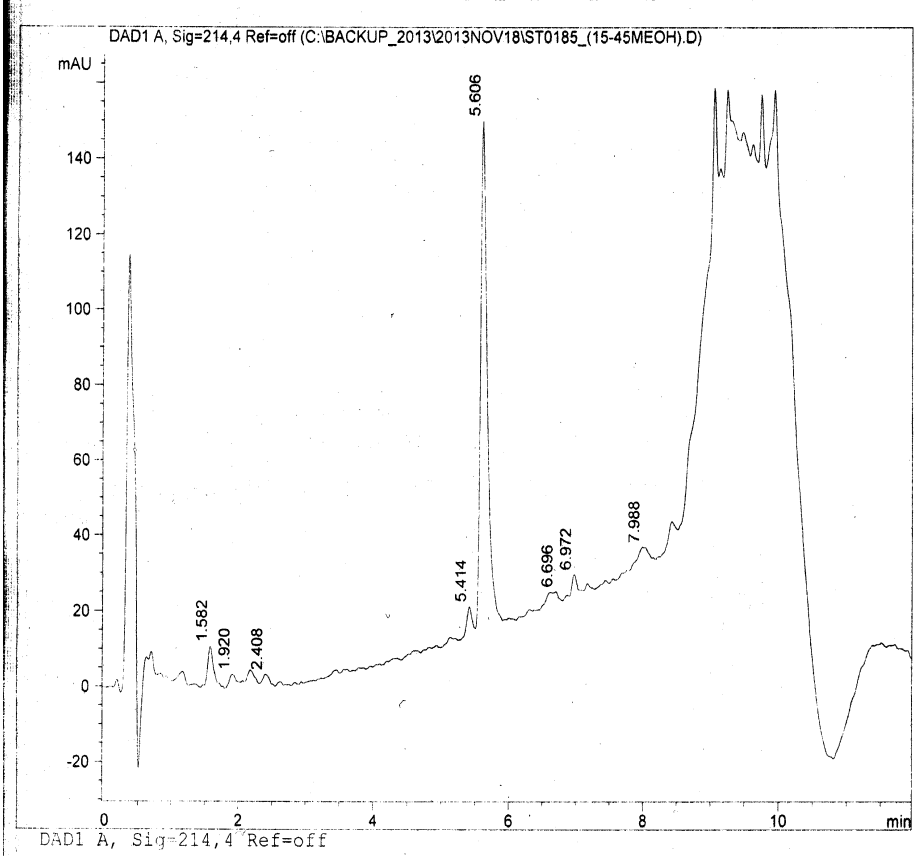

DAD1 A, Sig=214,4 Ref=off

Ret. Time	Height	Area	Area %
1.582	10.670	64.785	5.507
1.920	2.792	16.023	1.362
2.179	3.429	22.165	1.884
2.408	2.713	16.809	1.429
5.414	6.892	32.963	2.802
5.606	134.109	920.440	78.247
6.696	2.949	35.258	2.997
6.972	5.243	23.045	1.959
7.988	4.310	44.832	3.811

H-w-A-AaF-f-K-NH2

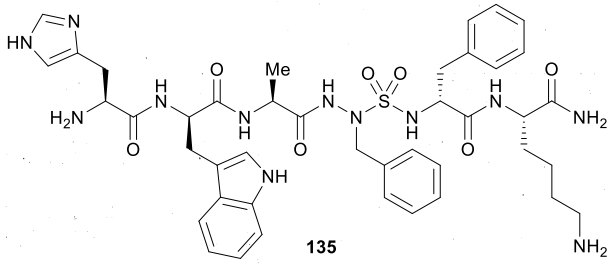

135

D-7000 HPLC System Manager Report

Analyzed: 01/11/10 12:40 PM
Reported: 01/11/10 01:47 PM
Processed: 01/11/10 01:47 PM

Data Path: H:\echantillons\DATA\0246\
Processing Method: Grad 05-80%MeOH 30min(40min)ST

System(acquisition): Sys 1
Series:0246
Application: echantillons
Vial Number: 3
Sample Name: SPST-7-1(P2)_5-80MeOH
Vial Type: UNK
Injection from this vial: 1 of 1
Volume: 5.0 ul
Sample Description: SPST-7-1(P2)_5-80MeOH

Chrom Type: Fixed WL Chromatogram, 214 nm

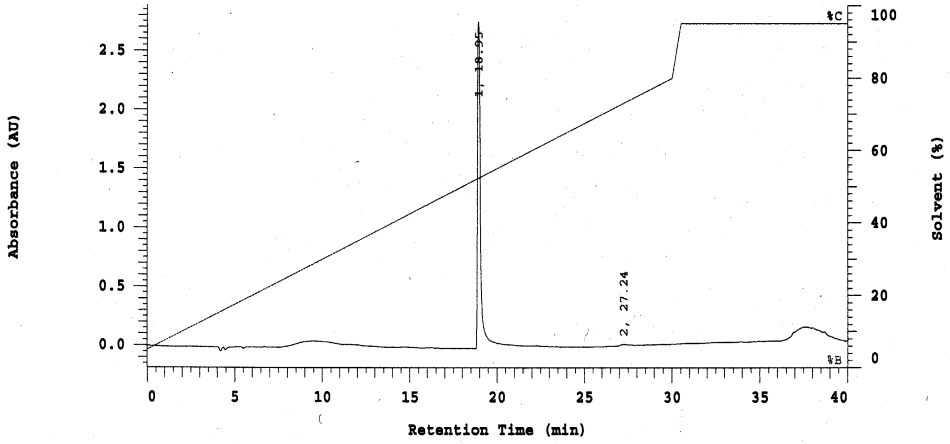

Acquisition Method: Grad 05-80%MeOH 30min(40min)ST
Column Type:
Developed by: Lubell
Pump A Type: L-7100
Solvent A: H2O 0.1% FA
Solvent B: MeCN 0.1% FA
Solvent C: MeOH 0.1% FA
Solvent D: Storage H2O/ORG 35/65 no FA
Method Description: grad 5 to 80% MeOH in 30 min, 10 min wash at 95% MeOH

Chrom Type: Fixed WL Chromatogram, 214 nm

Peak Quantitation: AREA
Calculation Method: AREA%

No.	RT	Area	Area %
1	18.95	15485900	98.771
2	27.24	192660	1.229
		15678560	100.000

H-w-A-AaF-L-K-NH2

Peak rejection level: 10000

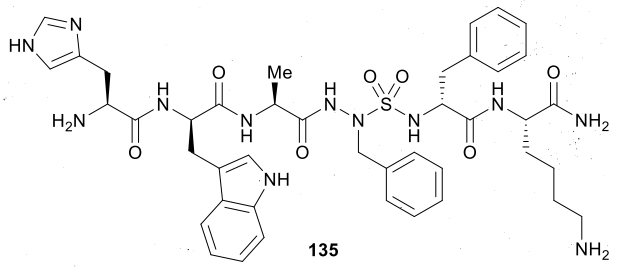

135

D-7000 HPLC System Manager Report

Analyzed: 01/11/10 10:55 AM
Reported: 01/11/10 01:48 PM
Processed: 01/11/10 01:45 PM

Data Path: H:\echantillons\DATA\0244\
Processing Method: Grad 05-80%MeCN 30min(40min)ST

System(acquisition): Sys 1
Series:0244
Application: echantillons
Vial Number: 3
Sample Name: SPST-7-1(P2)_5-80MeCN
Vial Type: UNK
Injection from this vial: 1 of 1
Volume: 5.0 ul
Sample Description: SPST-7-1(P2)_5-80MeCN

Chrom Type: Fixed WL Chromatogram, 214 nm

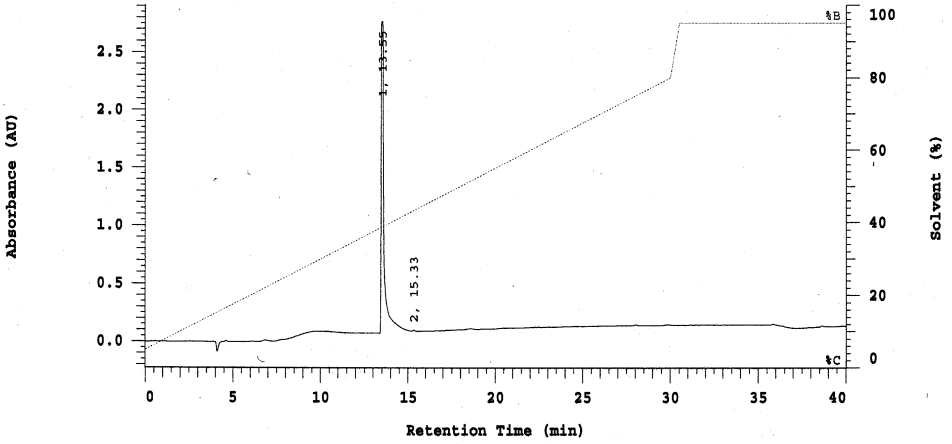

Acquisition Method: Grad 05-80%MeCN 30min(40min)ST
Column Type:
Developed by: Lubell
Pump A Type: L-7100
Solvent A: H2O 0.1% FA
Solvent B: MeCN 0.1% FA
Solvent C: MeOH 0.1% FA
Solvent D: Storage H2O/ORG 35/65 no FA
Method Description: grad 5 to 80% MeCN in 30 min, 10 min wash at 95% MeCN

Chrom Type: Fixed WL Chromatogram, 214 nm

Peak Quantitation: AREA
Calculation Method: AREA%

No.	RT	Area	Area %
1	13.55	16142720	99.809
2	15.33	30920	0.191
		16173640	100.000

H-His-Ala-Trp-Me-Phe-Sta-Phe-Lys-NH2

Peak rejection level: 10000

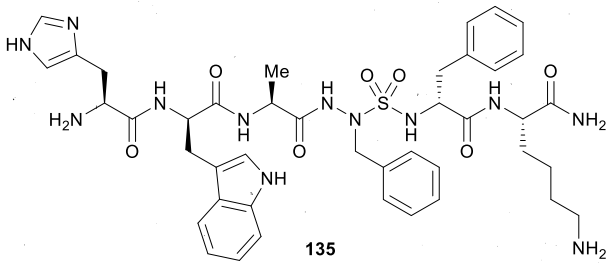

135

Page Indicator 1 / 1

Data File name: C:\BACKUP_2013\2013SEPT20\ST0148_(5-80MEOH3).D
Date:20 September 2013
Acq method: C:\CHEM32\1\METHODS\LC_05_80_14MN_MEOH_

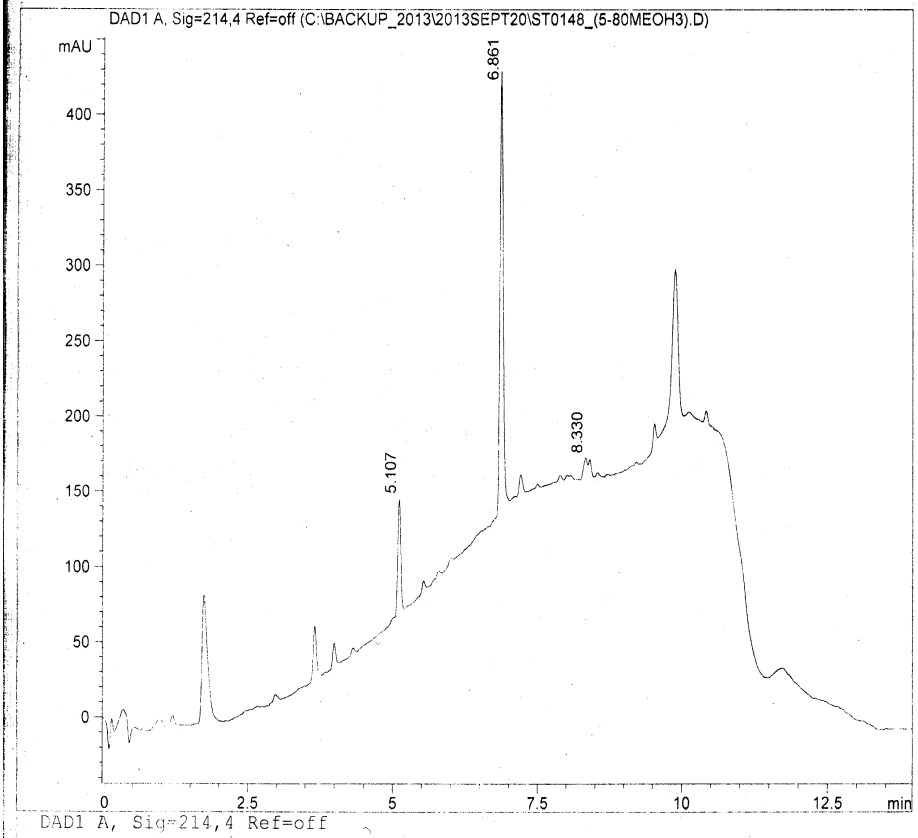

DAD1 A, Sig=214,4 Ref=off

Ret. Time	Height	Area	Area %	
5.107	76.188	265.569	17.328	Alloc-A-AαG-β-K-NH2
6.861	295.947	1151.118	75.109	Alloc-A-AαF(4-F)-β-K-NH2
8.330	14.771	115.910	7.563	Alloc-A-AαF(4-F)-(4-F-Bn)β-K-NH2

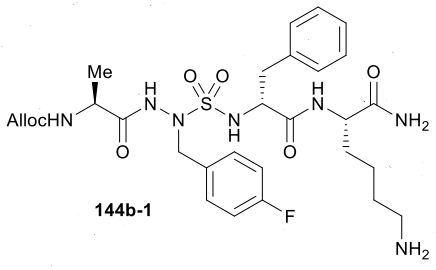

144b-1

Data File name: C:\BACKUP_2013\2013SEPT23\ST0150_(5-80MEOHS).D
Date:23 September 2013
Acq method: C:\CHEM32\1\METHODS\LC_05_80_14MN_MEOH_

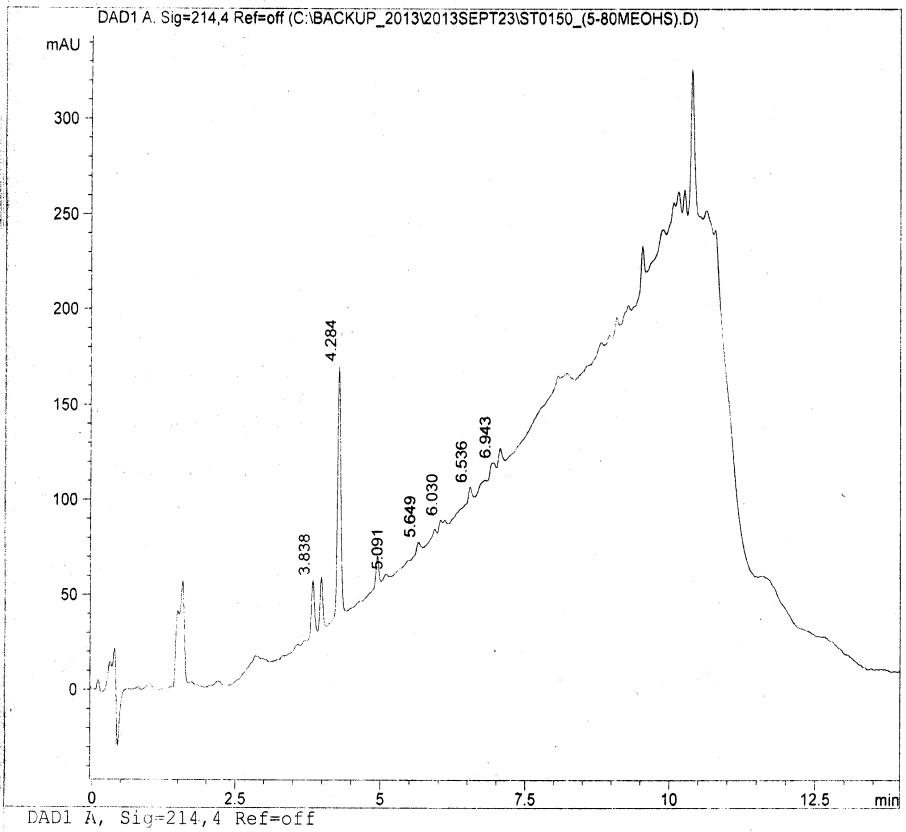

DAD1 A, Sig=214,4 Ref=off

Ret. Time	Height	Area	Area %
3.838	29.255	102.843	10.995
3.985	27.560	90.503	9.676
4.284	131.594	508.474	54.362
4.944	15.444	50.025	5.348
5.091	3.378	17.532	1.874
5.649	4.593	16.791	1.795
5.928	3.550	13.897	1.486
6.030	5.322	30.296	3.239
6.536	7.291	25.182	2.692
6.791	2.237	21.071	2.253
6.943	4.774	28.430	3.039
7.053	8.349	30.312	3.241

A-Aa-F(4-F)-f-K-NH2

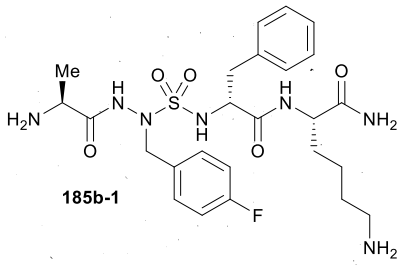

185b-1

Data File name: C:\BACKUP_2014\2014JULY30\LDY84_(20-80MEOH).D
Date:31 July 2014
Acq method: C:\CHEM32\1\METHODS\LC_20_80_14MN_MEOH_

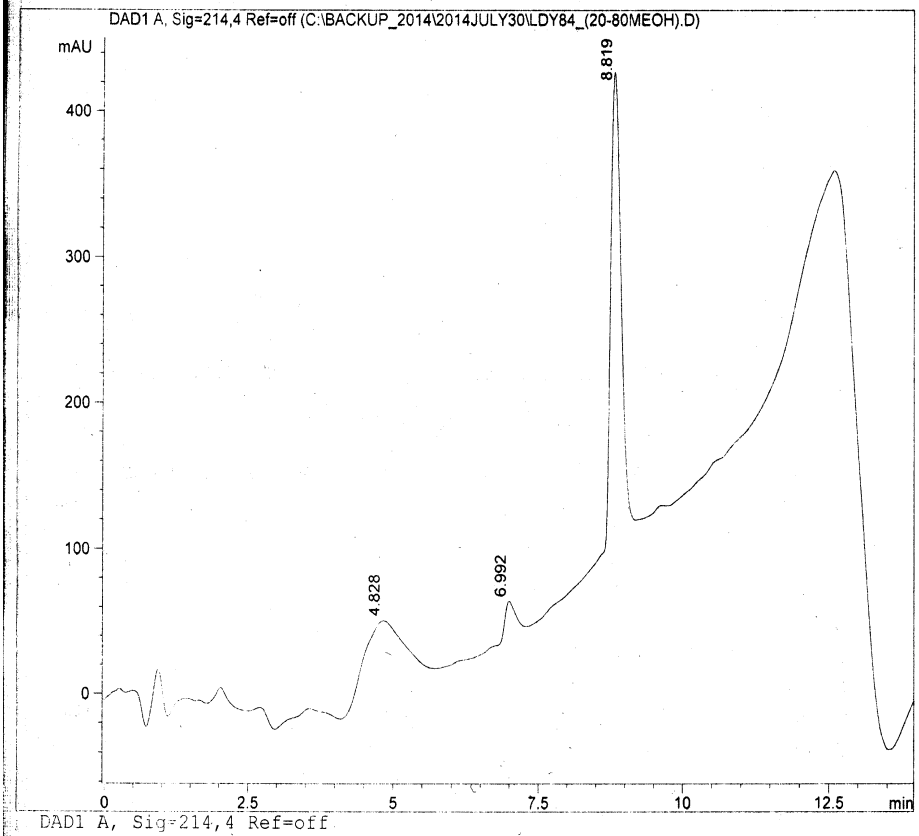

DAD1 A, Sig=214,4 Ref=off

Ret. Time	Height	Area	Area %
4.828	53.121	2536.508	36.781
6.992	25.422	311.783	4.521
8.819	324.004	4047.920	58.698

A-w-A-AaF(4-F)-f-k-NH2

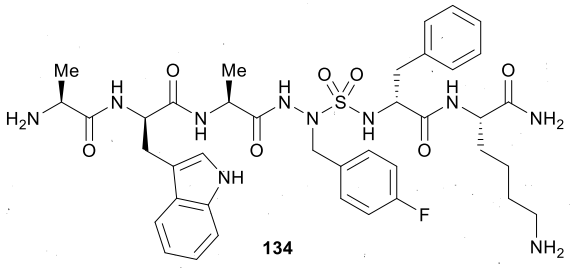

134

Data File name: C:\BACKUP_2014\2014AUG13\WDL-LDY-88-LC_20_80_14MN_MEOH_ST_ ->
Date:13 July 2014
Acq method: C:\CHEM32\1\METHODS\LC_20_80_14MN_MEOH_

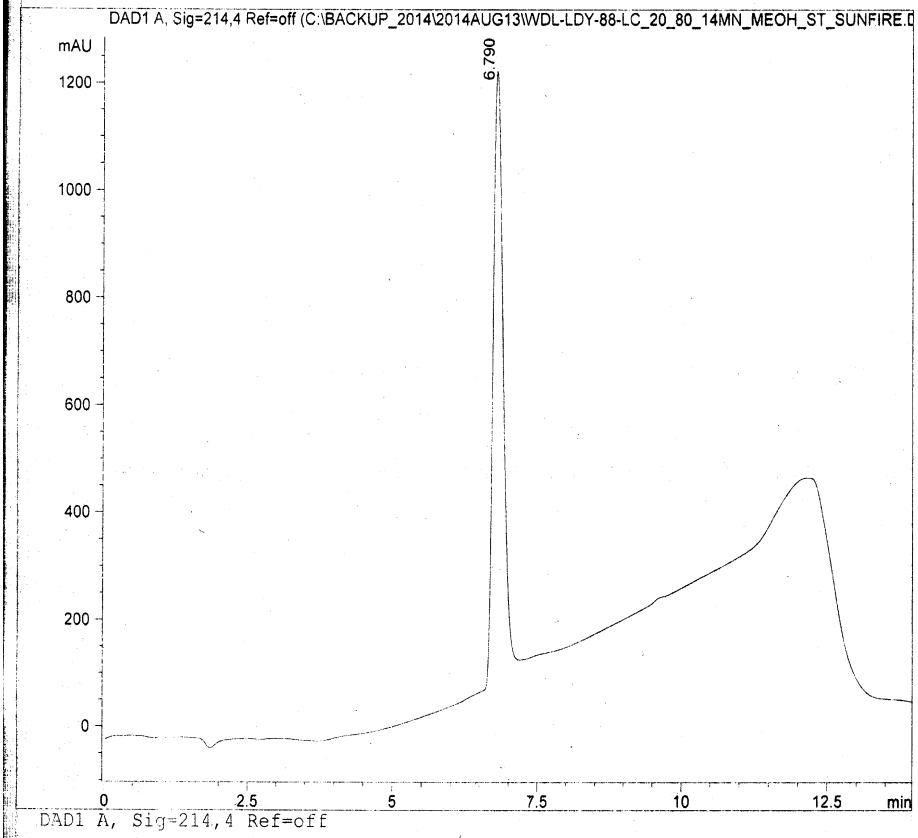

DAD1 A, Sig=214,4 Ref=off

Ret. Time	Height	Area	Area %
6.790	1136.814	13696.925	100.000

A-w-A-Aof(4-F)-f-k-NH2

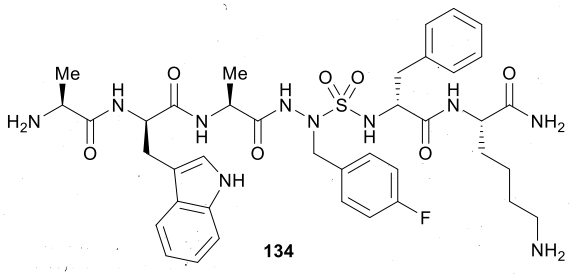

134

Data File name: C:\BACKUP_2014\2014AUG13\WDL-LDY-84-10-80-ACN-14MIN.D
Date:13 July 2014
Acq method: C:\CHEM32\1\METHODS\LC_10_80_14MN_ACN_S

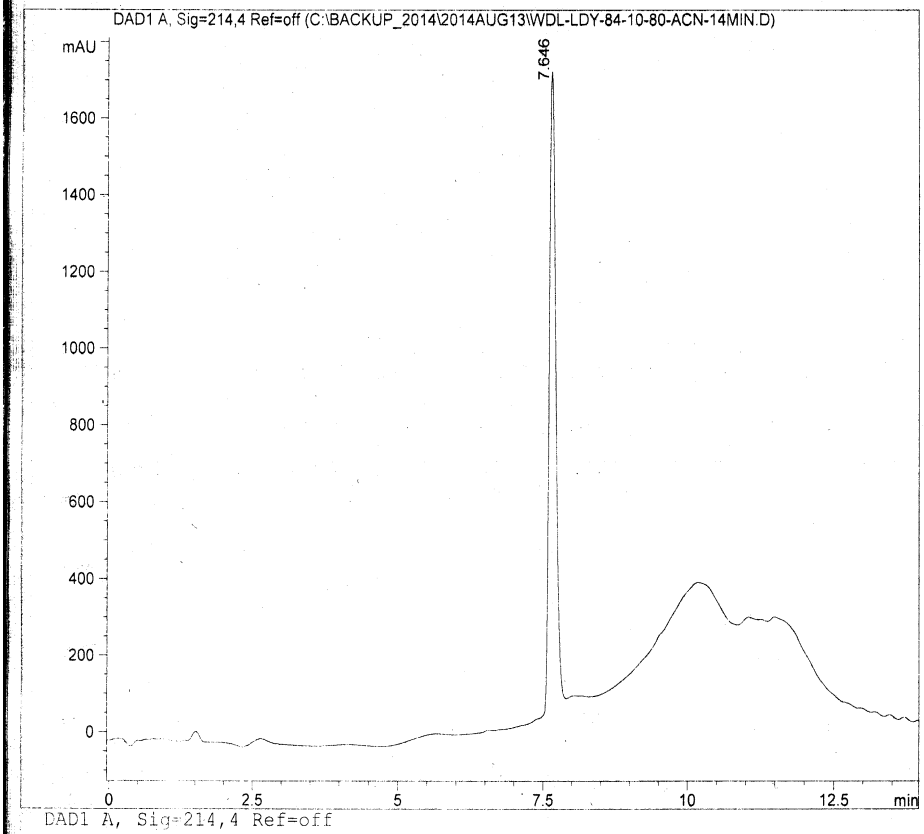

DAD1 A, Sig=214,4 Ref=off

Ret. Time	Height	Area	Area %
7.646	1664.685	13041.017	100.000

A-w-A-AaF(4-F)-f-K-NH2

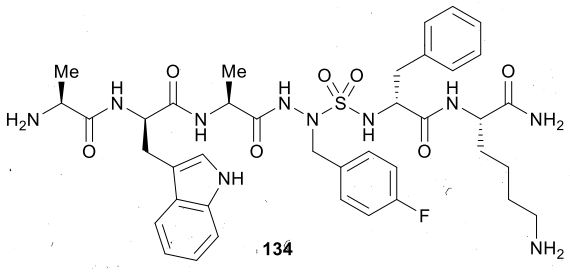

134

Data File name: C:\BACKUP_2013\2013SEPT30\ST0159_(5-80MEOH2).D
Date:30 September 2013
Acq method: C:\CHEM32\1\METHODS\LC_05_80_14MN_MEOH_

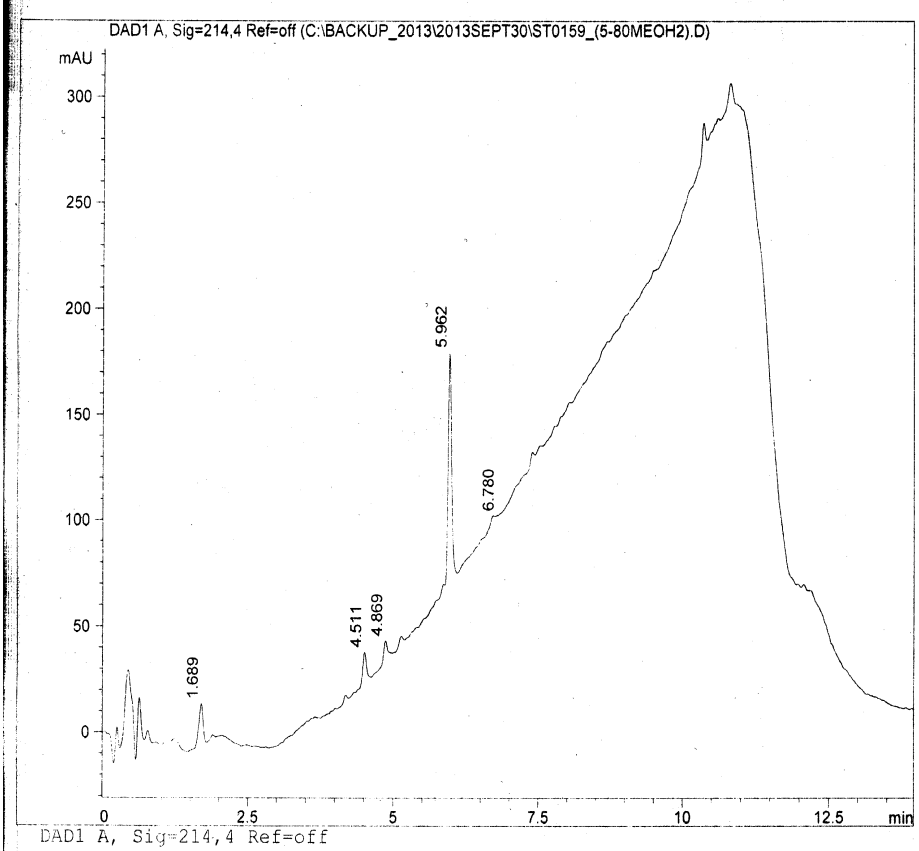

DAD1 A, Sig=214,4 Ref=off

Ret. Time	Height	Area	Area %
1.689	19.618	100.595	14.688
4.511	14.422	59.982	8.758
4.869	9.950	46.795	6.833
5.140	4.143	18.421	2.690
5.962	107.530	434.741	63.478
6.780	1.505	24.335	3.553

H-w-A-Aa[F(4-F)]-L-K-NH2

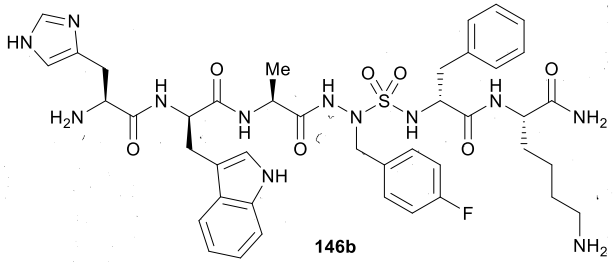

146b

Data File name: C:\BACKUP_2013\2013OCT01\ST0161_(5-80MEOH_PK).D
Date:4 October 2013
Acq method: C:\CHEM32\1\METHODS\LC_05_80_14MN_MEOH_

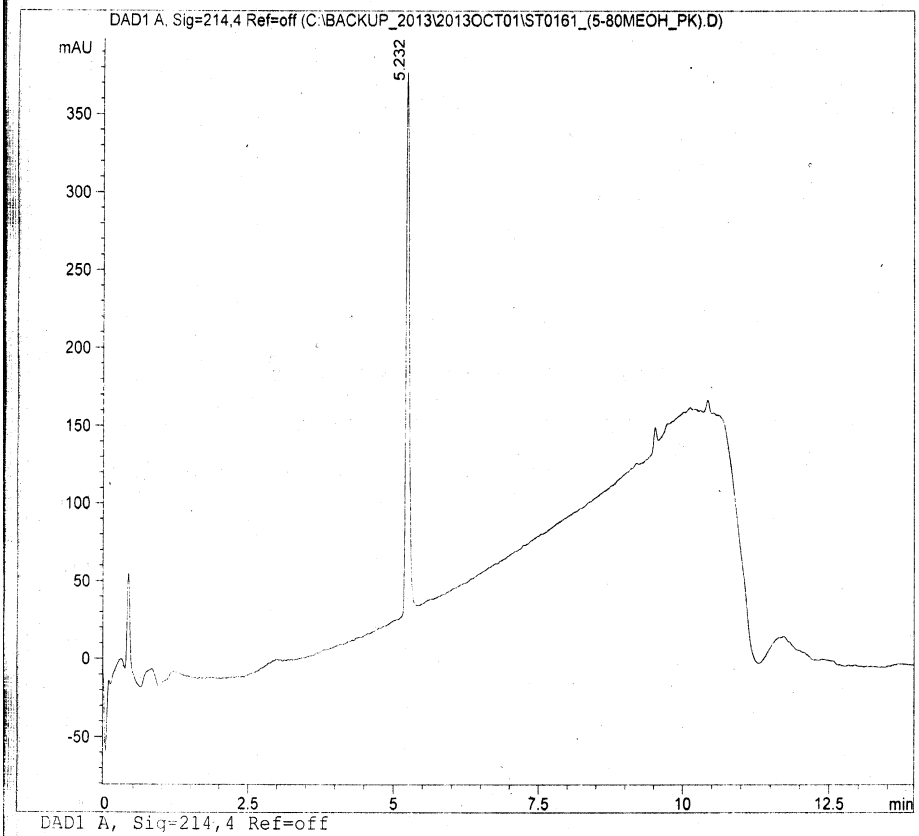

DAD1 A, Sig=214,4 Ref=off

Ret. Time	Height	Area	Area %
5.232	350.911	1375.343	100.000

H-w-A-A$_a$F(4-F)-$\mathcal{L}$-K-NH$_2$

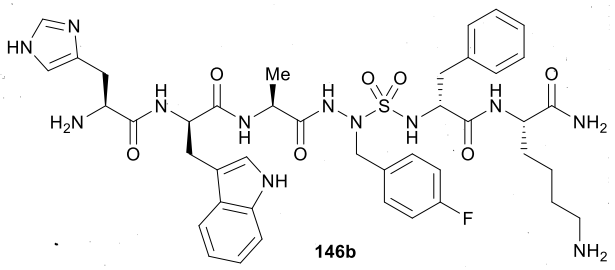

146b

Data File name: C:\BACKUP_2013\2013OCT01\ST0161_(5-80ACN_PK).D
Date:4 October 2013
Acq method: C:\CHEM32\1\METHODS\LC_05_80_14MN_ACN_S

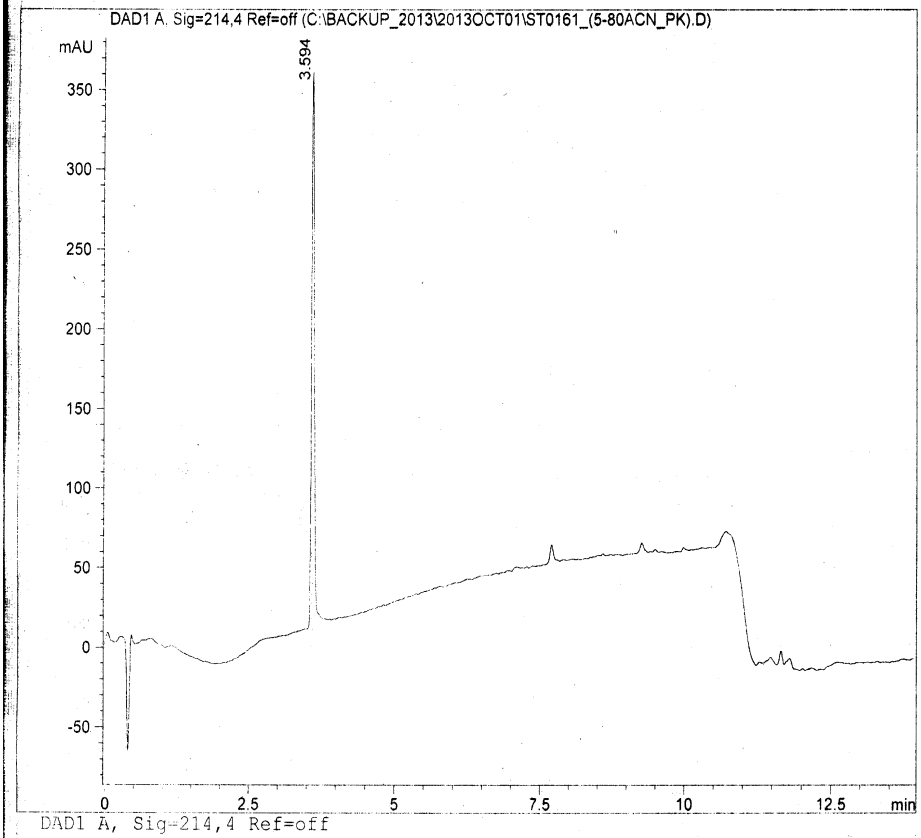

DAD1 A, Sig=214,4 Ref=off

Ret. Time	Height	Area	Area %
3.594	351.151	1173.098	100.000

H-w-A-AoF(4-F)-L-K-NH2

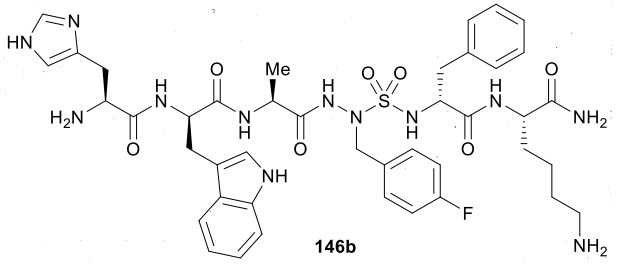

146b

Data File name: C:\CHEM32\1\DATA\2015MAR27\ST0381-3_10-80MEOH.D
Date:27 March 2015
Acq method: C:\CHEM32\1\METHODS\LC_10_80_14MN_MEOH_

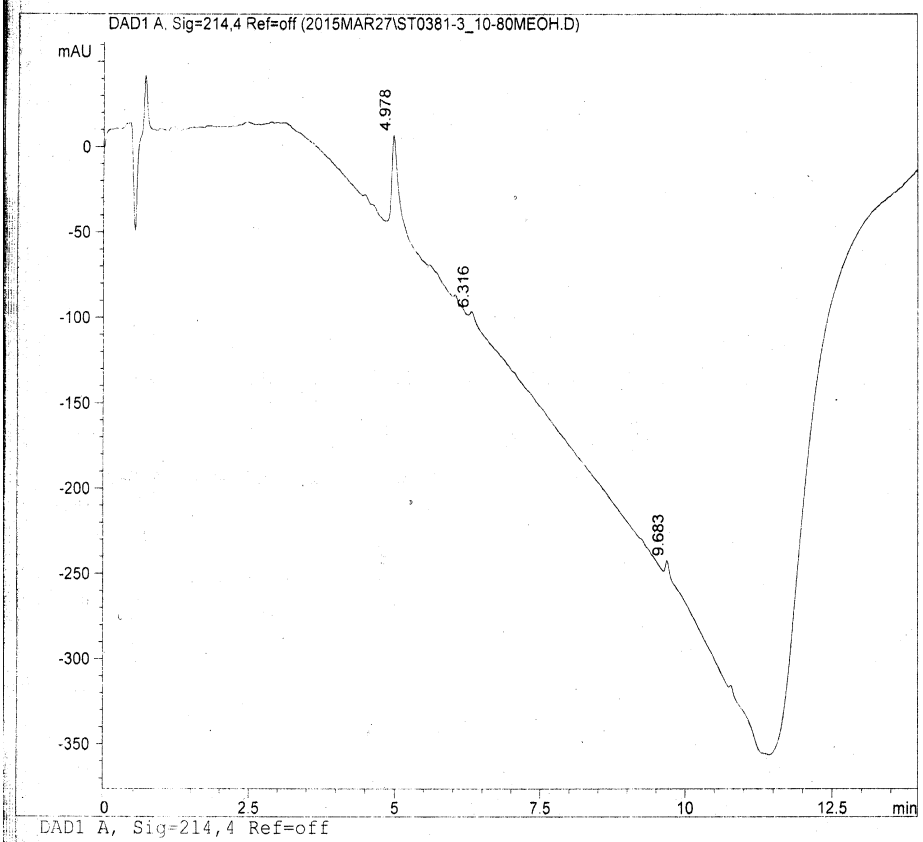

DAD1 A, Sig=214,4 Ref=off

Ret. Time	Height	Area	Area %
4.978	56.509	509.474	85.874
6.036	2.889	11.373	1.917
6.316	5.489	33.571	5.658
9.683	9.101	38.864	6.551

Y-A-H-w-A-Aaf(4-F)-f-K-NH2

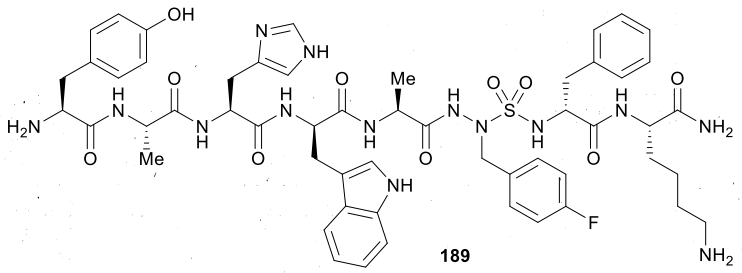

189

Data File name: C:\CHEM32\1\DATA\2015APRIL20\ST0382_PK5-80MEOH.D
Date:20 April 2015
Acq method: C:\CHEM32\1\METHODS\LC_05_80_14MN_MEOH_

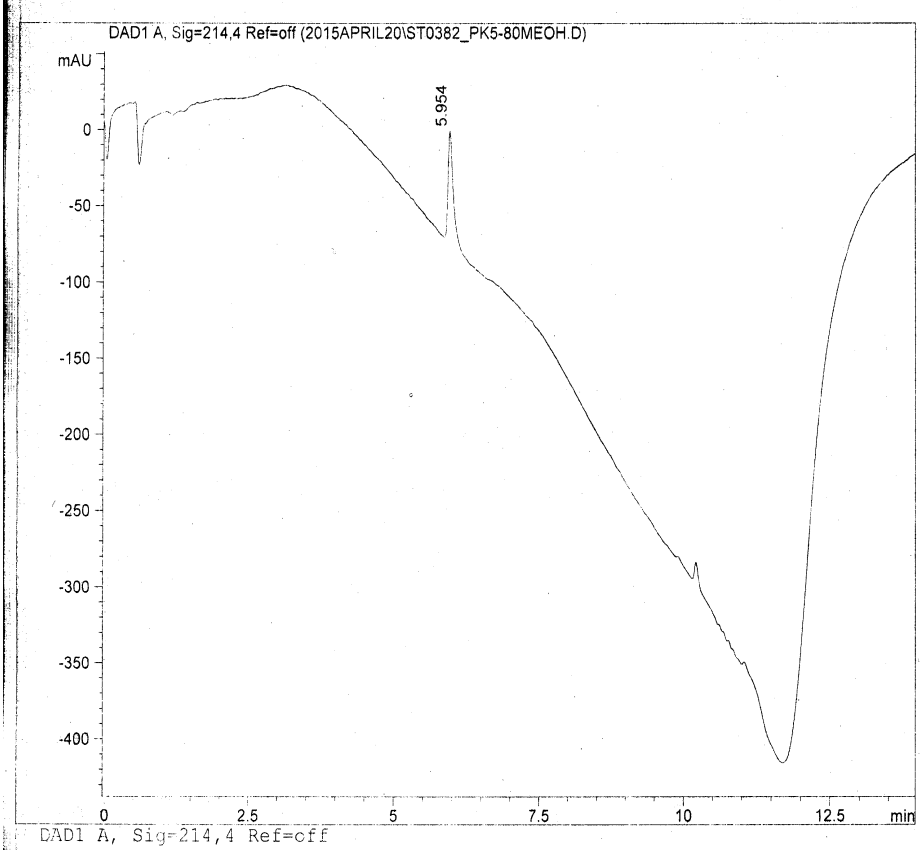

DAD1 A, Sig=214,4 Ref=off

Ret. Time	Height	Area	Area %
5.954	73.467	461.835	100.000

Y-A-H-W-A-AaF(4-F)-L-K-NH2

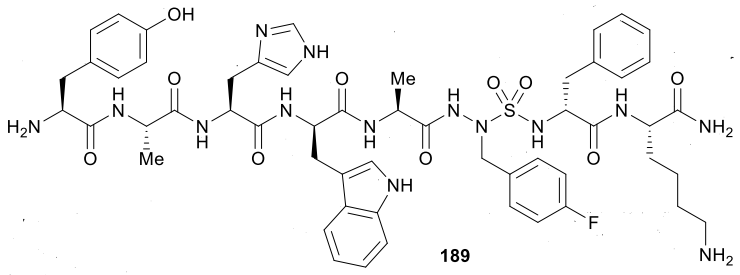

189

Data File name: C:\CHEM32\1\DATA\2015APRIL20\ST0382_PK5-80ACN.D
Date:20 April 2015
Acq method: C:\CHEM32\1\METHODS\LC_05_80_14MN_ACN_S

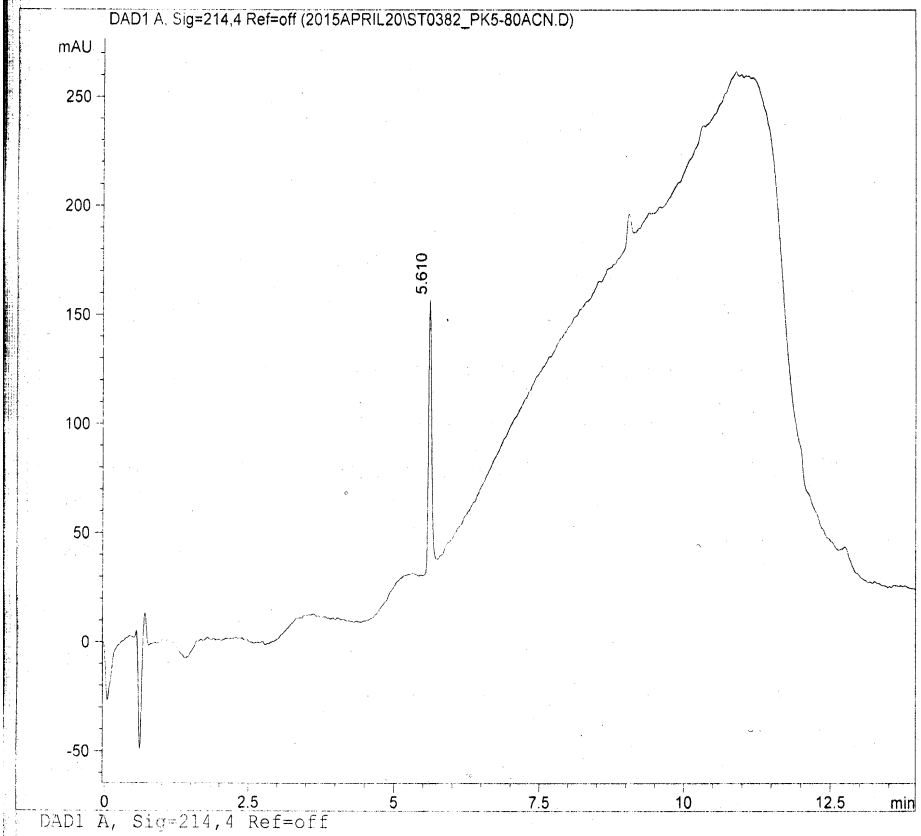

DAD1 A, Sig=214,4 Ref=off

Ret. Time	Height	Area	Area %
5.610	122.997	445.014	100.000

Y-A-H-w-A-AoF(4-F)-L-K-NH2

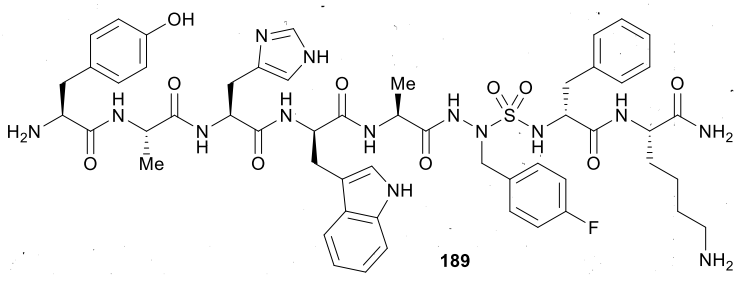

189

Data File name: C:\BACKUP_2013\2013SEPT20\ST0149_(5-80MEOH3).D
Date:20 September 2013
Acq method: C:\CHEM32\1\METHODS\LC_05_80_14MN_MEOH_

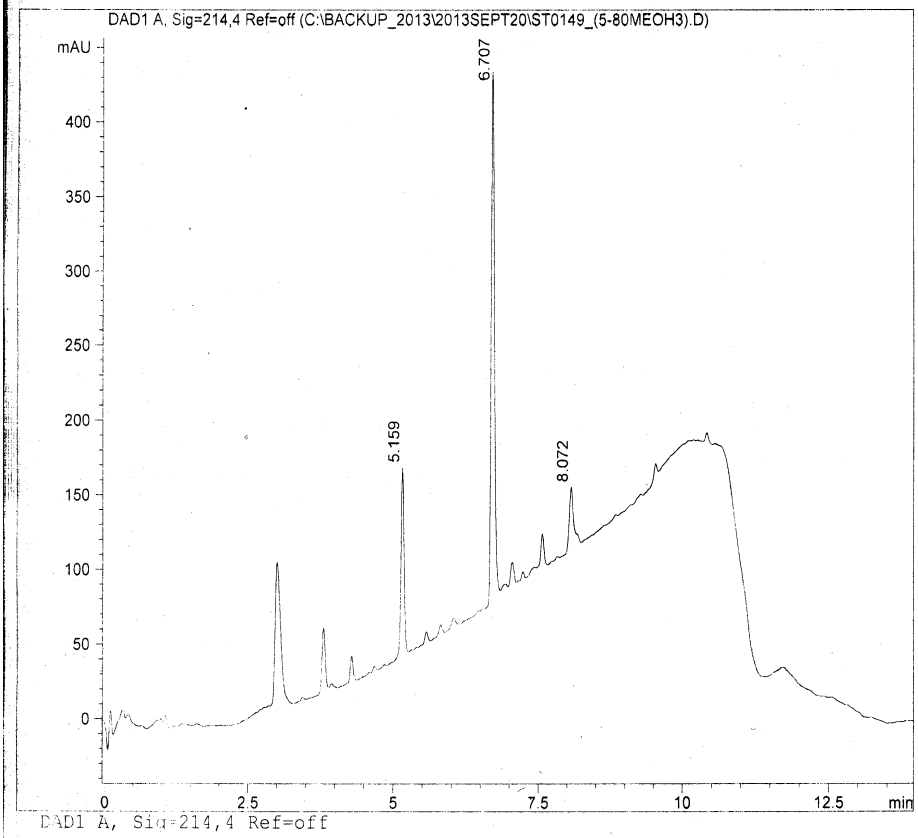

DAD1 A, Sig=214,4 Ref=off

Ret. Time	Height	Area	Area %	
5.159	125.675	460.409	22.249	Alloc-A-AaF-f-K-NH2
6.707	356.143	1372.814	66.341	Alloc-A-AaF(4-MeO)-f-K-NH2
8.072	42.767	236.112	11,410	Alloc-A-AaF(4-MeO)-(4-MeO-Bn)f-K-NH2

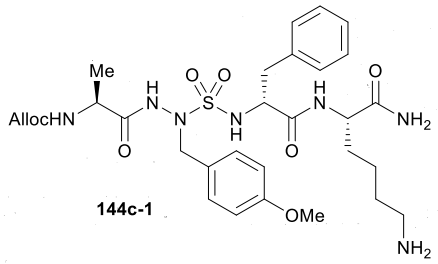

144c-1

Data File name: C:\BACKUP_2013\2013SEPT25\ST0155_(5-80MEOHS).D
Date:26 September 2013
Acq method: C:\CHEM32\1\METHODS\LC_05_80_14MN_MEOH_

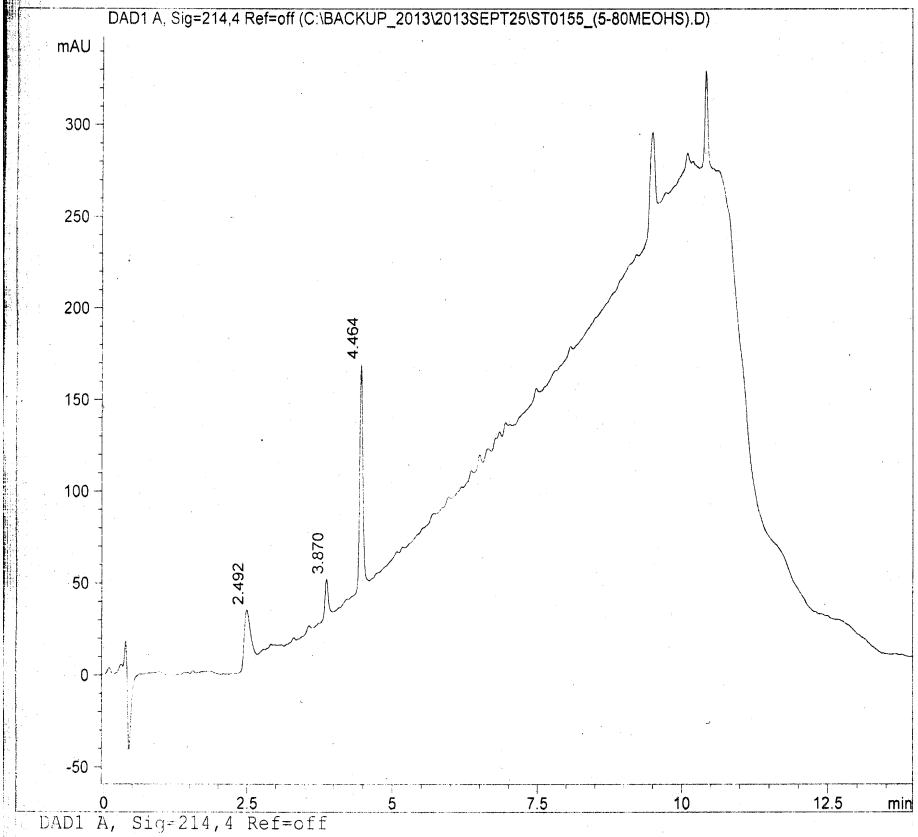

DAD1 A, Sig=214,4 Ref=off

Ret. Time	Height	Area	Area %
2.492	30.071	214.058	28.039
3.870	21.210	85.278	11.171
4.464	122.842	464.083	60.790

A-Asf(4-MeO)-f-K-NH_2

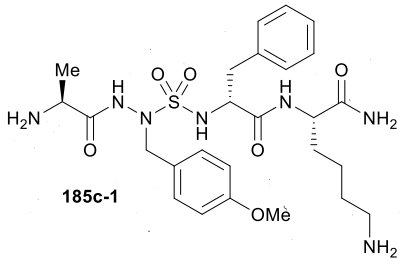

185c-1

Data File name: C:\BACKUP_2013\2013OCT07\ST0166_(5-80MEOH).D
Date:7 October 2013
Acq method: C:\CHEM32\1\METHODS\LC_05_80_14MN_MEOH_

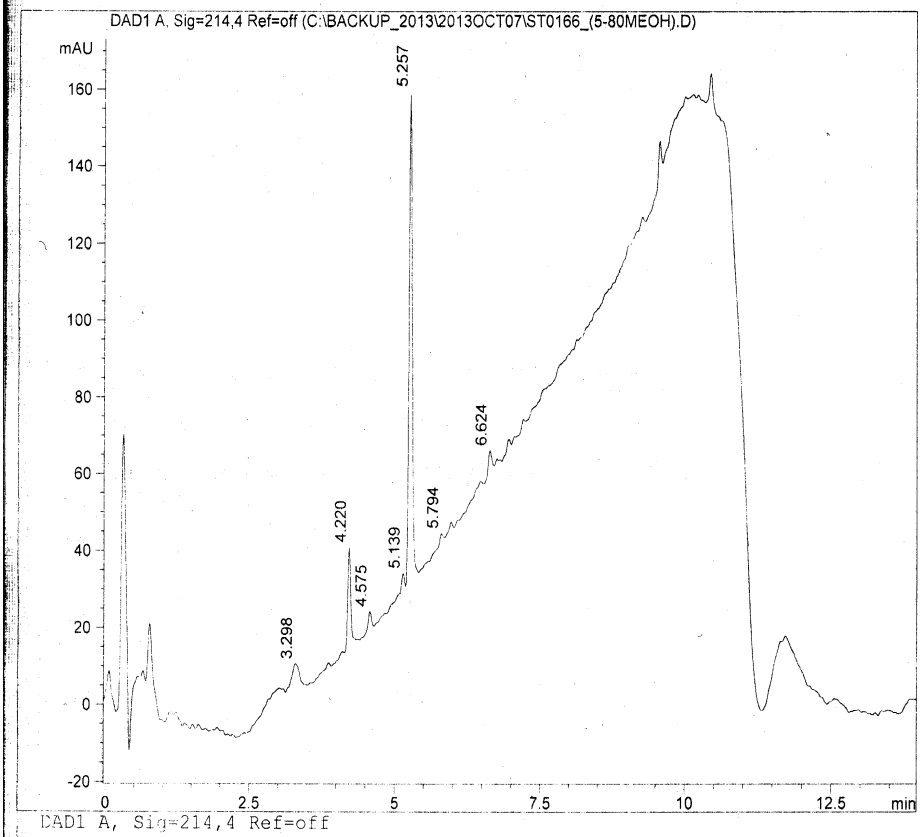

DAD1 A, Sig=214,4 Ref=off

Ret. Time	Height	Area	Area %
3.298	5.993	48.868	7.121
4.220	26.335	94.489	13.769
4.575	5.125	20.313	2.960
5.139	3.784	10.598	1.544
5.257	127.253	478.339	69.704
5.794	2.080	5.329	0.777
5.962	2.030	7.028	1.024
6.624	5.750	21.283	3.101

H-W-A-AcF(4-MeO)-L-K-NH2

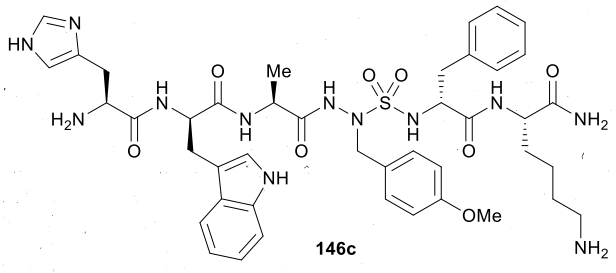

146c

Data File name: C:\BACKUP_2013\2013OCT21\ST0171_(PK15-45MEOH).D
Date:21 October 2013
Acq method: C:\CHEM32\1\METHODS\LC_15_45_14MN_MEOH_

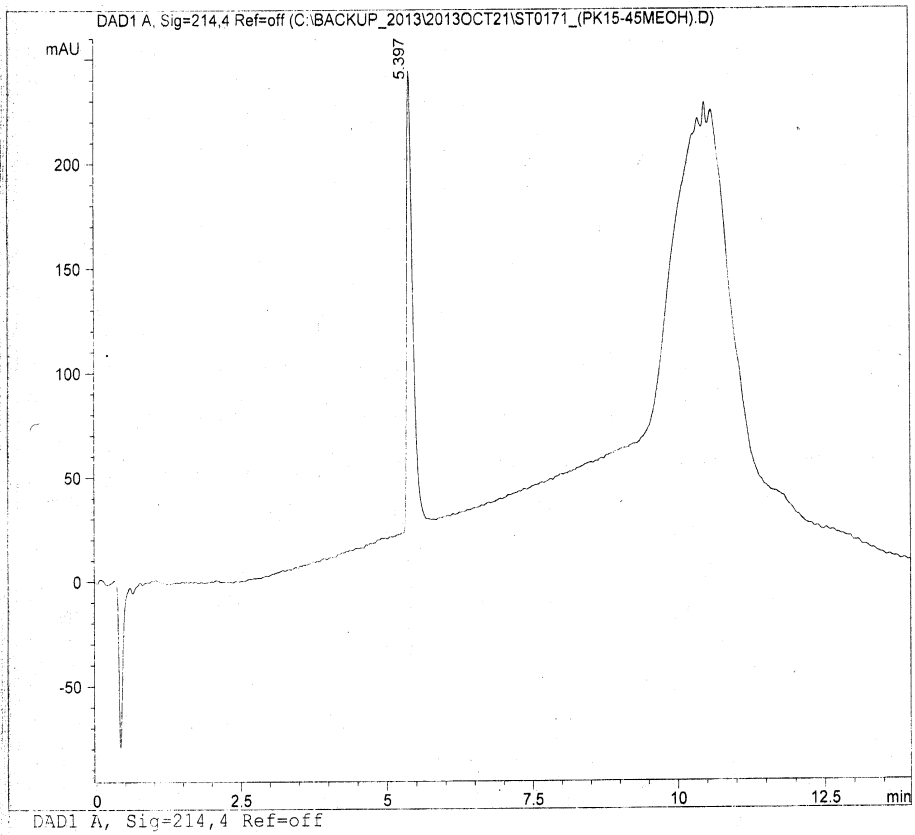

DAD1 A, Sig=214,4 Ref=off

Ret. Time	Height	Area	Area %
5.397	220.424	1589.335	100.000

H-w-A-AaF(4-MeO)-f-K-NH2

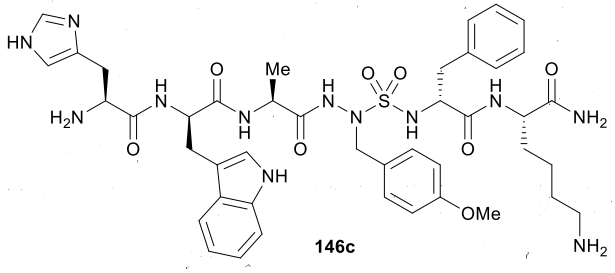

146c

Data File name: C:\BACKUP_2013\2013OCT21\ST0171_(PK10-30ACN).D
Date:21 October 2013
Acq method: C:\CHEM32\1\METHODS\LC_10_30_14MN_ACN_S

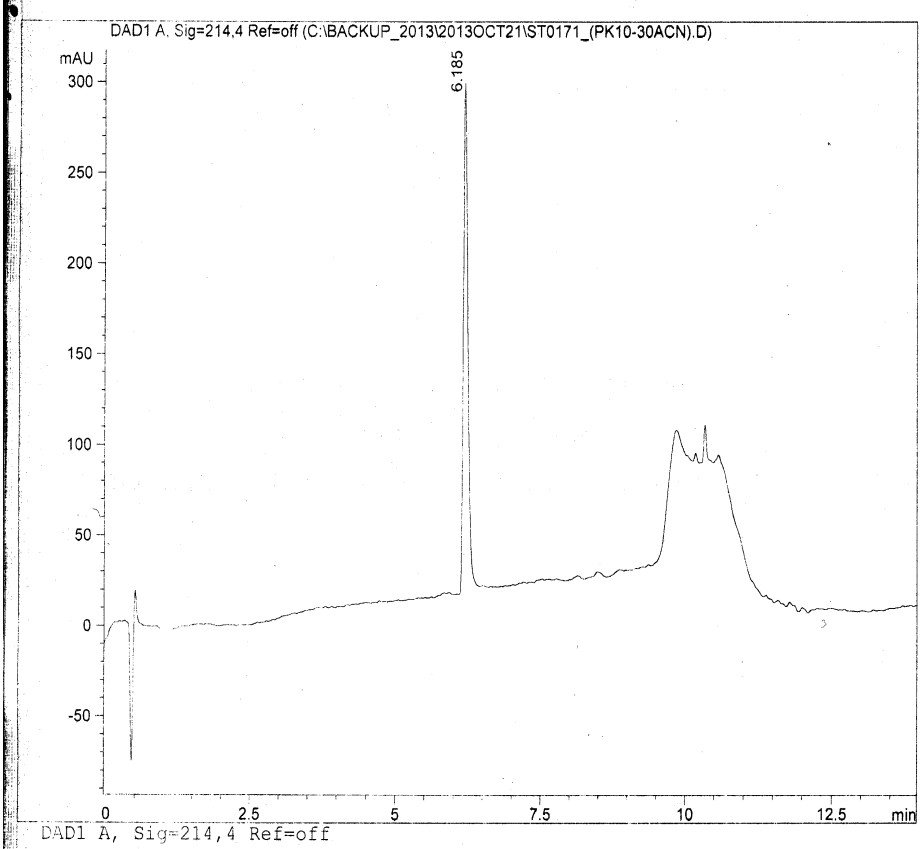

DAD1 A, Sig=214,4 Ref=off

Ret. Time	Height	Area	Area %
6.185	280.980	1508.167	100.000

H-w-A-Aa2F(4-meO)-L-K-NH2

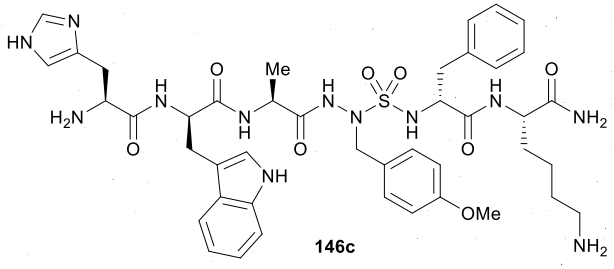

146c

Data File name: C:\BACKUP_2013\2013SEPT23\ST0152_(5-80MEOHS).D
Date:24 September 2013
Acq method: C:\CHEM32\1\METHODS\LC_05_80_14MN_MEOH_

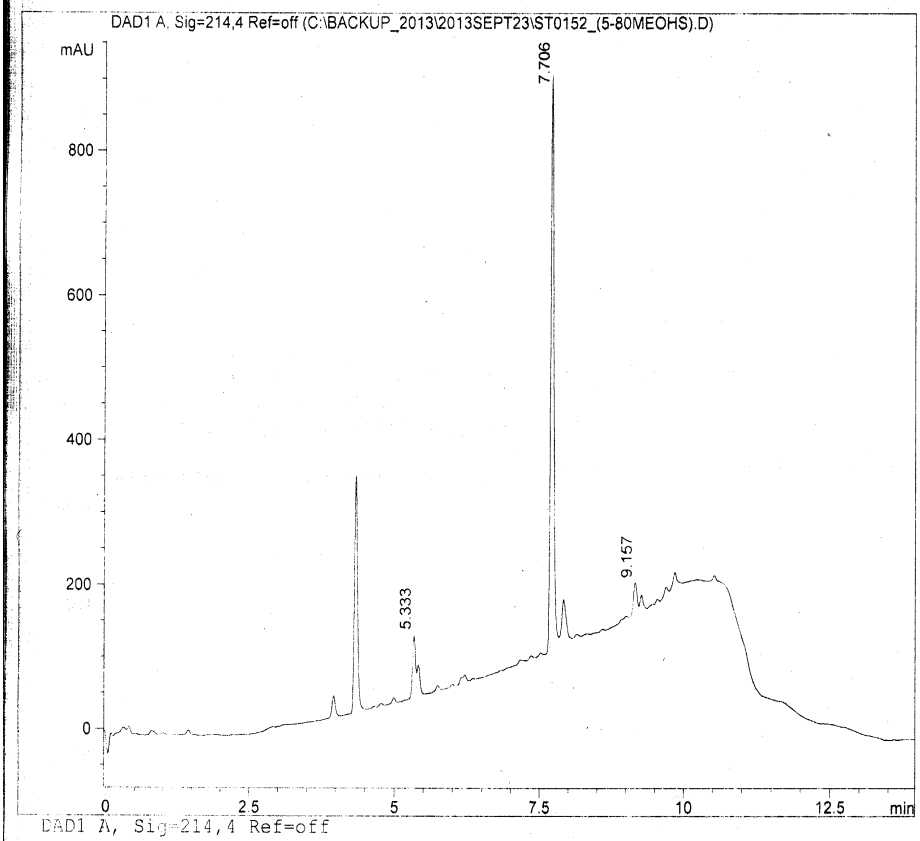

DAD1 A, Sig=214,4 Ref=off

Ret. Time	Height	Area	Area %	
5.333	85.603	436.000	11.926	Alloc-A-AaG-f-K-NH_2
7.706	794.198	2952.758	80.767	Alloc-A-AaA(2-Naphthyl)-f-K-NH_2
9.157	44.028	267.133	7.307	Alloc-A-AaA(2-Naphthyl)-(2-Naphthylmethyl)f-K-NH_2

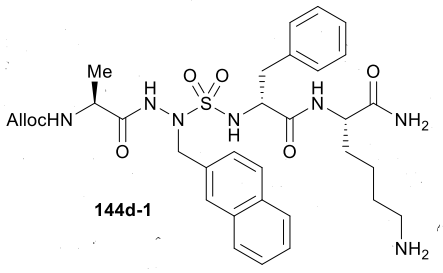

144d-1

Data File name: C:\BACKUP_2013\2013SEPT25\ST0156_(5-80MEOHS).D
Date:26 September 2013
Acq method: C:\CHEM32\1\METHODS\LC_05_80_14MN_MEOH_

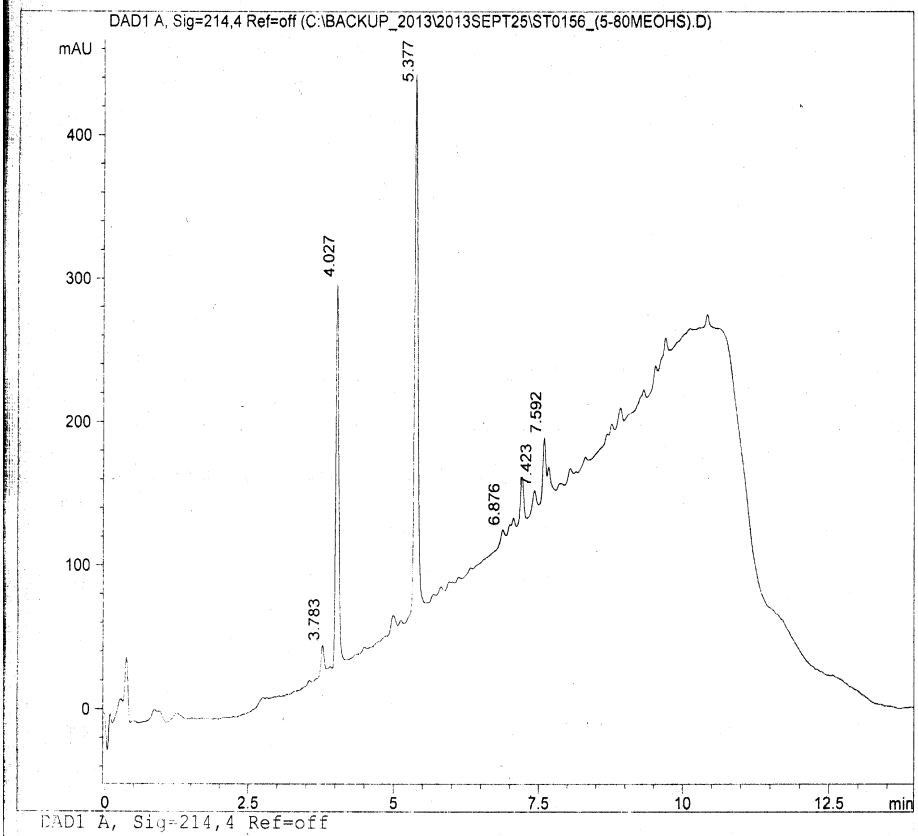

DAD1 A, Sig=214,4 Ref=off

Ret. Time	Height	Area	Area %
3.783	19.174	63.933	2.142
4.027	267.518	932.891	31.261
5.377	378.030	1527.307	51.179
6.876	7.988	33.276	1.115
7.059	7.409	37.910	1.270
7.207	30.568	106.897	3.582
7.423	13.056	53.121	1.780
7.592	43.223	228.890	7.670

A-A$_{sA}$A(2-Naphthyl)-L-K-NH$_2$

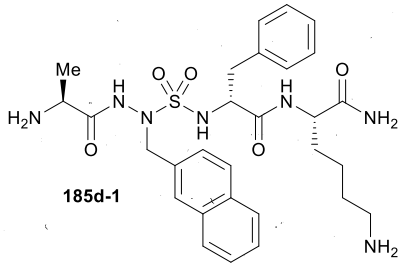

185d-1

Data File name: C:\BACKUP_2013\2013OCT21\ST0172_(PK25-55MEOH).D
Date:21 October 2013
Acq method: C:\CHEM32\1\METHODS\LC_25_55_14MN_MEOH_

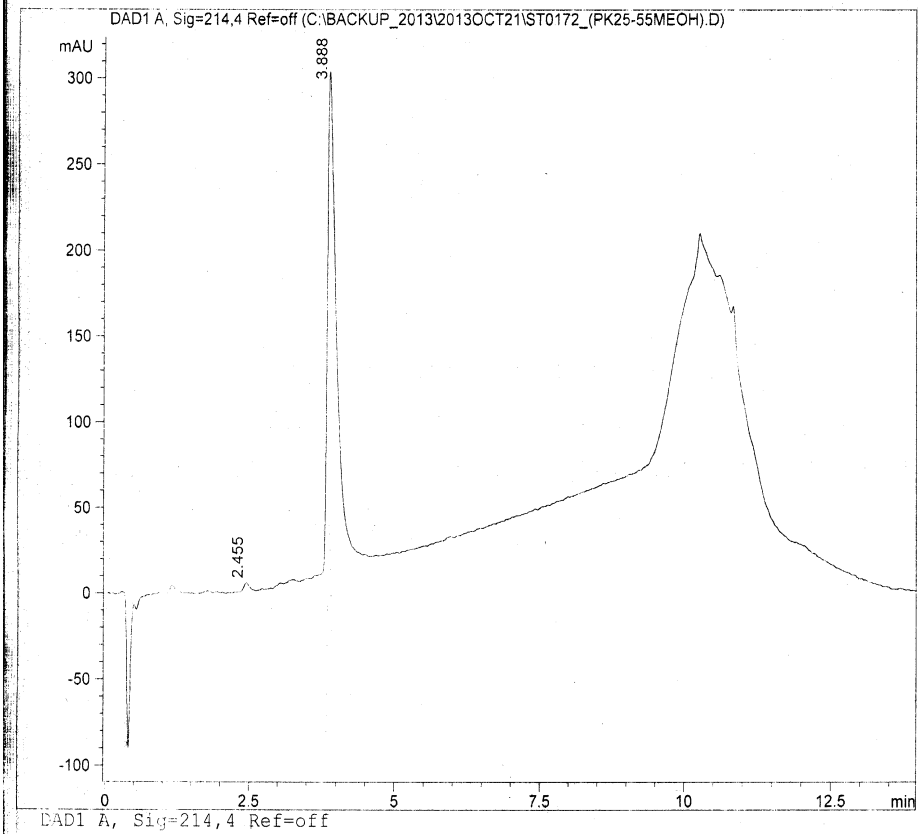

DAD1 A, Sig=214,4 Ref=off

Ret. Time	Height	Area	Area %
2.455	5.726	42.913	1.342
3.888	291.200	3154.309	98.658

H-w-A-AzaA(2-Naphthyl)-f-K-NH_2

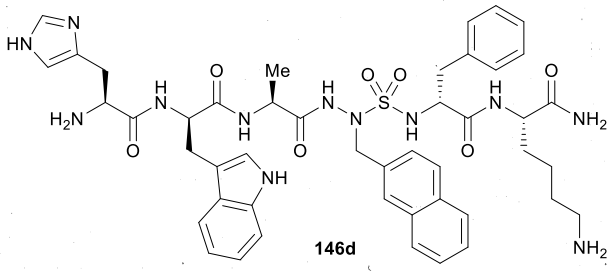

146d

Data File name: C:\BACKUP_2013\2013OCT07\ST0167_(5-80MEOH).D
Date:7 October 2013
Acq method: C:\CHEM32\1\METHODS\LC_05_80_14MN_MEOH_

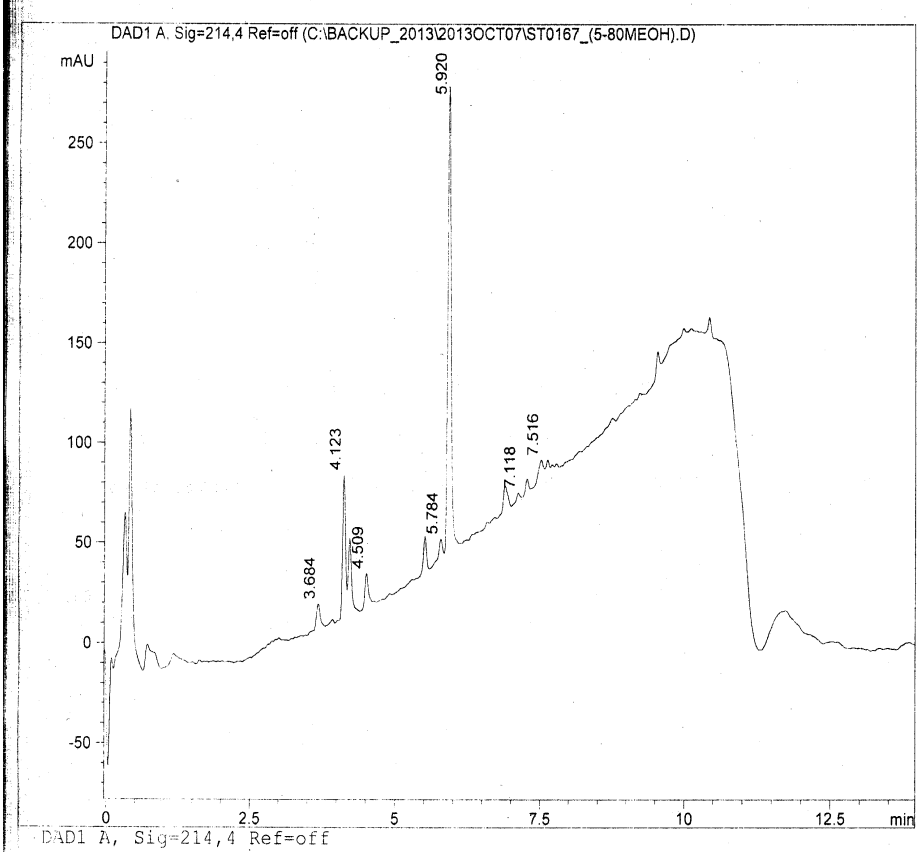

DAD1 A, Sig=214,4 Ref=off

Ret. Time	Height	Area	Area %
3.684	12.393	56.996	3.236
4.123	71.555	404.414	22.961
4.509	17.195	74.617	4.236
5.512	17.928	62.696	3.560
5.784	8.954	29.146	1.655
5.920	233.886	913.110	51.842
6.890	12.708	61.328	3.482
7.118	4.133	14.016	0.796
7.270	6.897	22.966	1.304
7.516	11.005	122.054	6.930

H-W-A-AmA(2-Naphthyl)-L-K-NH2

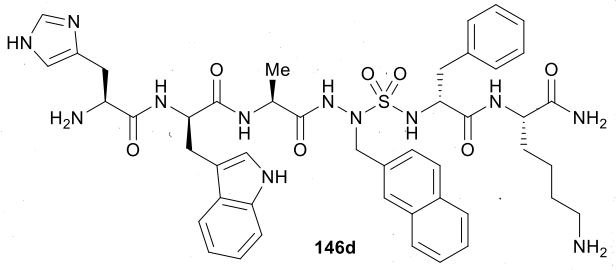

146d

Data File name: C:\BACKUP_2013\2013OCT21\ST0172_(PK15-35ACN).D
Date:21 October 2013
Acq method: C:\CHEM32\1\METHODS\LC_15_35_14MN_ACN_S

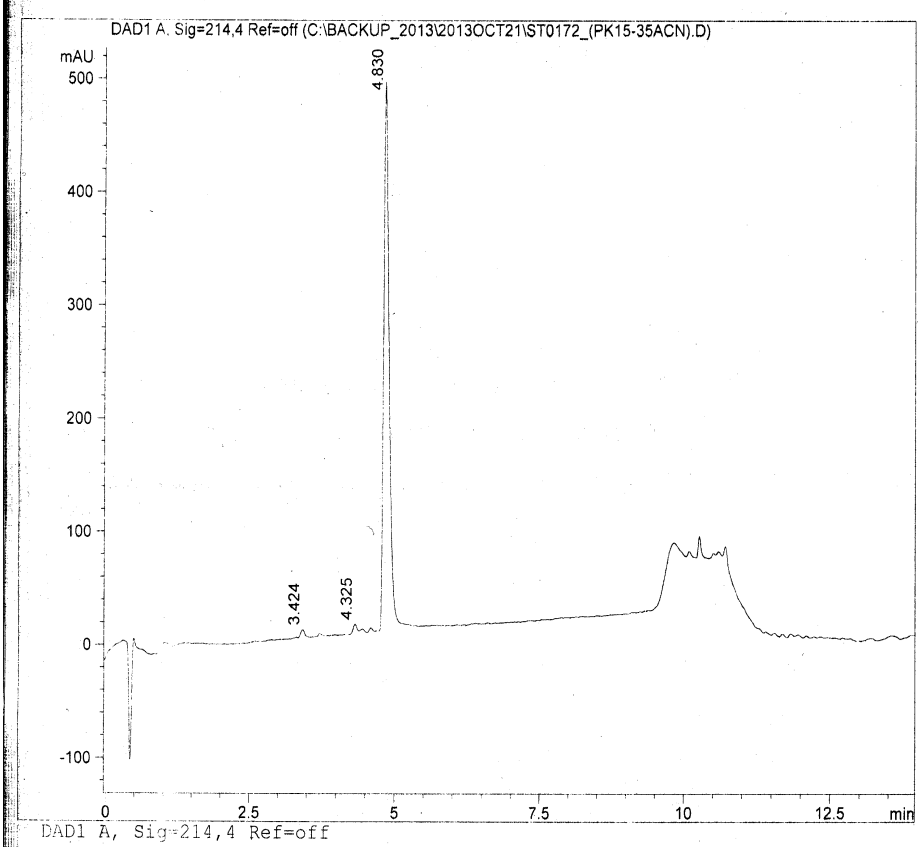

DAD1 A, Sig=214,4 Ref=off

Ret. Time	Height	Area	Area %
3.424	6.332	26.025	0.816
4.325	7.040	27.106	0.850
4.830	484.855	3135.502	98.334

H-w-A-Aza(2-Naphthyl)-L-K-NH2

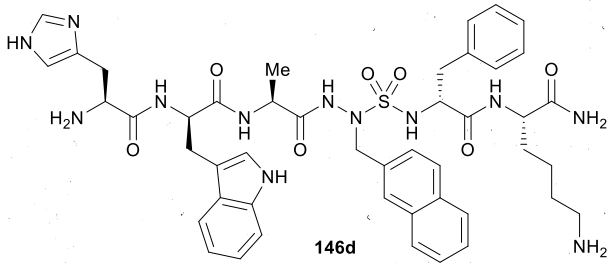

146d

Data File name: C:\BACKUP_2013\2013OCT01\ST0162_(5-80MEOHS).D
Date:1 October 2013
Acq method: C:\CHEM32\1\METHODS\LC_05_80_14MN_MEOH_

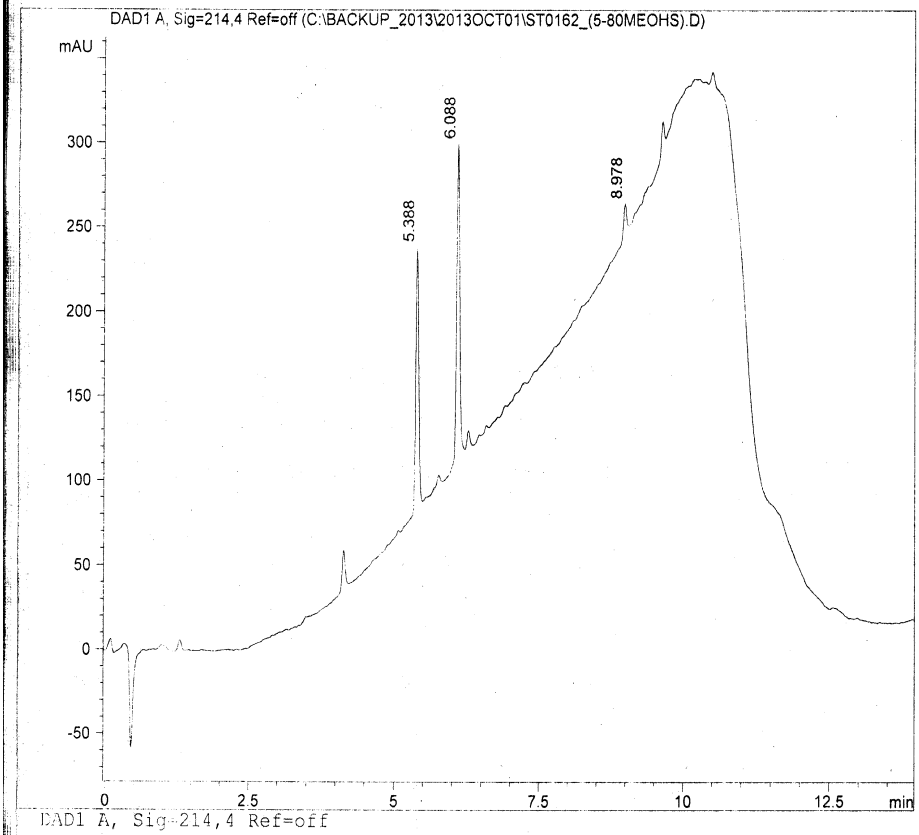

DAD1 A, Sig=214,4 Ref=off

Ret. Time	Height	Area	Area %	
5.388	155.569	555.995	41.747	Alloc-A-AaG-ℓ-K-NH_2
6.088	188.762	704.813	52.921	Alloc-A-AaY-ℓ-K-NH_2
8.978	19.636	71.007	5.332	Alloc-A-AaY-(4-HO-Bn)ℓ-K-NH_2

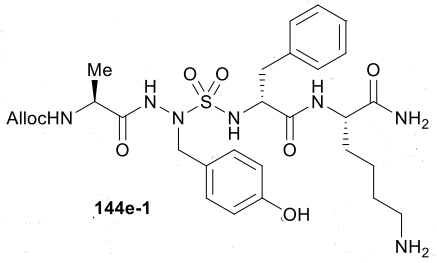

144e-1

Data File name: C:\BACKUP_2013\2013OCT07\ST0165_(5-80MEOH).D
Date:7 October 2013
Acq method: C:\CHEM32\1\METHODS\LC_05_80_14MN_MEOH_

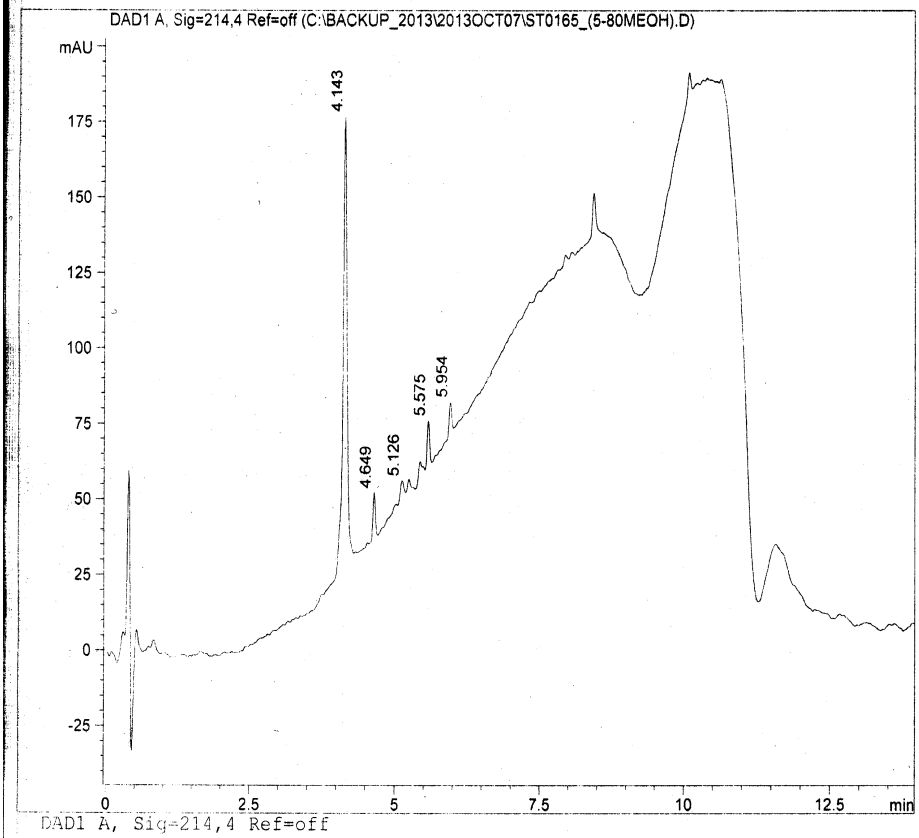

DAD1 A, Sig=214,4 Ref=off

Ret. Time	Height	Area	Area %
4.143	149.447	736.682	80.641
4.649	15.387	44.520	4.873
5.126	5.904	22.473	2.460
5.243	4.278	15.926	1.743
5.435	5.629	21.294	2.331
5.575	14.937	41.174	4.507
5.954	10.668	31.469	3.445

A-Ac-Y-L-K-NH_2

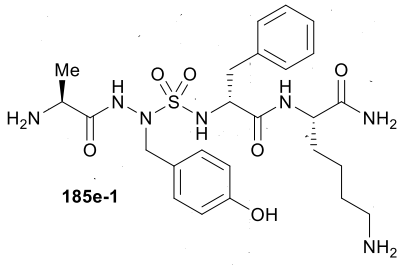

185e-1

Data File name: C:\BACKUP_2013\2013OCT15\ST0170_(10-40MEOH).D
Date:16 October 2013
Acq method: C:\CHEM32\1\METHODS\LC_10_40_14MN_MEOH_

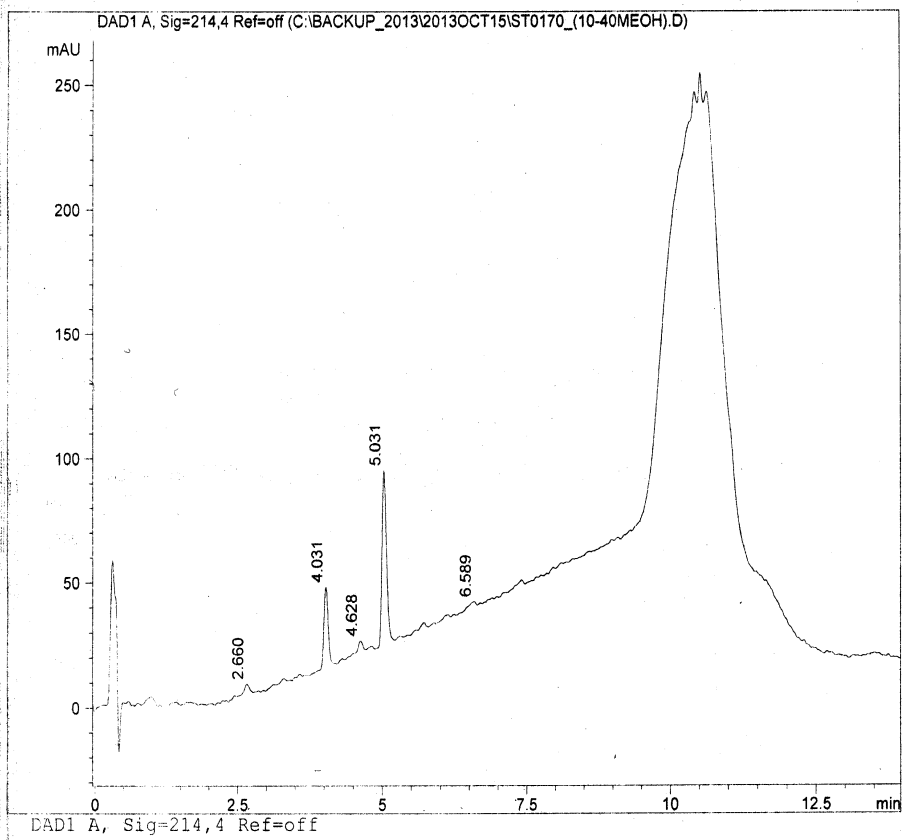

DAD1 A, Sig=214,4 Ref=off

Ret. Time	Height	Area	Area %
2.660	3.571	18.573	3.125
4.031	32.210	162.362	27.316
4.628	4.341	21.647	3.642
5.031	69.816	371.979	62.583
6.589	2.043	19.815	3.334

H-w-A-Aₚ-Y-β-K-NH₂

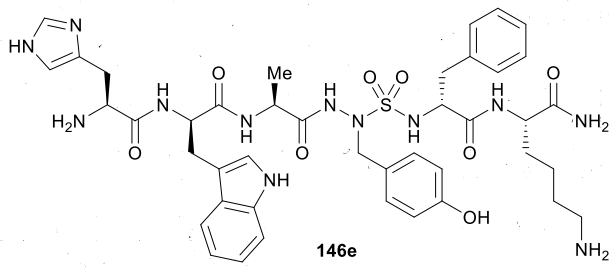

146e

Data File name: C:\BACKUP_2013\2013OCT30\ST0174_(PK15-45MEOH).D
Date:29 October 2013
Acq method: C:\CHEM32\1\METHODS\LC_15_45_12MN_MEOH_

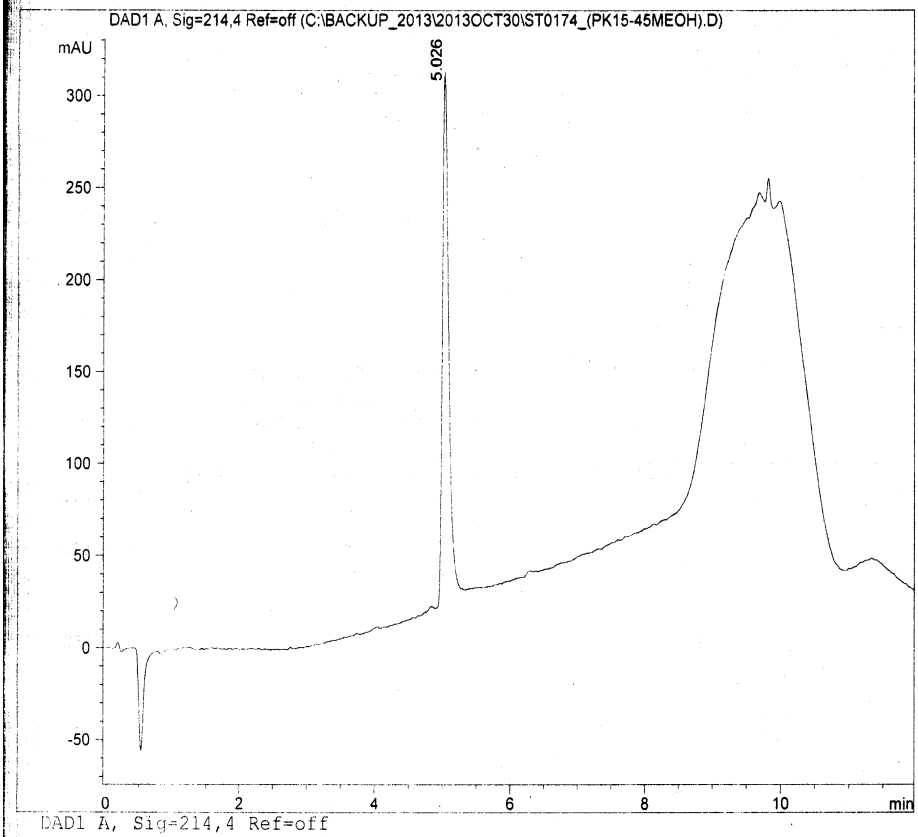

DAD1 A, Sig=214,4 Ref=off

Ret. Time	Height	Area	Area %
5.026	288.579	1851.172	100.000

H-W-A-Aₐ-Y-f-K-NH₂

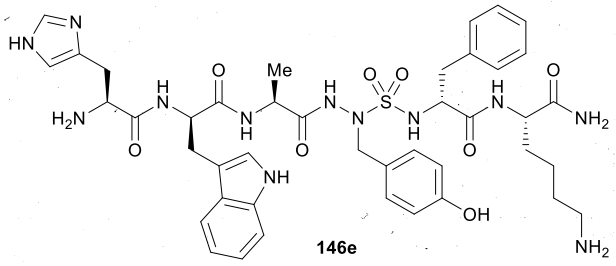

146e

Data File name: C:\BACKUP_2013\2013OCT30\ST0174_(PK15-40ACN).D
Date:29 October 2013
Acq method: C:\CHEM32\1\METHODS\LC_15_40_12MN_ACN_S

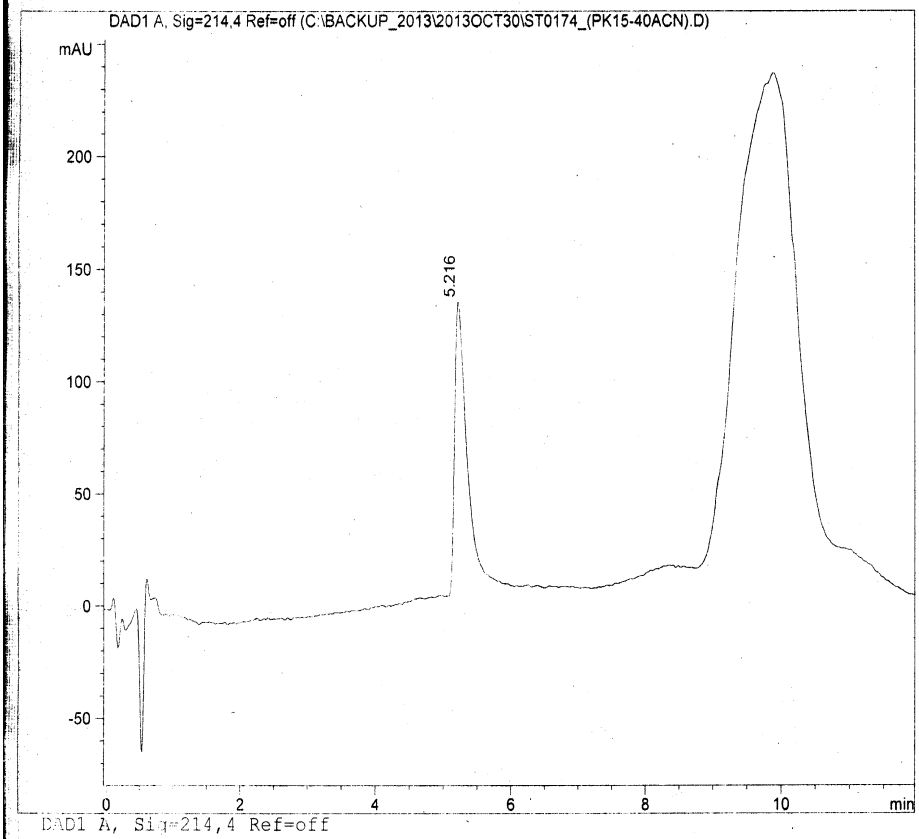

DAD1 A, Sig=214,4 Ref=off

Ret. Time	Height	Area	Area %
5.216	130.438	1676.003	100.000

H-w-A-Aa-Y-f-K-NH2

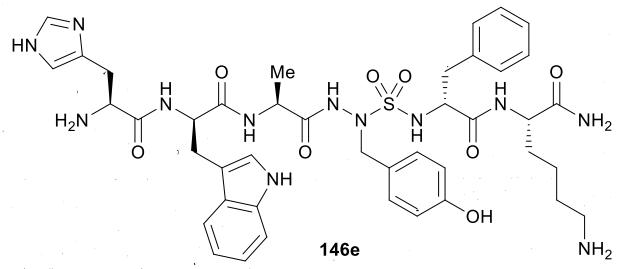

146e

Data File name: C:\CHEM32\1\DATA\2015MAR06\ST0369_5-90MEOH_12MN.D
Date:6 March 2015
Acq method: C:\CHEM32\1\METHODS\LC_05_90_20MN_MEOH_

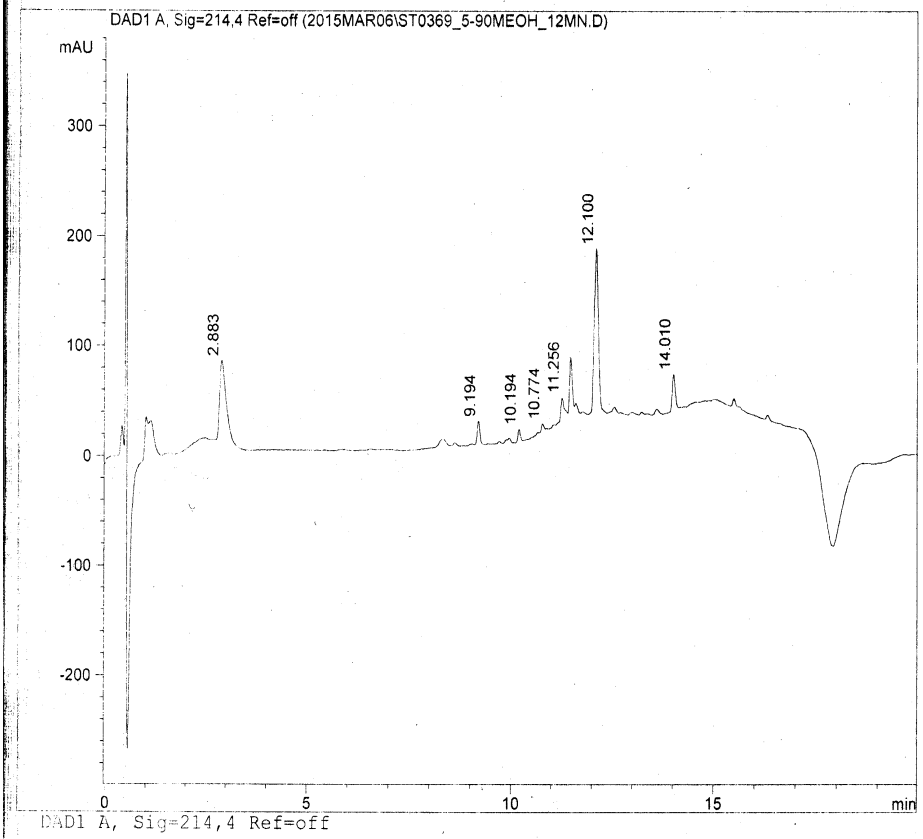

DAD1 A, Sig=214,4 Ref=off

Ret. Time	Height	Area	Area %	
2.883	74.591	852.401	31.385	Ac-f-K-NH2
9.194	21.666	101.844	3.750	
10.194	12.881	61.604	2.268	
10.774	7.850	37.740	1.390	
11.256	19.564	101.188	3.726	
11.466	52.219	306.093	11.270	
12.100	149.459	1079.040	39.730	Alloc-w-AoG-N-f-K-NH2
14.010	33.117	176.042	6.482	

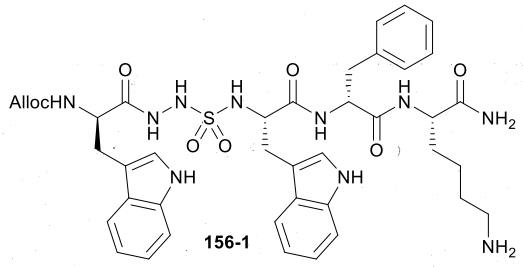

156-1

Data File name: C:\CHEM32\1\DATA\2015MAR11\ST0370_20-80MEOH_20MN.D
Date:11 March 2015
Acq method: C:\CHEM32\1\METHODS\LC_20_90_20MN_MEOH_

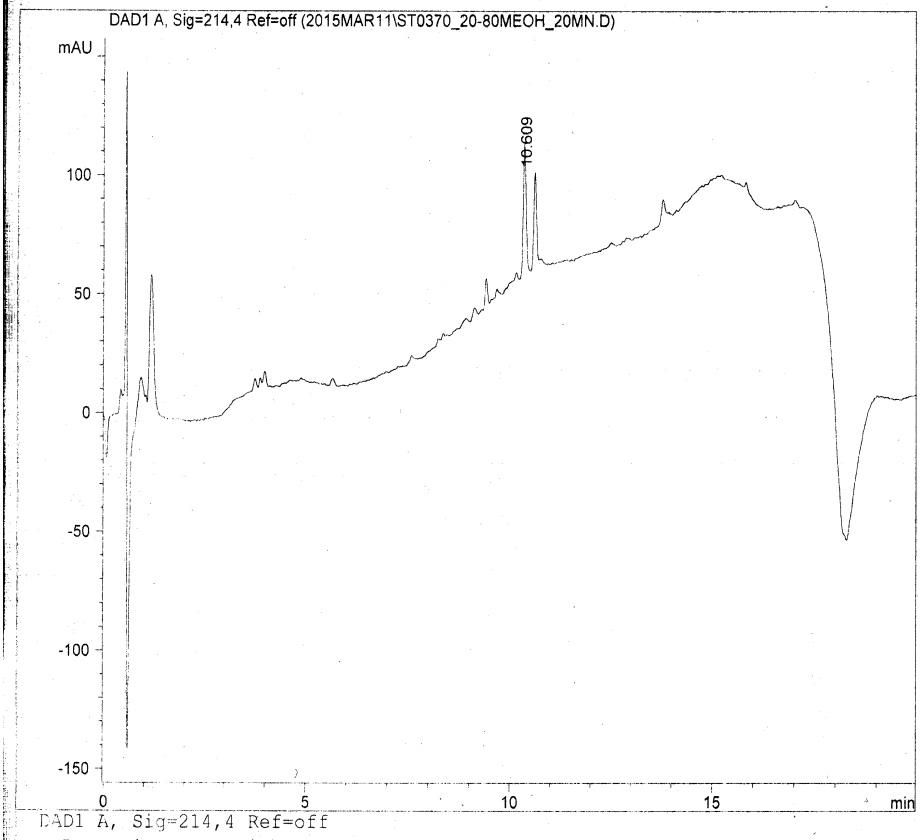

DAD1 A, Sig=214,4 Ref=off

Ret. Time	Height	Area	Area %	
10.349	55.087	274.519	60.180	Alloc-w-AsA-W-f-K-NH2
10.609	39.626	181.642	39.820	Alloc-w-AsG-W-f-K-NH2

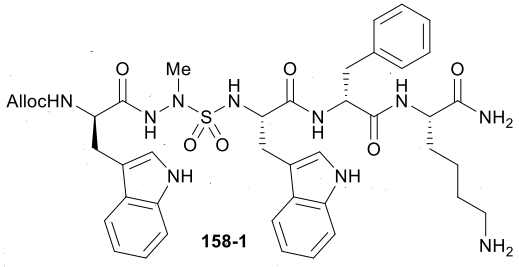

158-1

Data File name: C:\CHEM32\1\DATA\2015MAR20\ST0377-1_10-80MEOH.D
Date:20 March 2015
Acq method: C:\CHEM32\1\METHODS\LC_10_80_14MN_MEOH_

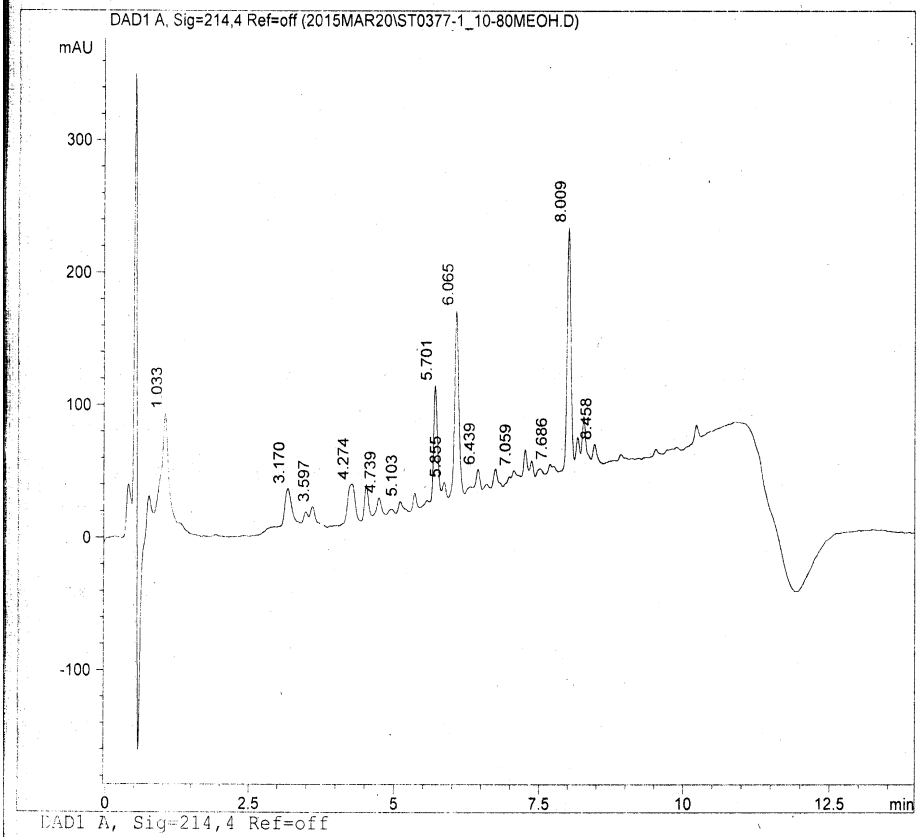

DAD1 A, Sig=214,4 Ref=off

Ret. Time	Height	Area	Area %
1.033	77.842	622.662	16.204
3.170	27.546	210.342	5.474
3.597	13.641	130.656	3.400
4.274	29.530	250.466	6.518
4.521	25.873	111.211	2.894
4.739	12.909	60.967	1.587
5.103	9.261	55.191	1.436
5.351	12.801	46.027	1.198
5.701	84.754	370.463	9.641
5.855	9.763	32.312	0.841
6.065	138.893	670.517	17.449
6.439	13.974	52.403	1.364
6.738	13.244	56.741	1.477
7.059	7.514	53.095	1.382
7.255	17.689	57.023	1.484
7.369	10.088	33.995	0.885
7.513	4.597	24.923	0.649
7.686	6.057	31.525	0.820
8.009	178.648	764.761	19.902
8.166	15.026	44.619	1.161
8.270	30.252	112.509	2.928
8.458	12.265	50.223	1.307

w-AoG-W-f-K-NH2
w-AoA-W-f-K-NH2